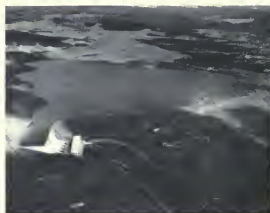




Copies of this bulletin at \$5.00 may be ordered from:

State of California  
DEPARTMENT OF WATER RESOURCES  
P.O. Box 94836  
Sacramento, CA 94236-0001

Make checks payable to:  
Department of Water Resources  
California residents add current sales tax.



ON THE COVER: Aerial view of Thermalito Forebay Dam, Powerplant, and Reservoir. See Figure 1 for location of Oroville-Thermalito facilities.

**Department of  
Water Resources**

**Bulletin 203-88**

# **The August 1, 1975 Oroville Earthquake Investigation**

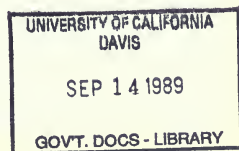
**Supplement to Bulletin 203-78**

**May 1989**

**Gordon K. Van Vleck  
Secretary for Resources  
The Resources  
Agency**

**George Deukmejian  
Governor  
State of  
California**

**David N. Kennedy  
Director  
Department of  
Water Resources**





**HARRY BOLTON SEED**  
1922—1989



*This bulletin is dedicated to the memory of Dr. Harry Bolton Seed. Dr. Seed, a member of the Special Consulting Board for the Oroville Earthquake, passed away shortly after completing the final review of the reports included in this bulletin.*

*Harry Seed was a giant in the field of geotechnical engineering and essentially pioneered all of the early and current methods used in geotechnical earthquake engineering. Many of the design and analysis methodologies used in the studies presented in this bulletin were developed from Dr. Seed's research during his thirty-eight year tenure at the University of California, Berkeley. Professor Seed has probably received more awards and honors than has any other civil engineer. Moreover, he was an extraordinary teacher who was able to impart knowledge to everyone with whom he came into contact.*

*Harry Seed had a special relationship with the Department of Water Resources. The Department sponsored much of his early research on the performance of soils and dams during earthquake shaking. He also supervised much of the modeling and testing performed at the Richmond Field Station during construction of the California State Water Project. Recently, the Department sponsored part of Dr. Seed's research in the performance of earthfill dams during recent earthquakes.*

*The Department benefited particularly from Harry Seed's guidance through his participation in several consulting boards. In addition to the Special Consulting Board for the Oroville Earthquake, he served on the Earthquake Analysis Board, which developed earthquake engineering criteria for the design of the State Water Project, and which was recently reconvened to provide guidance to our Division of Safety of Dams. He also served on several boards for the Department—relative to specific dams, including Auburn Dam, San Luis Dam, and O'Neill Forebay Dam.*

*Harry Seed had a unique gift for balancing the various needs of the public to achieve the greatest public good at minimum cost. Many individual members of the Department's staff were guided by and benefited from personal exchanges with him.*

*It is fitting that we take this opportunity to honor a man whose wisdom and abilities have had such a lasting impact on the activities of the California Department of Water Resources.*

*We will miss him.*



## FOREWORD

On August 1, 1975, an earthquake of Richter Scale magnitude of 5.7 occurred about 7.5 miles southwest of Oroville Dam. As reported in Department of Water Resources Bulletin 203-78 (February, 1979), the Oroville-Thermalito facilities demonstrated their ability to withstand the seismic loading of the earthquake. There was no structural damage; there was some superficial damage to a few secondary facilities.

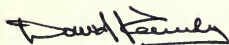
Following the earthquake, the Department established a Special Consulting Board, consisting of nine experts in the fields of seismology, geology, and dam design, to review the Department's investigations and to make recommendations for further investigations.

Bulletin 203-88 provides seismic re-evaluations of the various Oroville-Thermalito structures not addressed in Bulletin 203-78. The bulletin is presented in six chapters. Following Chapter I, "Introduction," Chapters II through VI provide seismic evaluations of these structures and facilities:

- II. Thermalito Powerplant Headworks
- III. Thermalito Afterbay Dam
- IV. Thermalito Afterbay Dam Concrete Structures
- V. Thermalito Forebay Dam
- VI. Bidwell Canyon and Parish Camp Saddle Dams and Effects of Possible Fault Movements in Oroville Project Dam Foundations

Chapters II through VI provide detailed technical presentations of the engineering re-evaluations for seismic stability of the structures and areas listed above. Conclusions and recommendations from each of those five chapters are summarized in Chapter I and supported in detail in the following chapters.

On the basis of this extensive re-evaluation of the Oroville-Thermalito facilities, the Department has concluded that those facilities pose no threat to public safety.



David N. Kennedy  
Department of Water Resources  
The Resources Agency  
State of California

SPECIAL CONSULTING BOARD  
FOR THE OROVILLE EARTHQUAKE

5 January 1989

Mr. John H. Lawder, Chief  
Division of Design and Construction  
Department of Water Resources  
1416 Ninth Street  
P.O. Box 942836  
Sacramento, California 94236-0001

Dear Mr. Lawder:

As requested, the Board has reviewed the following chapters of Bulletin 203-88, Supplement to Bulletin 203-78 "The August 1, 1975 Oroville Earthquake Investigations."

Chapter 1, Introduction, July 1988

Chapter 2, Seismic Evaluation of the Thermalito Power Plant Headworks

Chapter 3, Thermalito Afterbay Dam Seismic Evaluation

Chapter 4, Thermalito Afterbay Dam Concrete Structures Seismic Evaluation

Chapter 5, Thermalito Forebay Dam Seismic Evaluation, July 1988

Chapter 6, Seismic Evaluation of Bidwell Canyon and Parish Camp Saddle  
Dams and Effects of Possible Fault Movements in Oroville Project Dams  
Foundations, July 1988.

A meeting was held in the DWR building in Sacramento on November 18, 1988 with members of your staff making explanatory presentations and answering final questions from the Board members. The responses were fully adequate.

Based on its reviews the Board concurs with the conclusions presented in Chapters 1-6 of Bulletin 203-88 and with the adequacy of the remedial measures proposed.

Respectfully submitted,



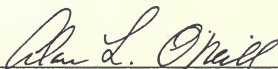
Clarence R. Allen



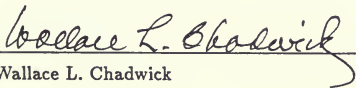
Thomas M. Leps



Bruce A. Bolt



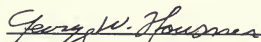
Alan L. O'Neill



Wallace L. Chadwick



H. Bolton Seed



George W. Housner

# CONTENTS

	Page
DEDICATION .....	ii
FOREWORD .....	v
FINAL REPORT FROM SPECIAL CONSULTING BOARD FOR THE OROVILLE EARTHQUAKE .....	vi
ENGINEERING CERTIFICATION .....	xl
ORGANIZATION .....	xli
CALIFORNIA WATER COMMISSION .....	xliii
 <b>CHAPTER I. INTRODUCTION</b> .....	 <b>1</b>
Background .....	1
Purpose .....	1
Description of the Oroville-Thermalito Facilities .....	1
The Investigating Organization .....	2
Summary Of Conclusions And Recommendations .....	3
Thermalito Powerplant Headworks (Chapter II) .....	3
Thermalito Afterbay Dam ( Chapter III) .....	3
Thermalito Afterbay Dam Concrete Structures (Chapter IV) .....	3
Thermalito Forebay Dam (Chapter V) .....	3
Bidwell Canyon and Parish Camp Saddle Dams (Chapter VI) .....	3
The Effects of Possible Fault Movements in Oroville Project Dam Foundations (Chapter VI) .....	3
Structural Modifications Made To Oroville-Thermalito Facilities .....	4
Department's Findings .....	4
 <b>CHAPTER II. SEISMIC EVALUATION OF THE THERMALITO POWERPLANT HEADWORKS</b> .....	 <b>5</b>
<b>PART 1</b> <b>LATERAL EARTHQUAKE FORCES FOR SAFETY EVALUATION</b> <b>OF THE THERMALITO POWERPLANT HEADWORKS</b>	
Introduction .....	5
Analysis Procedure .....	7
Computational Steps .....	7
Evaluation of the Procedure .....	8
Lateral Earthquake Forces .....	9
System and Ground Motion Properties .....	9
Computation of Earthquake Forces .....	9
Recommendations for Safety Evaluation .....	10
<b>PART 2</b> <b>EVALUATION OF STRESSES DUE TO LATERAL EARTHQUAKE FORCES</b>	
Review of Critical Stresses .....	29
Conclusions .....	30
References (for Chapter II) .....	31

## CONTENTS (Continued)

	Page
<b>CHAPTER III. THERMALITO AFTERBAY DAM, SEISMIC EVALUATION</b> .....	33
<b>1. SUMMARY</b> .....	33
Conclusions .....	33
Background .....	33
Concept and Progress of Investigations .....	34
Summary of Findings .....	35
<b>2. DESCRIPTION OF DAM AND FOUNDATION</b> .....	36
General .....	36
Embankment .....	36
Embankment Design .....	36
Embankment Materials .....	38
Foundation .....	38
Construction and Reservoir Filling .....	40
<b>3. EXPLORATION, SAMPLING, FIELD, AND LABORATORY TESTING</b> .....	41
Previous Foundation Exploration and Testing .....	41
1976 Drilling, Sampling, and Testing .....	41
1978 Drilling, Sampling, and Testing .....	41
1978 Standard Penetration Testing .....	42
1978 "Undisturbed" Sampling .....	42
Downhole Shear Wave Velocity Testing and Seismic Refraction Survey .....	44
1979-80 Investigations .....	47
Deep Foundation Borings .....	47
1979-80 Shear Wave Velocity Tests .....	47
1979-80 Standard Penetration Testing and Pitcher Barrel Sampling .....	47
1981-82 Investigations .....	49
Standard Penetration Testing .....	49
SPT Energy Calibration .....	51
Blowcount Correction for SPT Procedural Differences .....	54
Cone Soundings .....	56
Piston Sampling .....	56
<b>4. EMBANKMENT AND FOUNDATION CONDITIONS</b> .....	68
General .....	68
Mehrten Foundation .....	104
Red Bluff Formation .....	104
Columbia Soil Area .....	104
Embankment .....	105
Shear Wave Velocity Test Results .....	105
Preliminary Criteria for Identifying Suspect Sites .....	106

## CONTENTS (Continued)

	Page
Suspect Sites Identified by SPT Boring Survey .....	107
Additional Explorations to Delimit Suspect Sites .....	107
Sites Selected for Analyses .....	107
A. Model 1 – (Station 107 (Site 1)) .....	107
B. Model 2 – Station 165 (Worksite 2) .....	118
C. Model 3 – Station 347 (Columbia Soil) .....	120
5. ANALYSIS OF STATIC STRESSES .....	126
6. EARTHQUAKE MOTIONS .....	134
Background .....	134
Foundation Characteristics .....	137
Stiff Soil Sites .....	137
Deep Soil Sites .....	137
Pertinent Faults .....	137
Selection and Scaling of Accelerograms .....	138
7. ANALYSIS OF EARTHQUAKE INDUCED DYNAMIC STRESSES .....	142
8. STATIC AND CYCLIC SHEAR STRENGTHS .....	149
Static Shear Strength .....	149
Cyclic Shear Strength .....	154
Remolded Samples .....	154
1981–82 Correlation of Cyclic Strength with SPT .....	161
Sample Disturbance .....	161
Residual Pore Pressure .....	162
Determination of Cyclic Strength .....	162
9. EVALUATION OF LIQUEFACTION POTENTIAL .....	163
Method of Analysis .....	163
Cyclic Shear Strength .....	163
Liquefaction and Excess Pore Pressures .....	166
10. POST EARTHQUAKE SLOPE STABILITY ANALYSES .....	170
General .....	170
Sliding Wedge Analyses for Complete Liquefaction of Foundation Sand Layer .....	170
Sliding Wedge Analyses for Complete Liquefaction of Foundation Sand Layer—Shear Resistance Included on the Ends of the Sliding Block .....	170
Horizontal Sliding Analysis for Station 12 .....	173
Stability Analyses of the Three Model Sections for Pore Pressures Generated Immediately After Earthquake Shaking .....	173
Stability Analyses of the Three Model Sections for Redistributed Pore Pressures After Earthquake Shaking .....	174



## CONTENTS (Continued)

	Page
<b>11. PREDICTION OF EMBANKMENT PERFORMANCE</b>	177
General Considerations	177
Low Potential for Loss of Life	178
General Approach in the Evaluation	178
Degree of Conservatism in Analysis	178
Case Histories of Embankments With Foundation Liquefaction	180
Age of Red Bluff Silty Sands	181
Comparison With Upper San Fernando Dam	181
Other Earthquake Effects	182
Predicted Performance For Magnitude 6.5 Earthquake	183
References for Chapter III	185
<b>ADDENDA TO CHAPTER III</b>	
A. List of Borings and Soundings	191
B. Static Stresses from Static Finite Element Analyses	217
C. Accelerograms	229
D. Results of Dynamic Response Analyses	233
E. Dynamic Testing	243
F. Trial Failure Surfaces Generated for Slope Stability Analyses	251
<b>CHAPTER IV. THERMALITO AFTERBAY DAM CONCRETE STRUCTURES, SEISMIC EVALUATION</b>	253
Introduction	253
General Discussion	253
Original Seismic Design	254
Western Canal and Richvale Irrigation District Outlet	254
Description and Past Performance	254
Failure Evaluation	254
Seismic Reanalysis	255
PG and E Lateral	257
Description and Past Performance	257
Seismic Reanalysis	257
Sutter Butte Outlet	258
Description and Past Performance	258
Failure Evaluation	258
Seismic Reanalysis	258
Afterbay River Outlet	258
Description and Past Performance	258
Failure Evaluation	259
Seismic Reanalysis	263
Conclusion	263

## CONTENTS (Continued)

	Page
<b>CHAPTER V. SEISMIC EVALUATION OF THERMALITO FOREBAY DAM</b> .....	265
<b>1. SUMMARY</b> .....	265
Conclusions .....	265
Background .....	265
Concept of Investigation .....	265
Chronological Summary of the Investigation .....	266
1976 .....	266
1978 .....	266
1979-1980 .....	266
1981-1984 .....	267
1984-1988 .....	268
Summary of Findings .....	268
<b>2. DESIGN, CONSTRUCTION, AND PERFORMANCE OF THERMALITO FOREBAY DAM</b> ..	271
General Description of Dam and Reservoir .....	271
Site Geology .....	271
Geologic Investigations During Design .....	273
Geologic Investigations During Construction .....	276
General Description of the Design and Construction of the Embankment .....	277
Main Dam .....	277
Ruddy Creek Dam .....	277
Low Dam .....	277
Foundation Conditions .....	280
Foundation Treatment .....	281
Construction Materials .....	281
Stability Analysis of the Embankment .....	286
Concrete Wingwall Dams .....	287
Approach Channel Wingwall .....	287
Approach Channel Dam .....	288
Design Considerations .....	288
Embankment Instrumentation .....	288
Seepage Control Measures During and After Construction .....	288
Cutoff Trench and Upstream Blanket .....	291
Channel H Blanket .....	293
Relief Well System .....	293
Tail Channel Seepage .....	295
Current Evaluation of the Embankment Performance .....	295
Piezometers .....	295
Embankment Toe Drain Outlets .....	295
Seepage Relief System .....	295
Tail Channel Seepage Area .....	299

## CONTENTS (Continued)

	Page
Crest and Embankment Monuments .....	300
Vertical and Horizontal Movements .....	300
General Conditions .....	300
Assessment of Performance .....	300
<b>3. EXPLORATION, SAMPLING, AND FIELD TESTING .....</b>	<b>305</b>
Introduction .....	305
Standard Penetration Test Procedure .....	305
SPT Blowcount Corrections for Use with Seed and Idriss (1982) Correlation .....	305
SPT Blowcount Corrections for Use with Seed (1987) Correlation .....	306
SPT Notation .....	306
Chronological Summary of Field Testing .....	306
1976 Program .....	306
1978 Program .....	308
1979-1980 Program .....	309
1981-1982 Program .....	309
Cone Penetrometer Soundings .....	311
1984 Program .....	311
Characteristics of Red Bluff Formation Soils .....	311
General Characteristics of Suspect Soil Sites .....	339
Installation of Piezometers .....	342
<b>4. LABORATORY TESTING AND EVALUATION .....</b>	<b>356</b>
General .....	356
Chronological Summary of Laboratory Testing—1976 Program .....	356
1978 Program .....	356
1979-1980 Program .....	356
1981-1982 Program .....	358
Introduction .....	358
Classification Testing —Red Bluff Sediments .....	358
Classification Testing —Low Blowcount Foundation Sands .....	359
Cyclic Triaxial Testing—Low Blowcount Foundation Sands .....	360
1984 Program .....	361
General .....	361
Static Triaxial Compression Tests .....	361
Post-Cyclic Triaxial Tests .....	363
<b>5. IDENTIFICATION AND MODELING OF CRITICAL AREAS .....</b>	<b>386</b>
Introduction .....	386
Identifying Potential Liquefaction Sites .....	386
Identification of Most Critical Area at the Main Dam .....	386
Identification of Most Critical Area at the Low Dam .....	386
Assumptions for Developing Simplified Models .....	386

## CONTENTS (Continued)

	Page
Simplified Foundation Model—Main Dam—Station 10-11 .....	402
Simplified Foundation Model—Low Dam—Station 112 .....	403
Simplified Embankment—Foundation Models .....	403
<b>6. STATIC STRESS ANALYSES .....</b>	<b>406</b>
Introduction .....	406
Method of Analysis .....	406
Models .....	406
Results .....	406
<b>7. DYNAMIC RESPONSE ANALYSES .....</b>	<b>411</b>
Introduction .....	411
Background on Earthquake Motions Used in Analyses .....	411
Earthquake Motions Adopted for Current Evaluation .....	414
Methods of Analysis .....	415
Results from Program SHAKE .....	420
Results from Program QUAD4 .....	421
Dynamic Shear Stresses Adopted for Evaluations .....	422
<b>8. DETERMINATION OF PREDICTED ZONES OF LIQUEFACTION .....</b>	<b>433</b>
General .....	433
Determination of Cyclic Loading Resistance .....	433
Determination of Liquefaction Factors of Safety .....	434
<b>9. POST-EARTHQUAKE SLOPE STABILITY ANALYSES .....</b>	<b>437</b>
Introduction .....	437
Post-Earthquake Shear Strengths .....	437
Clayey Embankment and Foundation Cap .....	437
Non-Liquefied Suspect Foundation Soils .....	437
Liquefied Suspect Foundation Soils .....	437
Slope Stability Analyses .....	439
Effect of Residual Shear Strength .....	442
<b>10. EVALUATION OF CONCRETE WINGWALL DAMS .....</b>	<b>445</b>
Introduction .....	445
Description of Concrete Wingwall Dams .....	445
Approach Channel Dam .....	445
Wingwall Dam .....	445
Concrete Mixes .....	447

## CONTENTS (Continued)

	Page
Pseudodynamic Sliding Analyses .....	447
General .....	447
Re-evaluation of Pseudodynamic Sliding .....	447
Approach Channel Dam .....	447
Wingwall Dam .....	448
Simplified Dynamic Tensile Stress Analyses .....	448
General .....	448
Analysis Parameters .....	451
Approach Channel Dam .....	451
Wingwall Dam .....	451
Computed Tensile Stresses .....	452
Performance of Concrete Dams During Earthquake Shaking .....	454
Predicted Deformations .....	454
Prediction of Performance .....	455
<b>11. PREDICTION OF EMBANKMENT PERFORMANCE .....</b>	<b>458</b>
General .....	458
Summary of Predicted Embankment Stability .....	458
Predicted Level of Permanent Earthquake-Induced Deformations .....	458
Predicted Effects Due to Differential Settlement and Embankment Cracking .....	459
Potential Cracking Due to Fault Displacement .....	459
Potential Cracking Due to Foundation Bedrock Profile .....	459
Potential Cracking at the Wingwall/Embankment Contact .....	463
Summary of Predicted Embankment Performance For Magnitude 6.5 Earthquake .....	464
Embankment Stability .....	464
Embankment Deformation .....	464
Embankment Cracking .....	465
References for Chapter V .....	466
<b>ADDENDA TO CHAPTER V</b>	
A. Glossary .....	474
B. Explorations For Thermalito Forebay Seismic Evaluations .....	477
C. Static Stress Finite Element Analyses .....	485
D. Cyclic Triaxial Test Summaries .....	497
E. Dynamic Stress Analyses .....	521
F. Examination Of The Performance Of Upper San Fernando Dam During The Earthquake Of February 9, 1971 .....	543
<b>I. INTRODUCTION (to Addendum F) .....</b>	<b>545</b>
Description of Upper San Fernando Dam .....	545
Earthquake of February 9, 1971 .....	545

## CONTENTS (Continued)

	Page
Earthquake-Induced Displacements .....	545
Earthquake-Induced Pore Pressure Changes .....	548
1973 Liquefaction Evaluation .....	548
 <b>II. 1971 POST-EARTHQUAKE DRILLING EXPLORATIONS</b> .....	 549
Introduction .....	549
Standard Penetration Testing .....	549
SPT Test Procedures .....	549
Procedural and Overburden Corrections to Measured SPT Blowcount .....	549
Corrected Post-Earthquake SPT Blowcounts .....	549
Average Pre-Earthquake SPT Blowcount .....	550
 <b>III. POST-EARTHQUAKE SLOPE STABILITY ANALYSES</b> .....	 557
General .....	557
Stability Model and Parameters .....	557
Determination of Residual Shear Strength .....	558
Comparison of Estimates of Residual Strength for Upper San Fernando Dam with Correlation Developed By Seed et al. (1988) .....	561
 <b>IV. CONCLUSIONS</b> .....	 562
References for Addendum F .....	563
 <b>CHAPTER VI. SEISMIC EVALUATION OF BIDWELL CANYON AND PARISH CAMP               SADDLE DAMS AND EFFECTS OF POSSIBLE FAULT MOVEMENTS               IN OROVILLE PROJECT DAM FOUNDATIONS</b> .....	   565
<b>1. EXECUTIVE SUMMARY</b> .....	565
Conclusions .....	565
Background .....	565
<b>2. SEISMIC EVALUATION OF PARISH CAMP SADDLE DAM</b> .....	565
<b>3. SEISMIC EVALUATION OF BIDWELL CANYON SADDLE DAM</b> .....	566
General .....	566
Embankment .....	566
Foundation .....	569
Seismic Evaluation .....	570

## CONTENTS (Continued)

	Page
<b>4. EFFECTS OF POSSIBLE FAULT MOVEMENTS ON OROVILLE PROJECT DAMS</b> .....	575
Possible Fault Movements .....	575
Evaluation of Possible Effects of Fault Movements .....	576
Oroville Dam .....	576
Bidwell Canyon Saddle Dam .....	576
Parish Camp Saddle Dam .....	579
Thermalito Diversion Dam, Thermalito Fish Barrier Dam, and Thermalito Powerplant Headworks .....	579
Thermalito Forebay and Afterbay Dams .....	579
References for Chapter VI .....	580
 <b>APPENDIX A. REPORTS PREPARED BY THE SPECIAL CONSULTING BOARD FOR THE OROVILLE EARTHQUAKE BETWEEN 1979 AND 1989</b> .....	 581

## FIGURES

No.	Page
<b>—Chapter I—</b>	
1. Location Map—Oroville—Thermalito Facilities .....	xliv
2. Thermalito Forebay Dam, Powerplant, and Reservoir .....	1
3. Thermalito Afterbay Dam and Reservoir .....	2
<b>— Chapter II —</b>	
4. Location Map, Thermalito Powerplant, Forebay, and Afterbay .....	6
5. Standard Values for $R_1$ — the Ratio of Fundamental Vibration Periods of the Dam with and without Water, Plotted against Depth of Water for Various Values of E, the modulus of elasticity for concrete ....	7
6. Standard Fundamental Period and Mode Shape of Vibration for Design of Concrete Gravity Dams .....	8
7. Standard Plots for Variation of $p_1$ over the depth of water .....	8
8. Horizontal Ground Acceleration Specified by DWR .....	10
9. Pseudo Acceleration Response Spectrum for the Ground Motion Specified by DWR; Damping = 5% ....	12
10. Transverse Section, Unit No. 1 .....	13
11. Thermalito Powerplant, Intake and Penstocks .....	15
12. Area Properties of Planes .....	16
13. Individual Loads on Planes .....	19
14. Cumulative Loads on Planes .....	22
15. Individual Loads on Planes .....	26
16. Moments on Planes—Earthquake Upstream/Earthquake Downstream .....	27
17. Maximum Tensile Stresses .....	28
18. Height of Pier .....	28

## CONTENTS (Continued)

### Figures (continued)

Page

#### — Chapter III —

#### — Section 2 —

19.	Vicinity Map of Thermalito Afterbay .....	37
20.	Typical Embankment Sections for Thermalito Afterbay .....	38
21.	Thermalito Afterbay Dam Alignment and Reservoir Area .....	39

#### — Chapter III, Section 3 —

22.	1978 Standard Penetration Testing at Thermalito Afterbay .....	43
23.	1978 Procedure Used in Obtaining Undisturbed Samples of Thermalito Afterbay Sands .....	44
24.	1978 Sampling of Thermalito Afterbay Sand Layers .....	45
25.	1979-80 Shear Wave Velocity Testing at Thermalito Afterbay Station 107 (Site-1) .....	46
26.	Typical Sampling Intervals .....	48
27.	Baffled Drag Bit Used for SPT Borings at Thermalito Afterbay Dam, 1981-82 .....	49
28.	Details and Photo of Split Barrel Sampler Used in Standard Penetration Testing at Thermalito Afterbay ..	50
29.	Comparison of SPT N Values Between 1981 Continental Borings and 1979 Caltrans Boring at Station 107 + 00 .....	51
30.	Comparison of SPT N Values Between 1981 Continental Borings and 1979 Caltrans Boring at Station 102 + 00 .....	51
31.	Configuration of SPT Hammers .....	52
32.	Comparison of Sampling Energy Dissipation and SPT Blowcounts .....	53
33.	Comparison of SPT N Values Delivered by Safety and Doughnut Hammers .....	54
34.	Standard Penetration Test N Values and Material Types for Piston Sampling Station 102 + 50 .....	57
35.	Standard Penetration Test N Values and Material Types for Piston Sampling Station 107N .....	58
36.	Standard Penetration Test N Values and Material Types for Piston Sampling Station 107S .....	59
37.	Standard Penetration Test N Values and Material Types for Piston Sampling Station 164 + 50 .....	60
38.	Standard Penetration Test N Values and Material Types for Piston Sampling Station 165 .....	61
39.	Standard Penetration Test N Values and Material Types for Piston Sampling Station 167 .....	62
40.	Standard Penetration Test N Values and Material Types for Piston Sampling Station 183 .....	63
41.	Standard Penetration Test N Values and Material Types for Piston Sampling Station 380 .....	64
42.	Standard Penetration Test N Values and Material Types for Piston Sampling Station 383 .....	65
43.	"Gregory Undisturbed Sampler" used in "Undisturbed" Sampling of Thermalito Afterbay Foundation Silty Sands .....	66
44.	Trimming Tool, Perforated and Solid Expendable Packers, and Transport Box used in 1981-82 "Undisturbed" Sampling .....	67



## CONTENTS (Continued)

### FIGURES (continued)

No.		Page
- Chapter III, Section 4 -		
45.	Thermalito Afterbay Dam Boring Profiles: Plan and Profiles .....	70
46.	Thermalito Afterbay Dam Boring Profiles: Saddle Dam—Station 10 .....	72
47.	Thermalito Afterbay Dam Boring Profiles: Station 10—Station 35 .....	74
48.	Thermalito Afterbay Dam Boring Profiles: Station 35—Station 59 .....	76
49.	Thermalito Afterbay Dam Boring Profiles: Station 59—Station 91 .....	78
50.	Thermalito Afterbay Dam Boring Profiles: Station 91—Station 119 .....	80
51.	Thermalito Afterbay Dam Boring Profiles: Station 119—Station 147 .....	82
52.	Thermalito Afterbay Dam Boring Profiles: Station 147—Station 174 .....	84
53.	Thermalito Afterbay Dam Boring Profiles: Station 174—Station 202 .....	86
54.	Thermalito Afterbay Dam Boring Profiles: Station 202—Station 229 .....	88
55.	Thermalito Afterbay Dam Boring Profiles: Station 229—Station 256 .....	90
56.	Thermalito Afterbay Dam Boring Profiles: Station 256—Station 284 .....	92
57.	Thermalito Afterbay Dam Boring Profiles: Station 284—Station 311 .....	94
58.	Thermalito Afterbay Dam Boring Profiles: Station 311—Station 337 .....	96
59.	Thermalito Afterbay Dam Boring Profiles: Station 337—Station 365 .....	98
60.	Thermalito Afterbay Dam Boring Profiles: Station 365—Station 396 .....	100
61.	Thermalito Afterbay Dam Boring Profiles: Station 396—Station 404 .....	102
62.	Strata Predicted from 1978 Seismic Refraction Survey at Thermalito Afterbay Station 173 (Site 2) .....	104
63.	Gradation Curves for Columbia Soil Area Gravels .....	105
64.	Gradation Range for Thermalito Afterbay Embankment Clay .....	105
65.	Downhole Shear Wave Velocity Results for Thermalito Afterbay Station 107 (Site 1) .....	106
66.	Results of Downhole and Crosshole Shear Wave Velocity Test at Thermalito Afterbay Station 107 (Site 1) .....	107
67.	Suspect Sites with Soils Having Low Enough SPT $N_{A1}$ Values to Require Additional Studies .....	108
68.	Corrected Penetration Resistance at Thermalito Afterbay Stations 102–112 (Site 1) .....	117
69.	Minimum Corrected SPT Resistance Within Borings Between Stations 106 and 108 .....	117
70.	Corrected Standard Penetration Resistance Along Toe Between Stations 106 and 108 .....	118
71.	Gradation Envelope of Samples Collected from Stations 102–110 Representing the Suspect Layer for Model 1 (Site 1) .....	118
72.	Gradation Characteristics of Low Blowcount Sands Between Stations 106 and 108 .....	119
73.	Model Developed for Analysis of Station 107 (Site 1) .....	119
74.	Minimum Corrected SPT Resistance Within Borings and Soundings Between Stations 164 and 171 .....	120

## CONTENTS (Continued)

### FIGURES (continued)

No.	Page
75. Corrected Standard Penetration Resistance Along Toe Between Stations 164 and 167 .....	120
76. Penetration Resistance of Explorations near Borehole 81A-167 SPT B .....	123
77. Gradation Envelope of Samples Collected from Stations 164-171 Representing Suspect Layer for Model 2 (Worksite 2) .....	124
78. Gradation Characteristics of Low Blowcount Sands Between Stations 164 and 167 .....	124
79. Model Section Developed for Analysis of Station 165 (Worksite 2) .....	125
80. Corrected SPT Resistance at Thermalito Afterbay Dam Stations 344 to 350 .....	125
81. Gradation Envelope of SPT Silty Sand Samples Collected from Stations 344 to 348 and Between Elevations 91-101 feet .....	126
82. Model Section Developed for Analysis of Station 347 (Columbia Soil) .....	126
- Chapter III, Section 5 -	
83. Finite Element Mesh used in Static Stress Analyses for Thermalito Afterbay Dam Station 107 (Site 1) ...	127
84. Finite Element Mesh used in Static Stress Analyses for Thermalito Afterbay Dam Station 165 (Worksite 2) .....	127
85. Finite Element Mesh used in Static Stress Analyses for Thermalito Afterbay Dam Station 347 .....	127
86. Flow Nets Assumed for Static Finite Element Analysis of Thermalito Afterbay Station 107 (Site 1) .....	129
87. Flow Nets Assumed for Static Finite Element Analysis of Thermalito Afterbay Station 165 (Worksite 2) .....	129
88. Flow Nets Assumed for Static Finite Element Analysis of Thermalito Afterbay Columbia Soil (Stations 348 and 351) .....	130
89. Thermalito Afterbay Station 107 (Site 1) Embankment and Foundation Profile with Stress-Strain Parameters used in Static Finite Element Analysis .....	130
90. Thermalito Afterbay Station 165 (Worksite 2) Embankment and Foundation Profile with Stress-Strain Parameters used in Static Finite Element Analysis .....	131
91. Thermalito Afterbay Station 347 (Columbia Soil Area) Embankment and Foundation Profile with Stress-Strain Parameters used in Static Finite Element Analysis .....	131
92. Contours of Effective Vertical Normal Stress and Alpha Values Determined from Static Finite Element Analysis of Thermalito Afterbay Station 107 (Site 1) .....	132
93. Contours of Effective Vertical Normal Stress and Alpha Values Determined from Static Finite Element Analysis of Thermalito Afterbay Station 165 (Worksite 2) .....	133
94. Contours of Effective Vertical Normal Stress and Alpha Values Determined from Static Finite Element Analysis of Thermalito Afterbay Station 347 (Columbia Soil Area) .....	134
- Chapter III, Section 6 -	
95. Lineaments, Faults, and Recorded Epicenters Around Thermalito Afterbay .....	135

## CONTENTS (Continued)

### FIGURES (continued)

No.	Page
96. Relationship of Thermalito Afterbay to Assumed Fault Projections .....	136
97. Design Accelerograms and Acceleration Response Spectra .....	140
98. Comparison of the Mean Spectrum of the Three Design Accelerograms to the Average Stiff Soil Site Spectrum .....	141
- Chapter III, Section 7 -	
99. Shake Soil Models for Thermalito Afterbay Station 107 (Site 1) .....	142
100. Shake Soil Models for Thermalito Afterbay Station 165 (Worksite 2) .....	143
101. Shake Soil Models for Thermalito Afterbay Station 347 (Columbia Soil Area) .....	143
102. Column 8 Material Properties for Thermalito Afterbay Station 107 (Site 1) .....	144
103. Column 1 Material Properties for Thermalito Afterbay Station 165 (Worksite 2) .....	145
104. Column 1 Material Properties for Thermalito Afterbay Station 347 (Columbia Soil Area) .....	145
105. Dynamic Response Motion Produced in Shake Analysis for Thermalito Afterbay Station 107 (Site 1) Using the Eureka Federal Building N79E Record .....	146
106. Dynamic Response Motion Produced in Shake Analysis for Thermalito Afterbay Station 107 (Site 1) Using the Hollywood Storage P.E. Lot N90° Record .....	147
107. Dynamic Response Motion Produced in Shake Analysis for Thermalito Afterbay Station 107 (Site 1) Using the McCabe School S50°W Record .....	147
108. Typical Shear Stress Time Histories and Equivalent Uniform Cycle Conversion .....	148
- Chapter III, Section 8 -	
109. Static Undrained Shear Strength Determined from CUE Triaxial Tests on Undisturbed Samples of Thermalito Afterbay Embankment and Foundation Silt/Clay .....	150
110. Static Drained Shear Strength Determined from CUE Triaxial Tests on Undisturbed Samples of Thermalito Afterbay Embankment and Foundation Silt/Clay .....	150
111. Comparisons of Drained Shear Strength Between Undisturbed Samples of Thermalito Afterbay Embankment and Values Used During Design .....	150
112. Static Shear Strengths Determined from CUE Triaxial Tests Performed on Samples of Thermalito Afterbay Foundation Silt/Clay from Station 347 (Columbia Soils Area) .....	151
113. Comparison of Drained Shear Strength Between Undisturbed Samples of Thermalito Afterbay Station 347 (Columbia Soils Area) and Values Used During Design .....	151
114. Static CUE Triaxial Test Results for Undisturbed Samples of Thermalito Afterbay Foundation Silty Sand ( $N_{A1} = 20$ blows/ft) .....	152
115. Static Shear Strength of Thermalito Afterbay Station 107 (Site 1) Foundation Silty Sand Determined by CUE Triaxial Compression Tests on Undisturbed Samples ( $N_{A1} = 20$ ) .....	152
116. Static CUE Triaxial Test Results for Undisturbed Samples of Thermalito Afterbay Foundation Silty Sands $N_{A1} \approx 7 \text{ blows/foot}$ .....	153

## CONTENTS (Continued)

### FIGURES (continued)

No.		Page
117.	Static Shear Strengths Determined from CUE Triaxial Tests Performed on Samples of Thermalito Afterbay Foundation Silty Sands Representing $N_{A1} \approx 7 \text{ blows/foot}$ .....	153
118.	Results of 1976 Cyclic Triaxial Tests on Thermalito Afterbay and Forebay Sands .....	155
119.	Cyclic Triaxial Test Results from "Undisturbed" 1978 Samples of Thermalito Afterbay Foundation Silty Sands .....	155
120.	Typical Cyclic Triaxial Test Records for 1978 Test Program on Station 107 (Site 1) Silty Sand Cyclic Triaxial Test Records for 1978 Test Program on Station 107 (Site 1) Silty Sand .....	156
121.	Comparison of Cyclic Triaxial Test Results from "Undisturbed" 1980 Samples of Columbia Soils with Results of Foundation Silty Sands from Sites 1 and 2 .....	157
122.	Thermalito Afterbay Cyclic Triaxial Test Results ( $\sigma_{sc} = 1.0 ksc, K_c = 1.0$ ) .....	157
123.	Thermalito Afterbay Cyclic Triaxial Test Results ( $\sigma_{sc} = 2.5 ksc, K_c = 1.0$ ) .....	158
124.	Thermalito Afterbay Cyclic Triaxial Test Results ( $\sigma_{sc} = 1.0 ksc, K_c = 1.5$ ) .....	158
125.	Thermalito Afterbay Cyclic Triaxial Test Results ( $\sigma_{sc} = 2.5 ksc, K_c = 1.5$ ) .....	159
126.	Figure 126. Comparison of Gradation Envelopes for Thermalito Afterbay Piston Samples and SPT Samples with $N_{A1} = 5 - 8$ blows/foot .....	159
127.	Comparison of Gradation Envelopes for Thermalito Afterbay Piston Samples and SPT Samples with $N_{A1} = 12 - 13$ blows/foot .....	160
128.	Comparison of Gradation Envelopes for Thermalito Afterbay Piston Samples and SPT Samples with $N_{A1} = 18 - 21$ blows/foot .....	160
129.	Comparison of Gradation Envelopes for Thermalito Afterbay Piston Samples and SPT Samples with $N_{A1} = 25 - 31$ blows/foot .....	160
130.	Comparison of Gradation Envelopes for Thermalito Afterbay Piston Samples and SPT Samples with $N_{A1} = 43 - 46$ blows/foot .....	160
131.	Comparison Between Thermalito Afterbay Cyclic Triaxial Test Results and SPT Resistance .....	161
132.	Determination of Liquefaction Potential from Seed and Idriss (1981) SPT Correlation .....	162

### - Chapter III, Section 9 -

133.	Procedure for Interpreting Cyclic Triaxial Test Data for Isotropically Consolidated ( $K_c = 1.0$ ) Samples .	164
134.	Procedure for Interpreting Cyclic Triaxial Test Data for Anisotropically Consolidated ( $K_c > 1.0$ ) Samples	164
135.	Cyclic Strength Curves for Thermalito Afterbay Foundation Silty Sands $N_{A1} = 7$ blows/foot .....	164
136.	Cyclic Strength Curves for Thermalito Afterbay Foundation Silty Sands $N_{A1} = 20$ blows/foot .....	164
137.	Comparison of Cyclic Strengths ( $\alpha = 0$ ) Used During Different Periods of the Investigation .....	165
138.	Results of Dynamic Analysis with $M_L = 6.5$ Earthquake for Sand Layer at Station 107 (Site 1) [Reservoir Elevation = 128 feet] .....	166

## CONTENTS (Continued)

### FIGURES (continued)

No.	Page
139. Results of Dynamic Analysis with $M_L = 6.5$ Earthquake for Sand Layer at Station 107 (Site 1) [Reservoir Elevation = 136.5 feet] .....	167
140. Results of Dynamic Analysis with $M_L = 6.5$ Earthquake for Sand Layer at Station 165 (Worksite 2) [Reservoir Elevation = 128 feet] .....	167
141. Results of Dynamic Analysis with $M_L = 6.5$ Earthquake for Sand Layer at Station 165 (Worksite 2) [Reservoir Elevation = 136.5 feet] .....	168
142. Results of Dynamic Analysis with $M_L = 6.5$ Earthquake for Sand Layer at Station 347 (Columbia Soil Area) [Reservoir Elevation = 128 feet] .....	168
143. Results of Dynamic Analysis with $M_L = 6.5$ Earthquake for Sand Layer at Station 347 (Columbia Soil Area) [Reservoir Elevation = 136.5 feet] .....	169
<b>- Chapter III, Section 10 -</b>	
144. Static Stability with Liquefied Sand Layer Horizontal Sliding .....	171
145. Assumed Forces of Dam Failure Section Including Shear Resistance on the Ends of the Sliding Block ...	172
146. Minimum Length of Section that Will Fail by Horizontal Sliding when Including Shear Resistance on Ends of Section .....	172
147. Horizontal Sliding Analysis for Station 12 (Reservoir Elevation 136.5 feet) .....	173
148. Post-Earthquake Stability Analyses (Downstream) for Model 1—Station 107 (Site 1)— Reservoir Elevation 136.5 feet .....	175
149. Post-Earthquake Stability Analyses (Downstream) for Model 2—Station 165 (Worksite 2)— Reservoir Elevation 136.5 feet .....	175
150. Post-Earthquake Stability Analyses (Downstream) for Model 3—Station 347 (Columbia Soil Area)— Reservoir Elevation 136.5 feet .....	176
<b>- Chapter III, Section 11 -</b>	
151. Comparison of Cyclic Triaxial Strengths of Thermalito Afterbay Silty Sands with Sands that have Withstood Strong Earthquake Shaking .....	182
152. Comparison of Thermalito Afterbay Dam with Analysis of Stability of Upper San Fernando Dam Immediately Following Earthquake Shaking .....	183
<b>- Chapter III, Addenda -</b> <b>(Addendum B)</b>	
153. Static Horizontal Normal Stresses, $\sigma_x$ (psf), for Station 107 .....	218
154. Static Vertical Normal Stresses, $\sigma_y$ (psf), for Station 107 .....	218
155. Static Major Principal Stresses, $\sigma_1$ (psf), for Station 107 .....	219
156. Static Minor Principal Stresses, $\sigma_3$ (psf), for Station 107 .....	219
157. Static Horizontal Shear Stresses, $\tau_{xy}$ (psf), for Station 107 .....	220

# CONTENTS (Continued)

## FIGURES (continued)

No.		Page
<b>Chapter III, Addendum F</b>		
158.	Static Maximum Shear Stresses, $\tau_{\max}$ (psf), for Station 107 .....	220
159.	Principal Stress Orientations for Station 107 .....	221
160.	Static Horizontal Normal Stresses, $\sigma_x$ (psf) for Station 165 .....	221
161.	Static Vertical Normal Stresses, $\sigma_y$ (psf) for Station 165 .....	222
162.	Static Major Principal Stresses $\sigma_3$ (psf), for Station 165 .....	222
163.	Static Minor Principal Stresses, $\sigma_3$ (psf), for Station 165 .....	223
164.	Static Horizontal Shear Stresses, $\tau_{xy}$ (psf), for Station 165 .....	223
165.	Static Maximum Shear Stresses, $\tau_{\max}$ (psf), for Station 165 .....	224
166.	Principal Stress Orientations for Station 165 .....	224
167.	Static Horizontal Normal Stresses, $\sigma_x$ (psf), for Station 347 .....	225
168.	Static Vertical Normal Stresses, $\sigma_y$ (psf), for Station 347 .....	225
169.	Static Major Principal Stresses, $\sigma_1$ (psf), for Station 347 .....	226
170.	Static Minor Principal Stresses, $\sigma_3$ (psf), for Station 347 .....	226
171.	Static Horizontal Shear Stresses, $\tau_{xy}$ (psf), for Station 347 .....	227
172.	Static Maximum Shear Stresses, $\tau_{\max}$ (psf), for Station 347 .....	227
173.	Principal Stress Orientations for Station 347 .....	228
174.	Time Histories for the Thermalito Afterbay Analysis .....	230
175.	Response Spectra for the Thermalito Afterbay Analysis .....	231
176.	Maximum Horizontal Accelerations, $a_{\max}$ (g), Determined from One-Dimensional Shake Analysis for Station 107 Using Eureka Federal Building Motion .....	233
177.	Maximum Horizontal Accelerations, $a_{\max}$ (g), Determined from One-Dimensional Shake Analysis for Station 107 Using the Hollywood Storage P.E. Lot Motion .....	234
178.	Maximum Horizontal Accelerations, $a_{\max}$ (g), Determined from One-Dimensional Shake Analysis for Station 107 Using the McCabe School Motion .....	234
179.	Maximum Horizontal Accelerations, $a_{\max}$ (g), Determined from One-Dimensional Shake Analysis for Station 165 Using the McCabe School Motion .....	235
180.	Maximum Horizontal Accelerations, $a_{\max}$ (g), Determined from One-Dimensional Shake Analysis for Station 347 Using the McCabe School Motion .....	235
181.	Maximum Dynamic Shear Stresses $\tau_{\max}$ (psf), Station 107 from Shake Analysis .....	236
182.	Maximum Dynamic Shear Stresses $\tau_{\max}$ (psf), Station 165 and 347 from Shake Analysis Using the McCabe School Motion .....	237

## CONTENTS (Continued)

### FIGURES (continued)

No.	Page
183. Typical Shear Stress Time Histories in Suspect Sand Layer from Station 107 Downstream Shake Profile (Column 8) .....	238
184. Typical Shear Stress Time History in Suspect Sand Layer from Station 165 Upstream Shake Profile (Column 1) .....	239
185. Typical Shear Stress Time History in Suspect Sand Layer from Station 165 Downstream Shake Profile (Column 1B) .....	239
186. Typical Shear Stress Time History in Suspect Sand Layer from Station 165 Crest Shake Profile (Column 4) .....	240
187. Typical Shear Stress Time History in Suspect Sand Layer from Station 347 Upstream Shake Profile (Column 1) .....	240
188. Typical Shear Stress Time History in Suspect Sand Layer from Station 347 Crest Shake Profile (Column 4) .....	241
189. Trial Failure Surfaces Generated for Station 107 .....	251
190. Trial Failure Surfaces Generated for Station 165 .....	252
191. Trial Failure Surfaces Generated for Station 347 .....	252

### Chapter IV

192. Western Canal and Richvale Canal Outlets .....	254
193. Western Canal and Richvale Canal Outlets—Isometric View .....	255
194. Vertical Tensile Stresses (in ksi) in the Reinforcing Steel, Generated by the Reanalysis Earthquake ....	256
195. Horizontal Tensile Stresses (in ksi) in the Reinforcing Steel, Generated by the Reanalysis Earthquake ...	256
196. Peak Horizontal Tensile Stresses at Elevation 134.6 in the Reinforcing Steel Generated by Various Lateral Force Coefficients Combined with Static Loads .....	256
197. Pacific Gas and Electric Company Outlet .....	257
198. Pacific Gas and Electric Company Outlet—Isometric View .....	258
199. Sutter-Butte Outlet .....	259
200. Sutter-Butte Outlet—Isometric View .....	260
201. Vertical Tensile Stresses (in ksi) in the Reinforcing Steel, Generated by the Reanalysis Earthquake ....	260
202. Horizontal Tensile Stresses (in ksi) in the Reinforcing Steel, Generated by the Reanalysis Earthquake ...	260
203. Peak Vertical Tensile Stresses at Elevation 118.45 in the Reinforcing Steel Generated by Various Lateral Force Coefficients Combined with Static Loads .....	261
204. River Outlet .....	261
205. River Outlet Headworks and Fish Barrier Weir—Isometric View .....	262
206. Reinforcing Steel Tensile Stress Generated by the Reanalysis Earthquake .....	262
207. Peak Reinforcing Steel Tensile Stresses at Elevation 120 Generated by Various Lateral Force Coefficients Combined with Static Loads .....	263



## CONTENTS (Continued)

### FIGURES (continued)

No.		Page
— Chapter V, —Section 2		
208.	General Location Map for Thermalito Forebay Dam .....	270
209.	Plan View of Thermalito Forebay Dam .....	272
210.	General Plan of Thermalito Forebay Main Dam Area .....	273
211.	Areal Geology for Thermalito Forebay Main Dam .....	274
212.	Geologic Sections along Thermalito Forebay Main Dam .....	275
213.	Typical Sections of Thermalito Forebay Main Dam, Low Dam, and Ruddy Creek Dam .....	278
214.	Sections of Thermalito Forebay Zoned Main Dam Between Stations 2+03 and 4+20 .....	279
215.	Summary of Total and Effective Design Shear Strengths Determined from CUE Triaxial Compression Tests of Zone 1F Soil Performed During Design .....	282
216.	Gradations of Triaxial Test Specimens of Zone 1F Soil Tested During Design .....	283
217.	Strength Results from Direct Shear Tests of Zone 2F Soil Conducted During Design .....	284
218.	Gradations of Direct Shear Test Specimens of Zone 2F Soil Tested During Design .....	285
219.	Summary of Slope Stability Analyses Performed during Design for Main Dam and Foundation of Thermalito Forebay Dam .....	288
220.	Summary of Slope Stability Analyses Performed during Design for Main Dam Sections of Thermalito Forebay Dam .....	289
221.	Summary of Slope Stability Analyses Performed during Design for Ruddy Creek and Low Dam Sections of Thermalito Forebay Dam .....	290
222.	Plan and Sections of Wingwall Dam .....	291
223.	Plan and Sections of Approach Channel Dam .....	292
224.	Wingwall Dam Envelopment by Forebay Main Dam Embankment .....	293
225.	Location of Tail Channel Seepage Area Downstream of Thermalito Forebay Dam .....	294
226.	Location of Piezometers and Toe Drain Outlets along Thermalito Forebay Dam .....	296
227.	Location of Seepage Relief System at Thermalito Forebay Dam .....	297
228.	Location of Survey Monuments at Thermalito Forebay Dam .....	298
229.	Location of Crest Monuments at Thermalito Forebay Ruddy Creek Area .....	299
230.	Vertical Movements Measured at Thermalito Forebay Main Dam Crest Monuments .....	301
231.	Vertical Movements Measured at Thermalito Forebay Main Dam Slope Monuments .....	301
232.	Horizontal Movements Measured at Thermalito Forebay Main Dam Crest Monuments .....	302
233.	Vertical Movements Measured at Thermalito Forebay Ruddy Creek Area Crest Monuments .....	302
234.	Horizontal Movements Measured at Thermalito Forebay Ruddy Creek Area Crest Monuments .....	303



## CONTENTS (Continued)

### FIGURES (continued)

No.		Page
<b>- Chapter V, Section 3 -</b>		
235.	Configuration of SPT Hammers (Adapted from Steinberg, 1981) .....	304
236.	Comparison of SPT N-Values Determined Using Donut and Safety Hammers .....	308
237.	Chart for Determining Values of $C_N$ (after Seed et al., 1985) .....	310
238.	Location of SPT Boreholes Drilled Between Stations 7 and 40 along Thermalito Forebay Dam .....	312
239.	Location of SPT Boreholes Drilled Between Stations 40 and 150 along Thermalito Forebay Dam .....	314
240.	Borehole Profile at Thermalito Forebay Dam Station 11+50—Borehole Profile at the Tail Channel ....	316
241.	Borehole Profiles from Thermalito Forebay Main Dam to Tail Channel .....	318
242.	Thermalito Forebay Dam Borehole Profiles—Station 7+00 to 56+50 .....	320
243.	Thermalito Forebay Dam Borehole Profiles—Station 56+50 to 69+00 .....	322
244.	Thermalito Forebay Dam Borehole Profiles – Station 69+00 to 81+00 .....	324
245.	Thermalito Forebay Dam Borehole Profiles – Station 81+00 to 93+00 .....	326
246.	Thermalito Forebay Dam Borehole Profiles – Station 93+00 to 105+00 .....	328
247.	Thermalito Forebay Dam Borehole Profiles – Station 105+00 to 117+00 .....	330
248.	Thermalito Forebay Dam Borehole Profiles – Station 117+00 to 129+00 .....	332
249.	Thermalito Forebay Dam Borehole Profiles – Station 129+00 to 141+00 .....	334
250.	Thermalito Forebay Dam Borehole Profiles – Station 141+00 to 151+00 .....	336
251.	Thermalito Forebay Dam Shear Wave Velocity Test Results – Station 11+50 (Boring TFS – 4) .....	343
252.	Thermalito Forebay Dam Shear Wave Velocity Test Results – Station 81+79 (Boring TFS-3A) .....	344
253.	Thermalito Forebay Dam Shear Wave Velocity Test Results – Station 10+00 (Boring 79-10) .....	345
254.	Thermalito Forebay Dam Piston Sampling Site – Station 10+00 Area, Piston Sampling Site .....	346
255.	Thermalito Forebay Dam Piston Sampling Site – Station 11+00 Area, Piston Sampling Site .....	347
256.	Thermalito Forebay Dam Piston Sampling Site – Station 13+00 Area, Piston Sampling Site .....	348
257.	Thermalito Forebay Dam Piston Sampling Site – Station 68+00 Area, Piston Sampling Site .....	349
258.	Thermalito Forebay Dam Piston Sampling Site – Station 74+00 Area, Piston Sampling Site .....	350
259.	Thermalito Forebay Dam Piston Sampling Site – Station 112+00 Area, Piston Sampling Site .....	351
260.	Thermalito Forebay Dam Piston Sampling Site – Station 113+00 Area, Piston Sampling Site .....	352
261.	Location of Piezometers Installed at Thermalito Forebay Main Dam .....	353
262.	Typical Standpipe Piezometer Installation at Thermalito Forebay Dam Between 1976 and 1984 .....	354
263.	Piezometer Levels Measured at Thermalito Forebay Dam Station 10-11 and 112 Areas .....	355
<b>- Chapter V, Section 4 -</b>		
264.	Summary of Gradations for SPT Samples Obtained from the Suspect Foundation Sands at the Thermalito Forebay Main Dam—Station 10-11 Area .....	359

## CONTENTS (Continued)

### FIGURES (continued)

No.	Page
265. Summary of Gradations for SPT Samples Obtained from the Suspect Foundation Sands at the Thermalito Forebay Main Dam – Station 112 Area .....	360
266. Comparison of Gradations Determined for Piston and SPT Samples Obtained at the Thermalito Forebay Dam Station 10 Sampling Site .....	361
267. Comparison of Gradations Determined for Piston and SPT Samples Obtained at the Thermalito Forebay Dam Station 13 Sampling Site .....	362
268. Comparison of Gradations Determined for Piston and SPT Samples Obtained at the Thermalito Forebay Dam Station 68 Sampling Site .....	363
269. Comparison of Gradations Determined for Piston and SPT Samples Obtained at the Thermalito Forebay Dam Station 74 Sampling Site .....	364
270. Comparison of Gradations Determined for Piston and SPT Samples Obtained at the Thermalito Forebay Dam Station 112 Sampling Site .....	365
271. Comparison of Gradations Determined for Piston and SPT Samples Obtained at the Thermalito Forebay Dam Station 113 Sampling Site .....	366
272. Comparison of Plasticity Results Determined for Piston and SPT Samples Obtained at Thermalito Forebay Dam .....	367
273. Triaxial Compression Test Results for 1984 Undisturbed Specimens of Thermalito Forebay Main Dam Embankment Material .....	368
274. Thermalito Forebay Drained Static Shear Strength Results from ICU Triaxial Tests of Main Dam Embankment Soil .....	369
275. Thermalito Forebay Undrained Static Shear Strength Results from ICU Triaxial Tests of Main Dam Embankment Soil .....	370
276. Thermalito Forebay Undrained Static Shear Strengths Determined from ICU Triaxial Tests of Main Dam Embankment Soil .....	371
277. ICU Triaxial Compression Test Results for 1984 Undisturbed Specimens of Thermalito Forebay Low Dam Embankment Soil .....	372
278. Thermalito Forebay Drained Static Shear Strength—Results from ICU Triaxial Tests of Low Dam Embankment Material .....	373
279. Thermalito Forebay Undrained Static Shear Strength—Results from ICU Triaxial Tests of Low Dam Embankment Soil .....	374
280. Thermalito Forebay Undrained Static Shear Strength—Results from ICU Triaxial Tests of Low Dam Embankment Soil .....	375
281. ICU Triaxial Compression Test Results for 1984 Undisturbed Specimens of Thermalito Forebay Clayey Foundation Cap Soil .....	376
282. Thermalito Forebay Drained Static Shear Strength—Results from ICU Triaxial Tests of Non-Liquefiable Clayey Foundation Cap Soil .....	377
283. Thermalito Forebay Undrained Static Shear Strength—Results from ICU Triaxial Tests of Non-Liquefiable Clayey Foundation Cap Soil .....	378

## CONTENTS (Continued)

### FIGURES (continued)

No.	Page
284. Thermalito Forebay Undrained Static Shear Strengths Determined from ICU Triaxial Tests of Non-Liquefiable Clay Cap Soil .....	379
285. ICU Triaxial Compression Test Results for 1984 Undisturbed Specimens of Thermalito Forebay Suspect SC/SM Foundation Sand .....	380
286. Thermalito Forebay Drained Static Shear Strength Results from ICU Triaxial Tests of Suspect Foundation SC/SM Sand .....	381
287. Thermalito Forebay Undrained Static Shear Strength Results from ICU Triaxial Tests of Suspect Foundation SC/SM Sand .....	382
288. Thermalito Forebay Undrained Static Shear Strengths Determined from ICU Triaxial Tests of Suspect Foundation SC/SM Sand .....	383
289. Post-Cyclic Static Triaxial Compression Test Results for 1984 Undisturbed Specimens of Thermalito Forebay Low Dam (Station 112) Suspect SC/SM Foundation Sand .....	384
290. Residual Shear Strength Determined From Post-Cyclic Triaxial Tests Performed on 1984 Specimens of Thermalito Forebay Low Dam (Station 112) Suspect SC/SM Foundation Sand .....	385
- Chapter V, Section 5 -	
291. Minimum Corrected SPT Resistance Measured within Borings Drilled at Thermalito Forebay Main Dam .....	387
292. Longitudinal Profile of Low Blowcount Sand Layer Between Stations 10 + 09 and 11 + 33 at Thermalito Forebay Main Dam Area .....	388
293. Cross-section Profile of Low Blowcount Sand Layer Between Stations 10 + 09 and 10 + 70 at Thermalito Forebay Main Dam Area .....	390
294. Cross-section Profile of Low Blowcount Sand Layer Between Stations 10 + 70 and 11 + 33 at Thermalito Forebay Main Dam Area .....	392
295. Cross-section Profile of Low Blowcount Sand Layer Between Embankment Toe to Tail Channel at Thermalito Forebay Main Dam Area .....	394
296. Longitudinal Profile of Low Blowcount Sand Layer Between Stations 111 and 113 at Thermalito Forebay Low Dam Area .....	396
297. Cross-section Profile of Low Blowcount Sand Layer Between Stations 111 and 113 at Thermalito Forebay Low Dam Area .....	398
298. Correlation Between SPT Resistance and Field Liquefaction Behavior of Sands under Level Ground Conditions During Magnitude 6.5 Earthquakes (modified from Seed and Idriss, 1982) .....	400
299. Corrected Standard Penetration Test Resistance for Suspect Sands Located Between Stations 10 and 12 at the Thermalito Forebay Main Dam .....	401
300. Cross-Section Profile of Corrected Standard Penetration Resistance for Foundation Sands Located Between Stations 108 and 118 at the Thermalito Forebay Low Dam .....	402
301. Corrected Standard Penetration Test Resistance for Foundation Sands Located Between Stations 111 and 113 at the Thermalito Forebay Low Dam .....	404
302. Simplified Embankment-Foundation Models Created for the Critical Sites along Thermalito Forebay Main and Low Dams .....	405

# CONTENTS (Continued)

## FIGURES (continued)

No.		Page
<b>- Chapter V, Section 6 -</b>		
303.	Finite Element Model and Mesh Used for Static Stress Analysis of the Thermalito Forebay Main Dam Model (Station 10-11 Area) .....	407
304.	Finite Element Model and Mesh Used for Static Stress Analysis of the Thermalito Forebay Low Dam Model (Station 112 Area) .....	407
305.	Assumed Flownets Used in Static Stress Analyses of Thermalito Forebay Dam Critical Models .....	408
306.	Distribution of Effective Vertical Normal Stress and Alpha Values Calculated for Thermalito Forebay Main Dam Model (Station 10-11 Area) .....	408
307.	Distribution of Effective Vertical Normal Stress and Alpha Values Calculated for Thermalito Forebay Low Dam Model (Station 112 Area) .....	409
308.	Pre-Earthquake Stress Conditions Determined for the Suspect Sand Layers in the Thermalito Forebay Main Dam Model (Station 10-11 Area) .....	409
309.	Pre-Earthquake Stress Conditions Determined for the Suspect Sand Layers in the Thermalito Forebay Low Dam Model (Station 112 Area) .....	410
<b>- Chapter V, Section 7 -</b>		
310.	Location of Faults in the Thermalito Area .....	412
311.	Average Values of Maximum Acceleration in Rock (after Seed and Idriss, 1982) .....	414
312.	Oroville Reanalysis Earthquake Acceleration Time History—Rock Motion .....	416
313.	Oroville Reanalysis Earthquake Acceleration Response Spectrum .....	416
314.	El Centro Earthquake Motion—Ground Motion .....	417
315.	El Centro Acceleration Response Spectrum .....	417
316.	Thermalito Forebay, Standard Modulus Reduction and Damping Curves (after Seed and Idriss, 1970) ...	418
317.	Thermalito Forebay Main Dam, Station 10-11 Area—Model and SHAKE Column Locations .....	419
318.	Thermalito Forebay Low Dam, Station 112 Area, Model and SHAKE Column Locations .....	419
319.	Thermalito Forebay Main Dam Acceleration Response—Computed from Program SHAKE using the Oroville Reanalysis Earthquake Rock Motion .....	420
320.	Thermalito Forebay Main Dam Acceleration Response—Computed from Program SHAKE using the El Centro Ground Motion Record .....	421
321.	Thermalito Forebay Low Dam Acceleration Response—Computed from Program SHAKE using the Oroville Reanalysis Earthquake Rock Motion .....	422
322.	Thermalito Forebay Main Dam Acceleration Response—Computed from Program SHAKE using the Modified El Centro Record .....	423
323.	Thermalito Forebay Main Dam Maximum Horizontal Accelerations—Determined from Program SHAKE analyses using the Oroville Reanalysis Earthquake .....	424
324.	Thermalito Forebay Main Dam Maximum Horizontal Accelerations—Determined from Program SHAKE analyses using the Modified El Centro Record .....	424

## CONTENTS (Continued)

### FIGURES (continued)

No.	Page
325. Thermalito Forebay Low Dam Maximum Horizontal Accelerations— Determined from the Oroville Reanalysis Earthquake .....	425
326. Thermalito Forebay Low Dam Maximum Horizontal Accelerations— Determined from Program SHAKE analyses using the Modified El Centro Record .....	425
327. Thermalito Forebay Main Dam—Horizontal Acceleration Time Histories Computed by Program QUAD4 using the Oroville Reanalysis Earthquake .....	426
328. Thermalito Forebay Main Dam—Horizontal Acceleration Time Histories Computed by Program QUAD4 using the Modified El Centro Record .....	427
329. Thermalito Forebay Low Dam—Horizontal Acceleration Time Histories Computed by Program QUAD4 using the Oroville Reanalysis Earthquake .....	428
330. Thermalito Forebay Low Dam—Horizontal Acceleration Time Histories Computed by Program QUAD4 using the Modified El Centro Record .....	429
331. Dynamic Horizontal Shear Stress Time Histories Computed in the Suspect Sand Layers at Thermalito Forebay Main Dam by SHAKE and QUAD4 using the Oroville Reanalysis Earthquake .....	430
332. Dynamic Horizontal Shear Stress Time Histories Computed in the Suspect Sand Layers at Thermalito Forebay Main Dam by Programs SHAKE and QUAD4 using the Modified El Centro Record .....	430
333. Dynamic Horizontal Shear Stress Time Histories Computed in the Suspect Sand Layers at Thermalito Forebay Low Dam by Programs SHAKE and QUAD4 using the Oroville Reanalysis Earthquake .....	431
334. Dynamic Horizontal Shear Stress Time Histories Computed in the Suspect Sand Layers at Thermalito Forebay Low Dam by Programs SHAKE and QUAD4 using the Modified El Centro Record .....	431
335. Thermalito Forebay Main Dam, Maximum Shear Stresses in the Suspect Layers .....	432
336. Thermalito Forebay Low Dam, Maximum Shear Stresses in the Suspect Layers .....	432
– Chapter V, Section 8 –	
337. Comparison of Cyclic Triaxial Test Results of Foundation SC/SM Material .....	435
338. Thermalito Forebay Main Dam (Station 10–11 Area) Factors of Safety Against Liquefaction .....	436
339. Thermalito Forebay Main Dam (Station 112 Area) Factors of Safety Against Liquefaction .....	436
– Chapter V, Section 9 –	
340. Relationship between Residual Shear Strength and Equivalent Clean Sand SPT Value of $(N_1)_{60}$ (after Seed et al., 1988) .....	438
341. Relationship between Residual Shear Strength and Equivalent Clean Sand Value of $(N_1)_{60}$ (after Von Thun, 1986) .....	440

## CONTENTS (Continued)

### FIGURES (continued)

No.	Page
342. Thermalito Forebay Main Dam—Summary of Critical Failure Surfaces Determined from Post-Earthquake Stability Analyses .....	440
343. Thermalito Forebay Low Dam—Summary of Critical Failure Surfaces Determined from Post-Earthquake Stability Analyses .....	441
344. Thermalito Forebay Main Dam—Critical Factors of Safety Vs. Residual Shear Strengths .....	443
345. Thermalito Forebay Low Dam—Critical Factors of Safety Vs. Residual Shear Strengths .....	444
– Chapter V, Section 10 –	
346. Static and Pseudo-Dynamic Forces Acting on Channel Dam – Typical Section .....	446
347. Static and Pseudo-Dynamic Forces Acting on Wingwall Dam – Typical Section .....	449
348. Approach Channel Dam—Modified Cross-Section of the Wingwall Dam used in Simplified Dynamic Tensile Stress Analyses .....	450
349. Wingwall Dam—Modeled Cross Section used in Simplified Dynamic Tensile Stress Analyses .....	452
350. Typical Distributions of Combined Static plus Maximum Dynamic Stresses Calculated for the Approach Channel Dam Monoliths .....	453
351. Typical Distributions of Combined Static plus Maximum Dynamic Stresses Calculated for the Wingwall Dam Monoliths .....	453
– Chapter V, Section 11 –	
352. Areal Geology for Thermalito Forebay Main Dam .....	460
353. Geologic Sections along Thermalito Forebay Main Dam .....	461
354. Detailed Bedrock Profile for Thermalito Forebay Main Dam along Section AA (Figures 352 and 353) ...	462
355. Comparison of Gradations for Thermalito Forebay Main Dam Embankment Soils .....	463
– Chapter V, Addendum C –	
356. Element Numbers for Finite Element Mesh of Thermalito Forebay Main Dam .....	487
357. Node Numbers for Finite Element Mesh of Thermalito Forebay Main Dam .....	487
358. Static Vertical Effective Normal Stresses, $\sigma_y'$ (tsf) for Thermalito Forebay Main Dam .....	488
359. Static Horizontal Effective Normal Stresses, $\sigma_x'$ (tsf) for Thermalito Forebay Main Dam .....	488
360. Static Major Effective Principal Stresses, $\sigma_1'$ (tsf) for Thermalito Forebay Main Dam .....	489
361. Static Minor Effective Principal Stresses, $\sigma_3'$ (tsf) for Thermalito Forebay Main Dam .....	489
362. Static Horizontal Effective Shear Stresses, $\tau_{xy}$ (tsf) for Thermalito Forebay Main Dam .....	490
363. Static Maximum Effective Shear Stresses, $\tau_{max}$ (tsf) for Thermalito Forebay Main Dam .....	490
364. Static Principal Stress Orientation for Thermalito Forebay Main Dam .....	491
365. Element Numbers for Finite Element Mesh of Thermalito Forebay Low Dam .....	492
366. Node Numbers for Finite Element Mesh of Thermalito Forebay Low Dam .....	492



## CONTENTS (Continued)

### FIGURES (continued)

No.		Page
367.	Static Vertical Effective Normal Stresses, $\sigma'_y$ (tsf) for Thermalito Forebay Low Dam .....	493
368.	Static Horizontal Effective Normal Stresses, $\sigma'_x$ (tsf) for Thermalito Forebay Low Dam .....	493
369.	Static Major Effective Principal Stresses, $\sigma'_1$ (tsf) for Thermalito Forebay Low Dam .....	494
370.	Static Minor Effective Principal Stresses, $\sigma'_3$ (tsf) for Thermalito Forebay Low Dam .....	494
371.	Static Horizontal Effective Shear Stresses, $\tau_{xy}$ (tsf) for Thermalito Forebay Low Dam .....	495
372.	Static Maximum Effective Shear Stresses, $\tau_{max}$ (tsf) for Thermalito Forebay Low Dam .....	495
373.	Static Principal Stress Orientation for Thermalito Forebay Low Dam .....	496

### - Chapter V, Addendum D -

374.	Typical Triaxial Test Records ( $K_c = 1.0$ ) .....	505
375.	Typical Cyclic Triaxial Test Records ( $K_c > 1.0$ ) .....	506
376.	1976 SC/CM Samples ( $\sigma'_{3c} = 1.0$ ksc, $K_c = 1.0$ ) .....	507
377.	1976 SC/SM Samples ( $\sigma'_{3c} = 3.0$ ksc, $K_c = 1.0$ ) .....	507
378.	1978 SC/SM Samples from Station 11 + 55 ( $\sigma'_{3c} = 1.0$ ksc, $K_c = 1.0$ ) .....	508
379.	1978 SC/SM Samples from Station 11 + 55 ( $\sigma'_{3c} = 3.0$ ksc, $K_c = 1.0$ ) .....	508
380.	1980 SP, SW, SM, SC Hand Carved Samples from Tail Channel ( $\sigma'_{3c} = 1.0$ ksc, $K_c = 1.0$ ) .....	509
381.	1980 SP, SW, SM, SC Hand Carved Samples from Tail Channel ( $\sigma'_{3c} = 1.0$ ksc, $K_c = 1.5$ ) .....	509
382.	1980 SP, SW, SM, SC Hand Carved Samples from Tail Channel ( $\sigma'_{3c} = 3.0$ ksc, $K_c = 1.0$ ) .....	510
383.	1981-82 SC/SM Samples from Station 10 ( $\sigma'_{3c} = 1.0$ ksc, $K_c = 1.0$ , $N_{A1} = 25, 28$ ) .....	510
384.	1981-82 SC/SM Samples from Station 10 ( $\sigma'_{3c} = 1.0$ ksc, $K_c = 1.0$ , $N_{A1} = 25, 28$ ) .....	511
385.	1981-82 SC/SM Samples from Station 10 ( $\sigma'_{3c} = 3.0$ ksc, $K_c = 1.0$ , $N_{A1} = 25, 28$ ) .....	511
386.	1981-82 SW/SM Samples from Station 13 ( $\sigma'_{3c} = 1.75$ ksc, $K_c = 1.0$ , $N_{A1} = 30, 33, 39$ ) .....	512
387.	1981-82 SW/SM Samples from Station 13 ( $\sigma'_{3c} = 2.0$ ksc, $K_c = 1.0$ , $N_{A1} = 30, 33, 39$ ) .....	512
388.	1981-82 SW/SM Samples from Station 13 ( $\sigma'_{3c} = 2.0$ ksc, $K_c = 1.5, 2.0$ , $N_{A1} = 33$ ) .....	513
389.	1981-82 SW/SM Samples from Station 13 ( $\sigma'_{3c} = 3.0$ ksc, $K_c = 1.5$ , $N_{A1} = 30, 33$ ) .....	513
390.	1981-82 SW/SM Samples from Station 13 ( $\sigma'_{3c} = 4.0$ ksc, $K_c = 1.0$ , $N_{A1} = 30, 33, 39$ ) .....	514
391.	1981-82 SC/SM Samples from Station 68 ( $\sigma'_{3c} = 0.6$ ksc, $K_c = 1.0$ , $N_{A1} = 17$ ) .....	514
392.	1981-82 SC/SM Samples from Station 68 ( $\sigma'_{3c} = 0.6$ ksc, $K_c = 1.0$ , $N_{A1} = 19$ ) .....	515
393.	1981-82 SC/SM Samples from Station 68 ( $\sigma'_{3c} = 1.0$ ksc, $K_c = 1.0$ , $N_{A1} = 19$ ) .....	515

# CONTENTS (Continued)

## FIGURES (continued)

No.		Page
394.	1981-82 SC/SM Samples from Station 74 ( $\sigma'_{3c} = 0.6ksc, K_c = 1.0, N_{A1} = 20$ )	516
395.	1984 SC/SM Samples from Station 112 ( $\sigma'_{3c} = 0.6ksc, K_c = 1.0$ )	516
396.	1984 SC/SM Samples from Station 112 ( $\sigma'_{3c} = 1.0ksc, K_c = 1.0$ )	517
397.	1981-82 SC/SM Samples from Station 112 ( $\sigma'_{3c} = 2.0ksc, K_c = 1.0, N_{A1} = 17, 26$ )	517
398.	1981-82 SC/SM Samples from Station 112 ( $\sigma'_{3c} = 2.0ksc, K_c = 1.25, N_{A1} = 26$ )	518
399.	1984 SC/SM Samples from Station 112 ( $\sigma'_{3c} = 3.0ksc, K_c = 1.0$ )	518
400.	1981-82 SC/SM Samples from Station 113 ( $\sigma'_{3c} = 2.0ksc, K_c = 1.0, N_{A1} = 20, 27$ )	519
401.	1981-82 CW/SM Samples from Station 113 ( $\sigma'_{3c} = 2.0ksc, K_c = 2.0, N_{A1} = 27$ )	519

## - Chapter V, Addendum E -

402a.	Maximum Horizontal Accelerations, $a_{max}$ (g), Computed by Program SHAKE Using the Oroville Reanalysis Earthquake—Main Dam	525
402b.	Maximum Horizontal Accelerations, $a_{max}$ (g), Computed by Program SHAKE Using the Modified El Centro Record—Main Dam	525
403a.	Maximum Horizontal Accelerations, $a_{max}$ (g), Computed by Program QUAD4 Using the Oroville Reanalysis Earthquake —Main Dam	526
403b.	Maximum Horizontal Accelerations, $a_{max}$ (g), Computed by Program QUAD4 Using the Modified El Centro Record—Main Dam	526
404a.	Comparison of Maximum Horizontal Accelerations Computed by Programs SHAKE and QUAD4 using the Oroville Reanalysis Earthquake—Main Dam	527
404b.	Comparison of Maximum Horizontal Accelerations Computed by Programs SHAKE and QUAD4 Using the Modified El Centro Record—Main Dam	527
405a.	Maximum Horizontal Shear Stresses, $(\tau_{xy})_{max}$ (psf), Computed by Program SHAKE Using the Oroville Reanalysis Earthquake—Main Dam	528
405b.	Maximum Horizontal Shear Stresses, $(\tau_{xy})_{max}$ (psf), Computed by Program SHAKE Using the Modified El Centro Record—Main Dam	528
406a.	Maximum Horizontal Shear Stresses, $(\tau_{xy})_{max}$ (tsf), Computed by Program QUAD4 Using the Oroville Reanalysis Earthquake—Main Dam	529
406b.	Maximum Horizontal Shear Stresses, $(\tau_{xy})_{max}$ (tsf), Computed by Program QUAD4 Using the Modified El Centro Record—Main Dam	529
407a.	Comparison of Maximum Horizontal Shear Stresses, $(\tau_{xy})_{max}$ (tsf), Computed by Programs SHAKE and QUAD4 Using the Oroville Reanalysis Earthquake—Main Dam	530
407b.	Comparison of Maximum Horizontal Shear Stresses, $(\tau_{xy})_{max}$ (tsf), Computed by Programs SHAKE and QUAD4 Using the Modified El Centro Record—Main Dam	530
408a.	Maximum Shear Strains, $\gamma_{max}$ (%), Computed by Program SHAKE Using the Oroville Reanalysis Earthquake—Main Dam	531



## CONTENTS (Continued)

### FIGURES (continued)

No.	Page
408b. Maximum Shear Strains, $\gamma_{\max}$ (%), Computed by Program SHAKE Using the Modified El Centro Record—Main Dam .....	531
409a. Maximum Shear Strains, $\gamma_{\max}$ (%), Computed by Program QUAD4 Using the Oroville Reanalysis Earthquake—Main Dam .....	532
409b. Maximum Shear Strains, $\gamma_{\max}$ (%), Computed by Program QUAD4 Using the Modified El Centro Record—Main Dam .....	532
410a. Comparisons of Maximum Shear Strains, $\gamma_{\max}$ (%), Computed by Programs SHAKE and QUAD4 Using the Oroville Reanalysis Earthquake—Main Dam .....	533
410b. Comparisons of Maximum Shear Strains, $\gamma_{\max}$ (%), Computed by Programs SHAKE and QUAD4 Using the Modified El Centro Record—Main Dam .....	533
411a. Maximum Horizontal Accelerations, $a_{\max}$ (g), Computed by Program SHAKE Using the Oroville Reanalysis Earthquake—Low Dam .....	534
411b. Maximum Horizontal Accelerations, $a_{\max}$ (g), Computed by Program SHAKE Using the Modified El Centro Record—Low Dam .....	534
412a. Maximum Horizontal Accelerations, $a_{\max}$ (g), Computed by Program QUAD4 Using the Oroville Reanalysis Earthquake—Low Dam .....	535
412b. Maximum Horizontal Accelerations, $a_{\max}$ (g), Computed by Program QUAD4 Using the Modified El Centro Record—Low Dam .....	535
413a. Comparisons of Maximum Horizontal Accelerations, Computed by Programs SHAKE and QUAD4 Using the Oroville Reanalysis Earthquake—Low Dam .....	536
413b. Comparisons of Maximum Horizontal Accelerations, Computed by Programs SHAKE and QUAD4 Using the Modified El Centro Record—Low Dam .....	536
414a. Maximum Horizontal Shear Stresses, $(\tau_{xy})_{\max}$ (psf), Computed by Program SHAKE Using the Oroville Reanalysis Earthquake—Low Dam .....	537
414b. Maximum Horizontal Shear Stresses, $(\tau_{xy})_{\max}$ (psf), Computed by Program SHAKE Using the Modified El Centro Record—Low Dam .....	537
415a. Maximum Horizontal Shear Stresses, $(\tau_{xy})_{\max}$ (psf), Computed by Program QUAD4 Using the Oroville Reanalysis Earthquake—Low Dam .....	538
415b. Maximum Horizontal Shear Stresses, $(\tau_{xy})_{\max}$ (psf), Computed by Program QUAD4 Using the Modified El Centro Record—Low Dam .....	538
416a. Comparison of Maximum Horizontal Shear Stresses, $(\tau_{xy})_{\max}$ , Computed by Programs SHAKE and QUAD4 Using the Oroville Reanalysis Earthquake—Low Dam .....	539
416b. Comparison of Maximum Horizontal Shear Stresses, $(\tau_{xy})_{\max}$ , Computed by Programs SHAKE and QUAD4 Using the Modified El Centro Record—Low Dam .....	539

## CONTENTS (Continued)

### FIGURES (continued)

No.	Page
417a. Maximum Shear Strains, $\gamma_{\max}$ (%), Computed by Program SHAKE Using the Oroville Reanalysis Earthquake—Low Dam .....	540
417b. Maximum Shear Strains, $\gamma_{\max}$ (%), Computed by Program SHAKE Using the Modified El Centro Record—Low Dam .....	540
418a. Maximum Shear Strains, $\gamma_{\max}$ (%), Computed by Program QUAD4 Using the Oroville Reanalysis Earthquake—Low Dam .....	541
418b. Maximum Shear Strains, $\gamma_{\max}$ (%), Computed by Program QUAD4 Using the Modified El Centro Record—Low Dam .....	541
419a. Comparisons of Maximum Shear Strain, $\gamma_{\max}$ , Computed by Programs SHAKE and QUAD4 Using the Oroville Reanalysis Earthquake—Low Dam .....	542
419b. Comparisons of Maximum Shear Strains, $\gamma_{\max}$ , Computed by Programs SHAKE and QUAD4 Using the Modified El Centro Record—Low Dam .....	542
— Chapter V, Addendum F —	
420. Cross-Section Through Upper San Fernando Dam (after Seed et al., 1973) .....	544
421. Plan View Of Upper San Fernando Dam .....	544
422. Upper San Fernando Dam—Settlement Records Before and After Earthquake .....	546
423. Upper San Fernando Dam—Horizontal Offset Before and After Earthquake .....	546
424. Upper San Fernando Dam—Settlement Records Before and After Earthquake .....	547
425. Recorded Pore Pressures—Upper San Fernando Dam (adapted from Seed et al., 1973) .....	547
426. Idealized Cross-Section Through Upper San Fernando Dam (after Serff et al., 1976) .....	548
427. Strain Potential in Hydraulic Fill—Upper San Fernando Dam (after Seed et al., 1973) .....	548
428. 1971 Borehole Locations at Upper San Fernando Dam—Plan View (after Seed et al., 1973) .....	551
429. 1971 Borehole Locations at Upper San Fernando Dam—Profile View (after Seed et al., 1973) .....	552
430. Ranges of Grain Size Distribution Curves for Sand, Hydraulic Fill (after Seed, et al., 1973) .....	553
431. Corrected SPT Blowcounts for Boreholes Drilled through the Upstream and Downstream Shell Zones of Upper San Fernando Dam .....	554
432. Mean and Median Corrected SPT Blowcount Values for Layers of Hydraulic Fill in Upper San Fernando Dam (Non-Clayey Soils only) .....	555
433. Post-Earthquake Stability Model—Upper San Fernando Dam .....	557
434. Upper San Fernando Dam—Undrained Shear Strength of Clay (after Seed et al., 1973) .....	559
435. Residual Shear Strength in Liquefied Zone, $S_r$ , (psf) .....	560
436. Upper San Fernando Dam, Post-EQ Stability Analysis—Location of Critical Failure Surfaces .....	560
437. Relationship Between Residual Strength and Equivalent Clean Sand Value of $(N_1)_{60}$ (after Seed et al., 1988) .....	561

## CONTENTS (Continued)

### FIGURES (continued)

No.		Page
— Chapter VI —		
438.	Vicinity Map—Bidwell Canyon and Parish Camp Saddle Dams .....	564
439.	Bidwell Canyon Saddle Dam—Plan, Profile, and Exploration .....	567
440.	Bidwell Canyon Saddle Dam—Sections and Details .....	568
441.	Bidwell Canyon Saddle Dam—Gradation Curves .....	569
442.	Bidwell Canyon Saddle Dam—Gradation Curves .....	570
443.	Bidwell Canyon Saddle Dam—Atterberg Limits .....	571
444.	Bidwell Canyon Saddle Dam—Atterberg Limits .....	571
445.	Bidwell Canyon Saddle Dam—Foundation Geology .....	572
446.	Changes in Crest Elevations of Bidwell Canyon Saddle Dam .....	573
447.	Lineaments and Faults in the Northwestern Sierra Foothills .....	574
448.	Bidwell Canyon Saddle Dam—West Dam Shear Zone Gradations .....	577
449.	Plan View of Bidwell Canyon Saddle Dam—West Dam Shear Zone Gradations .....	578
450.	Cross Section AA of Bidwell Canyon Saddle Dam Along West Dam Shear Zone .....	578

### Tables

#### — Chapter II —

1.	Lateral Earthquake Forces Including Hydrodynamic Effects .....	10
2.	Lateral Earthquake Forces Excluding Hydrodynamic Effects .....	11
3.	Physical Properties of Block No. 1—Thermalito Powerplant .....	14
4.	Overturning Moments, Kip-ft .....	15
5.	Distances from Neutral Axis to Extreme Fiber .....	15
6.	Maximum Stresses Including Hydrodynamic Effects .....	29
7.	Maximum Stresses Excluding Hydrodynamic Effects .....	30

#### —Chapter III, Part 2 —

8.	Thermalito Afterbay Dam Statistics .....	36
9.	Embankment Materials Properties—Design Values .....	39
10.	Embankment Materials Properties—As-Built Values .....	40

#### —Chapter III, Part 3 —

11.	Energy Before Impact for Thermalito Afterbay SPT Hammers .....	52
12.	Estimated Effect of SPT Procedures on Blowcount, Thermalito Afterbay vs. Seed and Idriss (1981) Correlation .....	55
13.	Preliminary Criteria for Identifying Suspect Sites .....	106
14.	Thermalito Afterbay Boreholes Delimiting Suspect Areas .....	109

# CONTENTS (Continued)

## Tables (Continued)

No.		Page
15.	Corrected SPT Blowcount ( $N_{A1}$ ) Distribution Along the Downstream Toe Between Stations 106—108 .....	116
16.	Corrected SPT Blowcount ( $N_{A1}$ ) Distribution Beneath Embankment Crest Between Stations 106—108 .....	116
17.	Corrected SPT Blowcount ( $N_{A1}$ ) Distribution Along the Downstream Toe Between Stations 164—167, Modified SPT Blowcount, $N_1$ .....	121
18.	Corrected SPT Blowcount ( $N_{A1}$ ) Distribution Beneath Embankment Crest Between Stations 164—170 .....	122
19.	Corrected SPT Blowcount ( $N_{A1}$ ) Distribution Between Stations 344—350, Modified SPT Blowcount, $N_1$ .....	122
—Chapter III, Part 6—		
20.	Ranges of Source-to-Site Horizontal Distances for Thermalito Afterbay Dam .....	138
21.	Comparison of Approaches for Selecting Earthquake Motion Parameters .....	139
22.	Recorded Accelerograms Selected for Developing Reevaluation Earthquake Motions .....	141
—Chapter III, Part 8—		
23.	Static Shear Strength Summary for Thermalito Afterbay Materials .....	153
24.	Determination of Cyclic Strength .....	163
—Chapter III, Part 9—		
25.	Application of Cyclic Triaxial Strength Curves .....	165
—Chapter III, Part 10—		
26.	Minimum Safety Factors for Pore Pressure Conditions Immediately After Earthquake Shaking .....	174
27.	Minimum Safety Factors for Wedge Analyses With Pore Pressure Distribution .....	177
—Chapter III, Part 11—		
28.	Degree of Conservatism in Components of the Seismic Stability Analysis .....	179
—Chapter III, Addendum E—Dynamic Testing—		
29.	Cyclic Triaxial Test Summary for 1978 Undisturbed Samples Tested at $\sigma'_{3c} = 0.5ksc$ and $K_c = 1.0$ .....	243
30.	Cyclic Triaxial Test Summary for 1978 Undisturbed Samples Tested at $\sigma'_{3c} = 1.0ksc$ and $K_c = 1.0$ .....	243
31.	Cyclic Triaxial Test Summary for 1978 Undisturbed Samples Tested at $\sigma'_{3c} = 1.0ksc$ and $K_c = 1.5$ .....	244

# CONTENTS (Continued)

## Tables (Continued)

No.		Page
—Chapter III, Addendum E—Dynamic Testing (Continued) —		
32.	Cyclic Triaxial Test Summary for 1978 Undisturbed Samples Tested at $\sigma'_{3c} = 3.0ksc$ and $K_c = 1.0$ . . . . .	244
33.	Cyclic Triaxial Test Summary for 1978 Remolded Samples Tested at $\sigma'_{3c} = 1.0ksc$ and $K_c = 1.0$ . . . . .	244
34.	Cyclic Triaxial Test Summary for 1978 Remolded Samples Tested at $\sigma'_{3c} = 1.0ksc$ and $K_c = 1.5$ . . . . .	245
35.	Cyclic Triaxial Test Summary for 1978 Remolded Samples Tested at $\sigma'_{3c} = 1.0ksc$ and $K_c = 1.0$ . . . . .	245
36.	Cyclic Triaxial Test Summary for 1978 Remolded Samples Tested at $\sigma'_{3c} = 1.0ksc$ and $K_c = 1.5$ . . . . .	246
37.	Cyclic Triaxial Test Summary for 1979–80 Undisturbed Samples Tested at $\sigma_{3c} = 0.5ksc$ and $K_c = 1.0$ . . . . .	246
38.	Cyclic Triaxial Test Summary for 1979–80 Undisturbed Samples Tested at $\sigma_{3c} = 1.0ksc$ and $K_c = 1.0$ . . . . .	246
39.	Cyclic Triaxial Test Summary for 1980–81 Undisturbed Samples Tested at $\sigma_{3c} = 1.0ksc$ and $K_c = 1.0$ . . . . .	246
40.	Cyclic Triaxial Test Summary for 1981–82 Undisturbed Samples Tested at $\sigma'_{3c} = 1.0ksc$ and $K_c = 1.5$ . . . . .	248
41.	Cyclic Triaxial Test Summary for 1981–82 Undisturbed Samples Tested at $\sigma'_{3c} = 2.5ksc$ and $K_c = 1.0$ . . . . .	249
42.	Cyclic Triaxial Test Summary for 1981–82 Undisturbed Samples Tested at $\sigma'_{3c} = 2.5ksc$ and $K_c = 1.5$ . . . . .	250
— Chapter V, Section 2 —		
43.	Summary of Geologic Units Exposed Along Thermalito Forebay Dam . . . . .	276
44.	Summary of Design Parameters Used in Slope Stability Analyses of Embankment Dam . . . . .	286
45.	Summary of Results for Slope Stability Analyses Performed During Design . . . . .	287
46.	Estimated Effects of Procedural Differences on SPT Blowcounts . . . . .	307
47.	Suspect Soil Characteristics at 1981–82 Piston Sampling Locations . . . . .	338
48.	Suspect Foundation Sites 2 ( $N_{A1} \leq 30$ ) Along Thermalito Forebay Dam . . . . .	340
49.	Standpipe Piezometers Installed at Thermalito Forebay Dam . . . . .	342
50.	Summary of Cyclic Test Results for Thermalito Forebay Dam Foundation Soils . . . . .	357
51.	Drained Static Shear Strength Summary . . . . .	358
52.	Undrained Static Shear Strength Summary . . . . .	358
53.	Average Peak Acceleration Predicted for Magnitude 6.5 Earthquake . . . . .	415
54.	Residual Shear Strengths Predicted Using the Seed et al. (1988) Correlations . . . . .	439
55.	Summary of Post–Earthquake Slope Stability Analysis . . . . .	441
56.	Summary of Pseudostatic Factors in Safety Against Sliding for Concrete Dam Monoliths . . . . .	448
57.	Summary of Maximum Tensile Stresses . . . . .	452
58.	Components of the Seismic Stability Analysis . . . . .	456
59.	Summary of Filter Parameters for Main Dam Embankment Soils . . . . .	464
60.	Cyclic Triaxial Test Summary for 1976 Undisturbed Samples . . . . .	500

## CONTENTS (Continued)

### Tables (Continued)

No.		Page
61.	Cyclic Triaxial Test Summary for 1978 Undisturbed Samples .....	500
62.	Cyclic Triaxial Test Summary for 1979-1980 Undisturbed Samples .....	501
63.	Cyclic Triaxial Test Summary for 1981-1982 Undisturbed Samples .....	502
64.	Cyclic Triaxial Test Summary for 1984 Undisturbed Samples .....	504
65.	Summary of 1971 Drilling Explorations at Upper San Fernando Dam .....	550
66.	1971 Post-Earthquake SPT Blowcount Data (Non-Clayey Soils) .....	556
67.	Computations of Earthquake-Induced Vertical Strains in Hydraulic Fill .....	556
68.	Determinations of Average Pre-Earthquake SPT Blowcounts in the Hydraulic Fill of Upper San Fernando Dam .....	556
69.	Soil Properties Assumed in Post-Earthquake Slope Stability Analyses of Upper San Fernando Dam .....	558
70.	As-Built Properties of Bidwell Canyon Saddle Dam .....	566

## ENGINEERING CERTIFICATION

Bulletin 203-88 was prepared under my direction as the professional engineer in direct responsible charge of the work, in accordance with the provisions of the Professional Engineers' Act of the State of California.

Keith G. Barrett  
Chief, Design Office  
Registered Civil Engineer  
Registration No. 13538



STATE OF CALIFORNIA  
George Deukmejian, Governor

THE RESOURCES AGENCY  
Gordon K. Van Vleck, Secretary for Resources

DEPARTMENT OF WATER RESOURCES  
David N. Kennedy, Director

Robert G. Potter  
Deputy Director

John P. Caffrey  
Chief Deputy Director

Lawrence A. Mullnix  
Deputy Director

Salle S. Jantz  
Assistant Director

Susan N. Weber  
Chief Counsel

DIVISION OF DESIGN AND CONSTRUCTION

John H. Lawder ..... Chief  
Keith G. Barrett ..... Chief, Design Office  
Kenneth H. Koefoed ..... Chief, Plants and Pipelines Branch  
William M. Verigin ..... Chief, Civil Design Branch  
William D. Hammond ..... Chief, Dam Projects Section  
Leslie F. Harder, Jr. .... Chief, Canals and Levees Section

AUTHORS

Chapter I

Frank Dubar ..... Dam Projects Section  
Leslie F. Harder, Jr. .... Canals and Levees Section

Chapter II

Anil K. Chopra ..... University of California, Berkeley  
Arnold E. Eskel ..... Plants and Pipelines Branch  
Terry L. Becker ..... Plants and Pipelines Branch

Chapter III

Leslie F. Harder, Jr. .... Canals and Levees Section  
Williams D. Hammond ..... Dam Projects Section  
Penny S. Ross ..... Canals and Levees Section  
James W. Kassel ..... Canals and Levees Section  
Linus K. Motumah ..... Canals and Levees Section

Chapter IV

Edgar R. Najera ..... Plants and Pipelines Branch

(Continued on next page)

## CONTENTS (Continued)

### ORGANIZATION ( Continued)

#### Chapter V

Leslie F. Harder, Jr. ....	Canals and Levees Section
William D. Hammond .....	Dam Projects Section
Michael W. Driller .....	Canals and Levees Section
Nekane Hollister .....	Canals and Levees Section

#### Chapter VI

William D. Hammond .....	Dam Projects Section
Stephen W. Chan .....	Dam Projects Section
Leslie F. Harder, Jr. ....	Canals and Levees Section

#### Geologic Studies and Evaluation

Mark J. McQuilkin .....	Project Geology Branch
Thomas C. Tidyman .....	Project Geology Branch

#### Drafting and Report Preparation

John T. Keller .....	Canals and Levees Section
Peter R. Buchwald .....	Canals and Levees Section

#### Typing and Editing

Mary Ann Benny .....	Civil Design Branch
Shelly Asbury .....	Civil Design Branch
Hide Nakajo .....	Civil Design Branch
Tia Skidmore .....	Civil Design Branch

#### Editorial and Production Service

Earl G. Bingham .....	Reports Administration, Division of Planning
-----------------------	--



State of California  
The Resources Agency  
Department of Water Resources

**CALIFORNIA WATER COMMISSION**

**Stanley M. Barnes, Chairman, Visalia**  
**Martin A. Matich, Vice Chairman, San Bernardino**

Harold W. Ball .....	La Mesa
Katherine B. Dunlap .....	Los Angeles
Clair A. Hill .....	Redding
James J. Lenihan .....	Mountain View
James M. Stubchaer .....	Santa Barbara
Audrey Z. Tennis .....	Chico
Jack G. Thomson .....	Bakersfield

**Orville L. Abbott**  
**Executive Officer and Chief Engineer**

**Tom Y. Fujimoto**  
**Assistant Executive Officer**

The California Water Commission serves as a policy advisory body to the Director of Water Resources on all California water resources matters. The nine-member citizen commission provides a water resources forum for the people of the State, acts as a liaison between the legislative and executive branches of State Government, and coordinates federal, state, and local water resources efforts.

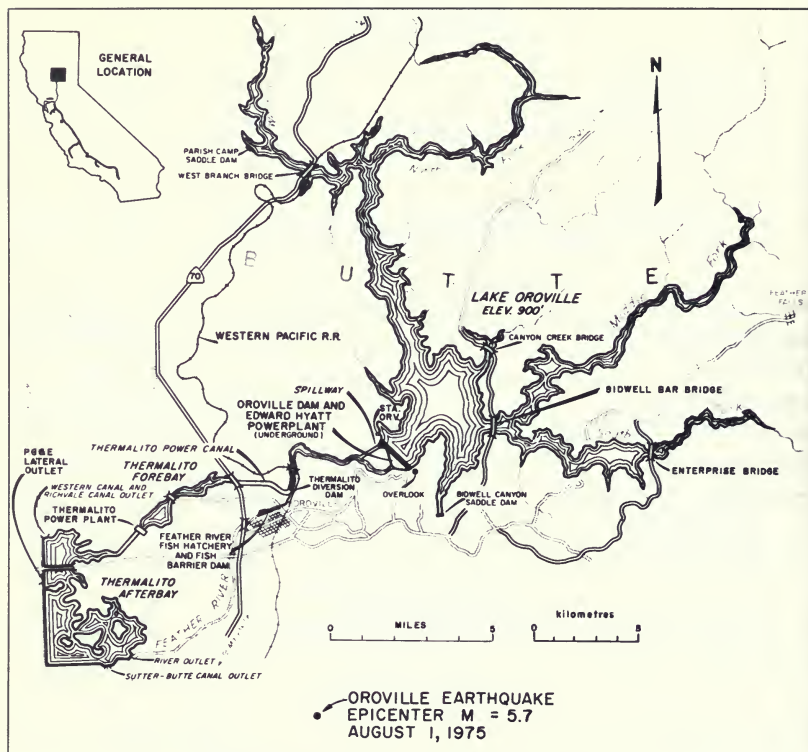


Figure 1. Location Map, Oroville-Thermalito Facilities

## CHAPTER I. INTRODUCTION

### Background

Oroville Dam is located on the Feather River in the foothills of the Sierra Nevada. The dam is 5 miles east of the city of Oroville and about 130 miles northeast of San Francisco.

On August 1, 1975, at 1320 hours, an earthquake of Richter Scale magnitude 5.7 occurred about 7.5 miles southwest of Oroville Dam. During the main event and the many aftershocks that followed, the Oroville-Thermalito facilities continued operating without interruption except for about a 45-minute shutdown of power generation.

Intensive investigations, originating from the Oroville Earthquake, were initiated to document the performance of the Oroville-Thermalito facilities during the 1975 earthquake, and to re-examine the ability of the facilities to withstand future earthquake shaking. Bulletin 203, published in April 1977, presented the results of investigations which documented the performance of the Oroville-Thermalito facilities during the 1975 Oroville earthquake sequence.

Bulletin 203-78, published in February 1979, presented the results of extensive geologic, seismologic, and geodetic investigations together with the engineering analyses performed in the seismic re-evaluations of Oroville Dam embankment, Oroville Dam Flood Control Outlet Structure, Thermalito Diversion Dam, and various secondary structures. Also included in Bulletin 203-78 was the Department's contingency plan for the Oroville-Thermalito facilities during a seismic emergency.

### Purpose

The purpose of this supplement, Bulletin 203-88, is to present the Department's seismic re-evaluations of the various Oroville-Thermalito project structures which were not addressed in Bulletin 203-78. These structures include Thermalito Powerplant Headworks, Thermalito Afterbay Dam, Thermalito Afterbay Dam Concrete Structures, Thermalito Forebay Dam, Bidwell Canyon Saddle Dam, and Parish Camp Saddle Dam. Also addressed in this bulletin is an evaluation of the effects of fault movements on the stability of dams in the Oroville-Thermalito area.

### Description Of The Oroville-Thermalito Facilities

Oroville Dam and its appurtenances, along with the Thermalito facilities, comprise a multiple purpose project, which includes water conservation, power generation, flood control, recreation, and fish and wildlife enhancement. Lake Oroville stores winter and spring runoff, which is released into the Feather River as necessary to supply project needs and commitments. The pumped-storage capability of the facilities permits maximum use of peaking power generation produced by the releases.

Water releases from Edward Hyatt Powerplant are largely diverted from the Feather River at the Thermalito Diversion Dam, a concrete gravity structure with a multiple radial gated crest section (see Figure 1). These diversions pass through Thermalito Power Canal and Thermalito Forebay, through the Thermalito Powerplant, and into Thermalito Afterbay (see Figures 2 and 3). The Thermalito Diversion Pool, Power Canal, and Forebay have a common water surface to accommodate flow reversals for the pumped-storage operation. Thermalito Afterbay stores the Plant discharges from Hyatt Powerplant and Thermalito Powerplant for possible off-peak



Figure 2. Thermalito Forebay Dam, Powerplant, and Reservoir

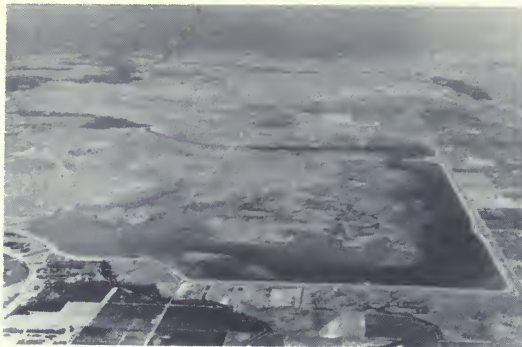


*Figure 3. Thermalito Afterbay Dam and Reservoir*

pumpback to Lake Oroville and for uniform flow releases to the Feather River.

Migrating salmon and steelhead are diverted from the river into the Feather River Fish Hatchery by the fish ladder at the Fish Barrier Dam, located approximately one-half mile downstream from Thermalito Diversion Dam.

### **The Investigating Organization**

On August 8, 1975, the Department of Water Resources convened its Consulting Board for Earthquake Analysis to review the post-earthquake situation and the preliminary data assembled. On September 11 and 12, 1975, a Special Consulting Board for the Oroville Earthquake, composed of nine members taken from the Consulting Board for Earthquake Analysis and additional consultants, was convened by the Department to review the Department's programs for data collection and evaluation of structural seismic safety. The Special Consulting Board currently consists of seven of the original nine Board members:

George W. Housner, Chairman  
 Clarence R. Allen  
 Bruce A. Bolt  
 Wallace L. Chadwick  
 Thomas M. Leps  
 Alan L. O'Neill  
 H. Bolton Seed

During the re-evaluation of the various structures, a smaller four-man board was formed from the Special Consulting Board to more expeditiously review the re-evaluations and provide guidance to Department staff. This so-called "mini board" consists of:

Wallace L. Chadwick  
 Thomas M. Leps  
 Alan L. O'Neill  
 H. Bolton Seed

Subsequent to the publication of Bulletin 203-78, the Special Consulting Board or its smaller "mini board" has met and/or issued reports a total of 10 times:

Dates	Board
February 26-27, 1979	Special Consulting Board
May 24-25, 1979	Special Consulting Board
August 14, 1980	Special Consulting Board
January 8-9, 1981	Special Consulting Board
March 18, 1982	Mini Board
July 1, 1982	Mini Board
November 15-16, 1983	Mini Board
October 19, 1984	Special Consulting Board
February 1, 1985	Special Consulting Board
November 18, 1988	Special Consulting Board

During these meetings, the Board has reviewed data, reports, and presentations by Department staff and has provided comments and guidance. Reports prepared by the Board are included in Appendix A.

## Summary Of Conclusions And Recommendations

Detailed technical presentations of the engineering re-evaluations for seismic stability are presented in the chapters which follow. Each chapter includes a description of the structure analyzed, selection of analysis method, analysis results, and conclusions. The conclusions and recommendations from Chapters II through VI follow:

### Thermalito Powerplant Headworks (Chapter II)

The stresses predicted by the analysis are within the allowable stresses of concrete and did not include the effect of the reinforcing steel. Consideration of the reinforcement would only serve to lower the stresses in the concrete.

One inch of vertical, sympathetic movement has been considered credible along a fault which lies beneath the bases of the penstocks. Although this may cause some cracking of the penstock, it would not result in damage to the headworks structure.

The traveling gantry crane is being provided with a tie-down system, which will be used during those periods when the crane is not in use. This will allow the crane to be fully operational immediately following the design earthquake.

DWR has therefore concluded that the Thermalito Powerplant headworks structure should safely withstand the ground motion specified by the Consulting Board; hence the structure should present no hazard to the general public under such an earthquake.

### Thermalito Afterbay Dam (Chapter III)

1. The strengths of foundation sands are higher than the values used in the preliminary (1981 Report) evaluation of Station 107.
2. The stability of the dam is satisfactory for the maximum earthquake shaking anticipated. Only minor cracking or movements are predicted for the postulated shaking. As an extra precaution, a short reach of dam with a sharp angle in the axis alignment has

been locally reinforced to supplement resistance to transverse cracking.

3. From a seismic safety standpoint, it is safe to restore full use of the reservoir, provided that the ground water piezometric level on the downstream side of the dam is controlled to prevent its rising above the ground surface for an extended period. To comply with this provision, a ground water pressure-relief system and a small berm have been added in short reaches along the downstream side of the dam.

### Thermalito Afterbay Dam Concrete Structures (Chapter IV)

Based on the present earthquake criteria and results from the analyses performed, the four Thermalito Afterbay concrete structures are considered safe when subjected to the reanalysis earthquake.

### Thermalito Forebay Dam (Chapter V)

1. The cyclic and residual strengths of the foundation sands are higher than the values used in preliminary studies performed between 1976 and 1984.
2. The stability of the dam is satisfactory for the maximum earthquake shaking anticipated. Only minor cracking or movements are predicted for the postulated shaking.
3. From a seismic safety standpoint, it is safe to continue full use of the reservoir.

### Bidwell Canyon and Parish Camp Saddle Dams (Chapter VI)

Bidwell Canyon Saddle Dam and Parish Camp Saddle Dam would perform satisfactorily during earthquake shaking as severe as the Oroville Reanalysis Earthquake ( $a_{max} = 0.6g$ ).

### The Effects of Possible Fault Movements in Oroville Project Dam Foundations (Chapter VI)

All of the Oroville Project Dams would perform satisfactorily if the postulated fault offsets in their foundations were to occur.

## **Structural Modifications Made To Oroville-Thermalito Facilities**

In order to provide additional protection to Thermalito Afterbay Dam, the Special Consulting Board recommended that the southwest corner of the reservoir embankment be reinforced, and that measures be implemented to assure that the water levels in the foundation immediately downstream of the dam remain no higher than the ground surface. To comply with these recommendations, the following was performed:

1. In 1986, an upstream buttress zone of gravel and cobbles was placed at the southwest corner of the dam between Stations 223 and 230. The buttress extends from foundation level up to the embankment crest and is up to 80 feet in width at crest elevation.
2. In 1985, a temporary well point system consisting of 20-foot deep well points, vacuum pumps, manifold pipe, and discharge lines were installed along the south side toe of the dam between Stations 275 and 295.
3. In 1986, a permanent relief well system was installed along the south toe of the dam between Stations 271 and 295. This system consists of fifty 20-foot deep relief wells, along with collector pipes, sumps, sump pumps, and discharge lines. This system was tested in

1986 and again in 1987 by holding the reservoir full for one to two weeks. In 1988, the temporary well point system was dismantled. The vacuum pumps and manifold pipe were removed, and most of the well points were abandoned in place with a surface seal. However, 78 well points between stations 282 and 290 were connected to the permanent relief system collector pipes. Piezometer observations made since then indicate that groundwater levels for full reservoir conditions will be below the ground surface along the south toe of the dam.

4. Fill material, between one and three feet thick, was placed on the ground surface along the west side of the dam, between Stations 170 and 176, to raise the ground surface elevation above the observed maximum ground water level.

The Department plans to carry out its recommendation, expressed in Chapter II, to provide a tie-down system for the traveling gantry crane on top of the Thermalito Powerplant Headworks structure. This work is expected to be completed in late 1989.

### **Department's Findings**

Based on the preceding conclusions from the investigations completed, the Department concludes that these facilities do not pose a threat to public safety.



## CHAPTER II

### SEISMIC EVALUATION OF THE THERMALITO POWERPLANT HEADWORKS

Chapter II is divided into two parts. Part 1 discusses the determination of the lateral earthquake forces acting on the Thermalito Powerplant headworks under the ground motion specified by the Department of Water Resources. Part 1 was prepared by Dr. Anil K. Chopra of the Uni-

versity of California, Berkeley. Part 2 addresses the determination of the stresses that occur in the headworks structure due to the earthquake forces, and an evaluation of the safety aspects of the structure to sustain those forces.

#### PART 1

### LATERAL EARTHQUAKE FORCES FOR SAFETY EVALUATION OF THE THERMALITO POWERPLANT HEADWORKS

#### Introduction

Following the Oroville earthquake of August 1, 1975, the California Department of Water Resources (DWR) decided to perform dynamic analysis of selected structures to provide the results needed to re-evaluate the safety of these structures against future earthquakes. This chapter is concerned with the analysis of Thermalito Powerplant Headworks, a concrete gravity structure, for the ground motion specified by DWR. A location map of Thermalito Powerplant is provided in Figure 4.

During the past twenty-five years, considerable progress has been made in the analysis of response of concrete gravity dams to earthquake ground motion. A general analytical procedure and computer program, wherein the effects of dam-water interaction and compressibility of water are included, is now available for two-dimensional finite element analysis of gravity-dam monoliths subjected to horizontal and vertical components of ground motion.<sup>1,2,\*</sup> This computer program has been employed in the dynamic analysis of Thermalito Diversion Dam for DWR.<sup>3</sup>

Although this procedure rigorously analyzes the earthquake response of gravity dam monoliths and has led to

results consistent with the damage to Koyna Dam during the December 11, 1967 earthquake, it was not considered to be the most appropriate approach for stress analysis of the Thermalito Powerplant Headworks structure. Unlike many gravity dams, this structure has major openings throughout. As a result, it was designed as a reinforced-concrete structure in contrast to most gravity dams, which are designed as plain, unreinforced mass concrete structures. Consequently, it is not reasonable to analyze a two-dimensional slice of the structure. On the other hand, a three-dimensional analysis, properly including hydrodynamic effects, is beyond the current state of the art.

After several discussions with DWR staff, it was concluded that the best approach would be to proceed as follows:

1. Based on the overall dynamic properties of the structure, recognizing the openings and other complexities, and including the hydrodynamic effects, estimate the lateral loads to represent the maximum effects of the earthquake ground motion.
2. Evaluate the capacity of the existing structure to safely carry these lateral earthquake loads and all other loads (except the pseudo-static earthquake loads) considered in the original design of the structure.

\*A numbered list of references is presented at the end of Chapter II.

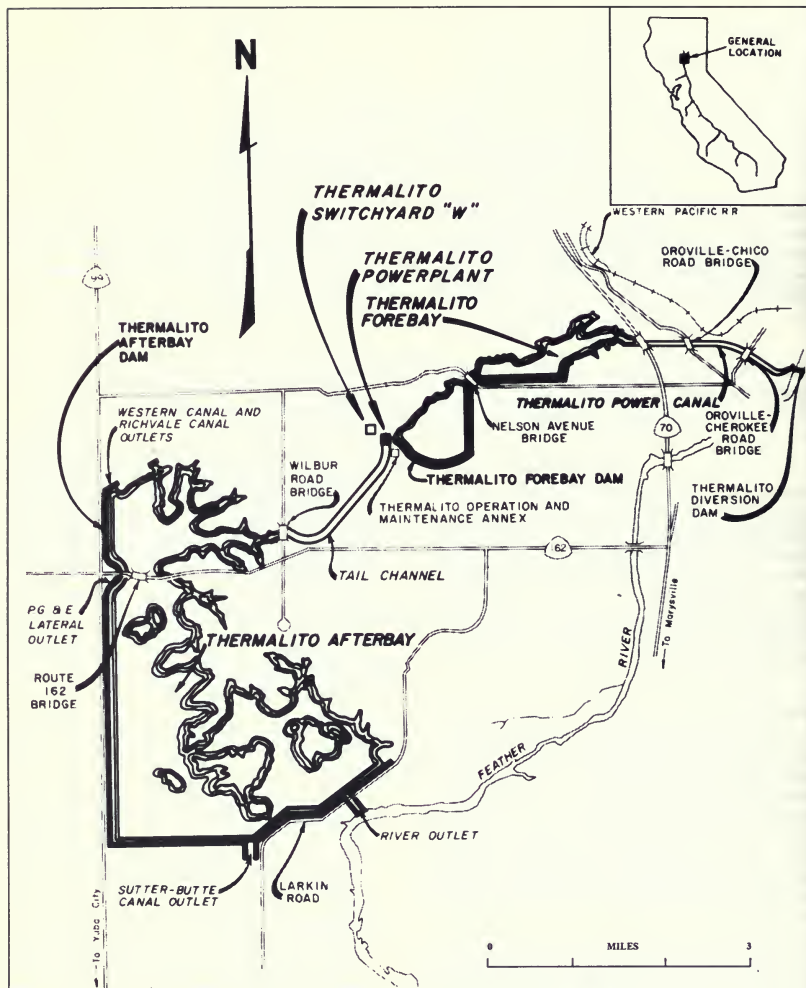


Figure 4. Location Map, Thermalito Powerplant, Forebay, and Afterbay



The recommended lateral earthquake forces are presented in Part 1 of this chapter. Also included are comments on the allowable tensile stresses to assist DWR in evaluating the structure.

### Analysis Procedure

A recent paper<sup>4</sup> presents a procedure for computing lateral earthquake forces to represent the maximum effects of earthquake ground motion on gravity dams. The following factors, important in the response of concrete gravity dams, are considered in the procedure: (1) fundamental period of vibration and mode shape of the dam, (2) effect of dam-water interaction on dynamic response characteristics of the dam, and (3) intensity and frequency characteristics of the ground motion. For this procedure the ground motion is characterized by its response spectrum. Based on rational simplifications and approximations, the following conclusion was reached:

### Computational Steps

The maximum effects of earthquake ground motion in the horizontal direction can be represented by a set of lateral forces, which should be considered to act in each direction—upstream and downstream—separately; their effects should be combined with those of all other design loads. These earthquake forces can be determined approximately by the following computational steps:

1. Compute  $T_s$ , the fundamental natural period of vibration of the dam in sec., without considering the influence of the stored water, from

$$T_s = 1.4 \frac{H_s}{\sqrt{E}} \quad (\text{Eq } 1)$$

in which  $H_s$  = height of the dam in feet; and  $E$  = modulus of elasticity (Young's modulus) of concrete in psi.

2. Compute  $\hat{T}_s$ , the fundamental period of vibration of the dam in sec., including the influence of the stored water, from:

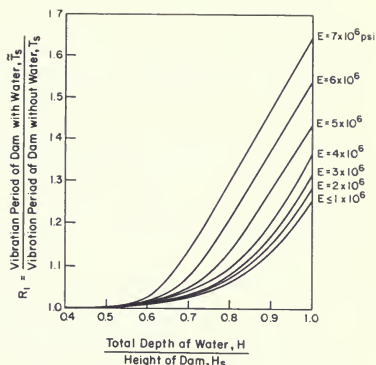


Figure 5. Standard Values for  $R_1$ —the Ratio of Fundamental Vibration Periods of the Dam with and without Water, Plotted against Depth of Water for Various Values of  $E$ , the modulus of elasticity for concrete

$$\hat{T}_s = R_1 T_s \quad (\text{Eq } 2)$$

in which  $R_1$  = period ratio determined from Figure 5 for the particular values of  $H$  and  $E$ ; and  $H$  = depth of stored water in feet.

3. Compute  $R_2$ , the ratio of the fundamental resonant period for the impulsive hydrodynamic pressure and  $\hat{T}_s$  computed in Step 2, from

$$R_2 = \frac{1}{\hat{T}_s} \frac{4H}{C} \quad (\text{Eq } 3)$$

where  $C$  = the velocity of sound in water (4,720 ft/sec.)

4. Compute  $f_s(z)$ , the lateral earthquake forces over the height of the dam including the hydrodynamic effects, from

$$f_s(z) = \alpha_1 \frac{S_a(\hat{T}_s)}{g} [w_s(z)\psi(z) + g\bar{p}_1(z)] \quad (\text{Eq } 4)$$

in which  $\alpha_1 = 4$ ,  $S_a(\hat{T}_s)$  = ordinate of the pseudo-acceleration response spectrum for the specified

earthquake for an appropriate damping value at period of vibration  $\bar{T}_s$  determined in Step 2;  $w_s(z)$  = weight per unit of the dam;  $\psi(z)$  = fundamental mode shape of the dam given in Figure 6. Corresponding to the value of  $R_2$  computed in Step 3 and for  $H/H_s = 1$ , the quantity  $g\bar{P}_1 = 1(z)$  is determined from Figure 7; the result is multiplied by the design value of  $(H/H_s)^2$  and substituted in Eq. 4.

5. The lateral earthquake forces without the hydrodynamic effects may be computed from:

$$f_s(z) = \alpha_2 \frac{S_a(\bar{T}_s)}{g} [w_s(z)\psi(z)] \quad (\text{Eq } 5)$$

in which  $\alpha_2 = 3$  and  $S_a(T_s)$  = ordinate of the pseudo-acceleration response spectrum at period of vibration  $T_s$  determined in Step 1.

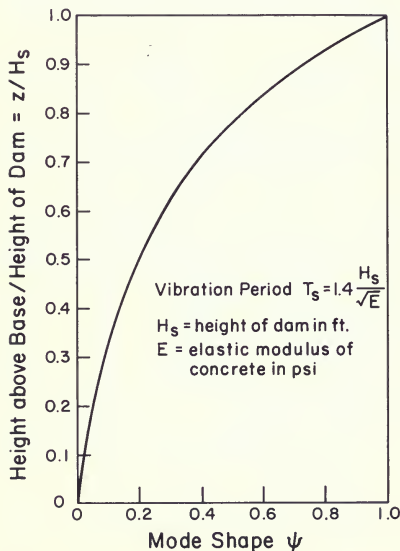


Figure 6. Standard Fundamental Period and Mode Shape of Vibration for Design of Concrete Gravity Dams

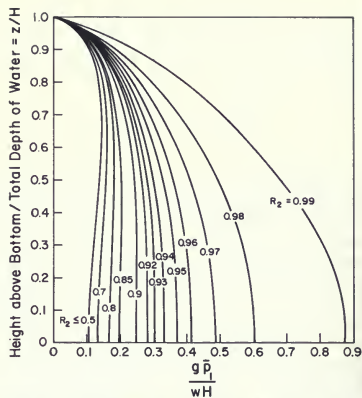


Figure 7. Standard Plots for Variation of  $\bar{P}_1$  over the depth of water for  $H/H_s = 1$  and various values of  $R_2 \equiv \bar{\omega}_s/\omega_f$

### Evaluation of the Procedure

Various approximations were introduced to develop the simplified analysis procedure summarized above, and these were individually checked to ensure that they would lead to acceptable results<sup>4</sup>. In order to provide an overall evaluation of the simplified analysis procedure, it was used to determine the stresses in Pine Flat Dam, and the results were compared with those from a computer analysis of response history in which the dam was idealized as a finite element system<sup>4</sup>.

Following the steps listed earlier, the lateral earthquake forces were computed for Pine Flat Dam. For purposes of stress calculations, the distributed gravity, hydrostatic, and earthquake loads were replaced by concentrated loads, in the same manner as in the traditional procedures for design calculations. The direct and bending stresses across horizontal sections were computed by elementary formulas for stresses in beams, also as in traditional procedures.

The history of response of Pine Flat Dam to the ground motion recorded at Taft during the Kern County earthquake of July 21, 1952—the response spectrum used for the simplified analyses was consistent with this ground motion—was obtained by the EADHI computer pro-

gram<sup>3</sup>. A dam monolith was idealized as a finite element system and the hydrodynamic effects were included in the analysis.

Comparison of results obtained from the two analyses demonstrated that the simplified analysis procedure summarized earlier leads to satisfactory results for maximum stress values on the downstream and upstream faces. It also leads to a satisfactory description of the distribution of stresses over the height of the dam.

## Lateral Earthquake Forces

### System and Ground Motion Properties

The headworks structure is described in Part 2 (of this chapter), prepared by DWR. Figures displaying the cross section details and dimensions at the centerline of the structure and the plan geometry and dimensions at several elevations are included with the description.

In the original analysis of the headworks, the structure was divided by five horizontal planes (one at the base, four above) resulting in five units. The weight of each unit and location of center of gravity of the unit were furnished by DWR. The lateral earthquake forces computed in this chapter refer to these five units.

The lateral forces are computed for the ground motion originally recommended by the Special Consulting Board to DWR (Figure 8). The pseudo-acceleration response spectrum for the ground motion for a 5 percent damping ratio (Figure 9) is used for these computations. This damping ratio is appropriate for concrete gravity dams.

### Computation of Earthquake Forces

The lateral earthquake forces are computed by following the steps listed in the preceding section:

1. For  $E = 5.0 \times 10^6$  psi and dam height  $H_s = 82.2$  ft., from Eq. 1:

$$\hat{T}_s = 1.4 \frac{82.2}{(\sqrt{5 \times 10^6})} = 0.051 \text{ sec.}$$

2. For  $E = 5.0 \times 10^6$  psi and  $H/H_s = 77.0/82.2 = 0.937$ , from Figure 5:

$$R_1 = 1.34$$

From Eq. 2:

$$\hat{T}_s = 1.34 (0.051) = 0.068 \text{ sec.}$$

3. From Eq. 3:

$$R_2 = \frac{1}{0.068} \frac{(4)(77)}{4720} = 0.96$$

4. Eq. 4 is replaced by its discrete form. The force acting on unit  $i$  is given by

$$f_{si} \alpha_1 \frac{S_a(\hat{T}_s)}{g} [w_{si} \psi_i + g \bar{P}_{li}] \quad (\text{Eq. 6})$$

where for this analysis:

$$\alpha_1 = 4$$

$S_a(\hat{T}_s)$  = ordinate of the pseudo-acceleration response spectrum at vibration period:

$$S_a(\hat{T}_s) = 0.78 \text{ g at } \hat{T}_s = 0.068 \text{ sec. (Figure 9)}$$

$g$  = acceleration of gravity

$w_{si}$  = weight of unit  $i$  (data provided by DWR)

$\psi_i$  = mode shape value at center of gravity of unit  $i$  (Figure 6)

$\bar{P}_{li} = \bar{P}_1(z)$  — determined as described earlier from Figure 7—integrated over unit  $i$ .

Based on the weight and the location of the center of gravity for each of the five units of the structure provided by DWR, the lateral forces using Eq. 6 are computed in Table 1.

5. Eq. 5 is replaced by its discrete form. The lateral force acting on unit  $i$  is given by:

$$f_{si} = \alpha_2 \frac{S_a(T_s)}{g} w_{si} \psi_i \quad (\text{Eq. 7})$$

where for this analysis:

$$\alpha_2 = 3$$

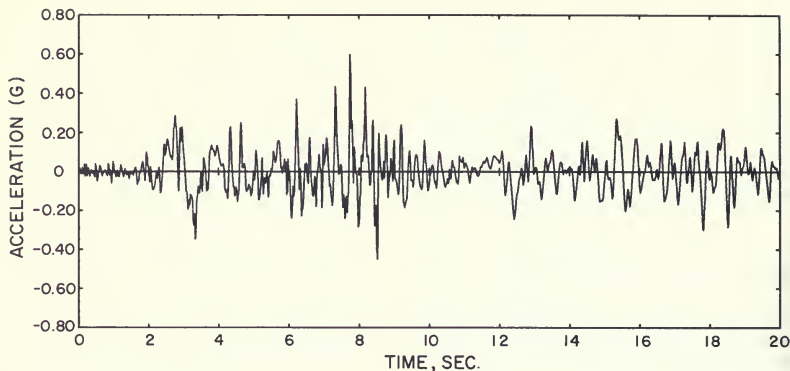


Figure 8. Horizontal Ground Acceleration Specified by DWR

### Recommendations for Safety Evaluation

Replace the earthquake forces considered in the original design of the structure by the forces presented in Tables 1 and 2. Using standard DWR procedures, evaluate the capacity of the existing structure to carry the revised earthquake forces and all other loads—self weight of the structure and equipment, hydrostatic forces, etc.—considered in the original design of the structure. The earthquake forces should be considered to act in each—upstream and downstream—direction separately. The reinforced concrete portions, as well as the plain mass concrete portions of the structure, should be analyzed for these loads. The results should be checked against the appropriate design criteria. The standard design criteria of DWR is appropriate for checking the reinforced concrete portions of the structure.

However, the following criteria are recommended for checking the plain, mass concrete portions of the structure: The compression and tensile stresses should not exceed the strength values in compression and tension, respectively. Usually, tensile stresses will control the evaluation, because they will be similar in magnitude to the compressive stresses, whereas the tensile strength of mass concrete is only about 10 percent of the compressive strength. The overturning and sliding stability criteria that were used in the original design of the structure need not be satisfied, because they have little meaning in the context of oscillatory response of dams due to earthquake motion.

Concrete strength in tension and in compression depends on the rate of loading, with increases up to 50 percent at loading rates representative of those the concrete may experience during earthquake motions of the dam.<sup>5-7</sup>

Table 1. Lateral Earthquake Forces Including Hydrodynamic Effects

Unit No. i	Height of c.g. Above Base (Plane 5-5), ft.	Weight $w_i$ , kips	Mode Shape $\psi_i$ at c.g.	$8\bar{P}_{11}$ , kips	Lateral Forces, kips $\frac{S_a(T_s)}{\alpha} \frac{a}{g} \{w_i \psi_i + 8\bar{P}_{11}\}$
1	79.42	2,645	0.909	6.6	7,392
2	70.27	3,228	0.636	422	7,611
3	60.04	2,645	0.430	606	5,376
4	37.80	16,214	0.174	3,395	19,240
5	10.64	17,361	0.028	2,643	9,737

**Table 2. Lateral Earthquake Forces Excluding Hydrodynamic Effects**

Unit No. 1	Height of c.g. Above Base (Plane 5-5), ft.	Weight $w_1$ , kips	Mode Shape $\psi_1$ at c.g.	Lateral Forces, kips $\frac{S_a(T)}{\alpha} \frac{g}{g} w_1 \psi_1$
1	79.42	2,645	0.909	5,410
2	70.27	3,228	0.636	4,620
3	60.04	2,645	0.430	2,559
4	37.80	16,214	0.174	6,348
5	10.64	17,361	0.028	1,094

Furthermore, the different types of tests that are available—direct tension, splitting tension, and flexural strength—generally yield different results for tensile strength. Because of its simplicity and ability to produce reliable results, the splitting tension test appears to be especially useful. Thus, the concrete strength values should be based on appropriate tension and compression tests on cores taken from the structure, at rates of loading representative of those the structure will experience in vibration due to earthquake motion.

At the present time, it is not practical to routinely perform cyclic tests with stress reversals on specimens under multi-axial states of stress; hence, monotonic tests are recommended to determine concrete strength. The data available for the structure are from compression tests on specimens during construction at normal, slow rates of loading. For preliminary evaluation, it is appropriate to allow a reasonable increase in the measured compressive strength, based on the available data<sup>5-7</sup>. For the faster loading rates during earthquakes, tensile strength may be taken as 10 percent of the compressive strength.

If the preliminary evaluation indicates that the design criteria are not satisfied, tension tests should be performed on cores taken from the structure to obtain more reliable estimates of the tensile strength of concrete.

Permitting significant tensile stresses, up to the tensile strength, is, of course, a major departure from the standard design criteria wherein little tension is permitted. However, evidence is available to support the recommended evaluation criteria that significant dynamic stresses in tension can be carried by sound concrete. In

addition to the data from laboratory tests mentioned earlier, evidence of the dynamic tensile strength of concrete was provided by the performance of three dams during earthquakes.

The ground motion experienced by Pacoima Dam during the San Fernando earthquake of 1971 must have been very intense; accelerations exceeding 1 g were recorded near the dam. Analyses of dynamic response of the dam, performed at the University of California, Berkeley, indicated that the dam must have developed maximum tensile stresses on the order of 750 psi. Yet, no evidence of cracking could be found on either face of the dam.

Analyses of Koyna Dam based on elastic behavior indicated tensile stresses almost three times the tensile strength of concrete, resulting in significant cracking of the dam. However, the dam survived the earthquake without any sudden release of water. Perhaps most interesting is the lack of damage to Crystal Springs Dam—a curved concrete gravity dam about 1,000 feet from the San Andreas Fault—during the great San Francisco earthquake of 1906.

Following the August 1, 1975 Oroville earthquake of Magnitude 5.7, the Department decided to evaluate the effects of an earthquake of Magnitude 6.5, centered approximately 4 miles away, on the Thermalito Powerplant headworks (Figures 10 and 11). The ground motion shown in Figure 8 (Part 1) was recommended by the DWR Special Consulting Board to represent the ground shaking (at the site) associated with the higher magnitude quake.

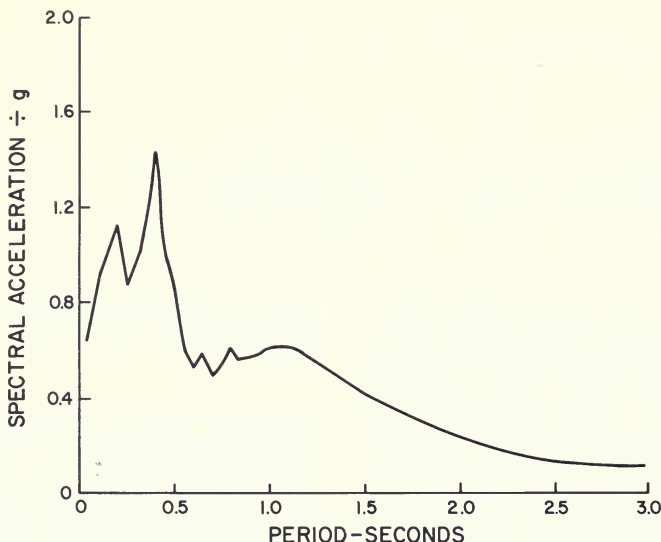


Figure 9. Pseudo-Acceleration Response Spectrum for the Ground Motion Specified by DWR; Damping = 5%

## PART 2 EVALUATION OF STRESSES DUE TO LATERAL EARTHQUAKE FORCES

A consulting agreement between Dr. Anil K. Chopra and DWR was made to cooperatively investigate the effects of the specified earthquake; the results are shown in this chapter. The plan was to first use a simplified approach to investigate the earthquake induced stresses in the structure, and then use a more refined method of analysis if the stresses were great enough to warrant it.

In the re-evaluation of the headworks structure, stresses due to static and seismic conditions were investigated separately and in combination. The concrete stresses were evaluated on the basis of the working stress method, disregarding the effect of the reinforcing steel. The following design criteria were used in the re-evaluation:

1. The maximum allowable tensile stresses for concrete shall not exceed 10 percent of the ultimate strength of the concrete. For this structure the maximum allowable tensile stress would be 10 percent (5,500 psi) = 550 psi.
2. The maximum compressive stress in the concrete shall not exceed 45 percent of the compressive strength:  $(0.45f'_c = 0.45 \times 5500 = 2475 \text{ psi})$  plus a 33-1/3 percent increase when combined with earthquake-induced forces.
3. The compressive and direct shear strength of the basaltic rock foundation is assumed equivalent to that of the structure concrete.





Table 3. Physical Properties of Block No. 1  
Thermalito Powerplant

Coordinates to Center of Gravity

<u>Mass of Unit</u>	<u>Total Wt. per Unit KIPS</u>	<u>X</u>	<u>Y</u>	<u>Z</u>
1	2645.28	25.89'	35.19'	2.78'
2	3228.12	24.16'	35.37'	11.93'
3	2644.80	25.77'	35.28'	22.16'
4	16214.06	41.55'	35.02'	44.40'
5	17360.86	42.71'	34.90'	71.56'
	<u>42093.12</u>			

Cumulative Loads

Coordinates to Center of Gravity

<u>Plane No.</u>	<u>Total Cumulative Wt. to Plane KIPS</u>	<u>X</u>	<u>Y</u>	<u>Z</u>
1-1	2645.28	25.89'	35.19'	2.78'
2-2	5873.40	24.94'	35.29'	7.81'
3-3	8518.20	25.20'	35.29'	12.26'
4-4	24732.26	35.92'	35.11'	33.33'
5-5	42093.12	38.73'	35.03'	49.10'

Neutral Axis by Area

$$I. = I_o + AX^2$$

<u>Plane No.</u>	<u>Total Area (ft<sup>2</sup>)</u>	<u>X</u>	<u>I (ft<sup>4</sup>)</u>
1-1	1783.74	23.95'	304614.30
2-2	1651.37	25.78'	229540.59
3-3	2140.64	27.45'	302996.38
4-4	3215.20	45.14'	1649183.56
5-5	5500.46	42.94'	3035580.12



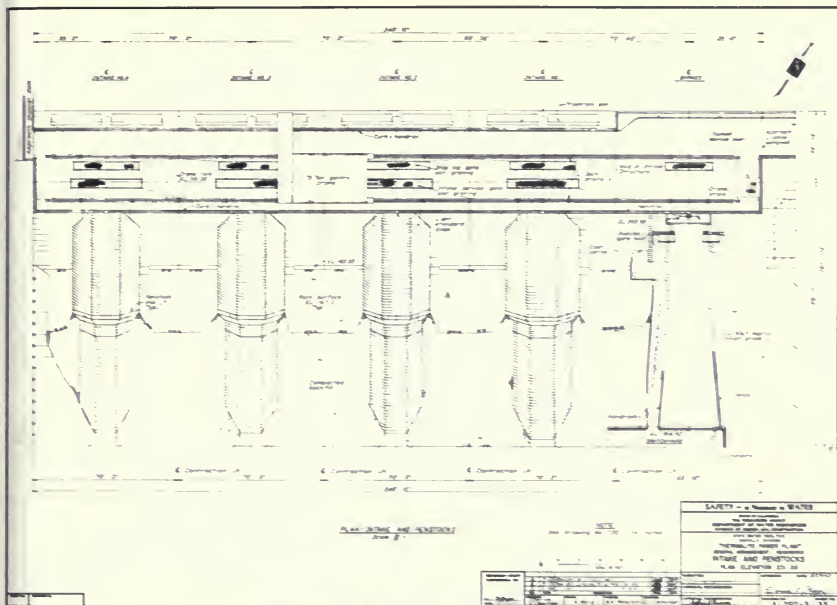


Figure 11. Thermalito Powerplant, Intake and Penstocks

Table 4. Overturning Moments, Kip-ft\*

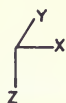
Level	Hydrostatic Moments	Self-Weight Moments	Dynamic Moments Including Hydrodynamic	Dynamic Moments Excluding Hydrodynamic
1-1	0	5,131.84 ↗	26,019.71	19,044.49
2-2	1,406.32 ↗	4,933.66 ↗	154,801.34	107,776.20
3-3	6,696.17 ↗	19,165.95 ↗	303,443.73	202,965.05
4-4	121,431.65 ↗	228,031.44 ↗	1,301,899.85	732,027.99
5-5	322,673.99 ↗	177,212.04 ↗	2,275,407.70	1,159,201.00

\* ↗ Indicates direction of moment on plane under consideration.

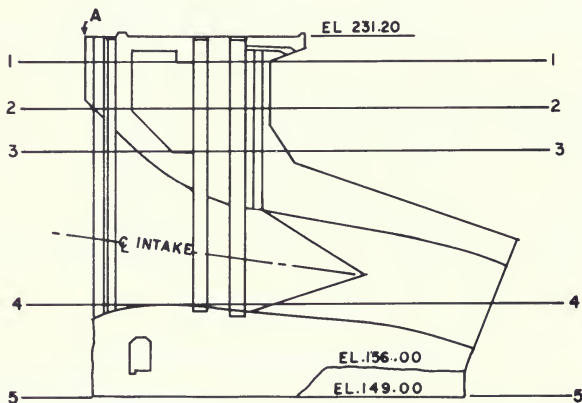
Table 5. Distances from Neutral Axis to Extreme Fiber

Level	Distance to Extreme Fiber (feet)	
	U/S	D/S
1-1	23.95	18.24
2-2	23.28	16.41
3-3	24.95	18.42
4-4	42.64	47.62
5-5	40.44	43.06

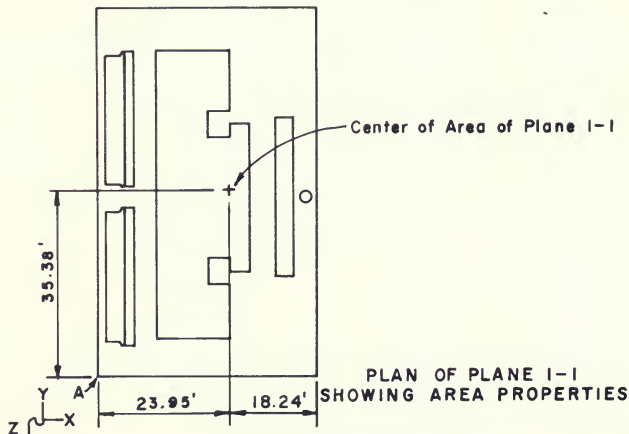
NOTE: Text continues on page 28.



# AREA PROPERTIES OF PLANES

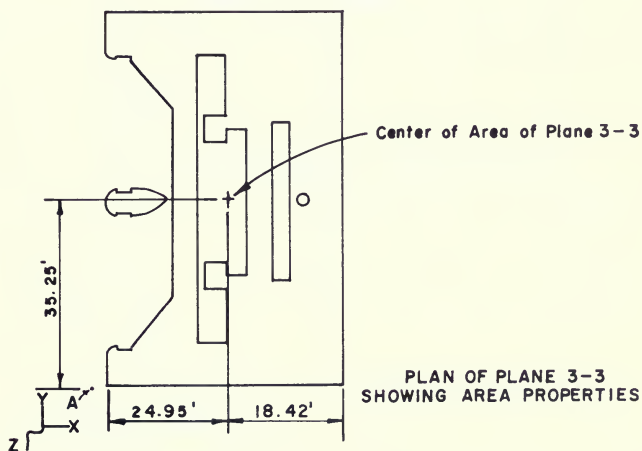
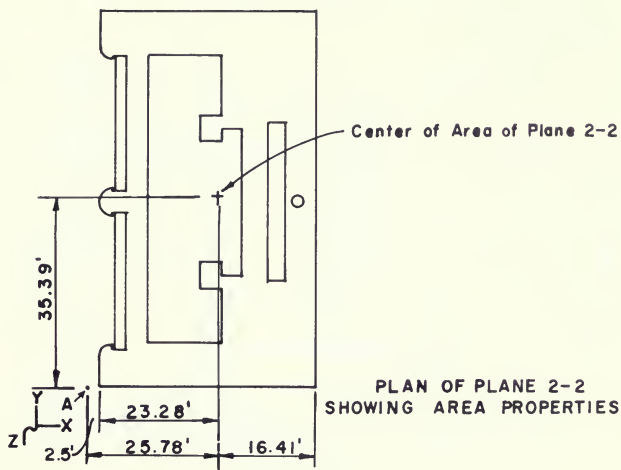


ELEVATION-INTAKE BLOCK NO. 1



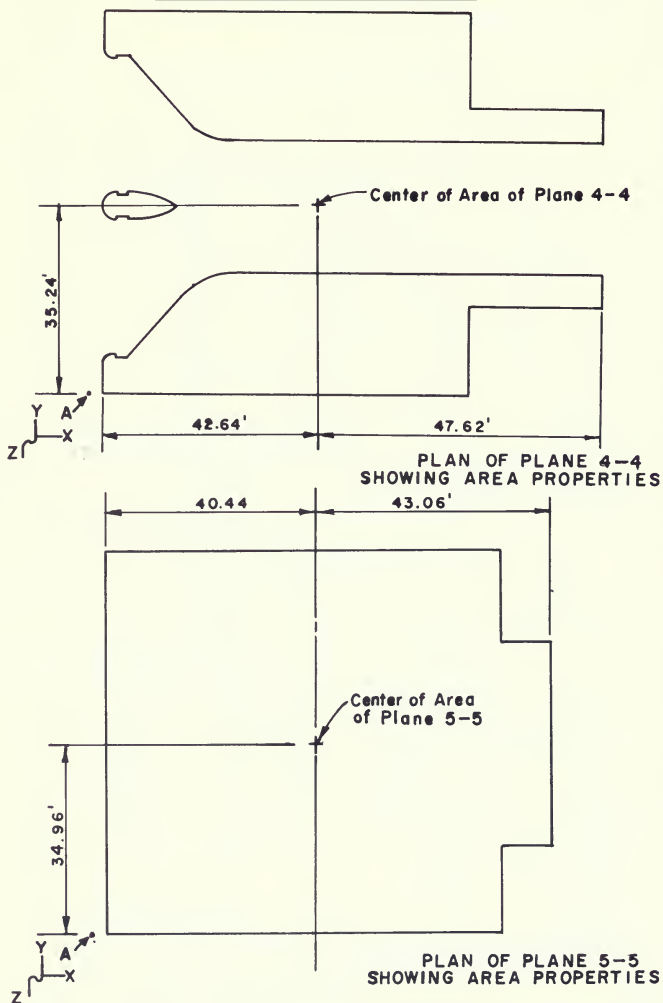
# AREA PROPERTIES OF PLANES

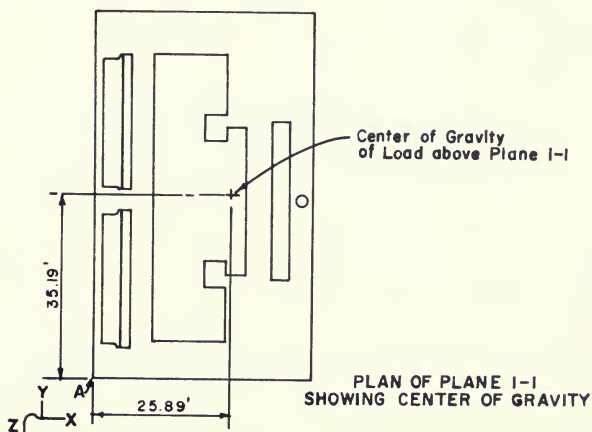
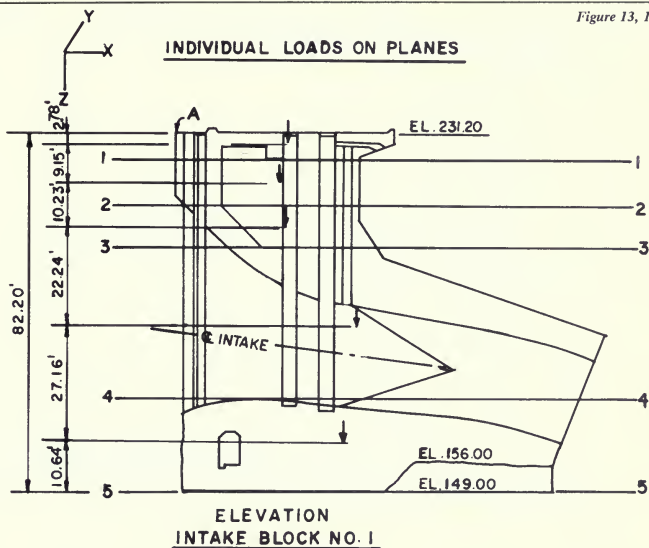
Figure 12, 2 of 3



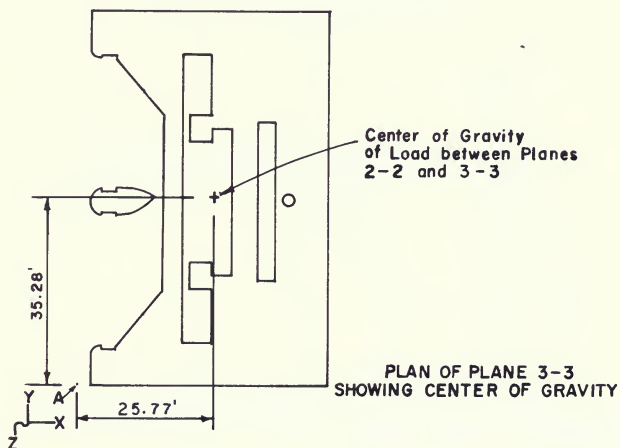
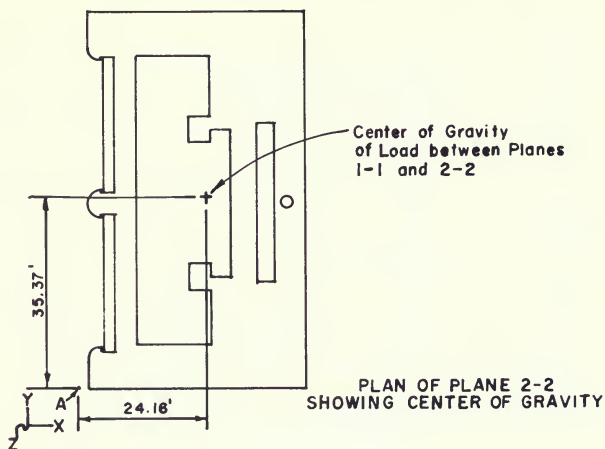
# AREA PROPERTIES OF PLANES

Figure 12, 3 of 3



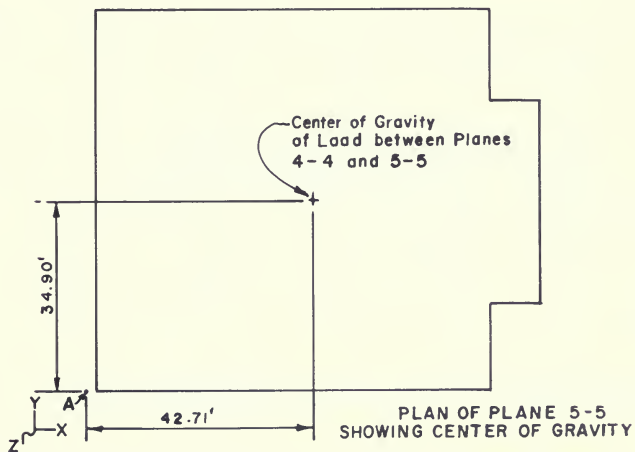
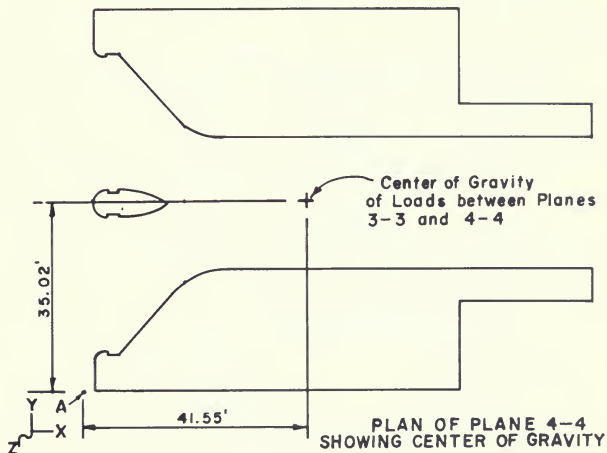


# INDIVIDUAL LOADS ON PLANES



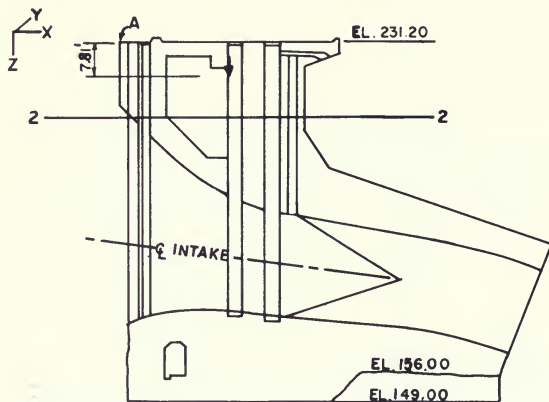
# INDIVIDUAL LOADS ON PLANES

Figure 13, 3 of 3

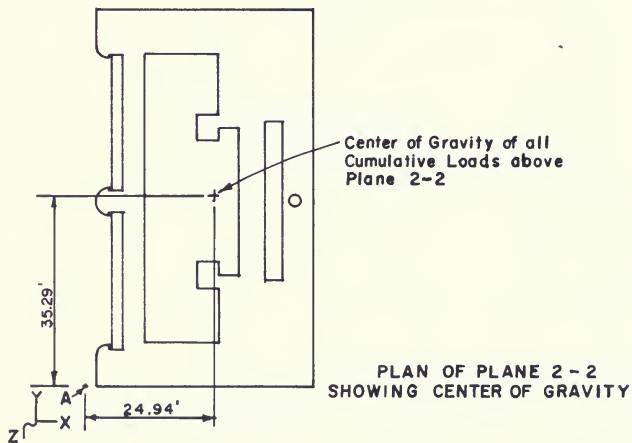


# CUMULATIVE LOADS ON PLANE 2-2

Figure 14, 1 of 4



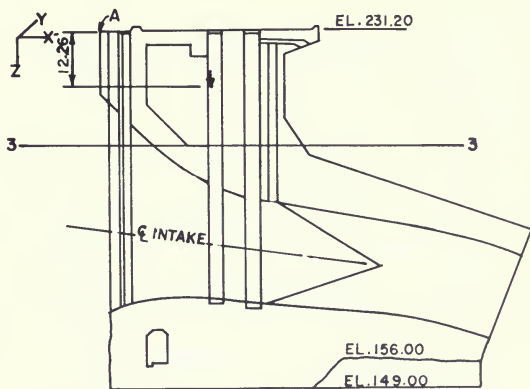
ELEVATION-INTAKE BLOCK NO. 1



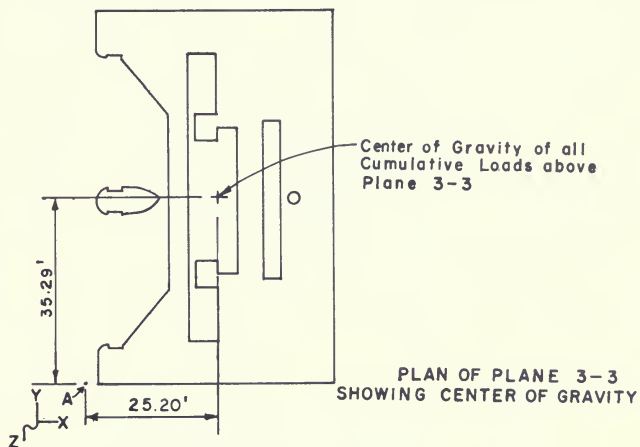


# CUMULATIVE LOADS ON PLANE 3-3

Figure 14, 2 of 4



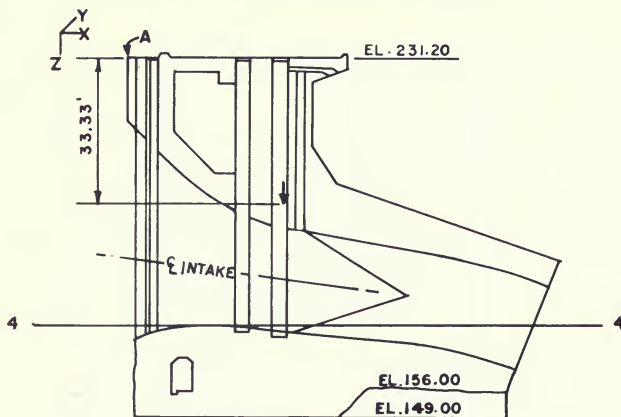
ELEVATION - INTAKE BLOCK NO. 1



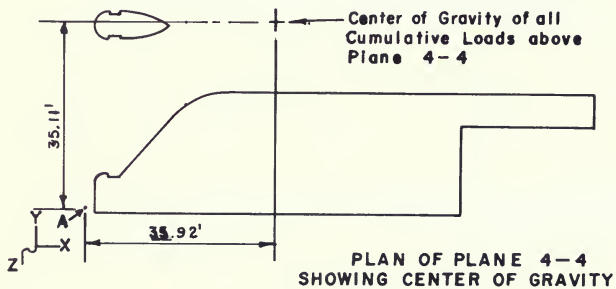
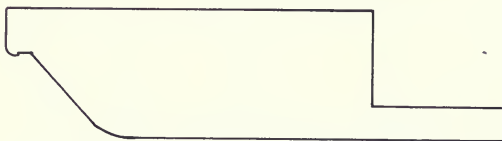
PLAN OF PLANE 3-3  
SHOWING CENTER OF GRAVITY

# **CUMULATIVE LOADS ON PLANE 4-4**

Figure 14, 3 of 4



**ELEVATION - INTAKE BLOCK NO. 1**



**PLAN OF PLANE 4-4  
SHOWING CENTER OF GRAVITY**

# CUMULATIVE LOADS ON PLANE 5-5

Figure 14, 4 of 4

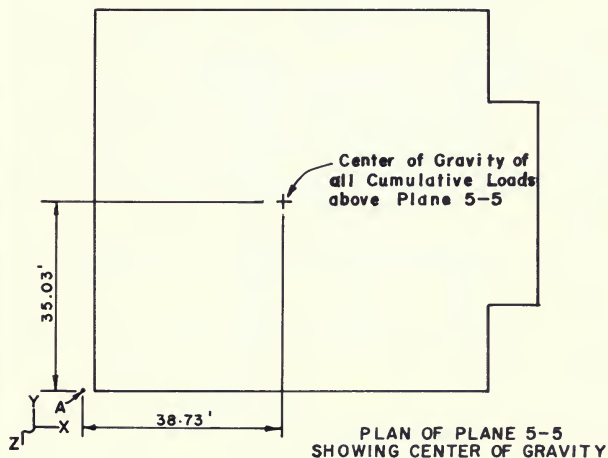
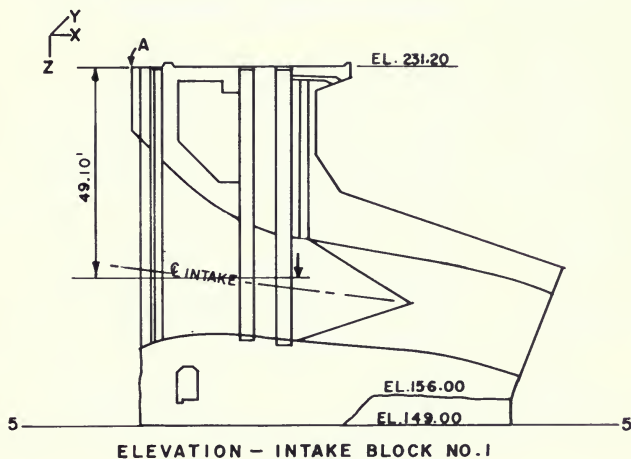
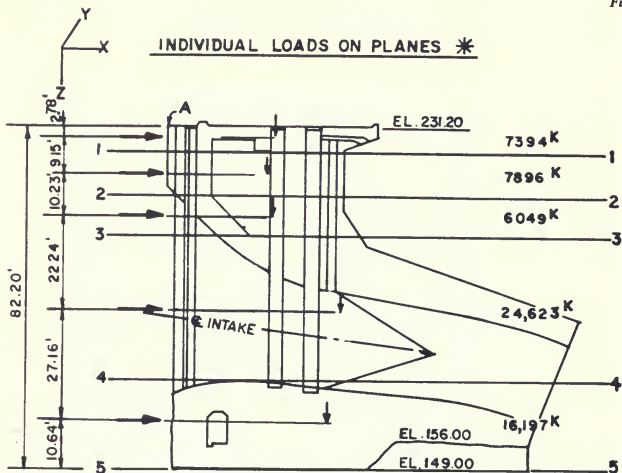
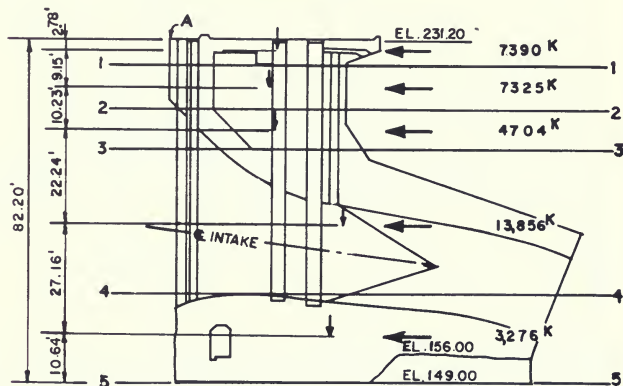


Figure 15



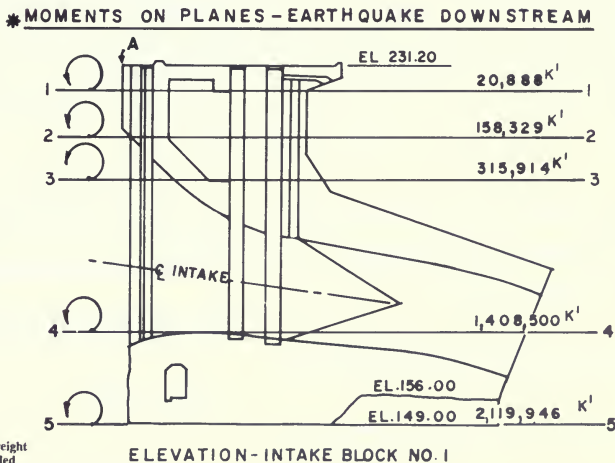
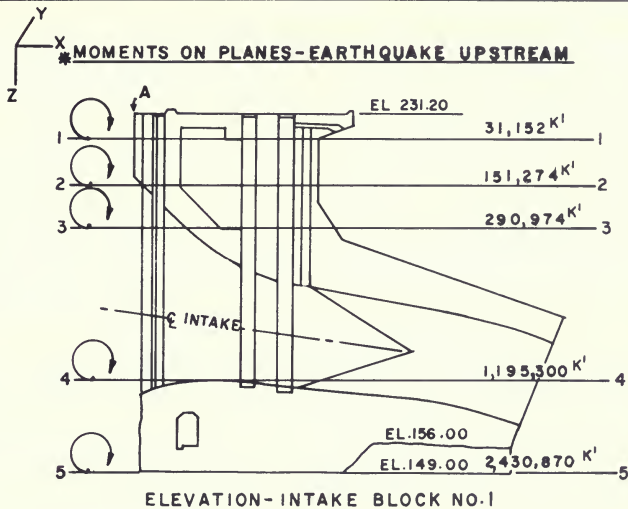
ELEVATION  
INTAKE BLOCK NO. 1



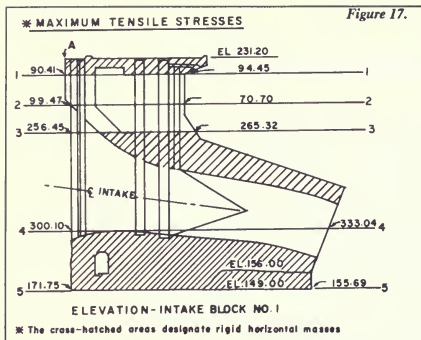
ELEVATION  
INTAKE BLOCK NO. 1

\*For Gravity Loads, see Table 3 —  
Hydrostatic and earthquake included

Figure 16



\*Hydrostatic, self-weight  
& earthquake included



The critical shear-resisting elements in the headworks structure occur between Elevations 231.20 and 209.43, and between Elevation 209.43 and the invert of the large water passage. An analysis was made to determine resisting elements between these two sets of levels, based on the assumption that the cross-hatched areas (see Figure 17) acted as rigid diaphragms fixing the ends of the piers, with the inflection point occurring at mid height of the pier as shown in Figure 18.

$$M = P \frac{H}{2}$$

$$f = \frac{Mc}{I} = \frac{P \frac{H}{2} \times .5d}{I}$$

$$f = \frac{PHd}{4I}$$

where:

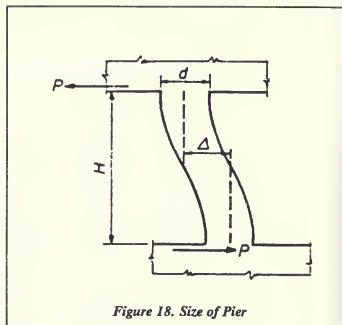
$I$  = moment of inertia of pier or wall being considered

$P$  = shear transferred between the diaphragms

$f$  = stress induced due to pier flexure

The stresses found due to pier flexure were combined in the proper manner with the stresses found due to overturning and gravity loads.

The stresses due to static loads (shown in Tables 6 and 7) are designated as  $S$  and are defined as follows:



$$S = \frac{P_v}{A} \pm \frac{(M_s + M_H)c}{I_1} \pm \frac{P_s Hd}{4I_2}$$

where:

$P_v$  = self weight resting on plane considered

$A$  = area of plane

$M_s$  = moment induced by self weight about the pier's neutral axis

$M_H$  = moment induced by hydrostatic loads about the pier's neutral axis

$P_s$  = load due to the hydrostatic loads

$I_1$  = moment of inertia of plane considered

$I_2$  = moment of inertia of individual pier under consideration

$c$  = distance from the neutral axis to the extreme fiber

The stresses due to dynamic loads (shown in Tables 6 and 7) are designated as  $E.Q.$  and are defined below:

$$E.Q. = \frac{MEc}{I_1} \pm \frac{PEHd}{4I_2}$$

where:

$P_E$  = the lateral earthquake loads (contained in Table 2 of Part I) distributed to individual resisting shear elements according to their relative rigidities.

$M_E$  = the moment due to the lateral load  $P_E$  about the neutral  $P_E$  axis of the shear element under consideration.



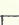

In addition to stresses due to flexure, overturning and gravity loads, shear stresses in the concrete structure and base rock were investigated and are discussed in the review of critical stresses.

## Review of Critical Stresses

As can be seen in Table 6, under static loading, no tensile stresses exist and the maximum concrete compressive stress is 68 psi. Under static and dynamic loading conditions, including hydrodynamic loads, the maximum concrete tensile stress is 333 psi. This occurs at the downstream face of the opening as shown in Figure 17. The maximum compressive stress of 432 psi, in Table 6 also, occurs on the downstream face of the opening.

The maximum average shear in the structure as a whole was found to be 99 psi, and the maximum shear in any individual member was found to be 113 psi.

Table 6. Maximum Stresses Including Hydrodynamic Effects\*

Unit No.	STATIC (S)		E.Q. 		E.Q. 		S + E.Q. 		S + E.Q. 	
	U/S	D/S	U/S	D/S	U/S	D/S	U/S	D/S	U/S	D/S
1	- 10.29	- 9.64	- 100.70	+ 104.09	+ 100.70	- 104.09	- 110.99	+ 94.45	+ 90.41	- 113.73
2	- 26.77	- 23.37	+ 126.23	- 94.06	- 126.23	+ 94.06	+ 99.47	- 117.43	- 153.00	+ 70.70
3	- 31.97	- 35.20	+ 288.43	- 300.52	- 288.43	+ 300.52	+ 256.45	- 335.72	- 320.40	+ 265.32
4	- 55.12	- 49.48	+ 355.22	- 382.52	- 355.22	+ 382.52	+ 300.10	- 432.01	- 410.34	+ 333.04
5	- 38.76	- 68.46	+ 210.51	- 224.15	- 210.51	+ 224.15	+ 171.75	- 292.60	- 249.27	+ 155.69

MAXIMUM TENSILE STRESS = 333.04 psi

MAXIMUM COMPRESSIVE STRESS = 432.01 psi

\* U/S in table designates upstream face

\* D/S in table designates downstream face

\*  Indicates direction of moment on plane under consideration

- = Compression

+ = Tension



**Table 7. Maximum Stresses Excluding Hydrodynamic Effects\***

Unit No.	STATIC (S)		E.Q. ↺		E.Q. ↻		S + E.Q. ↺		S + E.Q. ↻	
	U/S	D/S	U/S	D/S	U/S	D/S	U/S	D/S	U/S	D/S
1	- 10.29	- 9.64	- 65.78	+ 68.26	+ 65.78	- 68.26	- 76.07	+ 58.62	+ 55.49	- 77.90
2	- 26.77	- 23.37	+ 87.32	- 64.92	- 87.32	+ 64.92	+ 60.55	- 88.28	- 114.08	+ 41.55
3	- 31.97	- 35.20	+ 192.24	- 200.33	- 192.24	+ 200.33	+ 160.27	- 235.53	- 224.22	+ 165.13
4	- 55.12	- 49.48	+ 195.80	- 211.15	- 195.80	+ 211.15	+ 140.68	- 260.64	- 250.92	+ 161.67
5	- 38.76	- 68.46	+ 107.24	- 114.19	- 107.24	+ 114.19	+ 68.48	- 182.65	- 146.00	+ 45.73

MAXIMUM TENSILE STRESS = 165.13 psi

MAXIMUM COMPRESSIVE STRESS = 260.64 psi

\* U/S in table designates upstream face  
 \* D/S in table designates downstream face

\* ↺ Indicates direction of moment on plane under consideration  
 - = Compression  
 + = Tension

The maximum compressive stress occurring on the basaltic rock foundation was found to be 301 psi, and the maximum shear stress in the rock was 128 psi under combined static and dynamic conditions.

An analysis was made to investigate the stresses induced in the wall of the downstream end of the water passage opening by the maximum overturning moment on the structure. The maximum concrete compressive stress was 940 psi, and the maximum tensile stress was 460 psi.

### Conclusions

The stresses predicted by the analysis are within the allowable stresses of concrete and did not include the effect of the reinforcing steel. Consideration of the reinforcement would only lower the stresses in the concrete.

One inch of vertical, sympathetic movement has been considered credible along a fault which lies beneath the bases of the penstocks. Although this may cause some cracking of the penstock, it would not result in damage to the headworks structure.

The traveling gantry crane is being provided with a tie-down system, which will be used during those periods when the crane is not in use. This will allow the crane to be fully operational immediately following the design earthquake.

DWR has therefore concluded that the Thermalito Powerplant headworks structure should safely withstand the ground motion specified by the Consulting Board; hence the structure should present no hazard to the general public under such an earthquake.

## REFERENCES

1. Chakrabarti, P., and Chopra, A.K., "A Computer Program for Earthquake Analysis of Gravity Dams Including Hydrodynamic Interaction," Report No. EERC 73-7, Earthquake Engineering Research Center, University of California, Berkeley, California, May 1973.
2. Chakrabarti, P., and Chopra, A.K., "Earthquake Analysis of Gravity Dams Including Hydrodynamic Interaction," *International Journal of Earthquake Engineering and Structural Dynamics*, Vol. 2, No. 2, Oct.—Dec. 1973, pp. 143-160.
3. Chopra, A.K., "Earthquake Response Analyses of Thermalito Diversion Dam," Report to Department of Water Resources, State of California, 1977.
4. Chopra, A.K., "Earthquake Resistant Design of Concrete Gravity Dams," *Journal of the Structural Division, ASCE*, Vol. 104, No. ST6, June 1978, pp. 953-971.
5. Hatano, T., and Tsutsumi, H., "Dynamical Compressive Deformation and Failure of Concrete Under Earthquake Load," Technical Report No. C-5904, Central Research Institute of Electric Power Industry, Tokyo, Sept. 1959.
6. Hatano, T., "Dynamical Behavior of Concrete Under Impulsive Tensile Load," Technical Report No. C-6002, Central Research Institute of Electric Power Industry, Tokyo, Nov. 1960.
7. Raphael, J.M., "The Nature of Mass Concrete in Dams," Douglas McHenry Symposium Volume, American Concrete Institute, Detroit, Michigan, 1978.



## CHAPTER III THERMALITO AFTERBAY DAM SEISMIC EVALUATION

### 1. SUMMARY

#### Conclusions

1. The strengths of foundation sands are higher than the values used in the preliminary (1981 Report) evaluation of Station 107.
2. The stability of the dam is satisfactory for the maximum earthquake shaking anticipated. Only minor cracking or movements are predicted for the postulated shaking. As an extra precaution, a short reach of dam, with a sharp angle in the axis alignment, has been locally reinforced to supplement resistance to transverse cracking (see Chapter I).
3. From a seismic safety standpoint, it is safe to restore full use of the reservoir, provided that the ground water piezometric level on the downstream side of the dam is controlled to prevent its rising above the ground surface for an extended period. To comply with this provision, a ground water pressure relief system and a small berm have been added in short reaches along the downstream side of the dam (see Chapter I).

#### Background

After the Oroville Earthquake of August 1, 1975, the Department of Water Resources, with the guidance of its Special Consulting Board, decided to evaluate the seismic stability of critical Oroville Project structures for much stronger earthquake shaking than had been considered during design.

Thermalito Afterbay Dam, completed in 1967 at a location about 11 miles west of Oroville Dam, is one of these critical structures. It is an 8-mile-long compacted clay embankment with a maximum height of 39 feet founded on deep alluvium. The dam creates an offstream storage reservoir with a capacity of 57,000 acre-feet. Its purpose is to both regulate discharge from Thermalito Powerplant for release back to the Feather River and hold water for pump-back into Oroville Reservoir.

The dam was designed in the early 1960's using standard practices of that time. Earthquake effects were accounted for by including in the stability analyses a 0.1g horizontal acceleration. Both upstream and downstream slopes were analyzed for several reservoir levels. In most locations the foundation was assumed to be stronger than the dam, and only failure surfaces within the dam were considered. A short reach of the dam at the southeast end is founded on soils which were considered slightly weaker than the embankment. Here, failure surfaces into the foundation were analyzed. The minimum safety factor found was 1.2 for the upstream slope with a 13.5 foot drawdown combined with the 0.1g horizontal acceleration.

The embankment performed well in all the shocks of the Oroville earthquake sequence. There were no accelerometers at the dam, but maximum accelerations have been estimated at 0.09g for the main shock. The only effect of the earthquake that could be found by inspection was a longitudinal crack near the top of the upstream slope on each side of the river outlet structure. The cause was assumed to be the difference in rigidity between the embankment and outlet structure. The cracks were minor, however, and were not investigated further.

Although the embankment performed well in the 1975 earthquake, a new seismic evaluation was considered necessary because of the discovery of closer active faults than had been previously identified, and the availability of new procedures for making the evaluations. Therefore, the Department undertook the investigation described in this report to estimate appropriate earthquake ground motions and the consequent behavior of the dam. To assist in the evaluations, the Department convened a special consulting board of foremost specialists in geology, seismology, dynamic analysis, and practical dam design. This board has provided guidance in completing the studies and has reviewed the findings.

## Concept and Progress of Investigations

The embankment and its foundation were to be re-evaluated for earthquakes ranging up to Magnitude 6.5, which would produce much stronger ground motions than those resulting from the 1975 Oroville Earthquake of Magnitude 5.7.

A basic assumption made at the outset by the Department was that the compacted sandy clay embankment and the sometimes cemented clayey surface layer of the foundation would perform satisfactorily during severe earthquake shaking. This assumption was based on the findings of Seed, Makdisi, and DeAlba (1977)\*, who studied the historical performance of dams subjected to strong earthquake shaking.

It was further assumed that the main threat to stability would come from loose foundation sands or silts, which might liquefy and cause a section of embankment to slide out. Therefore, the investigative efforts were directed toward locating loose soil layers in the foundation, assessing their liquefaction potential, and evaluating the effects of foundation liquefaction on stability of the embankment.

The Department carried out the investigations in several stages between 1976 and 1982. Each stage consisted of drilling boreholes into the foundation to perform in situ testing or to obtain samples for laboratory tests. Throughout these stages, analyses were performed to predict the liquefaction potential of the foundation sands. The stages of the evaluation are summarized as follows:

**1976 Investigations.** Limited field studies and analyses confirmed the existence of potentially liquefiable sands in the foundation. Explorations used inadequate sampling procedures and incomplete sampling coverage to properly define the material properties necessary for performing analyses.

**1978 Investigations.** This stage of the evaluation was concerned with determining representative material properties necessary for performing the analyses. Intense sampling and testing were performed at four sites along the dam's length (Stations 107, 173, 203, and 281). A major discrepancy in the cyclic strengths showed up during this

stage. Cyclic triaxial tests made in the laboratory on samples of low blowcount silty sands indicated twice the strength predicted by Standard Penetration Test (SPT) correlations. It was also concluded during this stage that the accelerogram used in the Oroville Dam seismic evaluation ( $a_{\max} = 0.6g$ ) was inappropriate because the Afterbay Dam is located farther from the fault than is Oroville Dam, and the foundation is soil instead of rock.

**August 1979.** The reservoir elevation was restricted to a maximum elevation of 131 feet until it could be demonstrated that the dam was completely safe.

**1979–80 Investigations.** The investigations in 1979–80 concentrated on performing deeper explorations for use in selecting appropriate earthquake motions and in drilling additional SPT borings at 1,000-foot spacings along the length of the dam. These additional borings were drilled to find any other sites with low SPT resistance sands.

The testing performed during the 1979–80 investigations provided enough information to develop accelerograms appropriate for analyzing the afterbay. The accelerograms developed were three surface motions recorded at stiff soil sites during 6.5 magnitude events, scaled to have peak accelerations of 0.35g.

One location, Station 107 (Site 1), was chosen for detailed analyses because it had the most extensive, low blowcount sand layer found. The height of the dam at Station 107 is 26 feet. Foundation characteristics were determined to a depth of 500 feet, and a series of one-dimensional dynamic response analyses was performed.

For the silty sands at Station 107, with normalized blowcounts of about 10, the cyclic triaxial test strengths were twice the values obtained from published SPT correlations. Furthermore, the cyclic triaxial strengths obtained at Station 173 (Site 2) with normalized blowcounts of about 27 were the same as at Station 107. This discrepancy had been originally found in 1978 and had not been resolved. There was very little justification at this time for using the higher laboratory strengths, and the Department believed that the strength inconsistencies might not be resolved by further studies. Therefore, to perform the analyses, the Department decided to use an intermediate strength that was equal to 80 percent of the laboratory strength. Subsequent information showed this to be an overly conservative decision.

For the postulated earthquake shaking, analyses predicted zones of liquefaction beyond the embankment

\* A list of references is presented at the end of Chapter III.

toes and under the upstream slope of the dam. This extent of liquefaction would lead to an upstream slide in the embankment and foundation. Because the SPT borings indicated other locations also had low blowcount foundation sands, the Department estimated that possibly up to six locations might fail during the earthquake. It was also concluded that the 1,000-foot spacing of SPT borings was too large to assure that all possible locations where sliding might occur were discovered.

**1981 Final Draft Report.** (Presented to the Board on January 8, 1981).

**1981–82 Investigations.** This was the final stage of the evaluation and was originally intended as remedial design investigations. The Department performed a test program, using vibroflotation to densify the foundation silty sands at two sites. A large exploration and testing program was also carried out in order to both identify all potentially weak locations and to resolve the discrepancy between the cyclic triaxial test and SPT correlations. The new exploration program included 200 boreholes, 200 cone penetrometer soundings, 130 cyclic triaxial tests, and studies of the SPT procedures.

The work carried out in 1981–82 at Thermalito Afterbay and studies published by Kovacs et al (1981) indicated a wide variability in SPT procedures, which can lead to different results. Studies showed that the procedures used at the afterbay produced lower blowcounts than would be produced using the procedures considered “standard American practice.” New data from Japan published by Tokimatsu and Yoshimi (1981) also indicated that for sands with the same blowcount, those with higher silt content perform better during earthquakes.

Those two very important results resolved the discrepancy in the cyclic strengths. The cyclic triaxial strengths were higher than previous SPT correlations because the low blowcount afterbay sands had significant amounts of fines and because the SPT procedures used at the afterbay produced lower than “normal” blowcounts. In addition, the laboratory strengths increased for sands with higher blowcounts—a trend that was not found in 1978.

During this final stage of investigation, the maximum spacing between SPT borings along the dam’s length was reduced to 250 feet. This survey disclosed 21 locations with potentially liquefiable soils having corrected blowcounts less than 25. Three locations, representing the worst conditions found, were chosen for detailed analysis.

One of these three was Station 107, the site that was analyzed in detail in 1980. This site was reanalyzed because the new results justified a 30-percent increase in cyclic strength. The same accelerograms were used in the analyses. Evaluations predicted limited amounts of liquefaction and deformation, but failure was not indicated for any location due to the postulated earthquake shaking.

### Summary of Findings

The investigations have provided information leading to the following findings:

1. Earthquake motions with maximum accelerations of 0.35g at the ground surface are appropriate for use in analyzing the seismic stability of Thermalito Afterbay Dam.
2. Vibroflotation did not increase the SPT N values or CPT resistance of the foundation sand, but caused some decreases, particularly underneath the embankment. Even worse, there were indications that voids developed at the contact between the top of the sand layer and bottom of the silt/clay cap (Reference 20).
3. A site-specific correlation was developed between the SPT blowcount and the cyclic triaxial strengths of recovered afterbay sands. This site specific strength relationship defines higher cyclic strengths than do pre-1981 correlations. However, the strength relationship is consistent with 1981 published correlations when differences in SPT procedures are accounted for.
4. Analyses employing cyclic strengths from recent SPT correlations predicted foundation liquefaction only beyond the toes or in small zones beneath the embankment crest for the three critical sections analyzed. This is significantly less liquefaction than was predicted for Station 107 in the 1980 analyses.
5. Slope stability analyses were performed for conditions immediately after the earthquake, using calculated residual pore pressures in the sand layers, drained strength in the sand layers, and undrained strengths in cohesive materials. The lowest safety factor found for the three analyzed sites was 1.4.
6. Stability analyses for a very simplified assumption of pore pressure redistribution following the earthquake yielded a minimum safety factor against sliding



of 1.3. However, the 1.3 value is extremely conservative because neither pore pressure dissipation into underlying dense sand and gravel layers nor residual shear strength of liquefied soils were taken into account.

7. Historical behavior of clay embankments during earthquakes indicates that the afterbay embankment and clay foundation layers would perform well during severe earthquakes. Although failures of clay embankments due to foundation liquefaction were found in published accounts of earthquake damage, the foundations did not have strong surface caps of silt and clay. Analyses indicate that the surface cap at

the Afterbay has a significant stabilizing effect. Most of the failures discussed in the literature occurred when the embankment sank into or slid on liquefied surface soil. The literature contained no examples of a clay embankment founded on a strong intact cap developing a failure during or immediately after an earthquake.

8. Pre-earthquake groundwater piezometric levels equal to the downstream ground surfaces were the highest levels considered in the seismic evaluation studies. The predicted satisfactory performance depends on keeping the groundwater surface below ground surface.

## 2. DESCRIPTION OF DAM AND FOUNDATION

### General

Thermalito Afterbay is a shallow offstream reservoir with a capacity of 57,040 acre-feet, contained by Thermalito Afterbay Dam on the south and west and by higher natural ground on the north and east. Water flows from Thermalito Forebay through Thermalito Powerplant, into the tail channel and then into the afterbay on the generating cycle and reverses during the pumping cycle (Figure 19). The afterbay has a maximum operating surface of Elevation 136.5 feet and a minimum operating elevation of 124 feet. In addition to the main dam, there is a 12-foot-high saddle dam about 1,000 feet-long at the northwest corner of the reservoir. Pertinent statistics relating to the main dam are presented in Table 8.

**Table 8**  
**Thermalito Afterbay Dam Statistics**

Embankment crest length:	8 miles
Embankment volume:	5 million yards <sup>3</sup>
Maximum height:	39 feet
Average height:	24 feet
Crest width:	30 feet
Crest elevation:	142 feet
Freeboard, maximum operating surface:	5.5 feet

### Embankment

#### Embankment Design

There are two different cross section— one on Red Bluff formation, and the other on Columbia Soil (one mile

length at the southeast end). Both are essentially homogeneous sections of compacted sandy clay.

The section on the Red Bluff Formation has a horizontal drain blanket under the downstream slope (Figure 20). Side slopes are 3 to 1 upstream and 2.5 to 1 downstream. The upstream slope protection consists of an 8-foot horizontal thickness of riprap overlying an 8-foot horizontal thickness of Zone 3 bedding. The downstream slope facing is a 10-foot horizontal thickness of gravel. A shallow foundation trench is provided just upstream of the dam axis. The blanket drain, which extends from the downstream toe half way to the dam axis, is a 1.5-foot-thick layer of Zone 3 drain material sandwiched between 1-foot layers of select Zone 1A filter. A 3-foot-thick, 100-foot-wide blanket of Zone 1A compacted material extends upstream from the toe in locations where the foundation trench would not bottom on impervious material at a depth of less than 10 feet. In these locations the trench extended only 5 feet deep. Approximately 9,200 feet of the afterbay foundation trench encountered conditions requiring upstream blanketing (Figure 21).

The section on the Columbia soil foundation has the Oroville-Willows road relocation incorporated into the downstream slope on an 55-foot-wide berm. No foundation trench or blanket drain is provided, but the top 3 feet of foundation was stripped out beneath the dam and 100 feet upstream. The resulting surface was scarified, moi-

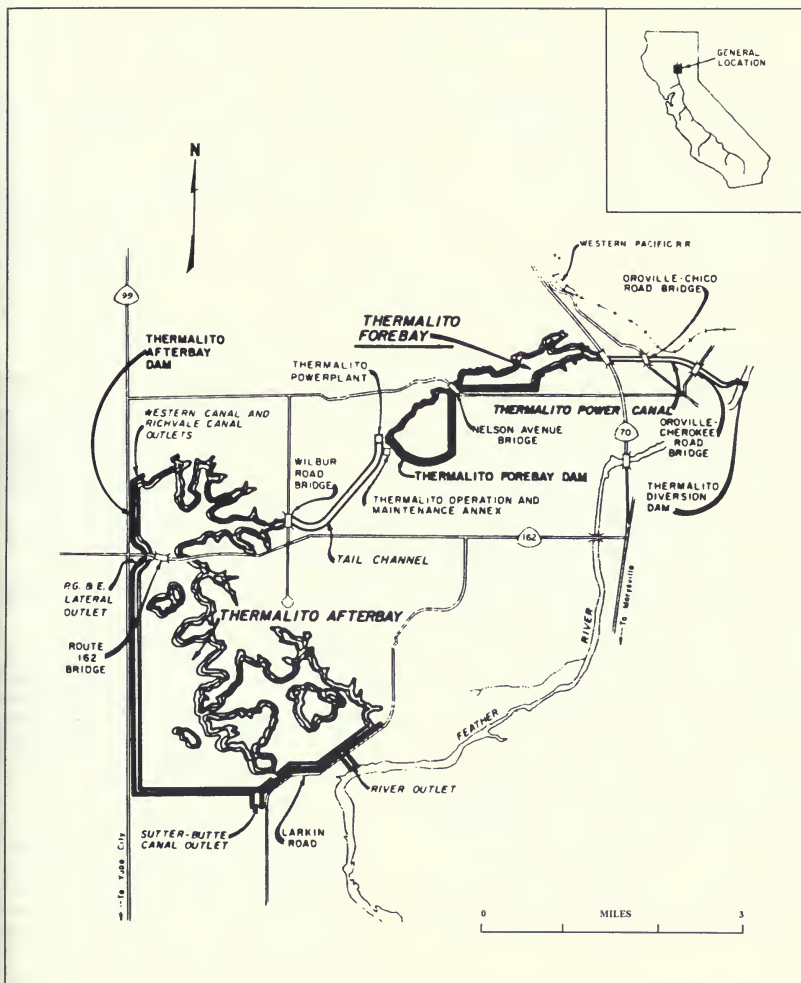


Figure 19. Vicinity Map of Thermalito Afterbay



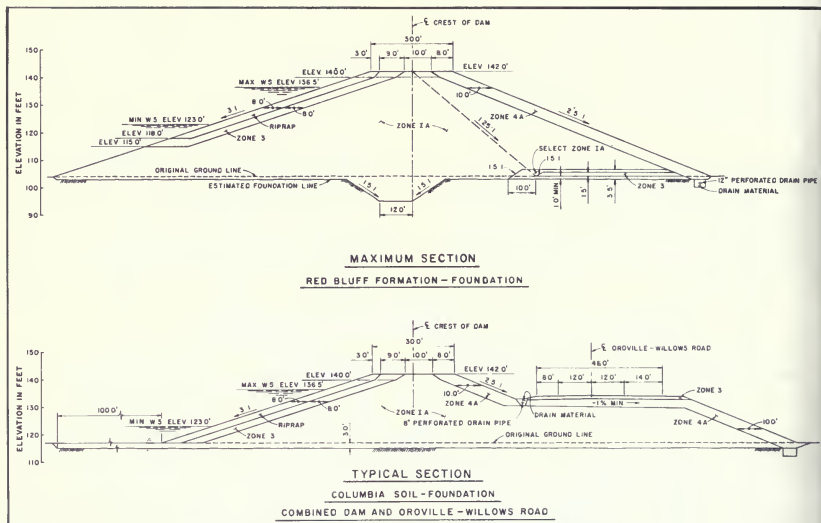


Figure 20. Typical Embankment Sections for Thermalito Afterbay

sture-conditioned, compacted, and covered with a 3-foot Zone 1A blanket.

### Embankment Materials

Tables 9 and 10 show the engineering properties of the embankment materials.

Zone 1A, the main section of the dam, consists of sand-silt-clay mixtures from the mandatory afterbay excavations and contractor-selected channel extension borrow areas. Select Zone 1A from the tail channel was used as filter layers for the blanket drain.

Zone 3 comprises sandy, coarse dredge tailings from the Oroville Dam reserve pervious borrow area, State Borrow Area Z. This material was used as riprap bedding and as the drain layer in the blanket drain.

The majority of Zone 4A, the downstream slope protection, was gravel obtained from the River Outlet Structure

area, with the rest from State Borrow Area Z and optional borrow areas.

Riprap was obtained from Power Canal and Oroville Spillway stockpiles and from the Cherokee Mine borrow area. The Cherokee Mine material consisted of rounded and poorly graded cobbles and boulders and therefore was mixed with rock from other sources or placed in areas not subject to severe wave action.

### Foundation

The afterbay is generally underlain by Red Bluff Formation except in the Columbia Soil area in the southeast corner. The Red Bluff deposits are fluvial (stream deposited) sediments, probably laid down by the ancestral Feather River. Owing to shifting stream courses and varying depositional conditions, a discontinuous mixture of clays, silt, silty sands and sandy gravels has accumulated over the years. Because of the erratic arrangement of the

Table 9. Embankment Materials Properties—Design Values

Zone	Soil Classification	"Drained" Shear Strength		Density (pcf)			Number of Tests	
		$\phi$	C-Tsf	Dry	Moist	Sat.	Triaxial Compression	Shear
1A	SC-CL	30	0.15	117	134	137	3	24
3	GP	45	0	155	161	165	*	
4A	GP	40	0	150	155	161	**	
Riprap		45	0	120	122	140	**	
Columbia Soil Area							2	6
Sutter Butte Outlet to River Outlet		30	0.10	96	122	124		
River Outlet to Western Canal		26	0.05	96	122	124		

\*Properties assumed the same as Oroville Dam Zone 2.

\*\*From Oroville Dam Design.

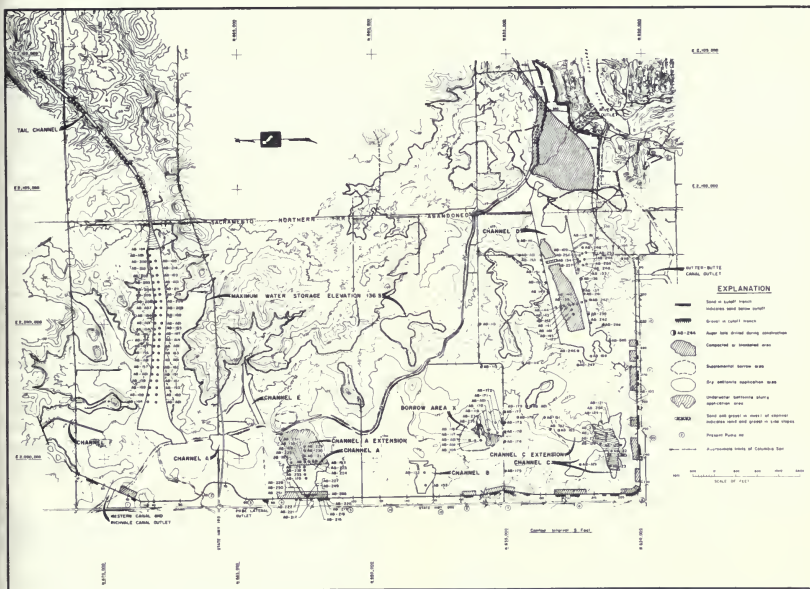


Figure 21. Thermalito Afterbay Dam Alignment and Reservoir Area

Table 10. Embankment Materials Properties—As-Built Values

Table 16. Embankment Materials Properties—As-Built Values							
Zone	Class	Field Dry Density			Average Moisture Content %	Average Compaction %	Number of Tests
		max pcf	avg pcf	min pcf			
1A	CL	133	107	76	$w_o$ -0.1	97	1108
3	GP	155	142	130	2.0	94	48
4A	GP		138		1.9	96	12
Columbia Soil Area 0-12 in. Before Construction							
			97		14.8		
After Construction							
			111		12.8 ( $w_o = 13.5$ )		
Columbia Soil Area 12-24 in. Before Construction							
			92		16.2	Note: $w_o$ denotes optimum moisture content.	
After Construction							
			110		14.3 ( $w_o = 14.3$ )		

various lenses of sediments, aquifer conditions vary widely throughout the area. The aquifer system in the area of the afterbay showed piezometric levels of 10 to 15 feet below the ground surface prior to reservoir filling. In general, this system is capped at the surface by a mixture of hardpan layers and slightly permeable weathered-in-place clays and silts.

Locally, streams have eroded through the surficial weathered zones and deposited unconsolidated fine-to coarse-grained alluvium ( $Q_{al}$ ) in the stream channels. Approximately 150 acres of recent alluvium known as the Columbia Soil area lies within the afterbay limits at the southeast corner. Most of the Columbia Soil is underlain at 10 to 15 feet by recent alluvium composed of relatively clean sand and gravel.

Older consolidated sediments (identified as the Mehrten Formation) lie immediately beneath the Red Bluff Formation and adjacent alluvial soils. The surface of the Mehrten Formation is probably erosional and slopes gently to the northwest.

### Construction and Reservoir Filling

A great variety of soil types were exposed during foundation preparation for the dam. Clean sand and minor local gravel required special treatment. In the Red Bluff founda-

tion materials, the 100-foot upstream clay blanket was constructed where sand or gravel were found to extend deeper than the foundation trench. The Columbia Soil area, which is underlain by gravel, was stripped to a 3-foot depth, scarified, moisture conditioned and compacted with four passes of a pneumatic roller over four passes of a tamping roller.

Initial storage in the afterbay began in November 1967. The water level was brought to Elevation 127 feet during December 1967 and January 1968. In early January, water levels in piezometers along Highway 99E began rising at a rapid rate and had reached ground level in some areas by early February.

In early February 1968, the afterbay water surface was lowered to Elevation 123 feet. Exposed sand areas in Channel A extension, Borrow Area X, Channel C, and Channel C extension were located and delineated. The sand zones covered larger areas than had been mapped in 1966. Apparently, subsequent borrow operations had enlarged the sand exposures.

Two shallow 6-inch wells were drilled at the toe of the dam in the wettest areas. Pump tests on these wells yielded aquifer permeabilities much greater than those determined during design exploration. A study of geologic, construction, and piezometric data indicated that the most probable sources were the channel excavations

on the east side of the afterbay. Therefore, in late February 1968, the afterbay water surface was dropped to the lowest possible level without pumping, Elevation 119 feet, and an attempt was made to seal suspected sources of seepage. Channel A extension and the pervious portion of Channel D were blanketed with 1.0 foot of compacted impervious borrow. Dry bentonite was spread, mixed, and rolled on the surface of the sandy areas of Borrow Area X and Channel C extension above water level. A bentonite slurry was pumped over submerged sandy areas. An attempt was made to place bentonite slurry over sand and gravel areas in the tail channel, but this operation was not completed due to spring rains.

### 3. EXPLORATION, SAMPLING, FIELD, AND LABORATORY TESTING

#### Previous Foundation Exploration and Testing

Drill logs were available for approximately 100 auger holes and 20 rotary borings located within a 600-foot strip centered on the dam axis. The auger holes—hand, flight, spin, and bucket—were primarily drilled before and during construction and ranged from 10 to 90 feet deep. The rotary holes were drilled generally in conjunction with the installation of the relief wells and ranged from 50 to 150 feet deep.

These previous holes were drilled primarily for the purposes of logging, permeability testing, and piezometer testing. There was little sampling and no Standard Penetration Testing performed.

#### 1976 Drilling, Sampling, and Testing

In the spring of 1976, eight rotary borings were made along the toe of the embankment, five along the west side and three along the south side. The borings are identified as boreholes D-1 to D-8. These borings, ranging from 16 to 26 feet in depth, were generally drilled with a 5-inch Pitcher barrel using drill mud. Fourteen samples were obtained with a 2.5-inch ID thick-wall sampler (area ratio = 0.56), mainly in suspect layers of sands and silty sands.

Thirteen Standard Penetration tests were also conducted. In most cases the testing was carried out immediately below sampling intervals. Measured penetration resistance varied from 7 to 50 blows per foot. It is unclear, however, whether the testing was conducted with a cathead-rope system or with a cable lift-clutch system.

The afterbay was then filled to Elevation 126 feet in March 1968. The ground water levels again rose to the ground surface in some locations. Because of power-production requirements and agricultural-water delivery obligations, the reservoir surface was not lowered again to attempt sealing of exposed pervious areas.

The problem of the high downstream water levels was solved in 1969 by the installation of a system of 15 irrigation-type wells. The afterbay water level was raised in stages to the maximum, Elevation 136.5 feet in May 1969. At full reservoir, 14 of the 15 pumps operated continuously, producing a total steady flow of 45 cubic feet per second.

Cyclic triaxial tests were run on 10 push sample specimens. Test specimens were extruded from sample tubes and trimmed to a 5-inch length to give a specimen height-to-diameter ratio of 2. Eight specimens were classified as silty sand and two were classified as silt. Measured dry densities ranged from 66 to 99 lb/ft<sup>3</sup>. The testing was performed at the Department of Water Resources Soils Laboratory. Tests were conducted at isotropically consolidated conditions for two values of consolidation stress—1 and 3 ksc.

#### 1978 Drilling, Sampling, and Testing

The 1976 explorations confirmed the existence of a highly lenticular foundation and the presence of substantial and potentially liquefiable sand layers. However, the cyclic strength results from the 1976 samples were considered unreliable due to the high probability of severe sample disturbance by the thick-walled sampler. In addition, measured SPT penetration resistance was questioned because of possible disturbance in borings by sampling procedures and incomplete records of test details.

The preliminary liquefaction analyses conducted in 1976 showed that additional information was required to perform an adequate study. The required information included knowledge of static shear strength of the embankment and foundation, representative cyclic strength of foundation sands, in situ soil moduli, soil depth to bedrock surface, and soil classification. To obtain this information, 27 borings were completed during the summer of 1978, with sampling and field testing as follows:

1. Concentrated exploration conducted at four sites judged from previous borehole logs to have the most extensive shallow sand layers:

Site 1	(Station 107)	Boreholes TAS 1 - 1E (6 borings)
Site 2	(Station 173)	Boreholes TAS 2 - 2M (13 borings)
Site 3	(Station 203)	Boreholes TAS 3 - 3E (6 borings)
Site 4	(Station 281)	Boreholes TAS 4 - 4A (2 borings)

2. At each of the four sites, at least one borehole through the embankment and into the foundation was drilled to obtain "undisturbed" samples of the embankment and foundation materials. Additional borings at the toe were made as necessary to obtain the best "undisturbed" samples from the sand layers and for performing Standard Penetration Testing.
3. At each site, downhole shear wave velocity tests were performed in both the embankment boring and a foundation boring at the toe.
4. At Stations 107 and 173 (Sites 1 and 2), standpipe piezometers were installed in an embankment boring and in a foundation boring at the toe. Another standpipe piezometer was installed in the embankment boring at Station 203 (Site 3).
5. At Station 173 (Site 2) on the west side of the afterbay, a seismic refraction survey was performed to determine if bedrock is within a 500-foot depth.

## 1978 Standard Penetration Testing

Standard Penetration Tests were carried out in boreholes near the downstream toe at the four sites. Tests were performed at about 4-foot-depth intervals. Borings were advanced by rotary drilling with a 5-or 6-inch tricone bit using bentonite drilling mud. A tricone bit was used because it deflected most of the drilling fluid to the side of the hole rather than toward the bottom. During the drilling of the last 6 inches of the hole, mud flow was reduced to minimize disturbance. After drilling was completed, mud was circulated for several minutes prior to sampling to remove any remaining cuttings.

The SPT utilized a 140-pound safety hammer falling 30 inches. For most tests, a 1-inch manila rope, wrapped twice around a rotating cathead, was used in the raising and releasing of the hammer (Figure 22). However, in some borings, a cable lift-clutch release system (safe-T-driver) was used in raising and dropping the hammer. The tests also employed a Caltrans split spoon sampler (shoe I.D. = 1-5/16 inches, barrel I.D. = 1-3/8 inches) and A rods.

Penetration resistance was determined by counting the number of hammer drops required for the samples to penetrate 18 inches. The penetration resistance, or N value, equaled the number of blows counted during the last 12 inches of penetration.

Gradation and density tests were performed on all SPT samples. Gradation results were used to classify the materials in the foundation in general, and to relate strength-test samples to each other and to the various types of soils in the foundation. Atterberg limits and specific gravity tests were run as needed to classify fine-grained soils and to determine void ratios.

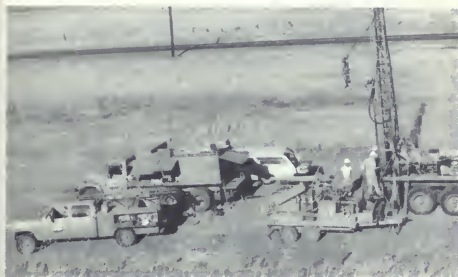
## 1978 "Undisturbed" Sampling

"Undisturbed" samples were obtained in different borings than the ones with SPT. "Undisturbed" clay samples were generally obtained with a Pitcher barrel using 36-inch lengths of 3-inch-diameter Shelby tubes. Although a few sands with high silt contents were sampled by a straight Shelby push, most sands were sampled with a stationary piston sampler. Piston samples were usually obtained within 50 feet of an SPT boring.

Borings were advanced in the same way as described for Standard Penetration Testing. After the drill bit was removed, the piston sampler was inserted in the hole. The sampler utilized 20- and 24-inch lengths of 3-inch-diameter Shelby tubes. When the sampler was flush with the bottom of the hole, the piston rod was clamped to the drill rig and the Shelby tube was pushed into the sand. A beveled E-rod was then jettied down beside the sample tube to the bottom of the sample depth (Figure 23). The sampler was then raised two feet as slowly as possible while at the same time drilling mud was pumped down the small rod to occupy the space vacated by the sample (Figures 23 and 24).

The sampler was lifted to the surface by a hydraulic drive system instead of a winch and cable. Before the bottom of

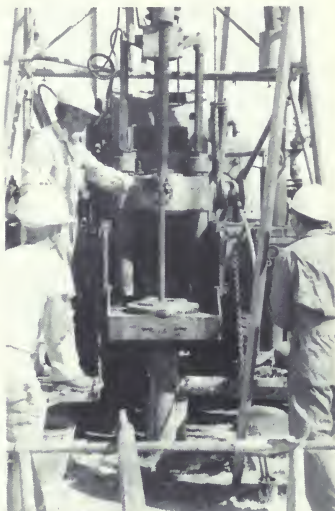




**SPT Testing Operation  
at Station 107 (Site 1)**



**140-Pound SPT Hammer  
(NOTE: Drilling Mud Recirculation in Background)**



**SPT Testing Using Cathead  
and Manila Rope**

*Figure 22. 1978 Standard Penetration Testing at Thermalito Afterbay*

the sample tube cleared the surface of the drill mud, the geologist reached down and dug out enough soil from the tip to insert a porous stone flush with the tube bottom. A red plastic cap punched with holes for drainage was then placed over the end of the tube and the sampler was raised out of the borehole.

After the sampler was unthreaded from the rod, any excess drill mud that had collected in the top of the sample tube was removed by carefully rotating the tube to a horizontal position and rinsing it with water with a wash bottle. The sample was then rotated back to the original vertical position. Next, the valve was opened to release the

piston suction and the tube was removed from the sampler. The top was then stuffed with either wet rags or lengths of wooden spacers and then capped with a perforated plastic cap. The samples were allowed to drain in their vertical positions for several hours before shipment to the lab.

Samples were shipped to the lab in padded wooden boxes, which allowed the tubes to remain upright. After arrival at the lab, the samples were kept upright until testing. Samples were generally extruded directly from the tubes (no sawing), encased in a rubber membrane, and moved into the triaxial cell. In a few cases, for sands with high silt

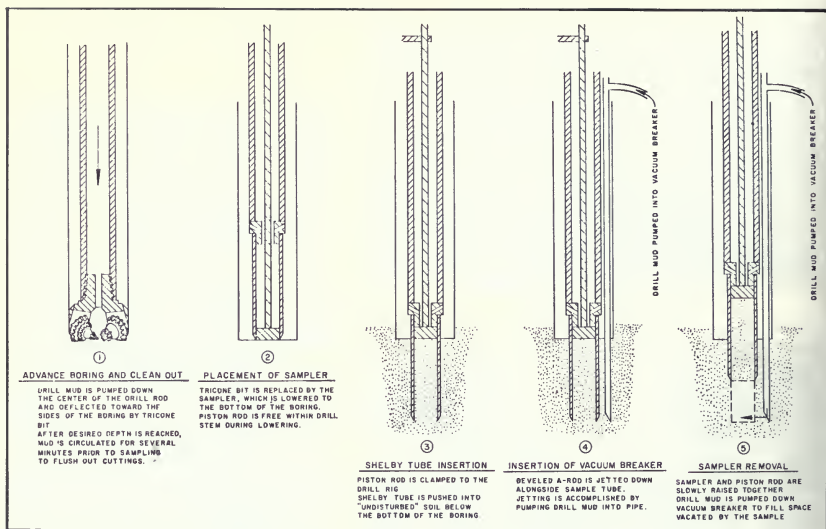


Figure 23. 1978 Procedure Used in Obtaining Undisturbed Samples of Thermalito Afterbay Sands

content, the tubes were first sawed into sections. Diameter measurements with a pi tape at top, middle, and bottom generally showed no slumping.

Static triaxial compression tests were run on 18 "undisturbed" specimens of embankment and foundation silts and clays from the four sites drilled, and on three specimens of foundation sand from Site 1. Stress-controlled cyclic triaxial tests were run on 33 isotropically-consolidated specimens of foundation sands from Stations 107 and 173 (Sites 1 and 2). Tests were also performed on remolded specimens, which were prepared to the same density by pluviation. A few of these test specimens were subjected, prior to testing, to 25, 60, and 120 cycles of low-level cyclic stresses. The specimens were allowed to dissipate excess pore pressures before the actual testing.

Gradation and density tests were run on all triaxial samples to relate sample strengths to each other and to the

blowcounts determined in the field. Relative density tests were also carried out for many of the "undisturbed" sand samples.

### Downhole Shear Wave Velocity Testing and Seismic Refraction Survey

Downhole shear-wave velocity tests were generally conducted the day after completion of a boring. The holes were uncased and usually partially or completely filled with drill mud. The tests were carried out by Caltrans personnel using the same techniques that were later used in downhole measurements made in 1979 (Figure 25). A wooden plank and hammer were used to generate SH waves. A probe containing three geophones was lowered in 5-foot increments. Within the probe, one geophone was oriented vertically, and the other two were oriented horizontally.



**Piston Sampler**



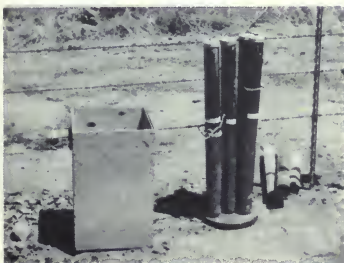
**Vacuum Breaker Tip**



**Jetting Vacuum Breaker Down  
Along Side of Sample Tube**



**Removal of Sampler After Sampling**



**Capped Shelby Tubes Allowed to  
Drain Before Shipment to Lab**



**Capped Tubes in Shipping Box**

*Figure 24. 1978 Sampling of Thermalito Afterbay Sand Layers*



The usual field procedure was to position the probe at the proper level within the hole and then force it against the side of the hole with an inflatable bladder. The plank, generally placed about 10 feet away from the hole and weighted by a vehicle, was struck horizontally on one or both ends with a wooden mallet to generate the shear waves. A vertical blow or blows was also struck on the ground near the end of the plank in order to obtain com-

pression wave arrival times. A signal recorder/plotter with a memory was used to record and enhance wave arrivals at the geophones.

The seismic refraction survey carried out at Station 173 (Site 2) was conducted to determine if the Sierran basement bedrock was within approximately 500 feet of the ground surface. A linear array of geophones was laid out



**Downhole Shear Wave Velocity Testing in Borehole 79-1078**



**Cal Trans Personnel Using Hammer and Plank Method in Downhole Shear Wave Velocity Tests**



**Woodward-Clyde Consultants Downhole Hammer Used in Crosshole Shear Wave Velocity Testing**



**Downhole Hammer Being Lowered into Cased Borehole**

*Figure 25. 1979-80 Shear Wave Velocity Testing at Thermalito Afterbay Station 107 (Site-1)*

in shallow boreholes at a 45-foot spacing along the embankment downstream toe. The energy source consisted of chemical explosives in a shallow borehole. The total length of the array was 1980 feet and was run in five segments. The results of the refraction study indicated that the minimum depth to bedrock is at least 500 feet.

### 1979–80 Investigations

Dynamic analyses completed by spring 1979 indicated that Station 107 (Site 1) might liquefy if the Oroville Reanalysis Earthquake ( $a_{\max} = 0.6g$ ) were used as the expected motion at the site. However, re-evaluation of this motion indicated that it was not appropriate for use in analyzing Thermalito Afterbay Dam. To determine an appropriate motion, additional studies were necessary at considerable depth. The Special Consulting Board for the Oroville Earthquake recommended specific studies for investigating the material properties at depth. The Board also recommended that additional SPT testing be carried out at Station 107 (Site 1) to aid in the evaluation of liquefaction potential beneath the dam. The Board went on to recommend that the embankment foundation in the Columbia Soil area also be examined for liquefaction potential.

The 1979–80 explorations consisted of the following:

1. Drilling three deep borings (300 to 500 feet deep) at Station 107 (Site 1) and one moderately deep boring (150 feet deep) at Station 300.
2. Performing crosshole and downhole shear-wave velocity testing in the deep borings at Station 107 (Site 1).
3. Drilling ten additional SPT borings at the toe and at the crest between Stations 102 and 112 to define the limits of the low blowcount sands at Site 1.
4. Drilling 29 additional shallow SPT borings (40-foot depths) into the Red Bluff Formation along the length of the dam to give a maximum spacing of 1,000 feet between SPT borings.
5. Drilling three Pitcher barrel sampling borings in the Columbia Soil area (Stations 351, 361, and 378).

### Deep Foundation Borings

Station 107 (Site 1) had been previously identified as probably the weakest foundation along the afterbay. This

was indicated by the low penetration resistances found at the site. Therefore, much of the additional investigations were targeted at this location. A deep boring was drilled about 120 feet downstream of the embankment toe. It was drilled to a depth of 505 feet. In addition, two 300-foot holes were drilled straddling the first deep hole for the purpose of conducting crosshole shear-wave velocity testing.

Disturbed sampling and logging were carried out in all three holes. Drilling was carried out with a 5-inch tricone bit. Disturbed sampling was conducted with the Caltrans SPT split spoon sampler until sandstone was encountered at about a 190-foot depth. Below this depth an NX core barrel with a diamond bit was used to obtain samples. After the desired depth was reached, the hole was reamed and expanded to about an 8.5-inch diameter. A PVC casing with a 4-1/4-inch inside diameter was then inserted and grouted into place with a low seismic-velocity grout.

The boring at Station 300 was carried out in the same manner except that the SPT split-spoon was terminated and intermittent NX coring and tricone drilling commenced at a depth of 85 feet. Since no shear-wave velocity tests were to be performed in this boring, no casing was installed.

### 1979–80 Shear Wave Velocity Tests

Downhole shear wave velocity tests were conducted by Caltrans personnel using the same basic techniques employed in the 1978 downhole tests. Crosshole shear-wave velocity tests were performed by Woodward-Clyde Consultants staff. A downhole hammer was inserted into one of the end boreholes, and geophones were placed in the other two holes (Figure 25). Tests were carried out at 5-foot depth increments. The process was repeated, but with the hammer located in the other end borehole. The boreholes were surveyed to obtain precise distances between the holes at different elevations.

### 1979–80 Standard Penetration Testing and Pitcher Barrel Sampling

Standard Penetration Testing performed in 1979–80 was carried out using the same methods employed during the 1978 program. The two exceptions were that only the rope and cathead system was used in 1979–80, and the testing interval was generally about 3 feet instead of 4 feet (Figure 26). All SPT samples were subjected to gradation and/or Atterberg limit testing.

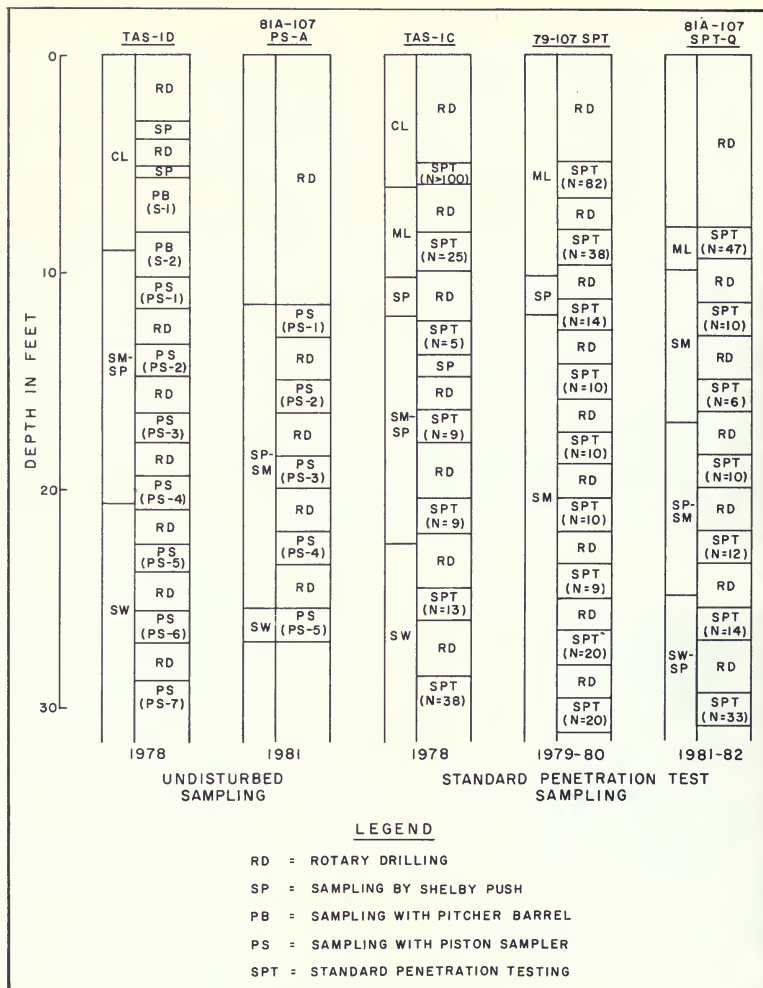


Figure 26. Typical Sampling Intervals

## 1981-82 Investigations

In previous explorations, drilling was carried out by Caltrans personnel and equipment. However, the size of the 1981-82 program necessitated contracting with a private drilling company. The contract driller, Continental Drilling Company, used four Mobile B-61 drill rigs, each supervised by a DWR geologist. Drilling began in July 1981 and was completed in April 1982.

The investigations consisted of 223 SPT borings, 26 borings for piston sampling of sands, and 211 electrical cone penetrometer (CPT) soundings. The purpose of these investigations was to identify all sites with loose foundation soils, which might liquefy and cause failure of the dam (suspect sites), and to delimit the extent of each suspect site.

Initial SPT borings were spaced at 250-foot intervals along the dam. Based on preliminary, conservative criteria, 21 suspect sites were identified. The extent of these sites was determined by additional, closer-spaced SPT borings and/or CPT soundings.

Two correlations were developed—one to relate SPT to CPT, and one to relate SPT to cyclic strengths of piston samples. To obtain reliable data for these correlations,

many tests and samples were required from closely spaced borings and soundings.

At the beginning of the investigations, each drill rig and crew made a SPT boring around two SPT borings made previously by Caltrans personnel. The purpose of these borings was to assure that the new drillers were obtaining similar SPT blowcounts (N values) both among themselves and with the blowcounts obtained by Caltrans. In addition, energy measurements were made for both doughnut SPT hammers and safety SPT hammers for free fall and rope-and cathode release.

### Standard Penetration Testing

The Standard Penetration Test (SPT) was the primary tool in this investigation and was performed, with a few exceptions, according to ASTM D-1586 specifications. All SPT borings were drilled with an 4.5-inch baffled drag bit. The baffles were arranged so that circulating drill fluid would be discharged to the side and upward (Figure 27) instead of downward where the flow might disturb the sand below. Bentonite drilling mud was used as the circulating fluid and all holes were uncased.

The SPT hammers were specified to be 140-pound safety hammers. Each hammer was weighed and determined to be within 4 pounds of the specification. Internal anvils



Upward  
Deflecting  
Baffle



Figure 27. Baffled Drag Bit Used for SPT Borings at Thermalito Afterbay Dam, 1981-82

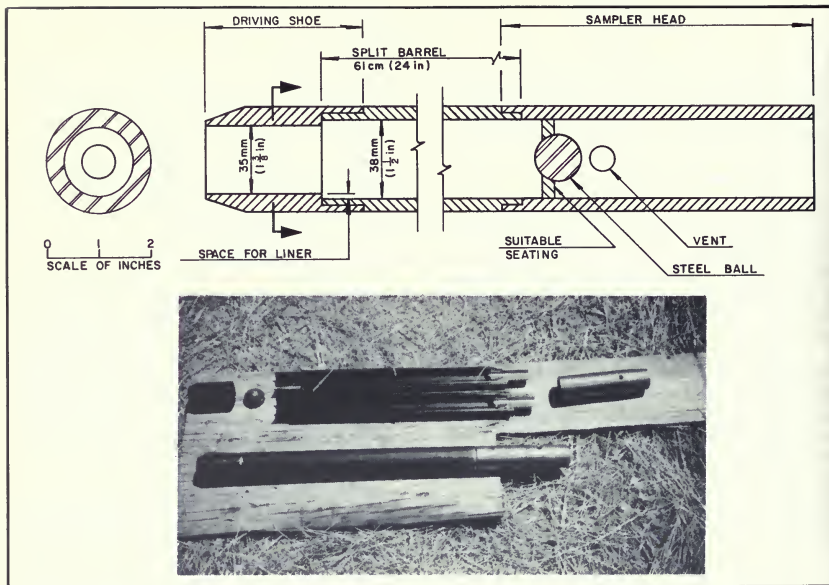


Figure 28. Details and Photo of Split Barrel Sampler Used in Standard Penetration Testing at Thermalito Afterbay

were inspected to assure that mushrooming of the anvil was not taking place.

The lifting mechanism for the SPT hammer was a rope and revolving cathead. The catheads were 8 inches in diameter and revolved between 90 and 150 rpm. Ropes were all "new" 1-inch manila ropes. Two wraps around the cathead were used for lifting the hammer. When a rope became significantly worn (usually after about 20 separate N-value determinations), the rope was replaced. This was done to provide uniformity of release because old ropes become too limp to throw clear of the cathead pulley, thereby causing more drag in the system and reducing the energy delivered to the drill rods. Ropes were stored in the cabs of the drill rigs at night and during rainfall.

Fall height of the hammers was specified to be 30 inches. Two hammers brought to the site by the contractor were

rejected because the total travel lengths were less than 30 inches. To aid the driller in dropping the hammer from the correct height, a stripe was painted on the hammer rod. Measurements and observations indicated that the operators were almost always within 1 inch of the correct height.

Samplers for the SPT testing were essentially the same as specified by ASTM D-1586 except that the sampler split barrel had a 1-1/2-inch I.D. (i.e., room for liners but no liners were used [Figure 28]). This change was adopted because research by Schmertmann (1979) indicates that most testing in the United States uses liner type samplers without liners. Another change to the usual SPT procedure was that mixtures of upset and parallel-walled NW drill rods were used instead of the traditional A rods. The two different NW rods have different thicknesses and, therefore, have about a 30 percent difference in weight.



Sampling intervals were usually every 36 inches, which allowed a clean-out interval of 18 inches between samples. Care was taken during the drilling operation to slow the bit rotation and fluid flow when the bit approached the sampling depth. When the bit reached the sampling depth, fluid circulation was maintained for a minimum time to flush out the cuttings. Drill rods were withdrawn with care to prevent caving.

After each SPT test, the recovered sample was field-classified by the DWR geologist and then bagged and sent to the laboratory for storage and/or additional classification testing.

Drillers for all four drill rigs were instructed on the importance of the SPT test and on its repeatability. To assure equivalence between the SPT N values from the four different rigs, comparison tests were carried out at two locations (Stations 104 + 50 and 107 + 00), where relatively uniform sand was encountered in a depth interval of about 3 to 10 to 25 feet. The distance between borings

was 6 feet. Figures 29 and 30 present the resulting blowcounts with results from previous tests by Caltrans. The average uncorrected blowcount in the sand layer is about 17 at Station 104 + 50 and about 13 at Station 107. Variations from the average are about  $\pm 3$  blows per foot at both stations and represent material variations as well as test variations.

### SPT Energy Calibration

Energy calibration of the SPT tests was conducted in two ways—by correlation with cone (CPT) resistance and by direct measurement. Of principal interest was the effect of using a safety hammer in the SPT investigations. More traditional American practice has included the use of a donut hammer in SPT investigations. Although both types of hammers weigh the same—140 pounds—the physical configurations differ considerably. The donut hammer is basically a compact donut-shaped weight falling on an anvil mounted between rod sections. The safety hammer is a longer cylinder which falls on an internal an-

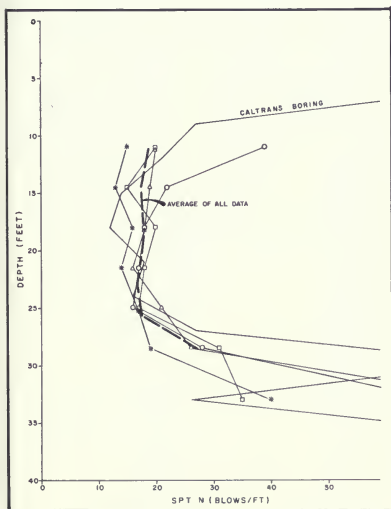


Figure 29. Comparison of SPT N Values Between 1981 Continental Borings and 1979 Caltrans Borings at Station 107 + 00

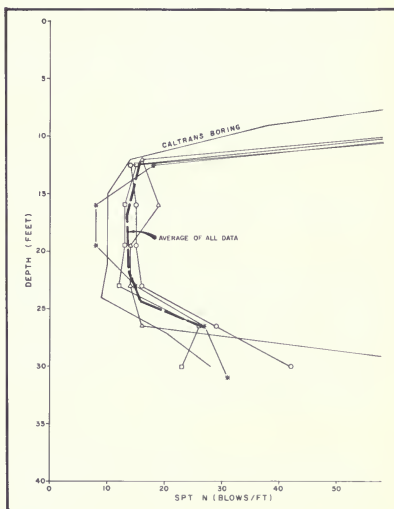


Figure 30. Comparison of SPT N Values Between 1981 Continental Borings and 1979 Caltrans Borings at Station 104 + 50

vil mounted on the end of the rod (Figure 31). Studies by Kovacs et al. (1981) have indicated that safety hammers are more efficient in transmitting energy to the drill rods than are donut hammers.

The calibration by CPT correlation was performed by ERTEC Western, Inc. for tests at Station 107 (Site 1). Cone resistances were used to calculate the theoretical energy dissipated into the soil during the SPT test. The process is described in detail by both Schmertmann (1979) and by Douglas, et al. (1981). Calculated energy dissipations are shown in Figure 32. Results indicate that the Thermalito safety hammer used with a rope and cathead imparts a relatively high energy to the soil when compared to an ERTEC donut hammer used with a rope and cathead. The results also indicate that the safety hammer is even slightly more efficient in delivering energy than an ERTEC free fall donut hammer:

$$\frac{\text{energy dissipated for DWR safety hammer with rope and cathead}}{\text{energy dissipated for donut hammer with rope and cathead}} \approx 1.55$$

$$\frac{\text{energy dissipated for DWR safety hammer with rope and cathead}}{\text{energy dissipated for ERTEC trip hammer (free-fall donut hammer)}} \approx 1.20$$

This correlation is supported by similar results obtained on a safety hammer reported by Bennett, et al. (1981).

The other method of calibrating the energy for the Thermalito SPT hammers was carried out at the afterbay by personnel from the National Bureau of Standards (NBS). Hammer velocities and rod forces were measured for SPT tests carried out through the crest at Station 107 (Site 1) and Station 168. Energies were measured for a safety hammer and a donut hammer for both rope-and-cathead and free-fall releases.

Unfortunately, it was not discovered until after the tests were completed that a mixture of upset and parallel-walled NW rods were used. This meant that a varying and unknown rod cross-sectional area was used in the tests, which made the energy measurements within the rods unreliable. Therefore, these results were not used. Velocity

measurements of the falling hammers, however, were not affected by this factor.

Table 11. Energy Before Impact for Thermalito Afterbay SPT Hammers

	Rope & Cathead Release	Free-Fall Release
% of Theoretical Maximum Energy (mean value)	70	98
Number of Data Points	138	16

Table 11 presents the results for hammer energy before anvil impact as determined by velocity measurements for both rope and cathead release and for free fall release. The energy results are expressed as percentages of the theoretical maximum (140 lb. hammer falling 30 inches = 4200 in-lb). As expected, free-fall releases were found to give essentially 100 percent (mean value = 98) of the theoretical maximum for both types of hammers. However, when released with a rope and cathead, rope

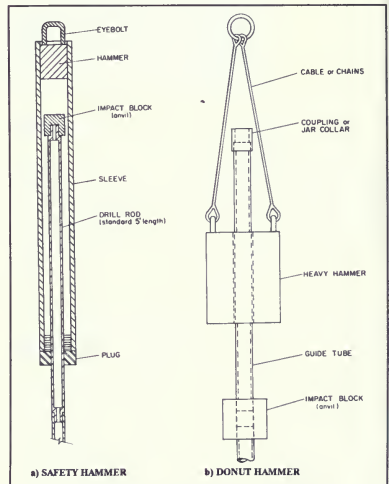


Figure 31. Configuration of SPT Hammers (Adapted from Steinberg, 1981)

friction decreases the energy before impact to about 70 percent. This is within the range found by Kovacs et al. (1981) for two turn rope and cathead releases using "new" rope.

Because the measurements of rod energies failed to produce reliable data on the effect of hammer type on the actual SPT blowcounts, SPT testing was performed at four sites using both the safety hammer and the donut hammer. Both hammers used the rope and cathead release with two wraps of a new rope. The tests penetrated mostly sands and silts. The uncorrected N values for each depth and hammer type were averaged for each site. Comparisons are shown in Figure 33 for the two hammer types. Although there is some scatter, the safety ham-

mer required only about 75 percent of the blows to penetrate a soil as did the donut hammer. This would indicate that the safety hammer is approximately 35 percent more efficient than the donut hammer in delivering energy to the sampler. This result is consistent with the findings of previous studies—Clarke (1969), Kovacs, et al. (1981) and Steinberg (1981). However, it is lower than the 1.55 ratio found by ERTEC in comparing CPT and SPT results.

Subsequent to the field investigations, it was learned that the SPT tests incorporated in published liquefaction correlations employed samplers with a constant 1.38 inch inside diameter, i.e., "no space for liners." Thus, the SPT tests performed at Thermalito, which used samplers with a larger I.D. in the spoon barrel, gave blowcounts that

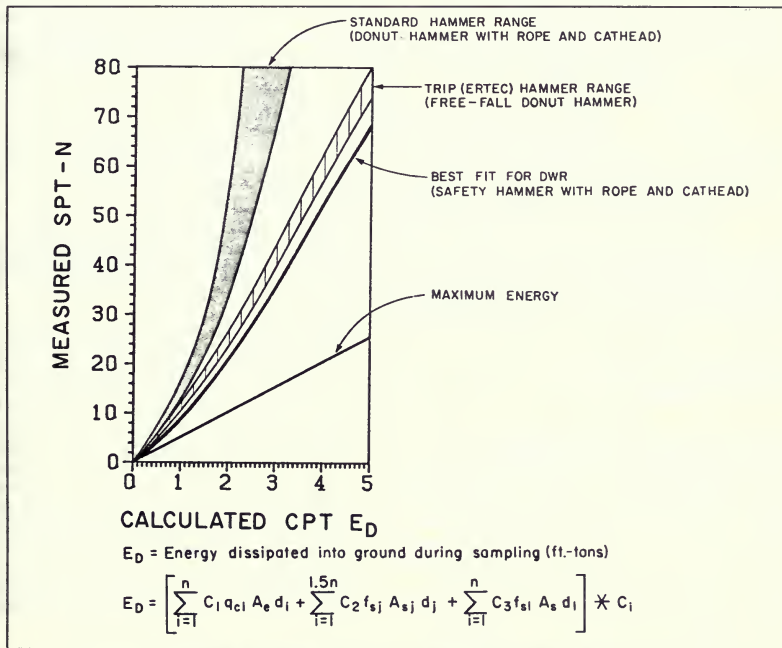


Figure 32. Comparison of Sampling Energy Dissipation and SPT Blowcounts (from ERTEC, 1981)



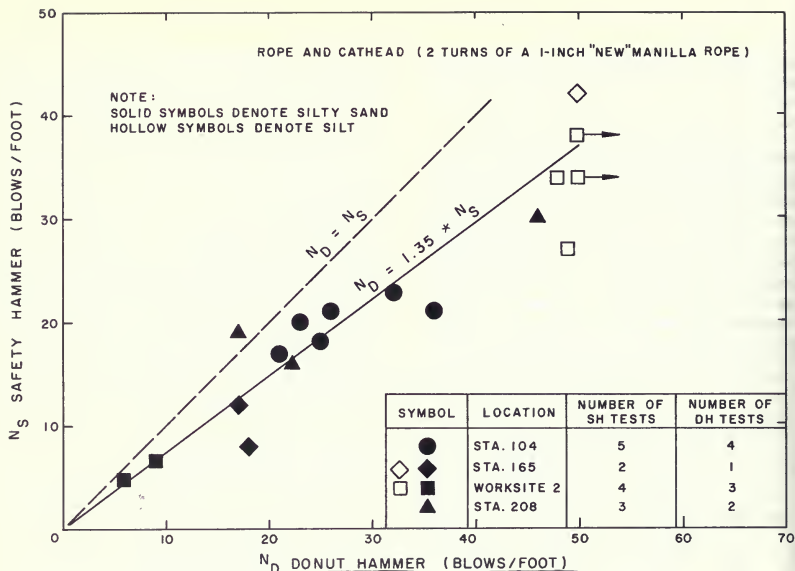


Figure 33. Comparison of SPT N Values Delivered by Safety and Donut Hammers

were too low. Although no tests were performed at the afterbay to examine this parameter effect, studies by Schmertmann (1979) indicate that having a larger I.D. in the spoon barrel during the SPT tests will reduce the blowcount in sands.

### Blowcount Correction for SPT Procedural Differences

The SPT correlation used to predict liquefaction resistance at Thermalito is the one developed by Seed and Idriss (1982). To account for procedural differences between the tests performed at Thermalito Afterbay Dam and the tests used in developing this correlation, correction factors were applied to the SPT blowcounts. These procedural differences principally involve the amount of hammer energy delivered to the drill rods and the configuration of the SPT sampler. In the Seed and Idriss (1982) correlation, the results were apparently intended for use with traditional American SPT hammer equipment, which has been a donut hammer (Figure 31). Typically, a donut hammer, when used with an "old" rope

wrapped two to three times around a rotating cathead, delivers to the drill rods approximately 45 percent of the theoretical free-fall energy of a 140-lb hammer falling 30 inches (see Kovacs et. al., 1981).

At Thermalito Afterbay Dam, safety hammers were used to obtain SPT blowcounts. Since safety hammers are more efficient than donut hammers in transmitting energy, the blowcounts need to be corrected (see Figures 32 and 33). Results showed that the safety hammers used at Thermalito had about 70 percent of the theoretical free-fall energy at hammer impact. Research has also shown that safety hammers are very efficient at transmitting energy at the hammer-anvil-rod contact and that this efficiency averages to about 95 percent. Consequently, the best estimate of rod energy delivered during the SPT testing at Thermalito is 67 percent of the theoretical free-fall energy ( $70\% \times 0.95 = 67\%$ ). This is substantially higher than the 45 percent commonly assumed for donut hammers.

The other principal difference between the Thermalito SPT procedures and the Seed and Idriss (1982) proce-

dures involves sampler configuration. The data in the Seed and Idriss (1982) correlation were collected with SPT samplers having a constant 1-3/8-inch inside diameter. However, the Thermalito SPT samplers have a 1-3/8-inch inside diameter at the shoe, but a 1.5-inch inside diameter within the barrel. The effect of having a larger sampler barrel can result in a 10 to 35 percent decrease in SPT resistance.

Table 12 summarizes the development of a correction factor to account for these procedural differences. Depending on what value is chosen to account for the effect of the different barrel sizes, the correction factor varies from 1.6 to 2.0. A correction factor of 1.5 was chosen conservatively to match the procedures used in the Seed and Idriss (1982) correlation. An additional correction factor,  $C_N$ , is also used to correct the blowcount for different overburden pressures.

Since several different expressions for SPT blowcounts are required in this bulletin, the following notation will be used:

N = Blowcount not corrected for either overburden pressure or for procedural differences.

$N_1$  = Blowcount corrected to 1 tsf overburden pressure, but not corrected for procedural differences. The correction factor for overburden pressures uses the relationship suggested by Seed and Idriss (1982).

$N_{A1}$  = Blowcount corrected for overburden pressure and procedural differences  $N_{A1} = 1.5 \times N_1$  (see Table 12). This is the blowcount value that would have been obtained had the SPT been performed by the same procedures used to develop the Seed and Idriss (1982) correlation.

**Table 12. Estimated Effect of SPT Procedures on Blowcount Thermalito Afterbay vs. Seed and Idriss (1982) Correlation**

SPT Procedure Employed at Thermalito Afterbay Dam	SPT Procedures for use with Seed and Idriss (1982) SPT Correlation**	Correction Factor*
Sampler driven by a 140-lb “ <i>Safety</i> ” Hammer raised 30 inches and released using 2 turns of a 1-in. “ <i>new</i> ” manilla rope around a rotating cathead. Energy delivered to the drill rods estimated to be about 67% of the theoretical free fall energy.	Sampler driven by a 140-lb. “ <i>Donut</i> ” Hammer raised 30 inches and released using 2 to 3 turns of a 1-in. “ <i>old</i> ” manila rope around a rotating cathead. Energy delivered to the drill rods estimated to be about 45% of the theoretical free fall energy.	1.49
Sampler consists of a 2.0-in. O.D. split spoon with an I.D. at the shoe of 1.38 inches and an I.D. within the barrel of about 1.5 inches.	Sampler consists of a 2.0-in. split spoon with a constant I.D. of 1.38 inches within both the shoe and the barrel.	1.1 to 1.35
Uncorrected Thermalito Afterbay SPT blowcounts are given the symbol N	TOTAL CORRECTION FACTOR FOR PROCEDURAL DIFFERENCES = $1.49 \times (1.1 \text{ to } 1.35)$ = 1.64 to 2.01  IN VIEW OF THE NECESSITY TO MAKE ASSUMPTIONS REGARDING PROCEDURES FOR THIS CORRELATION, A CONSERVATIVE VALUE OF 1.5 WAS ADOPTED.  Thermalito Afterbay blowcounts corrected by the 1.5 factor to this set of procedures and also corrected for overburden pressure are given the symbol $N_{A1}$	

Notes: \*Denotes that this correction factor is the value needed to correct Thermalito Afterbay SPT blowcounts for a procedural difference in order to be used with this correlation.

\*\*Denotes that the hammer energies appropriate for use with this correlation had to be estimated.

## Cone Soundings

Over 200 continuous electrical cone soundings were performed along the Afterbay length by ERTEC Western, Inc. At several locations, CPT soundings were made within a few feet of SPT borings in order to develop a correlation between SPT and CPT specifically for the afterbay soils and test procedures. The correlation was developed by ERTEC Western, Inc. and can be approximated by the following:

$$N = q/6 \text{ for } F < 1$$

$$N = q/4 \text{ for } F > 1$$

where:  $q$  = cone resistance in tsf and

$F$  = friction ratio in percent (%)

To get an equivalent corrected blowcount to use in the Seed and Idriss (1982) correlation, the following expression is used:

$$N_{A1}^* = (q/4) \cdot C_N$$

where:

$N_{A1}^*$  = equivalent corrected blowcount

$q$  = cone resistance in tsf

$C_N$  = overburden correction factor  
used by Seed and Idriss (1982)

Cone soundings were used principally to delimit the extents of soils found to have low SPT  $N$  values. Sounding profiles are presented in References 24, 25, and 35, along with details concerning the procedures used.

## Piston Sampling

Piston sampling was carried out at four general areas (Stations 104–108, Stations 164–166, Station 183, and Stations 380–383). These locations were picked for sampling because they had foundation soils with the lowest SPT blowcounts or cone resistance found along the afterbay and because the soils were relatively uniform over a large area.

To develop a correlation between cyclic strength and SPT, the uniformity of  $N$  values was first determined by drilling 3 to 4 SPT borings in triangular or linear patterns with 12- to 16-foot spacings between borings. If the  $N$  values were similar, piston sampling boreholes were then located between SPT borings with a minimum 6-foot distance between adjacent borings. The SPT  $N$  values and the locations of the borings are shown in Figures 34 through 42.

**Figures 34 — 42 follow**

**Text continues on page 66**

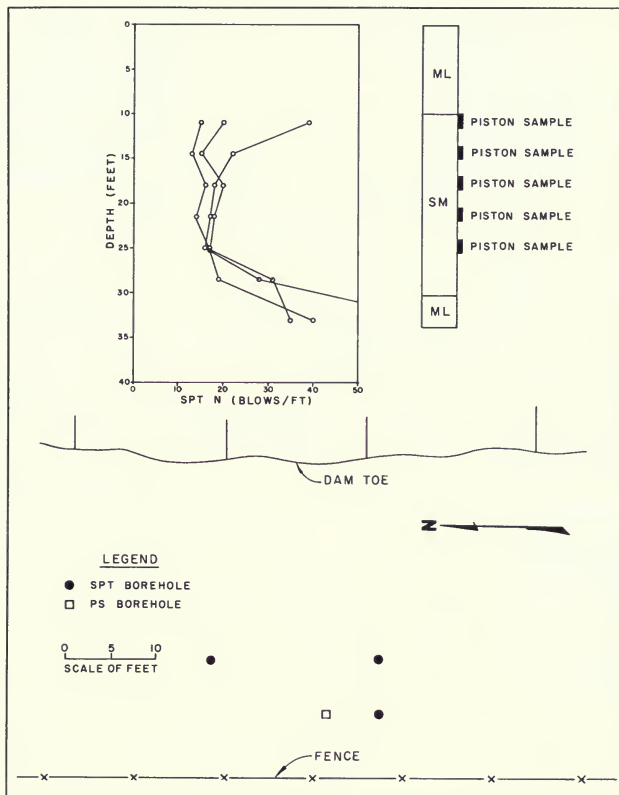


Figure 34. Standard Penetration Test N Values and Material Types for Piston Sampling Station 104 + 50

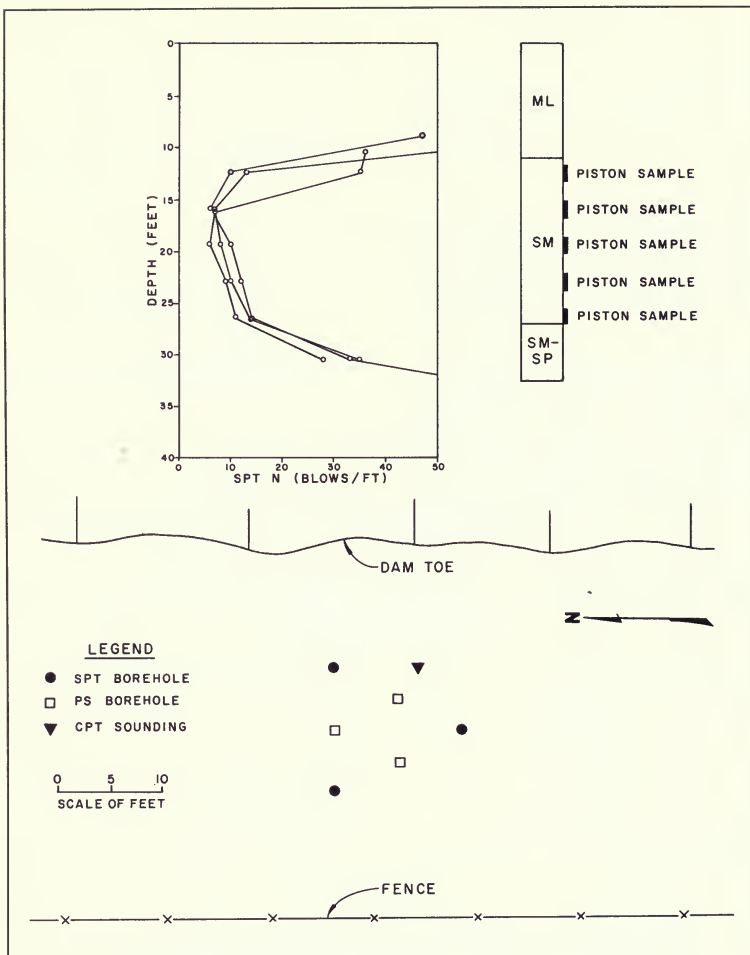


Figure 35. Standard Penetration Test N Values and Material Types for Piston Sampling Station 107N

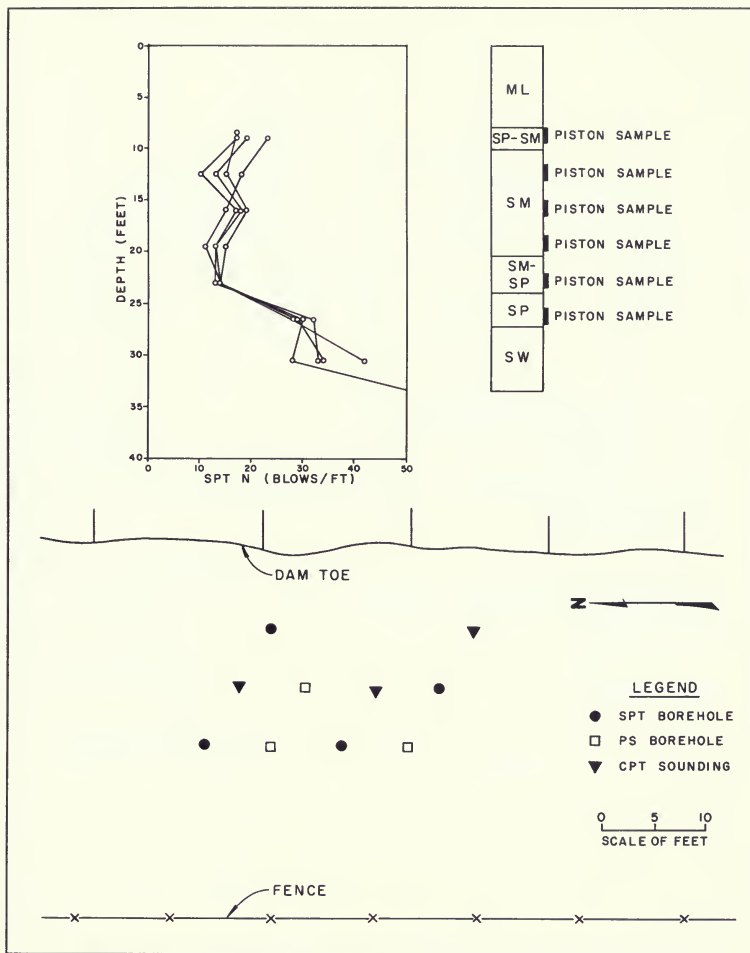


Figure 36. Standard Penetration Test N Values and Material Types for Piston Sampling Station 107S

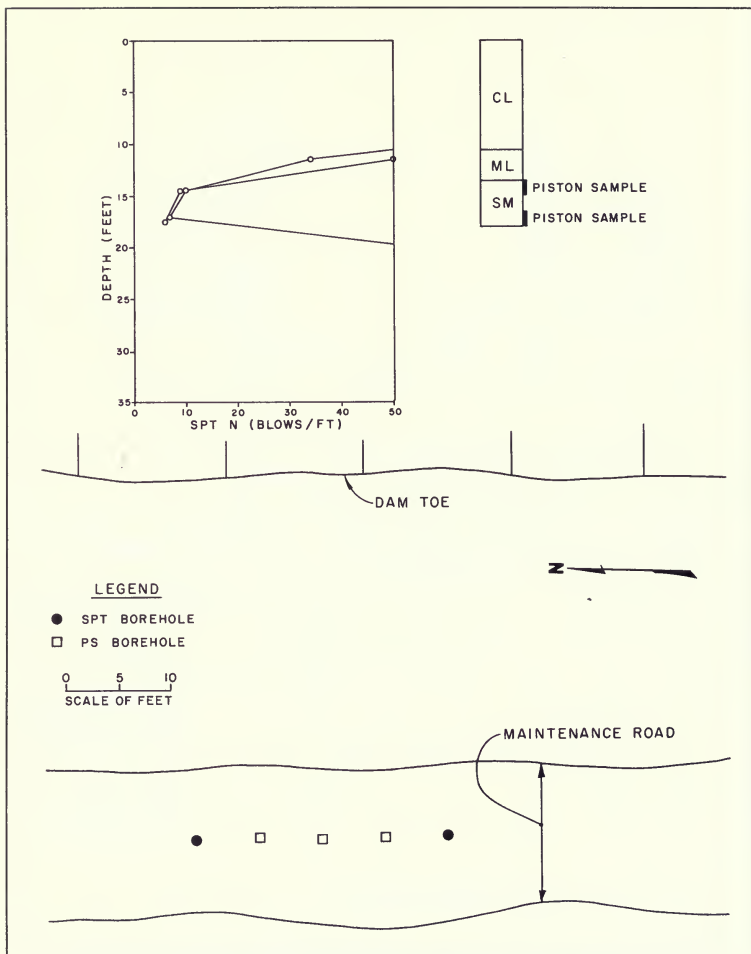


Figure 37. Standard Penetration Test N Values and Material Types for Piston Sampling Station 164+50

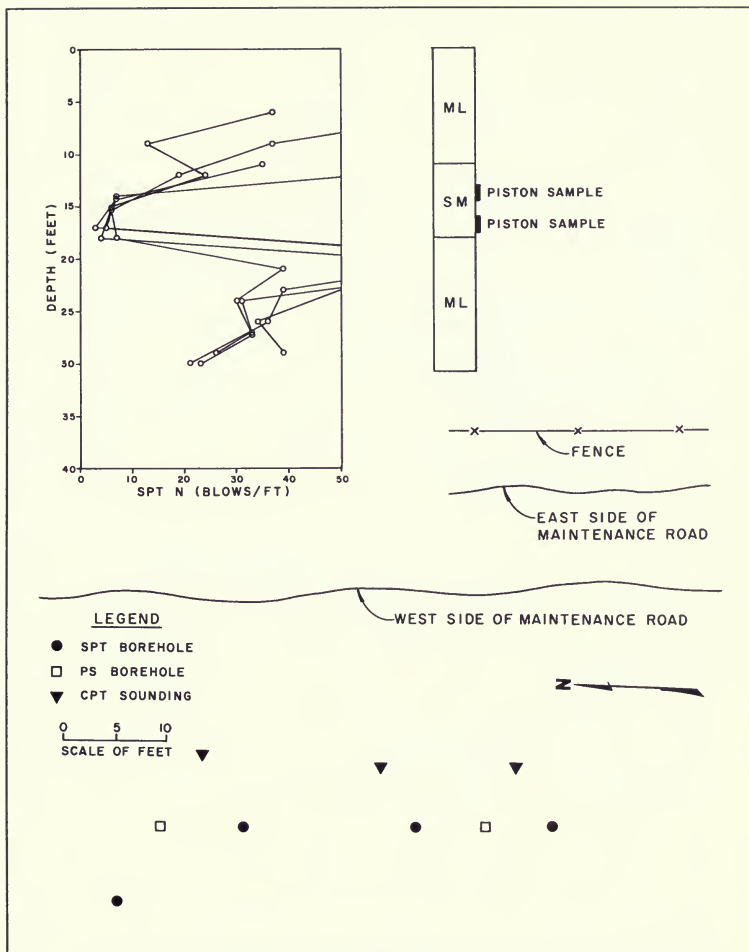


Figure 38. Standard Penetration Test N Values and Material Types for Piston Sampling Station 165



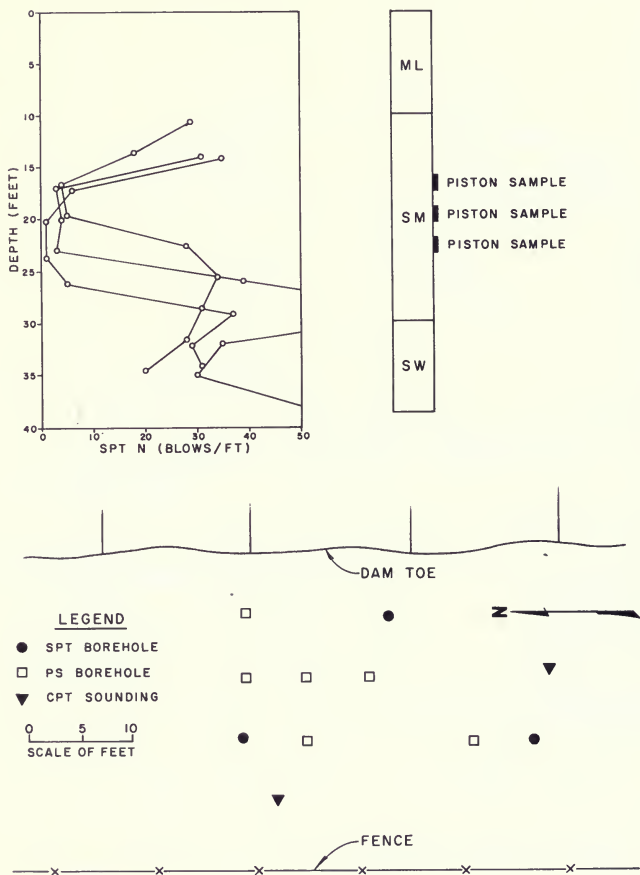


Figure 39. Standard Penetration Test N Values and Material Types for Piston Sampling Station 167



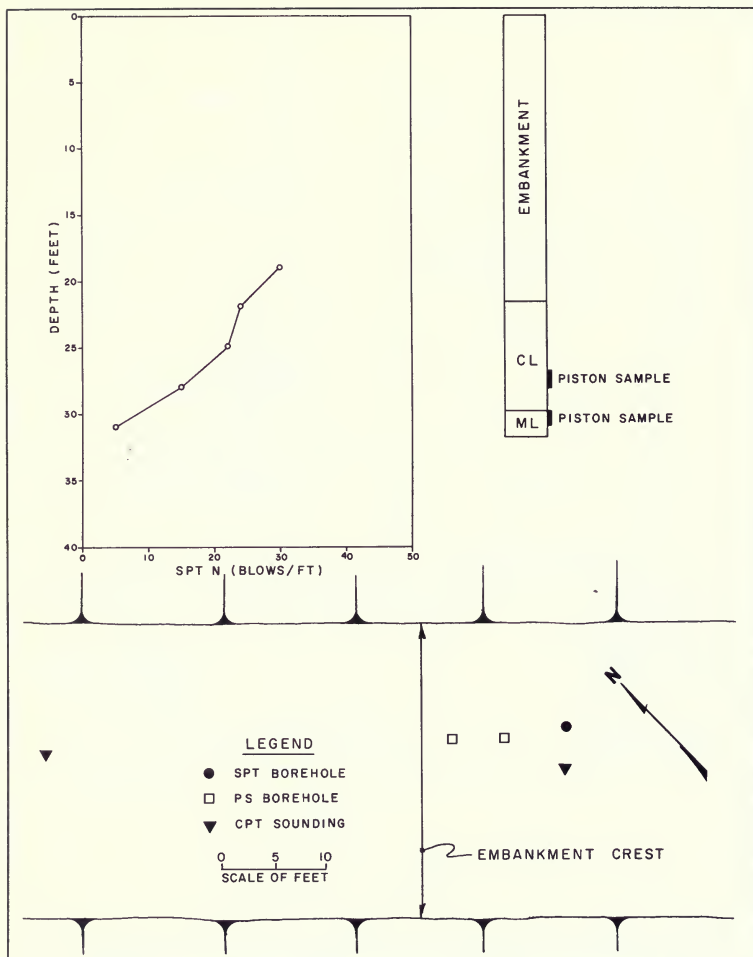


Figure 41. Standard Penetration Test N Values and Material Types for Piston Sampling Station 380

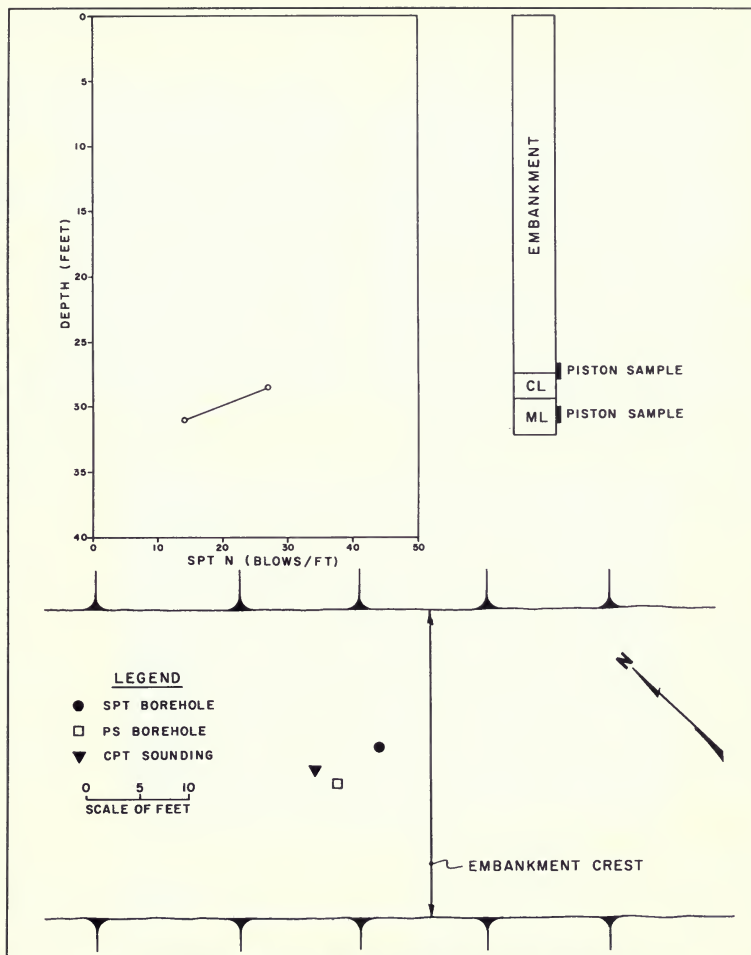


Figure 42. Standard Penetration Test N Values and Material Types for Piston Sampling Station 383

Piston sampling borings were drilled in basically the same manner as were the SPT borings. The only difference was that a 6-inch baffled drag bit was used instead of a 4.5-inch bit. Piston samples were taken with a hydraulically-operated piston sampler known as a Gregory Undisturbed Sampler (GUS) (Figure 43). This sampler used 3-inch-diameter Shelby tubes with no swedging. The Shelby tubes were 18 inches long and consisted of lacquered steel, galvanized steel, epoxied steel, and stainless steel. Stainless steel and epoxied steel tubes seemed to work the best in preventing the sample from rusting fast to the side of the tube and were, therefore, used for the majority of the samples.

Piston samples were taken at the same depth intervals as SPT tests to provide the best comparisons. After the desired depth was reached and the drill cuttings were flushed out, the bit was removed and the piston sampler was inserted into the hole. Water was used as the hydraulic fluid to operate the sampler and push the Shelby tube into the ground. Completion of the push was recognized by the start of water flowing out of the borehole, revealing that the hydraulic release vents of the sampler had been opened. As in 1978, a vacuum release tube was then inserted into the hole along the outside of the sampler and used to break the vacuum at the bottom of the hole during sampler removal by slowly pumping water into the tube as the sample was withdrawn.

The sampler was then carefully raised from the bottom of the hole with the winch and cable. When the sampler reached the top of the hole, and before the Shelby tube cleared the surface of the drill fluid, a solid expandable packer was inserted into the bottom of the tube to prevent the sample from being sucked out when lifting the tube out of the fluid. After the sampler was raised out of the water, the geologist drilled a small diameter vent hole in the upper end of the sample tube releasing the vacuum. The tube was then carefully removed from the sampler.

After labeling, the tube was then carried in a vertical position to a work area. Disturbed material or cuttings were removed from the top end of the Shelby tube with a special trimming tool (Figure 44). This tool also created a flat surface at the top of the sample for seating an expandable perforated packer (Figure 44). Filter paper was placed between the soil and packer. Measurements from the top of the tube to the soil and to the packer were recorded and a plastic cap was used to cover the top of the

tube. The cap was taped in place and the tube was carefully inverted.

A similar procedure for soil trimming was performed at the tip end of the Shelby tube. However, a solid expandable packer, without filter paper was used (Figure 44). Measurements from the tip of the tube to the soil and to the packer were also recorded.

The tube was then placed, still in the inverted vertical position (tip end up), into a specially designed foam-padded

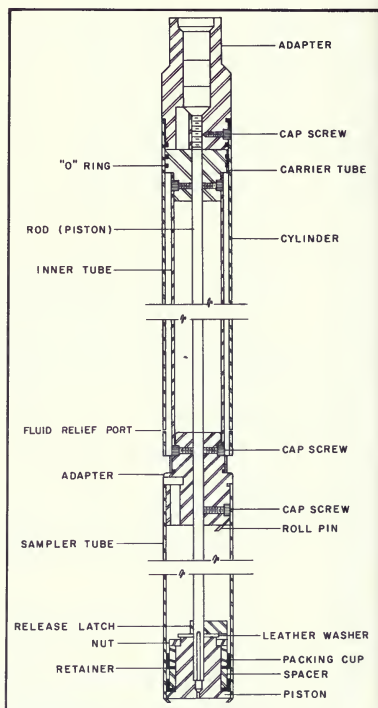
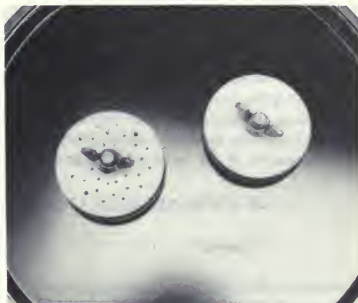


Figure 43. "Gregory Undisturbed Sampler" used in "Undisturbed" Sampling of Thermalito Afterbay Foundation Silty Sands



**Trimming Tool**



**Perforated and Solid Expandable Packers**



**Specially Designed Foam-Padded Transport Box**

*Figure 44. Trimming Tool, Perforated and Solid Expandable Packers, and Transport Box Used in 1981-82 "Undisturbed" Sampling*

transport box (Figure 44). The solid packer at the tip was loosened to allow drainage through the perforated packer at the top end of the tube (bottom of box). Any water draining out was collected in the space between the perforated packer and the plastic cap.

The samples were allowed to drain for a week or more before transport. The drainage requirement was established so that capillary forces within the sands would help minimize disturbance. Immediately before each sample was moved to the laboratory, the plastic cap was removed to enable measurements of the water collected during

drainage. The cap was then replaced, and the sample was placed back into the sample box. The solid packer was tightened before transport.

Before transport, the box was tied down onto a mattress in the vehicle to further prevent disturbance. In the laboratory, measurements of soil and packer movements, and any drainage occurring during transportation and storage, were recorded. These measurements indicated no detectable movements or drainage caused from transporting the samples to the laboratory.

## 4. EMBANKMENT AND FOUNDATION CONDITIONS

### General

The locations and borehole profiles of the drilling investigations are shown in Figures 45 through 61. For purposes of displaying the information, some boreholes were left out when holes at the same station were already displayed. In addition to data received from recent investigations, information from well hole logs, piezometer holes, and preconstruction holes have been used. Also

shown for recent boreholes are the SPT *N* values in blows per foot. These blowcounts have not been corrected for either overburden pressure or procedural differences. All soils have been classified using the Unified Soil Classification System. Where laboratory data have been used to classify the soils within the borehole, the symbol *L* (laboratory) has been added to the top of the soil profiles. For other profiles, the symbol *F* (field) is used, meaning visual classification only.



**NOTE:**

**Figures 45 through 61 follow;  
the text continues on page 104.**

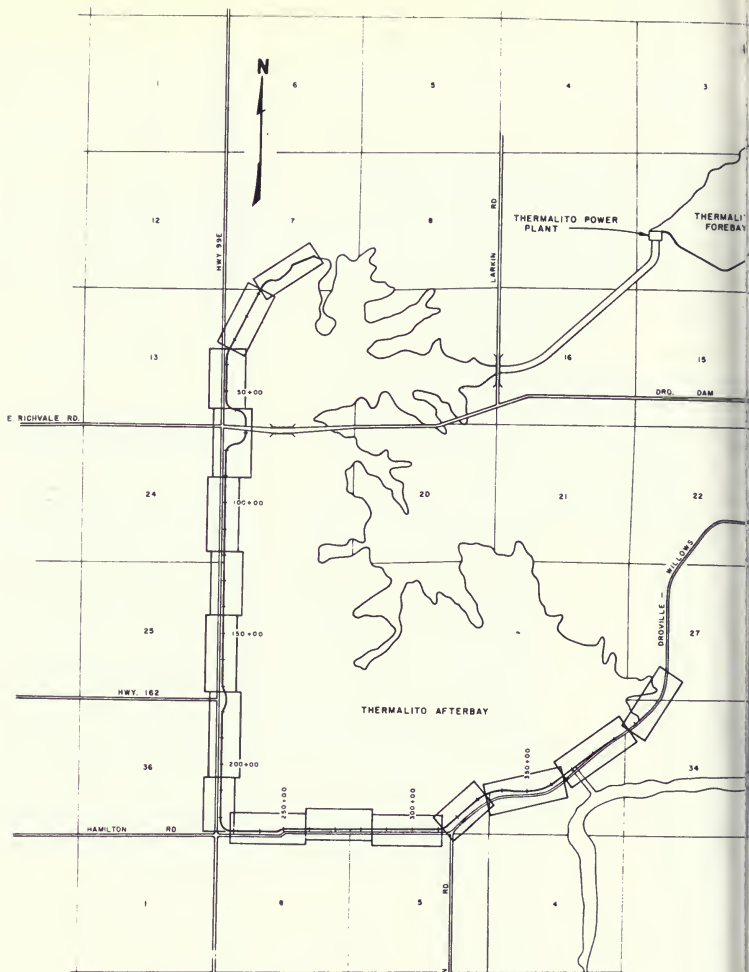
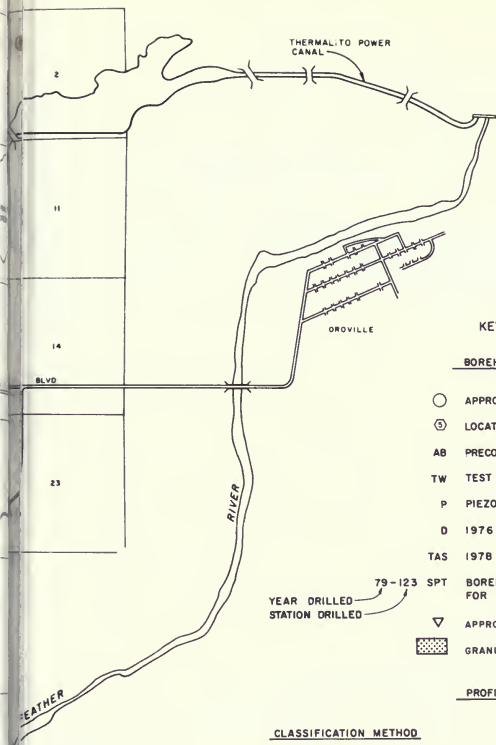


Figure 45. Thermalito Afterbay Plan



## KEY TO FIGURES

### BOREHOLE IDENTIFICATION

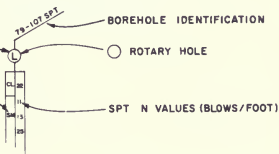
- APPROXIMATE BOREHOLE LOCATION
- ⑤ LOCATION OF PUMPBACK WELLS
- AB PRECONSTRUCTION BOREHOLE
- TW TEST WELL
- P PIEZOMETER HOLE
- D 1976 BOREHOLE FOR SEISMIC INVESTIGATION
- TAS 1978 BOREHOLE FOR SEISMIC INVESTIGATION
- 79-123 SPT BOREHOLE DRILLED FOR STANDARD PENETRATION TEST FOR SEISMIC INVESTIGATION (1979-81)
- ▽ APPROXIMATE CONE SOUNDING LOCATION (CPT)
- ▨ GRANULAR SOILS

### PROFILE IDENTIFICATION

#### CLASSIFICATION METHOD

L - LABORATORY  
F - FIELD

UNIFIED SOIL CLASSIFICATION  
SYMBOL



Dam Boring Profiles  
and Profiles

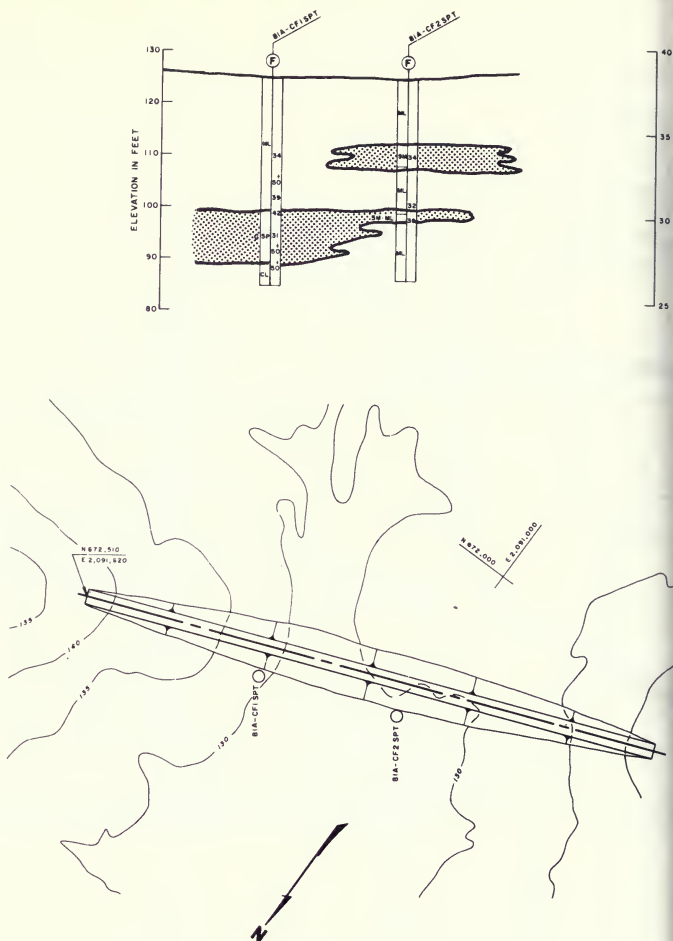
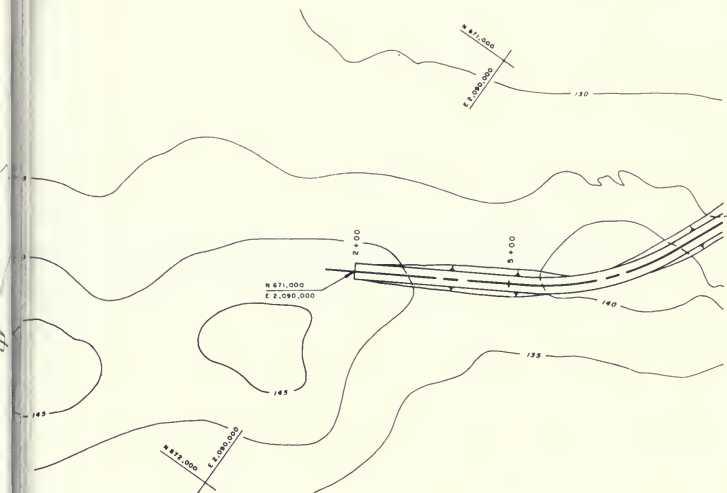


Figure 46. Thermalito Afterbay  
Saddle Dam—



Dam Boring Profiles  
Station 10

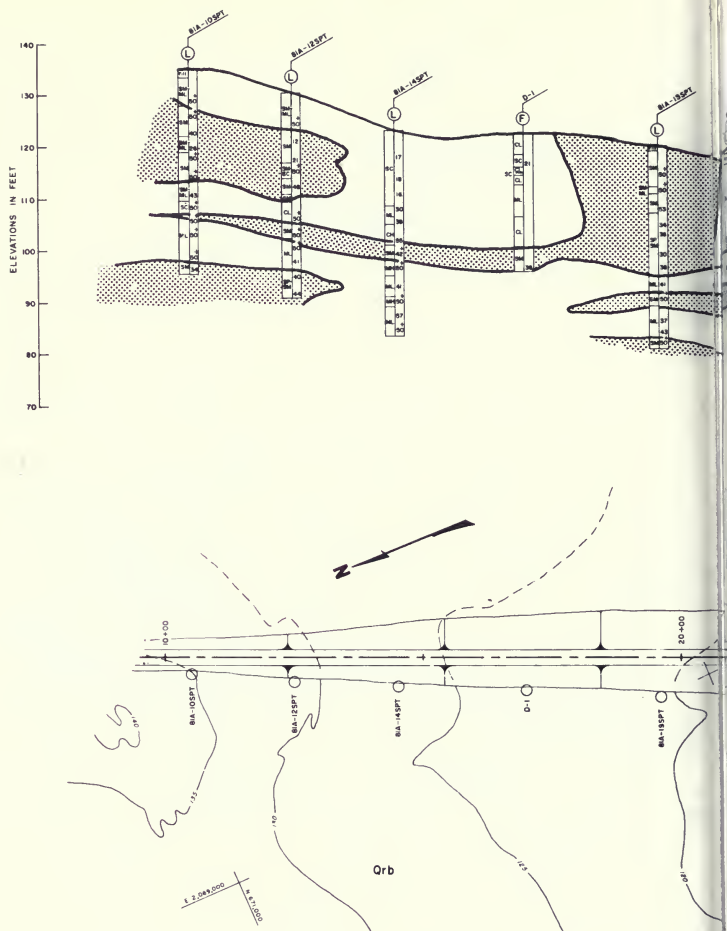
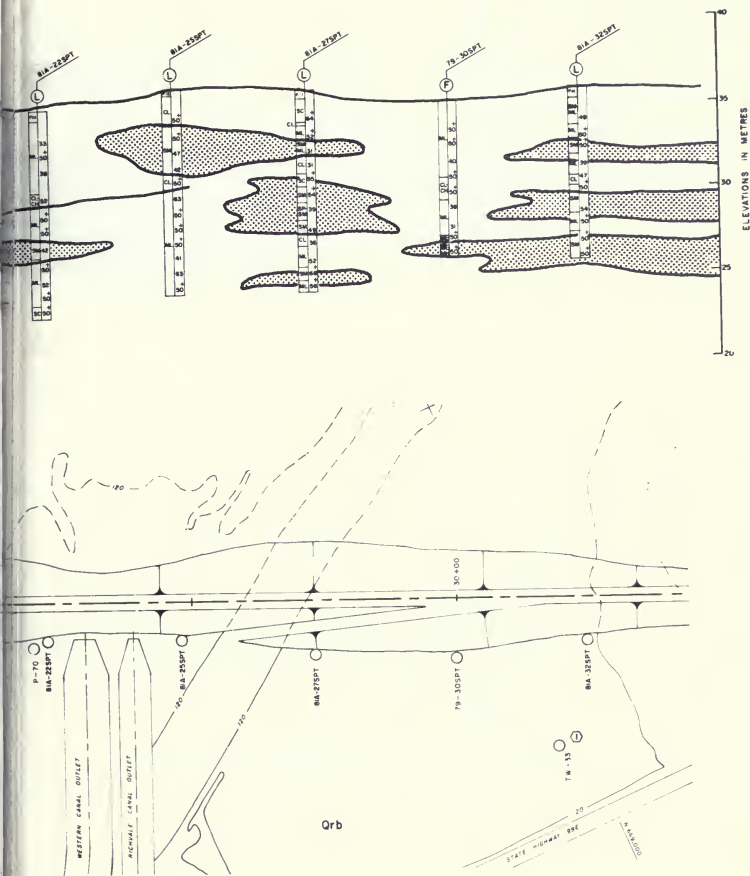


Figure 47. Thermalito Afterbay  
Station 10—



Dam Boring Profiles  
Station 35



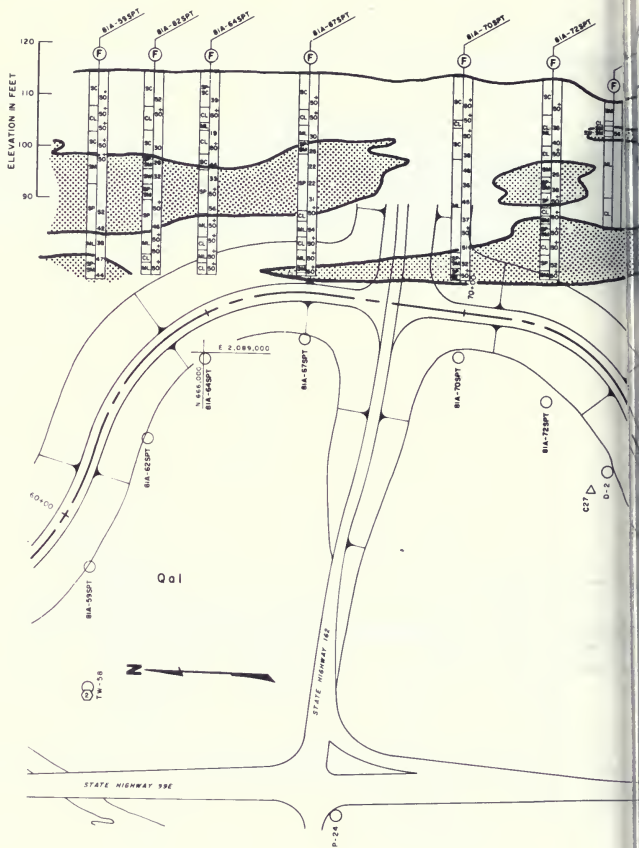
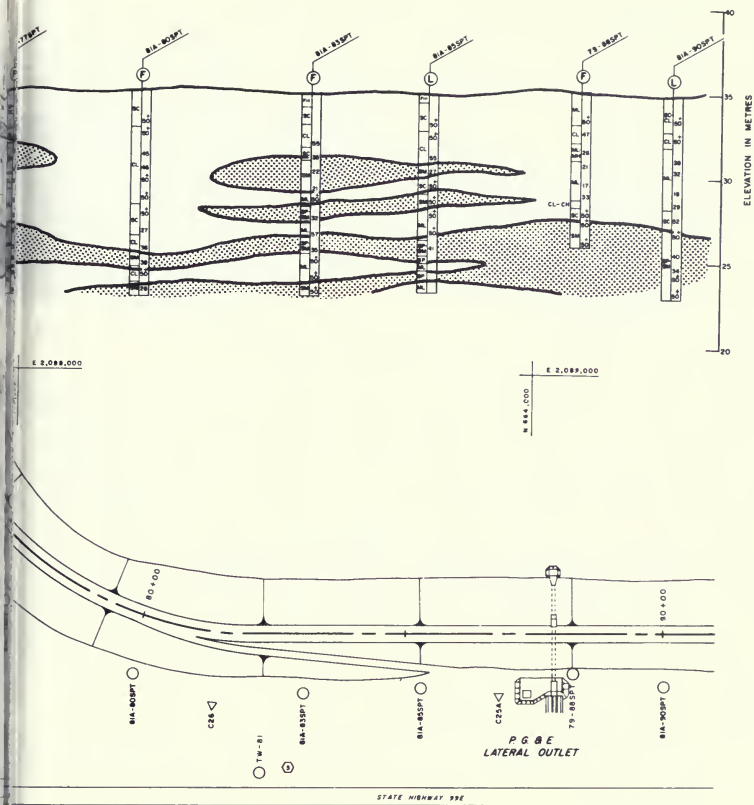
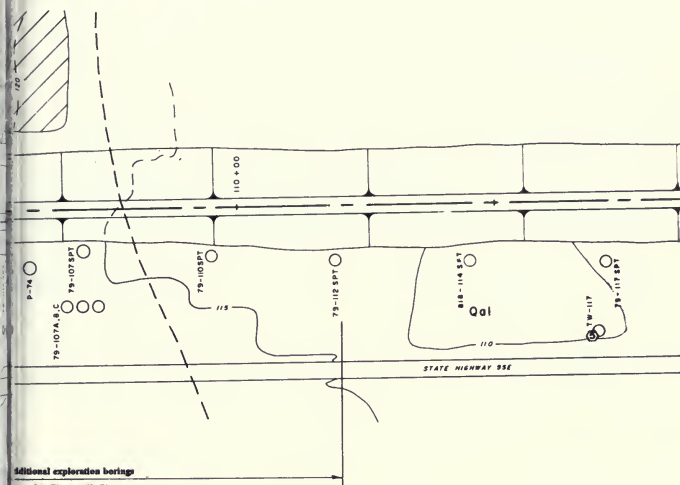
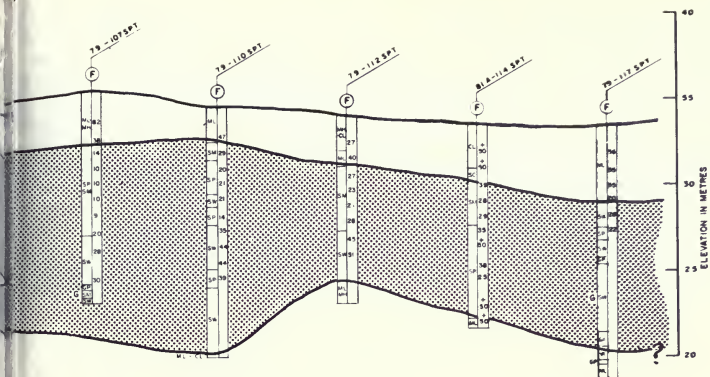


Figure 49. Thermalito Afterbay Station 59—



Dam Boring Profiles  
Station 91





Dam Boring Profiles  
Station 119

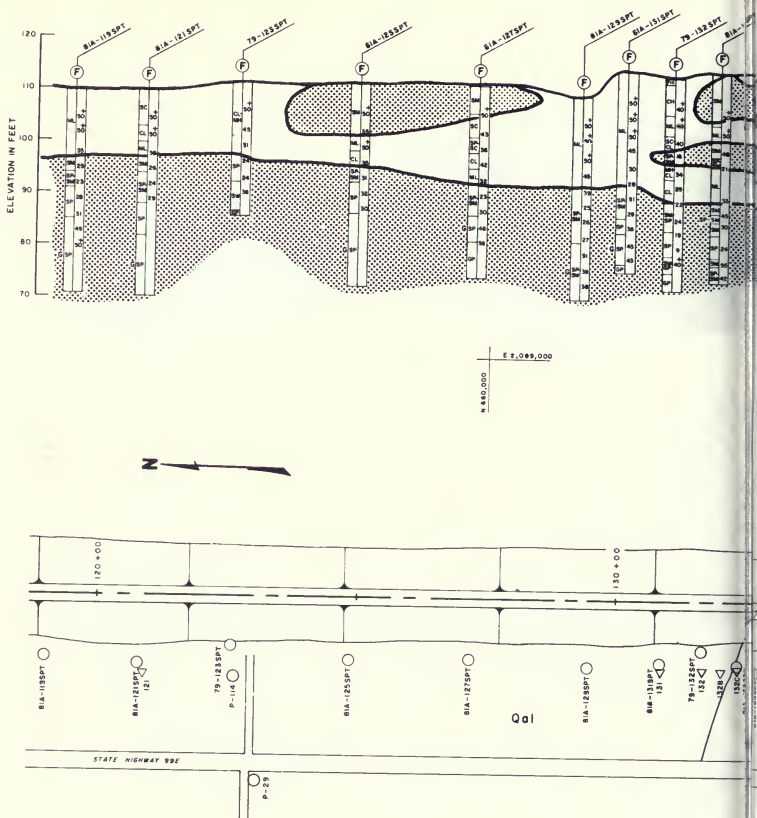
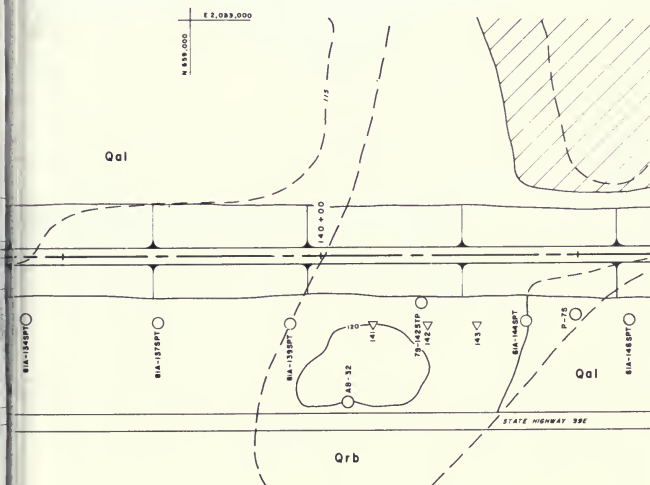
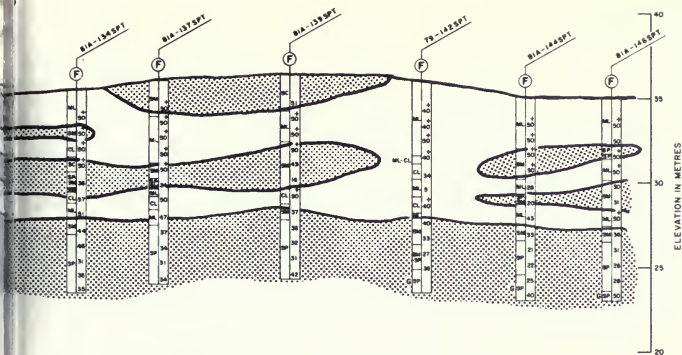


Figure 51. Thermalito Afterbay  
Station 119—



Dam Boring Profiles  
Station 147

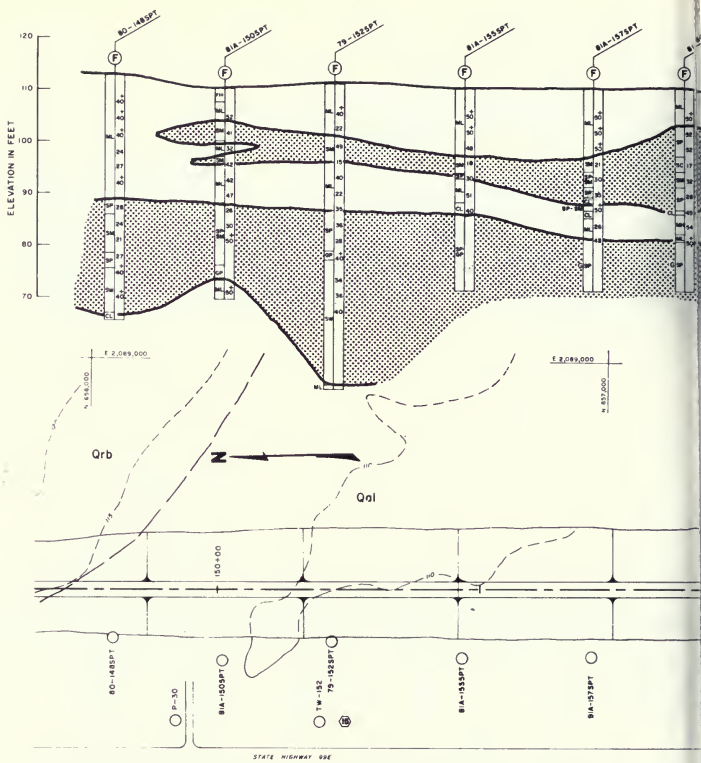
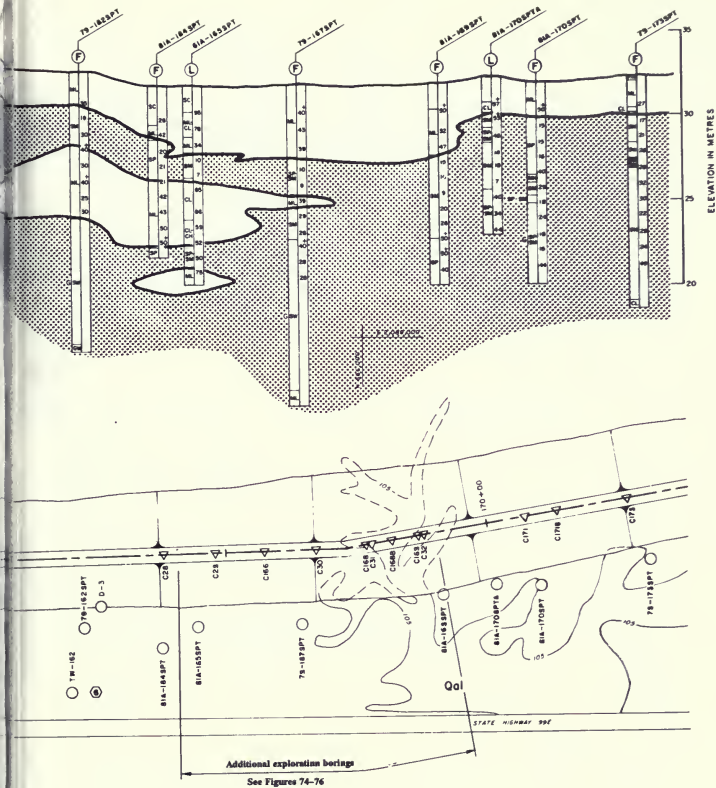


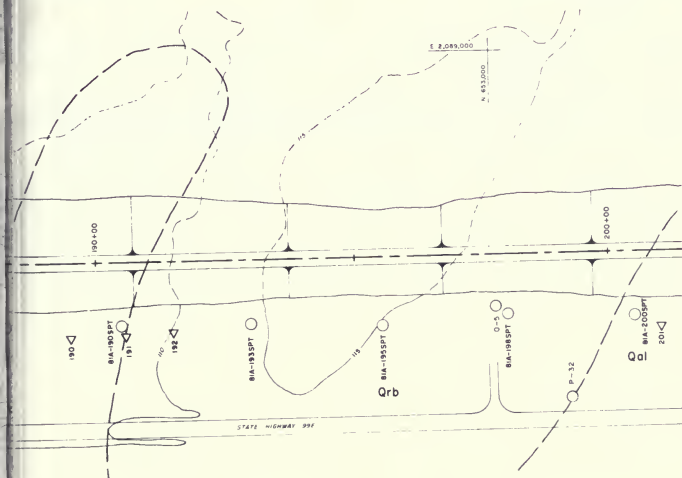
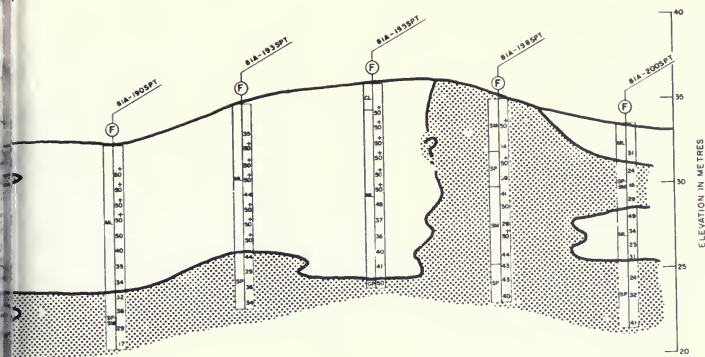
Figure 52. Thermalito Afterbay  
Station 147—





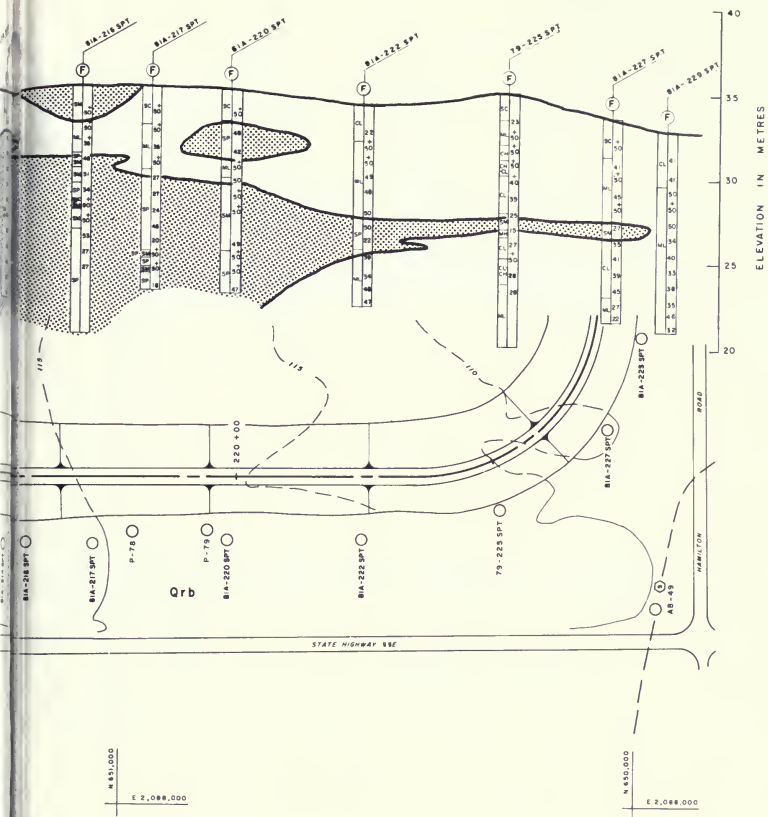
Dam Boring Profiles  
Station 174





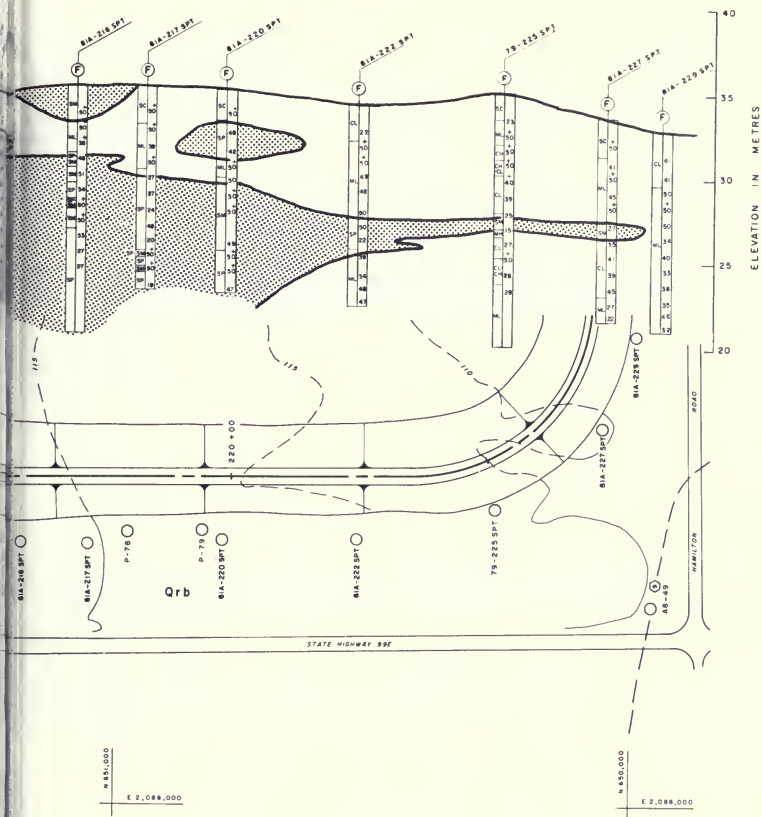
Dam Boring Profiles  
Station 202





Dam Boring Profiles  
Station 229





Dam Boring Profiles  
Station 229

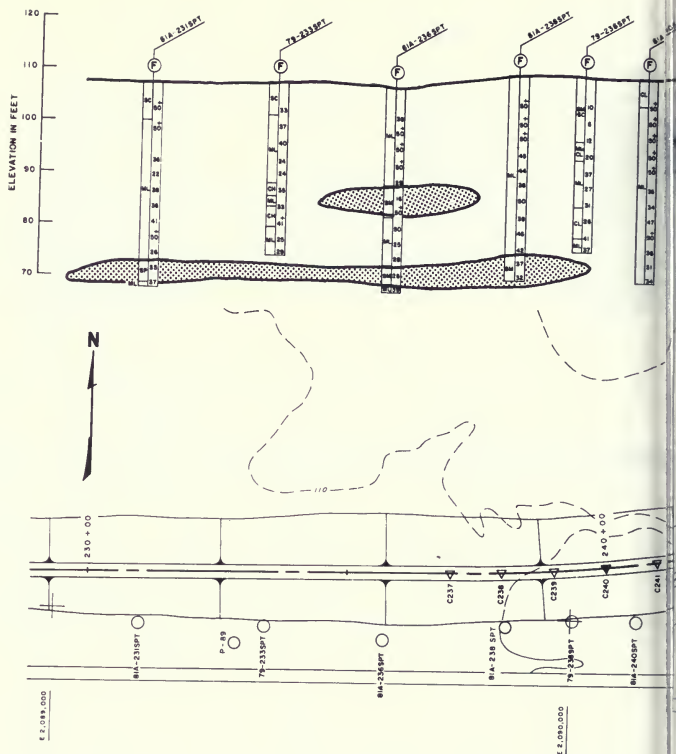
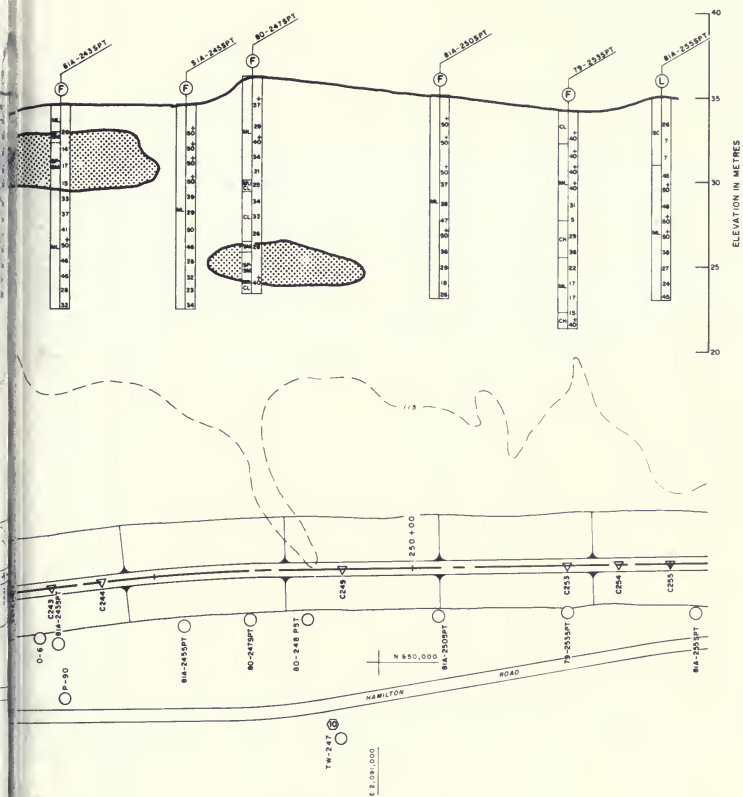


Figure 55. Thermalito Afterbay  
Station 229—





Dam Boring Profiles  
Station 256

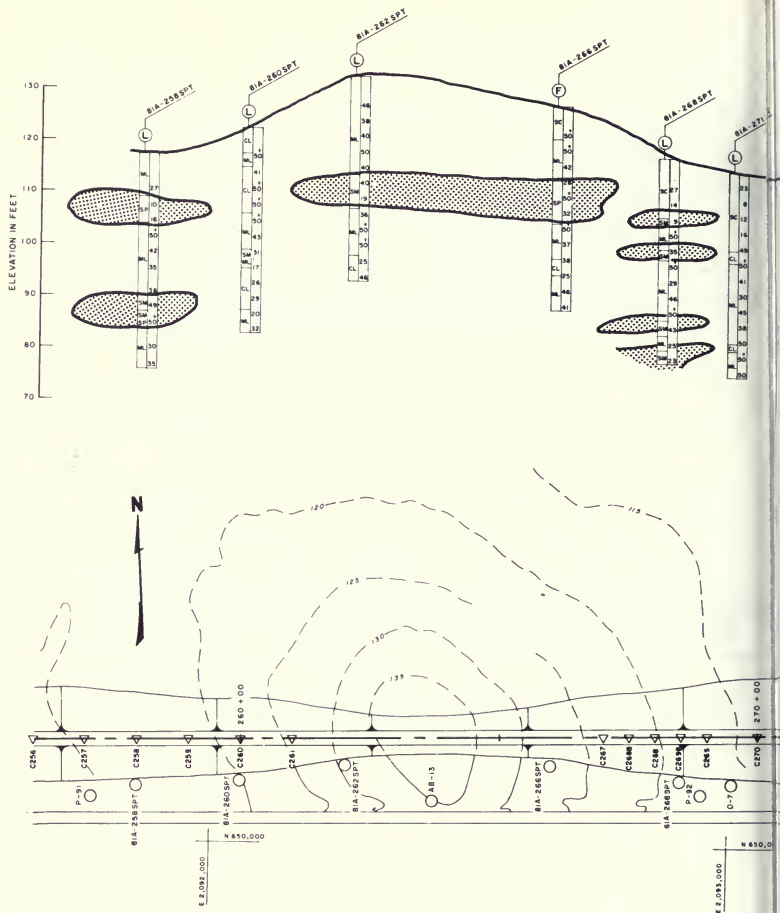
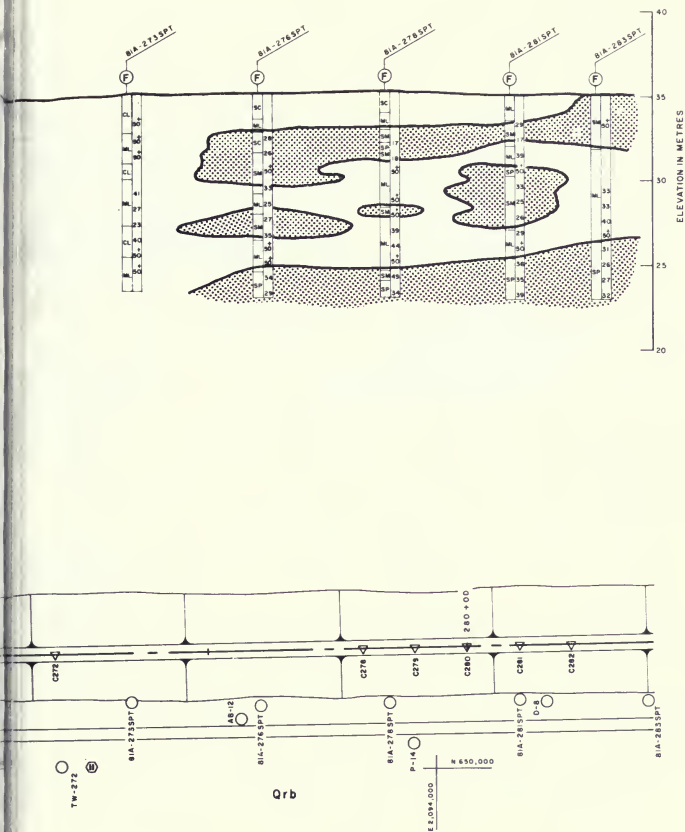


Figure 56. Thermalito Afterbay  
Station 256—



Dam Boring Profiles  
Station 284



### Dam Boring Profiles Station 311

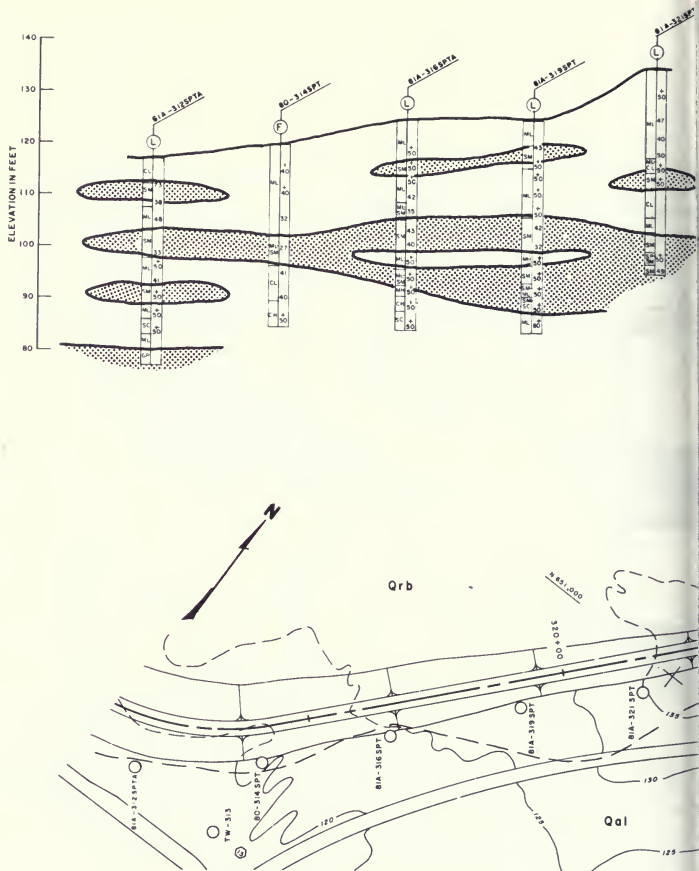
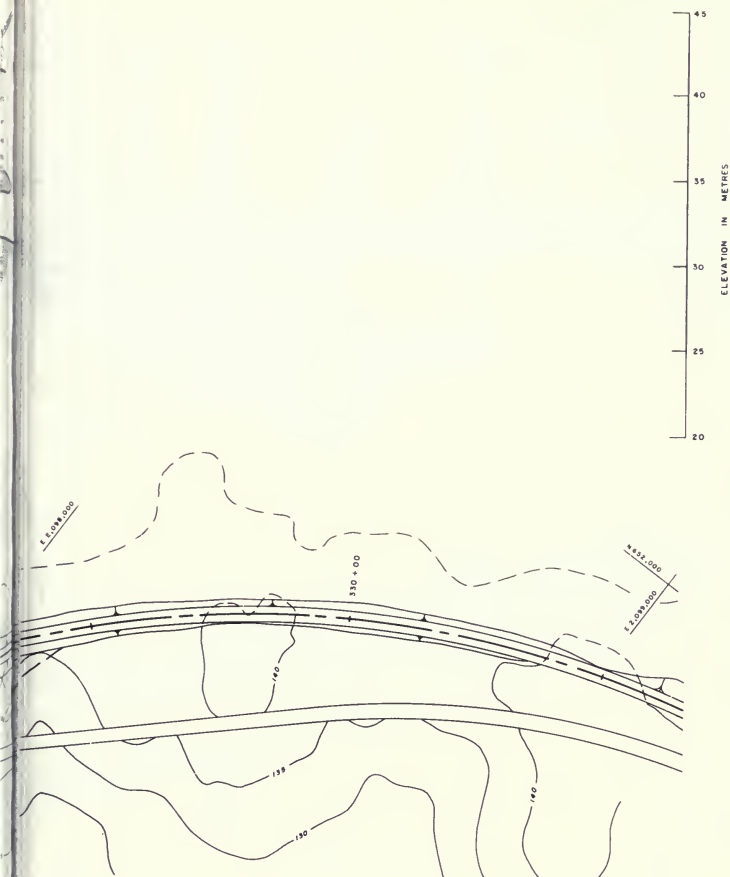


Figure 58. Thermalito Afterbay  
Station 311—



Dam Boring Profiles  
Station 337

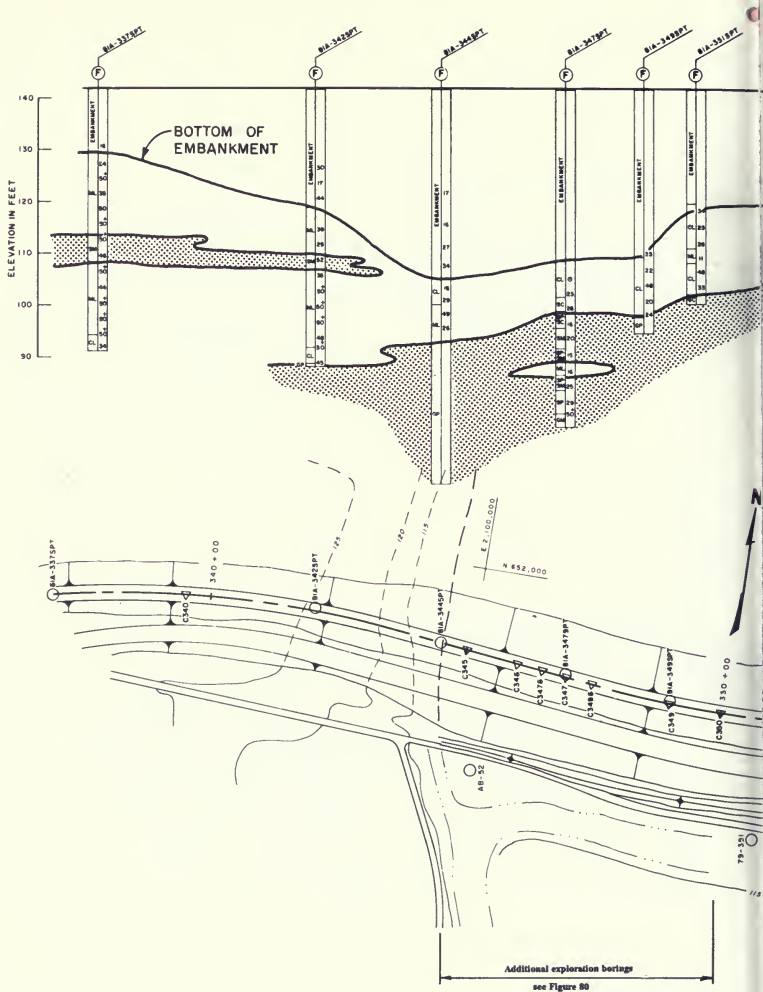


Figure 59. Thermalito Afterbay  
Station 337—





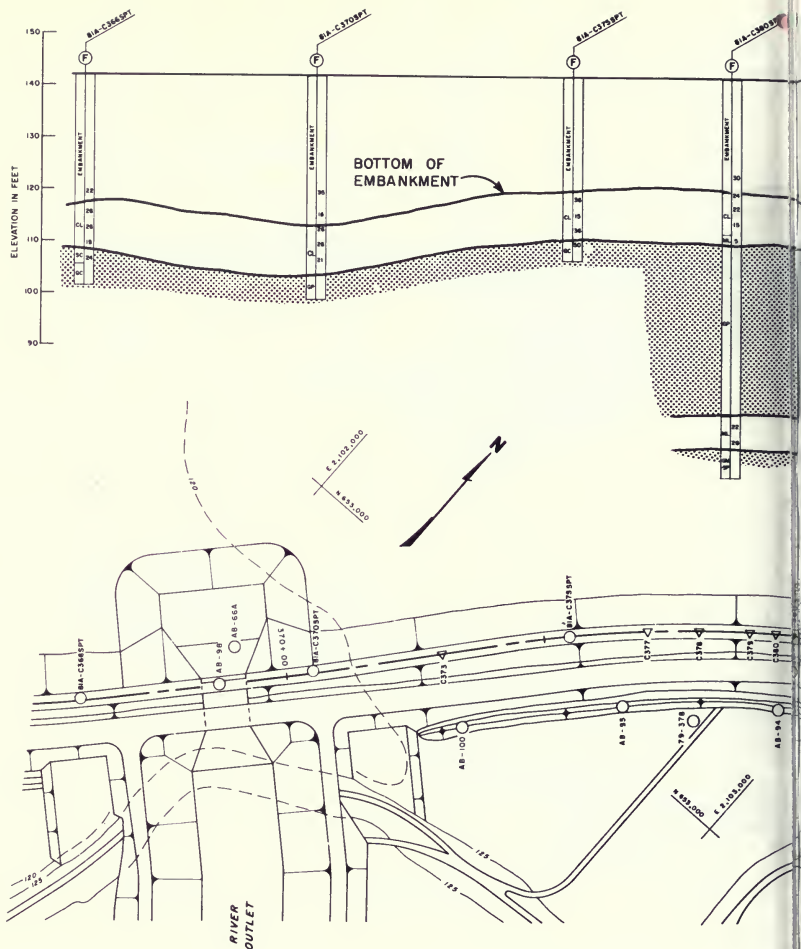
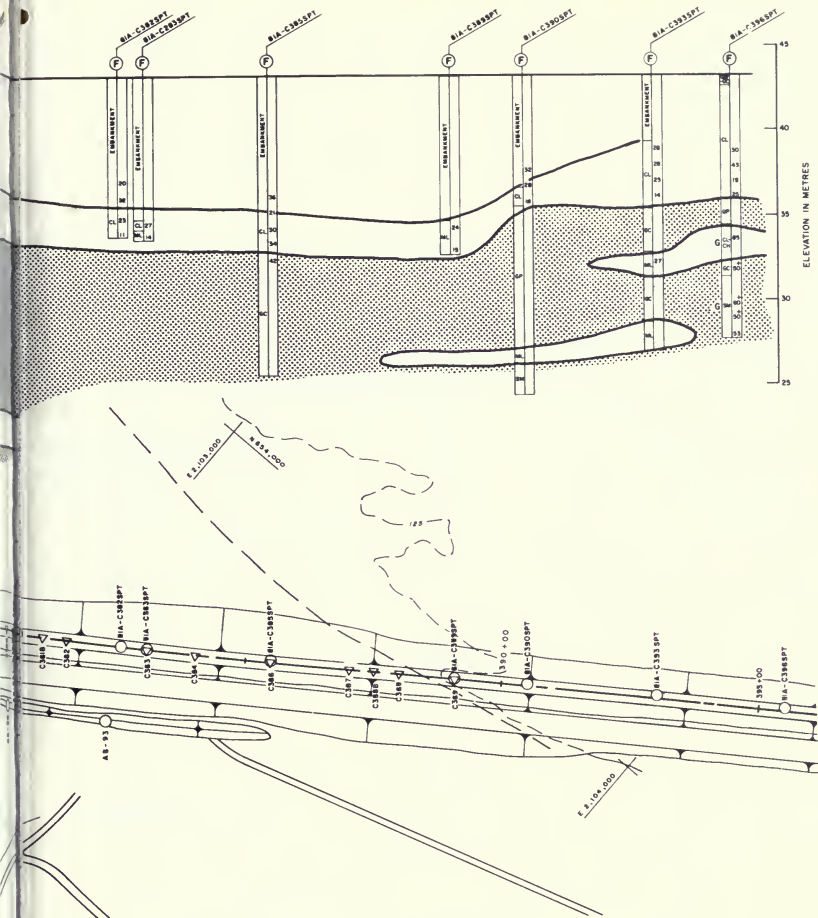


Figure 60. Thermalito Afterbay  
Station 365—



Dam Boring Profiles  
Station 396

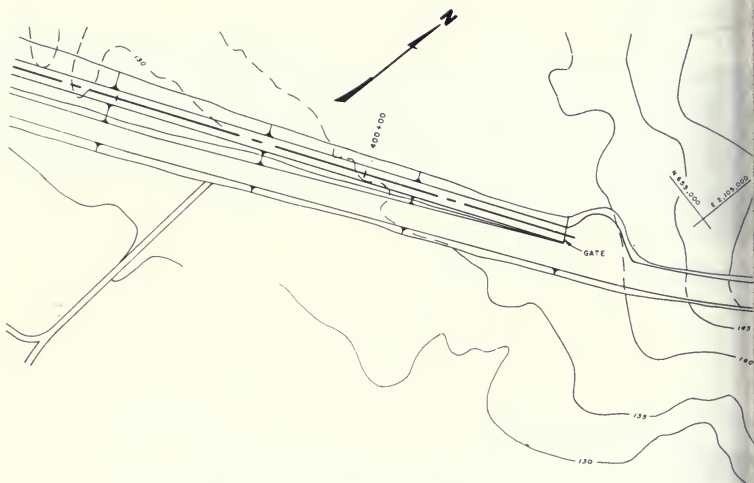
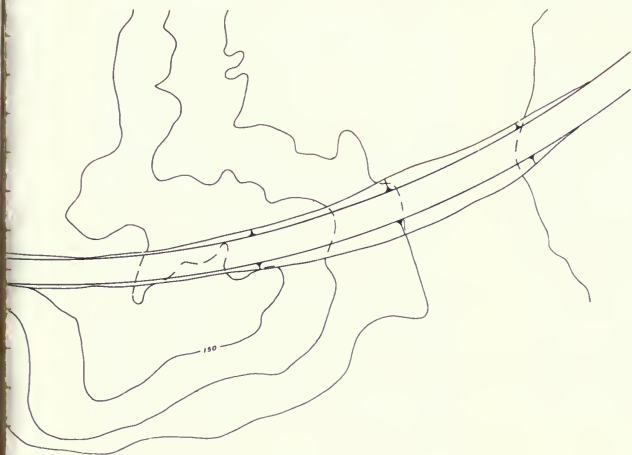


Figure 61. Thermalito Afterbay  
Station 396—



**Dam Boring Profiles  
Station 404**

## Mehrten Foundation

A formation tentatively identified as the Mehrten Formation was encountered in seven boreholes along the afterbay (AB-50, AB-66A, TW-313, 79-107A, 79-107B, 79-107C, 79-300 SPT). The depth to the surface of this formation ranges from 70 feet at Station 368 (River Outlet) to 190 feet at Station 107 (Site 1). Near the afterbay, the surface of the Mehrten Formation dips gently toward the northwest.

The formation is composed of alternating lenses of silty sandstone and sandy siltstone. It is weakly cemented and contains few fractures. Most of the boreholes into this formation penetrated only a few meters. However, the 500-foot hole at Station 107 (79-107B) penetrated more than 300 feet into this formation. The only noticeable change in the core samples retrieved was an increase in dry density with depth. At a depth of 190 feet, the surface of the formation, the dry density was about 76.7 lb/ft<sup>3</sup>. At a depth of 500 feet, the bottom of the hole, the dry density had increased to 102.5 lb/ft<sup>3</sup>.

The Mehrten Formation appears to extend beneath the entire afterbay. In addition to its presence in the seven boreholes, the formation was detected in the seismic refraction survey carried out at Station 173 (Site 2) in 1978 (Figure 62). The refraction survey identified a material with a compressive wave velocity of 7600 ft/sec at an aver-

age depth of 185 feet. This is a typical velocity for well-consolidated sedimentary material, and the depth is close to that of the Mehrten surface for this location.

The refraction survey was unable to detect the thickness of the Mehrten or the depth to basement bedrock. However, exploration studies for fossil fuels have indicated that hard rock lies at least 3,300 feet beneath the ground surface. An oil and gas exploration hole was drilled in 1944 about 1 mile southwest of Station 107 (Site 1). Although the logging may be imprecise, it indicates layers of siltstones, sandstones, shales, and conglomerates to a depth of several thousand feet. At a depth of 3,470 feet, serpentine was found. Corroborating evidence was found in the mid 70's by another oil exploration using seismic refraction surveys. The seismic surveys also indicated that basement rock is located about 3,300 feet beneath the ground surface near Station 107 (Site 1).

## Red Bluff Formation

Thermalito Afterbay Dam is founded on Red Bluff Formation from Station 0 to Station 344, about 80 percent of its length. The Red Bluff Formation was deposited as alluvial sediments having a great variety of soil types which vary considerably, both vertically and horizontally. Soils can be correlated over broad areas, but more often are difficult to match-up over short distances because of the many local variations. Red Bluff Formation is of Pleistocene Age and has remained in a relatively stable depositional-erosional environment for a large part of the million years or so since deposition. This lengthy duration of surface weathering is largely responsible for the extensive hardpan and soil profile development.

In general, the Red Bluff soils have about a 10-foot surface cap of silt or clay with thin lenses of clay pan or hard pan (Figures 46 through 59). These lenses have very high strength but are not continuous throughout the foundation. Beneath the silt-clay cap are layers of partially consolidated silt, clay, sand, and gravel down to the surface of the Mehrten Formation.

## Columbia Soil Area

Thermalito Afterbay Dam is founded on the Columbia Soil from about Station 344 to 390 (Figures 60 and 61). Boreholes into this more recent alluvium reveal 8- to 15-foot-thick layers of silt and lean clay overlying a thick bed of gravel. In some boreholes, 3-foot lenses of silty and poorly graded sands were found between the silt/clay

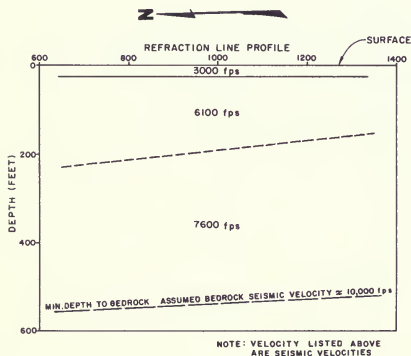


Figure 62. Strata Predicted from 1978 Seismic Refraction Survey at Thermalito Afterbay Station 173 (Site 2)

and the gravel. Between Stations 342 and 390, the gravel layer appeared to be quite thick and extend most, if not all, of the way down to the Mehrten Formation. East of Station 390, the gravel layer seemed to thin out to be replaced with other soils.

The upper few feet of the gravel layers were sampled in bucket auger holes (AB93-AB103) in 1965. Although there was a fair amount of variation, most of the material was classified as GM-GP. The samples were found to have between 7 and 17 percent passing the No. 200 sieve (74 microns). Gradations of these samples are shown in Figure 63.

### Embankment

The embankment was sampled at the four sites studied in 1978 and at another location (Station 286) in 1980. Classification test results made on sampled material reveal a sandy clay with a liquid limit of about 39 and a plasticity index of about 18. The gradation curves for the collected samples are shown in Figure 64.

### Shear Wave Velocity Test Results

Downhole shear-wave velocity testing was performed in 1978 at the four investigation sites (Stations 107, 173, 203, and 281). The clay embankment had a measured range of between 740 to 1340 fps. The foundation soils had a greater range with different materials and depths.

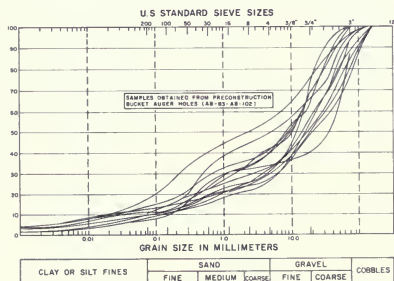


Figure 63. Gradation Curves for Columbia Soil Area Gravels

The minimum was 775 ft/sec and occurred within the low SPT blowcount sand layer at Station 107 (Site 1). This would yield a  $K_{2\max}$  value of about 70 for the sand. This value is not consistent with a loose sand since a  $K_{2\max}$  value of 70 had been considered typical of a dense sand.

Additional studies were performed in an attempt to clear up this inconsistency. When the 500-foot borehole was drilled 120 feet downstream of the embankment toe at the same location, the same loose silty sand layer was encountered. The downhole shear wave velocity measured for the sand in this hole was essentially the same as that measured previously (Figure 65). As a further check, a crosshole survey was performed at the deep hole. The results showed a basic agreement between the downhole and crosshole results, with the crosshole giving slightly higher ( $\approx 20$  percent) velocities for certain layers (Figure 66).

The crosshole testing revealed velocities as high as 3000 ft/sec within the Red Bluff material. These high velocities were found only within two gravel layers and are not considered unusual. Other soil types both below and above the two gravel layers had shear-wave velocities of less than 2200 ft/sec.

In the upper 100 feet of the Mehrten Formation, shear wave velocities were between 2350 to 2850 ft/sec.

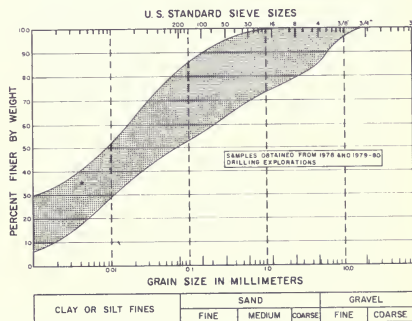


Figure 64. Gradation Range for Thermalito Afterbay Embankment Clay

## Preliminary Criteria for Identifying Suspect Sites

Suspect foundation conditions are sands or silts with low blowcounts, identified by the SPT survey with borings at 250-foot intervals (see Table 13). Conservative blowcount criteria were adopted initially because the site-specific SPT-cyclic strength correlation would not be completed before completion of the explorations.

Sands were considered suspect if the corrected blowcount,  $N_{A1}$ , was less than 25. Silts have greater liquefaction resistance than sands (Tokimatsu and Yoshimi, 1981). Therefore, silts were considered suspect only if the corrected blowcount was less than 15.

Clayey sands (SC) were considered liquefiable only if they contained less than 20 percent of 0.005 mm sizes (Seed & Idriss, 1982).

**Table 13. Preliminary Criteria for Identifying Suspect Sites**

Sand (SP, SW, SM, SC)	$N_{A1} < 25$ blows/ft <20% passing 0.005 mm
Silt (ML, MH)	$N_{A1} < 15$ blows/ft

The criteria were considered conservative because preliminary data were beginning to suggest that the Thermalito SPT procedure was producing lower blowcounts than other SPT procedures commonly used. This possibility was consistent with apparent higher strengths from tests of 1978 undisturbed samples than from SPT correlations and by relatively high shear wave velocities.

Suspect sites, as classified by these criteria, required further investigation—either additional exploration to delimit the extent, additional analyses, or both. Additional

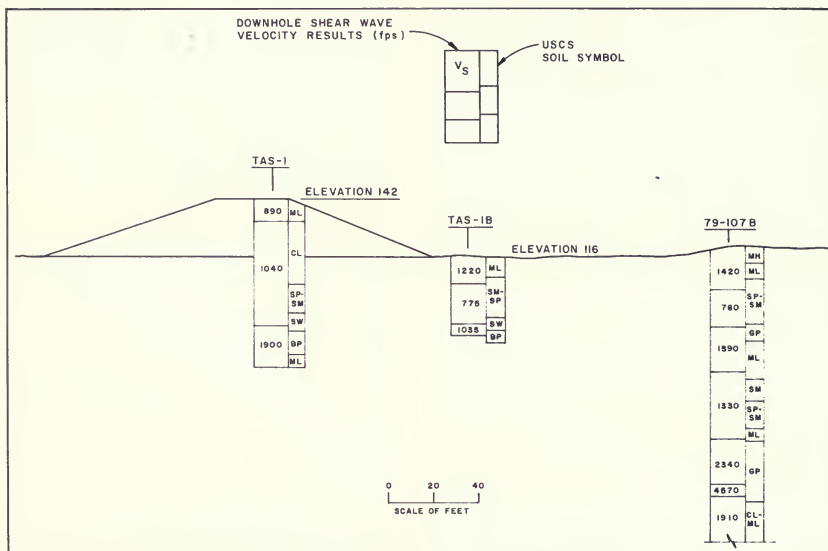


Figure 65. Downhole Shear Wave Velocity Results at Thermalito Afterbay Station 107 (Site-1)



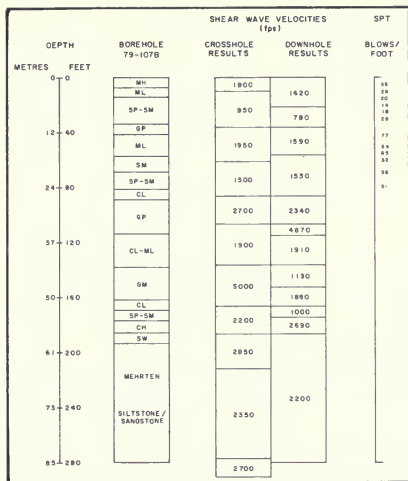


Figure 66. Results of Downhole and Crosshole Shear Wave Velocity Test at Thermalito Afterbay Station 107 (Site 1)

analyses would include the newly developed site-specific correlation between cyclic strength and SPT.

### Suspect Sites Identified by SPT Boring Survey

Of more than 160 SPT borings at 250-foot spacing, 19 encountered sand (SP, SW, SM) with  $N_{A1} < 25$ ; one encountered clayey sand (SC) with  $N_{A1} < 25$ ; and one encountered silt (ML, MH) with  $N_{A1} < 15$ . In some cases only one blowcount out of several in a sand layer was less than 25. The 21 suspect sites disclosed by the survey are shown in Figure 67.

### Additional Explorations to Delimit Suspect Sites

The Station 12 site was not explored further because the embankment height was only 12 feet and was determined to be stable even if the thin silty sand layer near the surface liquefied from toe to toe (Section 10).

The remaining 20 sites were subjected to additional explorations by electrical cone soundings, SPT borings, or

piston sampling. The cone soundings and SPT borings were used to delimit each remaining suspect site. The piston sampling was used in determining cyclic strengths for different blowcounts. Table 14 lists the suspect sites and additional explorations at each.

### Sites Selected for Analyses

Three sites were selected for liquefaction and stability analyses. These sites were chosen because they represented the worst conditions identified along the dam.

#### A. Model 1 – Station 107 (Site 1)

This site was chosen because it has the thickest low blowcount sand layer found in the Red Bluff Formation. In the 1979-80 drilling program, SPT borings were placed at both the crest and the downstream toe at 250-foot intervals at this site to delimit the horizontal extent of this suspect sand. Figure 68 illustrates the corrected blow counts taken from the crest and the toe between Stations 102 and 112. This figure reveals a low blowcount sand between approximately elevations 90 and 105 feet which extends along the axis of the dam about 750 feet.

The lowest corrected blowcount,  $N_{A1}$ , shown in Figure 68 is about 15 in a toe boring at Station 107. Because of the low blowcounts, this area was further explored in the 1981-82 program. Five crest SPT borings and 19 toe SPT borings were placed between Stations 106 and 108. Figure 69 shows the locations of these borings along with the lowest corrected blowcount found in each boring. Contour lines of minimum blowcounts have been drawn in the figure assuming a gradational change in penetration resistance between borings. Figure 69 indicates that corrected blowcounts less than 15 occupy only a relatively narrow area in the foundation between Stations 106 + 60 and 106 + 84.

Table 15 presents the corrected blowcounts in the suspect sands between Stations 106 and 108 for toe borings. Figure 70 presents a plot of these corrected blowcounts as a function of borehole depth. Shown in Figure 70 is a rectangle bracketing the blowcounts selected for a statistical analysis. Unusually high blowcounts or blowcounts performed in cohesive material (silt or clay) were not included in the statistical process. Included in the statistical analysis were the lower blowcounts in the narrow region between Stations



**Table 14. Thermalito Afterbay Boreholes Delimiting Suspect Areas**

Suspect Area	Exploration	Station	Dam Height (feet)	Depth (feet)	Suspect Material (USCS)	$N_{A1}$ or $N_{A1}^*$ (blows/foot)	Model Representation
I	81A-12 SPT (I)	12 + 50	12	8-10	SM	19	**
	80-102 SPT	102 + 00		5-30	ML & SM	> 30	
	80-102 SPT	102 + 00		5-30	ML & SM	> 30	
	79-105 SPT	104 + 50		12-24	SM	18-30	
	80-105 SPT	104 + 50		12-24	SM-SP	18-30	
II	79-109 SPT (I)	107 + 00	26	8-25	SM	14-30	MODEL 1 ( $N_{A1} = 20$ )
	80-107 SPT (I)	107 + 00		8-25	SM	18-30	
	79-110 SPT	109 + 50		18	SP-SM	23	
	80-110 SPT	109 + 50		12-24	SM	15-30	
	79-112 SPT	112 + 00		5-40	SM + ML	> 30	
(Additional Explorations – 30 SPT Borings, 6 Piston Sampling Borings, 20 Cone Soundings, see Figures 68, 69 and 70)							
	81A-131 SPT	130 + 81		15-35	ML & SM	> 45	
	81A-131 CPT	130 + 87		30-40	SM	> 50x	
	81A-132 CPT	131 + 62		32-40		> 50x	
III	79-132 SPT (I)	131 + 62	27	32-33	SP-SM	14	**
	81A-132 CPTB	132 + 02		32-40	SM	> 50x	
	81A-132 SPT	132 + 31		30-40	SP-SM	> 30	
	81A-132 CPTC	132 + 37		30-40	SM or ML	> 30x	
	81A-141-CPT	141 + 00		10-30	CL	> 20x	
IV	79-142 SPT (I)	142 + 00	24	10-22	SM-ML	9	**
	81A-142 CPT	142 + 06		10-30	CL	> 20x	
	81A-143 CPT	143 + 00			ML	> 20x	

(Continued on next page)

**Table 14. Thermalito Afterbay Boreholes Delimiting Suspect Areas (Continued)**

Table 14. Hermito Altiplano Boreholes Demarcating Suspect Areas (Continued)								
Suspect Area	Exploration	Station	Dam Height (feet)	Depth (feet)	Suspect Material (USCS)	$N_{A1}$ or $N_{A1}$ *	Model Representation	
V	81A-164 SPT	163 + 68	35	10-30		> 39	MODEL 2	
	81A-C164 SPT	163 + 68		10-30		> 21		
	81A-167 SPTH	164 + 68		13-20		SM		11-13
	81A-C165 SPT	164 + 68		10-30		> 27		
	81A-166 SPT	165 + 50		18	SM	5	$N_{A1}$ = 40 US	
	81A-C166 SPT	165 + 68		10-30	SM	> 38	$N_{A1}$ = 20 M	
	79-167 SPT (I)	166 + 40		13-19	SM	11-19	$N_{A1}$ = 10 DS	
	81A-167 SPTC	166 + 65		17-21	SM	7-9		
	81A-C167 SPT	166 + 68		10-30	SM	> 38		
	81A-167 SPT N	166 + 73		12-25		25-30		
(Additional Explorations – 17 SPT Borings, 8 Piston Sampling Borings, 25 Cone Soundings – See Figures 74, 75, and 76)								
VI	81A-C168 SPT	167 + 68		13-22	SP-SM	> 38	1 ( $N_{A1}$ = 20) and 2 ( $N_{A1}$ = 40,20,10)	
	81A-168 SPTA	168 + 09				15-27		
	81A-C169 SPT	168 + 68				> 23		
	81A-168 SPTB	168 + 59		13-22	SM	10-23		
	81A-169 SPT	168 + 95		14-22	SM	16-29		
	81A-C170 SPT	169 + 68		13-23	SM	20-26		
	81A-170 SPTA	170 + 00		14-22	SP-SM	12-33		
VII	81A-C171 CPT	170 + 74	37	15-28	SM	14-30x	1 ( $N_{A1}$ = 20)	
	81A-170 SPT(I)	170 + 82		29-34	SP-SM	21-27		
	CP-171 E1	171 + 20		10-40	SP-SM	> 30x		
	81A-C171 CPTB	171 + 38		20-30	SM-ML	22-30x		
	81A-C173 CPT	172 + 74		24-27	SM	14x		
	79-173 SPT	173 + 00		5-35	SP-SM	27-50		
	(Additional Explorations – 13 SPT and Piston Sampling Borings and 4 Cone Soundings)							

(Continued on next page)

Table 14. Thermalito Afterbay Boreholes Delimiting Suspect Areas (Continued)

Suspect Area	Exploration	Station	Dam Height (feet)	Depth (feet)	Suspect Material (USCS)	$N_{A1}$ or $N_{A1}$ * (blows/foot)	Model Representation
VIII	79-178 SPT (I)	178 + 06	35	6-12	SM	18-23	1 ( $N_{A1}$ = 20)
	81A-179 CPT	179 + 00		5-12	ML	> 15x	
	81A-C179 CPT	179 + 31		6	ML & CL	10x	
	81A-180B CPT	179 + 50		6-10	ML & CL	> 10x	
	81A-180 SPT A	180 + 09		6-11	SM	19-30	
	81A-180 SPT	180 + 25		6-11	SM	20-25	
	81A-180 CPT	180 + 31		6-10	ML	10x	
	81A-C180 CPT	180 + 31		12	ML	> 20x	
	81A-180 SPTB	180 + 41		6-13	SM	19-45	
	81A-181 CPTB	180 + 50		5-11	ML	> 20x	
	81A-181 CPT	181 + 00		9-10	SM	12x	
	81A-C181 CPT	181 + 31		6-15	CL	> 20x	
	81A-182 CPTB	181 + 50		0-15	CL	> 20x	
	81A-182 CPT	182 + 00		22-37	SM	12-30x	
	81A-183 SPTA	182 + 59		22-38	SM	> 30	
	81A-183 SPT (I)	182 + 83		22-45	SP-SM	16-30	
	81A-183 CPT	182 + 89		25-48	SM	10-20x	
	81A-183 SPTB	183 + 07		23-45	SM	21-50	
	81A-184 CPT	183 + 70		25-43	SM	14-30x	
	(Additional Explorations – 3 Piston Sampling Borings, 1 SPT Boring, and 4 Cone Soundings)						
IX	81A-190 CPT	189 + 50	34	30-50	SM	> 20x	1 ( $N_{A1}$ = 20)
	81A-190 SPT (I)	190 + 50		37-40	SP-SM	22	
	81A-191 SPT	190 + 56		30-50	SW (G)	> 20x	
	81A-192 CPT	191 + 50		30-50	SW	> 20x	

(Continued on next page)

**Table 14. Thermalito Afterbay Boreholes Delimiting Suspect Areas (Continued)**

Suspect Area	Exploration	Station	Dam Height (feet)	Depth (feet)	Suspect Material (USCS)	$N_{A1}$ or $N_{A1}$ * (blows/foot)	Model Representation
X	81A-200 SPT	200 + 50	33	5-17	ML & SM	> 30	1 ( $N_{A1}$ = 20)
	81A-201 CPT	201 + 00		5-15	ML & CL	> 15x	
	81A-202B CPT	201 + 50		5-15	CL & ML	> 15x	
	81A-C202 CPT	202 + 00		5-15	CL	> 15x	
	81A-202 CPT	202 + 00		5-15	CL	> 25x	
	81A-C203 CPT	203 + 00		5-15	SM	> 15-23x	
	81A-203 CPT	203 + 00		6-14	CL & ML	> 25x	
	79-203 SPT (I)	203 + 04		7-12	SM	21	
	81A-C204 CPT	204 + 00		5-12	CL & SM	> 20x	
	81A-204 CPT	204 + 00		5-15	CL	> 25x	
	81A-205 SPT	205 + 28		5-35	ML	> 50	
(Additional Explorations – 6 SPT and Sampling Borings, 4 Cone Soundings)							
XI	81A-207 CPT	206 + 50	32	10-30	CL,ML,SM	> 25x	1 ( $N_{A1}$ = 20)
	81A-207B CPT	207 + 00		20-30	CL	> 30x	
	81A-207 SPT	207 + 40		20-30	CL,ML,SM	> 30	
	81A-207 SPTA	207 + 46		20-30	ML & SM	> 25	
	81A-208 SPT (I)	207 + 52		23-28	SM-SP	18-27	
	81A-208 SPTB	207 + 58		23-28	SM	12-15	
	81A-208 SPTC	207 + 64		23 = 28	SM	23-27	
	81A-208 CPT	207 + 70		22-27	SM	16-25x	
	81A-209 CPT	208 + 50		22-26	SM	14-27x	
	81A-210 SPT	209 + 76		22-30	SM	> 27	
	81A-210 CPT	209 + 82		22-30	SM	12-35x	
XII	81A-214 SPT	214 + 10	29	30-40	SM	> 30	1 ( $N_{A1}$ = 20)
	81A-215 SPT (I)	214 + 60		30-40	SM	18	
	81A-216 SPT	215 + 90		30-40	SM	> 30	

(Continued on next page)

Table 14. Thermalito Afterbay Boreholes Delimiting Suspect Areas (Continued)

Suspect Area	Exploration	Station	Dam Height (feet)	Depth (feet)	Suspect Material (USCS)	$N_{A1}$ or $N_{A1}$ * (blows/foot)	Model Representation
XIII	81A-C237 CPT	237+00	32	5-12	ML & CL	>30x	$(N_{A1} = 40, 20, 10)$
	81A-238 SPT	238+00		5-12	ML	>50	
	81A-C238 CPT	238+00		5-12	ML, CL & SM	>20x	
	CP-238-E4	238+28		5-16	SM & CL	>30x	
	81A-C239 CPT	239+00		5-15	ML & CL	>50x	
	79-238 SPT (I)	239+23		4-10	SM	6-13	
	CP-238-E2	239+28		4-10	CL & SM	5-10x	
	CP-238-E3	239+38		4-10	CL & SM	10x	
	81A-C240 CPT	240+00		5-15	ML & CL	>20x	
	81A-240 SPT	240+50		5-20	ML	>40	
	CP-238 E5	240+57		5-20	ML & SM	>20x	
(Additional Explorations - 2 Cone Soundings)							
XIV	81A-C242 CPT	242+00	29	5-30	ML & CL	>17x	1 ( $N_{A1} = 20$ )
	81A-C-243 CPT	243+00		5-30	CL & ML	>30x	
	81A-243 SPT(I)	243+00		8-16	SM	24-36	
	81A-C244 CPT	244+00		5-30	ML	>20x	
	81A-245 SPT	245+00		5-30	ML	>40	
XV	81A-C257 CPT	257+00	24	8-14	ML & CL	8-20x	1 ( $N_{A1} = 20$ )
	81A-C258 CPT	258+00		8-14	ML & CL	>15x	
	81A-258 SPT(I)	258+00		8-13	SM	16-33	
	81A-C259 CPT	259+00		5-30	ML & CL	>20x	
	81A-C260 CPT	260+00		5-20	ML	17x	

(Continued on next page)

**Table 14. Thermalito Afterbay Boreholes Delimiting Suspect Areas (Continued)**

Suspect Area	Exploration	Station	Dam Height (feet)	Depth (feet)	Suspect Material (USCS)	$N_{A1}$ or $N_{A1}$ * (blows/foot)	Model Representation
XVI	81A-C268 CPTB	267 + 50	25	5-20	ML,CL,SM	> 30x	1 ( $N_{A1}$ = 20)
	81A-C268 CPT	268 + 00		5	ML & CL	16x	
	81A-C269 CPTB	268 + 50		5-15	CL	> 10x	
	81A-268 SPT(I)	268 + 50		12	SC	21	
	81A-C269 CPT	269 + 00		8	ML & CL	14x	
	81A-C270 CPT	270 + 00		4-10	ML	> 15x	
	81A-271 SPT	271 + 05		7-14	SC	14-34	
	81A-C272 CPT	272 + 00		4-12	CL & ML	> 10x	
XVII	81A-C279 CPT	279 + 00	27		CL	> 20x	**
	TAS 4A (I)	279 + 83		8-13	SM	20	
	81A-C280 CPT	280 + 00		3-13	ML	12-30	
	81A-281 SPT	281 + 00		9	ML	26	
	D-8 (I)	281 + 63		8-11	SM	12	
	81A-C282 CPT	282 + 00		3-15	ML	> 12x	
	81A-283 SPT	283 + 50		5-20	ML & SM	> 40	
	XVIII	81A-C344 SPT		344 + 50	25		
81A-C346 SPT		346 + 44				> 30	
81A-347h SPT		346 + 90	12-22	CL/SM		7/22	
81A-C347 SPT(I)		347 + 00	20-35	SM-ML		16-22	
81A-348 SPT		347 + 90	20-23	CL/ML		20/14	
81A-C348 SPT		348 + 06	21-24	SM		20-28	
81A-C349 SPT		349 + 00	13-18	CL		> 20	
(Additional Explorations – 7 Cone Soundings, 2 Preconstruction Borings – See Figure 80)							
XIX	81A-C350 SPT		25			> 25	3 ( $N_{A1}$ = 21)
	81A-C351 SPT(I)	351 + 00		5-10	SM-ML	15	
	81A-C352 SPT	352 + 00		5-12	CL-SC	> 20	
	81A-C353 SPT	353 + 00		6-8	CL-ML	20	
(Additional Explorations – 3 Soundings)							



**Table 14. Thermalito Afterbay Boreholes Delimiting Suspect Areas (Continued)**

Suspect Area	Exploration	Station	Dam Height (feet)	Depth (feet)	Suspect Material (USCS)	$N_{A1}$ or $N_{A1}$ *	Model Representation
XX	81A-C360 CPT	360+00			CL	> 15x	
	81A-C361 SPT(I)	361+00	22	13-16	SC	23	3 ( $N_{A1} = 21$ )
	81A-C362 SPT	361+94		13	SM	18	
	81A-363 SPT	362+94				> 30	
(Additional Explorations - 5 Cone Soundings)							
XXI	81A-C378 CPT	378+00		4	ML & CL	10x	
	81A-C379 CPT	379+00		8-13	ML	4x	
	81A-C380 CPT	379+50		6	ML	13x	
	81A-C380 CPTB	380+00		6-8	CL & ML	9x	
	81A-C380 SPT(I)	380+50		5-13	CL	6-20	
	81A-C381 CPT	380+50	22	8	CL	7x	**
	81A-C381 CPTB	381+00		8	CL	4x	
	81A-C382 CPT	381+50		8	CL	7x	
	81A-C382 SPT	381+56		8	SC	14	
	81A-C383 CPT	383+00		4-9	ML & CL	2x	
	81A-C383 SPT	383+06		8	ML	18	
(Additional Explorations - 2 Piston Sampling Borings)							

- NOTES: 1. \*\* = See Explanation  
 2. x =  $N_{A1}$  Values for CPT explorations were determined from the ERTEC correlations for Thermalito Afterbay.  
 3. (I) = Initial exploration  
 4. Depth = Depth below original ground surface at toe.

Explanations

Station

12+50	Not subjected to additional explorations because analyses indicated that the 12-foot embankment would not fail even if the thin silty sand layer near the surface were to liquefy from toe to toe (Section 10).
131+62 142+00 281+00	Suspect material was indicated during a previous exploration but could not be found during the 1981-82 exploration program. Therefore, this layer was considered to be either nonexistent or very small in extent and not analyzed.
362+00 380+00	Suspect material was not found in the initial SPT borehole survey but in additional borings and soundings performed subsequently in the same area.

**Table 15**  
**Corrected SPT Blowcount ( $N_{A1}$ ) Distribution Along the Downstream Toe Between Stations 106–108**  
**(Blows/ft)**

Borehole	Station	Depth, ft				
		12.5	16	19.5	23	26.5
81A–107 SPT J	105 + 86	29	23	23	25	36
81A–107 SPT H	106 + 15	35	28	25	25	21
81A–107 SPT G	106 + 33	47	23	21	20	24
81A–107 SPT F	106 + 48	35	19	21	21	20
81A–107 SPT D	106 + 60	25	13	11	15	17
81A–107 SPT Q	106 + 60	20	11	18	20	21
81A–107 SPT R	106 + 72	68	13	14	16	21
81A–107 SPT S	106 + 72	47	23	18	18	24
81A–107 SPT A	106 + 84	29	24	23	20	39
81A–107 SPT C	106 + 84	35	15	14	25	41
81A–107 SPT B	106 + 84	27	28	26	26	44
81A–107 SPT E	106 + 93	31	36	25	23	24
81A–107 SPT T	106 + 96	27	28	16	21	44
81A–107 SPT P	107 + 06	20	24	18	20	50
81A–107 SPT N	107 + 20	35	28	19	23	44
81A–107 SPT M	107 + 26	20	32	23	21	48
81A–107 SPT L	107 + 32	25	34	23	23	42
81A–107 SPT K	107 + 42	29	36	26	23	45
81A–107 SPT U	107 + 72	41	38	28	34	62 +

**Table 16**  
**Corrected SPT Blowcount ( $N_{A1}$ ) Distribution Beneath Embankment Crest Between Stations 106–108**  
**(Blows/ft)**

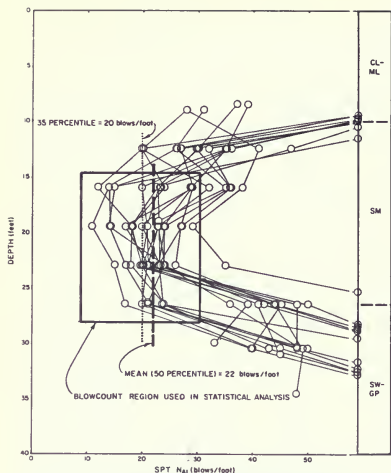
Borehole	Station	Depth, ft				
		39.5	42.5	45.5	48.5	51.5
81A–C107–B	105 + 26	24	30	25	36	35
81A–C107–C	106 + 76	22	37	43	47	62
80–107A SPT	106 + 82	22	18	20	20	35
81A–C107 SPT D	106 + 88	29*	33	30	37	53
81A–C107 SPT E	106 + 97	24*	32	32	36	53
81A–C107 SPT A	107 + 46	13*	50 +	26	30	45

\* Denotes material as being clay

106 + 60 and 106 + 84. The mean value (50th–percentile) of this blowcount set in toe borings was found to be 22. The 35–percentile blowcount was found to be 20 blows per foot (this means that approximately two thirds of the toe blowcounts are equal to or higher than this blowcount). The 35–percentile value is an accepted characterization for seismic analyses, maintains adequate conservatism, and was adopted for the toe borings at this site.

Table 16 presents the corrected blowcounts for the suspect sand found in crest borings. These blowcounts were found to be generally higher than those along the toe. Only one corrected blowcount in sand was found to be less than 20 blows per foot. The thickness of the low blowcount sand beneath the crest was also not as thick as it was found along the downstream toe. Although a higher blowcount could have been justified for the sand beneath the crest, it was decided





to conservatively characterize the entire layer as being 20 blowcount silty sand.

The gradation range for the suspect sand is shown in Figure 71. Figure 72 presents the  $D_{50}$  values and percentage of fines for the blowcounts shown in the bracketed region in Figure 70. The mean  $D_{50}$  is 0.31 millimeters and the mean percentage of fines is 18 percent.

The model developed for this site is shown in Figure 73. This model represents equivalent or worse conditions than exist at most of the suspect sites listed in Table 14.

#### B. Model 2 — Station 165 (Worksite 2)

This site was chosen for analysis because it contained the weakest material found along the dam and because the embankment height at this location (35 feet) was close to the maximum height. The suspect sand at this site was originally encountered in a downstream toe boring in 1979 at Station 167. In the 1981–82 investigation, seven crest and 18 downstream

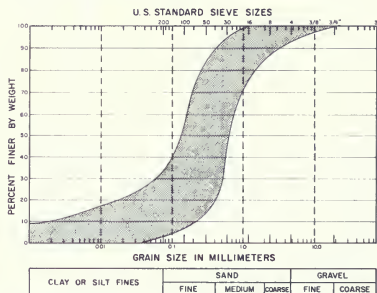
toe SPT borings were placed between Stations 165 and 171.

Figure 74 shows the locations of these borings along with the *lowest* corrected blowcount in each boring. Also shown are the locations of cone soundings used to supplement the SPT borings, together with the *lowest* equivalent blowcount,  $N_{A1}^*$ , for each sounding. Contour lines of minimum blowcounts have been drawn assuming gradational changes in blowcounts between borings.

Tables 17 and 18 (pages 121 and 122) present the corrected blowcounts for both toe and crest SPT borings between Stations 164 and 167. Figure 74 shows blowcounts of less than 10 along the toe between Stations 164 + 50 and 167 + 00. The blowcounts from borings within this length are shown in Figure 75.

Shown in this figure is a boring, Borehole 81A-167SPTB, which has two blowcounts as low as 2. These two-blowcount measurements, however, are found at depths where most of the other borings show relatively high penetration resistance.

Shown in Figure 76 is a plan view of the eleven borings and cone soundings within a 33-foot radius of this two-blowcount boring, together with the corrected blowcounts found in these explorations. Figure 76 shows that the corrected blowcounts for all of the nearby explorations are at least five blows per foot with some greater than 20. Sampling borings adjacent



*Figure 71. Gradation Envelope of Samples Collected from Stations 104-110 Representing Suspect Layer for Model 1 (Site 1)*

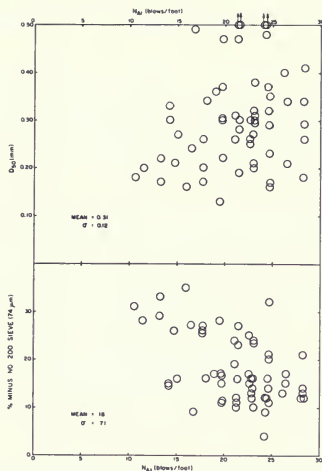


Figure 72. Gradation Characteristics of Low Blowcount Sands Between Stations 106 and 108

to the two-blowcount boring show dense silt at the same depths where the blowcounts of two were obtained. It was therefore concluded that the two-blowcount boring produced values not representative of the layer and that the 2-blowcount measurements result from a small and isolated pocket of weak materials. It should be noted that no other borehole drilled at the afterbay found corrected blowcounts lower than five.

Shown in Figure 75 is the bracketed region of blowcounts that was used in a statistical analysis of the toe blowcounts. As at Station 107, unusually high blowcounts were not included in the statistical process. Also not included were the very low blow counts at the 23- to 26-foot depths, which were not representative of the layer. The mean corrected blowcount for the suspect layer in these toe borings was found to be 12 blows per foot. The 35-percentile blowcount for these blowcounts was found to be 10 blows per foot.

Although low blowcounts were found along the downstream toe, Figure 74 shows that much higher blowcounts were found along the crest. The contours of minimum blowcount in Figure 74 are drawn assuming a gradational change in blowcounts between borings. This is a reasonable assumption since none of the borings along the toe suddenly changed from very low to very high, i.e., no borings with blowcounts less than 10 were found next to borings greater than 25. These contours of minimum blowcount indicate that blowcounts beneath the dam are not lower than 10 blows per foot. At the same station where the low blowcounts in Figure 75 were found, the lowest corrected blowcounts through the crest are 38.

For the length where very low blowcounts were found (Station 164 + 50 - 167), the suspect sand layer was modeled with three characterizations of blowcount resistance. Upstream of the crest, the suspect sand layer was assigned a corrected blowcount of 40. Downstream from about the embankment toe, the layer was assigned a corrected blowcount of 10. The 10-blowcount characterization was determined from the 35

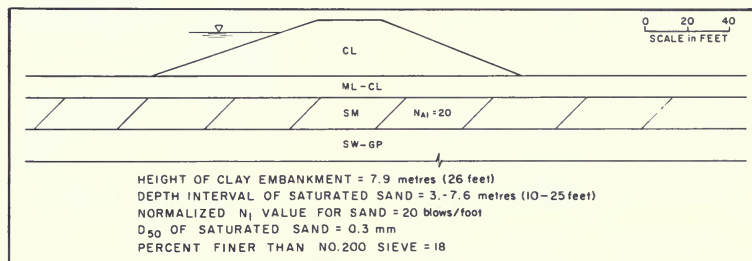


Fig. 73. Model Developed for Analysis of Station 107 (Site 1)

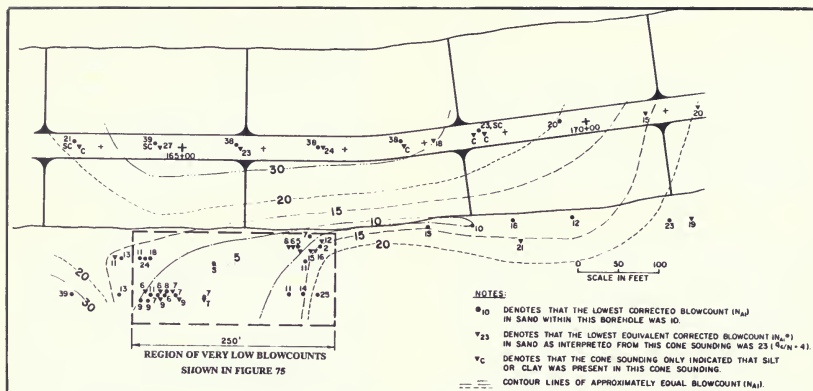


Figure 74. Minimum Corrected SPT Resistance Within Borings and Soundings Between Stations 164 and 171

percentile blowcount for toe borings in the area of lowest penetration resistance (Figures 74 and 75). For the middle region beneath the downstream slope, the blowcount was assigned a value of 20 blows per foot. This value was developed from the contour lines of minimum blowcount shown in Figure 75.

The gradation ranges for the suspect sands are shown in Figure 77. Figure 78 presents the  $D_{50}$  values and percentage of fines for samples whose blowcounts are shown in the bracketed region in Figure 75. The mean  $D_{50}$  is 0.20 millimeters and the mean percentage of fines is 25 percent.

The model developed for this site is shown in Figure 79.

### C. Model 3 – Station 347 (Columbia Soil)

This site was chosen because it is the most critical location in the Columbia Soil Area. Unlike the sections in the Red Bluff Formation, the Columbia Soil Area embankments incorporate a downstream berm. Figure 80 shows the material types and normalized blowcounts from SPT borings made between Stations 344 and 350.

The general description of the foundation material is a 10- to 15-foot thickness of silt and clay overlying a thick gravel layer. At certain locations, a low blowcount silty

sand layer exists between these two materials. Figure 80 shows at Borehole 81A-C347-SPT an apparent channel or depression eroded into the gravel and filled with low blowcount silts and sands. However, this channel or depression must be less than 100 feet wide because boreholes and cone soundings straddling this borehole

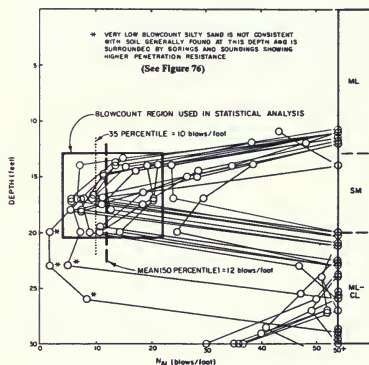


Figure 75. Corrected Standard Penetration Resistance Along Toe Between Stations 164 and 167

50 to 100 feet away did not find it. Borings along the downstream toe also failed to find it.

Figure 80, however, shows low blowcounts in material between Elevations 93 and 97 feet in boreholes between Stations 348 and 349. Table 19 presents the corrected blowcounts and material types between Stations 344 and 350 for Elevations 91 and 101 feet. The gradations of the sandy materials are shown in Figure 81.

Despite the large non-homogeneity of material at this elevation and station, it was decided to analyze for the possibility of a continuous low blowcount sand layer. Therefore, a model was developed that had a 9-foot thickness with an assigned corrected blowcount of 21. This blowcount was obtained by taking the mean of all blowcounts between Elevations 91 and 101 feet, which

were obtained in sandy material and which were less than 30 blows per foot. This characterization is considered extremely conservative.

Figure 81 presents the gradation range of silty sands found between Stations 344 and 348 and between Elevations 91 and 101 feet. The mean  $D_{50}$  for these samples was found to be 0.13 millimeters and the mean percentage of fines is 34 percent. The model developed for this site is shown in Figure 82.

The models for these three sites all incorporate a degree of conservatism in the characterizations of blowcounts. If mean blowcounts had been adopted instead, then the cyclic strengths assigned to the layer would be expected to be between 20 to 50 percent higher.

**Table 17. Corrected SPT Blowcount ( $N_{A1}$ ) Distribution Along the Downstream Toe Between Stations 164—167 (blows/ft)]**

Borehole	Station	Depth, ft			
		14-15	17-18	20-21	23
81A-165 SPT D	164 + 53	17	11		
81A-167 SPT L	164 + 54	13	9	70 +	84 +
81A-165 SPT E	164 + 59	24	24		
81A-165 SPT A	164 + 60	16	10	70 +	60
81A-165 SPT F	164 + 65	29	18		
81A-167 SPT H	164 + 66	11	13	68	50
81A-165 SPT B	164 + 78	7	7	70 +	70 +
81A-167 SPT K	164 + 83	13	6	70 +	66
81A-165 SPT C	164 + 85	16	8	61	70 +
81A-167 SPT G	164 + 95	11	7	70 +	51
81A-167 SPT F	165 + 30	27	7	82	54
81A-166 SPT	165 + 50	28	5	70 +	71
81A-167 SPT D	166 + 40	19	20	11	64
81A-167 SPT A	166 + 49	60	6	7	5*
79-167 SPT	166 + 55	19	11	66	47
81A-167 SPT E	166 + 56	21	20	14	60 +
81A-167 SPT C	166 + 65	35	7	9	47
81A-167 SPT N	166 + 73	38	30	25	94
81A-167 SPT B	166 + 79	67	11	2*	2*

\*Denotes very low blowcount sand that is not inconsistent with the soil generally found at this depth and that is surrounded by borings and soundings showing higher penetration resistance (see Figure 76 on page 123).

**Note:** Tables 18, 19, and Figures 76—82 follow

**Table 18. Corrected SPT Blowcount ( $N_{A1}$ ) Distribution Beneath the Embankment Crest  
Between Stations 164—170  
(blows/ft)**

Borehole	Station	45-46	47-49	50-52	53-55	56-58
81A-C164 SPT	163 + 68	21	52	39	36	33
81A-C165 SPT	164 + 68	41	39	50 +	49	49
81A-C166 SPT	165 + 68	50 +	50 +	50 +	50 +	50 +
81A-C167 SPT	166 + 68	50 +	50 +	38	45	50 +
81A-C168 SPT	167 + 68	50 +	44	38	50 +	43
81A-C169 SPT	168 + 68		38	26	23	38
81A-C170 SPT	169 + 68	50 +	24	26	20	22

**Table 19. Corrected SPT Blowcount ( $N_{A1}$ ) Distribution Between Stations 344—350  
(blows/ft)**

Borehole	Location	Station	Elevation, ft			
			98-101	95-97	93-94	91
81A-C344SPT	Crest	344 + 50	55 ML	29 ML	70 + G	G
AB-52	D/S Toe	≈345	SM	ML	SM	G
P-98	D/S Toe	≈346	CL	G		
81A-C346SPT	Crest	346 + 44	50 +	34 ML	70 SM	
81A-347SPT	D/S Toe	346 + 90	CL	7 CL	22 SM	70 + G
81A-C347SPT	Crest	347 + 00	32 SC	18 SM	21 SC	16 SM
81A-348SPT	D/S Toe	347 + 90	20 CL	14 ML	G	
81A-C348SPT	Crest	348 + 06	56 ML	20 SM	28 SM	
81A-C349SPT	Crest	349 + 00	27 CL	G		
81A-C350SPT	Crest	350 + 00	47 ML			

Note: CL denotes clay  
ML denotes silt  
SC denotes clayey sand  
SM denotes silty sand  
G denotes gravel

Assumed value for a possible silty sand layer between Elevations 90-99:

$$N_{A1} = 21, D_{50} = 0.13$$





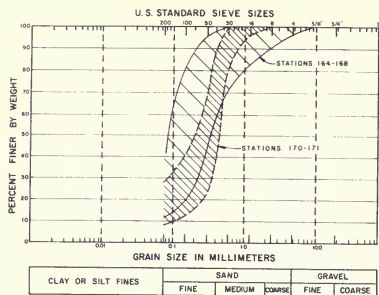


Figure 77. Gradation Envelope of Samples Collected from Stations 164-171 Representing Suspect Layer for Model 2 (Worksite 2)

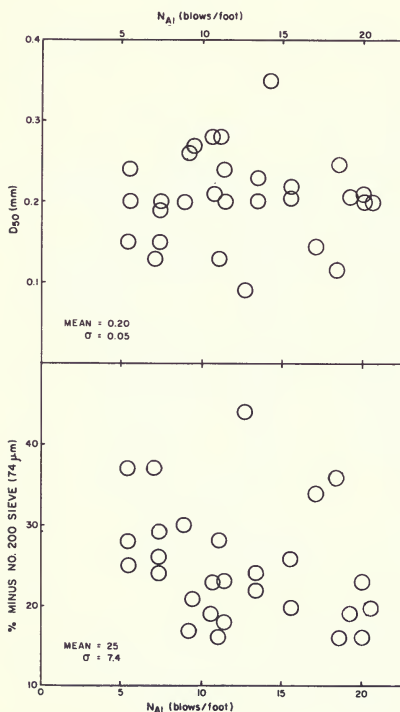


Figure 78. Gradation Characteristics of Low Blowcount Sands Between Stations 164 and 167

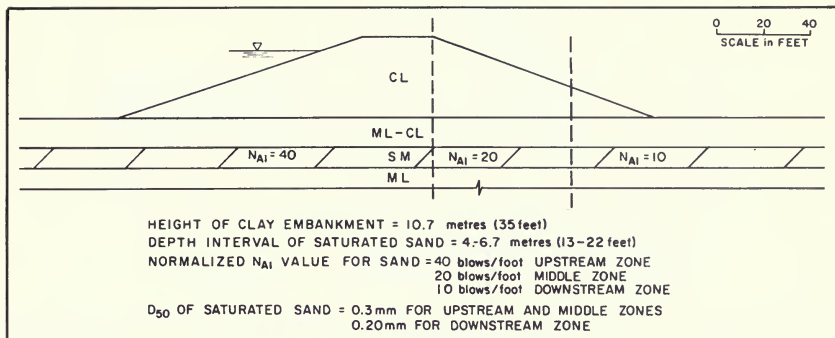


Figure 79. Model Section Developed for Analysis of Station 165 (Worksite 2)

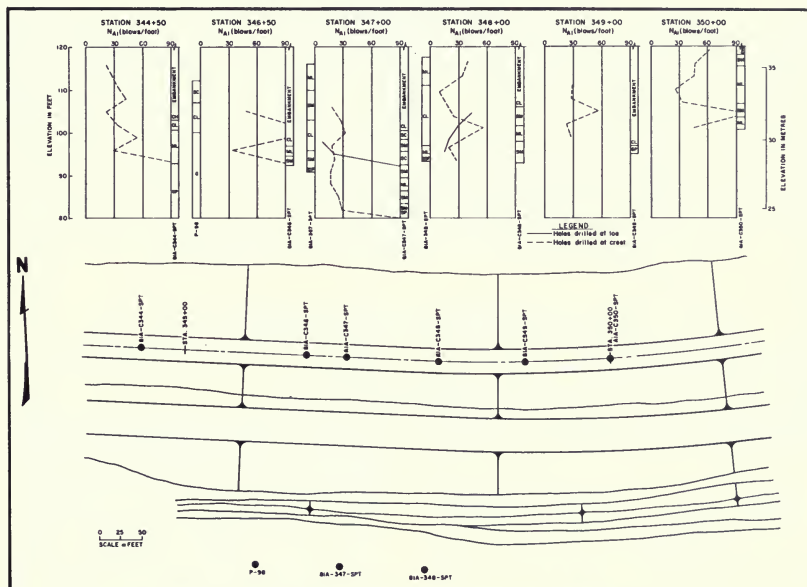


Figure 80. Corrected SPT Resistance at Thermalito Afterbay Dam Stations 344 to 350

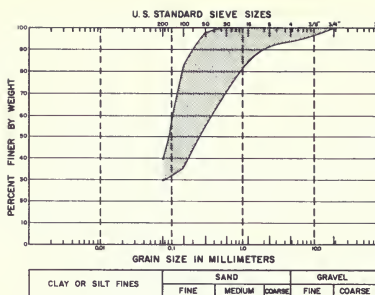


Figure 81. Gradation Envelope of SPT Silty Sand Samples Collected from Stations 344 to 348 and between Elevations 91-101 feet

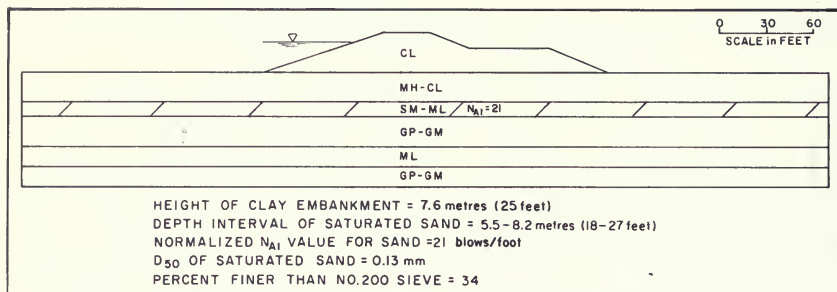


Figure 82. Model Section Developed for Analysis of Station 347 (Columbia Soil)

## 5. ANALYSIS OF STATIC STRESSES

The behavior of an embankment dam subjected to dynamic loading is significantly influenced by the stress conditions existing in the embankment prior to earthquake shaking. Therefore, a reasonable estimate of the static stresses must be made to determine the embankment's dynamic stability.

To estimate the static stresses, the finite element method was chosen. Finite element meshes were constructed to represent the geometry and conditions existing at each of the three suspect locations chosen for analysis. Each mesh extends all the way through the upper soils formation down to the surface of the Mehrten Formation. Figures 83 through 85 show the meshes used in the static

stress analyses for Station 107 (Site 1), Station 165 (Worksite 2), and Station 347 (Columbia Soil).

Two static finite element analyses were carried out for each mesh. One was for a full reservoir, Elevation 136.5 feet, and the other was for a lowered reservoir, Elevation 128 feet. The downstream water levels for the lower reservoir condition (Elevation 128 feet) were determined by piezometers installed at each of the three critical sites. Since groundwater levels were unavailable for conditions when the reservoir was held full (Elevation 136.5 feet) for a sustained period, downstream water levels for full reservoir were estimated. The downstream water levels used in the seismic analyses are listed on page 128.

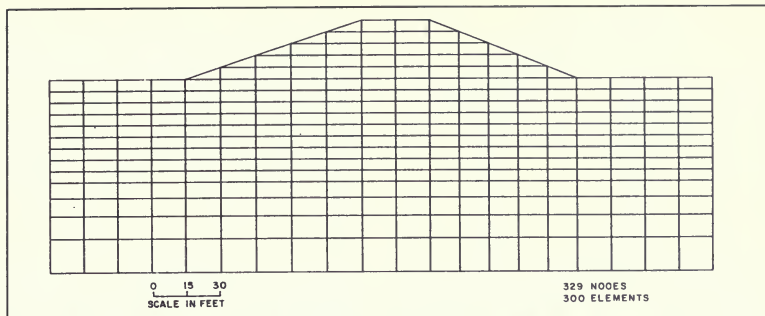


*Figure 83. Finite Element Mesh Used in Static Stress Analysis for Thermalito Afterbay Dam Station 107 (Site 1)*

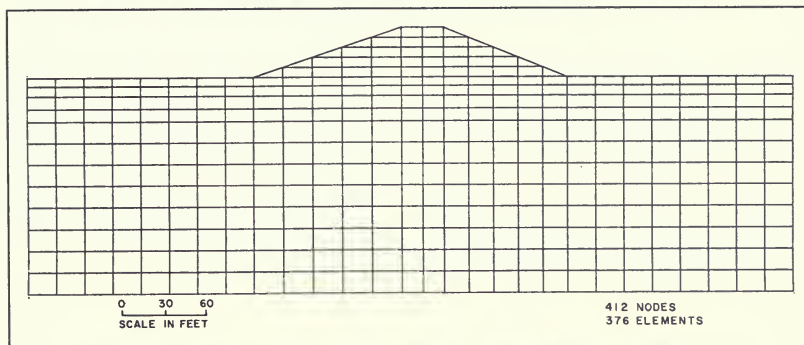


*Figure 84. Finite Element Mesh Used in Static Stress Analysis for Thermalito Afterbay Dam Station 165 (Site 1)*

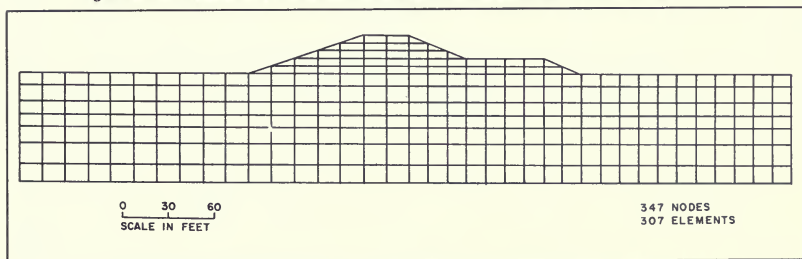


*Figure 85. Finite Element Mesh Used in Static Stress Analysis for Thermalito Afterbay Dam Station 347*

(From page 126)

Site	Reservoir Elevation	Depth Below Ground Level for Downstream Water Level
Station 107	128.0 feet	8 feet
	136.5 feet	6 feet
Station 165	128.0 feet	6 feet
	136.5 feet	0 feet
Station 347	128.0 feet	0 feet
	136.5 feet	0 feet

Flow nets were constructed to represent the two different seepage conditions by using a transformed section and assuming a horizontal permeability equal to 16 times the vertical permeability. The flow nets developed for each location are shown in Figures 86 through 88.

For each reservoir elevation, seepage and buoyancy forces were simulated by equivalent nodal forces. An in-house computer program, NODALFOR, was used to calculate these equivalent nodal forces. The calculated seepage and buoyancy forces were used in the subsequent static finite element analyses.

Computer program TWIST was used in the calculation of static stresses. TWIST is an in-house, improved version of program 4-CST and uses a quadrilateral element that is subdivided into two incompatible linear strain triangles. The program uses linear material properties.

Soil parameters necessary for the static analysis consisted of soil density, Young's modulus, and Poisson's ratio. Densities were obtained from values determined from recovered samples. Young's modulus and Poisson's ratio values were calculated from hyperbolic stress strain parameters used to define the initial tangent modulus and Poisson's ratio of similar soils. These parameters were obtained for similar soils from typical values published by Wong and Duncan (1974). The values chosen for each analysis are presented in Figures 89 through 91.

Studies by Lee and Idriss (1975) have shown that linear elastic gravity turn-on analyses predict virtually the same static stress distribution as the more sophisticated non-linear analyses by computer programs such as ISBILD. These studies have also shown that the results are not overly influenced by the choice of material properties.

In analyzing liquefaction potential for dams, the Seed-Lee-Idriss Method assumes that the stresses on the horizontal plane govern behavior. Therefore, the items of interest from a static stress analysis are the vertical effective normal stress ( $\sigma_y'$ ) and the horizontal shear stress ( $\tau_{xy}$ ). The horizontal shear stress is usually represented by the alpha value. The alpha value is the ratio of horizontal shear stress to vertical effective normal stress. Contours of the vertical normal stresses and the alpha values for the models analyzed are displayed in Figures 92 through 94 for both reservoir conditions.

Figures 86 through 94 follow.

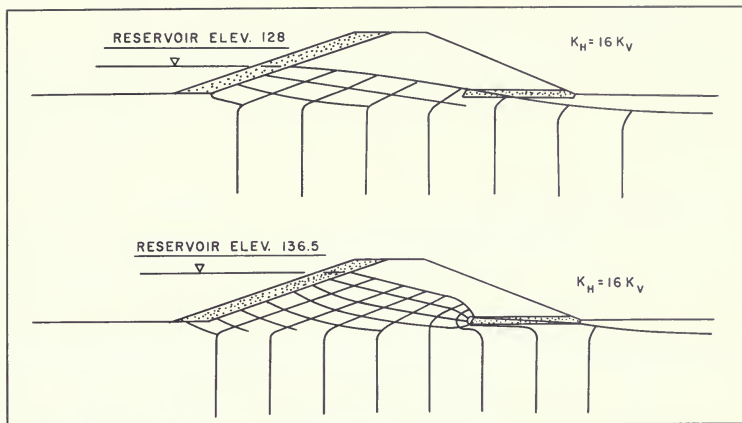


Figure 86. Flow Nets Assumed for Static Finite Element Analysis of Thermalito Afterbay Station 107 (Site 1)

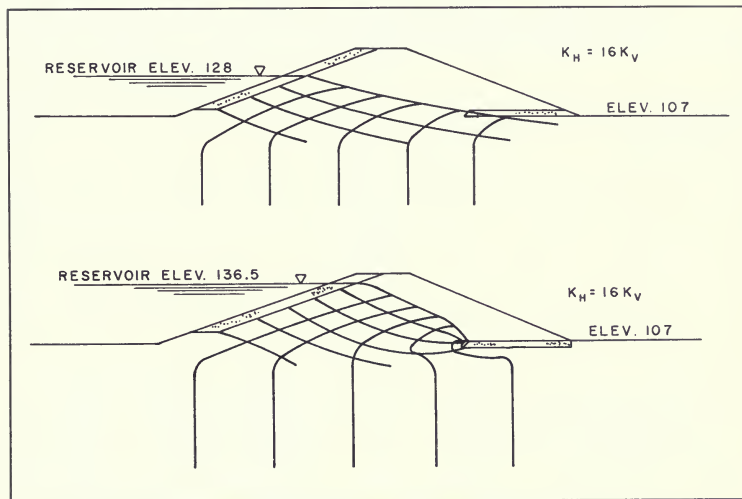


Figure 87. Flow Nets Assumed for Static Finite Element Analysis of Thermalito Afterbay Station 165 (Worksite 2)

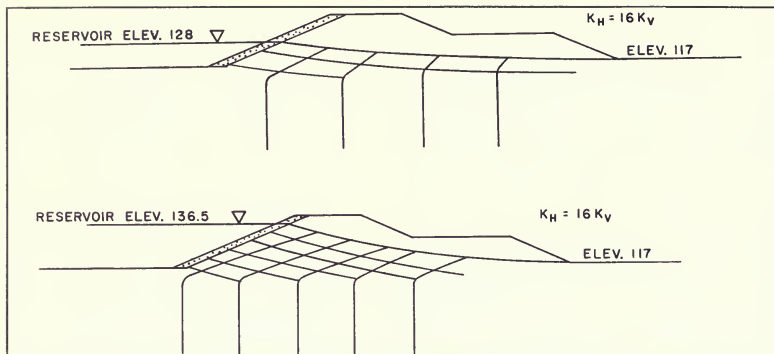


Figure 88. Flow Nets Assumed for Static Finite Element Analysis of Thermalito Afterbay Columbia Soil (Stations 348 and 351)

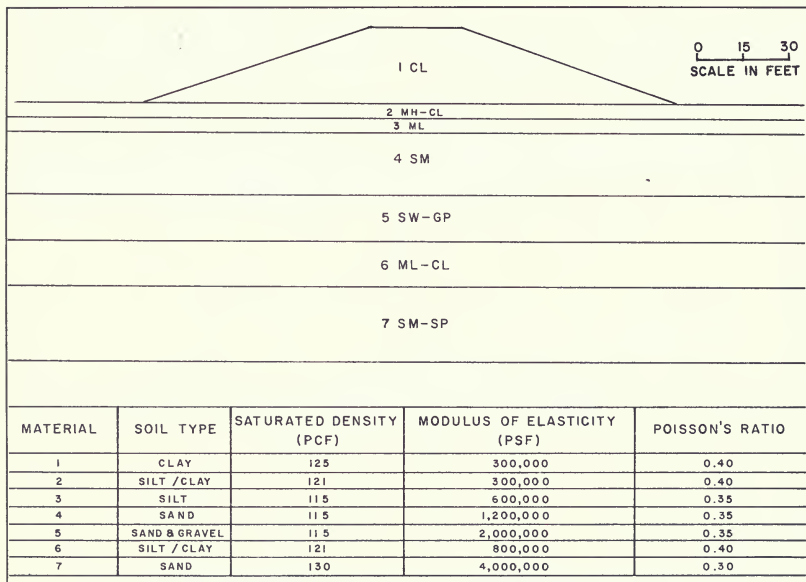


Figure 89. Thermalito Afterbay Station 107 (Site 1) Embankment and Foundation Profile with Stress-Strain Parameters Used in Static Finite Element Analysis



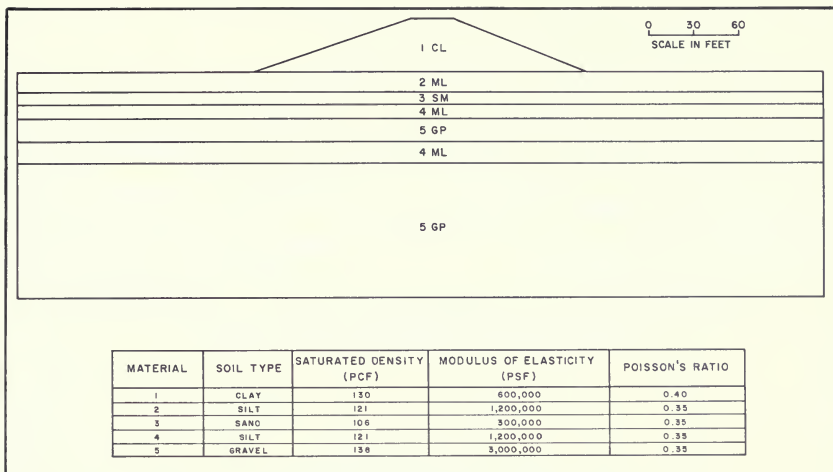


Figure 90. Thermalito Afterbay Station 165 (Worksite 2) Embankment and Foundation Profile with Stress-Strain Parameters Used in Static Finite Element Analysis

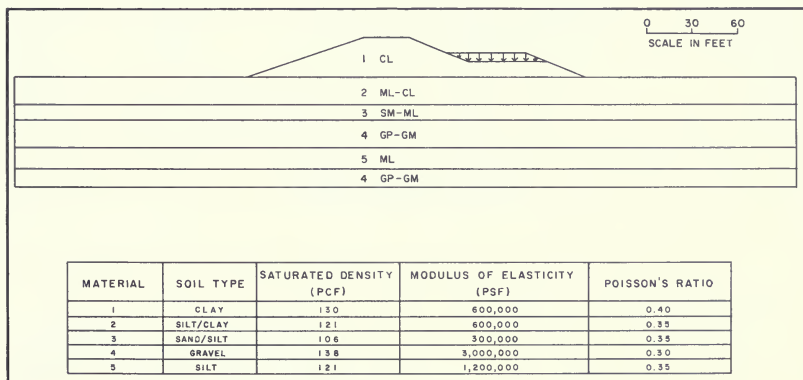


Figure 91. Thermalito Afterbay Station 347 (Columbia Soil Area) Embankment and Foundation Profile with Stress-Strain Parameters Used in Static Finite Element Analysis

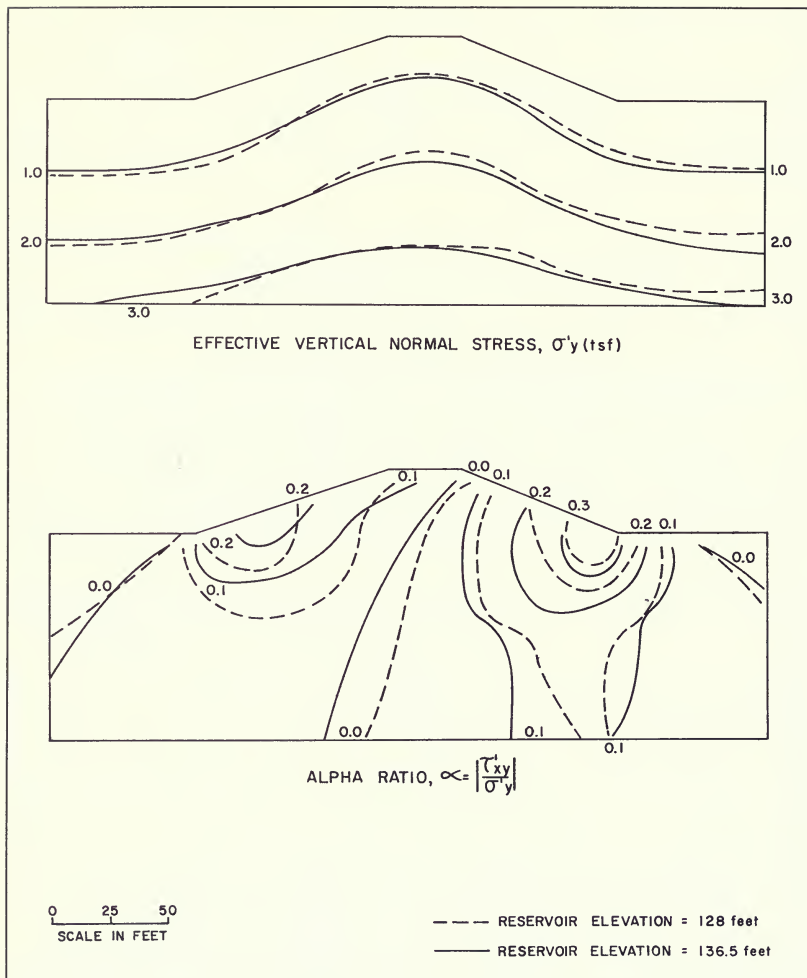


Figure 92. Contours of Effective Vertical Normal Stress and Alpha Values Determined from Static Finite Element Analysis of Thermalito Afterbay Station 107 (Site 1)

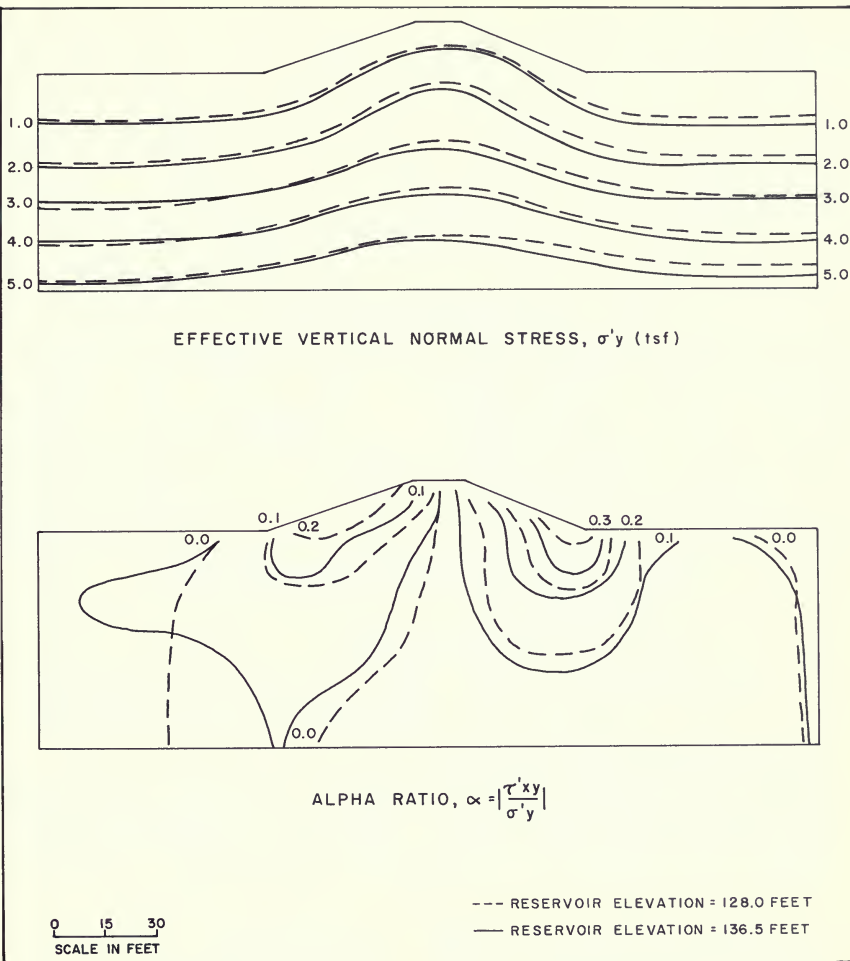


Figure 93. Contours of Effective Vertical Normal Stress and Alpha Values Determined from Static Finite Element Analysis of Thermalito Afterbay Station 165 (Worksheet 2)

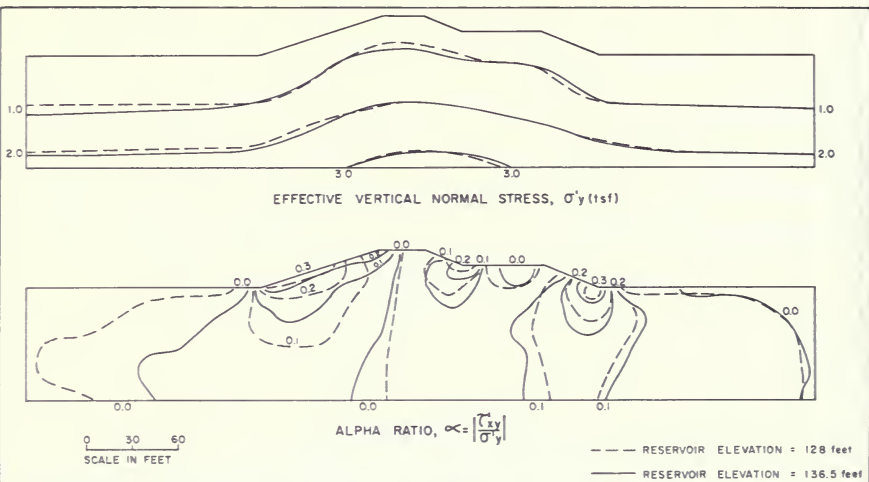


Figure 94. Contours of Effective Vertical Normal Stress and Alpha Values Determined from Static Finite Element Analysis of Thermalito Afterbay Station 347 (Columbia Soil Area)

## 6. Earthquake Motions

### Background

On August 1, 1975, a Richter Magnitude 5.7 earthquake occurred approximately 7.5 miles southwest of Oroville Dam near the town of Palermo. The earthquake sequence and associated surface cracking revealed a previously unidentified "active" fault (Figure 95.) A detailed discussion of the geological and seismological studies performed is presented in Chapters II, III, and IV of Bulletin 203-78.

Shortly after the 1975 Oroville Earthquake, the Special Consulting Board for the Oroville Earthquake recommended that the original appraisals of probable future regional seismicity in the site areas be revised. In a report dated August 11, 1975, the Board stated:

"... In view of the developments, it is appropriate to consider that earthquakes ranging up to Magnitude 6.5 may occur within a few miles of the [Oroville] dam site. . ."

Consequently, a program for the dynamic structural analysis of critical structures within the Oroville-Thermalito complex was implemented. The structures defined as critical and included in the program were identified in Bulletin 203-78 as:

- Oroville Dam
- Oroville Dam Spillway
- Thermalito Diversion Dam
- Thermalito Powerplant Headworks
- Thermalito Forebay Dam
- Thermalito Afterbay Dam

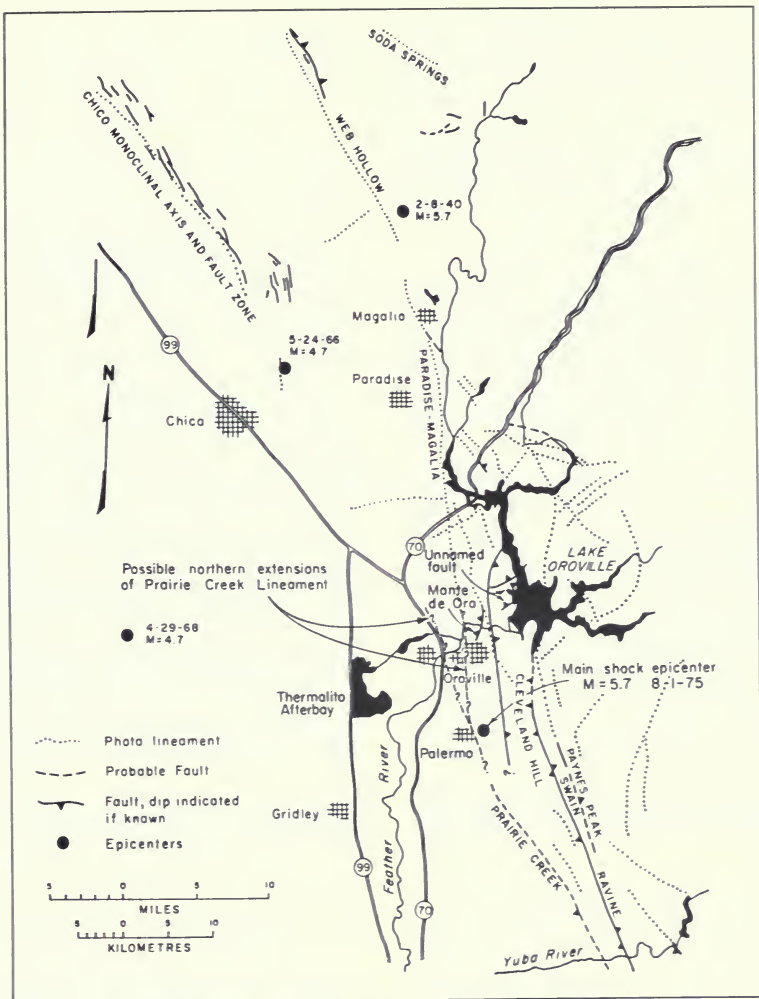


Figure 95. Lineaments, Faults, and Recorded Epicenters Around Thermalito Afterbay

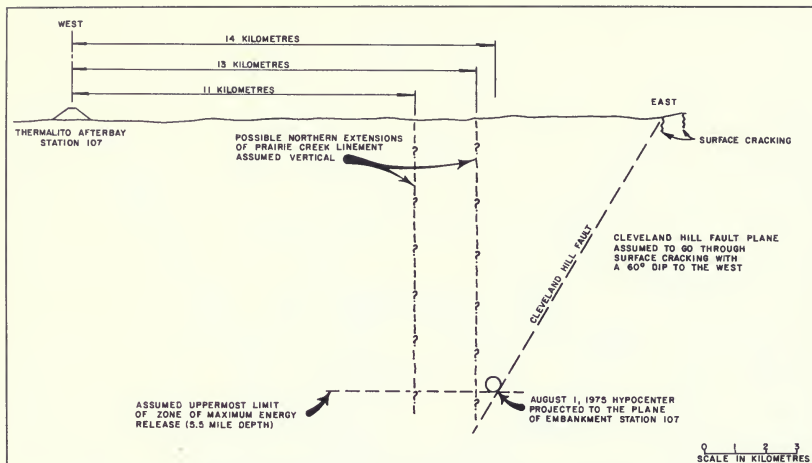


Figure 96. Relationship of Thermalito Afterbay to Assumed Fault Projections

An earthquake accelerogram or accelerograms were needed for analyzing the stresses induced by the postulated future Magnitude 6.5 earthquake. In a report dated September 12, 1975, the Board recommended:

"... that an appropriate earthquake motion for re-evaluation of structures critical to public safety in the Oroville-Thermalito complex would be one producing a peak acceleration of 0.6g and having characteristics similar to those developed near Pacoima Dam during the San Fernando earthquake of February 9, 1971..."

The Board also stressed in that report that this 6.5 magnitude represented a very conservative loading condition:

"... the Special Board emphasizes that the hypothetical maximum earthquake of Magnitude 6.5 mentioned in the Earthquake Board's report of 11 August 1975 is considered to be a very unlikely event and is intended to be used for safety review. Furthermore, it is our judgment that any earthquake significantly stronger than the Magnitude

5.7 event of 1 August 1975 is improbable in the near future. ..."

The motion finally developed was a combination of the 1971 Pacoima Dam S 16 E record and the first ten seconds of the 1952 Taft S 69 E record. The motion was scaled to have a peak acceleration of 0.6g and a total duration of 20 seconds. This motion was used to analyze Oroville Dam, Oroville Dam Spillway, the Thermalito Diversion Dam, and the Thermalito Powerplant Headworks, and was identified as the Oroville Reanalysis Earthquake. Further details concerning this motion are presented in Chapter V of Bulletin 203-78.

In 1976, the Board was asked if new information concerning the seismicity of the region had altered the original recommendation of analyzing for a future Magnitude 6.5 event. In a report dated November 23, 1976, the Board responded with the following statements:

"... Since the last meeting of the Board, substantial investigations of past and potential future seismic activity along the western Sierra Nevada have been made by the Department of Water Resources, by Woodward Clyde Consultants, and by the U. S. Army Corps of Engineers. We are not

aware that these investigations have produced any information to date which would cause the Board to change the earthquake motion it recommended in its response to Question No. 4 in the report of 12 September, 1975 for seismic re-evaluation of the Oroville-Thermalito Structures. . . .”

“... the most critical portions appear, at this time, to be some locations along the Thermalito Forebay and Afterbay Dams. Accordingly, it is recommended that locations of critical sections of these dams be determined on the basis of the existence of low density soils, particularly loose sands, in the foundation. Field sub-surface explorations, followed by analyses of these sections under the effects of the ‘re-evaluation earthquake’ should be carried out on an urgent basis and, where potential instability may be indicated, corrective designs should be developed and the construction accomplished as soon as possible.”

The initial analyses of Thermalito Afterbay Dam in 1976-78 were conducted using the Oroville Reanalysis Earthquake motion as the applied loading. By the spring of 1979, after further consideration by the Department of Water Resources (DWR) staff and the Special Consulting Board, it was decided that the Oroville Reanalysis Earthquake motion was not appropriate for use in analyzing the Thermalito Afterbay Dam. Two characteristics of the Thermalito Afterbay Site formed the basis for that decision:

1. Thermalito Afterbay Dam is significantly farther away from potential earthquake sources than either Oroville Dam or Thermalito Diversion Dam.
2. Thermalito Afterbay Dam is founded on soil, not on rock as are Oroville Dam and Thermalito Diversion Dam.

These characteristics would considerably modify not only the level but the spectral content of ground motions at the site.

In their report dated May 13, 1979, the Board suggested that a free-field ground surface motion of about three quarters the Oroville Reanalysis Earthquake motion would be appropriate if the dam were founded on rock. However, since the structure is founded on soil, further definition of the dynamic properties of the underlying soil would be required before appropriate ground mo-

tions could be developed. The Board went on to suggest specific investigations of the site and also suggested that useful information would be gained if a preliminary seismic evaluation were carried out using the 1940 El Centro accelerogram as the free-field surface ground motion at the afterbay.

As a result of the foregoing, an extensive program was undertaken to further define the foundation characteristics at depth and to estimate the appropriate ground motions for the afterbay.

### Foundation Characteristics

As described in Section 4, the afterbay is founded on Red Bluff Formation or on alluvial soils overlying Red Bluff Formation. Beneath the Red Bluff Formation lies the older, more consolidated Mehrten Formation. Depths to the Mehrten vary from about 65-200 feet. The shear wave velocity of the Mehrten Formation is somewhere between 2,200-2,850 ft/sec within the upper 100 feet at Station 107 (Site 1).

Several empirical studies, such as those by Seed et al. (1975), and Idriss and Power (1978) have subdivided soil sites into two basic categories:

#### - *Stiff Soil Sites:*

Composed of stiff soils underlain by a rock-like material. The rock-like material is considered to be shale-like or sounder, as evidenced by a shear wave velocity of about 2,500 ft/sec. The depth to rock-like material is no greater than 150-200 feet.

#### - *Deep Soil Sites:*

These sites contain more than about 200-250 feet of soil above a rock-like material.

Using these definitions, the Mehrten Formation can be classified as a rock or rock-like material. The foundation profiles along the Afterbay Dam are, therefore, classed as stiff soil sites.

### Pertinent Faults

The Cleveland Hill Fault is the fault which ruptured in 1975 and is the only known active fault in the area. It has a northerly trend and dips approximately 60 degrees to the west. Figure 95 shows the location of the afterbay relative to the Cleveland Hill Fault.

**Table 20. Ranges of Source-to-Site Horizontal Distances for Thermalito Afterbay Dam**

Fault	Source-to-Site Horizontal Distances, miles		
	Station		
	107	165	347
Cleveland Hill	9	9	6
Possible Prairie Creek Lineament Extension Trending Through Oroville	8	8	6
Possible Prairie Creek Lineament Extension Trending Near Thermalito Forebay	7	7.5	5.5

Subsequent to the initial evaluations of earthquake motions, additional consideration was given to the Prairie Creek Lineament. This lineament ends about 8 miles south of Oroville. However, the bedrock fault zone may be assumed to extend northward, concealed by the onlapping valley sediments (Reference 17). Evidence suggesting northward extension of the "Prairie Creek Lineament Fault Zone" includes (1) a linear array of local lurch crack sites along this extension; (2) the occurrence of a few deep aftershocks northwest of Oroville which coincide with this alignment; (3) apparent stratigraphic discontinuities or abrupt changes in stratigraphic gradients across the extension, and, (4) if extended far enough, the occurrence of several faults which do cut Cenozoic units and trend in the same direction as the extension. It is assumed that this fault zone is capable of producing the same magnitude earthquake postulated for the Cleveland Hill Fault.

The Prairie Creek Lineament Fault Zone is probably steeply dipping or vertical, possibly merging with the westerly dipping Cleveland Hill Fault at depth. Figures 95 and 96 illustrate the relationship of the Afterbay Dam with both the Cleveland Hill Fault and the possible extension of the Prairie Creek Lineament Fault Zone.

Table 20 lists the range of horizontal distances from the three modeled sites to the two fault zones. The horizontal distances to the Cleveland Hill Fault were determined by assuming a depth of 5.5 miles to the energy source and projecting vertically to the surface. Two horizontal distance ranges are shown in Table 20 for the Prairie Creek Lineament Fault Zone, one for a possible extension trending near Thermalito Forebay, the other for a possible extension trending through the town of Oroville (see Figures 95 and 96).

The numbers in Table 20 show that the source-to-site horizontal distances for the three modeled sites range be-

tween 5 to 9 miles. The source-to-site distances from the other suspect sites all fall within this range. A single source-to-site horizontal distance of 7 miles was selected for all sites along the afterbay. This would mean that sites along Highway 99, such as Station 165, have been analyzed with accelerations that are slightly too high, and that sites near Station 347 (river outlet) have been analyzed with accelerations that are slightly too low. However, the differences are considered minor. For a 7-mile distance, a 1-mile change would alter the maximum acceleration by approximately 0.03g.

### Selection and Scaling of Accelerograms

Current practice is to estimate appropriate ground motion characteristics from correlations developed from recorded earthquake accelerograms. The significant parameters for estimating these characteristics are the magnitude of the earthquake, distance from energy source to site, and foundation characteristics of the site. These characteristics can then be used to choose and modify existing records to be used as the loading for the site in question.

The selection of a 6.5 magnitude was recommended by the Special Consulting Board. The Department interpreted this selection as being very conservative for the conditions at Oroville. The Board's comments support this interpretation. In selecting ground motion parameters for a 6.5 magnitude event, the Department decided to use mean values for peak acceleration and spectral content. Although it has become increasingly common to use an 84th percentile (mean plus one standard deviation) instead of the mean for either peak acceleration or the spectral content, it was judged, with the conservatism already included in the selection of the 6.5 magnitude,



**Table 21. Comparison of Approaches for Selecting Earthquake Motion Parameters**

Magnitude	Spectral Content	Peak Acceleration $a_{max}$ (g)	$R = (\tau_{eq}/\tau_{max}) \times 15 \text{ cycles}$	Average Acceleration $R \cdot a_{max}$ (g)
6.5	(mean)	0.35 (mean)	0.56 (mean)	0.20
6.25	(mean)	0.41 (mean + $\sigma$ )	0.49 (mean)	0.20

that additional conservatism in the earthquake motion parameters was inappropriate.

For a stiff soil site located 7 miles horizontally away from the causative energy source, the mean value for peak acceleration according to Seed and Idriss (1982) would be about 0.35g. The ratio ( $R$ ) of equivalent stress for 15 uniform cycles ( $\tau_{eq}$ ) to the peak stress derived from a magnitude 6.5 time history ( $\tau_{max}$ ) would be about 0.56 (Reference 41). These values were adopted together with a mean spectral content for the earthquake motions used in re-analyzing Thermalito Afterbay Dam.

Alternatively, the Department could have selected the same parameters by going through a slightly different approach. If the Department had selected a less conservative magnitude, such as 6.25, for re-evaluating Thermalito Afterbay Dam, then extra conservatisms in either peak acceleration or spectral content would be appropriate. The 84th percentile value for peak acceleration for a 6.25 magnitude event would be about 0.41g and the ratio ( $R$ ) of equivalent stress for 15 cycles to the peak stress from a 6.25 magnitude event would be about 0.49 (Reference 41).

For comparison between the two approaches, the value that is appropriate to be compared is the average acceleration. The average acceleration is the product of the peak acceleration ( $a_{max}$ ) and the equivalent stress ratio ( $R$ ) for 15 cycles. Table 21 illustrates how the average acceleration ( $R \cdot a_{max}$ ) is the same (0.20) for either approach. In effect, the design earthquake parameters used in this study are equivalent to the use of 84th percentile values corresponding to a magnitude 6.25 event.

Three accelerograms have been used to analyze Thermalito Afterbay Dam. Three motions were considered

necessary to account for the variability in frequency content, number of significant cycles, and total duration. The motions chosen were ground surface accelerograms recorded on soil during earthquakes with Richter magnitudes of about 6.5 and at source-to-site distances of 10 to 22 miles. Ground motions recorded on soil were picked because there are more such motions available appropriate to the earthquake magnitude and site distance than rock motions. In addition, the suspect sand layers are closer to the soil surface than the deeper rock boundary. The characteristics of the three accelerograms are listed in Table 22. All three accelerograms were scaled to have a peak acceleration of 0.35g.

Figure 97 shows the three selected accelerograms scaled to a 0.35g peak acceleration. The lengths are limited to the first 20 seconds to make the duration consistent with the Oroville Reanalysis Earthquake. The corresponding acceleration response spectra are also shown, along with the average response spectrum for stiff soil sites (Seed et al., 1974).

The predominant period varies from about 0.25 to 0.4 seconds, and the shapes of the spectra are similar and close to the average spectrum for stiff soil sites. Figure 98 shows the mean acceleration spectrum of the three selected accelerograms together with the average stiff soil spectrum developed by Seed et al (1974). The natural periods of the embankment models range between 0.3 and 0.7 seconds. Within this range, the mean of the three accelerogram spectra exceed the average stiff soil site spectrum (Seed et al, 1974) by zero to 25 percent. Therefore there is an extra conservatism in the spectral content.

The number, amplitude, and frequency of large acceleration pulses vary for the three acceleration records. It was concluded that averaging the cyclic shear stresses pro-

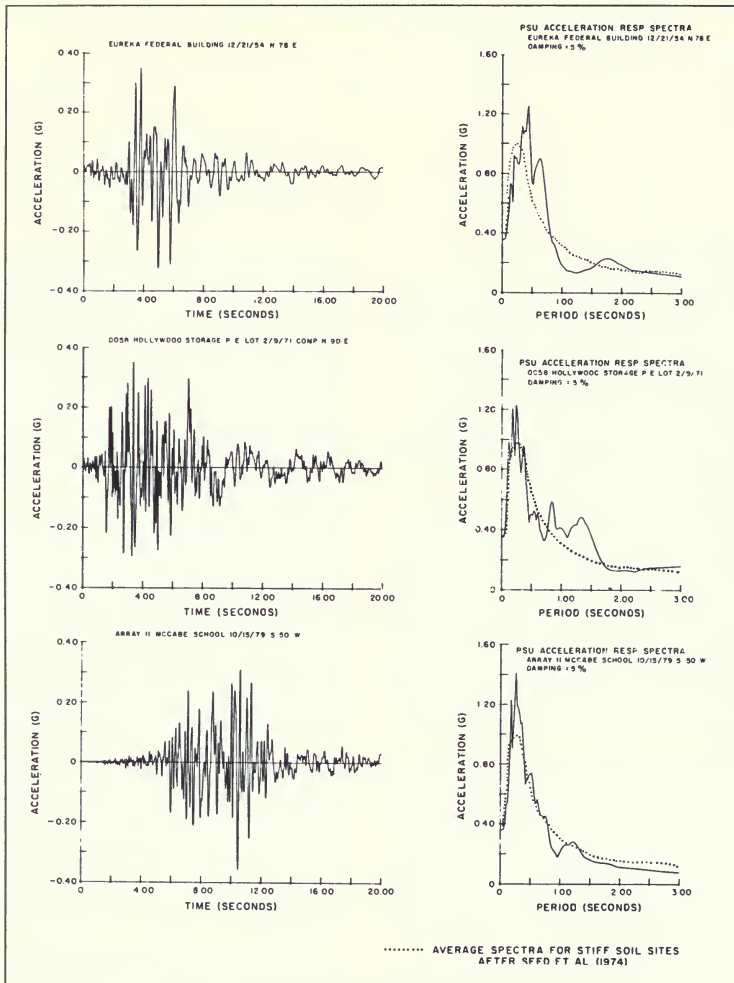
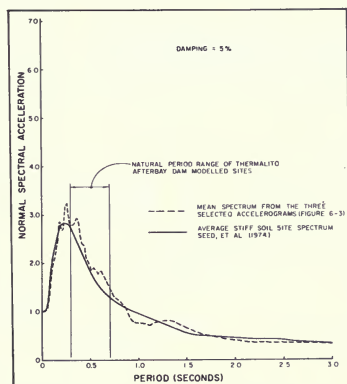


Figure 97. Design Accelerograms and Acceleration Response Spectra

**Table 22**  
**Recorded Accelerograms Selected for Developing Re-evaluation Earthquake Motions**

Earthquake	Station Location	Estimated Soil Depth (feet)	Approximate Source Distance (miles)	Original Peak Acceleration (g)	Scaling Factor to Obtain 0.35 Peak Acceleration	Instrument Component Bearing
Eureka 12/21/54 ( $M_L=6.6$ )	Eureka Federal Building	250	16	0.26	1.36	N79E
San Fernando 2/09/71 ( $M_L=6.6$ )	Hollywood Storage P.E. Lot	200	22	0.21	1.66	N90E
Imperial Valley 10/15/79 ( $M_L=6.4$ )	McCabe School Array 11	?	10	0.38	0.93	S50W

References: 1) Hudson and Brady (1971)  
2) Brady et al. (1980)  
3) Seed et al. (1974)



*Figure 98. Comparison of the Mean Spectrum of the Three Design Accelerograms to the Average Stiff Soil Site Spectra*

duced by the three accelerograms will reasonably account for overall frequency content and duration of strong shaking for earthquake magnitudes up to 6.5 occurring 7 miles from a stiff soil site.

A draft report describing the selection of proposed motions was sent to members of the Board. Their comments are contained in an August 14, 1980 letter from Professor George Housner, Chairman:

"The committee on Thermalito Dam has reviewed the draft copy of the section "Design Earthquake of the Thermalito Afterbay Dam—Evaluation of Seismic Stability Report. The following steps are planned for the analysis:

(1) A surface ground motion having 0.35g peak acceleration will be specified for the ground surface in the vicinity of Thermalito Dam. This ground motion will be in the form of magnitude  $6.5 \pm$  earthquakes.

(2) A corresponding base rock motion will be determined at depth so that when this is used as input

the calculated surface motion will reproduce the specified 0.35g recorded accelerogram. The stresses and strains in the materials beneath the surface of the ground will be calculated and the ability of the soil to survive under these deformations will be analyzed.

(3) The same base rock input motion will be used to excite a soil column beneath the dam, including the dam overburden. The calculated stresses and

strains will then be used to determine the ability of the soil material to survive.

The Committee feels that the foregoing is an appropriate method of analyzing the ability of the soil material to survive the dynamic stresses and strains. Several ground surface accelerograms should be used in the analysis, and one of these should be a record obtained on relatively hard ground."

## 7. ANALYSIS OF EARTHQUAKE INDUCED DYNAMIC STRESSES

The approach used to determine the dynamic stresses in the suspect silty sand layers was to conduct a set of one-dimensional dynamic response analyses for each of the three model sections. Analyses were carried out using several soil columns in the embankment and foundation. Eight soil columns were used at Station 107(Site 1) as illustrated in Figure 99. Station 165 (Worksite 2) involved seven columns as shown in Figure 100; and the upstream and downstream sides were analyzed separately because of the distinct difference in SPT  $N_{A1}$  value of the founda-

tion sand. Station 347 in the Columbia Soil Area was modeled using five columns as shown in Figure 101.

These one-dimensional analyses were chosen instead of two-dimensional finite element methods because of the smaller time and cost requirements. Studies such as those by Vrymoed and Calzascia (1978) and Smith (1979) have indicated that such an approach gives reasonably good agreement with the more sophisticated techniques of the finite element method. Another reason for the choice of

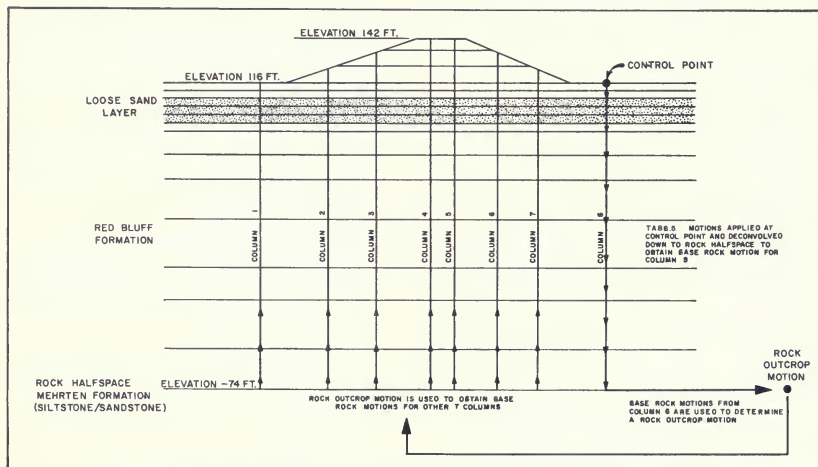


Figure 99. Shake Soil Models for Thermalito Afterbay Station 107 (Site 1)

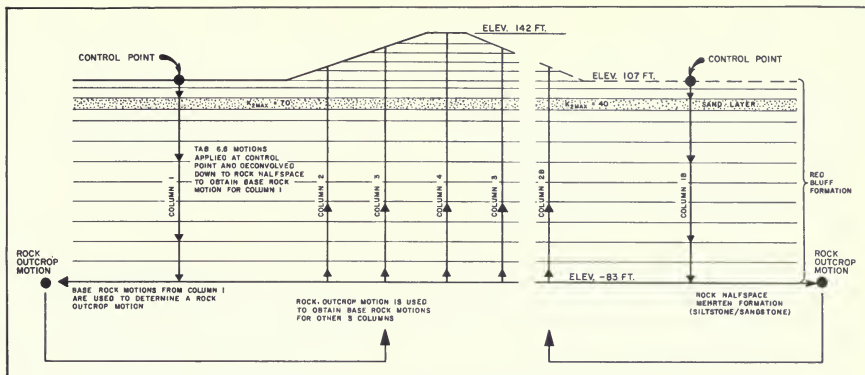


Figure 100. Shake Soil Models for Thermalito Afterbay Station 165 (Worksite 2)

the one-dimensional analysis was the necessity of deconvolving input ground surface motions down to base rock.

The computer program used in the analyses was program SHAKE, which was developed by Schnabel, et al. (1972). SHAKE vertically propagates shear waves through horizontally layered deposits by solution of the wave equation. To represent the non-linearity of dynamic soil properties, the equivalent linear method and an iterative process is used. The solution of the wave equation is done in the frequency domain with the complex response method.

The shear wave velocity results were used to define the dynamic shear modulus at low strain. Average modulus reduction and damping curves for sands and clays re-

ported by Seed and Idriss (1970) were used to represent the modulus and damping values at higher strain levels. The surface of the Mehrten Formation was adopted as base rock. A shear-wave velocity of 2,600 feet/sec was employed to represent the average stiffness of the rock half space (Mehrten). The material properties of the foundation soil columns are presented in Figure 102 through 104.

For Station 107 (Site 1), analyses were made for each of the three surface motions for the postulated 6.5 magnitude event. Each motion was input at the surface of column 8 and deconvolved down to base rock. The base rock motion is the motion at the surface of the Mehrten beneath 190 feet of overburden. The base rock motion was then converted into an outcrop rock motion, which is what

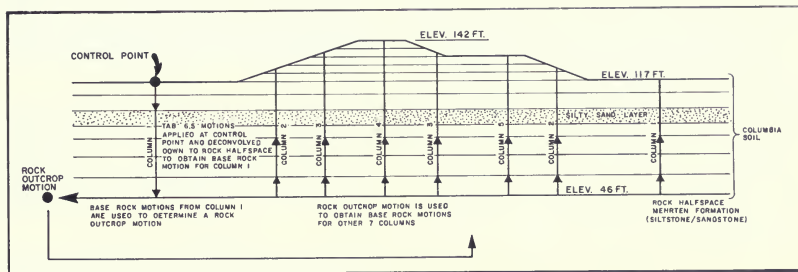


Figure 101. Shake Soil Models for Thermalito Afterbay Station 347 (Columbia Soil Area)

DEPTH (ft)	LAYER	MATERIAL	$\delta$ (pcf)	MODULUS REDUCTION AND DAMPING CURVE	MODULUS FACTOR	SHEAR WAVE VELOCITY AT LOW STRAIN (fps)	
10	1	CLAY	121	1	$S_u = 2.94$	$V_s = 1220$	REO BLUFF FORMATION
	2	SILT	115	1	$S_u = 2.42$	$V_s = 1220$	
	3	SAND	115	2	$K_{EMAX} = 85$	$V_s = 773$	
	4	SAND	115	2	$K_{EMAX} = 76$	$V_s = 775$	
	5	SAND	115	2	$K_{EMAX} = 69$	$V_s = 775$	
	6	SAND	115	2	$K_{EMAX} = 64$	$V_s = 775$	
40	7	SAND- GRAVEL	125	2	$K_{EMAX} = 380$	$V_s = 1950$	REO BLUFF FORMATION
50	8	SILT	121	1	$S_u = 6.49$	$V_s = 1950$	
70	9	SAND	125	2	$K_{EMAX} = 163$	$V_s = 1500$	
100	10	GRAVEL	135	2	$K_{EMAX} = 481$	$V_s = 2700$	
120	11	CLAY- SILT	130	1	$S_u = 6.62$	$V_s = 1900$	
150	12	GRAVEL	135	2	$K_{EMAX} = 476$	$V_s = 3000$	
180	13	SAND- CLAY	130	2	$K_{EMAX} = 226$	$V_s = 2200$	MEHRTEN FORMATION
190	14		115		$V_s = 2600$		

Figure 102. Column 8 Materials Properties for Thermalito Afterbay Station 107 (Site 1)

would occur at the surface of the Mehrten if there were no soil overburden.

The rock outcrop motion was then converted into seven base rock motions, for the overburden conditions of the seven other soil columns. These base rock motions represent the acceleration time histories at the surface of the Mehrten Formation beneath the appropriate overburden layers. The base rock motions were then propagated upward to obtain the response of the overlying soils. The process is illustrated in Figures 99 through 101. The resulting motions produced in the analyses are illustrated for columns 4 and 8 at Station 107 (Site 1) for all three accelerograms in Figures 105 through 107. This procedure has been used for projects in studies by Schnabel, et al. (1972), Seed, et al. (1974), and Pyke, et al. (1978).

The three sets of analyses produced time histories of induced shear stress for the sand layers of concern. Typical time histories are shown in Figure 108. In order to relate to cyclic triaxial test strengths, the irregular time histories were converted into 15 equivalent uniform cycles of stress with amplitudes equal to 56 percent of the peak values. This conversion was based upon values suggested by Seed and Idriss (1981).

For Station 107 (Site 1) the prediction of liquefaction potential in the sand layer at any one location employed the mean value of the three equivalent shear stresses from the design motions. The other two models were analyzed for only the McCabe School surface motion. This motion was chosen for three reasons:

1. Its acceleration response spectrum best matched the average spectrum for stiff soil sites (Figure 97).

- It required the least scaling of accelerations.
- At Station 107 (Site 1), the shear stresses induced by this motion were close to the mean of the stresses

produced by all three motions.

As at Station 107 (Site 1), the control point at the other two models for applying the motion was the surface of the foundation beyond the toe (Figures 100 and 101).

DEPTH (ft)	LAYER	MATERIAL	$\gamma$ (pcf)	MODULUS REDUCTION AND DAMPING CURVE	MODULUS FACTOR	SHEAR WAVE VELOCITY AT LOW STRAIN (fps)	
10	1	SILT	121	1	$S_u = 2.50$	$V_s = 1220$	RED BLUFF FORMATION
20	2	SILT	115	1	$S_u = 2.50$	$V_s = 1220$	
30	3	SAND	115	2	$E_{max} = 40\%$	$V_s = 525$	RED BLUFF FORMATION
40	4	SILT	115	1	$S_u = 2.50$	$V_s = 1220$	
50	5	GRAVEL	125	2	$E_{max} = 280$	$V_s = 1950$	RED BLUFF FORMATION
60	6	SILT	121	1	$S_u = 6.49$	$V_s = 1950$	
70	7	GRAVEL	125	2	$E_{max} = 165$	$V_s = 1500$	RED BLUFF FORMATION
80							
90							RED BLUFF FORMATION
100	6	GRAVEL	135	2	$E_{max} = 461$	$V_s = 2700$	
110							RED BLUFF FORMATION
120	9	SILT	130	1	$S_u = 6.62$	$V_s = 1900$	
130							RED BLUFF FORMATION
140	10	GRAVEL	135	2	$E_{max} = 476$	$V_s = 3000$	
150							RED BLUFF FORMATION
160							
170	11	GRAVEL	130	2	$E_{max} = 226$	$V_s = 2200$	RED BLUFF FORMATION
180							
12							MEHRTEN FORMATION
115							MEHRTEN FORMATION
$V_s = 2600$							MEHRTEN FORMATION

\*  $E_{max} = 70$  was used for this sand layer rest of the downstream slope segment.

Figure 103. Column 1 Material Properties for Thermalito Afterbay Station 165 Station 165 (Worksheet 2)

DEPTH (ft)	LAYER	MATERIAL	$\gamma$ (pcf)	MODULUS REDUCTION AND DAMPING CURVE	MODULUS FACTOR	SHEAR WAVE VELOCITY AT LOW STRAIN (fps)	
10	1	SILT-CLAY	115	1	$S_u = 2.42$	$V_s = 1220$	COLUMBIA SOIL
20	2	SILT-CLAY	115	1	$S_u = 2.42$	$V_s = 1220$	
30	3	SILT-SAND	115	2	$E_{max} = 70$	$V_s = 730$	COLUMBIA SOIL
40	4	GRAVEL	135	2	$E_{max} = 486$	$V_s = 1953$	
50	5	GRAVEL	155	2	$E_{max} = 486$	$V_s = 2126$	COLUMBIA SOIL
60	6	SILT	120	1	$S_u = 4.90$	$V_s = 1700$	
70	7	GRAVEL	155	2	$E_{max} = 504$	$V_s = 2456$	COLUMBIA SOIL
80							
6							MEHRTEN FORMATION
115							MEHRTEN FORMATION
$V_s = 2600$							MEHRTEN FORMATION

Figure 104. Column 1 Material Properties for Thermalito Afterbay Station 347 (Columbia Soil Area)

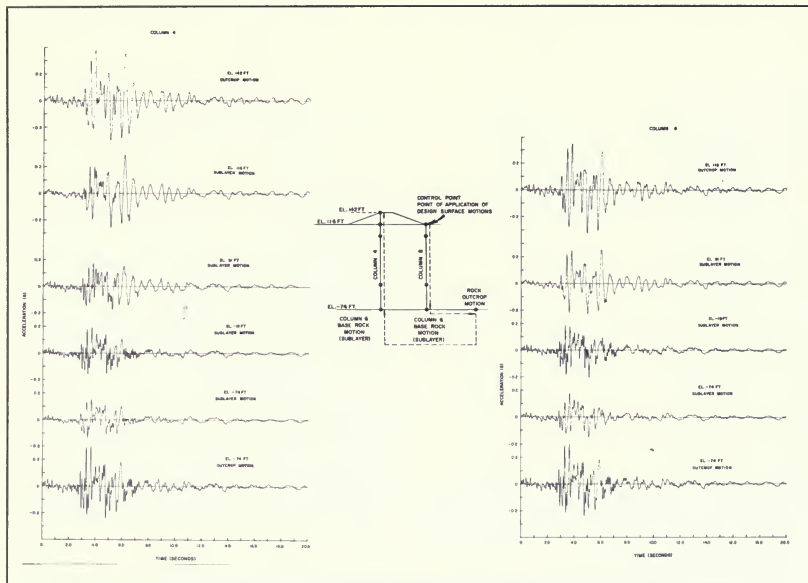


*Figure 105. Dynamic Response Motion Produced in Shake Analysis for Thermalito Afterbay Station 107 (Site 1) Using the Eureka Federal Building N79E Record*



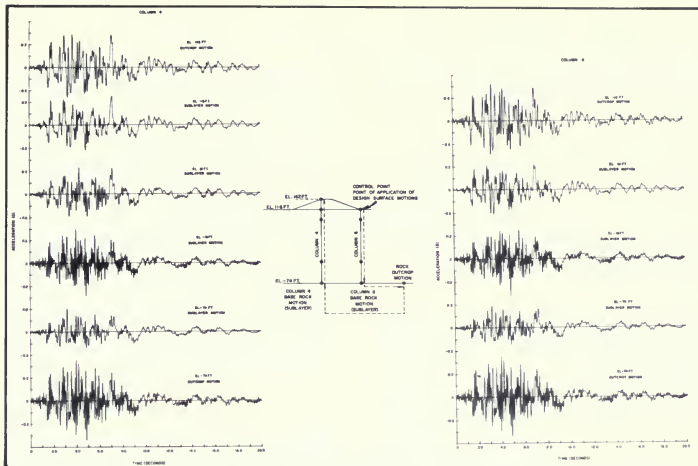


Figure 106. Dynamic Response Motion Produced in Shake Analysis for Thermalito Afterbay Station 107 (Site 1) Using the Hollywood Storage P.E. Lot N90°E Record

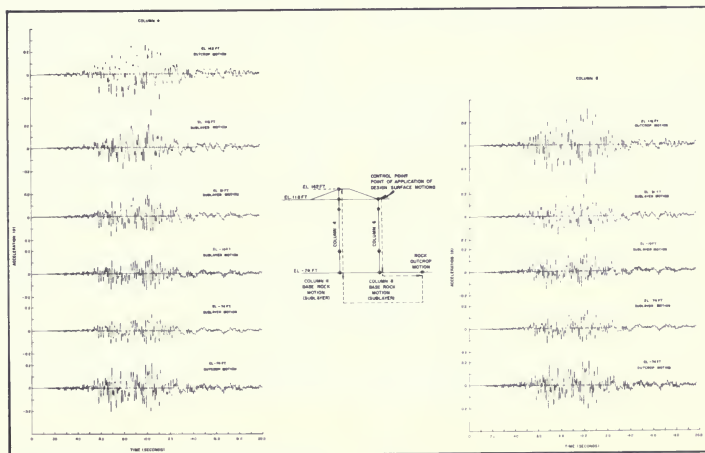
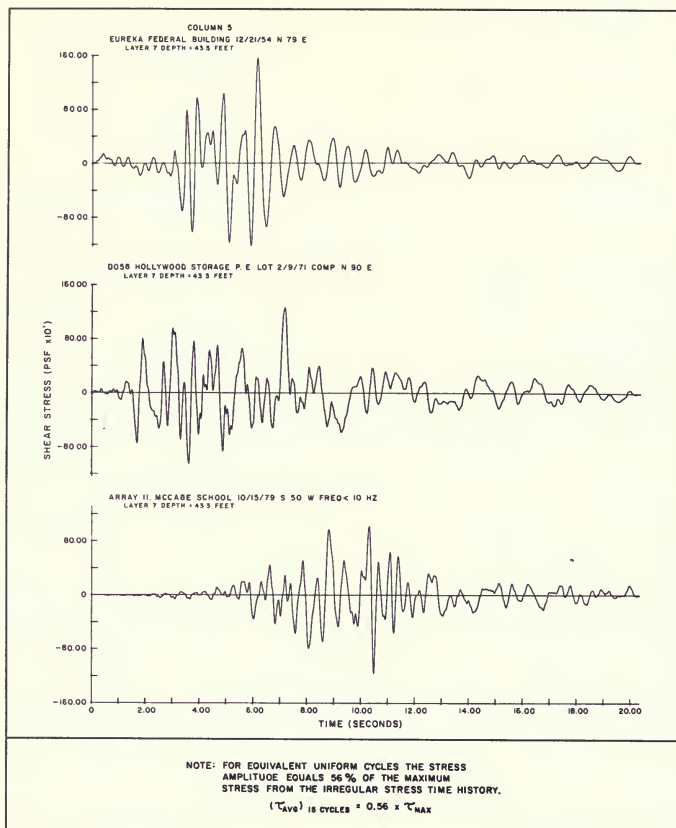


Figure 107. Dynamic Response Motion Produced in Shake Analysis for Thermalito Afterbay Station 107 (Site 1) Using the McCabe School S50°W Record



*Figure 108. Typical Shear Stress Time Histories  
and Equivalent Uniform Cycle Conversion*

## 8. STATIC AND CYCLIC SHEAR STRENGTHS

In earlier evaluations, two methods were used to define the cyclic strength of the foundation sands at Thermalito Afterbay. One method used results from cyclic triaxial tests performed on piston samples recovered in 1978; the other used empirical correlations between the development of liquefaction during earthquakes and SPT resistance. These two methods gave much different results with the SPT correlation indicating much weaker strengths. It was thought that the differences might be attributed to sampling and testing imperfections with the recovered piston samples and/or flawed interpretations of the SPT. It was also considered possible that the SPT correlation, developed mainly for clean sands, might not be appropriate for the silty sands found at Thermalito Afterbay. However, very little data were available prior to 1981 regarding the effect of fines on SPT resistance and liquefaction potential.

For the 1981 analyses, precautions were taken to minimize imperfections in the sampling and testing phases. As mentioned previously, a site specific correlation was developed between the Standard Penetration Test resistance determined in the field and the cyclic strength determined in the laboratory. In addition, more information regarding the question of gradation effects became available when Tokimatsu and Yoshimi (1981) published their SPT correlations.

### Static Shear Strength

The static shear strength for embankment and foundation soils was determined by performing several series of consolidated-undrained triaxial compression tests with pore pressure measurements:

1. Eleven tests were carried out in 1978 on Pitcher barrel samples of the embankment clay from four locations (Stations 107, 173, 203, and 281).
2. Twenty-three tests were carried out in 1978 on Pitcher barrel samples of the silt/clay cap within the Red Bluff Formation from four locations (Stations 107, 173, 203, and 281).
3. Three tests were carried out in 1978 on piston samples of the silty sand ( $N_{A1} \approx 20$ ) found at Station 107 (Site 1).
4. Five tests were carried out in 1980 on Pitcher barrel samples of embankment clay from Station 286.
5. Ten tests were carried out in 1981 and 1982 on piston samples of silty sand ( $N_{A1} \approx 7$ ) from Station 166 (Worksite 2).
6. Twenty-one tests were carried out in 1982 on Pitcher barrel samples of the silty/clay cap in the Columbia Soil Area between Stations 346 and 363.

Results from the triaxial compression tests are shown in Figures 109 and 110 for the embankment clay and Red Bluff Formation silt/clay cap. A comparison of the drained strength found in 1978 and 1980 with the drained strength used in design is presented in Figure 111 and shows the design strength to be significantly lower.

Results for tests made on the Columbia Soil are summarized in Figure 112. Figure 113 presents a comparison of the drained strength determined in 1981 with the strength used in design. This comparison also shows the design strengths to be significantly lower than what was determined in this program.

Figure 114 shows deviator stresses and pore pressures plotted against axial strain for the 1978 tests of the silty sand ( $N_{A1} \approx 20$ ) (from Station 107 (Site 1)). Also shown are the results of a test for the silty sand from Lower San Fernando Dam, which liquefied during the 1971 San Fernando Earthquake ( $M_L = 6.6$ ). The plots indicate good agreement between the two types of materials and show medium dense sand behavior with a tendency to dilate at strains above 1 percent. Figure 115 summarizes some of the data in the form of mohr diagrams.

Figure 116 shows deviator stresses and pore pressures plotted against axial strain for the 1982 tests of the silty sand ( $N_{A1} \approx 7$ ) from Station 166 (Worksite 2). The plots show a loose sand with virtually no tendency to dilate with increased levels of strain. Figure 117 shows some of the same data plotted in the form of p-q diagrams.

Table 23 summarizes all of the static shear strengths.

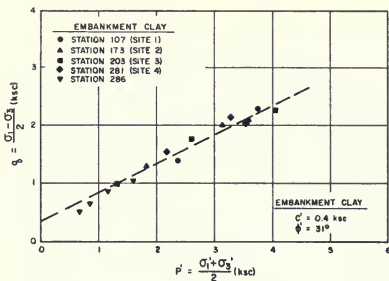
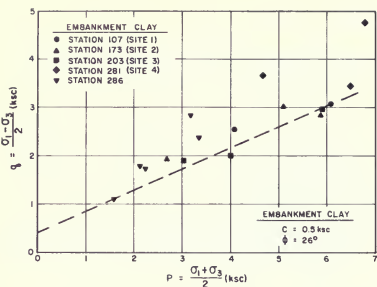


Figure 109. Static Undrained Shear Strength Determined from CUE Triaxial Tests on Undisturbed Samples of Thermalito Afterbay Embankment and Foundation Silt/Clay

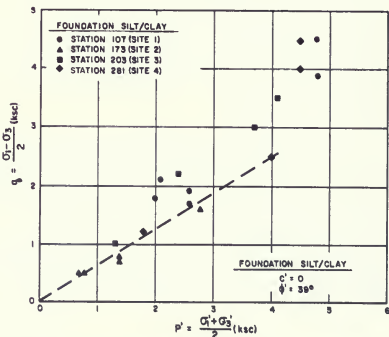


Figure 110. Static Drained Shear Strength Determined from CUE Triaxial Tests on Undisturbed Samples of Thermalito Afterbay Embankment and Foundation Silt/Clay

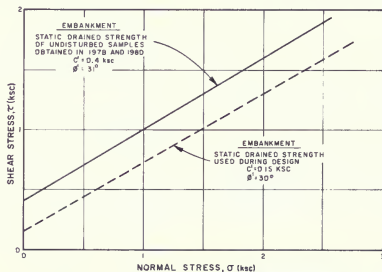
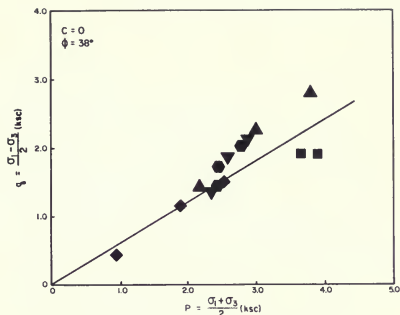
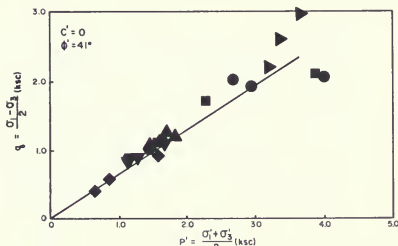


Figure 111. Comparisons of Drained Shear Strength Between Undisturbed Samples of Thermalito Afterbay Embankment and Values Used During Design



STATIC UNDRAINED STRENGTH

Figure 112. Static Shear Strengths Determined from CUE Triaxial Tests Performed on Samples of Thermalito Afterbay Silt/Clay from Station 347 (Columbia Soils Area)



STATIC DRAINED STRENGTH

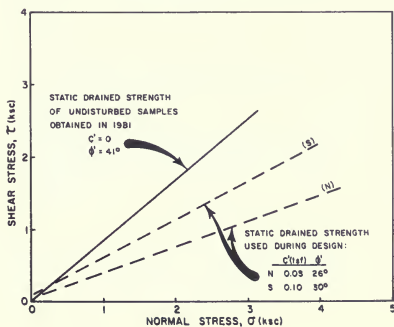


Figure 113. Comparisons of Drained Shear Strength Between Undisturbed Samples of Thermalito Afterbay Station 347 (Columbia Soils Area) and Values Used During Design

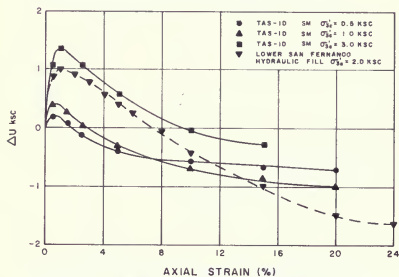
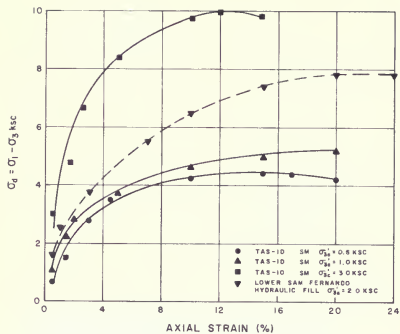


Figure 114. Static CUE Triaxial Test Results for Undisturbed Samples of Thermalito Afterbay Foundation Silty Sand ( $N_{A1} \approx 20$  blows/foot)

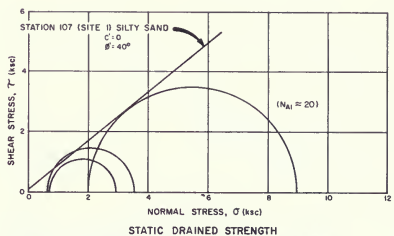
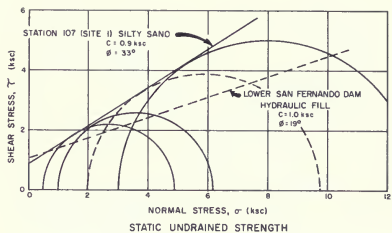


Figure 115. Static Shear Strength of Thermalito Afterbay Station 107 (Site 1) Foundation Silty Sand Determined by CUE Triaxial Compression Tests on Undisturbed Samples ( $N_{A1} \approx 20$ )

Table 23. Static Shear Strength Summary for Thermalito Afterbay Materials

	$C(\text{ksc})$	$\phi^{(o)}$	$C'(\text{ksc})$	$\phi'^{(o)}$
Embankment Clay	0.5	26	0.4	31
Foundation Silt/Clay (Red Bluff)	0	37	0	39
Foundation Silt/Clay (Columbia)	0	38	0	39
Foundation Silty Sands ( $N_{A1} = 20$ )	0.9	33	0	40
Foundation Silty Sands ( $N_{A1} = 7$ )	0	18	0	37

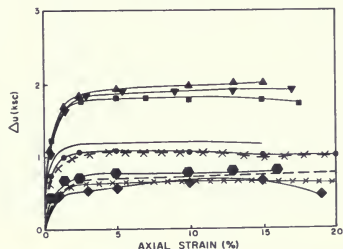
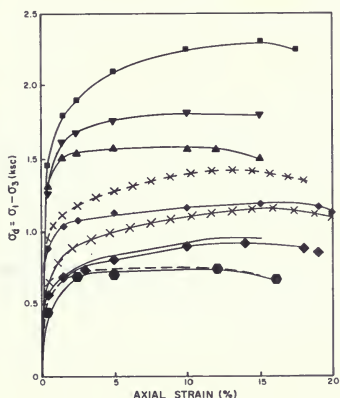


Figure 116. Static CUE Triaxial Test Results for Undisturbed Samples of Thermalito Afterbay Foundation Silty Sands ( $N_{A1} \approx 7$  blows/foot)

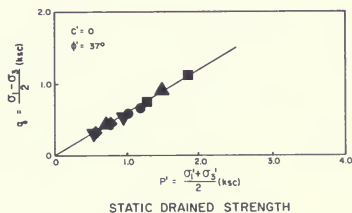
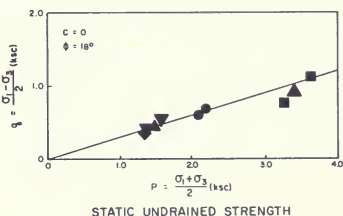


Figure 117. Static Shear Strengths Determined from CUE Triaxial Tests Performed on Samples of Thermalito Afterbay Foundation Silty Sands ( $N_{A1} \approx 7$  blows/foot)

## Cyclic Shear Strength

The cyclic shear strength of suspected liquefiable soils was determined by performing numerous cyclic triaxial tests on recovered piston and Pitcher barrel samples:

1. Fourteen tests were performed in 1976 on recovered samples of sandy soils from different sites around Thermalito Afterbay Dam. The samples were obtained using the DWR thick-walled sampler and probably came from deposits with an average corrected blowcount of about 38. The consolidation conditions used were:

$\sigma'_{3c}(ksc)$	$K_c$	No. of Tests
1.0	1.0	8
3.0	1.0	6

2. Thirty-six tests made in 1978 on recovered piston samples of silty sand from Station 107 (Site 1,  $N_{A1} \approx 20$ ) and Station 173 (Site 2,  $N_{A1} \approx 40$ ). Twenty-eight tests were also performed on reconstituted samples from both sites that were constructed to the approximate density of "Undisturbed" samples by pluviation through air. In addition, a few of the remolded specimens were subjected to intervals of small cycles of stress prior to actual testing. Consolidation conditions used consisted of the following:

### "UNDISTURBED" SAMPLES

$\sigma'_{3c}(ksc)$	$K_c$	No. of Tests
0.5	1.0	6
1.0	1.0	11
1.0	1.5	2
3.0	1.0	17

Remolded Samples  
(See next column)

$\sigma'_{3c}(ksc)$	$K_c$	No. of Tests
1.0	1.0	8
3.0	1.0	6

3. Four tests were made in 1980 on recovered Shelby push samples of Columbia Soil Area silty sands and clay (Stations 351 and 361). The consolidation conditions used were:

$\sigma'_{3c}(ksc)$	$K_c$	No. of Tests
0.5	1.0	1
1.0	1.0	3

4. One hundred twenty six tests were made in 1981 and 1982 on recovered piston samples of sands. In addition, eight tests were made on some low blowcount silts and clays from the Columbia Soil Area. This program was instigated to develop a site-specific correlation between blowcounts and cyclic triaxial strengths for Thermalito Afterbay. Therefore, these tests were performed on materials representing corrected blowcounts between 7 and 46. The consolidation conditions used were:

$\sigma'_{3c}(ksc)$	$K_c$	No. of Tests
1.0	1.0	47
1.0	1.5	18
2.5	1.0	39
2.5	1.5	22

The test results for the 1976 program are shown in Figure 118 for the development of  $\pm 5$  percent axial strain. Since these samples were taken with the thick-walled sampler, severe disturbance probably resulted. In addition, the cyclic strength did not correlate well with SPT resistance at the sampling sites. Therefore, these results were not used in subsequent analyses.

Test results from the "undisturbed" 1978 samples are shown in Figure 119 (failure was defined as 10 percent axial strain). The results indicate that the silty sands from



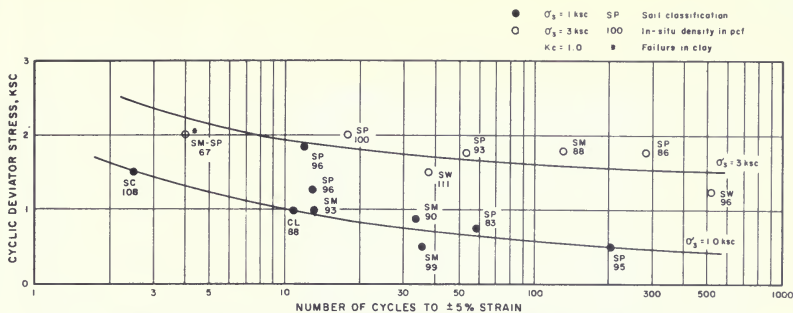


Figure 118. Results of 1976 Cyclic Triaxial Tests on Thermalito Afterbay and Forebay Sands

Station 107 (Site 1,  $NA1 \approx 20$ ) give about the same strength as the relatively clean sands from Station 173 (Site 2,  $NA1 \approx 38$ ). A typical test trace for the Station 107 (Site 1,  $NA1 \approx 20$ ) silty sand is shown in Figure 120. With soils having drastically different blowcounts giving virtually identical strengths, the question of sample disturbance was raised. In addition, since the piston sampling was usually carried out approximately 50 feet away from the SPT borings, the blowcounts might not have been representative of the material sampled.

The sampling and testing in 1980 of the Columbia Area soils yielded relatively high strengths compared to the 1978 "undisturbed" strengths (Figure 121). However, these samples were obtained using Shelby pushes and transported without the same special care as the 1978

samples. Furthermore, these sample strengths could not be correlated to blowcounts because no SPT borings were performed in the areas of the sample borings. Therefore, these four tests were also not used in subsequent analyses.

The results of the testing performed in 1981 and 1982 on recovered piston samples are shown in Figures 122 through 125 for the four consolidation conditions tested (failure was defined as 10 percent axial strain). Not all of the tests are shown since some samples had excessive disturbance due to freezing experiments or sampling mistakes. A complete list of test results, however, is presented in Addendum E. The figures show a definite increase in strength with increasing blowcount—a trend not found in 1978. The gradations of both the SPT samples and the corresponding cyclic triaxial specimens are shown in Figures 126 through 130.

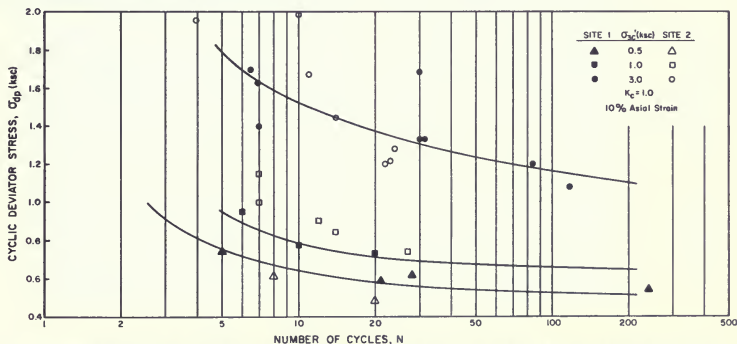
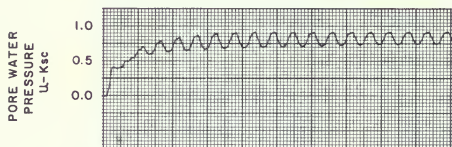
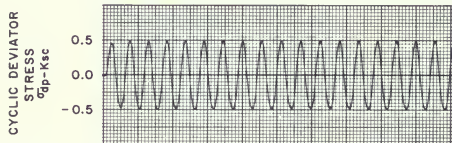
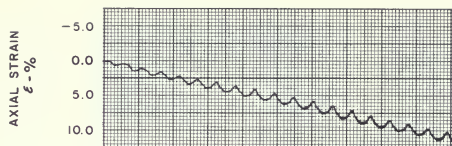
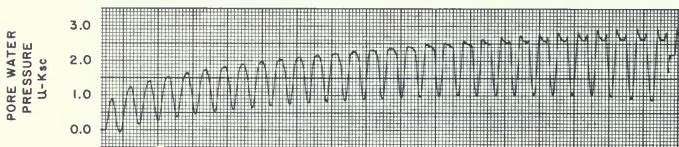
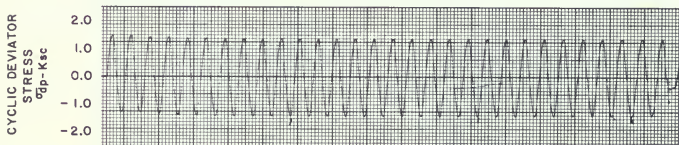
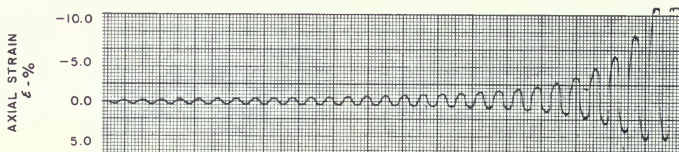


Figure 119. Cyclic Triaxial Test Results from "Undisturbed" 1978 Samples of Thermalito Afterbay Foundation Silty Sands



ANISOTROPICALLY-CONSOLIDATED SAMPLE ( $K_c=1.5$ )



ISOTROPICALLY-CONSOLIDATED SAMPLE ( $K_c=1.0$ )

Figure 120. Typical Cyclic Triaxial Test Records for 1978 Test Program on Station 107 (Site 1) Silty Sand

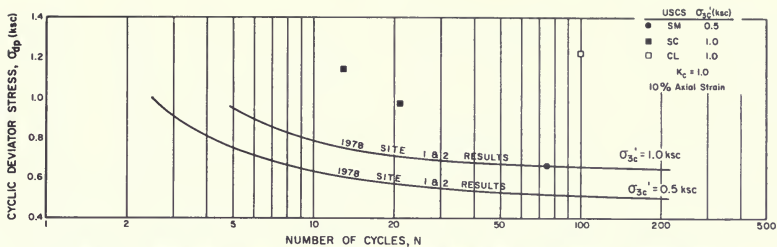


Figure 121. Comparison of Cyclic Triaxial Test Results from "Undisturbed" 1980 Samples of Columbia Soils with Results from 1978 Samples of Foundation Silty Sands from Sites 1 and 2

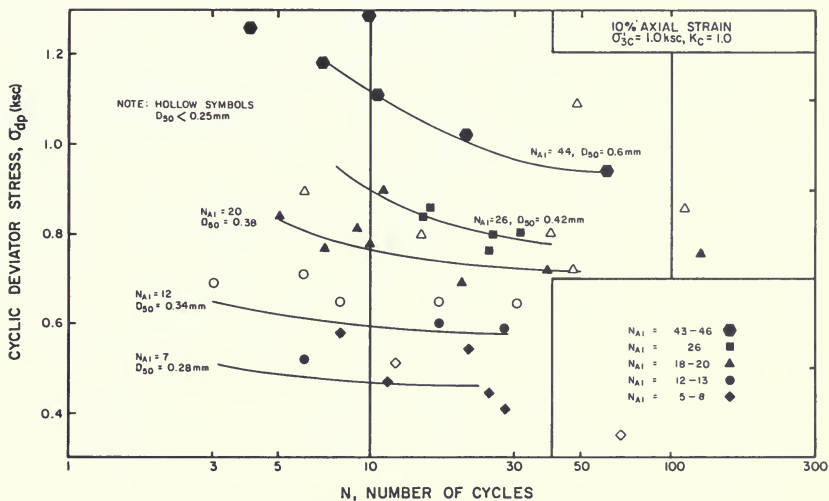


Figure 122. Thermalito Afterbay Cyclic Triaxial Test Results

$$(\sigma'_{3c} = 1.0 \text{ ksc}, K_c = 1.0)$$

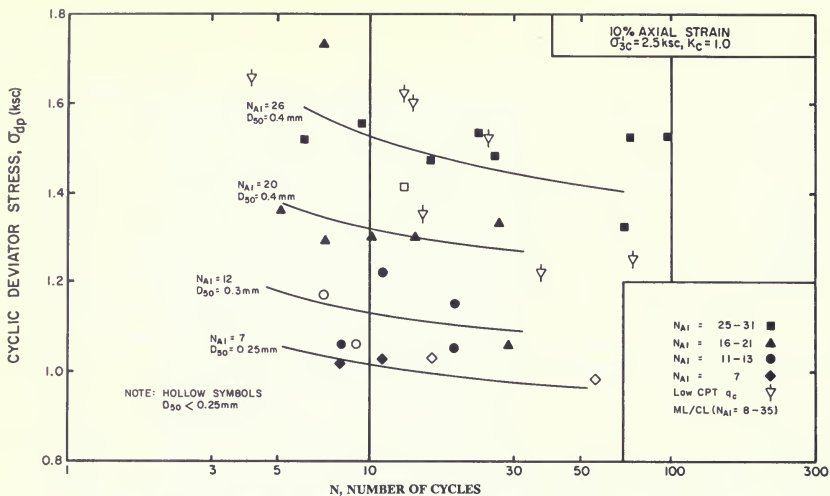


Figure 123. Thermalite Afterbay Cyclic Triaxial Test Results

( $\sigma'_{3c} = 2.5 \text{ ksc}$ ,  $K_c = 1.0$ )

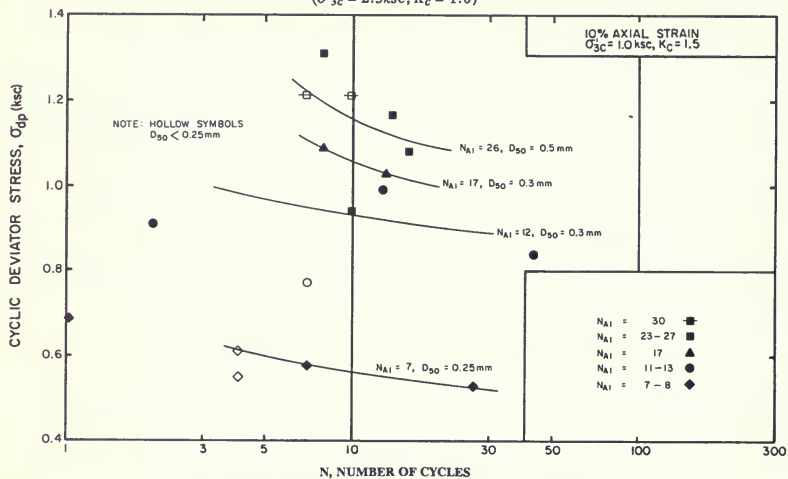


Figure 124. Thermalite Afterbay Cyclic Triaxial Test Results

( $\sigma'_{3c} = 1.0 \text{ ksc}$ ,  $K_c = 1.5$ )

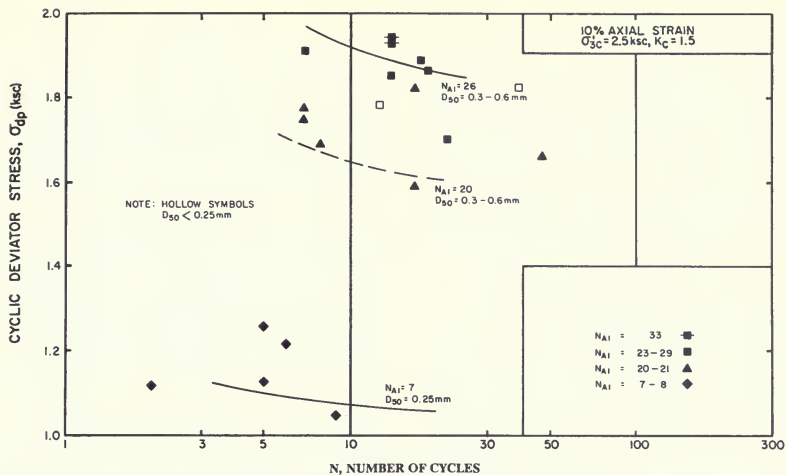


Figure 125. Thermalito Afterbay Cyclic Triaxial Test Results

$$(\sigma'_{3c} = 2.5 \text{ ksc}, K_c = 1.5)$$

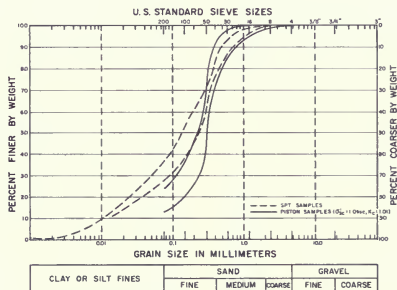


Figure 126. Comparison of Gradation Envelopes

for Thermalito Afterbay Piston Samples and SPT Samples with

$$N_{A1} = 5-8 \text{ blows/foot}$$

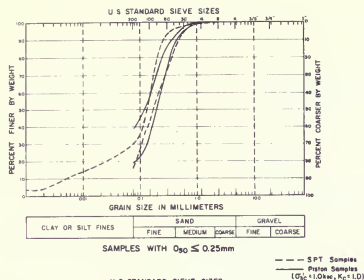


Figure 127. Comparison of Gradation Envelopes for Thermalito Afterbay Piston Samples and SPT Samples with  $N_{A1} = 12-13$  blows/foot

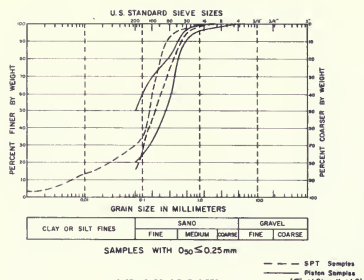


Figure 128. Comparison of Gradation Envelopes for Thermalito Afterbay Piston Samples and SPT Samples with  $N_{A1} = 18-21$  blows/foot

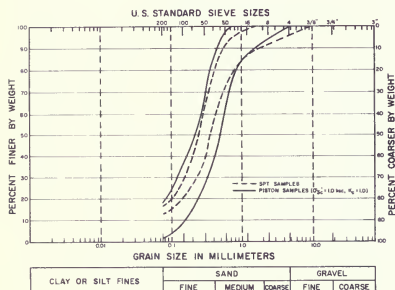


Figure 129. Comparison of Gradation Envelopes for Thermalito Afterbay Piston Samples and SPT Samples with  $N_{A1} = 25-31$  blows/foot

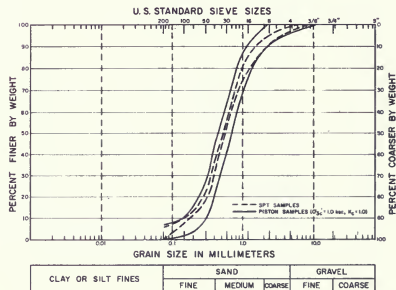


Figure 130. Comparison of Gradation Envelopes for Thermalito Afterbay Piston Samples and SPT Samples with  $N_{A1} = 43-46$  blows/foot

## 1981-82 Correlation of Cyclic Strength with SPT

The basic approach in this investigation was to search for weak sandy soils using the SPT and then to define the cyclic strength of the soils by the cyclic triaxial test. The resulting correlation was then used to define the strength of soils at other locations where only SPT resistance was known.

Empirical correlations between earthquake-induced liquefaction and the SPT resistance have been developed for locations all over the world. The two most recent and prominent correlations are those developed by Tokimatsu and Yoshimi (1981) and by Seed and Idriss (1981). Both of these are somewhat interrelated since some of the data and methods are shared between the two studies.

To compare the SPT cyclic strength correlation developed at Thermalito Afterbay to the correlations developed from field liquefaction, a correction was applied to the data. Since almost all field data come from level ground and depths of 30 feet or less, only one triaxial consolidation ( $\sigma'_{3c} = 1.0 \text{ ksc}$ ,  $K_c = 1.0$ ) was appropriate for use in the comparisons. A  $C_r$  correction of 0.57 was applied to the triaxial strength obtained from Figure 122 to correct to level ground conditions. As described in Section 3, the SPT blowcounts have already been corrected for procedural differences.

The cyclic triaxial strength correlation with SPT blowcount developed for Thermalito Afterbay is shown in Figure 131. Each data point represents the corrected strength at 15 cycles. This strength is plotted against the corrected blowcount that represents the layer where the sand samples were obtained. The Thermalito Afterbay data points show the average  $D_{50}$  of the samples tested in the laboratory. Also shown are the lower bound curves from the Seed and Idriss (1982) study. A lower bound curve represents the boundary between "liquefaction" and "no liquefaction" observations of sites which have withstood strong earthquake shaking. The lower bound curves are considered a field measurement of cyclic strength.

In general, Figure 131 shows reasonable agreement between Thermalito Afterbay data and the field SPT correlations. The coarser Thermalito Afterbay data points at

$N_{A1}$  equal to 7 and 12 have somewhat higher strengths than predicted by the lower bound curves for the same gradation ranges in the field studies. Although this might be a result of sample densification, it must be noted that the Thermalito data are quite close to the borderline of the different gradation ranges. In addition, the lower bound curves represent conservative interpretations of the data because the correlations show some non-liquefied sites lying above the lower bound curves (zone of predicted "liquefaction").

## Sample Disturbance

"Undisturbed" tube samples were obtained of the silty sands in 1981-82 using a hydraulic piston sampler. Except for freeze sampling, which was considered impractical for sands having high silt content, this method is considered to cause the least disturbance in sampling sands within boreholes. Great care was used in the sampling, transportation, and specimen preparation process. Nevertheless, there was probably some densification of the low blowcount sand during sampling and sample handling. This effect would increase the strength determined by the triaxial test. There was probably also some loosening of the high blowcount sands during sampling and sample handling. Sample loosening would cause a decrease in the strength determined by the cyclic triaxial test. This disturbance effect might explain why there are some discrepancies in Figure 131. At low blowcounts, the after-

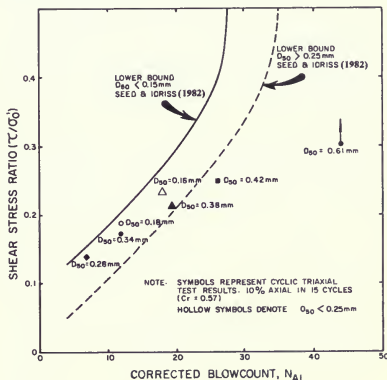


Figure 131. Comparison Between Thermalito Afterbay Cyclic Triaxial Test Results and SPT Resistance



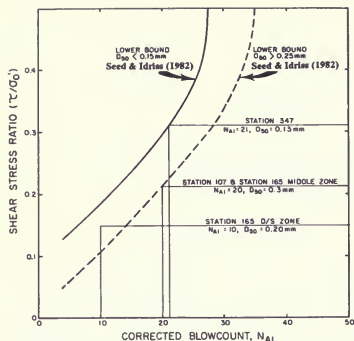


Figure 132. Determination of Liquefaction Potential from Seed and Idriss (1982) SPT Correlation

bay triaxial test results give somewhat higher strengths than predicted by the Seed and Idriss (1982) SPT correlation. At high blowcounts, the triaxial test results give much lower strengths than the SPT correlation.

There is also another disturbance effect. Sampling and sample handling tends to reduce the interparticle stability induced by long-term loading and/or seismic strain. This effect always results in a reduction of strength. For loose sands, this reduction of interparticle stability would have a counter-balancing effect against sample densification. For dense sands, reduction of interparticle stability would magnify the loosening effect during sampling.

According to studies by Singh, et al. (1979), sampling of natural sand deposits having relative densities of about 60 percent would result in a net decrease in strength by about 15 percent. In other words, the reduction of interparticle stability would outweigh the strength increase due to densification. The inter particle stability could be a significant strength component for the afterbay sands since the estimated age of the deposits ranges up to 3.5 million years. It is also possible that densification in the low blowcount afterbay sands may be reduced due to the high silt content (10 – 40 percent).

Thus, the cyclic triaxial test strengths for the low blow-count sands may not be too high after all. However, since all of the disturbance effects for high density sands result in a decrease in strength, the triaxial test results for corrected blowcounts over 25 are concluded to be too low.

## Residual Pore Pressure

Residual pore pressures were examined in an effort to evaluate the strength of foundation sands that did not completely liquefy. Pore pressure development was estimated using the residual pore pressures at the end of each cycle of the triaxial test. The pore pressures developed initially during the tests were relatively high when compared to shake table results on clean sands. This may have been due to the test or the difference in gradations. This rapid rise in pore pressure made it difficult to extrapolate pore pressure ratios of 40 percent and 60 percent to 15 cycles since these ratios usually developed in less than five cycles. Therefore, extrapolations were made conservative. These extrapolations remain very conservative when compared to the standard pore pressure development curves recommended by Seed and Idriss (1982).

## Determination of Cyclic Strength

Figure 132 displays the determination of cyclic strength for the three modeled sites from the Seed and Idriss (1982) correlation. Table 24 compares the cyclic strengths for the three modeled sites determined by both the cyclic triaxial test results and the Seed and Idriss (1982) SPT correlation. Cyclic strengths determined by the laboratory test approach for the three sites were obtained by interpolating the data points in Figure 131.

Although there is some justification for using the laboratory strengths, it was decided to conservatively adopt the lower of the two strengths for each site. Actually, the amount of conservatism is minor. Table 24 also presents the adopted strength values. For Station 107, the two approaches predict the same strength. For Station 165, the strength determined by the SPT correlation is only about 6 percent less than the cyclic triaxial strength for the downstream zone. Only at Station 347 does the SPT correlation predict higher strength; and this difference is only about 19 percent.



**Table 24. Determination of Cyclic Strength**

Site	(blows/feet)	$D_{50}$ (mm)	SPT ( $\tau/\sigma'_0$ )	C3X ( $\tau/\sigma'_0$ )	Adopted ( $\tau/\sigma'_0$ )
Station 107	20	0.31	0.21	0.21	0.21
Station 165					
Middle Zone	20	0.30	0.21	0.21	0.21
D/S Zone	10	0.20	0.15	0.16	0.15
Station 347	21	0.13	0.31	>0.26	0.26

Notes:

SPT ( $\tau/\sigma'_0$ ) denotes cyclic stress ratio predicted by Seed and Idriss (1982) SPT correlation (See Figure 132).

C3X ( $\tau/\sigma'_0$ ) denotes cyclic stress ratio predicted by cyclic triaxial tests  $\sigma'_{3c} = 1.0$  ksc,  $K_c = 1.0$ ,

$C_r = 0.57$ —see Figure 131.

## 9. EVALUATION OF LIQUEFACTION POTENTIAL

### Method of Analysis

Liquefaction potential is usually determined by comparing predicted stresses with cyclic strengths. In the Seed-Lee-Idriss method, strengths and stresses are compared by assuming that the horizontal plane in the field and the  $45 + \phi'/2$  degree plane (45 degrees for isotropically consolidated tests) in the triaxial sample are critical. To be equivalent, both planes must have the same effective normal and shear stresses before dynamic loading. A safety factor against liquefaction is defined as:

$$\text{Safety Factor} = \frac{\text{Uniform cyclic shear stress on } 45 + \phi'/2 \text{ degree plane required to cause liquefaction or a specified amount of strain in N cycles}}{\text{N equivalent uniform cycles of shear stress induced by the earthquake on the horizontal plane}}$$

However, other methods have been proposed. A method suggested by Leps (1973) proposes predicting liquefaction potential by assuming that the major principal consolidation stress is the critical condition that must be matched between the field and the laboratory specimen. A method suggested by Bennett (1977) proposes to use the mean normal consolidation stress as the critical condition.

Studies by Vaid and Finn (1979) indicate that if the cyclic loading resistance were measured in terms of the combined shear stress (static + cyclic), more consistent laboratory results would be produced (an increase in resistance with increase in static stress was always noted irrespective of relative density or shear strain level of interest). Other researchers—Casagrande (1975) and Castro (1976)—suggest that liquefaction potential be determined by critical-state soil mechanics.

Using the different procedures will no doubt give different answers for some projects. However, all have limitations and the only one that has been calibrated against known embankment behavior during earthquake shaking is the Seed-Lee-Idriss method. This is the method that was chosen for analyzing the afterbay dam. That it seems to work is no doubt due to compensating errors. This also points to the danger of improving the accuracy of a single component in that it may eliminate a compensating effect and lead to an erroneous end result.

### Cyclic Shear Strength

Table 24 (in Section 8) shows the selection of cyclic shear strength as the lower value from either the laboratory triaxial tests or the SPT correlation. However, the strengths presented in Table 24 are only applicable for shallow, level ground conditions. To describe the strengths for

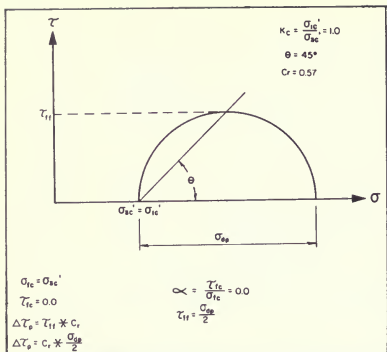


Figure 133. Procedure for Interpreting Cyclic Triaxial Test Data for Isotropically Consolidated ( $K_c = 1.0$ ) Samples

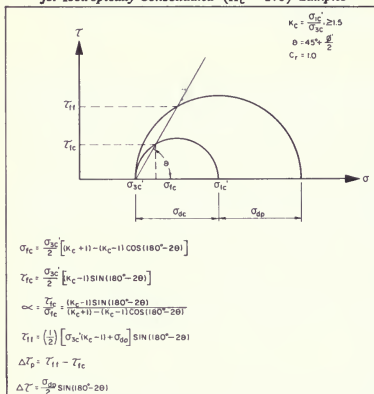


Figure 134. Procedure for Interpreting Cyclic Triaxial Test Data for Anisotropically Consolidated ( $K_c > 1.0$ ) Samples

other consolidation conditions, additional information is needed.

The cyclic triaxial test results in Section 8 describe the strengths for a range of consolidation conditions. Cyclic strength curves are developed from cyclic triaxial data by the Seed Lee-Idriss method illustrated in Figures 133 and 134. Shown in Figures 135 and 136 are cyclic strength curves developed from laboratory results for  $N_{A1}$  equal

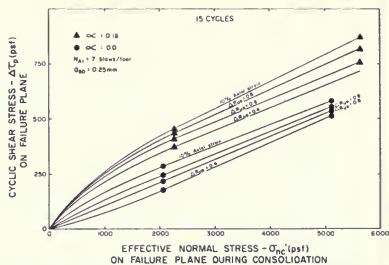


Figure 135. Cyclic Strength Curves for Thermalito Afterbay Foundation Silty Sands ( $N_{A1} \approx 7$  blows/foot)

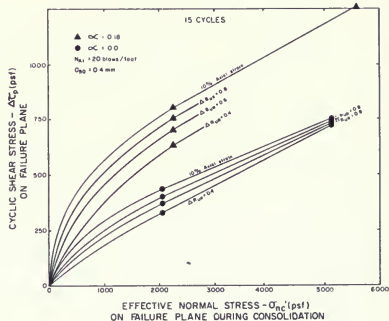


Figure 136. Cyclic Strength Curves for Thermalito Afterbay Foundation Silty Sands ( $N_{A1} \approx 20$  blows/foot)

to 7 and  $N_{A1}$  equal to 20. Failure was defined as 10 percent axial strain occurring in 15 cycles. Also shown are curves for residual pore pressure ratios of 40, 60, and 80 percent.

All of the isotropically consolidated ( $K_c = 1.0$ ),  $\alpha = 0.0$ ) triaxial test results were reduced by multiplying by a  $C_r$  correction equal to 0.57.

**Table 25: Application of Cyclic Triaxial Strength Curves**

Site	Cyclic Strength* Stress Ratio Adopted	Cyclic Strength Curves Applied	Stress Ratio of Curves Applied	Correction Factor Applied to Strength Curves
Station 107	0.21	Figure 136 ( $N_{A1} = 20$ )	0.21	$(0.21/0.21)=1.00$
Station 165 Middle Zone	0.21	Figure 136 ( $N_{A1} = 20$ )	0.21	$(0.21/0.21) = 1.00$
Downstream Zone	0.15	Figure 135 ( $N_{A1} = 7$ )	0.14	$(0.15/0.14)=1.07$
Station 347	0.26	Figure 136 ( $N_{A1} = 20$ )	0.21	$(0.26/.21)=1.24$

\*The stress ratio listed is applicable to an effective overburden pressure of 1 ksc and an alpha value of zero.

The curves in Figure 136 are directly applicable to Station 107 and to the middle zone at Station 165. This is because both the SPT correlation and the laboratory results predict the same strength (Table 23). However, the downstream zone at Station 165 and the sand at Station 347 cannot directly use the curves in Figures 135 and 136. Corrections to the curves are required.

Correct strengths for use in the analyses are obtained by multiplying the strength curves in Figures 135 and 136 by factors to yield the strengths adopted in Table 24. For example, the stress ratio adopted in Table 24 for Station 347 was chosen to be 0.26 ( $\sigma_n' = 1 \text{ ksc}$ ,  $\alpha = 0$ ). The stress ratio for 10 percent axial strain obtained from Figure 136 equals 0.21 ( $\sigma_n' = 1 \text{ ksc}$ ,  $\alpha = 0$ ). To use the strength curves in Figure 136 for the suspect sand at Station 347, a correction factor equal to 1.24 ( $0.26/0.21$ ) is applied. Table 25 presents the strength curves used to analyze the three modeled sites and the correction factors used in applying the strength curves.

Figure 137 compares the strengths used at different times for Station 107 (Site 1). During the investigation for the 1980 analysis of Station 107 (Site 1), only 80 percent of the cyclic triaxial strength values obtained from the 1978 exploration program were used. In 1980, it was

not realized that the SPT procedures used in the investigation produced blowcounts which were too low to be used with published SPT correlations. At that time, it was believed that the appropriate blowcount for the suspect sand at this site was equal to 10. Since there was such a large difference (in 1980) between the laboratory strengths and the SPT correlation, the reduced laboratory strength value was used in that analysis. After the

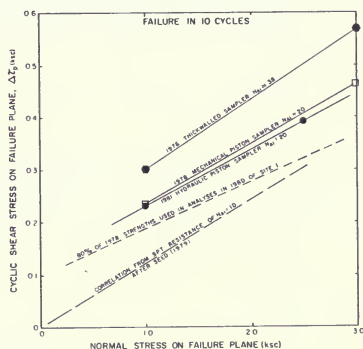


**Figure 137. Comparison of Cyclic Strengths ( $\alpha = 0$ ) Used During Different Periods of the Investigation**

1981-82 investigation program, however, it was shown that the appropriate blowcount was equal to 20 and that laboratory strengths for this site were correct all along (Section 3 and Section 8).

### Liquefaction and Excess Pore Pressures

Figures 138 through 143 show the predicted safety factors for 10 percent axial strain, and the induced residual pore pressures, in the low blowcount sand layers at the three critical sites for the postulated earthquake shaking. For elements with safety factors greater than 1.0, induced residual pore pressures were estimated from the pore pressure curves. The upstream zone of the suspect sand layer

at Station 165 had such high blowcounts ( $N_{A1} = 40$ ) that it was assumed that no liquefaction could develop there. Therefore, Figures 140 and 141 present assumed values for liquefaction safety factors ( $> 2.0$ ) and residual pore pressure ratios ( $< 0.2$ ) for this zone of high penetration resistance.

In general, liquefaction develops in the foundation sand layers beneath the embankment crest and beyond the embankment toes. Beneath the slopes of the embankment, all locations show some buildup of excess pore pressures, but not complete liquefaction. The extent of liquefaction is not significantly influenced by the reservoir elevation.

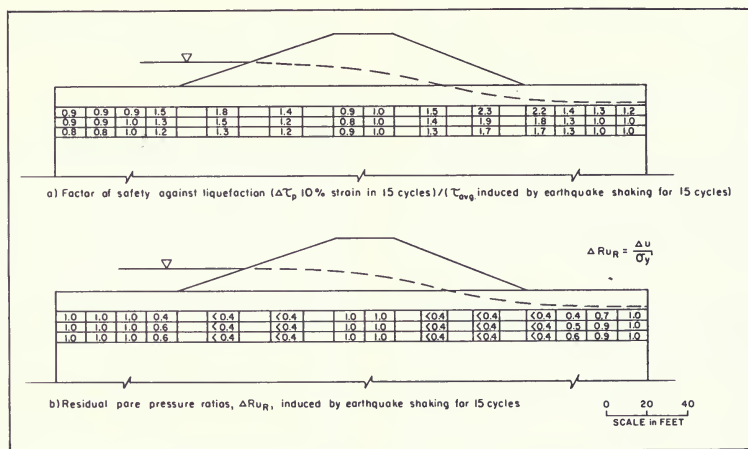


Figure 138. Results of Dynamic Analysis with  $M_L = 6.5$  Earthquake for Sand Layer at Station 107 (Site 1)  
(Reservoir Elevation = 128 feet)

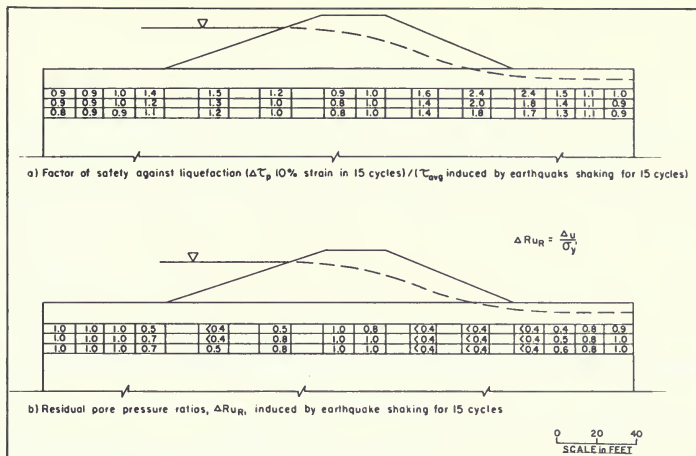


Figure 139. Results of Dynamic Analysis with  $M_L = 6.5$  Earthquake for Sand Layer at Station 107 (Site 1) (Reservoir Elevation 136.5 feet)

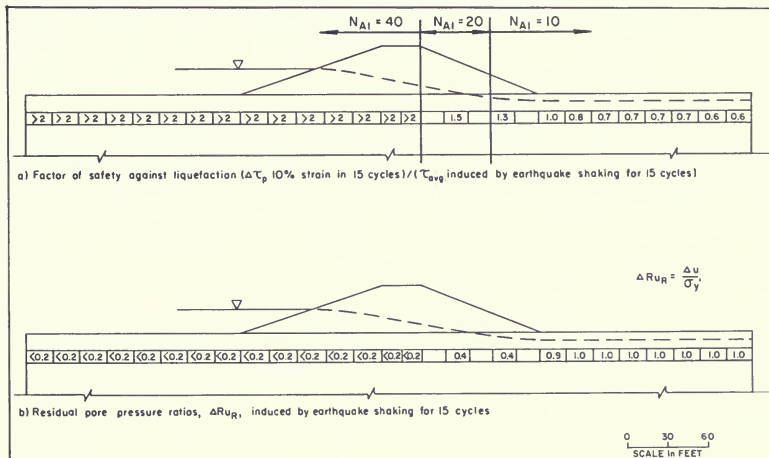


Figure 140. Results of Dynamic Analysis with  $M_L = 6.5$  Earthquake for Sand Layer at Station 165 (Worksite 2) (Reservoir Elevation 128 feet)

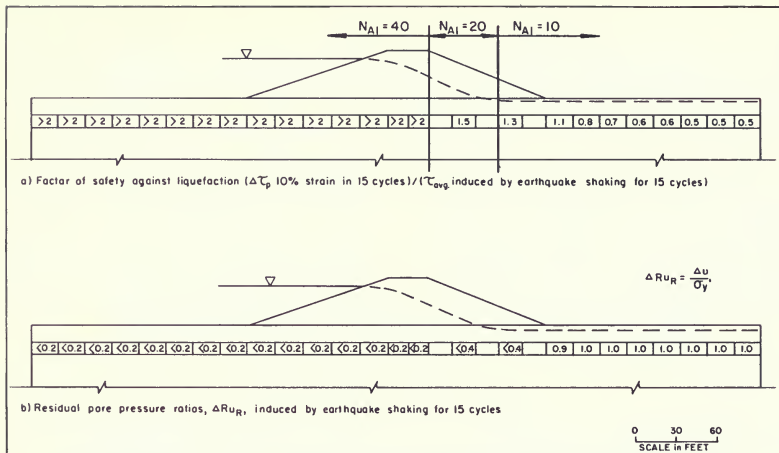


Figure 141. Results of Dynamic Analysis with  $M_L = 6.5$  Earthquake for Sand Layer at Station 165 (Worksite 2) (Reservoir Elevation 136.5 feet)

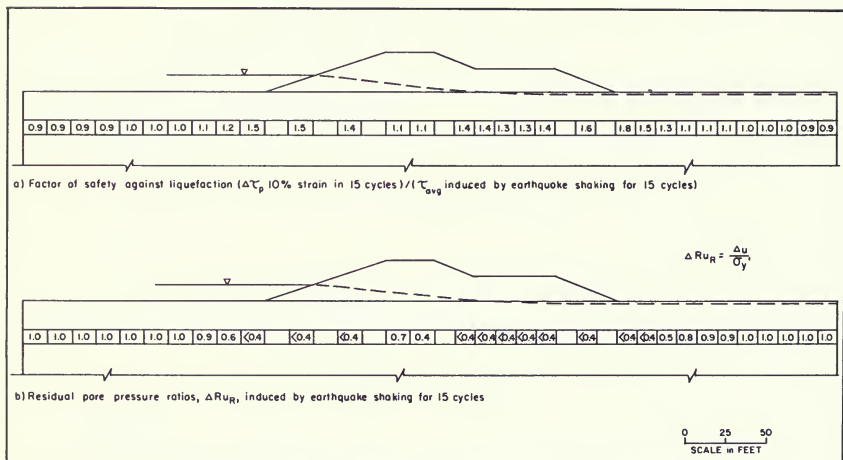


Figure 142. Results of Dynamic Analysis with  $M_L = 6.5$  Earthquake for Sand Layer at Station 347 (Columbia Soil Area) (Reservoir Elevation 128 feet)

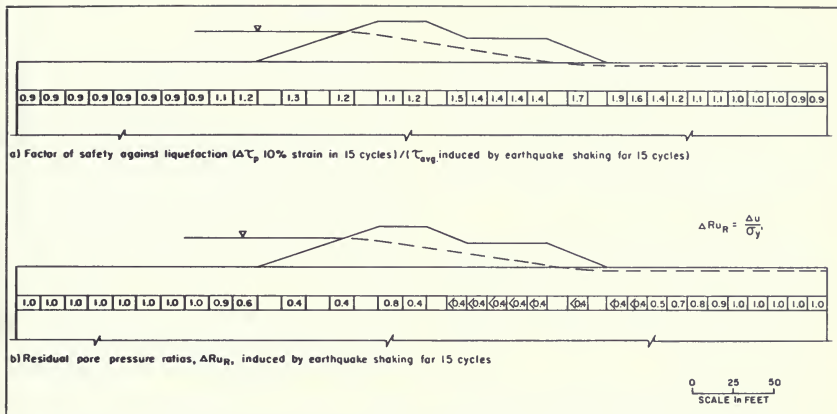


Figure 143. Results of Dynamic Analysis with  $M_L = 6.5$  Earthquake for Sand Layer at Station 347 (Columbia Soil Area)  
(Reservoir Elevation 136.5 feet)

## 10. POST EARTHQUAKE SLOPE STABILITY ANALYSES

### General

The development of large zones of liquefaction in portions of an embankment or embankment foundation does not necessarily lead to a failure of the dam. For example, according to Seed, et al. (1973), Upper San Fernando Dam developed almost complete liquefaction throughout the central portion of the embankment during the 1971 San Fernando earthquake ( $M_L = 6.6$ ), but total movements of only about 6 feet or less resulted.

To examine the post-seismic slope stability of the embankment for different locations around the afterbay, several different types of analyses were performed.

1. Sliding horizontal wedge analyses were performed, assuming complete liquefaction of a horizontal foundation sand layer.
2. Additional sliding horizontal wedge analyses were performed considering the shear resistance on the ends, in an effort to determine the minimum length of liquefied dam foundation which would cause a failure.
3. Circular sliding and wedge analyses were performed for the three model sections analyzed, using residual pore pressures remaining immediately after the postulated earthquake.
4. Wedge analyses were carried out for average redistributions of the excess pore water pressure generated by the earthquake.

### Sliding Wedge Analyses for Complete Liquefaction of Foundation Sand Layer

Wedge analyses were carried out for horizontal sliding of the embankment on a completely liquefied foundation (Figure 144). Active and passive forces were calculated by the Rankine Theory. Calculations considered the following variables:

1. Two embankment heights – 26 and 39 feet.
2. Four thicknesses of surface silt/clay 5, 10, 15, and 20 feet.

3. Three reservoir elevations – 124, 128, and 136.5 feet.
4. Three downstream depths to groundwater – 0, 5, and 10 feet.

The calculated safety factors for this set of analyses are also shown in Figure 144. Calculations indicate that for either height of dam, a horizontal sliding failure similar to the Sheffield Dam failure would probably result for most locations along the afterbay if a sand layer completely liquefied beneath the embankment. For this mode of failure, a surface silt/clay cap of between 15 to 30 feet thickness over the liquefied layer would be required to prevent sliding.

### Sliding Wedge Analyses for Complete Liquefaction of Foundation Sand Layer—Shear Resistance Included on the Ends of the Sliding Block

An important factor to consider in stability analyses is the length of a liquefied layer along the dam axis. If the zones of liquefaction extended only a few tens of feet along the dam axis, the dam would probably not fail because the end resistances would be sufficient to prevent sliding.

Slope stability analyses are usually conducted on the assumptions that the modeled section represents conditions over a very long length of dam and that shear resistances on the ends of a sliding mass can be ignored. To examine the importance of the end resistances, the simple horizontal sliding analyses were redone assuming shear resistances on the ends. The assumed forces are illustrated in Figure 145.

Calculation results are shown in Figure 146 in terms of the minimum longitudinal length of liquefied foundation required to cause a slide (factor of safety = 1.0) under full reservoir conditions. The downstream ground water elevation was assumed to be at the ground surface. The minimum length of foundation liquefaction which would cause a failure for any location along the afterbay was calculated to be about 380 feet.

As an aid in interpreting the results of this analysis, the calculation method was applied to the failure of Sheffield Dam. This failure was believed to be due to downstream horizontal sliding on an almost completely liquefied sand



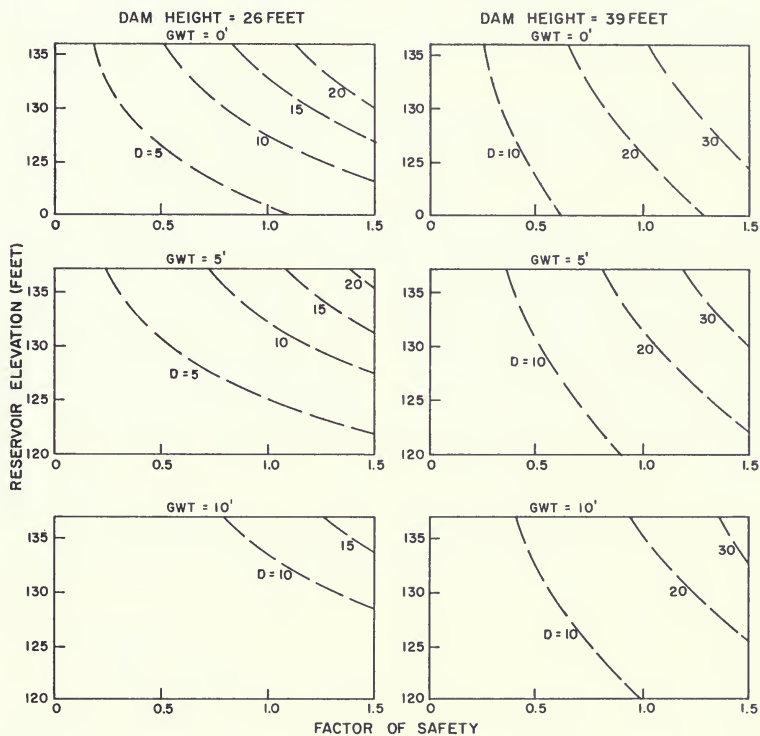
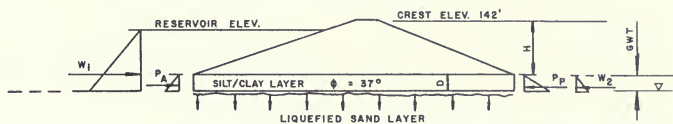


Figure 144. Static Stability with Liquefied Sand Layer Horizontal Sliding

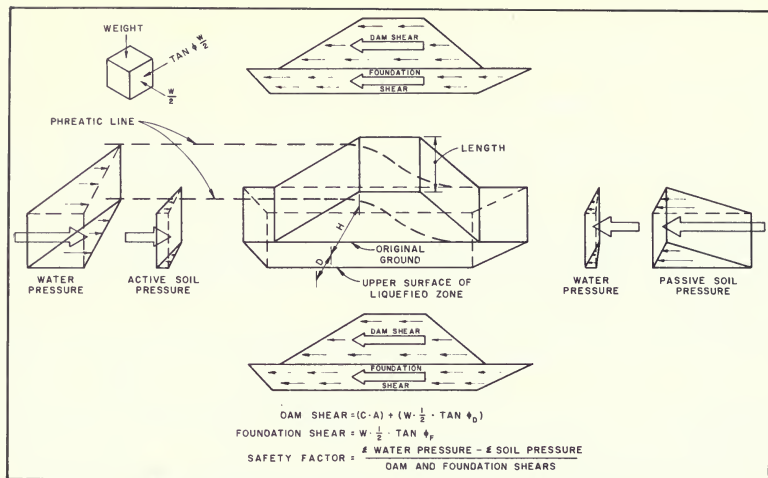


Figure 145. Assumed Forces of Dam Failure Section Including Shear Resistance on the ends of the Sliding Block

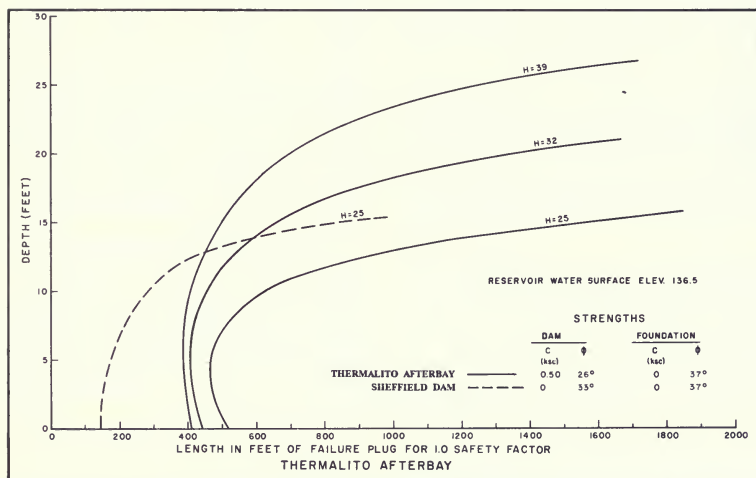


Figure 146. Minimum Length of Section that will Fail by Horizontal Sliding when Including Shear Resistance on Ends of Section

layer at the base of the 25-foot-high dam. Depth of water in the reservoir was about 15 to 18 feet. Total length of dam was 700 feet, of which a 300-foot section was involved in the sliding. This proves that a section as short as 300 feet can slide, but does not prove that a shorter section would not slide. Calculations showed that a minimum length of 140 feet of liquefied foundation would cause failure (Figure 146). The strength used for the embankment material was a  $\phi$  equal to 33 degrees and a cohesion intercept of zero (Sheffield embankment material had a drained strength of  $\phi' = 34.5^\circ$ ,  $c' = 0$ ).

The calculations agreed with observed behavior in that a failure of over 140 feet resulted. However, the accuracy of the numbers from these calculations is open to question. It must be noted that horizontal sliding may not necessarily be the most critical mode of failure and that the calculations represent only rough estimates of real behavior. Therefore, in this evaluation, the minimum length of liquefaction which would cause a failure was assumed to be 250 feet rather than the calculated 380 feet.

### Horizontal Sliding Analysis for Station 12

A boring at Station 12 + 50 (81A-1-SPT) revealed a corrected blowcount of 21 in silty sand ( $D_{50} = .35$  mm, minus #200 sieve size = 20 percent). The embankment is only 12 feet high at this location. Rather than carry out additional

analyses or detailed explorations, a horizontal sliding stability analysis was conducted on the assumption that the entire layer had liquefied. This was a very conservative assumption in light of subsequent analyses for other sites, which indicated only partial liquefaction in foundation layers.

The analyses is displayed in Figure 147 for full reservoir and a downstream ground water elevation at the ground surface. The calculated safety factor is 1.23 for the assumption of complete foundation liquefaction, but would be much higher for partial foundation liquefaction.

### Stability Analyses of the Three Model Sections for Pore Pressures Generated Immediately After Earthquake Shaking

Circular sliding and wedge analyses were performed for Stations 107, 165, and 347 for the residual pore pressures remaining immediately after the earthquake. These analyses used assumed values for residual pore pressures. These assumed values were obtained during an earlier stage of the investigation and are slightly higher than those in pore pressures presented in Figures 138 through 143. Use of these pore pressures add a degree of conservatism to the slope stability analyses. The analyses were conducted for reservoir Elevations 128 and 136.5 feet and for both upstream and downstream directions.

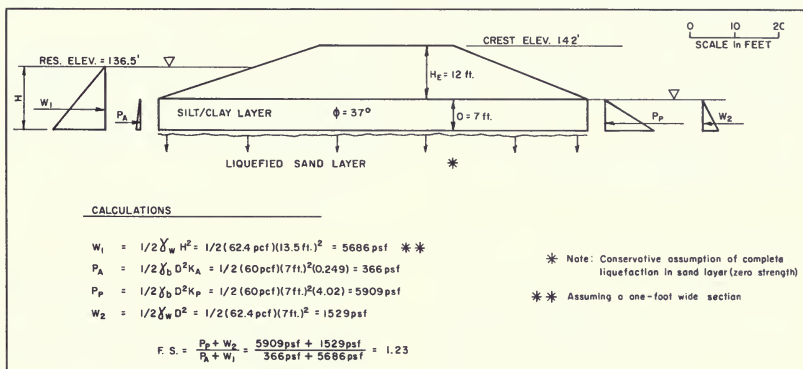


Figure 147. Horizontal Sliding Analysis for Station 12 (Reservoir Elevation = 136.5 feet)

**Table 26: Minimum Safety Factors for Pore Pressure Conditions  
Immediately After Earthquake Shaking**

Location	Reservoir Elevation (ft)	Direction	F.S. Wedge Sliding	F.S. Circular Sliding
Station 107	128	Upstream	2.2	2.3
		Downstream	—	2.3
	136	Upstream	—	1.8
		Downstream	1.8	2.1
Station 165	128	Upstream	2.9	2.7
		Downstream	—	2.1
	136.5	Upstream	—	2.8
		Downstream	1.4	1.8
Station 347	128	Upstream	3.1	3.3
		Downstream	—	3.4
	136.5	Upstream	—	3.0
		Downstream	3.0	3.6

The actual strength within the nonliquefied zones in the sand immediately after the earthquake would be quite high since the conditions would correspond to undrained loading. After a short time had passed, water would be able to flow and the strength of the sand would correspond to a drained loading condition. Therefore, for these analyses, the drained strengths of the sands were used together with generated pore water pressures to represent the strength of the sand. However, because of the low permeability of the materials and the rapid nature of the loadings, the undrained strengths were used for the embankment clay and the surface silt/clay cap. Strength values used were based on tests of undisturbed samples (Section 8) and shown in Figures 148 through 150. For the slope stability analyses of the Station 165 model, the strength corresponding to a corrected blowcount of seven was conservatively used for the entire sand layer.

Wedge analyses were carried out using computer program STABL, which uses Carter's adaptation of the modified Bishop Method. Two separate phreatic surfaces were input. One was for the steady state seepage condition to define pore pressures in the clay embankment and silt/clay cap. The other surface represented the pore pressure in the sand layer immediately after the earthquake.

Circular sliding analyses were carried out with computer program BISHOP, which uses the modified Bishop Method. The only basic change in the input between the two programs was that program BISHOP does not accept a second phreatic surface. Therefore, lowered friction angles for different zones in the sand layer were used (e.g., if the residual pore pressure ratio was 80 percent, then the tangent of the friction angle was made to be only 20 percent of the actual tangent value).

The safety factor results of these analyses are shown in Table 26. In general, the wedge and circular sliding analyses gave similar minimum safety factors with the wedge analyses giving slightly lower numbers in some cases. The lowest safety factor was 1.4 for downstream sliding under full reservoir at Station 165.

#### **Stability Analyses of the Three Model Sections for Redistributed Pore Pressures After Earthquake Shaking**

Pore water pressure dissipation and redistribution after earthquake shaking is a very complex process. Many complex developments are being produced simultaneously. These include shearing and the compression or dilation of the sand, flow of water from high pressures to low pressures, and effects of variable permeabilities on the flow patterns.

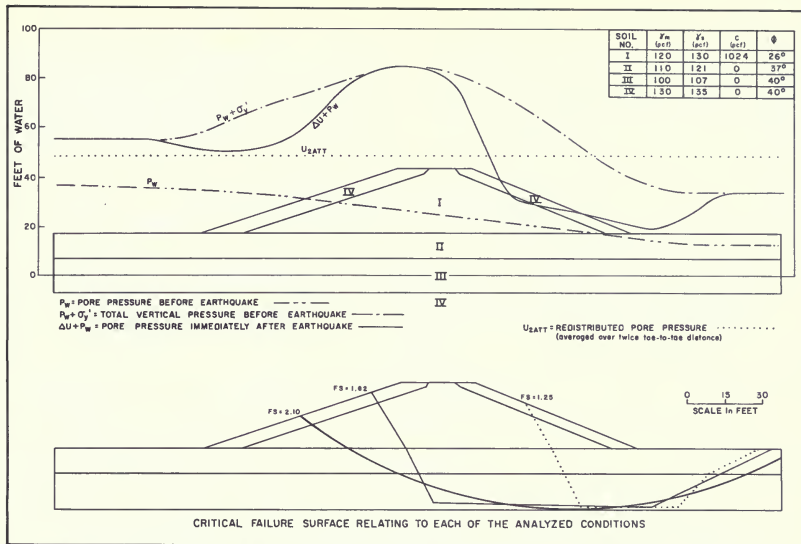


Figure 148. Post Earthquake Stability Analyses (Downstream) for Model 1—Station 107 (Site 1)—Reservoir Elevation = 136.5 feet

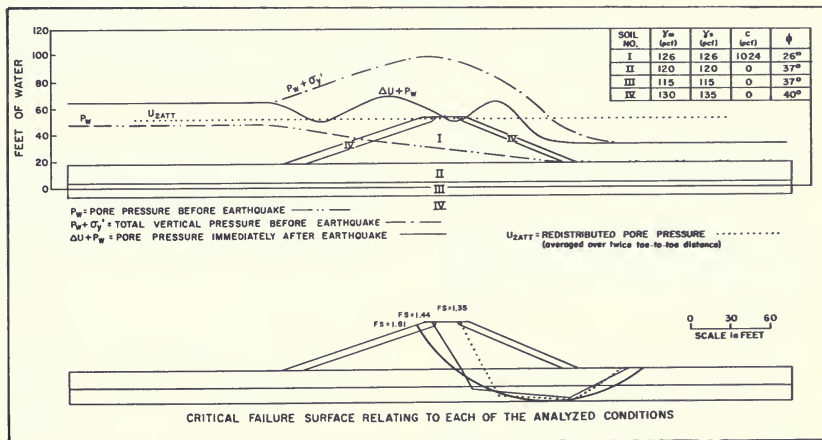


Figure 149. Post Earthquake Stability Analyses (Downstream) for Model 2—Station 165 (Worksite 2)—Reservoir Elevation = 136.5 feet

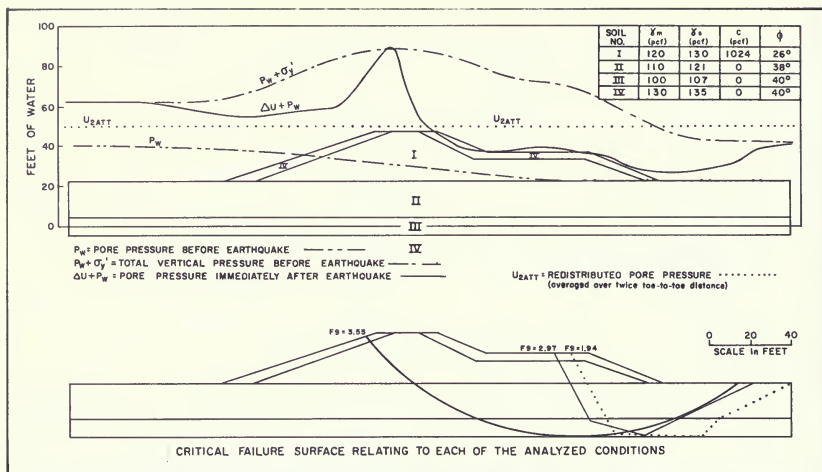


Figure 150. Post Earthquake Stability Analyses (Downstream) for Model 3—Station 347 (Columbia Soil Area)—Reservoir Elevation = 136.5 feet

For Thermalito Afterbay, the dissipation and redistribution of pore pressures for the three stations modeled was carried out by assuming the following:

1. No change in pore pressure due to post seismic shearing (probably conservative, since, according to Seed [1979], Lower San Fernando Dam sands were thought to have developed negative pore pressures).
2. No dissipation of pore pressures to other soil layers (probably conservative at Stations 107 and 347 since the weak sands lie above dense gravel layers, which would probably dissipate some of the excess pressure).
3. Pore pressures were assumed to redistribute to an average value that was constant for the entire sand layer. The pore pressures were averaged over twice the toe-to-toe horizontal distance for the embankment with the averaging zone centered on the centerline of the embankment.

As noted in the preceding section, the pore pressures used for conditions immediately after earthquake shaking were slightly higher than those actually calculated in Section 9. Therefore these analyses are somewhat conservative.

The minimum safety factors calculated for the redistributions are shown in Table 27. The critical failure surfaces for the three models are illustrated in Figures 148 through 150 for both average redistributions of pore pressure and for the pore pressures immediately after the earthquake.

The absolute minimum safety factor for the models and conditions analyzed was 1.3. This was calculated for the redistribution averaged over twice the toe-to-toe distance at Station 107. Averaging pore pressures is considered to give a conservative representation of post-earthquake stability.

Only wedge analyses were carried out for redistributed pore pressures. As before, the wedge analyses were conducted with program STABL. The redistributed pore pressures were input this time as the second phreatic surface for the sand layer. The material properties were kept

the same as in the preceding analyses, except for one modification where the average redistributed pore pressures exceeded the total vertical pressure, the friction angle was made to be zero to avoid negative shear resistances in that layer.

**Table 27: Minimum Safety Factors for Wedge Analyses  
With Pore Pressure Distribution**

Location	Reservoir Elevation ( ft )	Direction	F.S. Pore Pressure Averaged Twice Toe-to-Toe Distance
Station 107	128	Upstream	
		Downstream	—
	136.5	Upstream	—
		Downstream	1.3
Station 165	128	Upstream	—
		Downstream	—
	136.5	Upstream	—
		Downstream	1.4
Station 347	128	Upstream	2.9
		Downstream	—
	136.5	Upstream	—
		Downstream	1.9

## 11. PREDICTION OF EMBANKMENT PERFORMANCE

### General Considerations

The accuracy of the evaluation tools used in this investigation and the extent of our knowledge of earthquake engineering are recognized as being in the infant stages of development. This is mainly due to the relative rarity of earthquake events and, therefore, chances to calibrate theories and analysis techniques. The relative lack of corroboration of major portions of analysis theories and techniques has produced differences in the theories available to engineers for use in evaluating seismic stability of embankment dams. In addition, our tools for characterizing soil (in situ testing, sampling, and laboratory testing) are restricted by physical limitations and errors. In some cases representative numbers are achieved only by compensating errors.

The complexity and limited knowledge of earthquake mo-

tions and soil response has forced many analysis simplifications and assumptions. Many times when faced with unknown parameters or limited information, conservative assumptions are made. Although this is frequently appropriate, making conservative simplifications or assumptions for each step of an analysis can lead to an unrealistic result. Furthermore, different engineers make different simplifications. It is for these reasons that seismic evaluations are sometimes considered more of an art than a science.

It should be noted that many engineers use analysis results simply as augmentations of their judgments. In this evaluation, numbers such as safety factors are used as relative indicators instead of precise measurements of safety. Safety factors should not be considered without being aware of the details and choices involved in the steps of the analysis.



## Low Potential for Loss of Life

Although Thermalito Afterbay Reservoir has a relatively large capacity of 57,000 acre-feet, the dam has a maximum height of only 39 feet and is located in an area of scattered farms. Inundation studies have shown that failure of the dam would cause widespread flooding of farmland. Three small communities—Biggs, Gridley, and Live Oak—are within the limits of the inundated area. State Highway 99 is also within 300 feet of the dam. However, because the area is so flat, water released from the reservoir would spread over a wide area and the depths would be small.

The potential for damage and loss of life is much lower than for Oroville Dam. Therefore, the Board suggested, and the Department considered, assigning a greater acceptable level of risk than that used for the Oroville Dam seismic re-evaluation. One way this could be done is to adopt a smaller magnitude earthquake, with a corresponding greater probability of occurrence. The Department decided to ignore the lower risk and adopt the same earthquake magnitude (6.5) used for the Oroville Dam seismic re-evaluation.

## General Approach in the Evaluation

The embankment is composed of compacted clayey soils and, given a stable foundation, would withstand with negligible damage the shaking associated with the adopted earthquake. This conclusion is based on the performance of clay dams during earthquake shaking as described by Seed, et al. (1977). The conclusion is also considered to apply to clayey soils in the foundation, particularly the weathered surface layer found in the Afterbay foundation. This surface layer is usually found to be border line silt-clay, often containing cemented hardpan sublayers.

That extensive layers of sand exist in the dam foundation was well known from all the investigations conducted for design, construction, and seepage control. The current investigation was aimed at determining whether any of these sands are loose enough to liquefy during earthquake shaking, and whether the liquefaction would be extensive enough to cause failure of the dam. Most of the effort has been to study the effects of liquefaction on stability, but other effects could lead to unsatisfactory performance also, e.g., excessive settlement into the liquefied sand or loss of sand from the foundation by sand boils.

The physical dimensions of the problem made the task very complicated. In order to judge if stability is satisfactory for the entire 8-mile length of the dam, the search for loose sands in the foundation had to be thorough enough to give reasonable assurance that no critical conditions were missed. The required thoroughness of the search is a difficult judgment in itself.

A large amount of analytical work was carried out to predict liquefaction and consequent stability conditions. The results are used along with a consideration of case histories, understanding of general soil behavior, and review of many other investigations, to predict the performance of the dam. Admittedly, the analytic results were weighted heavily in these predictions. A greater reliance on past experience would have been preferred; however, relating to observed past behavior can be misleading without careful analyses to account for the different conditions between the case at hand and the observed behavior.

An additional point that should be noted is that the water levels in the foundation downstream of the dam are maintained by the operation of fifteen agricultural pumps, some of which are pumping continuously. The maximum pre-earthquake downstream piezometric level considered in this evaluation was at the ground surface elevation. If future changes in the operation of the reservoir and/or pump system resulted in piezometric levels significantly higher than the ground surface for extended periods, the conclusions reached in this bulletin may not apply.

## Degree of Conservatism in Analysis

The seismic stability analysis of Thermalito Afterbay Dam employed procedures consistent with the approach most widely adopted in this country, the Seed-Lee-Idriss Method. This method has been successfully calibrated against a few dams that have sustained strong earthquake shaking (Sheffield, Lower San Fernando, Upper San Fernando, and Chabot). Nevertheless, for every step in the evaluation, techniques and parameter choices had to be made. The choices adopted are believed to be either reasonable or conservative. Although in some steps the selected choices represent average values and not conservative values, sufficient conservatism was put in other steps that the overall evaluation can be considered conservative. Extreme conservatism in every step (taking the worst possible assumption) would lead to the conclusion of potential failure for most structures and would do so for the Afterbay Dam.



Table 28. Degree of Conservatism in Components of the Seismic Stability Analysis

Component	Range of Values	Values Selected	Assessment
<b>I. EARTHQUAKE LOADING</b>			
a) Critical Fault	<ul style="list-style-type: none"> <li>Prairie Creek Lineament (12-15 km away)</li> <li>Cleveland Hill Fault (13-18 km away)</li> </ul>	Cleveland Hill Fault (15 km away)	No significant difference
b) Maximum Event	<ul style="list-style-type: none"> <li>Magnitude 5.7</li> <li>Magnitude 6.5</li> </ul>	Magnitude 6.5	Conservative
c) Peak Acceleration	<ul style="list-style-type: none"> <li>Scale up 1975 Peak from Magnitude 5.7 to Magnitude 6.5</li> <li>Mean Value from Published Correlations for Magnitude 6.5 Strike-Slip and Thrust Faults</li> <li>Mean + 1 Standard Deviation Value from Published Correlations for Magnitude 6.5 Strike-Slip and Thrust Faults</li> </ul>	Mean Value from Published Correlations for Magnitude 6.5 Strike-Slip and Thrust Faults	Average
d) Accelerograms	<ul style="list-style-type: none"> <li>Modified 1975 Oroville Record</li> <li>Average Response from 3 Magnitude 6.5 Strike-Slip and Thrust Records</li> <li>Maximum Response from 3 Magnitude 6.5 Strike-Slip and Thrust Records</li> </ul>	Avg Response from 3 Magnitude 6.5 Strike-Slip and Thrust Records	Average
<b>II. CYCLIC STRENGTH</b>			
a) Characterization of In-situ Sand	<ul style="list-style-type: none"> <li>Mean SPT Blowcount</li> <li>Lowest SPT Blowcount</li> </ul>	35-Percentile SPT Blowcount	Conservative
b) Method of Determining Cyclic Strength	<ul style="list-style-type: none"> <li>Cyclic Triaxial Strength Curve</li> <li>Modification of Cyclic Triaxial Strength Curves to Match SPT Strength Correlation</li> </ul>	Modification of Cyclic Triaxial Strength Curves to Match SPT Strength Correlation	Conservative
c) Pore Pressure Development	<ul style="list-style-type: none"> <li>Limited Triaxial Data</li> <li>Published Simple Shear Curves</li> </ul>	Limited Triaxial Data	Conservative
<b>III. PREDICTION OF LIQUEFACTION</b>			
a) Method	<ul style="list-style-type: none"> <li>Seed-Lee-Idriss (Horizontal Plane)</li> <li>Casagrande Castro (Critical Void Ratio)</li> <li>Laps/Bennet (<math>\sigma_1</math> and/or <math>\sigma_m</math>)</li> </ul>	Seed-Lee-Idriss	*
b) Dynamic Analysis	<ul style="list-style-type: none"> <li>Equivalent Linear Total Stress</li> <li>Non-Linear Effective Stress</li> </ul>	Equivalent Linear Total Stress	*
<b>IV. POST-EARTHQUAKE STABILITY</b>			
a) Interpretation of Static Triaxial Compression Tests	<ul style="list-style-type: none"> <li>Lower Bound, Curve Through Data</li> <li>Average Curve Through Data</li> </ul>	Average Curve Through Data	Average
b) Strength of Sand Following Earthquake Shaking	<ul style="list-style-type: none"> <li>Zones With 10% Compressive Strain Potential Have Zero Strength. All other Zones Have Full Strength and Zero Excess Pore Pressure.*</li> <li>Zones Which Develop 100% Excess Pore Pressure Have Residual Viscous Strength. All Other Zones Have Reduced Strengths Due to Excess Pore Pressure.</li> <li>Zones Which Develop 10% Compressive Strain Potential Have Reduced Strengths Due to Excess Pore Pressures</li> </ul>	Zones Which Develop 10% Compressive Strain Potential Have Zero Strengths. All Other Zones Have Reduced Strengths Due to Excess Pore Pressure	Conservative
c) Pore Pressure Redistribution	<ul style="list-style-type: none"> <li>Dissipation and Dilation Force Pore Pressures in Non-Liquefied Areas to Drop to Pre-Earthquake Conditions</li> <li>Pore Pressures Redistributed to an Average Constant Value Across the Sand Layer</li> </ul>	Pore Pressures Redistributed to an Average Constant Value Across the Sand Layer	Extremely Conservative
Net Stability Factor = 1.3			Conservative

\*Value is integral part of procedure (Seed-Lee-Idriss) calibrated against observed behavior of Chabot, Sheffield, Lower San Fernando, and Upper San Fernando dams.

The components and parameters of the analysis are summarized in Table 28. An overall degree of conservatism cannot be obtained from the table since conservatism is more a matter of judgment than of statistics. Furthermore, the components are not directly proportional to each other, i.e., a 20 percent increase in cyclic shear strength will not produce a 20 percent increase in the post-earthquake stability safety factor. Nevertheless, since most of the components are assessed as conservative, the final stability factor of safety (1.3) can be accepted as conservative.

A further conservatism should also be noted. When the evaluation of Thermalito Afterbay Dam was performed, there was insufficient information from available case histories to justify a non-zero residual shear strength in completely liquefied sands. Consequently, the post-earthquake slope stability analyses performed for the three critical sites employed zero residual shear strengths (i.e., 100 percent pore pressures and zero cohesion) for foundation soil areas predicted to have complete liquefaction. By the time this bulletin was written, however, recent interpretations of post-earthquake sliding in liquefied soils showed that a significant residual shear strength could have been justified for the afterbay soils. This would have increased significantly the post-earthquake slope stability factors of safety (see analyses for Thermalito Forebay Dam in Chapter V).

### Case Histories of Embankments With Foundation Liquefaction

Many small embankments have experienced strong earthquake shaking. These include small dams, railroad and highway embankments, and river and canal levees. Studies of performance have been made mainly in the United States and Japan. These studies tend to be biased by the tendency to report behavior only for damaged structures.

Damage reports from strong earthquakes include small embankments that failed due to liquefaction of the foundation. These structures include highway and railroad embankments in Alaska, canal levees in El Centro, river levees in Japan, and the Sheffield Dam near Santa Barbara. However, none of these embankments was founded on surface silt/clay caps overlying the liquefiable sand layers:

1. Sheffield Dam was a 25-foot-high earth embankment that failed during the 1925 Santa Barbara Earthquake. The earthquake was considered a Richter Magnitude 6.3 event with an epicenter about 7 miles away from the damsite. Peak accelerations were estimated by Seed et al. (1967) to be about 0.15g (probably too low by subsequent correlations). Failure was attributed to earthquake-induced liquefaction of loose silty sand near the base of the dam. This resulted in a 300-foot length of dam sliding about 100 feet downstream.
2. The Hosorogi railroad embankment suffered extensive damage during the 1948 Fukui Earthquake. This silty/clay embankment was constructed on soft organic silt. The embankment had a maximum height of about 28 feet and experienced horizontal earthquake accelerations as high as 0.45g. According to Ambraseys (1960):  
  
 "The embankment in most places slumped to 40 percent of its original height while it was displaced horizontally by as much as its full width. Cross sections of the embankment after the earthquake show that it was first broken into blocks by the shock and the unequal subsidence of its foundation, and it was then flattened to a shapeless mass of earth blocks. The foundation sunk considerably and rows of rice plant on both sides of the embankment were heaved up and compressed at the toes of the slopes. In many places the structure flowed out, leaving the tracks in the air. At other points the track was turned upside down by the flow of the fill material, which in places moved 50 feet from its original position. The type of failure generally observed along the Hosorogi embankment indicates clearly a base failure and spreading of the fill; the fundamental cause being the soft foundation material. The fact that the collapse was due to base failure is best illustrated by the evidence that houses built on soft ground near Kitagata-mura sunk more than three feet into the ground but sustained absolutely no damage to the roof and structural members."
3. According to Seed (1968), highway embankments in the 1964 Alaska Earthquake ( $M_s = 8.6$ ) suffered extensive cracking due to liquefaction of the foundation silts and lateral spreading. The example quoted

shows a highway embankment about 12 feet high that developed large longitudinal centerline cracks and some transverse cracks. It was postulated that the lateral movement of this embankment was limited because liquefaction did not extend across the entire base of the embankment.

These are the only reported examples found for similar-sized embankments that developed significant damage during earthquakes. All of these embankments were founded directly on the soils, which lost strength and, being older, were probably not as well constructed as Thermalito Afterbay Dam.

To our knowledge, there are no reported performance cases with the same conditions as the Afterbay—a liquefied sand layer capped by an impervious layer on which the embankment is built.

The historical documented evidence is too limited to use as a basis for predicting behavior for the specific conditions at the Afterbay. However, it is encouraging that case histories could not be found where liquefaction at depth caused failure of an embankment on a confining impervious surface layer.

### Age of Red Bluff Silty Sands

The suspect silty sands in the Red Bluff Formation are estimated to be approximately 450,000 years old (Pleistocene Epoch). Earthquake induced failures have generally occurred in much younger Holocene deposits. Statistical

studies by Youd and Perkins (1978) indicate that alluvial and flood plan deposits of the Pleistocene Epoch have a low probability of developing liquefaction induced ground failure.

### Comparison With Upper San Fernando Dam

The level of permanent earthquake-induced deformations that might be produced Thermalito Afterbay Dam can be estimated by examining the performance of Upper San Fernando Dam during the 1971 San Fernando Earthquake ( $M_L = 6.6$ ). The Upper San Fernando Dam is a hydraulic fill embankment, which was shaken severely by the 1971 earthquake. Investigations indicated that the earthquake produced peak ground accelerations of about 0.6g at the dam site and induced zones of liquefaction within the hydraulic fill. Despite development of the liquefied zones, the dam suffered average deformations of about 6 feet of horizontal movement and about 2.5 feet of settlement (see Seed et al., 1973; Addendum F in Chapter V).

The most critical site along Thermalito Afterbay Dam is the Station 107 (Site 1) location. Both the Station 107 suspect sands and the Upper San Fernando Dam hydraulic fill were analyzed to have liquefied zones following earthquake shaking. However, because the Station 107 sands were found to have higher cyclic shear strength (see Figure 151), the amount of predicted liquefaction was less for this site than at upper San Fernando Dam (Figure 152). The following chart compares the two structures:

Parameter	Thermalito Afterbay Dam Station 107 Site	Upper San Fernando Dam
Height of Embankment (feet)	26	70
Thickness of Liquefiable Zone (feet)	15	40
Liquefiable Soil	Silty Sand $N_{A1} = 20$	Silty Sand & Sandy Silt $N_{A1} = 10 - 14$
Earthquake	$M = 6.5$ $a_{max} = 0.35g$	$M = 6.6$ $a_{max} = 0.6g$

A review of the materials and loading for the two sites indicates that the predicted deformations will be much less at Thermalito Afterbay than those sustained at Upper San Fernando Dam. Factors indicating this include (1) much lower earthquake loading, (b) much smaller thickness of liquefiable materials, (c) higher

SPT blowcounts, and (d) smaller amounts of predicted liquefaction at Thermalito Afterbay than at Upper San Fernando Dam. In light of these comparisons, judgment would suggest that only about 0.5 feet of settlement and 1 foot of lateral movement would be predicted for locations along Thermalito Afterbay Dam.

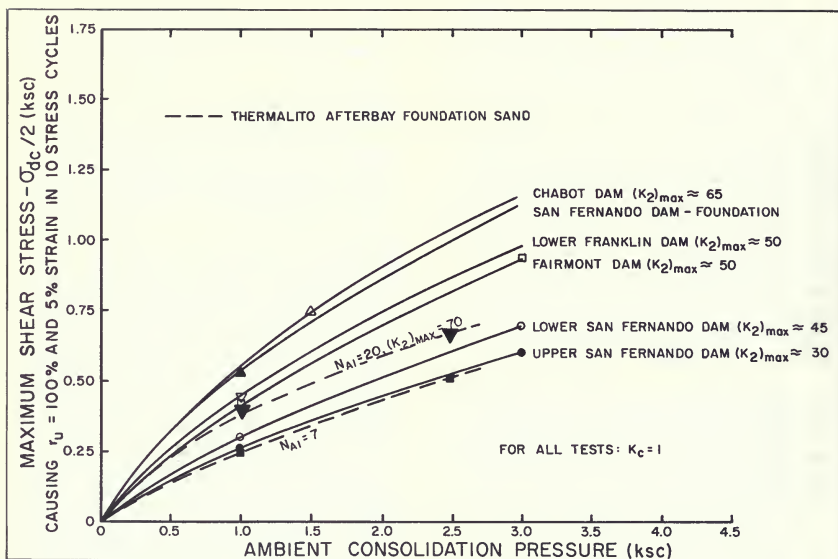


Figure 151. Comparison of Cyclic Triaxial Strengths of Thermalito Afterbay Silty Sands with Sands that have Withstood Strong Earthquake Shaking

### Other Earthquake Effects

Unacceptable performance other than shear slides is sometimes associated with liquefaction of foundation sand. In the case of a dam, the consequences could be:

- The embankment sinking into liquefied sand, resulting in loss of freeboard.
- Differential settlement or sinking at the end of an area of foundation liquefaction could cause transverse cracks subject to seepage and erosion.
- Liquefied sand "flowing" out from under the dam and surfacing in sand boils, causing excessive settlement—loss of freeboard.

It is very unlikely that any of the above consequences would develop at Thermalito Afterbay because of the strong impervious layer that overlies the sand.

Additional possible sources of unacceptable behavior are local reaches of the dam where there exist sharp downstream angles in the axis alignment, such as the 90-degree bend at Station 225. These locations may possibly develop large displacements and transverse cracking due to out-of-phase and different directions of response to any earthquake shaking. Although this behavior is also considered unlikely for the anticipated level of earthquake motions, the Department reinforced the Station 225 bend with an upstream fillet buttress (See Chapter I).

## Predicted Performance For Magnitude 6.5 Earthquake

The behavior of clay embankments during earthquakes indicates that the afterbay embankment and clay foundation layers would perform well during severe earthquakes, in the absence of adverse foundation behavior. For limited extents along the dam's length, analyses pre-

dict liquefaction in some foundation sands beneath the dam crest and beyond the toes for the postulated earthquake shaking. The surface cap of silt and clay has a substantial stabilizing effect since the minimum safety factor against sliding is 1.3 using a conservative assumption of zero residual shear resistance in the liquefied sands. Historical evidence is generally consistent with this finding. Only minor cracking or movements are predicted for the postulated shaking.

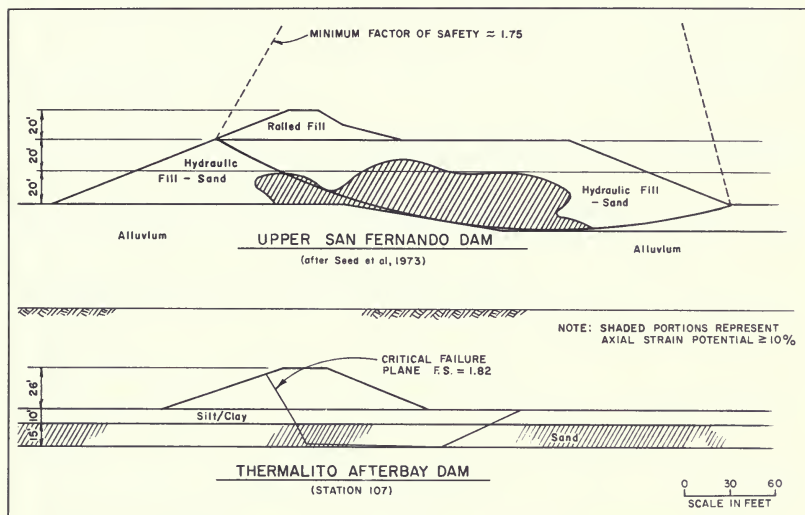


Figure 152. Comparison of Thermalito Afterbay Dam with Analysis of Stability of Upper San Fernando Dam Immediately Following Earthquake Shaking.



## REFERENCES FOR CHAPTER III

1. Ambraseys, N. N. (1960), "On the Seismic Behavior of Earth Dams," *Proceedings of the Second World Conference on Earthquake Engineering*, Japan, 1960.
2. Banerjee, Nani G.; Seed, H. Bolton; and Chan, Clarence K. (1979), "Cyclic Behavior of Dense Coarse-Grained Materials in Relation to the Seismic Stability of Dams," Earthquake Engineering Research Center, Report No. UCB/EERC-79/13, University of California, Berkeley.
3. Bennett, M. J.; Youd, T. L.; Harp, E. L.; and Weiczorek, G. F. (1981), "Subsurface Investigation of Liquefaction, Imperial Valley Earthquake, California, October 15, 1979," U. S. Geological Survey Open File Report 81-502, 1981.
4. Bennett, W. J. (1977), "Dynamic Analysis Proposal", Office Memorandum, Division of Safety of Dams, Department of Water Resources.
5. Brady, A. G.; Perez, V.; and Mork, P. N. (1980), "The Imperial Valley Earthquake, October 15, 1979. Digitization and Processing of Accelerograph Records." Seismic Engineering Data Report 80-703. United States Geological Survey, Menlo Park, California, April.
6. California Department of Transportation (1979), "Report of Down-Hole Shear Wave Investigation at Thermalito Afterbay and Forebay." Report Prepared for the Department of Water Resources.
7. California Department of Transportation (1980), "Down-Hole Shear Wave Velocity Results for Thermalito Afterbay." Data Report Prepared for the Department of Water Resources.
8. California Department of Water Resources (1962), "Basic Data Compilation Report—Exploration Drilling— Thermalito Afterbay", August 31, 1962.
9. California Department of Water Resources (1964), "Interim Exploration Data, Soil Permeability Investigation— Thermalito Forebay and Afterbay." April 9, 1964.
10. California Department of Water Resources (1965a), "Thermalito Forebay and Afterbay Geology and Construction Materials Data." Project Geology Report D-48, May 1965.
11. California Department of Water Resources (1965b), "Interim Exploration Data, Columbia Soil Area, Thermalito Afterbay," August 18, 1962.
12. California Department of Water Resources (1968a), "Final Geologic Report on Foundation Conditions and Grouting Thermalito Forebay and Afterbay—Appendix A to Final Construction Report," Project Geology Report No. C-31, July 1968.
13. California Department of Water Resources (1968b), "Final Construction Report on Thermalito Forebay and Afterbay—Oroville Division," August 1968.
14. California Department of Water Resources (1969), "Thermalito Afterbay Seepage Control Memorandum Report," August 1969.
15. California Department of Water Resources (1973), "Thermalito Afterbay—Draft Final Design Report", 1973.



16. California Department of Water Resources (1977), "Performance of the Oroville Dam and Related Facilities During the August 1, 1975 Earthquake," Bulletin 203-78.
17. California Department of Water Resources (1979), "The August 1, 1975 Oroville Earthquake Investigations," Bulletin 203-78.
18. California Department of Water Resources (1983a), "Basic Data Report—Exploration For Seismic Stability re-evaluation —Thermalito Forebay and Afterbay." Project Geology Report.
19. California Department of Water Resources (1983b), "Soils Laboratory Report—Laboratory Test Results for Seismic Stability Re-evaluation —Thermalito Forebay and Afterbay."
20. California Department of Water Resources (1983c), "Thermalito Afterbay—Vibroflotation Test Program to Densify Foundation Sands."
21. Casagrande, A., "Liquefaction and Cyclic Deformation of Sands – A Critical Review (1975)." Paper Presented at the Fifth Panamerican Conference on Soil Mechanics and Foundation Engineering, Buenos Aires, Argentina, November 1975.
22. Clark, K. R. (1969), "Research on Undisturbed Sampling of Soils, Shales, Air Drilling Techniques, and Data on Penetration Resistance Testing—Third Progress Report on Soil Sampling Research." Report No. EM-770, United States Department of the Interior, Bureau of Reclamation, July.
23. Douglas, B. J.; Olsen, R. S.; and Martin, G. R. (1981), "Evaluation of the Cone Penetrometer Test for Use in SPT-Liquefaction Potential Assessment." Preprint From the ASCE Annual Convention, St. Louis, October 1981.
24. Ertec Western, Inc. (1981), "Cone Penetrometer Test Investigations and Analyses, Thermalito Afterbay, Oroville, California." Report Submitted to the State of California, Department of Water Resources, July.
25. Ertec Western, Inc. (1982), "Cone Penetrometer Test Investigations and Analyses, Thermalito Afterbay Vibroflotation Program, Oroville, California." Report Submitted to the State of California, Department of Water Resources, January.
26. Hudson, E. E. and Brady, A. G. (1971), "Strong Motion Earthquake Accelerograms—Digitized and Plotted Data," Vol. II – Part A, Report No. EERL 71-50, Earthquake Engineering Research Laboratory, California Institute of Technology, Pasadena, California, September.
27. Idriss, I. M. and Power, M. S. (1978), "Peak Horizontal Accelerations, Velocities, and Displacements on Rock and Stiff Soil Sites for Moderately Strong Earthquakes." Submitted to the Bulletin of the Seismological Society of America for possible publication.
28. Kovacs, W. D. (1981), "Results and Interpretation of SPT Practice Study," Geotechnical Testing Journal, GTJODJ, Vol. 4, No. 3, September.
29. Kovacs, W. D.; Salomone, L. S.; and Yokel, F. Y. (1981), "Energy Measurement in the Standard Penetration Test", NBS Building Science Series 135, National Bureau of Standards, Washington, D. C.
30. Lee, Kenneth L. and Idriss, Izzat M. (1975) "Static Stresses by Linear and Nonlinear Method." Journal of the Geotechnical Engineering Division, American Society of Civil Engineers, 101, No. GT9, September.



31. Leps, Thomas M. (1973), "Butt Valley Dam—Evaluation of Seismic Stability." Report for Pacific Gas and Electric Company by Thomas M. Leps, Inc., August 1973.
32. National Bureau of Standards (1983), "SPT Energy Evaluations (Performed at Thermalito Afterbay, Oroville, California, January 11–12, 1982)." Report Submitted to the Department of Water Resources.
33. Pyke, Robert M.; Knuppel, Lee A.; and Lee, Kenneth L. (1978), "Liquefaction of Hydraulic Fill." Journal of the Geotechnical Engineering Division, American Society of Civil Engineers, 104, No. GT11, November.
34. Sarmiento, John (1981), "U. S. Geological Survey Cone Penetration Program for Thermalito Afterbay, Oroville California." U. S. Geological Survey Report MS-98, Menlo Park, California.
35. Schmertmann, John H. (1979), "Statics of SPT." Journal of the Geotechnical Engineering Division, American Society of Civil Engineers, 105, GT5, May.
36. Schnabel, P. B.; Lysmer, John; Seed, H. Bolton (1972), "SHAKE, a Computer Program for Earthquake Response Analysis of Horizontally Layered Sites." Earthquake Engineering Research Center, Report No. EERC 72-12, University of California, Berkeley.
37. Seed, H. Bolton (1968), "Landslides During Earthquakes Due to Soil Liquefaction." Journal of the Soil Mechanics and Foundations Division, American Society of Civil Engineers, 92, SM3, March.
38. Seed, H. B. (1976), "Evaluation of Soil Liquefaction Effects During Earthquakes." Presented at the ASCE Annual Convention and Exposition, Philadelphia, PA September–October 1.
39. Seed, H. Bolton (1979), "Considerations in the Earthquake-Resistant Design of Earth and Rockfill Dams," *Geotechnique*, 29, No. 3.
40. Seed, H. B.; and Idriss, I. M. (1970), "Soil Moduli and Damping Factors for Dynamic Response Analyses." Earthquake Engineering Research Center, Report No. EERC 70-10, University of California, Berkeley, December.
41. Seed, H. B.; and Idriss, I. M. (1982), "Ground Motions and Soil Liquefaction During Earthquakes," monograph, Earthquake Engineering Research Institute, Berkeley, California, 1982.
42. Seed, H. B.; Idriss, I. M.; Makdisi, F. I.; and Banerjee, N. (1975), "Representation of Irregular Stress Time Histories by Equivalent Uniform Stress Series in Liquefaction Analyses." Earthquake Engineering Research Center, Report No. EERC 75-29, University of California, Berkeley, October.
43. Seed, H. B.; Lee, K. L.; and Idriss, I. M. (1969), "An Analysis of the Sheffield Dam Failure." Journal of the Soil Mechanics and Foundations Division, ASCE, Vol. 95, No. SM6, November.
44. Seed, H. B.; Lee, K. L.; Idriss, I. M.; and Makdisi, F. I. (1973), "Analysis of the Slide in the San Fernando Dams During the Earthquake of February 9, 1971." Earthquake Engineering Research Center, Report No. 73-2, University of California, Berkeley, June.
45. Seed, H. B.; Makdisi, F. I.; and DeAlba, P. (1978), "Performance of Earth Dams During Earthquakes." Journal of the Geotechnical Division, ASCE, Vol. 104, No. GT7, September.
46. Seed, H. B.; Murarka, R.; Lysmer, J.; and Idriss, I. M. (1975), "Relationships Between Maximum Acceleration, Maximum Velocity, Distance from Source, Local Site Conditions for Moderately Strong Earthquakes." Earthquake Engineering Research Center, Report No. EERC 75-17, University of California, Berkeley.

47. Seed, H. B.; Ugas, C.; and Lysmer, J. (1974), "Site Dependent Spectra for Earthquake-Resistant Design." Earthquake Engineering Research Center, EERC74-11, University of California, Berkeley.
48. Singh, S.; Seed, H. B.; and Chan (1979), "Undisturbed Sampling and Cyclic Load Testing of Sands." Earthquake Engineering Research Center, Report No. UCB/EERC 79/33, University of California, Berkeley, December.
49. Smith, D. (1979), "Dynamic Analysis of Castaic Dam." Office Report, Department of Water Resources, Division of Safety of Dams.
50. Steinberg, S. (1981), "Energy Calibration and Hammer Influence on SPT." Paper Presented at the Engineering Foundation Conference on Updating Subsurface Sampling of Soils and Rocks and Their Insitu Testing, Santa Barbara, California, January 3-8, 1982.
51. Tokimatsu, K.; and Yoshimi, H., "Field Correlation of Soil Liquefaction With SPT and Grain Size." Proceedings—International Conference on Recent Advances in Geotechnical Earthquake Engineering and Soil Dynamics, St. Louis, MO, April 26 – May 2.
52. Trifunac, M. D. and Brune, J. N., (1970), "Complexity of Energy Release During the Imperial Valley, California, Earthquake of 1940." Bulletin of the Seismological Society of America, Vol. 60, No. 1, February.
53. Vaid, Y. P. and Finn, W. D. Liam (1979), "Effect of Static Shear on Liquefaction Potential." Journal of the Geotechnical Engineering Division, ASCE, Vol. 105, GT10, October
54. Vrymoed, J. L., and Calzascia, E. R. (1978), "Simplified Determination of Dynamic Stresses in Earth Dam," Proceedings of the ASCE Geotechnical Engineering Division Specialty Conference on Earthquake Engineering and Soil Dynamics, Pasadena, CA, June.
55. Wong, K. S., and Duncan, J. M. (1974), "Hyperbolic Stress-Strain Parameters for Nonlinear Finite Element Analysis of Stress and Movements in Soil Masses." Report No. TE-74-3, University of California, Berkeley.
56. Woodward-Clyde Consultants (1980), "Shear Wave Velocity Measurements at Oroville, California." Report Submitted to the Department of Water Resources, July.
57. Youd, T. L., and Perkins, D. M. (1978), "Mapping Liquefaction-Induced Ground Failure Potential." Journal of the Geotechnical Engineering Division, ASCE, Vol. 104, No. GT4, April.

## **ADDENDA TO CHAPTER III**

**A. List of Borings and Soundings**

**B. Static Stresses from Static Finite Element Analyses**

**C. Accelerograms**

**D. Results of Dynamic Response Analyses**

**E. Dynamic Testing**

**F. Trial Failure Surfaces Generated for Slope Stability Analyses**



## ADDENDUM A

### LIST OF BORINGS AND SOUNDINGS

The drilling and sampling procedures performed at Thermalito Afterbay are described in detail in Section 3 of Chapter 3. From 1976—1972, more than 500 explorations were placed along the length of the dam. This addendum contains a list consisting of the following:

#### 1. Exploration Identification

SV, D, SPT = Standard Penetration Test Boring

CP, CV, CPT = Cone Penetrometer Test Sounding

M = mechanical; E = electrical

PS = Stationary Piston Sampling Boring

PB = Pitcher Barrel Sampling Boring

(Three borings, 79—361, and 79—378 were performed by Selby Push.)

#### 2. Station

Station of hole location along the dam axis (feet)

#### 3. Location

Location and distance of hole along dam section—usually with reference to crest centerline, toe, or maintenance road centerline.

#### 4. Tested By

Organization that performed the exploration. The following organizations participated in the explorations:

- a. California Department of Transportation (Caltrans)
- b. Continental Drilling Company
- c. Ertec Western, Inc.
- d. United States Geological Survey

#### 5. Date Tested

Actual dates on which the exploration was performed

#### 6. Spacing

Distance (feet) of the exploration from the exploration upstation.

**Thermalito Afterbay Seismic Explorations**  
**Borings from the 1976, 1978, 1979-80, and 1981-82 Investigations**

Exploration	Station	Location	Tested By	Date Tested	Spacing (feet)
81A-CF1 SPT		14' W/O DS Toe	Continental	10/15/81	N/A
81A-CF2 SPT		13' " "	Continental	10/14/81	N/A
81A-10 SPT	10+50	6' " "	Continental	7/22,23/81	N/A
81A-12 SPT	12+50	8' " "	Continental	7/23,24/81	200
81A-14 SPT	14+53	7' " "	Continental	7/22,23/81	203
D-1	17+00	5' " "	Caltrans	3/22,23/76	247
81A-19 SPT	19+60	10' " "	Continental	7/27,28/81	260
81A-22 SPT	22+20	7' " "	Continental	7/7,8/81	260
81A-25 SPT	24+80	6' " "	Continental	7/9,10/81	260
81A-27 SPT	27+40	8' " "	Continental	7/13,14/81	260
79-30 SPT	30+00	9' " "	Caltrans	10/23/79	260
81A-32 SPT	32+50	8' " "	Continental	7/14,15/81	250
81A-35 SPT	35+00	10' " "	Continental	7/16,17/81	250
81A-37 SPT	37+50	10' " "	Continental	7/20,21/81	250
79-40 SPT	40+01	5' " "	Caltrans	10/23,24/79	251
81A-42 SPT	42+50	7' " "	Continental	7/28,29/81	249
81A-45 SPT	45+00	4' " "	Continental	7/29,30/81	250
81A-47 SPT	47+50	5' " "	Continental	7/30/81	250
79-50 SPT	49+98	5' " "	Caltrans	10/24/79	248
81A-52 SPT	52+50	5' " "	Continental	8/3/81	252
81A-55 SPT	55+00	5' " "	Continental	8/4-6/81	250
79-57 SPT	57+23	5' " "	Caltrans	10/31/79	223
81A-59 SPT	59+50	3' " "	Continental	8/6,7,10/81	227

**Thermalito Afterbay Seismic Explorations**  
**Borings from the 1976, 1978, 1979-80, and 1981-82 Investigations**

Exploration	Station	Location	Tested By	Date Tested	Spacing (feet)
81A-62 SPT	62+00	7' W/O DS Toe	Continental	8/10,11/82	250
81A-64 SPT	64+50	5' " "	Continental	8/12/81	250
81A-67 SPT	67+00	7' " "	Continental	8/13/81	250
81A-70 SPT	70+00	15' " "	Continental	8/14,17/81	300
81A-72 SPT	72+50	20' " "	Continental	8/20/81	250
D-2	74+88	At DS Toe	Caltrans	3/23,24/76	238
81A-C27 CPT	75+00	C-Maintenance Road	Ertec	10/23/81	12
81A-77 SPT	77+50	25' W/O DS Toe	Continental	8/17,18/81	250
81A-80 SPT	80+10	25' " "	Continental	8/21/81	260
81A-C26 CPT	81+50	C-Maintenance Road	Ertec	10/23/81	140
81A-83 SPT	83+00	30' W/O DS Toe	Continental	8/24,25/81	150
81A-85 SPT	85+30	25' " "	Continental	8/25,26/81	230
81A-C25A CPT	86+80	C-Maintenance Road	Ertec	10/23/81	150
79-88 SPT	88+25	8.5' W/O DS Toe	Caltrans	10/71-21/81	145
81A-90 SPT	90+00	35' " "	Continental	8/26,27/81	175
81A-92 SPT	92+50	30' " "	Continental	8/27/81	250
81A-95 SPT	95+00	44' " "	Continental	8/27/81	250
81A-C24 CPT	96+40	C-Maintenance Road	Ertec	10/23/81	140
81A-98 SPT	98+20	35' W/O DS Toe	Continental	9/1/81	180
81A-100 SPT	100+00	35' " "	Continental	9/2/81	180
79-102 SPT	102+00	15' " "	Caltrans	10/16/79	200
80-102 SPT	102+00	8-1/2' E/O C-Crest	Caltrans	3/27/80	
81A-104 PB-A	104+10	22' W/O DS Toe	Continental	7/2/81	210

**Thermalito Afterbay Seismic Explorations**  
**Borings from the 1976, 1978, 1979-80, and 1981-82 Investigations**

Exploration	Station	Location	Tested By	Date Tested	Spacing (feet)
81A-104 SPT-F	104+16	21' W/O DS Toe	Continental	8/17,18/81	6
81A-104 SPT-G	104+16	47' " "	Continental	8/19/81	
81A-104 SPT-L	104+22	21' " "	Continental	4/15/82	6
80-104 SPT	104+28	8-1/2 E of $\bar{C}$ -Crest	Caltrans	3/26,27/80	6
81A-104-PS-A	104+28	27' W/O DS Toe	Continental	8/14-17/81	
81A-104-SPT-J	104+28	15' " "	Continental	3/26/82	
81A-104 SPT-K	104+34	15' " "	Continental	3/30-4/12/82	6
81A-104 SPT-A	104+34	21' " "	Continental	7/2/81	
81A-104 SPT-E	104+34	27' " "	Continental	7/21/81	
81A-104 SPT-H	104+40	15' " "	Continental	3/10,11/82	6
81A-104 SPT-B	104+40	21' " "	Continental	7/6/81	
81A-104 SPT-C	104+40	27' " "	Continental	7/8-14/82	
81A-104 SPT-M	104+46	15' " "	Continental	4/16/82	6
81A-104 SPT-D	104+46	21' " "	Continental	7/17-20/81	
79-104 SPT	104+50	22' " "	Caltrans	10/18/79	4
81A-C1 CPT	105+83	7' " "	Ertec	10/24/81	137
CV1-21	105+83	11' " "	Ertec	2/2/82	
81A-107 SPT-J	105+86	15' " "	Continental	7/28/81	3
81A-C2 CPT	105+97	15' " "	Ertec	10/22/81	11
81A-C3 CPT	106+11	7' " "	Ertec	10/22/81	14
CV1-22	106+11	11' " "	Ertec	2/2/82	
81A-107 SPT-H	106+15	15' " "	Continental	7/27/81	4
81A-C15 CPT	106+26	6' W/O $\bar{C}$ -Crest	Ertec	10/24/81	11



**Thermalito Afterbay Seismic Explorations**  
**Borings from the 1976, 1978, 1979-80, and 1981-82 Investigations**

Exploration	Station	Location	Tested By	Date Tested	Spacing (feet)
81A-C107 SPT-B	106+26	℄-Crest	Continental	9/21-23/81	
81A-C4 CPT	106+30	8' W/O DS Toe	Ertec	10/22/81	4
81A-C5 CPT	106+30	22' W/O DS Toe	Ertec	10/22/81	
CV1-20	106+30	18-1/2' W/O DS Toe	Ertec	2/2/82	
CV1-C1	106+32	℄-Crest	Ertec	2/1/82	2
81A-107 SPT-G	106+33	15' W/O DS Toe	Continental	7/24/81	1
SV1-9	106+40	9' " "	Continental	1/18/81	7
81A-C6 CPT	106+45	8' " "	Ertec	10/22/81	5
81A-C7 CPT	106+45	22' " "	Ertec	10/22/81	
CV1-17	106+45	11-1/2' W/O DS Toe	Ertec	10/24/81	
CV1-18	106+45	9-1/2 " "	Ertec	10/23/81	
CV1-19	106+45	8' " "	Ertec	10/23/81	
81A-107 SPT-F	106+48	13' " "	Continental	7/23/81	3
81A-107 SPT-D	106+60	13' " "	Continental	7/20/81	12
81A-107 PS-E	106+60	18' " "	Continental	11/6/81	
81A-107 SPT-Q	106+60	24' " "	Continental	8/6/81	
TAS-1C	106+62	37' " "	Caltrans	8/15/78	2
CP-107-M1	106+64	8' " "	USGS	5/19/81	2
81A-107 PS-A	106+66	22' " "	Continental	9/10-11/81	2
81A-107 PS-G	106+66	15' " "	Continental	11/5/81	
CP-107-E3	106+68	13' " "	Ertec	5/28/81	2
CP-107-E2	106+68	8' " "	USGS	5/19/81	
81A-107 SPT-R	106+72	19' " "	Continental	8/7/81	4

**Thermalito Afterbay Seismic Explorations**  
**Borings from the 1976, 1978, 1979-80, and 1981-82 Investigations**

Exploration	Station	Location	Tested By	Date Tested	Spacing (feet)
81A-107 PS-D	106+72	24' W/O DS Toe	Continental	7/20/81	
81A-107 SPT-S	106+72	31' " "	Continental	8/10/81	
CP-107-M2	106+74	8' " "	USGS	5/19/81	2
81A-C107 SPT-C	106+76	7' E/O $\xi$ -Crest	Continental	9/23-25/81	2
CP-107-E4	106+78	13' W/O DS Toe	Ertec	5/28/8	2
CP-107-E1	106+78	8' " "	USGS	5/19/81	
CV1-C2	106+80	5' E/O $\xi$ -Crest	Ertec	2/1/82	2
80-107A SPT	106+80	10-1/2' E/O $\xi$ Crest	Caltrans	3/28-31/80	
TAS-1B	106+82	8' W/O DS Toe	Caltrans	7/13-14/78	2
79-107A SPT	106+83	124' " "	Caltrans	8/27/79	1
TAS-1A	106+84	11' W/O $\xi$ -Crest	Caltrans	7/11/78	1
81A-107 SPT-A	106+84	25' W/O DS Toe	Continental	7/6/81	
81A-107 SPT-C	106+84	14' " "	Continental	7/17/81	
SV1C-1	106+84	3' E/O $\xi$ -Crest	Continental	12/22,23,30/81	
81A-C16 CPT	106+85	6' " "	Ertec	10/24/82	1
79-107 SPT	106+86	18' W/O DS Toe	Caltrans	9/28-10/1/79	1
CP-107A-M1	106+87	10-1/2' E/O $\xi$ -Crest	USGS	5/20/81	1
81A-C107 SPT-D	106+88	$\xi$ -Crest	Continental	9/28-29/81	1
81A-107 SPT-B	106+90	25' W/O DS Toe	Continental	7/7/81	1
SV1C-2	106+91	3' W/O $\xi$ -Crest	Continental	12/31/81, 1/4-6/82	1
80-107 SPT	106+91	9' W/O $\xi$ -Crest	Caltrans	3/20-25/80	
81A-107 SPT-E	106+93	19' W/O DS Toe	Continental	7/20-21/82	2
CV1-C3	106+94	3' W/O $\xi$ -Crest	Ertec	12/17/81	1

**Thermalito Afterbay Seismic Explorations**  
**Borings from the 1976, 1978, 1979-80, and 1981-82 Investigations**

Exploration	Station	Location	Tested By	Date Tested	Spacing (feet)
CP-107A-E1	106+94	10-1/2' E/O $\xi$ -Crest	USGS	5/21/81	
CP-107A-E3	106+95	5-1/2' E/O $\xi$ -Crest	Ertec	5/28/81	1
81A-107 SPT-T	106+96	13' W/O DS Toe	Continental	8/11/81	1
SV1-1	106+96	19' W/O DS Toe	Continental	12/23-28/81	
SV1-2	106+96	22' W/O DS Toe	Continental	12/28-30/81	
SV1-3	106+96	16' W/O DS Toe	Continental	12/30/81	
81A-C107 SPT-E	106+97	6' E/O $\xi$ -Crest	Continental	9/30-10/1/81	1
TAS-1	107+00	11' W/O $\xi$ -Crest	Caltrans	7/5-7/78	3
SV1-4	107+00	11' " "	Continental	12/31/81	
CV1-14	107+00	19' " "	Ertec	2/1/82	
CV1-16	107+00	16' " "	Ertec	2/1/82	
79-107B SPT	107+00	124' " "	Caltrans	8/7-24/79	
81A-C8 CPT	107+02	13' " "	Ertec	10/22/81	2
CV1-13	107+03	16' " "	Ertec	2/1/82	1
CV1-15	107+03	13' " "	Ertec	2/1/82	
81A-107 SPT-P	107+06	19' " "	Continental	8/5/81	3
SV1-5	107+09	9' " "	Continental	1/5/82	3
TAS-1D	107+10	8' " "	Caltrans	8/23,24/78	1
SV1-6	107+12	11' " "	Continental	1/5-6/82	3
CV1-11	107+13	16' " "	Ertec	2/1/82	1
81A-C9-CPT	107+13	6' " "	Ertec	10/23/81	
81A-C10-CPT	107+13	19' " "	Ertec	10/22/81	
CV1-12	107+16	9' " "	Ertec	2/1/82	3

**Thermalito Afterbay Seismic Explorations**  
**Borings from the 1976, 1978, 1979-80, and 1981-82 Investigations**

Exploration	Station	Location	Tested By	Date Tested	Spacing (feet)
CV1-8	107+16	6' W/O E-Crest	Ertec	12/18/81	
79-107C SPT	107+17	124' " "	Caltrans	9/19/79	1
81A-107 SPT-N	107+20	17' " "	Continental	8/4/81	1
81A-C11-CPT	107+23	13' " "	Ertec	10/23/81	3
TAS-1E	107+24	8' " "	Caltrans	8/24,25/78	1
CV1-10	107+24	16' " "	Ertec	2/1/82	
CV1-9	107+26	16' " "	Ertec	2/1/82	2
81A-107 PS-F	107+26	18' " "	Continental	11/3-4/81	
81A-107 SPT-M	107+26	7' " "	Continental	8/3/81	
SV1-8	107+26	11' W/O DS Toe	Continental	1/15/81	
81A-107 PS-B	107+29	12' " "	Continental	10/2-5/81	3
CV1-7	107+30	6' " "	Ertec	12/18/81	1
81A-107 SPT-L	107+32	19' " "	Continental	7/31/81	2
81A-C12A CPT	107+36	13' " "	Ertec	10/23/81	4
CV1-3	107+38	12' " "	Ertec	12/17/81	2
81A-107 PS-C	107+39	20' " "	Continental	11/2-3/81	1
SV1-7	107+39	14' " "	Continental	1/7-8/81	
CV1-4	107+40	9' " "	Ertec	12/17/81	1
CV1-6	107+41	6' " "	Ertec	12/18/82	1
CV1-C4	107+41	6' W/O E-Crest	Ertec	2/1/82	
CV1-5	107+42	9' W/O DS Toe	Ertec	12/17/81	1
81A-107 SPT-K	107+42	13' " "	Continental	7/30/81	
CV1-6B	107+43	6' W/O DS Toe	Ertec	12/18/81	1

**Thermalito Afterbay Seismic Explorations**  
**Borings from the 1976, 1978, 1979—80, and 1981—82 Investigations**

Exploration	Station	Location	Tested By	Date Tested	Spacing (feet)
SV1C-3	107+43	£-Crest	Continental	1/3/82	
CV1-6A	107+44	6' W/O DS Toe	Ertec	12/18/81	1
81A-C13 CPT	107+45	6' " "	Ertec	10/23/81	1
81A-C107 SPT-A	107+46	£-Crest	Continental	9/16-18/81	1
81-C17 CPT	107+47	6' W/O £-Crest	Ertec	10/24/81	1
81A-C14 CPT	107+66	12' W/O DS Toe	Ertec	10/22/81	19
CV1-2	107+66	12' " "	Ertec	12/17/81	
CV1-1A	107+68	12' " "	Ertec	12/17/81	2
81A-107 SPT-U	107+72	12' " "	Continental	9/2,3/81	4
79-110-SPT	109+50	20' " "	Caltrans	10/17/79	178
80-110 SPT	109+50	6' E/O £-Crest	Caltrans	3/25-26/80	
79-112 SPT	112+00	16' W/O DS Toe	Caltrans	10/17/79	250
81A-114 SPT	114+50	35' " "	Continental	9/3, 9/81	250
79-117 SPT	117+17	39' " "	Caltrans	11/29,30/79	267
81A-119 SPT	119+00	35' " "	Continental	9/10,11,14/81	183
81A-121 SPT	120+80	35' " "	Continental	9/24-16/81	180
81A-11 CPT	120+86	£-Maintenance Road	Ertec	1/29/82	6
79-123 SPT	122+60	7' W/O DS Toe	Caltrans	11/1/79	174
81A-125 SPT	124+88	35' W/O DS Toe	Continental	9/16-18/81	228
81A-127 SPT	127+16	35' " "	Continental	9/18-21/81	228
81A-129 SPT	129+45	36' W/O DS Toe	Continental	9/21-22/81	229
81A-131 SPT	130+81	40' " "	Continental	1/25-26/82	136
81A-131 CPT	130+87	£-Maintenance Road	Ertec	1/31/82	6

**Thermalito Afterbay Seismic Explorations**  
**Borings from the 1976, 1978, 1979-80, and 1981-82 Investigations**

Exploration	Station	Location	Tested By	Date Tested	Spacing (feet)
81A-132 CPT	131+62	E-Maintenance Road	Ertec	1/31/82	75
79-132 SPT	131+68	11' W/O DS Toe	Caltrans	11/2/79	6
81A-132B CPT	132+02	E-Maintenance Road	Ertec	1/31/82	34
81A-132 SPT	132+31	46' W/O DS Toe	Continental	1/26-27/82	29
81A-132C CPT	132+37	E-Maintenance Road	Ertec	1/31/82	6
81A-134 SPT	134+26	46' W/O DS Toe	Continental	9/22,23/81	189
81A-137 SPT	136+84	48' " "	Continental	9/24/81	258
81A-139 SPT	139+42	53' " "	Continental	9/25/81	258
81A-141 CPT	141+00	E-Maintenance Road	Ertec	1/31/82	158
79-142 SPT	142+00	9' W/O DS Toe	Caltrans	11/25/79	100
81A-142 CPT	142+06	E-Maintenance Road	Ertec	1/31/82	6
81A-143 CPT	143+00	E-Maintenance Road	Ertec	1/31/82	94
81A-144 SPT	144+00	48' W/O DS Toe	Continental	9/28/81	100
81A-146 SPT	146+00	43' " "	Continental	9/28/81	200
80-148 SPT	148+04	13' " "	Caltrans	7/24,25/80	204
81A-150 SPT	150+09	40' " "	Continental	9/30/81	205
79-152 SPT	152+17	5-1/2' W/O DS Toe	Caltrans	11/6/79	208
81A-155 SPT	154+68	36' W/O DS Toe	Continental	10/1/81	251
81A-157 SPT	157+18	35' W/O DS Toe	Continental	10/2/81	250
81A-160 SPT	159+68	38' " "	Continental	10/5/81	250
CP-162-E1	161+94	E-Maintenance Road	Ertec	5/29/81	226
79-162 SPT	162+19	38' W/O DS Toe	Caltrans	11/27/79	25
D-3	162+50	At DS Toe	Caltrans	3/24/76	31

**Thermalito Afterbay Seismic Explorations**  
**Borings from the 1976, 1978, 1979-80, and 1981-82 Investigations**

Exploration	Station	Location	Tested By	Date Tested	Spacing (feet)
81A-164 SPT	163+68	75' W/O DS Toe	Continental	10/1/81	118
81A-C164 SPT	163+68	C-Crest	Continental	10/9,12/81	
81A-C28 CPT	163+74	C-Crest	Ertec	10/24/81	6
81A-167 SPT-J	164+27	80' W/O DS Toe	Continental	10/5/81	53
81A-165 SPT	164+29	42' " "	Continental	7/15,16/81	2
CP-165-E1	164+31	C-Maintenance Road	Ertec	5/29/81	2
81A-165 PS-A	164+35	42' W/O DS Toe	Continental	8/12/81	4
81A-164 PS-B	164+41	42' " "	Continental	8/13/81	6
81A-164 PS-C	164+47	41' " "	Continental	9/9,10/81	6
81A-164 SPT-D	164+53	40' " "	Continental	11/20/81	6
81A-167 SPT-L	164+54	88' " "	Continental	10/16/81	1
SV2-3	164+58	85' " "	Continental	11/20,21/82	4
81A-164 SPT-E	164+59	40' " "	Continental	1/20/81	1
81A-164 PS-D	164+59	84' " "	Continental	11/9/81	
CV2-9	164+59	91' " "	Ertec	2/2/82	
CV2-10	164+59	95' " "	Ertec	2/2/82	
CV2-11	164+59	97' " "	Ertec	2/2/82	
CV2-12	164+59	98' " "	Ertec	2/2/82	
81A-164 SPT-A	164+62	91' W/O DS Toe	Continental	11/9,10/81	3
81A-C18 CPT	164+62	77' " "	Ertec	10/23/81	
CV2-7	164+62	81' " "	Ertec	2/2/82	
CV2-8	164+62	95' " "	Ertec	2/2/82	
81A-165 SPT-F	164+65	40' " "	Continental	11/20/81	3

**Thermalito Afterbay Seismic Explorations**  
**Borings from the 1976, 1978, 1979-80, and 1981-82 Investigations**

Exploration	Station	Location	Tested By	Date Tested	Spacing (feet)
81A-167 SPT-H	164+66	80' W/O DS Toe	Continental	10/2/81	1
81A-C165 SPT	164+68	5' E/O $\bar{C}$ -Crest	Continental	10/15/81	2
81A-C29 CPT	164+74	$\bar{C}$ -Crest	Ertec	10/24/81	6
CV2-5	164+74	77' W/O DS Toe	Ertec	2/2/82	
CV2-6	164+74	85' " "	Ertec	2/2/82	
81A-165 SPT-B	164+78	80' " "	Continental	11/10, 11/81	4
81A-167 SPT-K	164+83	80' " "	Continental	10/19/81	5
SV2-2	164+83	77' " "	Continental	1/19, 20/82	
SV2-4	164+84	76' " "	Ertec	2/2/82	1
81A-164 SPT-C	164+85	75' " "	Continental	11/11/81	
CV2-3	164+86	75' " "	Ertec	2/2/82	2
81A-C19 CPT	164+87	74' " "	Ertec	10/23/81	1
81A-C20 CPT	164+87	86' " "	Ertec	10/23/81	
CV-2	164+87	86' " "	Ertec	2/2/82	
81A-164 PS-E	164+88	80' " "	Continental	11/9/81	1
PV2-A	164+90	77' " "	Continental	2/2, 3/82	
SV2-4	164+90	83' " "	Continental	1/22/82	4
SV2-1	164+92	77' " "	Continental	1/18/82	2
81A-167 SPT-G	164+95	80' " "	Continental	10/1/81	3
81A-C21 CPT	165+03	74' " "	Ertec	10/23/81	
CV2-1	165+03	83' " "	Ertec	2/2/82	
81A-C22 CPT	165+10	86' " "	Ertec	10/23/81	7
81A-167 SPT-F	165+30	80' " "	Continental	9/30/81	20



**Thermalito Afterbay Seismic Explorations**  
**Borings from the 1976, 1978, 1979-80, and 1981-82 Investigations**

Exploration	Station	Location	Tested By	Date Tested	Spacing (feet)
81A-C23 CPT	165+40	80' W/O DS Toe	Ertec	10/23/81	10
81A-C166 SPT	165+68	3' E/O $\xi$ -Crest	Continental	10/23-29/81	28
81A-C166 CPT	165+74	$\xi$ -Crest	Ertec	12/15/81	6
81A-167 SPT-D	166+30	68' W/O DS Toe	Continental	9/3-8/81	56
CP-167-M2	166+41	20' " "	USGS	5/21/81	11
CP-167-E2	166+45	20' " "	USGS	5/21/81	4
79-167 SPT	166+46	43' " "	Caltrans	11/29/76	1
81A-167 PS-D	166+49	14' " "	Continental	1/29/82	3
81A-167 PS-E	166+49	8' " "	Continental	2/1/82	
81A-167 PST-A	166+49	18' " "	Continental	8/20,21/81	
81A-166 SPT-A	166+50	42' " "	Continental	8/26/81	1
CP-167-E4	166+51	26' " "	Ertec	5/29/81	1
81A-167 PS-C	166+55	13' " "	Continental	1/28/82	3
81A-167 PS-A	166+55	18' " "	Continental	8/27/81	
81A-167 SPT-E	166+56	68' " "	Continental	9/8,9/81	
81A-167 SPT-M	166+61	68' " "	Continental	3/15,16/82	5
81A-167 PS-F	166+61	12' " "	Continental	3/15,16/82	
CP-167-M1	166+65	25' " "	USGS	5/20/81	4
81A-167 SPT-C	166+65	6' " "	Continental	8/25/81	
81A-C167 SPT	166+68	$\xi$ -Crest	Continental	1/13,14/82	3
CP-167-E1	166+71	25' W/O DS Toe	USGS	5/20/81	3
81A-167 PS-B	166+73	18' " "	Continental	10/5-6/81	2
81A-167 SPT-N	166+73	68' " "	Continental	3/15/82	

**Thermalito Afterbay Seismic Explorations**  
**Borings from the 1976, 1978, 1979-80, and 1981-82 Investigations**

Exploration	Station	Location	Tested By	Date Tested	Spacing (feet)
81A-C30 CPT	166+74	£-Crest	Ertec	10/24/81	1
CP-167-E3	166+76	13' W/O DS Toe	Ertec	5/29/81	2
81A-167 SPT-B	166+79	18' " "	Continental	8/21-24/81	3
81A-167 PB-A	166+79	26' " "	Continental	7/16/81	
81A-C168 CPT	167+62	£-Crest	Ertec	1/30/82	83
81A-C168 SPT	167+68	4' E/O £-Crest	Continental	12/10-22/81	6
81A-C31 CPT	167+74	£-Crest	Ertec	10/24/81	6
81A-168 SPT-A	68+09	9' W/O DS Toe	Continental	8/28-31/81	35
81A-C168B CPT	168+12	£-Crest	Ertec	2/1/82	3
81A-168 SPT-B	168+59	12' W/O DS Toe	Continental	8/28-31/81	47
81A-C169 CPT	168+62	£-Crest	Ertec	1/30/82	3
81A-C169 SPT	168+68	4' E/O £-Crest	Continental	12/7-9/81	6
81A-C32 CPT	168+74	£-Crest	Ertec	10/24/81	6
81A-169 SPT	168+95	7' W/O DS Toe	Continental	10/5-6/81	21
CP-169-E1	169+22	31' " "	Ertec	5/29/81	27
81A-C170 SPT	169+68	3' E/O £-Crest	Continental	12/1-4/81	46
81A-170 SPT-A	170+00	34' W/O DS Toe	Continental	11/12-13/81	32
81A-C171 CPT	170+74	£-Crest	Ertec	12/15/81	74
81A-170 SPT	170+82	31' W/O DS Toe	Continental	10/5-6/81	8
CP-171-E1	171+20	29' " "	Ertec	5/29/81	38
81A-C171B CPT	171+38	£-Crest	Ertec	2/1/82	18
TAS-2M	172+58	35' W/O DS Toe	Caltrans	8/17/78	120
81A-C173 CPT	172+74	£-Crest	Ertec	12/15/81	16

**Thermalito Afterbay Seismic Explorations**  
**Borings from the 1976, 1978, 1979—80, and 1981—82 Investigations**

Exploration	Station	Location	Tested By	Date Tested	Spacing (feet)
TAS2L	172+78	34' W/O DS Toe	Caltrans	8/16/78	4
TAS-2C	172+80	13' " "	Caltrans	7/11-12/78	6
CP-173-M1	172+94	33' " "	USGS	5/19/81	9
TAS2B	172+98	11' W/O Rd $\bar{C}$ Crest	Caltrans	7/10/78	4
CP-173-E1	172+99	33' W/O DS Toe	USGS	5/19/81	5
CP-173-E2	172+99	28' " "	Ertec	5/29/81	
79-173 SPT	173+00	30' " "	Caltrans	11/6,7/79	1
TAS2A	173+00	11' " "	Caltrans	6/29/78	1
TAS2	173+03	8' W/O Rd $\bar{C}$ Crest	Caltrans	6/26-28/78	3
TAS2E	173+19	34' W/O DS Toe	Caltrans	7/25,26/78	16
TAS2G	173+22	33' " "	Caltrans	7/27/78	3
CP-173-E3	173+27	33' " "	Ertec	5/29/81	5
TAS-2F	173+24	34' " "	Caltrans	7/26,27/78	3
TAS-2H	173+35	33' " "	Caltrans	7/27,28/78	9
TAS-2J	173+39	33' " "	Caltrans	7/31-8/2/78	4
TAS-2D	173+40	13' " "	Caltrans	7/12,13/78	1
TAS-2K	173+44	33' " "	Caltrans	8/2,3/78	4
81A-175 SPT	175+33	35' " "	Continental	10/6/81	185
CP-175-E1	175+42	35' " "	Ertec	5/29/81	9
79-178 SPT	177+67	34' " "	Caltrans	11/20-21/78	225
CP-178-M1	178+07	29' " "	USGS	5/20/81	40
CP-178-E1	178+12	29' " "	USGS	5/20/81	5
CP-178-E2	178+12	32' " "	Ertec	5/29/81	

**Thermalito Afterbay Seismic Explorations**  
**Borings from the 1976, 1978, 1979-80, and 1981-82 Investigations**

Exploration	Station	Location	Tested By	Date Tested	Spacing (feet)
D-4	178+25	5' W/O DS Toe	Caltrans	3/25/76	13
CP-178-E3	178+38	32' " "	Ertec	5/29/81	13
81A-179 CPT	179+00	E-Maintenance Road	Ertec	12/15/81	62
81A-C179 CPT	179+31	E-Crest	Ertec	1/30/82	31
81A-180B CPT	179+50	E-Crest	Ertec	1/31/82	19
81A-180 SPT-A	180+09	100' W/O DS Toe	Continental	11/11/81	59
81A-180 SPT	180+25	29' " "	Continental	10/7/81	16
81A-180 CPT	180+31	E-Maintenance Road	Ertec	12/16/81	6
81A-C180 CPT	180+31	E-Crest	Ertec	1/30/82	
81A-180 PS-A	180+35	48.5' W/O Fence	Continental	11/10/81	4
81A-180 SPT-B	180+41	48.5' W/O Fence	Continental	11/10, 11/81	6
81A-181B CPT	180+50	E-Maintenance Road	Ertec	1/31/82	9
81A-181 CPT	181+00	E-Maintenance Road	Ertec	12/16/81	50
81A-C181 CPT	181+31	E-Crest	Ertec	1/30/82	31
81A-182B CPT	181+50	E-Maintenance Road	Ertec	1/31/82	19
81A-182 CPT	182+00	E-Maintenance Road	Ertec	12/16/82	50
81A-183 SPT-A	182+59	25' W/O DS Toe	Continental	1/28, 29/82	59
81A-183 SPT	182+83	25' W/O DS Toe	Continental	10/8/81	24
81A-183 CPT	182+89	E-Maintenance Road	Ertec	12/16/81	6
81A-183 PS-A	182+93	25' W/O DS Toe	Continental	3/3-4/82	4
81A-183 PS	183+00	25' " "	Continental	3/2-3/82	7
81A-183 SPT-B	183+07	25' " "	Continental	226-3/2/82	7
81A-184 CPT	183+70	E-Maintenance Road	Ertec	12/16/81	63

**Thermalito Afterbay Seismic Explorations**  
**Borings from the 1976, 1978, 1979-80, and 1981-82 Investigations**

Exploration	Station	Location	Tested By	Date Tested	Spacing (feet)
81A-185 SPT	185+41	31' W/O DS Toe	Continental	10/9/81	171
79-188	188+00	27' " "	Caltrans	11/7/79	259
81A-190 CPT	189+50	E-Maintenance Road	Ertec	12/16/81	150
81A-190 SPT	190+50	35' W/O DS Toe	Continental	10/12/81	
81A-191 CPT	190+56	E-Maintenance Road	Ertec	12/16/81	6
81A-192 CPT	191+50	E-Maintenance Road	Ertec	12/16/81	94
81A-193 SPT	193+00	44' W/O DS Toe	Continental	9/29-30/81	150
81A-195 SPT	195+50	57' " "	Continental	9/28,29/81	250
D-5	197+75	5' " "	Caltrans	3/25-26/76	225
81A-198 SPT	198+00	43' " "	Continental	9/25-28/81	25
CP-198-E1	198+04	42' " "	Ertec	5/29/81	4
81A-200 SPT	200+50	25' " "	Ertec	9/24-25/81	246
81A-201 CPT	201+00	E-Maintenance Road	Ertec	1/31/82	50
81A-202B CPT	201+50	E-Maintenance Road	Ertec	1/31/82	50
81A-C202 CPT	202+00	E-Crest	Ertec	1/30/82	50
81A-202 CPT	202+00	E-Maintenance Road	Ertec	1/30/82	
81A-C203 CPT	203+00	E-Crest	Ertec	1/30/82	100
81A-203 CPT	203+00	E-Maintenance Road	Ertec	1/30/82	
TAS-3	203+00	10' W/O E-Crest	Caltrans	7/17-19/78	
79-203 SPT	203+04	32' W/O DS Toe	Caltrans	11/29/79	4
CP-203-M1	203+04	37' " "	USGS	5/21/81	
TAS-3A	203+05	6.5' " "	Caltrans	7/19/78	1
CP-203-E1	203+11	32' " "	USGS	5/21/81	6

**Thermalito Afterbay Seismic Explorations**  
**Borings from the 1976, 1978, 1979-80, and 1981-82 Investigations**

Exploration	Station	Location	Tested By	Date Tested	Spacing (feet)
CP-203-E2	203+14	32' W/O DS Toe	Ertec	5/29/81	2
TAS-3D	203+25	36' " "	Caltrans	8/8/78	14
TAS-3C	203+55	36' " "	Caltrans	8/7,8/78	30
TAS-3B	203+66	37' " "	Caltrans	8/4/78	11
TAS-3E	203+86	36' " "	Caltrans	8/17,18/78	20
CP-203-E2	203+14	32' " "	Ertec	5/29/81	2
81A-C204 CPT	204+00	℄-Crest	Ertec	1/30/82	86
81A-204 CPT	204+00	℄-Maintenance Road	Ertec	1/30/81	
81A-205 SPT	205+28	35' W/O DS Toe	Continental	9/23,24/81	128
81A-207 CPT	206+50	℄-Maintenance Road	Ertec	12/16/81	122
81A-207B CPT	207+00	℄-Maintenance Road	Ertec	2/2/82	50
81A-207 SPT	207+40	33' W/O DS Toe	Continental	11/20/81	40
81A-207 SPT-A	207+46	33' " "	Continental	11/23/81	6
81A-208 SPT	207+52	33' " "	Continental	9/22,23/81	6
81A-208 SPT-B	207+58	33' " "	Continental	11/19-20/81	6
81A-208 SPT-C	207+64	33' " "	Continental	11/18-19/81	6
81A-208 CPT	207+70	℄-Maintenance Road	Ertec	12/16/81	6
81A-209 CPT	208+50	℄-Maintenance Road	Ertec	12/16/81	80
81A-210 SPT	209+76	39' W/O DS Toe	Continental	9/21-22/81	126
81A-210 CPT	209+82	℄-Maintenance Road	Ertec	2/2/82	6
79-212 SPT	212+00	36' W/O DS Toe	Caltrans	11/8/79	218
81A-214 SPT	214+10	40' " "	Continental	11/24,25/81	210
81A-215 SPT	214+60	42' " "	Continental	9/21/81	50

**Thermalito Afterbay Seismic Explorations**  
**Borings from the 1976, 1978, 1979—80, and 1981–82 Investigations**

Exploration	Station	Location	Tested By	Date Tested	Spacing (feet)
81A-216 SPT	215+90	44' W/O DS Toe	Continental	1/28,29/82	130
81A-217 SPT	217+20	51' " "	Continental	9/16,17/81	130
81A-220 SPT	219+80	51' " "	Continental	9/15/81	260
81A-222 SPT	222+40	49' " "	Continental	11/14/81	260
79-225 SPT	225+00	9' SW/O DS Toe	Caltrans	11/8/79	260
81A-227 SPT	226+83	16.5' S/O DS Toe	Continental	9/10,11/81	183
81A-229 SPT	228+66	12' S/O DS Toe	Continental	9/9,10/81	183
81A-231 SPT	231+00	12' " "	Continental	4/8,9/8	234
79-233 SPT	233+40	8' " "	Caltrans	11/13/79	240
81A-236 SPT	235+70	12' " "	Continental	9/4/81	230
81A-C237 CPT	237+00	£-Crest	Ertec	1/30/82	130
81A-238 SPT	238+00	10' S/O DS Toe	Continental	9/3/81	100
81A-C238 CPT	238+00	£-Crest	Ertec	12/15/81	
CP-238-E4	238+28	11' S/O DS Toe	Ertec	15/29/81	28
81A-C239 CPT	239+00	£-Crest	Ertec	1/30/82	72
79-238 SPT	239+23	6' S/O DS Toe	Caltrans	11/28/79	23
CP-238-E1	239+28	6' " "	USGS	5/20/81	5
CP-238-E2	239+28	12' " "	Ertec	5/29/81	
CP-238-M1	239+33	6' " "	USGS	5/20/81	5
CP-238-E3	239+38	26' " "	Ertec	5/29/81	5
81A-C240 CPT	240+00	£-Crest	Ertec	12/15/81	62
81A-240 SPT	240+50	14' S/O DS Toe	Continental	9/2/81	50
CP-238-E5	240+57	13' " "	Ertec	5/29/81	7

**Thermalito Afterbay Seismic Explorations**  
**Borings from the 1976, 1978, 1979—80, and 1981-82 Investigations**

Exploration	Station	Location	Tested By	Date Tested	Spacing (feet)
81A-C241 CPT	241+00	£-Crest	Ertec	1/30/82	43
81A-C242 CPT	242+00	£-Crest	Ertec	12/15/81	100
D-6	242+75	At DS Toe	Caltrans	3/26-29/76	75
81A-C243 CPT	243+00	£-Crest	Ertec	1/30/81	25
81A-243 SPT	243+00	23-S/O DS Toe	Continental	9/1/82	
81A-C244 CPT	244+00	£-Crest	Ertec	12/15/81	100
81A-245 SPT	245+00	19' S/O DS Toe	Continental	8/31/81	100
80-247 SPT	246+80	14' " "	Caltrans	7/23/80	180
81A-C249 CPT	248+65	£-Crest	Ertec	12/15/81	185
81A-250 SPT	250+50	12.5' S/O DS Toe	Continental	8/28/81	185
81A-C253 CPT	253+00	£-Crest	Ertec	1/30/82	250
79-253 SPT	253+00	6' S/O DS Toe	Caltrans	11/13,14/79	
81A-C254 CPT	254+00	£-Crest	Ertec	12/17/81	100
81A-C255 CPT	255+00	£-Crest	Ertec	1/29/82	100
81A-255 SPT	255+50	11.5' S/O DS Toe	Continental	8/27/81	50
81A-C256 CPT	256+00	£-Crest	Ertec	12/17/81	50
81A-C257 CPT	257+00	£-Crest	Ertec	1/29/82	100
81A-C258 CPT	258+00	£-Crest	Ertec	12/17/81	100
81A-258 SPT	258+00	12' S/O DS Toe	Continental	8/26/81	
81A-C259 CPT	259+00	£-Crest	Ertec	1/29/82	100
81A-C260 CPT	260+00	£-Crest	Ertec	12/17/81	100
81A-260 SPT	260+00	12.5' S/O DS Toe	Continental	8/25/81	
81A-C261 CPT	261+00	£-Crest	Ertec	1/29/82	100



**Thermalito Afterbay Seismic Explorations**  
**Borings from the 1976, 1978, 1979-80, and 1981-82 Investigations**

Exploration	Station	Location	Tested By	Date Tested	Spacing (feet)
81A-262 SPT	262+00	14' S/O DS Toe	Continental	8/24/81	100
81A-266 SPT	266+00	13' " "	Continental	8/21-24/81	400
81A-C267 CPT	267+00	ℰ-Crest	Ertec	1/29/82	100
81A-C268B CPT	267+50	ℰ-Crest	Ertec	2/2/82	50
81A-C268 CPT	268+00	ℰ-Crest	Ertec	12/17/81	50
81A-C269B CPT	268+50	ℰ-Crest	Ertec	2/2/82	50
81A-268 SPT	268+50	13' S/O DS Toe	Continental	8/20,21/81	
81A-C269 CPT	269+00	ℰ-Crest	Ertec	1/29/82	50
D-7	269+50	3' S/O DS Toe	Caltrans	3/29/76	50
81A-C270 CPT	270+00	ℰ-Crest	Ertec	12/17/81	50
81A-271 SPT	271+05	6' S/O DS Toe	Continental	8/19,20/81	105
81A-C272 CPT	272+00	ℰ-Crest	Ertec	12/17/81	95
81A-273 SPT	273+50	5' S/O DS Toe	Continental	3/18/81	150
81A-276 SPT	276+02	16' " "	Continental	8/17/81	252
81A-C278 CPT	278+00	ℰ-Crest	Ertec	12/17/81	198
81A-278 SPT	278+50	11' S/O DS Toe	Continental	8/11,12/81	50
81A-C279 CPT	279+00	ℰ-Crest	Ertec	2/1/82	50
TAS-4A	279+83	18' S/O DS Toe	Caltrans	8/22/78	83
81A-C280 CPT	280+00	ℰ-Crest	Ertec	12/17/81	17
CP-280-M1	280+00	15' S/O DS Toe	USGS	5/22/81	
TAS-4	281+00	13' S/O ℰ-Crest	Caltrans	7/20,21/78	100
81A-C281 CPT	281+00	ℰ-Crest	Ertec	2/1/82	
81A-281 SPT	28+00	15' S/O DS Toe	Continental	10/13/81	

**Thermalito Afterbay Seismic Explorations**  
**Borings from the 1976, 1978, 1979-80, and 1981-82 Investigations**

Exploration	Station	Location	Tested By	Date Tested	Spacing (feet)
D-8	281+63	4' S/O DS Toe	Caltrans	3/30,31/76	63
81A-C282 CPT	282+00	£-Crest	Ertec	12/16/81	37
81A-283 SPT	283+50	13' S/O DS Toe	Continental	8/13/81	150
81A-C285 CPT	285+00	£-Crest	Ertec	12/15/81	150
80-286 SPT	286+35	11' N/O £-Crest	Caltrans	7/22,23/80	135
81A-288 SPT	288+14	15' S/O DS Toe	Continental	8/14/81	179
79-290 SPT	289+87	4' " "	Caltrans	11/14,15/79	173
81A-292 SPT	292+29	6' " "	Continental	8/7/81	242
81A-295 SPT	295+00	14' " "	Continental	8/5/81	271
81A-297 SPT	297+32	18' " "	Continental	8/4/81	232
79-300 SPT	299+97	23' " "	Caltrans	11/15-20/79	265
81A-302 SPT	302+50	21' " "	Continental	7/24-27/81	253
80-305 SPT	304+95	12' " "	Caltrans	7/24/80	245
81A-308 SPT	307+89	19' " "	Continental	7/22,23/81	294
79-310 SPT	310+00	7' " "	Caltrans	11/9/79	211
81A-312 SPT	312+00	25' " "	Continental	7/8/81	200
80-314 SPT	313+54	8' SE/O DS Toe	Caltrans	7/25/80	154
81A-316 SPT	316+50	10' SE/O DS TToe	Continental	7/13,14/81	296
81A-319 SPT	319+00	16' S/O DS Toe	Continental	7/14-17/81	250
81A-321 SPT	321+50	25' " "	Continental	7/17/81	250
81A-C337 SPT	337+00	5' N/O £-Crest	Continental	12/22,23/81	1550
81A-C340 CPT	339+50	£-Crest	Ertec	12/15/81	250
81A-C342 SPT	342+00	4' N/O £-Crest	Continental	10/28-30/81	250

**Thermalito Afterbay Seismic Explorations**  
**Borings from the 1976, 1978, 1979-80, and 1981-82 Investigations**

Exploration	Station	Location	Tested By	Date Tested	Spacing (feet)
81A-C344 SPT	344+50	7' N/O $\xi$ -Crest	Continental	10/27-11/3/81	250
81A-C345 CPT	345+00	$\xi$ -Crest	Ertec	1/29/82	50
81A-C346 CPT	346+00	$\xi$ -Crest	Ertec	12/15/81	100
81A-C346 SPT	346+44	3' N/O $\xi$ -Crest	Continental	3/5-8/82	44
81A-C347B CPT	346+50	$\xi$ -Crest	Ertec	2/1/82	6
81A-347 SPT	346+90	190' S/O $\xi$ -Crest	Continental	4/21/82	40
81A-C347 CPT	347+00	$\xi$ -Crest	Ertec	12/15/81	10
81A-C347 SPT	347+00	5' N/O $\xi$ -Crest	Continental	10/30-11/2,3/81	
81A-C348B CPT	347+50	$\xi$ -Crest	Ertec	1/31/82	50
81A-348 SPT	347+90	190' S/O $\xi$ -Crest	Continental	4/21/82	40
81A-C348 CPT	348+00	$\xi$ -Crest	Ertec	12/15/81	10
81A-C348 SPT	348+06	2' N/O $\xi$ -Crest	Continental	1/22-26/82	6
81A-C349 CPT	349+00	$\xi$ -Crest	Ertec	1/29/82	94
81A-C349 SPT	349+00	6' N/O $\xi$ -Crest	Continental	11/3-5/81	
81A-C350 CPT	350+00	$\xi$ -Crest	Ertec	1/29/82	100
81A-C350 SPT	350+00	5' S/O $\xi$ -Crest	Continental	3/18,19/82	
81A-C351 SPT	351+00	5' N/O $\xi$ -Crest	Continental	12/18-22/81	100
79-351	351+00	23' S/O DS Toe	Caltrans	10/30/79	
81A-C351 CPT	351+06	$\xi$ -Crest	Ertec	1/29/82	6
81A-C352 SPT	352+00	9' N/O $\xi$ -Crest	Continental	3/23,24/82	94
81A-C353 SPT	353+00	4' " "	Continental	3/17,18/82	100
81A-C354 CPT	354+00	$\xi$ -Crest	Ertec	1/29/82	100
81A-C354 SPT	354+00	12' N/O $\xi$ -Crest	Continental	3/25/82	

**Thermalito Afterbay Seismic Explorations**  
**Borings from the 1976, 1978, 1979-80, and 1981-82 Investigations**

Exploration	Station	Location	Tested By	Date Tested	Spacing (feet)
81A-C355 CPT	354+50	£-Crest	Ertec	1/31/821	50
81A-C356 SPT	356+00	6' N/O £-Crest	Continental	11/11/81	150
81A-C357 CPT	358+00	£-Crest	Ertec	1/30/82	200
81A-C359 SPT	358+56	3' N/O £-Crest	Continental	1/26,27/82	56
81A-C360 CPT	360+00	£-Crest	Ertec	1/30/82	144
81A-C361 SPT	361+00	5' N/O £-Crest	Continental	12/17,18/81	100
79-361	361+00	32' S/O DS Toe	Caltrans	10/30/79	
81A-C361 CPT	361+06	£-Crest	Ertec	1/30/82	6
81A-C362 SPT	361+94	4' N/O £-Crest	Continental	3/8,9/82	88
81A-C362 CPT	362+00	£-Crest	Ertec	1/30/82	6
81A-C363 SPT	362+94	5' N/O £-Crest	Continental	3/9,10/82	94
81A-C364 CPT	363+50	£-Crest	Ertec	12/15/81	56
81A-C366 SPT	366+00	4' W/O £-Crest	Continental	12/14-16/81	250
81A-370 SPT	370+50	7' " "	Continental	12/10-14/81	150
81A-C373 CPT	373+00	£-Crest	Ertec	12/15/81	250
81A-C375 SPT	375+50	5' W/O £-Crest	Continental	12/7-9/81	250
81A-C377 CPT	377+00	£-Crest	Ertec	1/29/82	150
81A-C378 CPT	378+00	£-Crest	Ertec	12/15/81	100
79-378	378+00	25' S/O DS Toe	Caltrans	10/31/79	
81A-C379 CPT	379+00	£-Crest	Ertec	1/29/82	100
81A-C380 CPT	379+50	£-Crest	Ertec	12/15/81	50
81A-C380B CPT	380+00	£-Crest	Ertec	1/29/82	50
81A-C380 PS-A	380+38	3' W/O £-Crest	Continental	1/22-26/82	38

**Thermalito Afterbay Seismic Explorations**  
**Borings from the 1976, 1978, 1979-80, and 1981-82 Investigations**

Exploration	Station	Location	Tested By	Date Tested	Spacing (feet)
81A-C380 PS	380+43	3' W/O $\xi$ -Crest	Continental	1/21,22/82	5
81A-C381 CPT	380+50	$\xi$ -Crest	Ertec	12/15/81	7
81A-C380 SPT	380+50	4' W/O $\xi$ -Crest	Continental	11/12-23/81	
81A-C381B CPT	381+00	$\xi$ -Crest	Ertec	1/29/82	50
81A-C382 CPT	381+50	$\xi$ -Crest	Ertec	12/15/81	50
81A-C382 SPT	381+56	3' W/O $\xi$ -Crest	Continental	1/27,28/82	6
81A-C383 CPT	383+00	$\xi$ -Crest	Ertec	12/15/81	144
81A-C383 PS	383+02	1' E/O $\xi$ -Crest	Continental	1/26,27/82	2
81A-C383 SPT	383+06	2' W/O $\xi$ -Crest	Continental	1/20,21/82	4
81A-C384 CPT	384+00	$\xi$ -Crest	Ertec	1/29/82	94
81A-C385 SPT	385+50	7' W/O $\xi$ -Crest	Continental	12/1-7/81	150
81A-C386 CPT	385+56	$\xi$ -Crest	Ertec	1/31/82	6
81A-C387 CPT	387+00	$\xi$ -Crest	Ertec	12/15/81	144
81A-C388B CPT	387+50	$\xi$ -Crest	Ertec	1/31/82	50
81A-C388 CPT	388+00	$\xi$ -Crest	Ertec	12/15/81	50
81A-C389 CPT	389+00	$\xi$ -Crest	Ertec	12/15/81	100
81A-C389 SPT	389+06	2' W/O $\xi$ -Crest	Continental	1/21,22/82	6
81A-C390 SPT	390+50	5' W/O $\xi$ -Crest	Continental	11/24-12/1/81	44
81A-C393 SPT	393+00	6' W/O $\xi$ -Crest	Continental	11/23-12/1/81	250
81A-C396 SPT	395+50	5' N/O $\xi$ -Crest	Continental	11/16,17/81	250



## ADDENDUM B

### STATIC STRESSES FROM STATIC FINITE ELEMENT ANALYSES

The static stresses presented in this appendix are values generated by the static finite element program TWIST. Stresses are presented in units of pounds per square foot and are shown for the three models analyzed (Stations 107, 165, and 347). Each model has the following stress components presented for the two reservoir elevations (128 and 136.5 feet) used in the analysis:

1. Static horizontal normal stresses,  $\sigma_x$  (psf)
2. Static vertical normal stresses,  $\sigma_y$  (psf)
3. Static major principal stresses,  $\sigma_1$  (psf)
4. Static minor principal stresses,  $\sigma_3$  (psf)
5. Static horizontal shear stresses,  $\tau_{xy}$  (psf)
6. Static maximum shear stresses  $\tau_{\max}$  (psf)
7. Principal stress orientations

In each of the following figures (Figures 153–173), the suspect sand layer is shown bracketed by a heavy dark line above and below the layer.

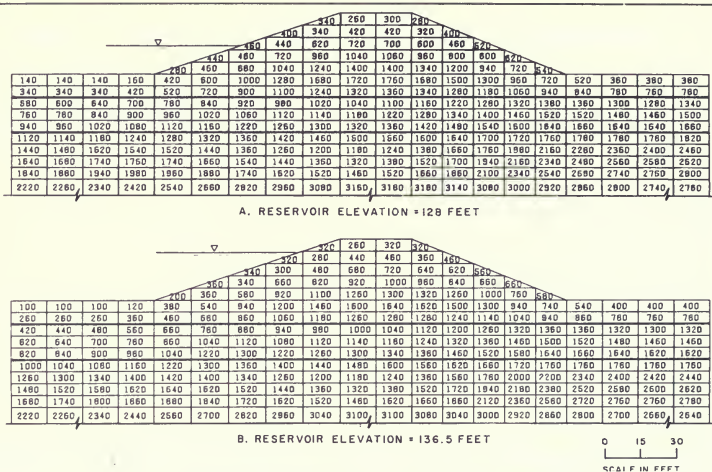


Figure 153. Static Horizontal Normal Stresses,  $\sigma_x$  (psf), for Station 107

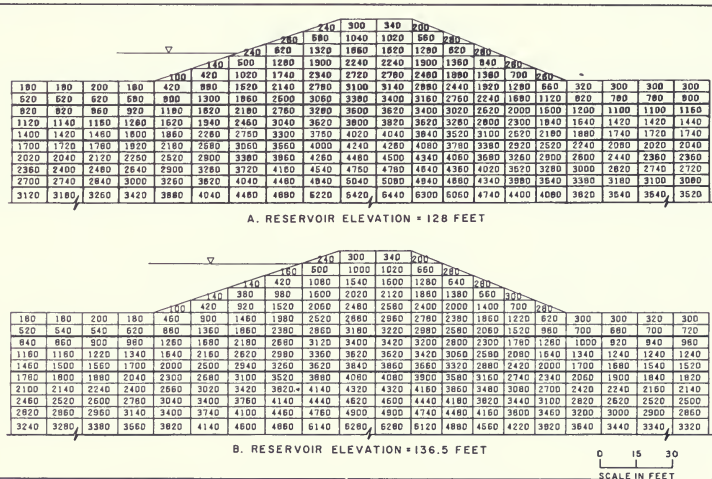


Figure 154. Static Vertical Normal Stresses,  $\sigma_y$  (psf), for Station 107



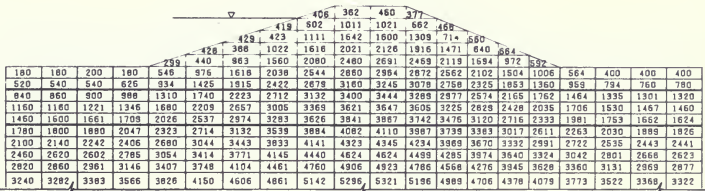
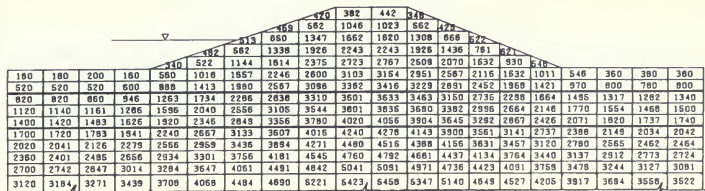


Figure 155. Static Major Principal Stresses,  $\sigma_1$  (psf), for Station 107

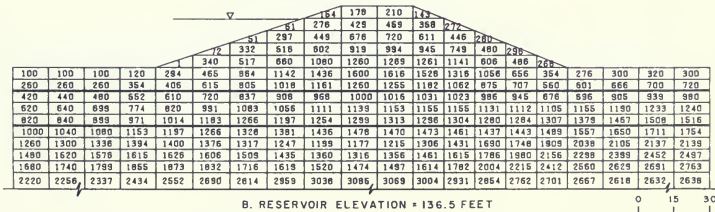
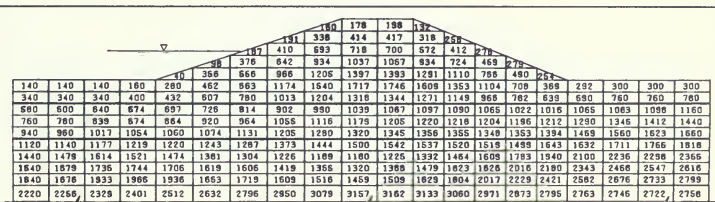


Figure 156. Static Minor Principal Stresses,  $\sigma_3$  (psf), for Station 107



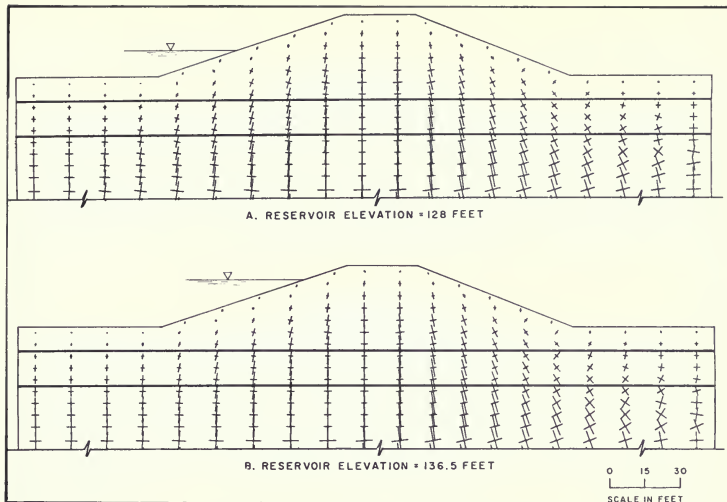


Figure 159. Principal Stress Orientations for Station 107

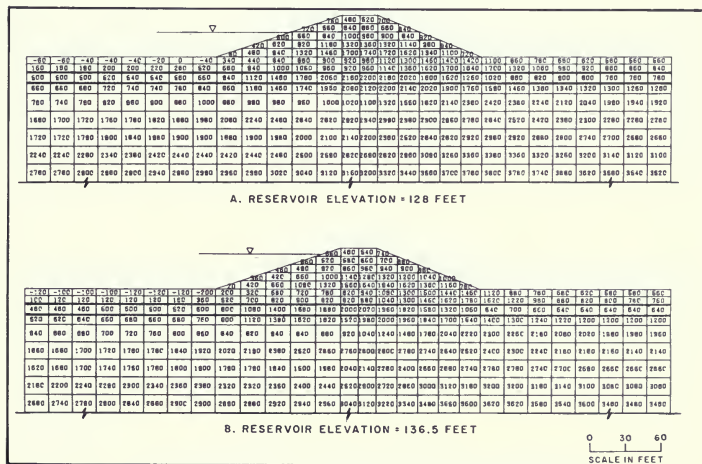


Figure 160. Static Horizontal Normal Stresses,  $\sigma_x$  (psf) for Station 165

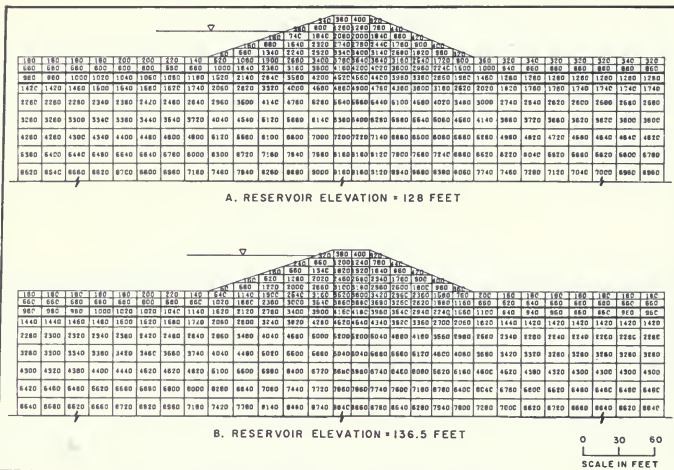


Figure 161. Static Vertical Normal Stresses,  $\sigma_y$  (psf) for Station 165

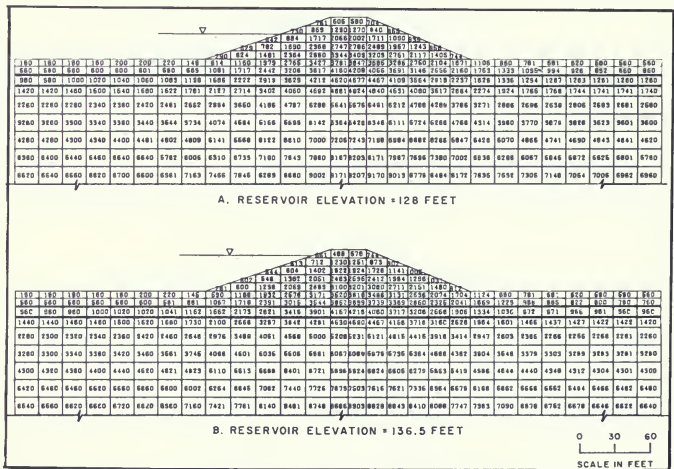
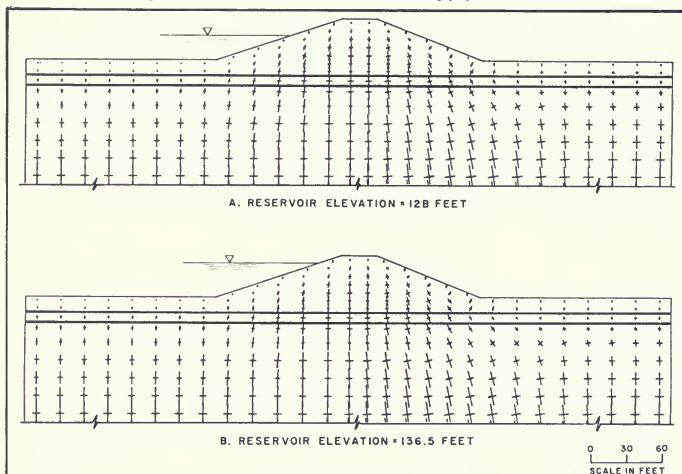
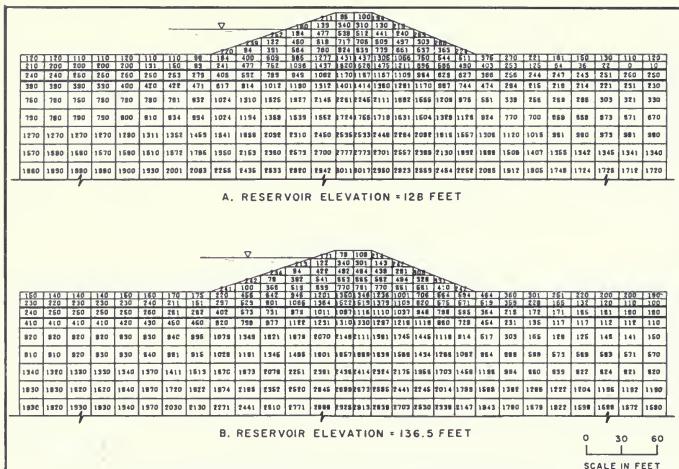


Figure 162. Static Major Principal Stresses,  $\sigma_1$  (psf), for Station 165







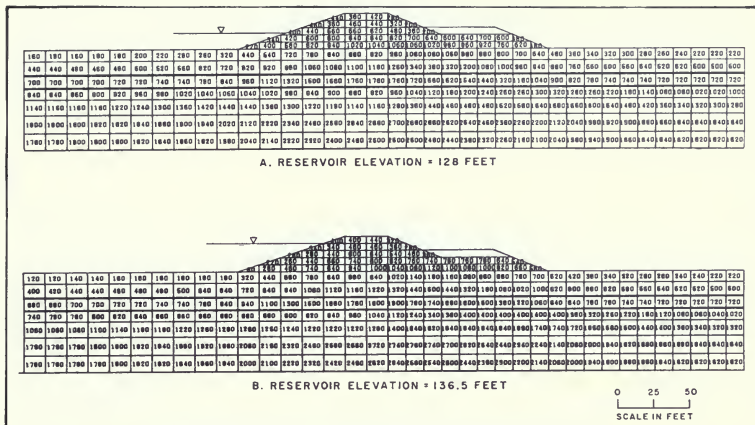


Figure 167. Static Horizontal Normal Stresses,  $\sigma_x$  (psf), for Station 347

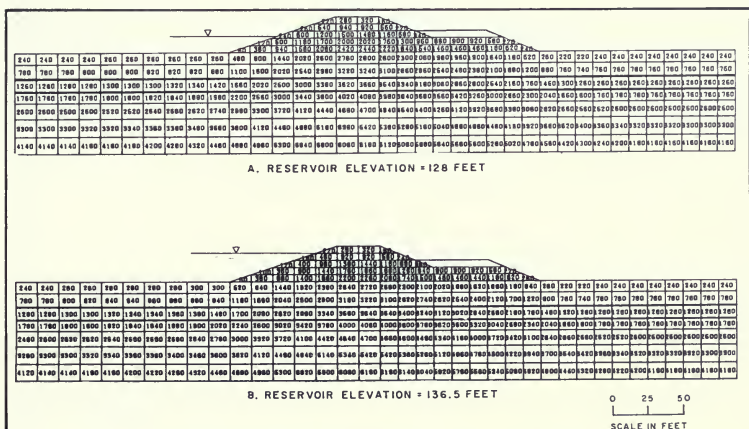


Figure 168. Static Vertical Normal Stresses,  $\sigma_y$  (psf), for Station 347

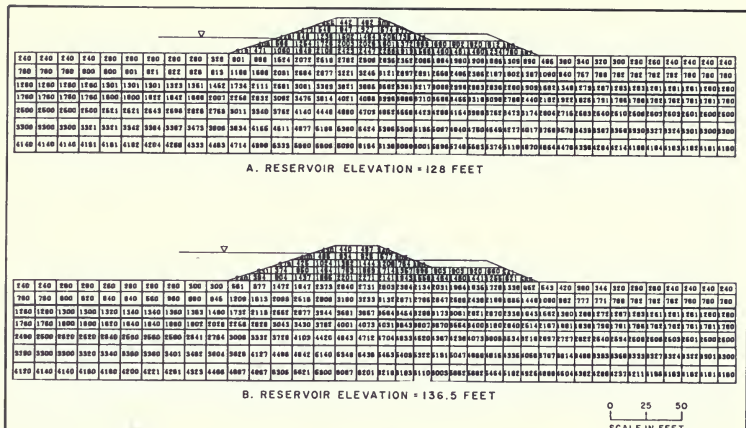


Figure 169. Static Major Principal Stresses,  $\sigma_1$  (psf), for Station 347

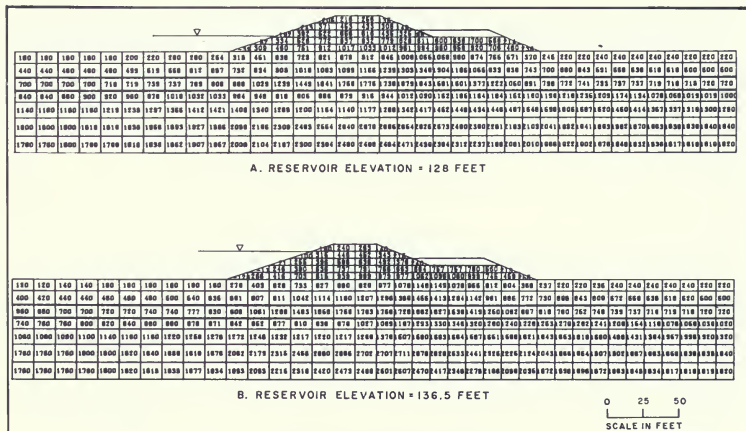


Figure 170. Static Minor Principal Stresses,  $\sigma_3$  (psf), for Station 347



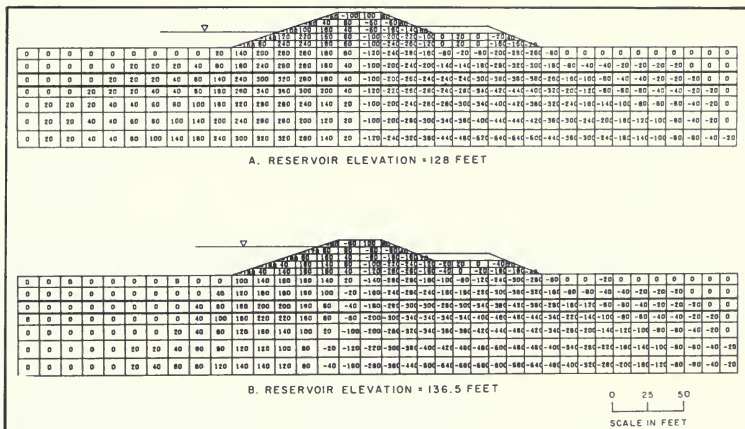


Figure 171. Static Horizontal Shear Stresses,  $\tau_{xy}$  (psf), for Station 347

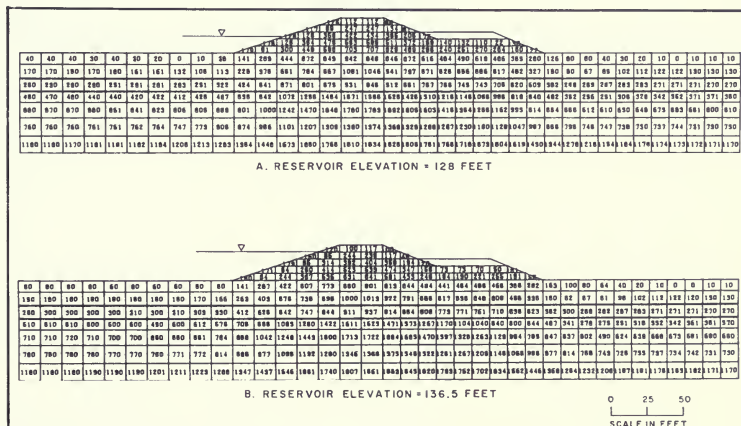


Figure 172. Static Maximum Shear Stresses,  $\tau_{\max}$  (psf), for Station 347

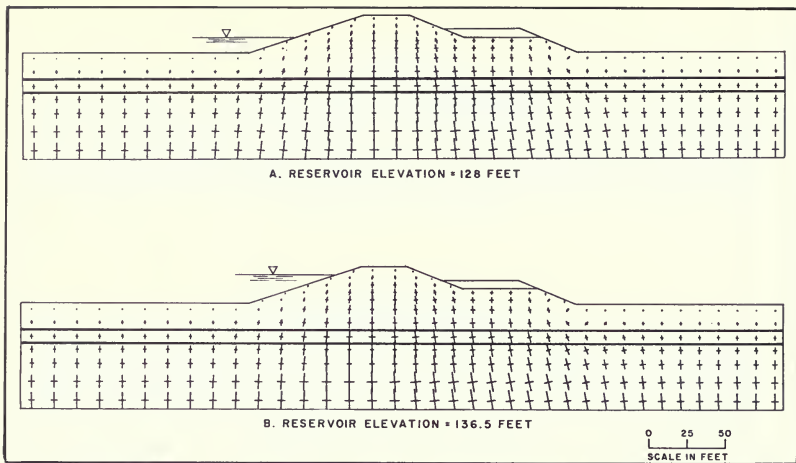


Figure 173. Principal Stress Orientations for Station 347

## **ADDENDUM C**

### **ACCELEROGRAMS**

Addendum C contains the time histories and response spectra for the three earthquake motions used in the seismic analyses of Thermalito Afterbay Dam (figures 174 and 175). Figure 174 presents the displacement, velocity, and acceleration time histories for each motion. Figure 175 presents the response spectra with damping ratios of 0.02, 0.05, 0.10, and 0.20.

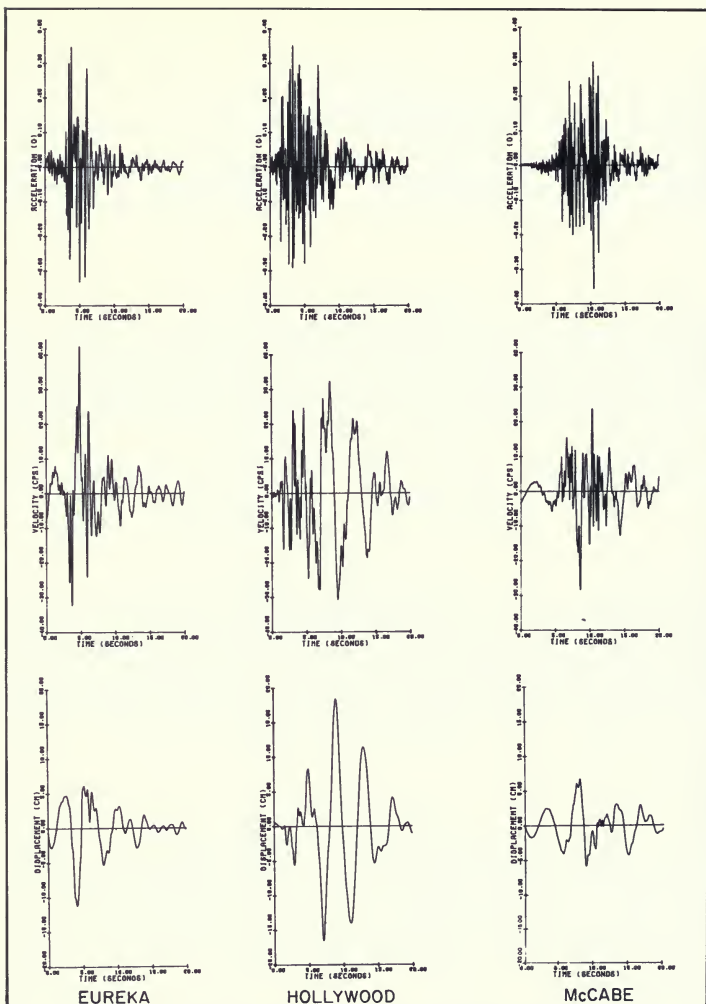


Figure 174. Time Histories for the Thermalito Afterbay Analysis

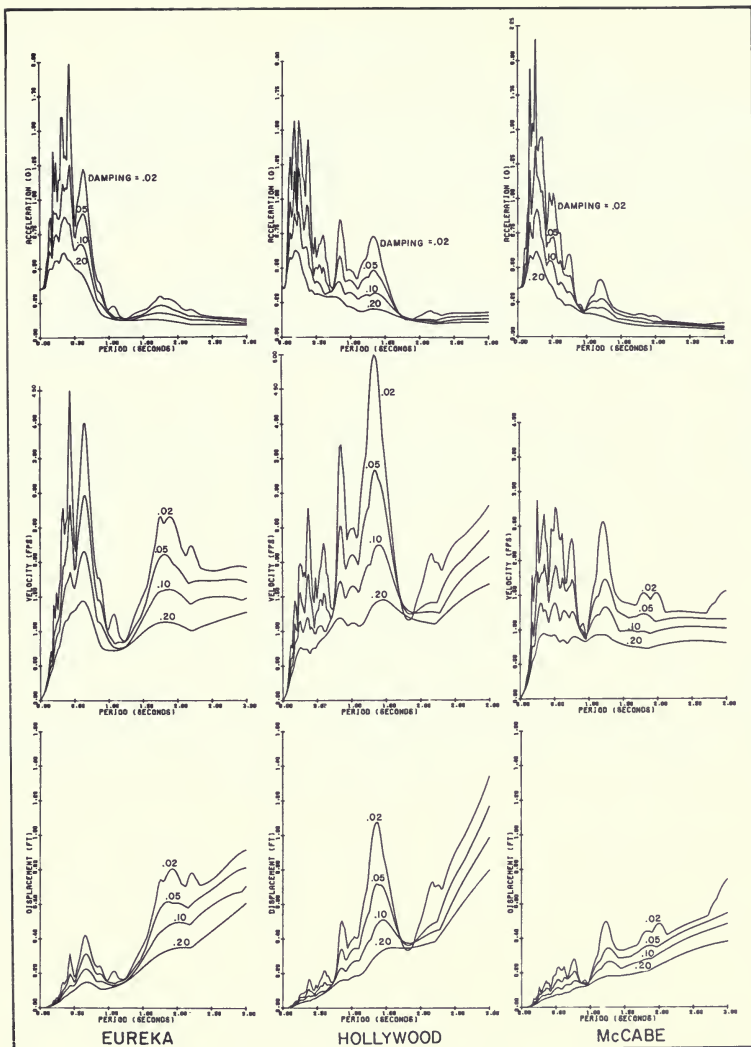


Figure 175. Response Spectra for the Thermalito Afterbay Analysis



## ADDENDUM D

### RESULTS OF DYNAMIC RESPONSE ANALYSES

Earthquake-induced dynamic stresses were calculated using a series of one-dimensional dynamic response analyses for each of the three models analyzed (Stations 107, 165, and 347). Program SHAKE was used in these three analyses. This addendum presents, for each model, the maximum horizontal accelerations along each SHAKE profile, the maximum dynamic shear stresses in the suspect sand layer and typical shear stress time histories produced in the suspect sand layer. Acceleration values are presented in units of gravity, and shear stresses are shown in units of pounds per square foot.

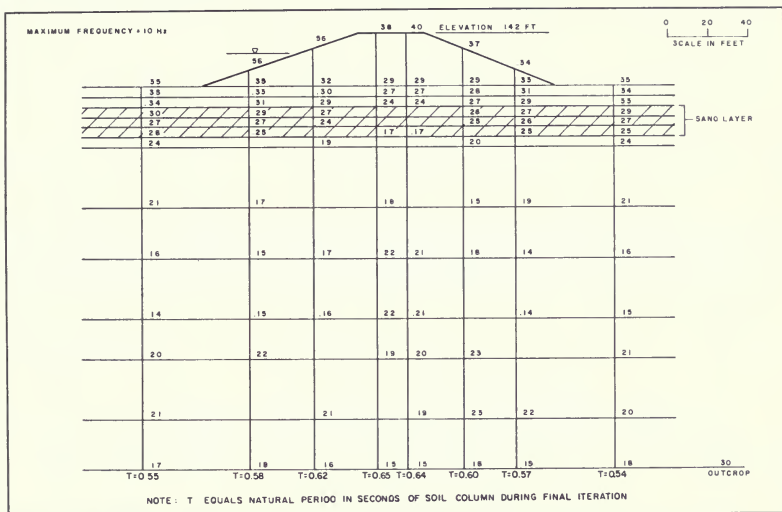


Figure 176. Maximum Horizontal Accelerations,  $a_{\max}$  (g), Determined from One-Dimensional Shake Analysis for Station 107 Using the Eureka Federal Building Motion

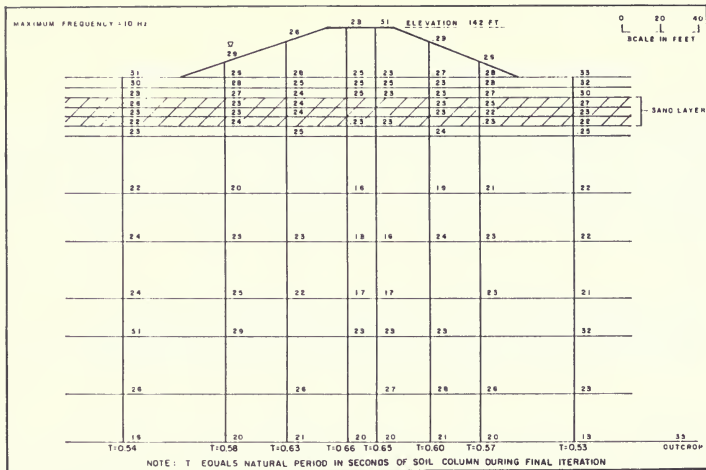


Figure 177. Maximum Horizontal Accelerations,  $a_{\max}$  (g), Determined from One-Dimensional Shake Analysis for Station 107 Using the Hollywood Storage P.E. Lot Motion

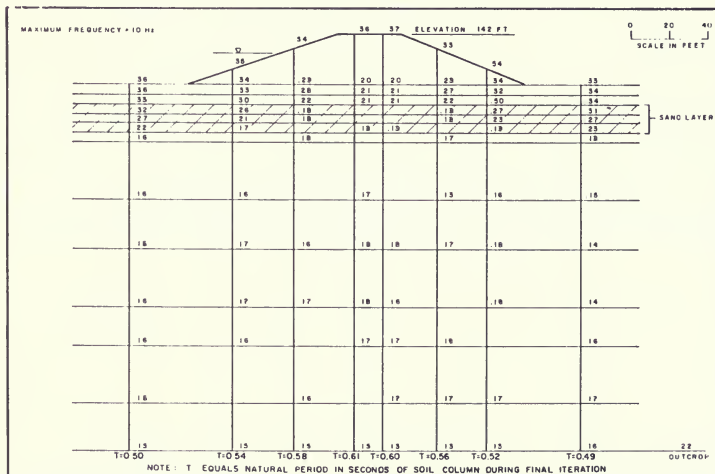


Figure 178. Maximum Horizontal Accelerations,  $a_{\max}$  (g), Determined from One-Dimensional Shake Analysis for Station 165 Using the McCabe School Motion



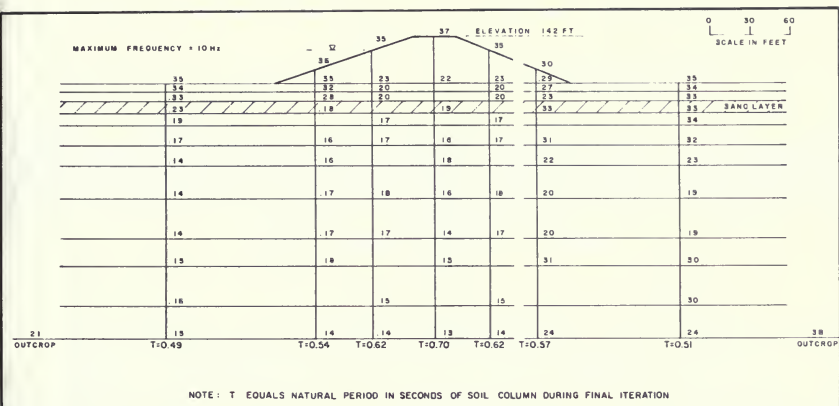


Figure 179. Maximum Horizontal Accelerations,  $a_{\max}$  (g), Determined from One-Dimensional Shake Analysis for Station 347 Using the McCabe School Motion

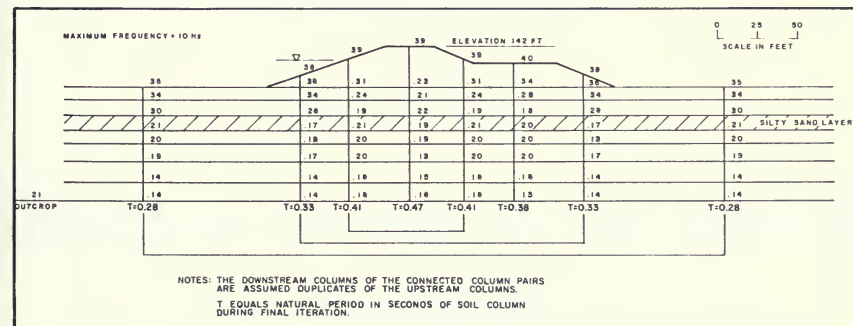


Figure 180. Maximum Horizontal Accelerations,  $a_{\max}$  (g), Determined from One-Dimensional Shake Analysis for Station 347 Using the McCabe School Motion

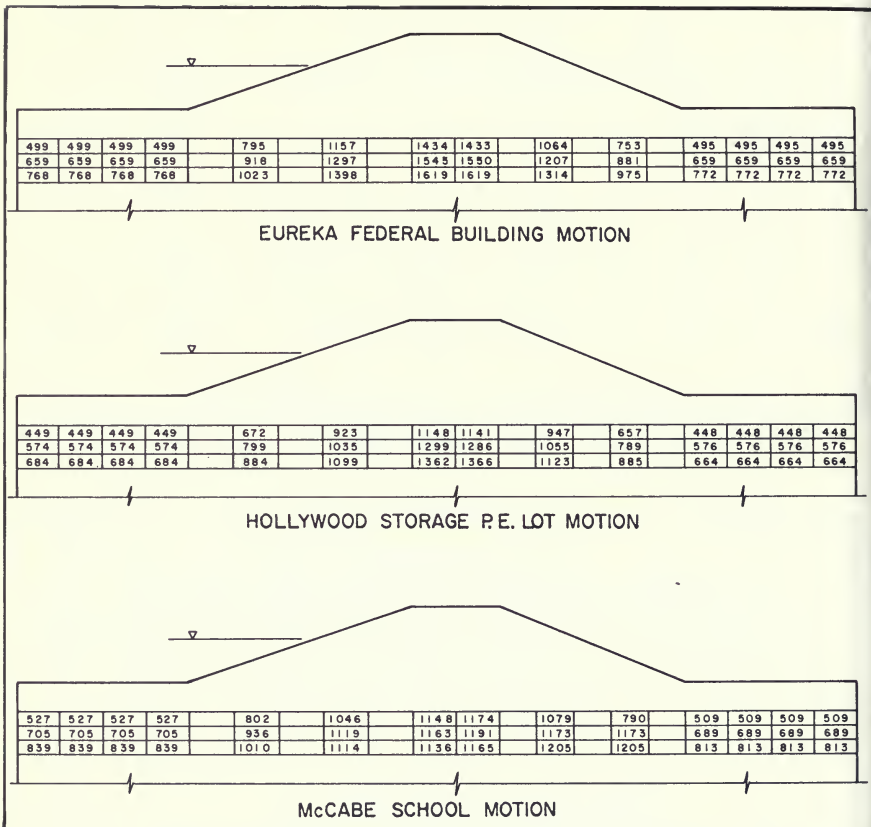


Figure 181. Maximum Dynamic Shear Stresses,  $\tau_{\max}$  (psf), Station 107 from Shake Analysis

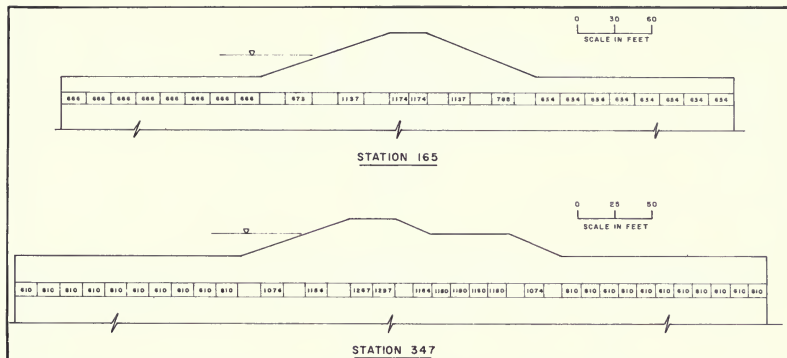


Figure 182. Maximum Dynamic Shear Stresses,  $\tau_{\max}$  (psf), Station 165 and 347 from Shake Analysis Using the McCabe School Motion

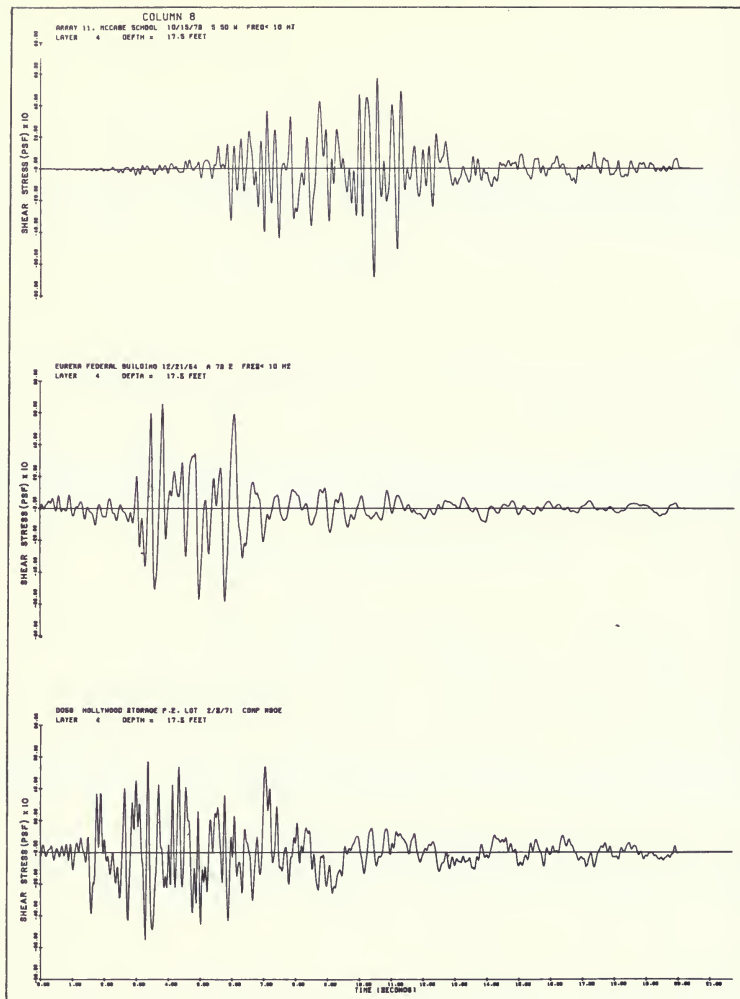


Figure 183. Typical Shear Stress Time Histories in Suspect Sand Layer from Station 107 Downstream Shake Profile (Column 8)

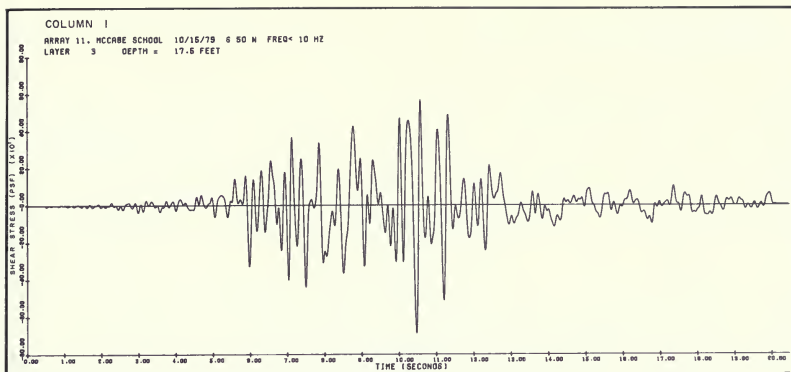


Figure 184. Typical Shear Stress Time History in Suspect Sand Layer from Station 165 Upstream Shake Profile (Column 1)

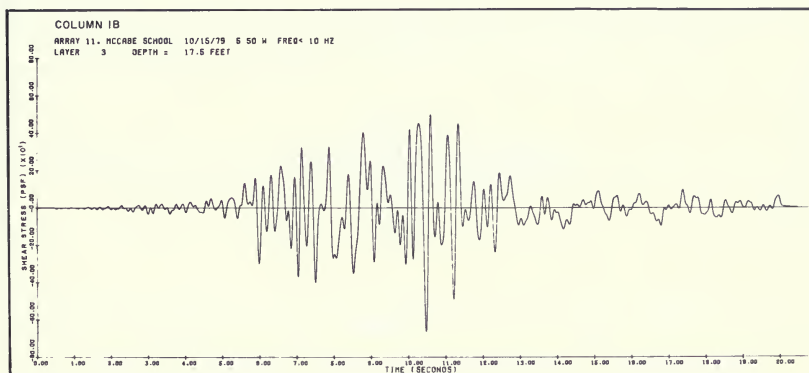


Figure 185. Typical Shear Stress Time History in Suspect Sand Layer from Station 165 Downstream Shake Profile (Column 1B)

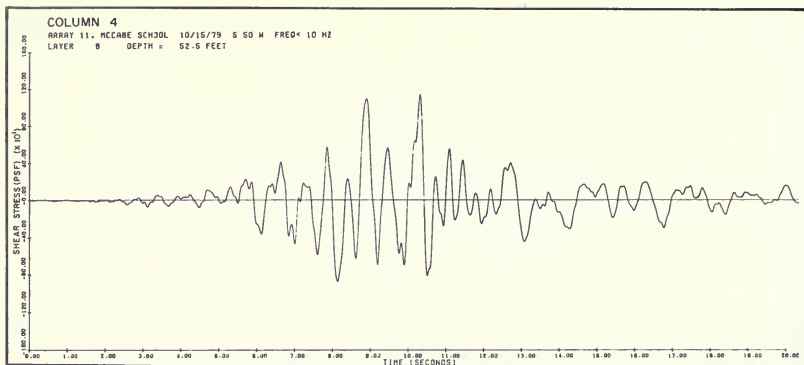
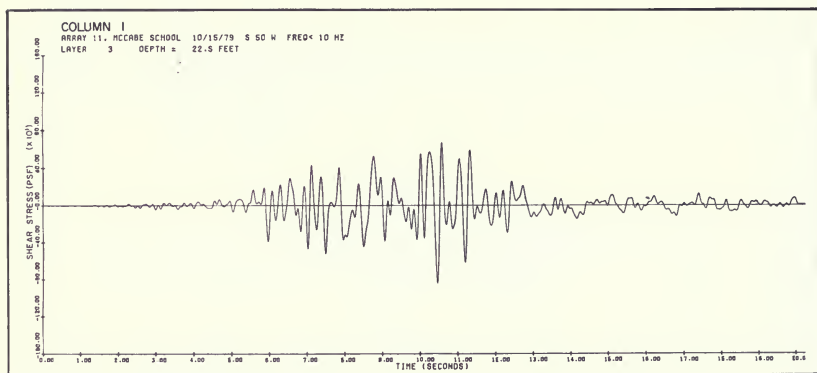
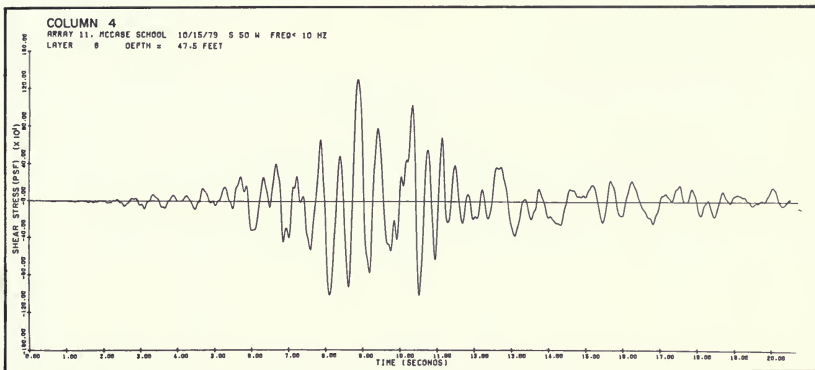


Figure 186. Typical Shear Stress Time History in Suspect Sand Layer from Station 165 Crest Shake Profile (Column 4)



187. Typical Shear Stress Time History in Suspect Sand Layer from Station 347 Upstream Shake Profile (Column 1)



*Figure 188. Typical Shear Stress Time History in Suspect Sand Layer from Station 347 Crest Shake Profile (Column 4)*





## ADDENDUM E DYNAMIC TESTING

Undisturbed samples collected from the weak foundation sand layers at the Afterbay were subjected to stress-controlled cyclic triaxial tests. In addition, a substantial number of cyclic triaxial tests were performed on remolded specimens made from the 1978 samples.

Addendum E presents a summary of cyclic triaxial tests performed between 1978 and 1982. They are organized by sampling year and consolidation conditions. Each summary tabulates the samples' particular information (i.e., depth, assigned blowcount value, material type, densities, and grain size), along with the test results (stress level, and number of stress cycles required to induce 5 percent strain and 10 percent strain.)

**Table 29. Cyclic Triaxial Test Summary for 1978 Undisturbed Samples Tested at  $\sigma'_{3c} = 0.5ksc$  and  $K_c = 1.0$**

Borehole	Depth (feet)	Field Sample	Lab ID	Assigned N <sub>A1</sub> (blows/ foot)	Dry Density (pcf)	Consol- idated Dry Density (psf)	% Minus #200 Sieve	D <sub>50</sub> (mm)	USCS Classifi- cation	B Value	$\sigma_{dp}$ (KSC)	N <sub>5</sub> (cycles)	N <sub>10</sub> (cycles)
TAS-1D*	11	PS-1	8-438C	20	93.9	94.5	13	0.50	SM,		0.55	216	240
TAS-1D*	20	PS-4	8-441B	20	74.4	75.2	17	0.17	SM		0.60	15	21
TAS-1E	11	PS-1	8-447C	20	100.6	101.3	7	0.67	SM-SM,		0.74	2	5
TAS-1E*	14	PS-2	6-448B	20	99.9	100.5	18	0.50	SM		0.62	18	28
TAS-2J*	13	PS-3	8-350C	40	91.0	91.7	4	0.30	SW	-	0.61	4	8
TAS-2K*	10	PS-2	8-360C	40	85.4	86.0	8	0.25	SM-SP	-	0.48	10	20

\* 10% strain extrapolated

**Table 30. Cyclic Triaxial Test Summary for 1978 Undisturbed Samples Tested at  $\sigma'_{3c} = 1.0ksc$  and  $K_c = 1.0$**

Borehole	Depth (feet)	Field Sample	Lab ID	Assigned N <sub>A1</sub> (blows/ foot)	Dry Density (pcf)	Consol- idated Dry Density (psf)	% Minus #200 Sieve	D <sub>50</sub> (mm)	USCS Classifi- cation	B Value	$\sigma_{dp}$ (KSC)	N <sub>5</sub> (cycles)	N <sub>10</sub> (cycles)
TAS-1D	13	PS-2	8-439B	20	89.8	90.5	14	0.30	SM	-	0.95	4.5	6
TAS-1D	14	PS-2	8-439C	20	70.5	71.6	25	0.26	SM	-	0.72	16	-
TAS-1D	16	PS-3	8-440B	20	80.6	82.0	11	0.42	SM-SP	-	0.77	7.5	10
TAS-1E*	16	PS-3	8-449B	20	80.2	81.2	12	0.33	SM-SP	-	0.73	15	20
TAS-2D	15	PS-3	8-279C	40	105.0	106.3	-	-	-	-	0.84	26	-
TAS-2F	25	PS-4	8-289	40	-	-	-	-	-	-	1.15	3.5	7
TAS-2F	28	PS-5	8-290	40	97.7	98.8	3	0.60	SP	-	1.00	5	7
TAS-2J	15	PS-4	8-351C	40	94.8	95.3	3	0.50	SP		0.72	9	27
TAS-2K	12	PS-3	8-361B	40	97.9	99.5	11	0.27	SM-SW	-	0.67	39	-
TAS-2K	12	PS-3	8-361C	40	97.3	98.1	4	0.51	SP	-	0.9	5	12
TAS-2K	21	PS-6	8-364C	40	104.6	105.5	-	-	-	-	0.84	6	14

\* 10% strain extrapolated

Table 31. Cyclic Triaxial Test Summary for 1978 Undisturbed Samples Tested at  $\sigma'_{3c} = 1.0ksc$  and  $K_c = 1.5$ 

Borehole	Depth (feet)	Field Sample	Lab ID	Assigned <sup>a</sup> Al (blows/foot)	Dry Density (pcf)	Consolidated Dry Density (pcf)	% Minus #200 Sieve	D <sub>50</sub> (mm)	USCS Classification	B Value	$\sigma_{dp}$ (KSC)	N <sub>5</sub> (cycles)	N <sub>10</sub> (cycles)
TAS-2D	12	PS-2	8-278C	40	90.4	92.7	-	-	-	-	1.23	27	-
TAS-2D	14	PS-3	8-279B	40	-	-	-	-	-	-	1.20	14	35

Table 32. Cyclic Triaxial Test Summary for 1978 Undisturbed Samples Tested at  $\sigma'_{3c} = 3.0ksc$  and  $K_c = 1.0$ 

Borehole	Depth (feet)	Field Sample	Lab ID	Assigned <sup>a</sup> Al (blows/foot)	Dry Density (pcf)	Consolidated Dry Density (pcf)	% Minus #200 Sieve	D <sub>50</sub> (mm)	USCS Classification	B Value	$\sigma_{dp}$ (KSC)	N <sub>5</sub> (cycles)	N <sub>10</sub> (cycles)
TAS-1D	17	PS-3	8-440C	20	83.5	85.8	12	0.30	SM-SW	-	1.40	6	7
TAS-1D	20	PS-4	8-441C	20	70.0	71.5	17	0.22	SM	-	1.20	82	85
TAS-1E*	14	PS-2	8-448C	20	89.7	91.6	18	0.27	SM	-	1.33	29	32
TAS-1E	17	PS-3	8-449C	20	75.3	77.3	12	0.31	SM-SP	-	1.69	5.5	6.5
TAS-1E*	19	PS-4	8-450B	20	69.0	71.7	16	0.18	SM	-	1.33	28	30
TAS-1E	20	PS-4	8-450C	20	72.5	74.7	12	0.21	SM-SP	-	1.08	115	118
TAS-1E*	23	PS-5	8-451C	20	90.8	93.8	11	0.50	SM-SW	-	1.62	3.5	7
TAS-1E	25	PS-6	8-452B	20	88.5	90.0	7	0.28	SP-SM	-	1.32	469	-
TAS-1E*	26	PS-6	8-452C	20	87.9	89.3	4	0.32	SP	-	1.68	29	30
TAS-2D*	20	PS-5	8-281	40	94.9	95.3	5	0.40	SP-SM	-	1.95	2	4
TAS-2K	16	FS-1	8-347C	40	98.4	100.5	6	0.41	SP-SM	-	1.27	22	-
TAS-2J*	30	PS-9	8-356C	40	97.7	99.4	3	0.80	SP	-	1.67	6	11
TAS-2J*	32	PS-10	8-357C	40	94.0	94.9	2	0.42	SP	-	1.99	5	10
TAS-2K*	23	PS-7	8-365C	40	111.4	112.7	35	0.37	SM	-	1.28	16	24
TAS-2K*	25	PS-8	8-366C	40	100.4	101.7	3	0.61	SP	-	1.20	15	22
TAS-2K	27	PS-9	8-367C	40	93.6	95.2	4	0.56	SP	-	1.21	20	23
TAS-2K*	29	PS-10	8-368C	40	93.3	94.9	6	0.59	SP-SM	-	1.44	7.5	14

\* 10% strain extrapolated

Table 33. Cyclic Triaxial Test Summary for 1978 Remolded Samples Tested at  $\sigma'_{3c} = 1.0ksc$  and  $K_c = 1.0$ 

Borehole	Depth (feet)	Field Sample	Lab ID	Assigned <sup>a</sup> Al (blows/foot)	Dry Density (pcf)	Consolidated Dry Density (pcf)	% Minus #200 Sieve	D <sub>50</sub> (mm)	USCS Classification	B Value	$\sigma_{dp}$ (KSC)	N <sub>5</sub> (cycles)	N <sub>10</sub> (cycles)
TAS-1D	16	PS-3	8-440B	-	84.9	87.5	11	0.42	SM-SP	-	0.50	5	9
TAS-1D**	17	PS-3	8-440BC	-	87.7	89.8	12	0.30	SM-SP	-	0.82	1.5	2
TAS-1E*	17	PS-3	8-449B	-	84.8	-	12	0.33	SM-SP	-	0.37	22	29
TAS-1E**	17	PS-3	8-449B	-	85.6	86.8	12	0.33	SM-SP	-	0.65	3.5	4.5
TAS-2J	15	PS-4	8-351C	-	96.0	95.3	3	0.50	SP	-	0.49	7.5	-

\* 10% strain extrapolated

\*\* intervals of induced cyclic stress prior to testing

Table 34. Cyclic Triaxial Test Summary for 1978 Remolded Samples Tested at  $\sigma'_{3c} = 1.0ksc$  and  $K_c = 1.5$

Borehole	Depth (feet)	Field Sample	Lab ID	Assigned $N_{A1}$ (blows/foot)	Dry Density (pcf)	Consolidated Dry Density (pcf)	% Minus #200 Sieve	D <sub>50</sub> (mm)	USCS Classification	B Value	$\sigma_{dp}$ (KSC)	N <sub>5</sub> (cycles)	N <sub>10</sub> (cycles)
TAS-1D	17	PS-3	8-440BC	-	87.3	89.4	12	0.30	SM-SP	-	1.27	1	1.5
TAS-1D	17	PS-3	8-440BC	-	87.6	90.8	12	0.30	SM-SP	-	0.50	8	16
TAS-1D	17	PS-3	8-440BC	-	87.8	93.1	12	0.30	SM-SP	-	0.41	55	-
TAS-1D*	20	PS-4	8-441C	-	71.2	74.4	17	0.22	SM	-	0.53	21	60
TAS-1E*	17	PS-3	8-449C	-	79.8	83.4	12	0.31	SM-SP	-	0.54	17	48

\* 10% strain extrapolated

Table 35. Cyclic Triaxial Test Summary for 1978 Remolded Samples Tested at  $\sigma'_{3c} = 1.0ksc$  and  $K_c = 1.0$

Borehole	Depth (feet)	Field Sample	Lab ID	Assigned $N_{A1}$ (blows/foot)	Dry Density (pcf)	Consolidated Dry Density (pcf)	% Minus #200 Sieve	D <sub>50</sub> (mm)	USCS Classification	B Value	$\sigma_{dp}$ (KSC)	N <sub>5</sub> (cycles)	N <sub>10</sub> (cycles)
TAS-1D	17	PS-3	8-440BC	-	85.7	90.6	12	0.30	SM-SP	-	1.17	7.5	8.5
TAS-1D**	17	PS-3	8-440BC	-	-	-	12	0.30	SM-SP	-	1.42	8	9
TAS-1D	17	PS-3	8-440C	-	89.2	93.7	12	0.30	SM-SW	-	1.00	18	20
TAS-1**	17	PS-2	8-448C	-	89.3	100.0	18	0.27	SM	-	1.30	46	49
TAS-2J	30	PS-9	8-356C	-	97.5	99.8	3	0.71	SP	-	1.57	1.5	3
TAS-2J*	30	PS-9	8-356C	-	98.7	100.7	3	0.71	SP	-	1.17	5	8
TAS-2J	30	PS-9	8-356C	-	98.8	101.3	3	0.71	SP	-	0.96	25	28
TAS-2J**	30	PS-9	8-356C1	-	99.2	101.1	3	0.71	SP	-	1.49	2.5	4
TAS-2J**	30	PS-9	8-356C-2	-	99.4	101.4	3	0.71	SP	-	1.49	5.5	8
TAS-2J**	30	PS-9	8-356C-3	-	99.5	101.9	3	0.71	SP	-	1.47	8.5	11
TAS-2J	32	PS-10	8-357C	-	93.8	95.2	2	0.39	SP	-	2.62	1.5	2
TAS-2J	32	PS-10	8-357C	-	94.9	-	2	0.39	SP	-	1.97	1.5	3.5
TAS-2J *	32	PS-10	8-357C	-	95.3	96.7	2	0.39	SP	-	1.25	4	7
TAS-2J *	32	PS-10	8-357C	-	93.9	95.8	2	0.39	SP	-	0.98	13	16

\* 10% strain extrapolated

\*\* intervals of induced cyclic stress prior to testing

Table 36. Cyclic Triaxial Test Summary for 1978 Remolded Samples Tested at  $\sigma'_{3c} = 1.0ksc$  and  $K_c = 1.5$ 

Borehole	Depth (feet)	Field Sample	Lab ID	Assigned $N_{Al}$ (blows/foot)	Dry Density (pcf)	Consolidated Dry Density (psf)	% Minus #200 Sieve	D <sub>50</sub> (mm)	USCS Classification	B Value	$\sigma_{dp}$ (KSC)	N <sub>5</sub> (cycles)	N <sub>10</sub> (cycles)
TAS-1D	17	PS-3	8-440BC	-	87.2	93.8	12	0.30	SM-SP	-	1.20	9	11
TAS-1D	20	PS-4	8-441C	-	72.6	78.7	17	0.22	SM	-	1.23	12	15
TAS-1D	20	PS-4	8-441C	-	74.0	84.1	17	0.22	SM	-	1.56	3	5
TAS-1E	17	PS-3	8-449C	-	78.1	81.4	12	0.31	SM-SP	-	1.21	17	20

Table 37. Cyclic Triaxial Test Summary for 1979-80 Undisturbed Samples Tested at  $\sigma'_{3c} = 0.5ksc$  and  $K_c = 1.0$ 

Borehole	Depth (feet)	Field Sample	Lab ID	Assigned $N_{Al}$ (blows/foot)	Dry Density (pcf)	Consolidated Dry Density (psf)	% Minus #200 Sieve	D <sub>50</sub> (mm)	USCS Classification	B Value	$\sigma_{dp}$ (KSC)	N <sub>5</sub> (cycles)	N <sub>10</sub> (cycles)
79-351*	12.0-13.0	S-9	79-748E	-			16	0.5	SM	0.95	0.67	33	75

Table 38. Cyclic Triaxial Test Summary for 1979-80 Undisturbed Samples Tested at  $\sigma'_{3c} = 1.0ksc$  and  $K_c = 1.0$ 

Borehole	Depth (feet)	Field Sample	Lab ID	Assigned $N_{Al}$ (blows/foot)	Dry Density (pcf)	Consolidated Dry Density (psf)	% Minus #200 Sieve	D <sub>50</sub> (mm)	USCS Classification	B Value	$\sigma_{dp}$ (KSC)	N <sub>5</sub> (cycles)	N <sub>10</sub> (cycles)
79-351*	13.3-14.5	S-10	79-349E	--	109.9	110.6	27	0.5	SC	0.95	1.14	5	13
79-351*	13.3-14.5	S-10	79-349D	--			27	0.4	SC	0.95	0.97	9	21
79-361*	9.1-10.0	S-8	79-754E	--			78	0.01	CL	0.95	1.22	65	100+

\*10% strain extrapolated

Table 39. Cyclic Triaxial Test Summary for 1981-82 Undisturbed Samples Tested at  $\sigma'_{3c} = 1.0ksc$  and  $K_c = 1.0$ 

Borehole	Depth (feet)	Field Sample	Lab ID	Assigned $N_{Al}$ (blows/foot)	Dry Density (pcf)	Consolidated Dry Density (psf)	% Minus #200 Sieve	D <sub>50</sub> (mm)	USCS Classification	B Value	$\sigma_{dp}$ (KSC)	N <sub>5</sub> (cycles)	N <sub>10</sub> (cycles)
81A-104PSA	10.3-11.7	1	738C	35	88.9	90.0	8	0.32	SP-SM	0.80	0.68	25	30
81A-104PSA	13.6-15.1	2	739C	24	79.8	81.1	10	0.30	SM-SP	0.86	0.76	16	25
	**13.6-15.1	2	739B	24	80.0	81.1	16	0.20	SM	?	0.81	54	?
81A-104PSA	†17.0-18.4	3	740C	24	80.3	81.3	2	0.30	SP	0.95	0.84	10	15
	†17.0-18.4	3	740B	24	82.7	82.8	8	0.30	SP-SM	0.96	0.92	5	8
81A-104PSA	20.5-21.8	4	741C	26	69.7	70.6	6	0.37	SP-SM	0.95	0.80	21	26
	20.5-21.8	4	741B	26	67.2	68.1	6	0.46	SP-SM	0.96	0.86	11	16
81A-104PSA	24.0-25.3	5	742C	26	75.3	76.0	5	0.37	SP	0.95	0.92	7	12
	24.0-25.3	5	742B	26	73.5	73.9	5	0.42	SP	0.94	0.80	24	32

**Table 39. Cyclic Triaxial Test Summary for 1981-82 Undisturbed Samples Tested at  $\sigma'_{3c} = 1.0 \text{ ksc}$  and  $K_c = 1.0$**   
(Continued)

Borehole	Depth (feet)	Field Sample	Lab ID	Assigned N <sub>al</sub> (blows/ foot)	Dry Density (pcf)	Consol- idated Dry Density (psf)	Z Minus #200 Sieve	D <sub>50</sub> (mm)	USCS Classifi- cation	B Value	$\sigma_{dp}$ (KSC)	N <sub>5</sub> (cycles)	N <sub>10</sub> (cycles)
81A-107PSA	11.5-12.8	1	1146C	20	84.2	85.9	11	0.36	SM-SP	0.94	0.69	17	20
	11.5-12.8	1	1146B	20	85.7	86.5	12	0.37	SM	0.95	0.72	30	38
81A-107PSA	15.0-16.5	2	1147C	12	75.1	75.8	12	0.36	SM	0.96	0.60	11	17
	15.0-16.5	2	1147B	12	83.5	85.2	14	0.32	SM	0.95	0.59	23	28
81A-107PSA	22.1-23.5	4	1149C	18	75.0	75.9	13	0.29	SM	0.95	0.77	5	7
	22.1-23.5	4	1149B	18	81.7	82.1	12	0.29	SM	0.95	0.83	4	5
81A-107PSA	25.5-26.6	5	1150C	21	67.6	68.7	8	0.45	SW-SM	0.95	0.90	6	11
	25.5-26.6	5	1150B	21	78.5	80.4	10	0.52	SM-SW	0.95	0.78	7	10
81A-107PSB	†11.5-12.7	2	1267C	23	70.3	74.1	20	0.17	SM	0.95	0.70	31	37
	†11.5-12.7	2	1267B	23	75.5	78.8	20	0.19	SM	0.95	0.97	25	29
81A-107PSC	25.8-26.9	6	1617C	44	89.5	89.8	0	0.66	SP	0.95	1.26	2.5	4
	25.8-26.9	6	1617B	44	93.3	94.1	2	0.72	SP	0.95	1.11	6	10.5
81A-107PSP	25.7-26.9	5	1625C	43	95.1	95.9	1	0.70	SP	0.95	1.18	4	7
	25.7-26.9	5	1625B	43	88.5	89.0	1	0.50	SP	0.95	1.29	6	10
81A-107PSP†	22.1-23.4	3	1628B	15	-	-	-	-	-	0.95	1.09	43	-
81A-165PSA	13.6-14.9	1	734C	18	79.2	81.1	27	0.15	SM	0.93	0.72	43	48
	13.6-14.9	1	734B	18	85.1	86.4	29	0.17	SM	0.95	0.86	100	107
81A-165PSA	16.5-17.9	2	735C	12	81.6	83.0	29	0.22	SM	0.90	0.71	4	6
	16.5-17.9	2	735B	12	84.4	85.8	20	0.22	SM	0.91	0.65	15	17
81A-165PSB	13.6-14.7	1	736C	18	79.8	81.4	22	0.15	SM	0.95	0.80	11	15
	13.6-14.7	1	736B	18	82.4	84.1	38	0.11	SM	0.90	1.09	43	49
81A-165PSB	16.6-17.9	2	737C	12	73.8	77.6	49	0.08	SM	0.95	0.64	25	31
	16.6-17.9	2	737B	12	79.4	80.7	26	0.21	SM	0.95	0.69	2	3
81A-165PSC	13.4-14.9	1	1151C	18	79.9	81.0	18	0.20	SM	0.95	0.90	5	6
	13.4-14.9	1	1151B	18	82.8	84.1	32	0.15	SM	0.97	0.80	35	40
81A-165PSC	16.5-18.0	2	1152C	12	66.2	69.2	37	0.14	SM	0.95	0.65	5	8
	16.5-18.0	2	1152B	12	77.5	79.9	23	0.23	SM	0.95	0.52	5	6
81A-167PSA	15.8-17.3	1	875C	7	80.2	81.2	16	0.25	SM	0.96	0.67	9	12
	15.8-17.3	1	875B	7	76.4	77.1	17	0.29	SM	0.95	0.54	18	21
81A-167PSA	19.0-20.5	2	876C	8	83.0	83.7	18	0.31	SM	0.96	0.51	10	12
	19.0-20.5	2	876B	8	89.9	90.6	19	0.22	SM	0.95	0.58	6	8
81A-167PSA	22.0-23.5	3	877C	5	72.0	73.0	14	0.32	SM	0.96	0.44	22	25
81A-167-PSD	19.0-22.4	2	623C	8	61.4	62.7	21	0.29	SM	0.95	0.405	22	28
	19.0-22.4	2	623B	8	62.7	63.7	20	0.25	SM	0.95	0.35	61	67

(continued on next page)

Table 39. Cyclic Triaxial Test Summary for 1981-82 Undisturbed Samples Tested at  $\sigma'_{3c} = 1.0ksc$  and  $K_c = 1.0$   
(Continued)

Borehole	Depth (feet)	Field Sample	Lab ID	Assigned N <sub>A1</sub> (blows/ foot)	Dry Density (pcf)	Consol- idated Dry Density (pcf)	% Minus #200 Sieve	D <sub>50</sub> (mm)	USCS Classifi- cation	B Value	$\sigma_{dp}$ (KSC)	N <sub>5</sub> (cycles)	N <sub>10</sub> (cycles)
81A-180PSA	†8.1-9.4	1	1635C	18	91.1	91.6	8	0.50	SP-SM	0.95	0.81	6	9
	†8.1-9.4	1	1635B	18	103.1	104.0	1	0.69	SP-SM	0.95	0.76	88	125+
81A-180PSA	11.1-12.3	2	1636C	46	98.9	100.0	7	0.49	SP-SM	0.95	1.02	12	21
	11.1-12.3	2	1636B	46	102.9	104.4	8	0.50	SP-SM	0.90+	0.94	30	56

\*\* intervals of induced cyclic stress prior to testing

† excessive disturbance due to sampling errors or freezing experiments

† † sample tested at Caltrans Laboratory

Table 40. Cyclic Triaxial Test Summary for 1981-82 Undisturbed Samples Tested at  $\sigma'_{3c} = 1.0ksc$  and  $K_c = 1.5$

Borehole	Depth (feet)	Field Sample	Lab ID	Assigned N <sub>A1</sub> (blows/ foot)	Dry Density (pcf)	Consol- idated Dry Density (pcf)	% Minus #200 Sieve	D <sub>50</sub> (mm)	USCS Classifi- cation	B Value	$\sigma_{dp}$ (KSC)	N <sub>5</sub> (cycles)	N <sub>10</sub> (cycles)
81A-107PSC	11.6-12.8	2	1613C	27	77.8	78.9	16	0.75	SM	0.95	1.31	5	8
	11.6-12.8	2	1613B	27	77.6	77.9	12	0.29	SM	0.95	0.94	7	10
81A-107PSD	21.9-23.1	2	1619C	17	85.1	85.8	9	0.35	SM-SP	0.95	1.09	5	8
	21.9-23.1	2	1619B	17	70.0	70.3	11	0.30	SM-SP	0.95	1.03	10	13
81A-107PSE	15.0-16.4	1	1630C	12	71.0	72.7	18	0.29	SM	0.96	0.98	11	13
	15.0-16.4	1	1630B	12	76.2	76.9	18	0.31	SM	0.95	0.91	1	2
81A-107PSF	11.6-12.9	1	1621C	30	65.9	67.1	18	0.21	SM	0.95	1.21	9	10
	11.6-12.9	1	1621B	30	61.8	62.8	30	0.17	SM	0.95	1.21	6	7
81A-107PSF	22.1-23.4	4	1624C	23	73.2	73.8	6	0.44	SP-SM	0.95	1.08	13	16
	22.1-23.4	4	1624B	23	73.4	74.1	6	0.42	SP-SM	0.95	1.17	12	14
81A-165PSD	13.0-14.5	1	1631C	13	82.6	84.5	20	0.25	SM	0.95	0.84	42	44
	13.0-14.5	1	1631B	13	81.8	83.1	22	0.17	SM	0.95	-	-	-
81A-165PSD	17.0-18.5	2	1632C	11	69.1	69.7	28	0.11	SM				
	17.0-18.5	2	1632B	11	73.4	73.8	29	0.11	SM	0.95+	0.77	4	7
81A-167-PSC	19.0-20.4	2	558B	8	59.6	60.6	19	0.31	SM	0.95	0.69	1	1
81A-167-PSF	16.0-17.4	1	976C	7	69.3	70.5	19	0.19	SM	0.95	0.61	3	4
	16.0-17.4	1	976B	7	75.3	76.2	16	0.26	SM	0.95	0.53	17	27
81A-167-PSF	19.0-20.4	2	977C	8	68.9	71.1	25	0.23	SM	0.95	0.55	2	4
	19.0-20.4	2	977B	8	70.8	73.2	23	0.25	SM	0.95	0.58	4	7

**Table 41. Cyclic Triaxial Test Summary for 1981-82 Undisturbed Samples Tested at  $\sigma'_{3c} = 2.5$  ksc and  $K_c = 1.0$**

Borehole	Depth (feet)	Field Sample	Lab ID	Assigned $N_{bl}$ (blows/foot)	Dry Density (pcf)	Consolidated Dry Density (pcf)	% Minus #200 Sieve	D <sub>50</sub> (mm)	USCS Classification	B Value	$\sigma_{dp}$ (KSC)	N <sub>5</sub> (cycles)	N <sub>10</sub> (cycles)
81A-107PSA	18.5-19.9	3	1148C	16	81.2	84.0	11	0.35	SM-SP	0.85	0.91	42	44
	18.5-19.9	3	1148B	16	83.4	85.6	11	0.40	SM-SP	0.95	1.06	25	29
81A-107PSB	+8.0-9.4	1	1266C	27	87.3	93.2	9	0.32	SM-SP	0.95	1.39	17	20
	+8.0-9.4	1	1266B	27	88.9	96.4	9	0.32	SM-SP	0.95	1.52	93	98
81A-107PSB	+15.1-16.3	3	1268C	32	81.1	83.2	6	0.37	SP-SM	0.95	1.26	31	35
	+15.1-16.3	3	1268B	32	75.2	77.1	10	0.37	SM-SP	0.95	1.45	17	20
81A-107PSB	+22.2-23.0	4	1269C	23	72.6	76.9	9	0.49	SP-SM	0.95	1.26	7	9
81A-107PSC	8.1-9.3	1	1612C	31	93.6	96.1	4	0.40	SP-SM	0.94	1.47	14	16
	8.1-9.3	1	1612B	31	88.4	89.5	6	0.38	SP-SM	0.95	1.48	23	26
81A-107PSC	18.7-19.9	4	1615C	25	69.0	71.3	8	0.26	SP-SM	0.95	1.32	65	70
	18.7-19.9	4	1615B	25	66.7	68.1	11	0.19	SM-SP	0.95	1.41	10	13
81A-107PSD	18.8-20.2	1	1618C	16	73.2	75.5	12	0.37	SM-SP	0.95	1.30	12	14
	18.8-20.2	1	1618B	16	73.7	75.3	11	0.38	SM-SP	0.95	1.33	25	27
81A-107PSF	15.0-16.4	2	1622C	31	73.1	74.8	5	0.44	SP-SM	0.95	1.52	70	74
81A-107PSF	15.0-16.4	2	1622B	31	73.7	75.3	6	0.33	SP-SM	0.95	1.53	21	24
	+18.5-19.9	3	1623B	20	-	-	-	-	SM	0.95	1.40	90	-
81A-107PSG	15.2-16.4	1	1626C	13	81.9	84.4	16	0.33	SM	0.95	1.06	7	8
81A-107PSG	15.2-16.4	1	1626B	13	84.0	86.3	21	0.26	SM	0.95	1.05	16	19
	18.4-19.8	2	1627C	12	69.2	70.9	15	0.31	SM	0.95	1.22	9	11
81A-107PSG	18.4-19.8	2	1627B	12	75.7	77.2	13	0.44	SM	0.95	1.15	16	19
	+22.1-23.4	3	1628C	15	-	-	-	-	SM	0.95	1.30	7	-
81A-107PSG	25.5-26.9	4	1629C	19	68.2	71.5	7	0.40	SP-SM	0.95	1.36	4	5
	25.5-26.9	4	1629B	19	75.1	77.6	7	0.42	SP-SM	0.95	1.29	5	7
81A-165PSE	16.3-17.6	2	1634C	7	73.2	76.9	26	0.18	SM	0.95	0.98	53	56
	16.3-17.6	2	1634B	7	76.0	79.7	24	0.20	SM	0.95	1.03	13.5	16
81A-167PSB	16.1-17.5	1	1271C	11	79.9	82.7	20	0.22	SM	0.95	1.17	5	7
	16.1-17.5	1	1271B	11	82.4	84.2	17	0.22	SM	0.95	1.06	7	9
81A-167PSE	16.0-17.3	1	561C	7	79.6	83.5	16	0.25	SM	0.94	1.02	7	8
	16.0-17.3	1	561B	7	82.8	84.5	14	0.25	SM	0.95	1.03	9	11
81A-183PS	41.1-41.8	4	981C	21	86.7	88.1	11	0.33	SM-SP	0.95	1.73	4	7
81A-183PS	44.2-45.3	5	982C	27	91.0	92.9	2	0.60	SP	0.95	1.52	4	6
	44.2-45.3	5	982B	27	96.1	97.1	4	0.56	SP	0.95	1.56	5	9
81A-183PSA	41.3-42.1	4	986C	21	94.1	91.3	6	0.75	SP-SM	0.95	1.34	5	8
81A-C380PSA	27.2-28.5	1	526C	20	108.6	111.4	81	-	CL	0.95	1.35	9	5
	27.2-28.5	1	526B	20	110.0	112.0	82	-	CL	0.92	1.21	21	35

(continued on next page)

**Table 41. Cyclic Triaxial Test Summary for 1981-82 Undisturbed Samples Tested at  $\sigma'_{3c} = 2.5 \text{ ksc}$  and  $K_c = 1.0$  (Continued)**

Borehole	Depth (feet)	Field Sample	Lab ID	Assigned $N_{Al}$ (blows/foot)	Dry Density (pcf)	Consolidated Dry Density (psf)	% Minus #200 Sieve	D <sub>50</sub> (mm)	USCS Classification	B Value	$\sigma_{dp}$ (KSC)	N <sub>5</sub> (cycles)	N <sub>10</sub> (cycles)
81A-C380PSA	30.1-31.2	2	527C	6	82.1	85.8	73	-	ML	0.95	1.25	70	75
	30.1-31.2	2	527B	6	91.1		78	-	ML				
81A-C383PS	17.4-28.5	1	528C	35	103.6	107.6	83	-	CL	0.95	1.52	16	25
	27.4-28.5	1	528B	35	105.0	108.7	84	-	CL	0.92	1.60	4	14
81A-C383PS	30.0-31.4	2	529C	18	95.9	98.0	51	-	CL	0.95	1.66	3	4
	30.0-31.4	2	529B	18	101.4	104.3	70	-	CL	0.95	1.62	10	13

† excessive disturbance due to sampling or freezing experiments

†† sample tested at Caltrans Laboratory

**Table 42. Cyclic Triaxial Test Summary for 1981-82 Undisturbed Samples Tested at  $\sigma'_{3c} = 2.5 \text{ ksc}$  and  $K_c = 1.5$**

Borehole	Depth (feet)	Field Sample	Lab ID	Assigned $N_{Al}$ (blows/foot)	Dry Density (pcf)	Consolidated Dry Density (psf)	% Minus #200 Sieve	D <sub>50</sub> (mm)	USCS Classification	B Value	$\sigma_{dp}$ (KSC)	N <sub>5</sub> (cycles)	N <sub>10</sub> (cycles)
81A-107PSB	15.0-16.3	3	1614C	33	80.4	81.7	6	0.45	SP-SM	0.95	1.94	10	14
	15.0-16.3	3	1614B	33	58.7	60.0	10	0.31	SM-SP	0.95	1.93	11	14
81A-107PSD	25.5-26.9	3	1620C	23	90.6	93.7	4	0.45	SP-SM	0.95	1.86	13	19
	25.5-26.9	3	1620B	23	56.5	58.5	7	0.57	SP-SM	0.95	1.89	15	18
81A-165PSE	†13.1-14.4	1	1633C	13	81.2	83.5	26	0.18	SM	-	-	-	-
	†13.1-14.4	1	1633B	13	83.9	85.9	24	0.60	SM	-	-	-	-
81A-167PSC	16.1-17.4	1	557C	7	75.0	78.1	17	0.21	SM	0.96	1.26	3	5
	16.1-17.4	1	557B	7	81.4	83.7	15	0.28	SM	-	1.22	5	6
81A-167PSC	19.0-20.4	2	558C	8	65.9	69.5	22	0.28	SM	0.95	1.13	3	5
81A-167PSD	15.4-17.3	1	622C	7	70.7	73.6	21	0.19	SM	0.95	1.12	1.5	2
	15.9-17.3	1	622B	7	79.2	81.4	13	0.27	SM	0.95	1.05	5	9
81A-183PS	32.0-33.2	1	979C	29	82.3	84.8	5	0.60	SP	0.95	1.91	5	7
	32.0-33.2	1	979B	29	84.6	87.3	10	0.25	SM-SP	0.95	1.85	9	14
81A-183PS	35.4-36.4	2	980C	21	89.7	91.9	4	0.36	SP	0.95	1.75	5	7
	35.4-36.4	2	980B	21	93.9	95.6	6	0.30	SP-SM	0.95	1.66	42	48
81A-183PSA	32.0-33.3	1	983C	29	83.1	84.7	5	0.17	SP	0.90	1.79	9	13
	32.0-33.3	1	983B	29	89.3	90.7	3	0.22	SP	0.93	1.83	34	40
81A-183PSA	35.3-36.4	2	984C	21	87.8	89.5	4	0.55	SP	0.95+	1.69	6	8
	35.3-36.4	2	984B	21	93.2	95.1	7	0.50	SP-SM	0.95	1.59	13	17
81A-183PSA	38.2-39.4	3	985C	21	87.0	88.6	4	0.47	SP	0.95	1.78	6	7
	38.2-39.4	3	985B	21	91.8	94.2	4	0.57	SP	0.95	1.82	14	17
81A-183PSA	44.3-45.1	5	987C	27	90.4	91.3	3	0.35	SP	0.95	1.71	16	20

† excessive disturbance due to sampling errors or freezing experiments



## ADDENDUM F

### TRIAL FAILURE SURFACES GENERATED FOR SLOPE STABILITY ANALYSES

Addendum F presents the coverage of trial surfaces generated for the wedge analyses of post-seismic slope stability. Shown in the following three figures (189-191) are typical trial surface coverages for the three models analyzed. Analyses shown are for the following conditions:

1. Reservoir Elevation = 136.5 feet;
2. Downstream sliding
3. Pore Pressures in sand layer redistributed over twice the toe-to-toe distance (Section 10)

Each figure displays between 11 to 18 failure surfaces with the base of each wedge forced through the suspect sand layer. Each surface shown is actually the critical surface of approximately 50 surfaces generated in the immediate area. Therefore, the most critical surface (shown as an asterisked line) gives the lowest safety factor from between 500 to 900 surfaces generated.

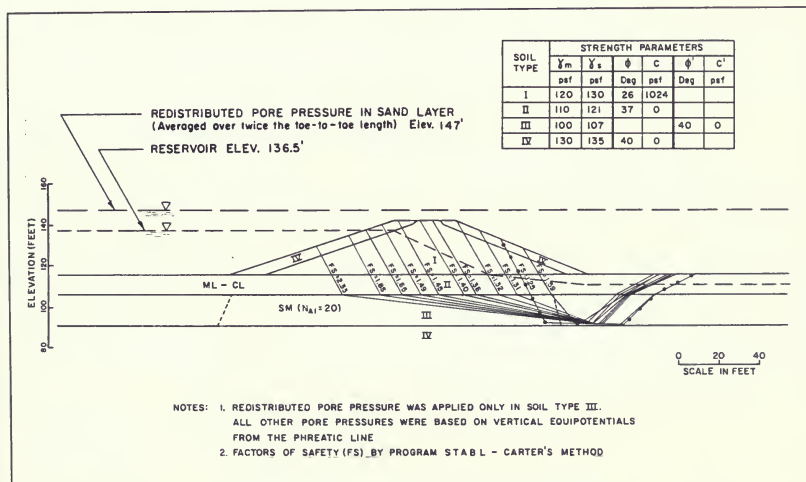


Figure 189. Trial Failure Surfaces Generated for Station 107

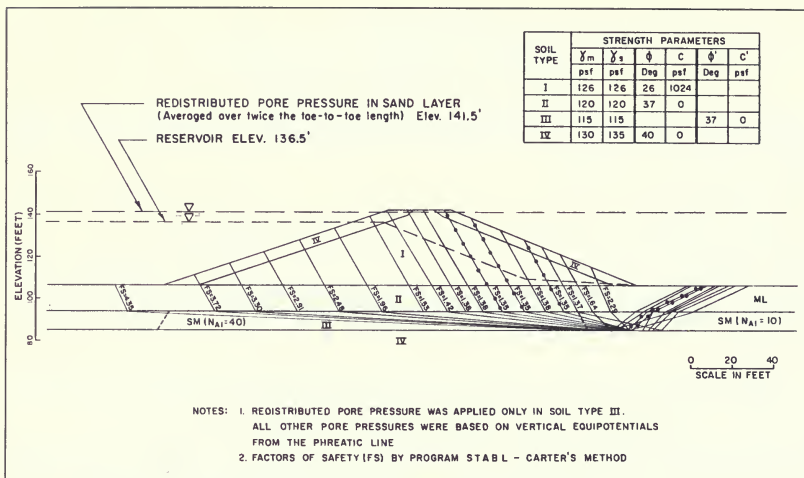


Figure 190. Trial Failure Surfaces Generated for Station 165

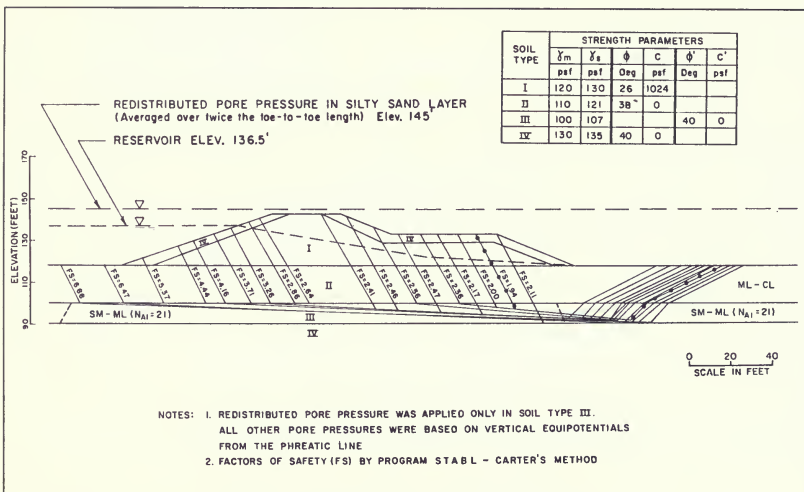


Figure 191. Trial Failure Surfaces Generated for Station 347

## CHAPTER IV

# THERMALITO AFTERBAY DAM CONCRETE STRUCTURES

### SEISMIC EVALUATION

#### Introduction

#### General Discussion

As a result of the August 1975 earthquake, the Department of Water Resources (DWR) decided to re-analyze the major structures of the Oroville complex, using the latest state-of-the-art dynamic analysis with the reanalysis earthquake described in Bulletin 203-78, Chapter V, Section 6\*. After a general re-evaluation, DWR also decided to re-examine noncritical structures—the Western Canal and Richvale Irrigation District Outlets, PGandE Lateral, Sutter Butte Outlet, and Thermalito River Outlet—along Thermalito Afterbay Dam (See Figure 4, Chapter II) using a pseudostatic analysis with lateral loads generated by the reanalysis earthquake.

The Department assumed that the most damaging earthquake motion would originate from the Cleveland Hills Fault, which is about 9 miles from the afterbay structures. The embankment was therefore re-analyzed on the basis of three earthquake motions (see Figure 97, Chapter III) originating from earthquakes of magnitude similar to the reanalysis earthquake, i.e., 6.5 on the Richter scale. These three motions were recorded at sites 10 to 22 miles from the energy source.

All three motions were scaled to a peak acceleration of 0.35g and were limited to the first 20 seconds to keep the duration consistent with the Oroville Reanalysis Earthquake. To select a reanalysis lateral inertial force coefficient for application to the concrete structures under combined earthquake and gravity loads, all three times histories were carefully examined; consequently, a uni-

form coefficient of 0.3 was selected. This is equivalent to a constant horizontal acceleration of 0.3g.

All structures were analyzed in two ways, i.e., using horizontal ground accelerations perpendicular to the water flow, and parallel to the water flow. The ground motion perpendicular to the water flow produced the highest tensile rebar stresses. The motion parallel to the water flow produced rebar stresses well below the yield stress and therefore is not considered a problem. Compressive concrete stresses obtained were well within the design criteria set by DWR and the special consulting board. Although the stresses obtained in the analysis are based on theoretical criteria, they are expected to be the highest that would be experienced during the earthquake postulated. The structures were also checked for sliding and were found to be safe in that respect.

Because sand layers were found in the afterbay area, the Department also investigated the possibility of liquefaction in the Thermalito Afterbay Dam foundation soils, caused by seismic ground vibrations. Boreholes were drilled along the toe on both sides of each concrete structure. The lowest normalized (to one-ton-per-square-foot overburden) standard penetration test blowcount in these boreholes was 20 in a silty soil and 24 in a sandy soil. Based on an analysis presented in Chapter II, these soils would not develop significant excess pore water pressure during the earthquake postulated. The bore holes are believed to be representative of the foundation soil under the structures, in which case, foundation liquefaction is not a problem.

Note: Curves on Figures 196, 203, and 207 should not be extrapolated. If it is desired to make an investigation for lateral forces greater than 0.3, a separate study should be conducted.

\*DWR Bulletin 203-78, *The August 1, 1975 Oroville Earthquake Investigations*, February 1975

### Original Seismic Design

The original seismic design of the noncritical structures was based on a pseudo-static analysis using a 0.1g uniform seismic acceleration combined with normal static loads. The hydrodynamic loads were determined by the Westergaard formula.

### Western Canal and Richvale Irrigation District Outlets

### Description and Past Performance

Each of these facilities (Figures 192 and 193) consists of a headworks structure with control gates; the Western Canal outlet has five 96-inch-diameter conduits; the Rich-

vale outlet has three 72-inch-diameter conduits. The facilities rest on a concrete slab base on a foundation of compact silt and silty sand. Each conduit is equipped with a slide gate at the upstream end to control flows and a Dall flow tube to measure the flows. The headworks structures are approximately 40 feet high. Both structures are built into the afterbay embankment.

An inspection of both structures following the August 1, 1975 earthquake revealed no damage.

### Failure Evaluation

Collapse of the outlet structures could result in some property damage, danger to motorists on Highway 99, which adjoins the afterbay dam, and some disruption to project operation.

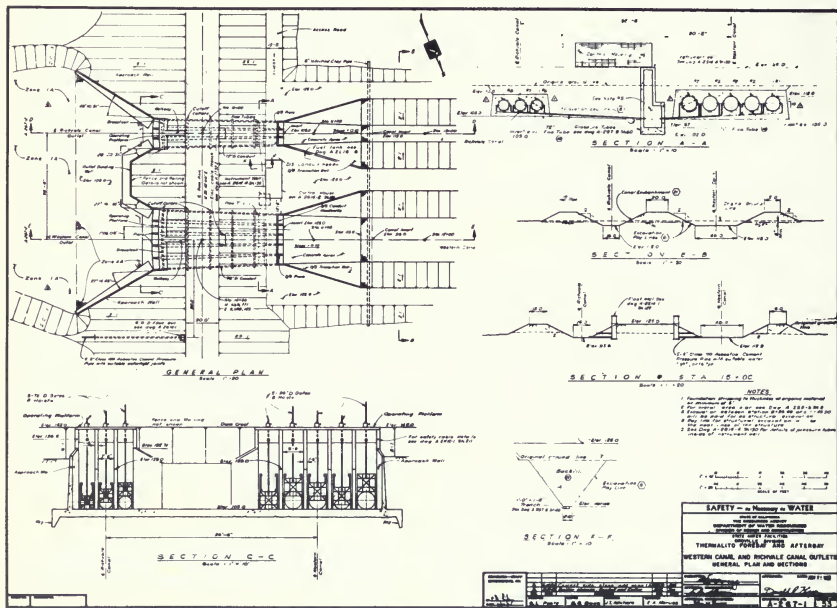


*Figure 192. Western Canal and Richvale Canal Outlet*

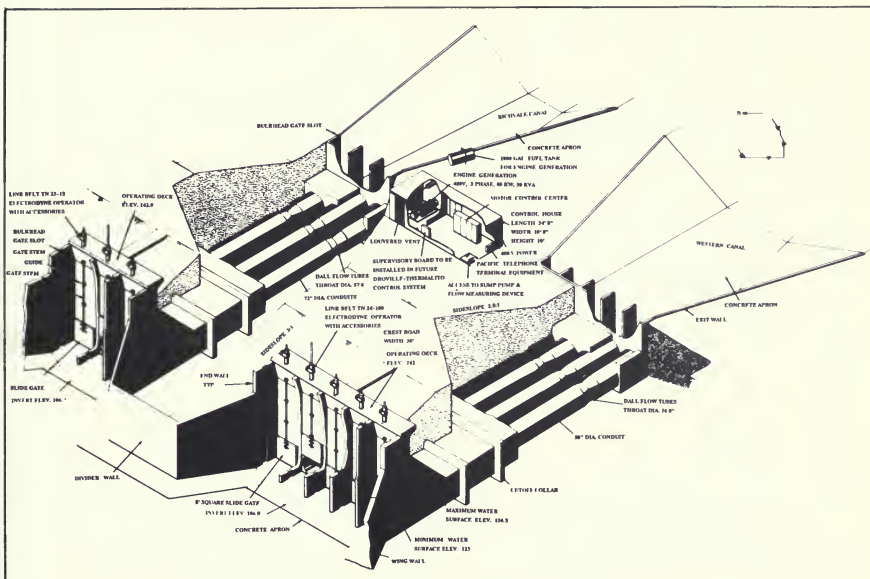


Figure 193. Western Canal and Richvale Canal Outlets—Isometric View

## Seismic Reanalysis

Both structures were checked using the reanalysis lateral inertial force coefficient of 0.3 (see "Introduction") combined with static loads. Rebar tensile stresses at different points in the structures were well within the established design criteria, except for a small area near the upstream end of the headworks end walls (Elevation 134.6 feet), where horizontal stresses reached 40 ksi. Figures 194 and 195 show these values with the earthquake acceleration perpendicular to the water flow.

Besides checking the end walls for the lateral inertial-force coefficient of 0.3 above, DWR also analyzed them using coefficients of 0.1 and 0.2. Figure 196 shows a plot of the resulting peak horizontal rebar tensile stresses at Elevation 134.6 feet. Vertical rebar stresses are similar and therefore are not shown.

On the basis of this analysis, both structures are considered safe.

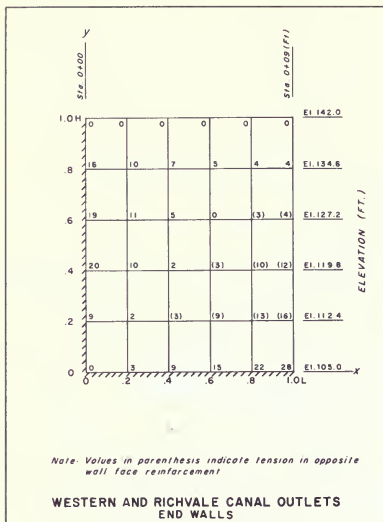


Figure 194. Vertical Tensile Stresses (in ksi) in the Reinforcing Steel, Generated by the Reanalysis Earthquake

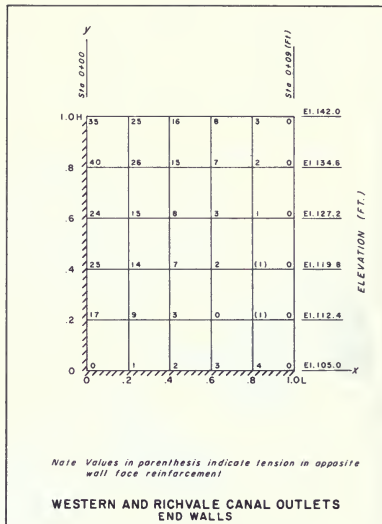


Figure 195. Horizontal Tensile Stresses (in ksi) in the Reinforcing Steel, Generated by the Reanalysis Earthquake

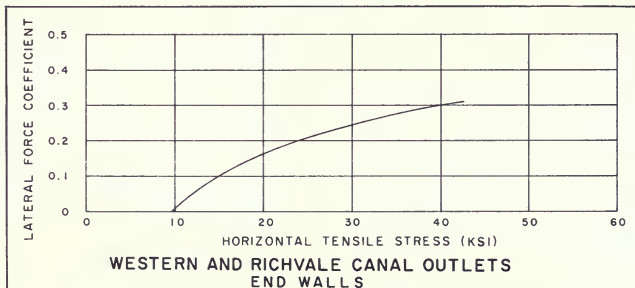


Figure 196. Peak Horizontal Tensile Stresses at Elevation 134.6 in the Reinforcing Steel Generated by Various Lateral Force Coefficients Combined with Static Loads

## PG and E Lateral

### Description and Past Performance

The PGandE Lateral (Figures 197 and 198) consists of a 30-inch-diameter conduit, a small intake training structure with provisions for bulkheading, a wetwall upstream of the dam axis containing a 30-inch-square slide gate for control and an outlet stilling box with a weir for measuring flow.

An inspection of the structure after the August 1, 1975 earthquake revealed no damage.

### Seismic Reanalysis

Collapse of the PG and E Lateral would result in minor damage, and only minor disruption to project operations. Therefore, no additional analysis was performed.

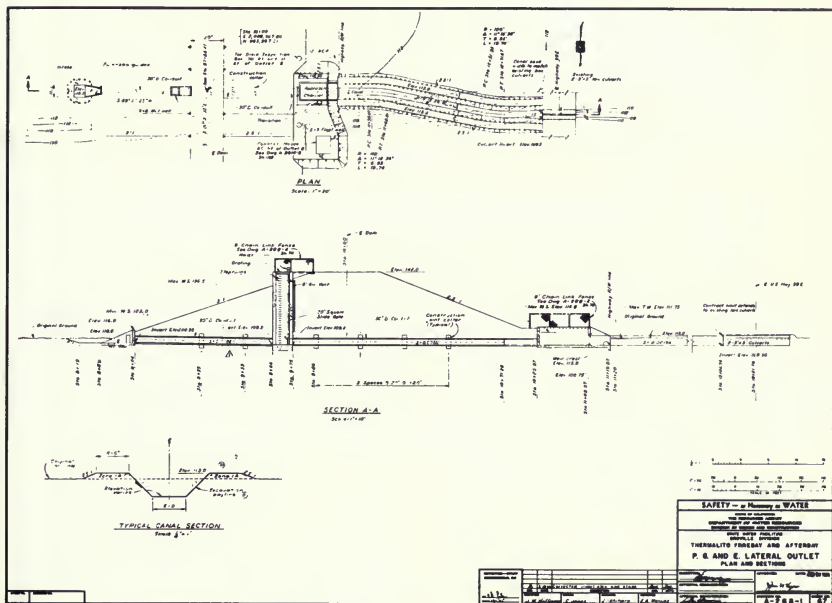


Figure 197. Pacific Gas and Electric Company Outlet



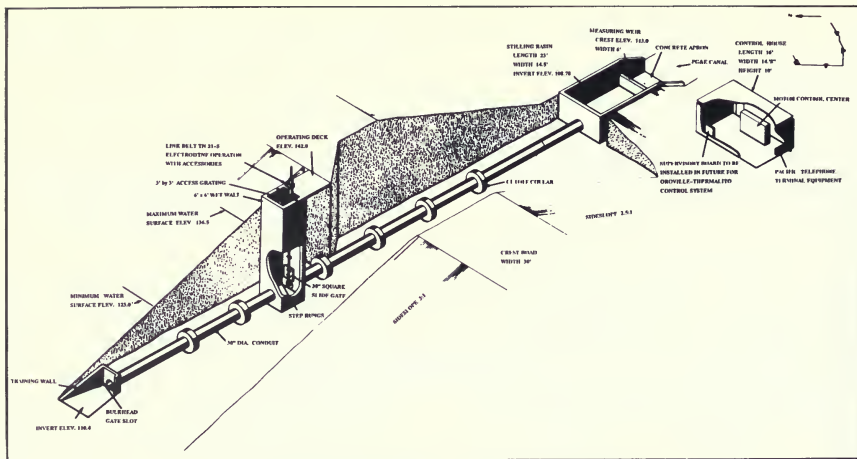


Figure 198. Pacific Gas and Electric Company Outlet, Isometric View

## Sutter Butte Outlet

### Description and Past Performance

The Sutter Butte Outlet (Figures 199 and 200) consists of four 7-foot-wide by 6-foot-high rectangular conduits founded on a concrete base slab, slide gates for control, a headwall with provisions for bulkheading, and an outlet channel approximately 1,200 feet long, connecting to the existing Sutter Butte Canal. The concrete slab overlies a 2-foot-thick drain blanket. Flow is measured by a weir located about 400 feet downstream of the conduit outlet. The gate structure is about 40 feet high. The foundation for this structure consists of compact clayey silt and fine sandy silt.

This structure was inspected after the August 1, 1975 earthquake; no damage was found.

### Failure Evaluation

A review of the consequences of total failure of this structure indicates little property damage, danger to motorists along the highway near the structure, and a possibility of some disruption in project operation.

## Seismic Reanalysis

This structure was investigated using the reanalysis lateral force coefficient of 0.3 combined with static loads. Rebar tensile stresses obtained at different locations in the structure were within the established design criteria. Figures 201 and 202 show expected vertical and horizontal tensile rebar stresses in the end walls, which are the members where higher stresses occurred with the earthquake acceleration perpendicular to the water flow.

Besides checking these walls for the lateral inertial force coefficient of 0.3, as above, DWR also analyzed them using coefficients of 0.1 and 0.2. Figure 203 shows a plot of the resulting peak vertical rebar tensile stresses at Elevation 118.45 feet. Horizontal rebar stresses are smaller and therefore are not shown. On the basis of this analysis, this structure is considered safe.

## Afterbay River Outlet

### Description and Past Performance

The River Outlet (Figures 204 and 205) is situated in the southeast corner of the afterbay (Figure 4, Chapter II). It consists of a headworks structure, 800 feet of trapezoidal



channel, with 31-foot-high training dikes, and a fish barrier weir. Before construction, the site of the headworks, channel, and weir was excavated to existing gravels, and then backfilled with well-graded gravels.

The headworks structure breaches the dam embankment. It consists of five 14-foot-square top-seal radial gates, a concrete breast wall, counterfort side walls, approach walls, and outlet walls. The radial gates are separated by 4.5-foot piers. A service bridge spans the structure over the gates, and a county bridge crosses the downstream part of the structure.

The channel outlet is an unlined trapezoidal section between the headworks and the fish barrier.

The fish barrier is a 12-foot-high concrete gravity ogee-shaped weir approximately 168 feet long. The structure includes a service bridge. The channel is paved for 130 feet downstream of the weir. Sheet pile cutoffs are placed upstream of the weir and at the downstream end of the paved channel.

An inspection of the concrete structures after the August 1, 1975 earthquake revealed no damage. The unlined channel training dikes suffered minor surface cracking but no structural failure.

### Failure Evaluation.

Complete structural failure of the headworks and fish barrier structures could cause temporary disruption in the project operations but should cause no property damage;

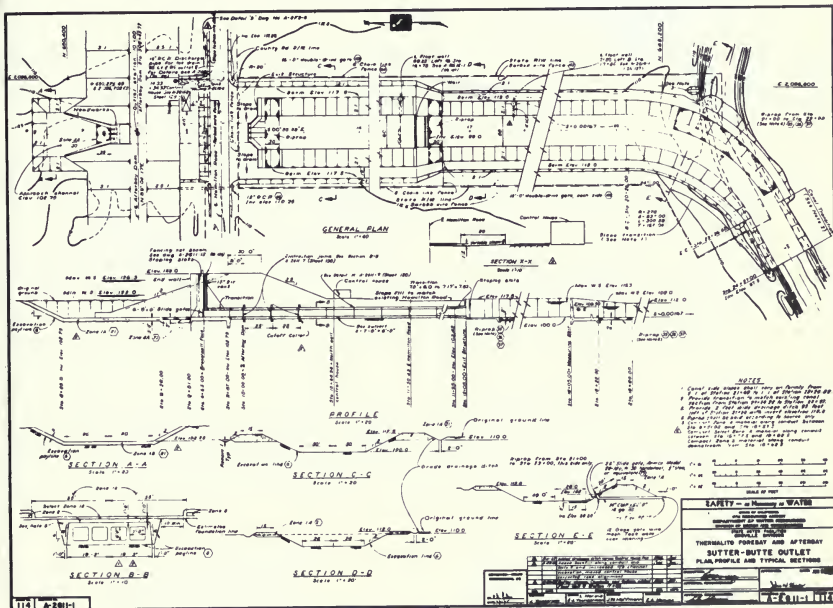
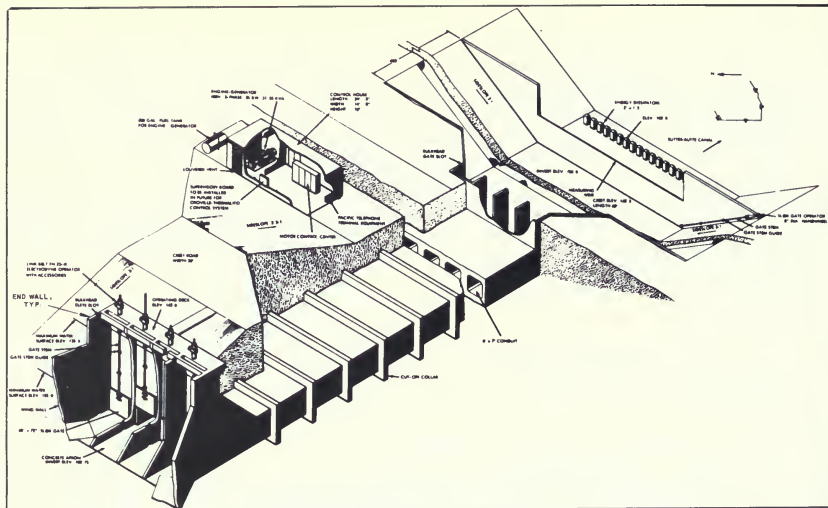
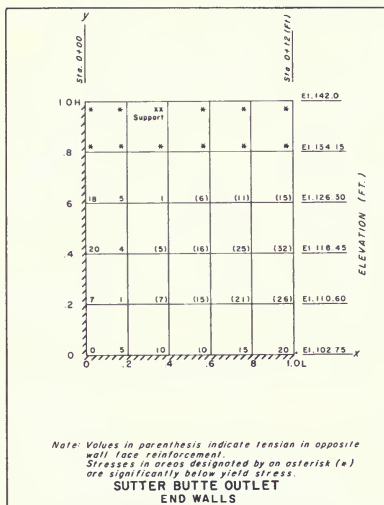


Figure 199. Sutter-Butte Outlet



**Figure 200. Sutter Butte Outlet, Isometric View**



*Figure 20I. Vertical Tensile Stresses (in ksi) in the Reinforcing Steel—Generated by the Reanalysis Earthquake*

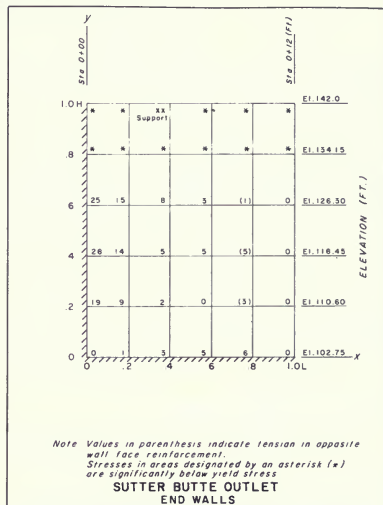


**Figure 202. Horizontal Tensile Stresses (in ksi) in the Reinforcing Steel—Generated by the Reanalysis Earthquake**

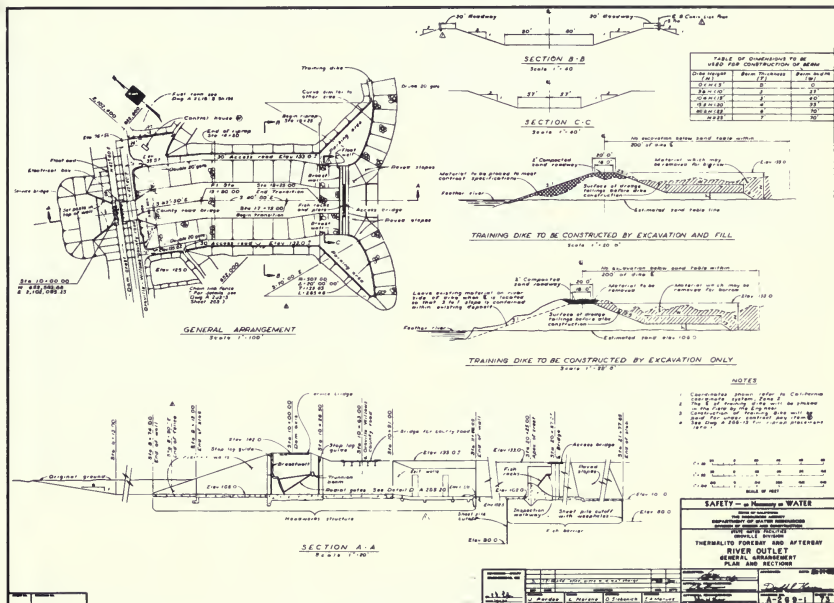
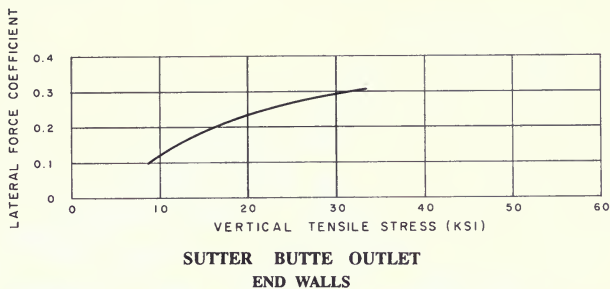


**Figure 204. River Outlet**



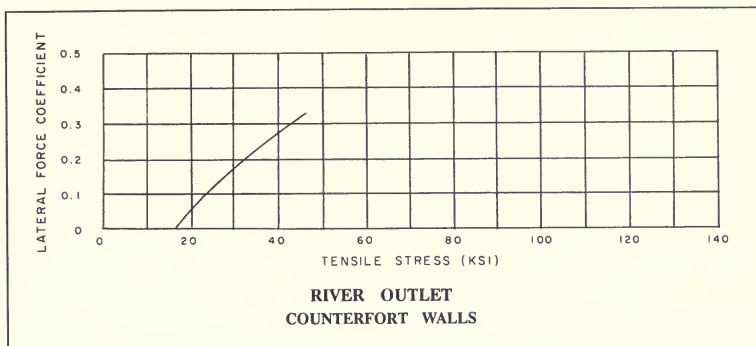


*Figure 207. Peak Reinforcing Steel Tensile Stresses at Elevation 120  
Generated by Various Lateral Force Coefficients Combined with Static Loads*

however, this type of failure could result in the release of a surge of water, endangering fishermen or others in or near the river.

Collapse of the training dikes alone would cause no property damage or disruption of project operations.

### Seismic Reanalysis

The headworks structure was investigated, applying the same criteria used in reanalysis of the other structures described in this chapter. The highest rebar tensile stresses encountered were in the counterfort walls located at either side of the radial gate complex. Figure 206 shows a cross section of these walls with rebar tensile stresses at different elevations for a lateral force coefficient of 0.3 combined with gravity loads.

The highest tensile stress found (42 ksi) was at Elevation 120 feet, where half of the vertical reinforcement is discontinued. This stress is slightly higher than the maximum

allowable tensile stress, but considering the transitory nature of the loading, it should not affect the integrity of the structure.

Figure 207 shows a plot of the highest rebar stresses resulting from earthquake and gravity loads in the counterforts at Elevation 120 feet versus various lateral force coefficients. Except for the value shown opposite the lateral coefficient of 0.3, stresses shown were extrapolated from other values obtained at a different counterfort wall elevation.

On the basis of this analysis, this structure is considered safe.

### Conclusion.

Based on the present earthquake criteria and results from the analyses performed, the four Thermalito Afterbay concrete structures are considered safe when subjected to the reanalysis earthquake.



## **CHAPTER V**

### **SEISMIC EVALUATION OF THERMALITO FOREBAY DAM**

#### **1. EXECUTIVE SUMMARY**

##### **Conclusions**

1. The cyclic and residual strengths of the foundation sands are higher than the values used in preliminary studies performed between 1976 and 1984.
2. The stability of the dam is satisfactory for the maximum earthquake shaking anticipated. Only minor cracking and minor movements are predicted for the postulated shaking.
3. From a seismic safety standpoint, it is safe to continue full use of the reservoir.

##### **Background**

On August 1, 1975, a moderate earthquake occurred near Oroville, California. This earthquake had a Richter magnitude of 5.7 and occurred along the Cleveland Hill Fault. Following the earthquake, the Department of Water Resources, along with their Special Consulting Board, decided to re-evaluate the seismic stability of all critical Oroville Project structures. This re-evaluation employed much stronger earthquake shaking than considered during design. Thermalito Forebay Dam is one of these critical structures.

Thermalito Forebay Dam was designed in the early 1960's using standard practices of the time. Earthquake effects were considered in the static slope stability analyses by utilizing a 0.1g horizontal acceleration. Shallow and deep failure surfaces in the embankment and foundations were considered for several reservoir levels. Since no drainage would occur during the earthquake, consolidated, undrained strengths were used. The minimum safety factor

was 1.1 for the downstream slope for both shallow and deep circles.

The embankment and adjacent concrete structures performed well in all the shocks of the 1975 Oroville Earthquake sequence. Inspection of the dam showed only two minor cracks near the crest of the Low Dam at Station 123+00.

Although the embankment withstood the 1975 earthquake, a new seismic evaluation was considered necessary. The 1975 Oroville Earthquake revealed active faults that were closer than those which had been considered in design. Also, since the early 1960's, new techniques had been developed for seismic evaluations. Therefore, this investigation was undertaken to determine the behavior of Thermalito Forebay Dam during a postulated future 6.5 magnitude earthquake.

##### **Concept of Investigation**

A basic assumption made for the study was that, given a competent foundation, the compacted silty, gravelly, clayey sand embankment and the dense clay to clayey sand surface layer of the foundation would perform satisfactorily during a magnitude 6.5 earthquake. This assumption was based on findings by Seed, Makdisi and DeAlba (1977) on the historical performance of dams subjected to strong earthquake motions.

The main mode of possible failure was assumed to be embankment slides through loose foundation sands or silts which had liquefied during the postulated earthquake. Therefore, the investigation centered on locating any loose sand and silt layers in the foundation, assessing their



liquefaction potential, and evaluating the effects of foundation liquefaction on the stability of the embankment.

Liquefaction potential of sand layers was estimated by comparing cyclic strength with earthquake-induced cyclic stress. Values of cyclic loading resistance were determined by using recent correlations between Standard Penetration Test (SPT) resistance and field behavior of soils during earthquakes. The results of cyclic triaxial tests were used to modify the correlated SPT strengths for different consolidation stress conditions. Earthquake-induced cyclic stresses were determined by dynamic response analyses using adopted earthquake motions.

To evaluate embankment stability following the earthquake, post-earthquake slope stability analyses were performed. These analyses employed reduced and/or residual shear strengths for the different soil materials in order to account for the effects of shaking.

In addition, a limited number of simplified analyses were performed to evaluate the performance of the two concrete wingwall dams connected to the power plant headworks structure. These analyses consisted of calculating sliding stability for pseudodynamic loading. Furthermore, simplified dynamic stress analyses were performed in order to determine the potential for excessive tensile stresses and cracking to develop within the concrete dams.

## **Chronological Summary of the Investigation**

### **1976**

The initial investigation was performed in 1976 and consisted of five borings along the 3 mile length of the dam. Within these borings, a few scattered SPT tests, were performed and a few samples were obtained using the DWR thick-walled sampler. A limited number of cyclic triaxial tests were conducted on specimens prepared from these samples.

### **1978**

The next phase of the investigation was conducted in 1978 and was targeted at identified foundation sand layers at the Main Dam and at Station 82 of the Low Dam. Several

borings were drilled along the toe of the dam to measure shear wave velocities, determine SPT resistance, and obtain undisturbed samples of the sandy soil. Special attention was given to sample handling and cyclic triaxial testing of these sand samples. Borings were also drilled through the dam crest in order to determine the extent of the sand layers beneath the dam.

Earthquake-induced cyclic stresses were predicted using one-dimensional dynamic response analyses. As recommended by the consulting board, the earthquake loading consisted of an acceleration time history formally titled the Oroville Reanalysis Earthquake ( $a_{\max} = 0.6g$ ). To model the stiffness of the foundation, the moduli determined from shear wave velocity tests were used in the upper 50 feet of the foundation profile and assumed values were used for greater depths.

The results of the evaluation indicated the possibility of liquefaction at the Main Dam. However, further consideration of probable fault capabilities led to the judgment that the Oroville Reanalysis Earthquake was inappropriate for the analysis. It was also decided that more information on the foundation was required before a final determination of appropriate earthquake ground motions could be made, and that a more thorough investigation along the full length of the dam was necessary to determine all locations with loose foundation sands.

### **1979–1980**

This phase of the investigation was conducted primarily to better define foundation conditions. A 500-foot-deep boring at the Main Dam was drilled to determine the type of foundation soils and depth to rock. Shear wave velocity tests were performed in this boring to define shear moduli to a 300-foot depth. Several borings with SPT tests were drilled to define the extent of low blowcount sands between the toe of the Main Dam and the tail channel. SPT borings were also spaced 1,000 feet apart along the full length of the Low Dam to locate any other sites with low blowcounts. Several hand carved samples were obtained at the Main Dam (Tail Channel Cut Slope) to determine the cyclic triaxial strength in the laboratory.

Evaluation of cyclic stresses utilized three earthquake motions: Modified Federal Building (Eureka, 1954), Modified Hollywood Storage Building (San Fernando,



1971), and Modified McCabe School (Imperial Valley, 1979). Each was scaled to a maximum acceleration of 0.4g. This peak acceleration value was lower than the 0.6g value used in previous analyses in order to account for the fact that Thermalito Forebay Dam is further from the Cleveland Hill Fault than is Oroville Dam.

The conclusion at the end of this phase was that the seismic stability of the dam would be satisfactory. However, the Consulting Board recommended that the relationship between SPT blowcount and cyclic loading resistance be better defined, and that the extent of loose foundation sand layers along the dam be determined.

### 1981–1984

SPT borings were drilled along the toe of the Main Dam at 100-foot spacings to define the areal extent of the low blowcount sands. Additional SPT borings were drilled through the crest of the Main Dam between Stations 9 and 12. Bag samples were obtained for every SPT test to determine the soil classifications. SPT borings were also used to identify areas to obtain undisturbed piston samples of soil representing specific SPT blowcounts.

Along the toe of the Low Dam, SPT borings were spaced at 250-foot intervals to locate and define the extent of loose foundation sands. Piston samples were obtained for cyclic strength testing in the laboratory. Classification tests were run on both SPT and piston samples.

Two critical sites, Station 10–11 (Main Dam) and Station 112 (Low Dam) areas, were explored in detail. These two sites were considered to have the worst conditions (lowest SPT blowcounts) along the Forebay Dam. In addition to the previously mentioned explorations, undisturbed samples of the clayey embankment and surface cap soils were obtained at these two sites and used for static and cyclic triaxial tests.

During this period, it was realized that many of the clayey sands encountered during the explorations were actually composed of weathered soil grains that easily break apart with remolding. In some cases, this meant that a soil that, perhaps existing and/or behaving in situ as a silty soil, could be classified in the field or in the laboratory as a clayey sand. For most situations, clayey soils are regarded as non-liquefiable. As a consequence of this realization,

it was decided to be conservative and simply assume that the clayey sands behave like silty sands and, therefore, are also suspect. Both of the critical sites at Stations 10–11 and Station 112 have low-blowcount clayey sand/silty sand layers.

Also, during this period of the investigation, a change was again made in the choice of accelerogram to be used in the dynamic response analyses. This change resulted from a re-evaluation of the Prairie Creek Lineament. Although this structure ends about 8 miles south of Oroville, a northern extension would pass within 2–3 miles of the Forebay Dam. Re-examination of this structure resulted in the assumption that this lineament extension poses the same earthquake threat to the Forebay Dam as does the Cleveland Hill Fault to Oroville Dam. Consequently, it was decided to use the Oroville Reanalysis Earthquake ( $a_{\max} = 0.6g$ ) in analyzing the Forebay Dam.

For the two critical sites, Stations 10–11 and Station 112, the following detailed studies were performed:

- a. Static stress analysis using the finite element method.
- b. One-dimensional dynamic response analyses using the Oroville Reanalysis Earthquake ( $a_{\max} = 0.6g$ ) to predict earthquake-induced cyclic stresses.
- c. Calculation of factors of safety against liquefaction and the levels of excess pore water pressures generated.
- d. Post-earthquake slope stability analyses using reduced soil strengths for non-liquefied soils and zero strengths for liquefied zones.
- e. Examination of the possibility of movements on transverse faults in the Main Dam right abutment basalt.
- f. Examination of the possible effects of the variability of the basalt rock beneath the alluvial foundation of the Main Dam.

The results of these calculations and a conclusion of adequate safety were presented in a draft report in October 1984 to both the Division of Safety of Dams and the consulting board.

After reviewing the 1984 draft report, the Division of Safety of Dams decided that the information contained in the report did not indicate that the dam would be stable in the event of a maximum credible earthquake on the Prairie Creek Lineament. At the same time, the consulting board stated that the use of the Oroville Reanalysis Earthquake scaled to 0.6g was overly conservative for use in analyzing Thermalito Forebay Dam. To resolve the concerns of these two groups, the following additional work was conducted:

- a. Performed additional finite element and one-dimensional dynamic response analyses for the two critical sites. These analyses employed both the Oroville Reanalysis Earthquake ( $a_{\max} = 0.6g$ ) and a modified El Centro record ( $a_{\max} = 0.55g$ ) as earthquake loadings. For each element of suspect sand, the higher of the two earthquake-induced stresses was used for computations of factors of safety against the development of liquefaction.
- b. The cyclic loading resistance of the suspect sands were defined using correlations between field performance and SPT resistance. The correlated strengths were extended to different consolidation stress conditions using results of cyclic triaxial tests performed for Thermalito Afterbay Dam.
- c. Factors of safety against liquefaction and estimates of generated excess pore water pressures were calculated for the suspect sand layers at the two critical sites by comparing earthquake-induced cyclic stresses to cyclic loading resistance.
- d. Post-earthquake slope stability analyses were performed using reduced soil strengths in non-liquefied soils and residual strengths in liquefied soils.
- e. A limited number of pseudodynamic sliding analyses were performed for the two concrete wingwall dams connected to the powerplant headworks structure. In addition, simplified dynamic stress calculations were performed in an effort to determine areas of potential excessive tensile stress and possible cracking.

### Summary of Findings

1. Fourteen sites were found along the Forebay Dam with foundation soils having corrected SPT blow-counts of less than 30.
2. Low blowcount soils generally consist of silty and/or clayey sands. Soil gradations, plasticity, and blow-counts vary greatly within a short distance, both horizontally and vertically.
3. The Earthquake-induced cyclic stresses calculated in the dynamic response analyses for the two critical sites using the Oroville Reanalysis Earthquake ( $a_{\max} = 0.6g$ ) are generally comparable (within 15 percent) with those calculated using the Modified El Centro record ( $a_{\max} = 0.55g$ ). Using the higher of the stresses from the two different earthquake loadings together with SPT cyclic strengths results in a prediction of liquefaction within the suspect layers beyond the upstream and downstream toes and in a central zone beneath the dam crest for the Main Dam dam model. For the Low Dam model there was a much greater amount of liquefaction predicted in the foundation beneath the upstream slope.
4. Employing zero strength for liquefied zones and considering the pore pressures induced in the non-liquefied zones, the post-earthquake slope stability safety factor for the Main Dam (Station 10–11) model is 1.8. The factor of safety for the same conditions at the Low Dam (Station 112) model is 1.2. Recent studies have shown that liquefied soils maintain residual shear strengths. Using recent correlations between SPT resistance and residual shear strength, post-earthquake slope stability analyses show that the minimum factor of safety against sliding at the Low Dam would increase to 1.6.
5. The faults in basalt foundation rock at the right end of the dam are considered inactive and do not present a hazard to the dam.
6. The shape of the basalt surface where it dips under the alluvium at the right end of the dam is no steeper than 1:1 and will not cause differential settlement cracking in overlying alluvium and embankment.
7. Pseudodynamic sliding analyses of the two concrete wingwall dams revealed factors of safety above unity

for horizontal seismic coefficients in excess of 60 percent of gravity. Predicted earthquake-induced tensile stresses in these two dams were less than 11 percent of the compressive strength of the concrete. Accordingly, since the dynamic tensile strength of concrete is often accepted as being equal to 15 percent of its compressive strength (see Reference 80), no sig-

nificant earthquake-induced cracking would be indicated.

8. The maximum permanent earthquake induced deformation in Thermalito Forebay Dam is predicted to be at the Station 112 (Low Dam) site. This deformation is expected to be less than 1 foot in any direction. No transverse cracking is predicted.

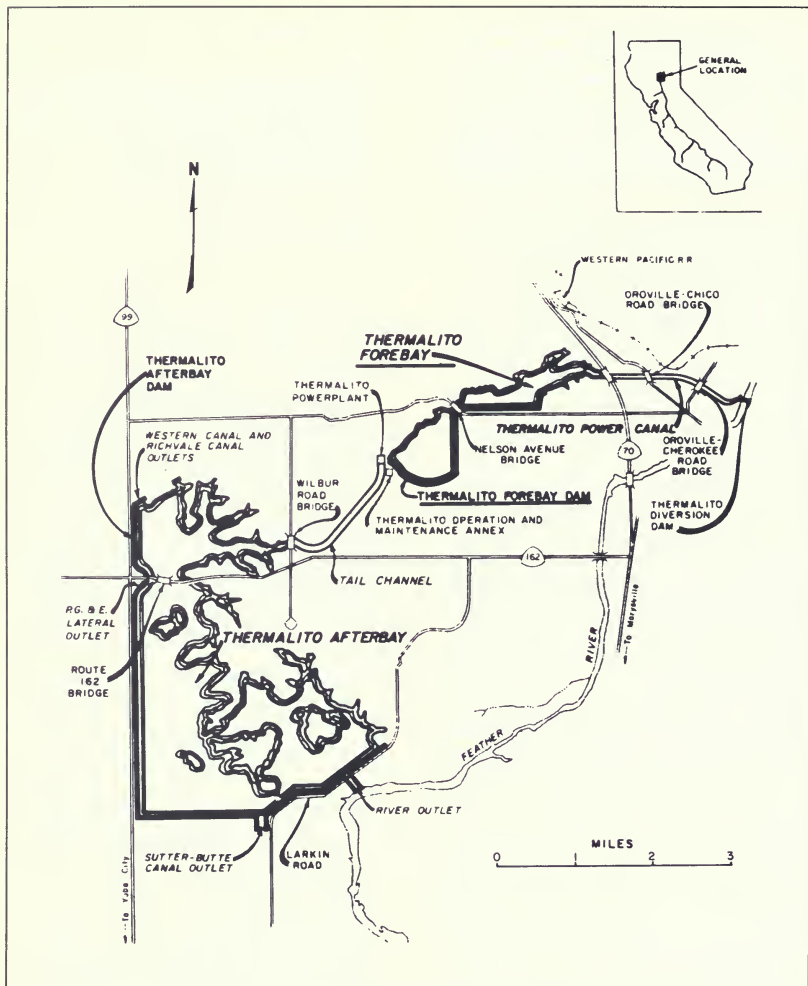


Figure 208. Thermalito Forebay Dam, General Location Map

## 2. DESIGN, CONSTRUCTION, AND PERFORMANCE OF THERMALITO FOREBAY DAM

### General Description of Dam and Reservoir

Thermalito Forebay is a relatively shallow 11,400 acre-foot offstream reservoir encompassed on the south and east by Thermalito Forebay Dam and by the Campbell Hills on the north and west. It is located in Sections 1, 2, 3, 10 and 11 T.N. 19N, R3E, Mount Diablo B&M, Butte County, approximately 3 miles west of the city of Oroville (Figure 208).

Thermalito Forebay Dam and reservoir is an integral part of the Oroville Division power complex, with Thermalito Powerplant located on its southwestern end and Thermalito Power Canal connected to its northeastern end. The 11,400 acre-feet of gross storage are divided into two major areas connected by a 400-foot channel (Channel H) which is bridged by Nelson Avenue (Figure 209). Channel H at Nelson Avenue and its extensions in both directions were excavated to provide hydraulic circulation through the reservoir and to furnish embankment materials.

The dam is principally an earth embankment structure approximately 15,900 feet long, with a maximum height of 71 feet and an average height of 25 feet. The crest of the dam is at Elevation 231.0, and the maximum normal water surface is Elevation 225.0.

A groundwater relief system is located at the downstream toe of the dam just south of Nelson Avenue between Stations 80 and 88. The system consists of relief wells, collector pipe, sump, pump and discharge line. The purpose of this system is to reduce high ground water levels that had developed in this area.

In the vicinity of the Thermalito Powerplant, the embankment dam is connected to the plant headworks structure by a concrete wingwall dam. The eastern portion of the wingwall dam is partially embedded within the embankment dam. Only in this vicinity was a zoned embankment placed. Another concrete wingwall dam—the Approach Channel Dam—is situated on the other side of the power plant headworks structure (See Figure 210).

### Site Geology

The surface geology of the Thermalito Forebay area consists of alluvium, Red Bluff sediments, basalt rubble, and layers of basalt and interflow strata.

Alluvium ( $Q_{al}$ ) is found along the drainages traversing the area and in the eastern portion of the Forebay. Along Grubb Creek at the site of the Main Dam and along Ruddy Creek at the east end of the reservoir, there was approximately 5 feet of alluvium. The alluvium in this area consists of loose gravelly silt with lenses of gravel. Minor gravel deposits also occur in the channels of numerous smaller drainages traversing the reservoir area.

The Red Bluff formation ( $Q_{rb}$ ) is exposed over most of the reservoir area with the exception of the northern and northeastern portions of the Forebay. This formation is a Plio-Pleistocene age flood plain deposit containing crudely stratified silty and clayey sands, silts, and clays with scattered lenses of clayey or silty gravel.

A series of southwesterly dipping basalt flows ( $T_v$ ) is exposed along the northern border of the reservoir area. These Tertiary-age basalt strata are collectively referred to as the Lovejoy formation. Based on Thermalito Powerplant drilling, three members of this series of hard, dense, slightly weathered, and strongly fractured basalts were delineated: Upper Basalt Flow ( $T_{vu}$ ), Middle Basalt Flow ( $T_{vm}$ ), and Lower Basalt Flow ( $T_{vl}$ ). Between the Middle ( $T_{vm}$ ) and Lower ( $T_{vl}$ ) Basalt Flows is the Lower Interflow Material ( $T_{ifl}$ ), a sedimentary deposit characterized by fine-grained volcanic sediments and basalt fragments. Outcrops of Interflow Materials ( $T_{ifl}$ ) and Upper Basalt ( $T_{vu}$ ) were not observed within the reservoir area but crop out in the Forebay power plant area. The basalt series is overlapped by the Red Bluff formation and is underlain by older consolidated sediments identified as the Ione formation. Overlying portions of the Lower Basalt ( $T_{vl}$ ), Middle Basalt ( $T_{vm}$ ), and Lower Interflow Material ( $T_{ifl}$ ) and overlapping into the Red

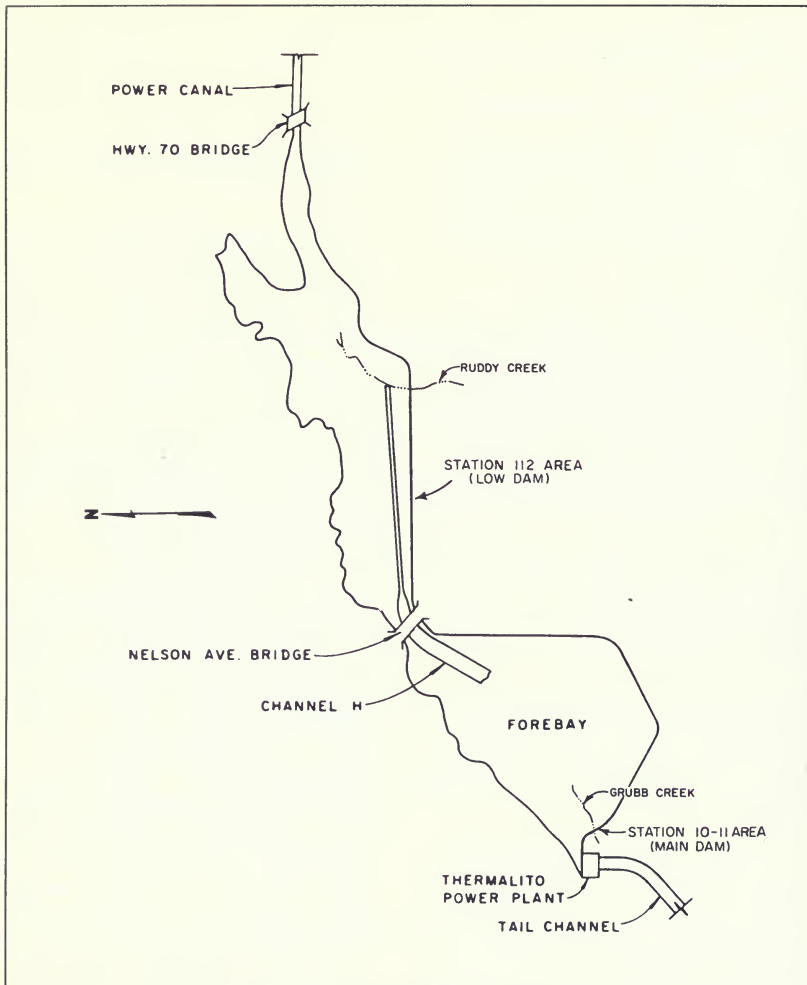


Figure 209. Thermalito Forebay Dam, Plan View

Bluff formation ( $Q_{rb}$ ) is a unit of Basalt Rubble ( $T_r$ ). The Basalt Rubble unit consists of loosely to moderately consolidated fragments of basalt in a clay matrix that resulted from talus-type deposition adjacent to steep slopes. The Basalt Rubble is contemporaneous with and interfingers with the Red Bluff stream deposits.

A steeply dipping fault zone striking NE-SW was exposed in the power plant excavation. This zone projects across the right abutment of the Main Dam. The fault zone consists of multiple faults with a net normal displacement. The southeast block is 40 to 60 feet lower than the northwest block. The shear zone does not displace the overlying Basalt Rubble ( $T_r$ ) or the Red Bluff formation ( $Q_{rb}$ ).

The geology in the vicinity of the Main Dam is presented in Figures 211 and 212, and the geologic units are summarized in Table 43.

## Geologic Investigations During Design

Geologic exploration for design of Thermalito Forebay began in April 1953 and extended to May 1965. Additional explorations were undertaken as construction and operation problems developed. Some of the explorations were initiated for other features of the Oroville-Thermalito Complex, but were used for the Forebay due to overlapping areas.

The initial design exploration in April 1953 consisted of three bucket auger holes for Oroville Dam embankment material within the Forebay area.

From January 1957 to August 1957, four flight auger and eleven bucket auger holes were drilled for preliminary materials exploration in the vicinity of the Forebay.

One rotary hole was drilled in August 1959 for preliminary foundation exploration at Ruddy Creek.

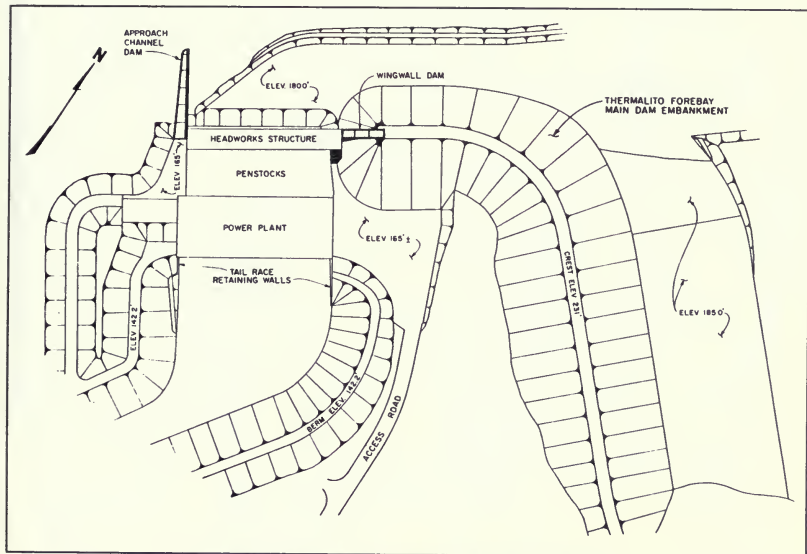
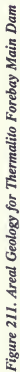
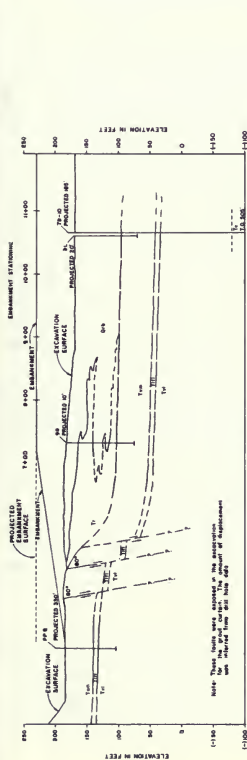


Figure 210. General Plan of Thermalito Forebay—Main Dam Area

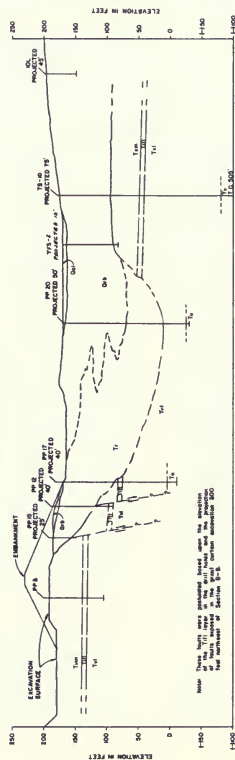




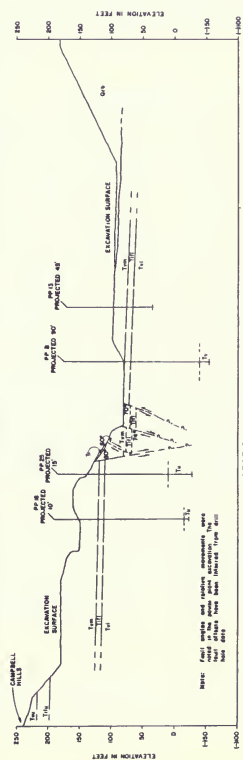




SECTION A-A



SECTION B-B



SECTION C-C

# EXPLANATION GEOLOGIC UNITS

Qa ALLUVIUM

Qb RED BLUFF FORMATION

Tr BASALT RUBBLE

Tua UPPER BASALT FLOW

Tui UPPER INTERFLOW

Tm MIDDLE BASALT FLOW

Tli LOWER INTERFLOW

Tl LOWER BASALT FLOW

T Undifferentiated Basalt Flow

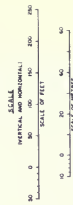
Correct

Fault showing up at surface and relative displacement

Inferred contact or fault

Insignificant data for interpretation

Anticline line and number



NOTE: For location of sections see Page 4

Figure 212. Geologic Sections along Thermalito Forebay Main Dam

**Table 43. Summary of Geologic Units Exposed Along Thermalito Forebay Dam**

Symbol	Unit	Description
<i>Qat</i>	Recent Alluvium	Unconsolidated mixtures of clays, silts, sands, and gravels.
<i>Qrb</i>	Red Bluff Formation	Loose to moderately consolidated mixtures of clays, silts, sands, and gravels.
<i>T<sub>r</sub></i>	Basalt Rubble	Loose to moderately consolidated basalt fragments in a clayey matrix. Locally includes blocks of basalt and interflow materials in the major zone.
<i>T<sub>vu</sub></i>	Upper Basalt Flow	Medium gray. Very fine-grained. Hard. Dense. Moderately to strongly fractured. Generally slightly to moderately weathered.
<i>T<sub>ifu</sub></i>	Upper Interflow	Tuffaceous silt and clay, overlying basalt breccia with a matrix of tuffaceous materials or soft tan amorphous mineral.
<i>T<sub>vm</sub></i>	Middle Basalt Flow	Medium gray. Very fine-grained. Hard. Dense. Moderately to strongly fractured. Generally slightly to moderately weathered.
<i>T<sub>ift</sub></i>	Lower Interflow	Basalt rubble cemented with tuffaceous sand or soft, tan amorphous mineral. Some lenses of dense tuffaceous sand, silt, and clay.
<i>T<sub>vl</sub></i>	Lower Basalt Flow	Medium light-gray. Fine-grained. Hard. Dense. Moderately to strongly fractured. Generally fresh.

From February 1963 to April 1964, six rotary holes were drilled for exploration of the Main Dam foundation. Thirteen bucket auger and twelve spin auger holes were also drilled for materials and foundation exploration for the Low Dam and five rotary holes were drilled for foundation exploration for Nelson Avenue Bridge. As an added safety factor, an extra borrow area was investigated in May 1964 by drilling five more bucket auger holes in an area near the power plant.

Two more rotary holes were drilled in the Ruddy Creek Dam foundation in April 1965 for more extensive foundation exploration and three rotary holes were drilled in May 1965, in an area above the Thermalito Diversion Dam, to provide a backup source for riprap.

The soil surface permeability in the Forebay was tested by surface infiltrometers in November and December 1957, and again in September through December 1958. A

foundation permeability test was taken in one hole in December 1958 and again in nine holes in April and May of 1964.

The groundwater surface configuration was measured in several wells every spring and fall from December 1957 to October 1959.

#### Geologic Investigation During Construction

During construction, ten more auger holes were drilled in Channel H in an attempt to locate coarse impervious "Select Zone 2F" transition material for the protection of the Zone 3 blanket drain.

In May 1967, four auger holes were drilled just upstream of the dam between Station 63+00 and 80+25 to check the thickness of the impervious cap. The holes were drilled where sand had been found in the exploration trench. Five auger holes were drilled in the Main Dam

foundation area at the same time for additional preconstruction exploration.

Nine test pits were excavated in the floor of Channel H to conduct crude field permeability tests and to obtain gradations for determining the extent of impervious blanketing required.

Eleven piezometers were installed downstream of the dam during construction.

### General Description of the Design and Construction of the Embankment

The Thermalito Forebay Dam is principally an earth embankment structure with a maximum height of 71 feet and an average height of about 25 feet. The 30-foot wide crest is at Elevation 231.0 and provides a 6-foot minimum freeboard. Figure 213 contains cross sections of the embankment dam along with design parameters.

The embankment is divided into three segments: the Main Dam, which begins at the gravity wingwall of Thermalito Powerplant and continues across Grubb Creek, the Ruddy Creek Dam across Ruddy Creek, and the Low Dam connecting these embankments and completing the enclosure.

The alignment of the dam was generally selected to minimize embankment height by locating on the highest natural topography. There are three notable exceptions. The desire to minimize the Nelson Avenue relocation costs controlled the alignment in that area. At the left abutment of both the Ruddy Creek Dam and Main Dam, the embankment was located upstream of natural high ground. This was done to blanket a possible pervious lense in the Ruddy Creek foundation and to keep the Main Dam away from the Tail Channel excavation to reduce the seepage potential and improve the stability of the Main Dam.

The descriptions of the segments are:

**Main Dam.** The Main Dam is 1,330 feet long and runs between Stations 2+08 and 15+37. It has a downstream slope of 2.5:1, upstream slopes varying from 1.75:1 to 3:1,

and consists of four zones. Zone 1F, the major portion of the embankment, is an impervious zone of compacted gravelly, silty and clayey sands. Zone 3 consists of pervious sandy, coarse, dredge tailings used in a 12-foot-wide transition zone within both upstream and downstream slopes and in an 18-inch-thick horizontal drain blanket in the downstream section. Zone 4F is a compacted gravel zone that is used on both slopes as slope protection. Between Stations 2+08 and 5+50 along the power plant approach channel, the upstream slope varies between 1.75:1 to 3:1. To provide upstream stability the 4F material was placed in variable width within the upstream slope (see Figures 213 and 214). Between Stations 5+50 and 15+37, the upstream slope continues at a 3:1 slope. An 8-foot wide zone of riprap above Elevation 218.0 protects against wave action.

**Ruddy Creek Dam.** The Ruddy Creek Dam is 1,730 feet long and runs between Stations 131+70 and 149+00. It has a maximum height of 45 feet, and has 2.5:1 slopes both upstream and downstream. The embankment consists of five zones, with Zones 3, 4F, and riprap being the same as the Main Dam. Zone 2F, the major portion of the embankment, is an impervious zone of compacted materials varying from sandy silts and clays to silty and clayey sands. A 1-foot-thick blanket of specially selected Zone 2F, is a transition zone surrounding the Zone 3 in the horizontal drain.

**Low Dam.** The Low Dam is 12,800 feet long and runs between Stations 38+50 and 131+70 and between Station 149+00 and the end of the line. It has a maximum height of 35 feet and 2.5:1 slopes both upstream and downstream. Its cross section is the same as Ruddy Creek Dam, with the exception that the Zone 4F material below the riprap and the Zone 3 material on the downstream slope are deleted. The Zone 3 blanket drain and Select Zone 2F are included where the dam is more than 17 feet high. Within the recreation area, exterior zones are eliminated wherever the recreation fill encompasses the dam embankment.

For most of the embankment, the designers intended to construct a basically homogeneous dam with locally available materials. Preliminary designs including zoned



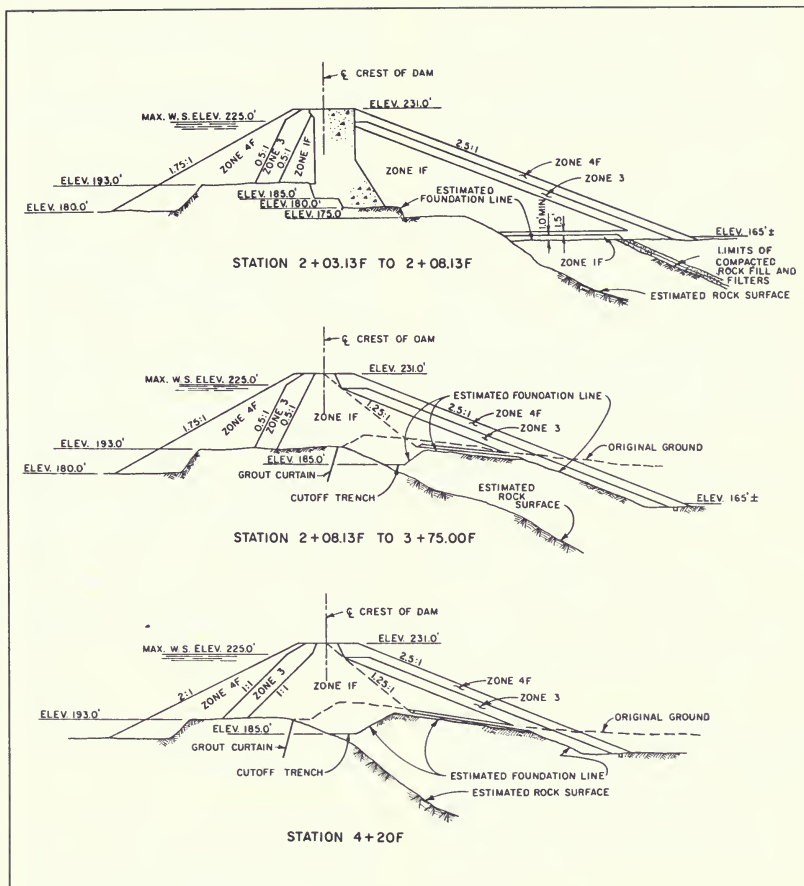


Figure 214. Sections of Thermalito Forebay Zoned Main Dam Between Stations 2+03 and 4+20

embankments with more dredge tailings and basalt were deemed too complicated for the height of the dam, and so the slopes were flattened and more common material was used. Zoned embankments and semi-zoned embankments were included where special conditions made them necessary. The upstream half of the Main Dam near the power plant (Stations 2 + 08 to 5 + 50) is a zoned embankment to minimize the encroachment into the approach channel. The sound basalt foundation in this area permitted use of a 1.75:1 slope, making the rather complicated construction worthwhile here and at the downstream shell contact with the power plant.

In the original design, the embankments were not provided with internal drains. However, the Division of Safety of Dams disagreed with both the designers and the Oroville Dam Consulting Board, who had reviewed the designs, and required blanket drains to be added. Safety of Dams required the changes because it did not approve homogeneous sections for modern dams and believed that the cohesion strength intercept found in the laboratory testing might not be present in all of the soil to be placed in the long embankment.

The dredge tailing deposit selected for the Thermalito Forebay and Afterbay Contract was unusually clean so pit run Zone 3, with selected relatively coarse impervious borrow for the subzone transition around it was used for the drain. Zone 1F in the Main Dam was found to be coarse enough in stockpile to not need the select subzone.

Asbestos cement drainage pipes are installed in trenches below the toe of the dams. In the Main Dam, the pipe is 12 inches in diameter and extends between Stations 2 + 03 and 15 + 37. In the Low Dam and Ruddy Creek Dam, the pipe is 8 inches in diameter and extends between Stations 54 + 00 and 155 + 00. Outlets are provided to natural or man-made water courses. The function of the toe drain in the Low and Ruddy Creek Dams is to channel unsightly seepage into natural water courses. The embankment-foundation contact was assumed to be the likely source of seepage. In the Main Dam, the drain was placed to assure that the phreatic surface between the dam and the tailrace channel will be maintained at or below the level assumed for design of the dam.

There is a 24-foot-wide road on the crest of the dam for maintenance purposes. The road surfacing material is a 4-inch layer of Class 2 aggregate base.

Access to the dam crest is at the end of the Low Dam near the power canal, Nelson Avenue, and Access Road "C" between the power plant and the recreation area.

### Foundation Conditions

The major portion of the Forebay embankment is founded on the Red Bluff formation ( $Q_{rb}$ ). This formation is lenticular in the Forebay area, and its composition ranges from silts and clays to gravelly, silty and clayey sands, with some clean sands and gravels.

The only portion of the dam not founded on the Red Bluff formation is a short reach along the approach channel, adjacent to the power plant. The upstream portion of the embankment in this area is founded on fresh in situ basalt; the downstream toe foundation is Basalt Rubble. At the point where the dam starts to curve out across Grubb Creek, the center part of the foundation is founded on the Basalt Rubble with the upstream and downstream portions on Red Bluff sediments. Beyond Station 9 + 20, the entire embankment is founded on Red Bluff formation.

The contact between the Red Bluff and basalt is a lens of basalt rubble. It coincides with the centerline of the dam as it parallels the approach channel, but is exposed to the water in the approach channel as the dam turns out across Grubb Creek.

The shear zone found in the power plant excavation projects into the right abutment of the Main Dam and may correlate with shears exposed in the dam foundation between Stations 5 + 00 and 7 + 00.

Undisturbed samples of the Red Bluff formation were obtained and tested for shear strength. In the power plant excavation the Red Bluff sediments were too coarse to sample. Samples from the lenses of hardpan were also not tested for shear strength because prior tests on similar material from Thermalito Afterbay had shown very high strengths. For these reasons, the shear strengths derived from the testing program and assigned to the foundation for the stability analyses were believed to be conservative.



The permeability testing of the Forebay area and observations of the power plant excavation showed that the Red Bluff formation is generally impervious, but that pervious lenses are present. The field permeability testing seemed to indicate that most of the pervious lenses were discontinuous. Nothing was identified in the explorations to indicate that there was any general change in permeability with depth. That is, the pervious lenses could occur at any depth. Unlike the Afterbay, the pre-project groundwater levels were generally 100 feet or more below the ground surface.

### Foundation Treatment

Foundation treatment for the basalt included having the entire core contact slush grouted. In addition, a three-stage single line grout curtain with a maximum depth of 100 feet was constructed. This curtain extends beneath the embankment dam from the easterly end of the concrete wingwall dam at Station 2+25 to Station 8+11 where the Red Bluff soils overlie the basalt. A primary objective of this extension was to grout the Basalt Rubble lens at the contact. The lens or wedge of Basalt Rubble overlies the Middle Basalt flow and interfingers with the Red Bluff sediments. The Basalt Rubble and the Middle and Lower Basalt flows were generally tight. Most of the grout was injected into the Lower Interflow Layer between the two basalt flows.

Where the Basalt Rubble was exposed in downstream portions of the dam foundation between Station 2+00 and 6+00, a 2-foot thick impervious layer was placed over the rubble.

For embankments founded on Red Bluff foundation, all topsoil and recent alluvium was stripped. This averaged 7 feet for the Main Dam and Ruddy Creek Dams and 6 inches for the Low Dam.

A 30-foot-deep cutoff trench is located near the upstream toe under the Main Dam (Station 6+00 to 14+00) which extends across Grubb Creek to seal horizontal sand lenses. The trench overlaps and is, in effect, an extension of the grout curtain in the Basalt foundation. During construction, the trench was deepened and extended to the east as far as it was safe to do so to cut off a clean sand lens exposed in the bottom of the trench. The

depth of the excavation and the steep side slopes determined the actual extent of the trench. This limit was accepted after examining the tail channel slope and reviewing the other seepage control features in the area. It was determined that the extended cutoff trench would increase the seepage path adequately to make the seepage exit into the tail channel without affecting the stability of the dam.

Relatively impervious random and wet waste material from the power plant excavation was used to blanket the entire reservoir floor to Elevation 185 upstream of the Main Dam. Although there was no specific design need for the blanket, it was considered a good use for the available material.

The trench under the Low and Ruddy Creek Dams labeled "cutoff trench" was primarily an exploration trench. It was deepened locally up to 10 feet to cut off sand lenses exposed in the excavation and it was used to identify the need for impervious blanketing in the reservoir area.

Foundation settlements were predicted to be negligible for the Low and Ruddy Creek Dams, and only 6 inches of camber is provided for the Main Dam for both embankment and foundation settlement.

### Construction Materials

The Thermalito Forebay Dam consists of six different zones of materials: Zones 1F, 2F, 3, 4F, 2F select, and riprap. In the early design stages, it became evident that there was an abundance of excavated material from the adjoining Thermalito features which could be used as embankment material. Much of the exploration for the power plant, tailrace and power canal served as materials exploration for Zones 1F and 2F. Mechanical analysis, Atterberg Limits, and specific gravity tests were run on most samples from the Red Bluff Formation which fell within the limits of anticipated borrow sources. These tests revealed gravelly, silty and clayey sands to sandy silts and clays.

**Zone 1F.** Zone 1F material came primarily from the Thermalito Powerplant excavation. Red Bluff material excavated above the water table was stockpiled by the power plant contractor for use by the dam contractor. This

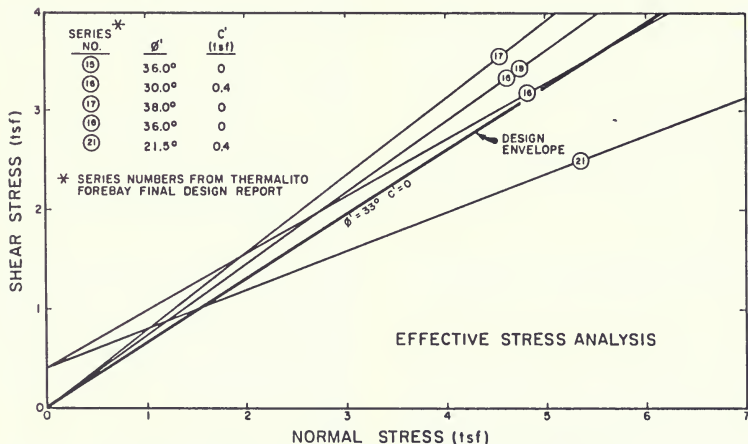
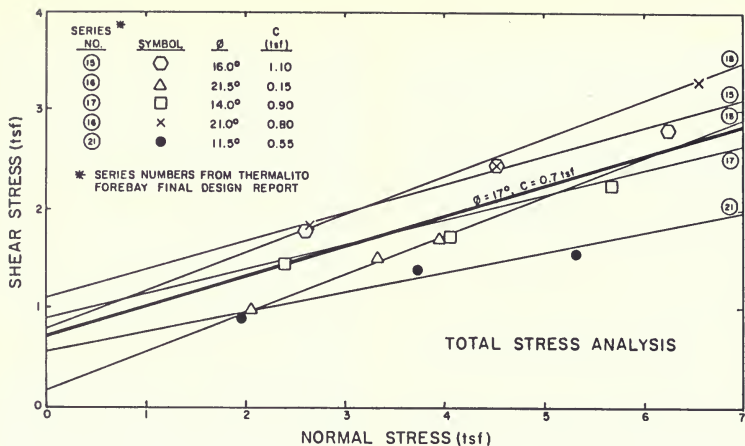


Figure 215. Summary of Total and Effective Design Shear Strengths Determined from CUE Triaxial Compression Tests of Zone 1F Soil Performed During Design



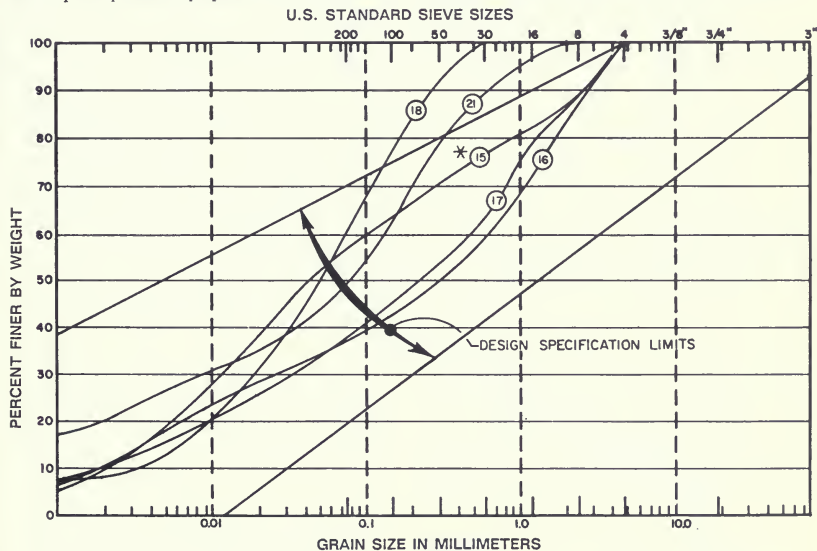
stockpile had to be supplemented with like material excavated from the reservoir floor because the contractor was allowed to use too much of the stockpiled material for Zone 2B and the bottom of the stockpile was too wet for use in the dam. Apparently, rainwater had percolated into the relatively loose stockpile during the three winters between the original excavation and use in the dam, and the impervious Red Bluff Formation blocked drainage from the bottom of the stockpile.

The closer gradation limits of Zone 1F, as compared to Zone 2F, were obtained by taking advantage of the mixing of the lenticular soil during stockpiling and re-handling of the materials. Composites of representative samples from the power plant were prepared to determine these

gradation limits and samples were taken from the stockpile prior to construction to verify the design limits.

For Zone 1F material, compaction tests were run on 22 samples from the tailrace area and one sample from the Zone 1F stockpile with a resulting average maximum density (DWR Standard) of 114 pcf and optimum water content of 16.3 percent.

Twelve consolidated, saturated, undrained triaxial shear test series with pore pressure measurements were run on representative samples from the tailrace limits. The remolded test specimens were recompacted to 97 percent relative compaction (DWR Standard) and were tested prior to the decision to stockpile and re-handle the material. Later, it was found that four series fell outside the



CLAY OR SILT FINES	SAND			GRAVEL	
	FINE	MEDIUM	COARSE	FINE	COARSE

\* SAMPLE REFERENCE NUMBERS FROM THERMALITO FOREBAY FINAL DESIGN REPORTS

NOTE: ONLY NO. 4 FRACTION WAS TESTED

Figure 216. Gradations of Triaxial Test Specimens of Zone 1F Soil Tested During Design

composite gradation curves, one series had inconclusive results, one series was not tested to DWR standards and one series was both inconclusive and fell outside the composite gradation envelope. Consequently, the remaining five series were used to determine the design strength parameters. An effective strength of 33 degrees and 0 cohesion, and a total strength of 17 degrees with a 0.7 tsf cohesion intercept, were chosen for design strength parameters. Figure 215 presents a comparison of the shear strength test results with the values adopted for design. The effective strength failure criterion was maximum obliquity. The total strength criterion was the lower of either peak deviator stress or the development of 20 percent axial strain. For some slope stability analyses, a lower total strength of 16 degrees with a 0.4 tsf cohesion intercept

cept was adopted. Gradation curves for the five test series are shown in Figure 216.

Twelve permeability tests were run on samples which fell within the composite grading limits; the results ranged from 0.3 to .00009 ft/day at 97 percent relative compaction (DWR Standard).

**Zone 2F.** The design concept for Zone 2F was to use essentially any of the Red Bluff material from the mandatory Channel H and tail channel excavations. The explorations had disclosed only minor amounts of pervious materials and it was believed that they would be blended with finer materials during excavation or could be placed in the outer portions of the zone. The blending concept appears

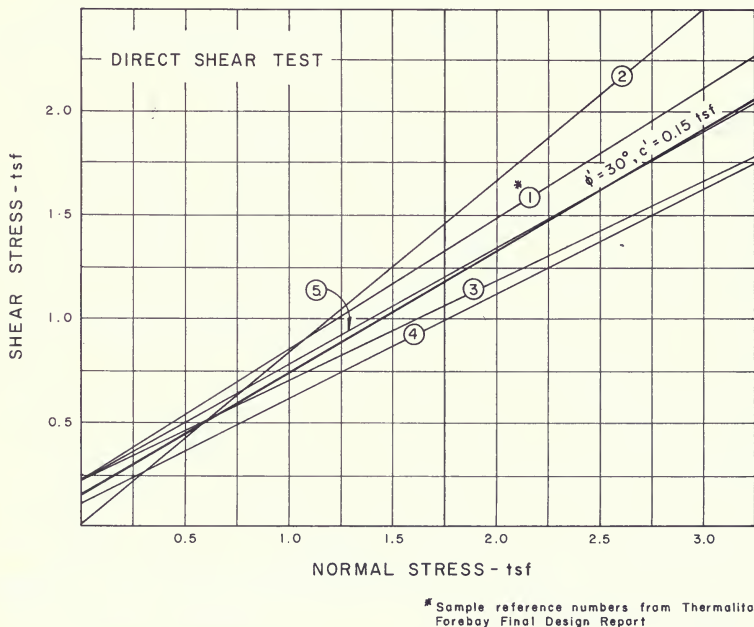
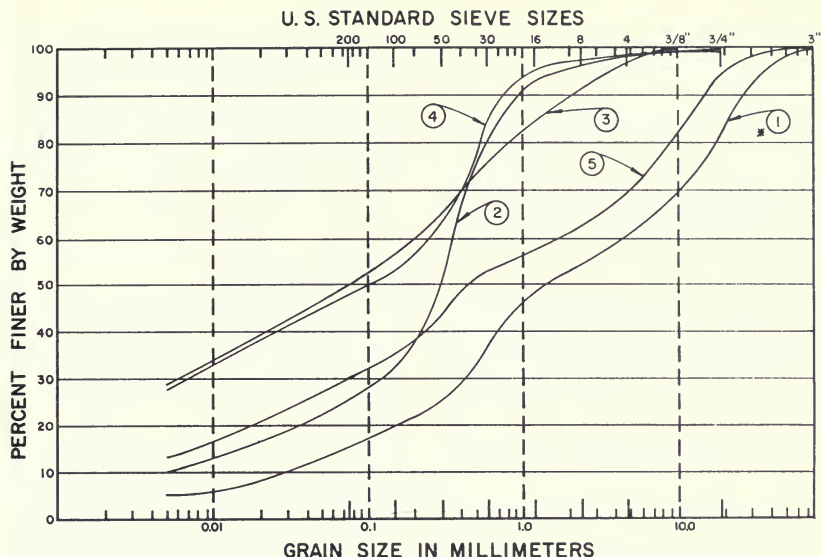


Figure 217. Strength Results from Direct Shear Tests of Zone 2F Soil Conducted During Design



CLAY OR SILT FINES	SAND			GRAVEL	
	FINE	MEDIUM	COARSE	FINE	COARSE

\* Sample reference numbers from Thermalito Forebay Final Design Report

NOTE: Only - 4 Fraction was tested

Figure 218. Gradations of Direct Shear Test Specimens of Zone 2F Soil Tested During Design

to have been valid. Pervious embankment materials were not a problem during construction. No attempt was made to route the material being placed in the embankment. Strength of the material was not a major consideration in determining its suitability for use in the zone because of the low height of the dam.

The 10 percent finer and coarser gradation limits were determined for all explored materials likely to be used in the dam. Five samples were selected from within these limits for testing with the direct shear test. The direct shear tests were set up at optimum moisture and 95 percent relative compaction (DWR Standard). The relative compaction used was lower than the 97 percent used for Zone 1F because of anticipated quality control problems

on the long dam. The samples were then saturated and sheared slowly. The direct shear tests results were checked against the Thermalito Afterbay direct shear testing, the Main Dam triaxial testing and published standard strengths before the design strength was selected (Figure 217). Gradation curves for the five samples are shown on Figure 218.

The Zone 1F stockpile was the source of the "Select Zone 2F" transition protecting the Zone 3 blanket drain.

**Zone 3.** Zone 3 was a sandy gravel obtained from the State Borrow Area Z located in the Oroville Dam reserve pervious borrow area. This part of the dredge tailing deposit characteristically had smaller rock sizes, more sand and

fewer fines than the rest of the deposit and was similar to Oroville Dam Zone 2.

Final design densities were assumed to be the same as those found in Oroville Dam Zone 2. The shear strength was assumed to be the same as that determined in Oroville Zone 2 tests performed at the relatively low confining pressures appropriate to Thermalito Forebay Dam (higher strength than used for Oroville). This strength had effective strength parameters of 45 degrees and zero cohesion.

**Zone 4F.** The source of Zone 4F material was the Thermalito Powerplant approach channel and an extension of the channel identified as Borrow Area Y. The approach excavation was stockpiled by the power plant contractor, and Borrow Area Y was excavated as needed for the dam construction.

The design parameters used for Zone 4F were based on a survey of the literature available at the time.

### Stability Analysis of the Embankment

The soil properties used in the slope stability analyses performed during design are summarized in Table 44. The stability analysis approach used was in accordance with Supervision of Dams' Technical Memorandum, "Earth Dam Stability," by Mr. W. A. Brown, with one exception. In addition to the slip circles, the infinite slope method was used to check the stability of the outside slopes of Zone 4F.

For seismic conditions, a pseudodynamic acceleration of 0.1g was applied horizontally in the most unfavorable direction for the particular section being analyzed. For deep circles through the foundation of the Main Dam and extending into the tail channel, the seismic force was applied at the center of mass rather than at the failure plane.

No failure circles were allowed to pass through the basalt foundation.

Both total and effective stress analyses were performed on the Main Dam section. Since the design strengths for Zone 2F in the Low and Ruddy Creek Dams were based on results from consolidated-drained direct shear tests, only effective stress analyses were performed for these embankments.

Zones 3, 4F and the riprap were assumed to be free draining, with respect to Zone 1F and Zone 2F. Steady state flow nets were drawn assuming a 9:1 ratio of horizontal to vertical permeability for the Zone 1F and 2F embankment. The Basalt Foundation was considered completely impervious where the rock surface was treated, and equal to the contiguous soil permeability where the surface was untreated. The Red Bluff foundation was considered to have the same permeability as Zone 1F and Zone 2F.

For the evaluation of rapid drawdown, the phreatic line was assumed to coincide with the full reservoir steady state seepage phreatic line through Zones 1F or 2F; and

**Table 44. Summary of Design Parameters Used in Slope Stability Analysis of Embankment Dam**

Zone	Density			$G_s$	Total Stress Analyses		Effective Stress Analyses	
					$\phi$	$C$	$\phi'$	$C'$
	Dry (pcf)	Moist (pcf)	Saturated (pcf)		degrees	tsf	degrees	tsf
1F	114	130	135	2.75	16	0.4	33	0
2F	109	126	134	2.75			30	0.15
3	155	161	164	2.91			45	0
4F	135	138	150	2.85			45	0
Riprap	125	127	144	2.85			45	0
Foundation	93	118	121	2.75	15	1.0	32	0.20

**Table 45. Summary of Results for Slope Stability Analyses Performed During Design**

Case	Location	Design Criteria	Analysis	Factor of Safety	
				Minimum Required	Minimum Computed
I	Upstream	Water Surface Elevation 225—phreatic line horizontal—static condition	Effective stress	1.5	1.9
II	Upstream	Case I with 0.1 g seismic factor	Effective stress	1.2	1.2
III	Downstream	Steady seepage—water surface elevation 225—flow net—static condition	Effective stress	1.5	1.6
IV	Downstream	Case II with 0.1 g seismic factor	Effective stress	1.2	1.2
			Total stress	1.1	1.1
V	Upstream	Rapid drawdown modified	Effective stress	1.1	1.4
			Total stress	1.0	2.0

The infinite slope analysis factors of safety were:

Factor of Safety

<u>Conditions</u>	<u>Minimum Required</u>	<u>Minimum Computed</u>
Static	1.5	1.75
Seismic Moist	1.1	1.40
Seismic Buoyant	1.1	1.22

to coincide with the upstream face of Zone 1F or 2F. The drawdown water surface was Elevation 195 for the Low and Ruddy Creek Dams and Elevation 185 for the Main Dam. Table 44 presents the design parameters used in the stability analyses.

Listed in Table 45 are the stability conditions analyzed using slip circles and the factors of safety required. Figures 219 through 221 present the critical circles and factors of safety for the different dam sections and stability conditions analyzed. The minimum factors of safety calculated for any dam for a particular stability condition are also presented in Table 45.

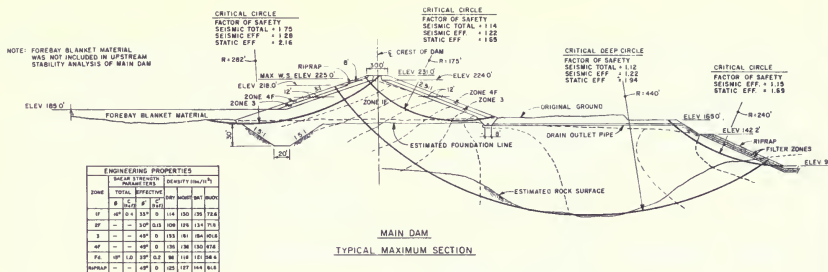
The computed infinite slope safety factors are for a 1.75:1 slope, which is the steepest upstream or downstream slope on the Forebay dam.

### Concrete Wingwall Dams

In addition to the embankment dam, a concrete headworks structure and two concrete wingwall dams act to store water in Thermalito Forebay Reservoir (See Figure 210). The concrete headworks structure was analyzed in 1979 and determined to be safe for future seismic loadings (see Chapter II of this bulletin).

#### Approach Channel Wingwall

The Approach Channel wingwall is a concrete gravity structure founded on the Middle Basalt Flow ( $T_{ym}$ ). This dam consists of three monoliths (A, B, & C) connected together and to the headworks structure by two 9-inch polyvinyl chloride waterstops which bracket a 5-inch asphalt seal. The first monolith (A) is connected to the power plant and the end monolith (C) butts up at a 0.2:1 slope against the Zone 1F material within the embankment dam at Station 2+08 (see Figure 222). The



embankment material wraps around portions of all three monoliths resulting in partially embedded structures.

Monoliths A and B are 35 feet long and Monolith C is 30 feet long. All three monoliths have crest elevations of 231 feet and have variable base elevations.

### Approach Channel Dam

The Approach Channel Dam is a concrete gravity structure also founded on the Middle Basalt Flow ( $T_{vm}$ ). This dam runs from the headworks structure 226 feet to the right abutment. The dam consists of six monoliths (A-1 through A-6) connected to each other and to the headworks structure by two 9-inch polyvinyl chloride waterstops which bracket a 5-inch asphalt seal. Monoliths A-1 through A-5 are 40 feet long; Monolith A-6 is 26 feet long. All six have a crest elevation of 231 feet and have variable base elevations. Monoliths A-1 and A-2 contain a grout and drainage gallery (see Figure 223).

### Design Consideration

Both concrete wingwall dams were founded on sound basalt rock ( $T_{vm}$ ) with the concrete designed to have a minimum compressive strength of 3000 psi. Special considerations included wrapping portions of the Approach Channel Wingwall monoliths with embankment material to prevent piping (see Figure 224) and to install the drainage gallery in two of the Approach Channel Dam monoliths to provide access to foundation relief drains. Since construction, the maximum flow from this gallery was 40 gpm (measured in 1970). Since 1970, the flow has tapered off to less than 1/4 gpm measured in 1984. The reason for this decrease is not readily apparent.

### Embankment Instrumentation

The instrumentation for monitoring structural performance of the dam consisted of a set of surface and crest monuments on the Main Dam and open-tube piezometers downstream of the dam. The toe drain outfalls were designed to allow measurement of seepage and are considered instruments. The surface and crest monuments were limited to the Main Dam which is the highest section and the closest to the Tail Channel excavation.

It was realized early in design that seepage from the Forebay could cause problems with the dam and the downstream area. Therefore, water wells in the area were monitored semiannually starting in 1957. The well network was supplemented with the open-tube piezometers during and after construction as discussed below.

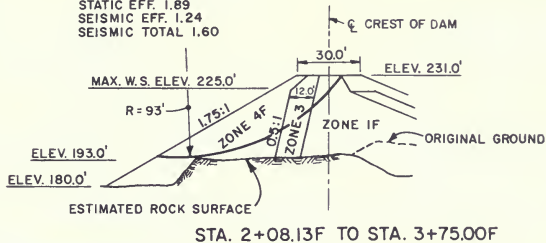
### Seepage Control Measures During and After Construction

Several seepage control measures were added during and after construction to supplement the seepage control features in the original design such as the grout curtain and cutoff trench at the main dam.

Reservoirs constructed on similar foundations had caused problems for others in the past so the well monitoring program was initiated early in design. The wells were supplemented with open tube piezometers around Thermalito Afterbay to better identify pre-project groundwater levels. Piezometers were not installed in the Forebay area at that time because the explorations had shown that the existing groundwater levels were below the practical depth of piezometers.

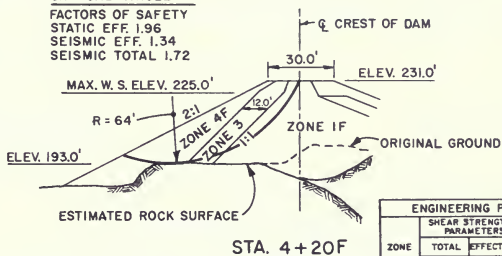
# CRITICAL CIRCLE

FACTORS OF SAFETY  
 STATIC EFF. 1.89  
 SEISMIC EFF. 1.24  
 SEISMIC TOTAL 1.60



# CRITICAL CIRCLE

FACTORS OF SAFETY  
 STATIC EFF. 1.96  
 SEISMIC EFF. 1.34  
 SEISMIC TOTAL 1.72



# ENGINEERING PROPERTIES

ZONE	SHEAR STRENGTH PARAMETERS				DENSITY (lb <sub>m</sub> /ft <sup>3</sup> )			
	TOTAL		EFFECTIVE		DRY	MOIST	SAT.	BUOY.
	$\phi$	C (tsf)	$\phi'$	C' (tsf)				
1F	16°	0.4	33°	0	114	130	135	72.5
2F	—	—	30°	0.15	109	126	134	71.5
3	—	—	45°	0	155	161	164	101.5
4F	—	—	45°	0	135	138	150	87.5
F4.	15°	1.0	32°	0.2	93	118	121	58.5
RIPRAP	—	—	45°	0	125	127	144	81.5

# CRITICAL CIRCLE

FACTORS OF SAFETY  
 STATIC EFF. 1.86  
 SEISMIC EFF. 1.27  
 SEISMIC TOTAL 2.10

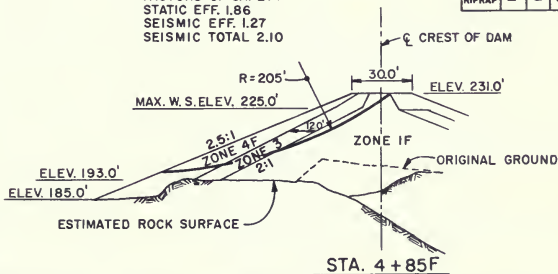
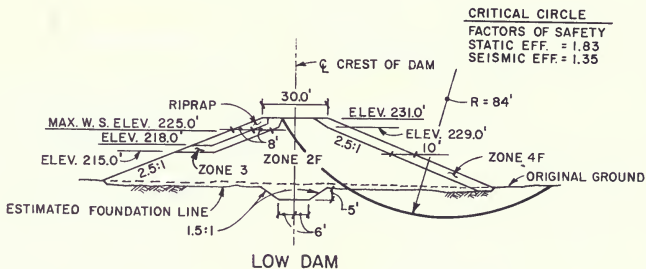
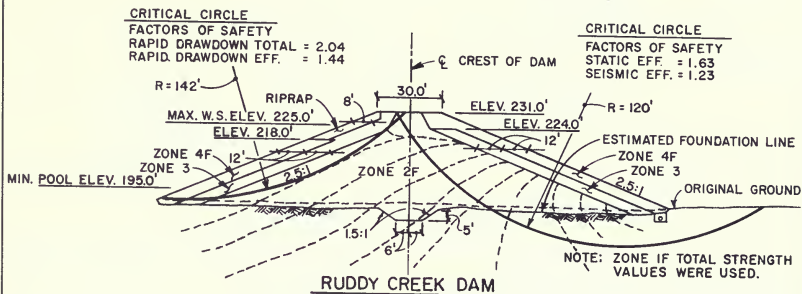


Figure 220. Summary of Slope Stability Analyses Performed during Design for Main Dam Sections of Thermalito Forebay Dam





ENGINEERING PROPERTIES									
ZONE	SHEAR STRENGTH PARAMETERS				DENSITY (lbs/ft. <sup>3</sup> )				
	TOTAL		EFFECTIVE		DRY	MOIST	SAT.	BUOY.	
	$\phi$	C (tsf)	$\phi'$	C' (tsf)					
1F	16°	0.4	33°	0	114	130	135	72.6	
2F	—	—	30°	0.15	109	126	134	71.6	
3	—	—	45°	0	155	161	164	101.6	
4F	—	—	45°	0	135	138	150	87.6	
Fd.	15°	1.0	32°	0.2	93	118	121	58.6	
RIPRAP	—	—	45°	0	125	127	144	81.6	

Figure 221. Summary of Slope Stability Analyses Performed during Design for Ruddy Creek and Low Dam Sections of Thermalito Forebay Dam



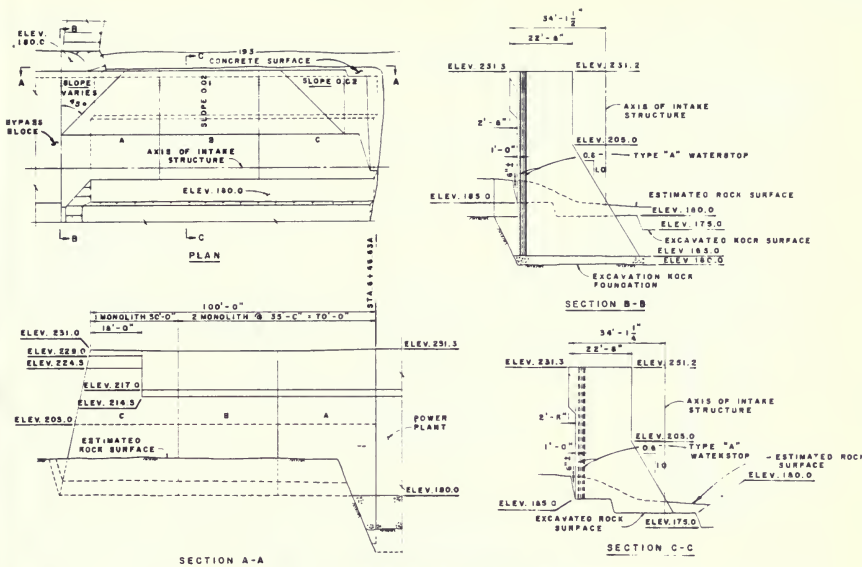


Figure 222. Plan and Sections of Wingwall Dam

The excavation for Thermalito Powerplant indicated that the Red Bluff Formation has a high horizontal permeability. Not only were there pervious lenses encountered, but there were significant seeps at the contact of two very impervious members. Concern was then focused on preventing water from entering into the pervious lenses. The basalt was identified as a possible point of entry. It was examined and deemed a marginal source of water and impractical to treat. The exploration was reviewed to assure that the Channel H excavation would not cut into any major pervious Red Bluff strata. On the basis of laboratory soil gradation testing, it was found that it would not. This may not have been a valid conclusion. In hindsight, field logs consistently indicated less silt and clay sizes in soil samples than did the laboratory tests. Later review showed that the testing procedures were probably breaking down larger-sized particles of weathered alluvium into fines. The permeability of the well-graded gravelly sands is very sensitive to the percentage of silt and clay.

## Cutoff Trench and Upstream Blanket

When sand was first discovered in the foundation of Thermalito Afterbay Dam, cutoff trench criteria were developed to treat the various conditions disclosed by the excavation. These criteria were carried over to the Forebay. The criteria as stated at the time for the Afterbay were:

1. Continue excavation, as noted in the Designers' Memorandum, to a 5-foot minimum depth to verify the existence of the compact, cemented silt and lean clay layer in the upper few feet of the Red Bluff formation.
2. If an impervious material is not found in the excavation at the minimum depth, auger from the bottom of the trench to determine whether an impervious layer can be reached within a reasonable excavation depth.

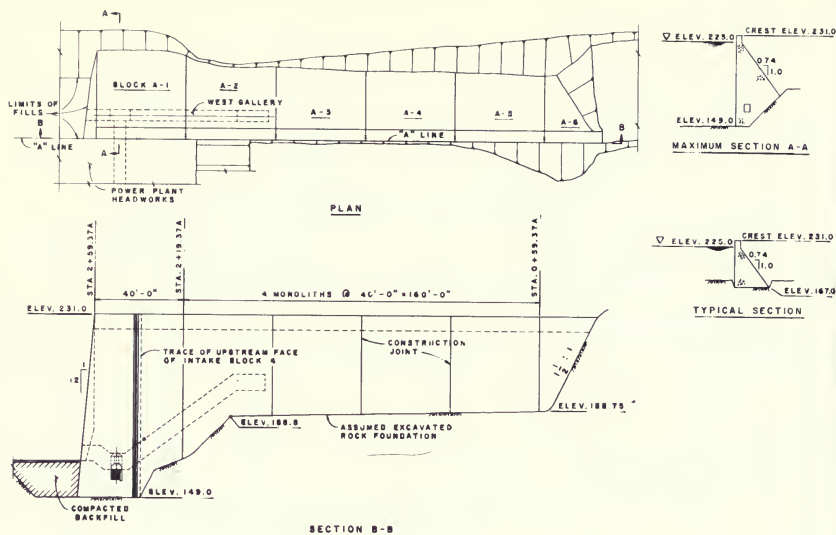


Figure 223. Plan and Sections of Approach Channel Dam

3. If augering shows that an impervious layer can be reached with continuance of the trench excavation to a maximum depth of an additional 5 feet, the excavation will be continued to the impervious layer.
4. If augering shows that an impervious layer cannot be reached within the additional 5 feet as noted in No. 3, or the pervious lens does not pinch out in a reasonable distance in a horizontal direction, the trench excavation will be stopped at 5 feet and a 3-foot-thick blanket of Zone 1A material will be placed upstream of the dam for a minimum distance of 100 feet normal to the dam axis.
5. In a direction parallel to the dam axis, the blanket will terminate at a distance of 100 feet beyond those points where augering in the exploration trench shows that the compact surface layer is found to satisfactorily meet the requirements as noted in Items 1, 2, and 3.
6. The area to be blanketed will be stripped of grass, scarified, moisture conditioned, and compacted before the Zone 1A material is placed. If the contractor's haul road, as it now exists, on the afterbay floor is within the 100-foot minimum blanket distance, it should be tied into the blanket and considered part of the blanket without further treatment.
7. All auger holes will be filled with impervious material and tamped in such a manner as to insure the integrity of the existing foundation.

The haul road mentioned above was not as continuous in the Forebay as it was in the Afterbay, where the blanket joined with the road provided a 150- to 200-foot wide impervious strip.

Open tube piezometers were installed downstream of the areas that were blanketed to check the effectiveness of the treatment.

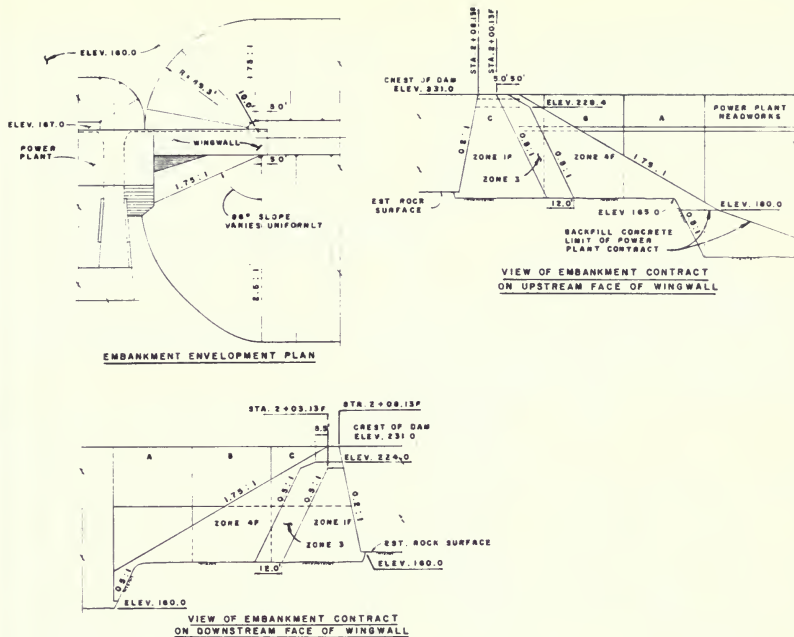


Figure 224. Wingwall Dam Envelopment by Forebay Main Dam Embankment

### Channel H Blanket.

Excavation to grade at Channel H exposed local areas of pervious sand and gravel below the zone of weathering. To estimate the permeability of these materials, samples were taken for mechanical analysis and seepage rates were observed by introducing water into the pits from which the samples were taken. The excavated channel was mapped to delineate materials of estimated similar permeability. An impervious blanket, 18 inches thick, was then compacted upon pervious materials on the channel invert and south cut slope.

The Channel H excavation exposed a distinct impervious cap of clay and clayey sand at the surface of the Red Bluff in this area. A similar situation occurred in the Oroville

Impervious Borrow Area directly to the south where the finer near-surface material had to be blended with the coarse material from below to meet the specification requirements. One explanation for the existence of this cap is that it was deposited as sand and gravel and had weathered in place.

During early operation, the specified minimum water surface was not maintained in the Forebay and some of the impervious blanket may have been eroded by the resultant high velocities of flow through the Forebay.

### Relief Well System

Water was first turned into the Forebay in mid-October 1967, but the reservoir was not brought to full operating

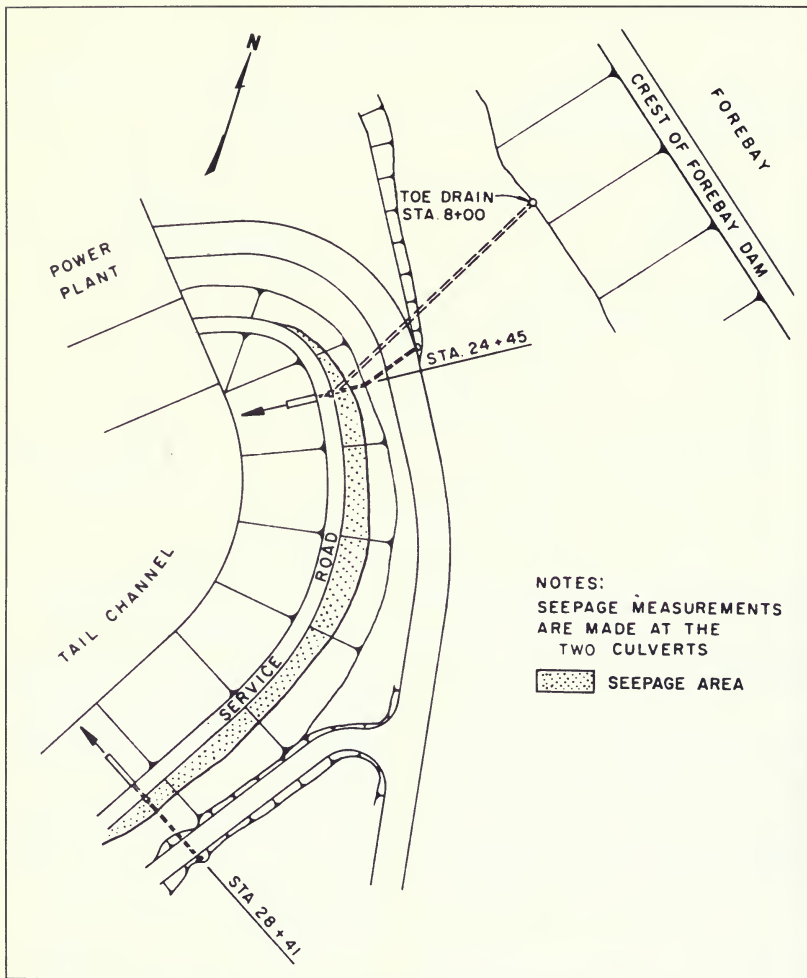


Figure 225. Location of Tail Channel Seepage Area Downstream of Thermalito Forebay Dam

level until early December 1967. On November 14, 1967, air was noted being forced out of piezometer P-63, just south of the Nelson Avenue Bridge. By December 18, 1967, the flow of air ceased as the water level in the piezometer had risen gradually to cover the perforated interval of pipe. During January and February 1968, the water level in P-63 rose at the rate of 3 to 4 feet per week. In order to provide pressure relief if the piezometric level rose to ground elevation, seven relief wells (P-116 through P-122) were drilled in the vicinity of P-63 in late February and early March 1968.

By early April 1968, the water level in P-63 had reached ground elevation, and one of the relief wells (P-118) began flowing.

The water level in P-63 continued to rise so a shallow trench was dug, and the relief wells were cut off in an attempt to lower the water level. There was considerable delay in obtaining the collector pipe ordered for the trench and it was left open approximately one year. A portable pump was used to lift the water back into the Forebay. This system was not effective in lowering the water level to the ground surface as desired, and a second series of eleven wells were installed in September 1968. After thorough cleaning and development, the wells were permitted to flow into the open ditch. In June 1969, this system was improved by cutting off the wells at about 4 feet below ground level and installing a 10-inch perforated asbestos cement pipe to interconnect the relief wells. A sump, 100 gpm submersible pump, and permanent 4-inch asbestos cement pipe discharge line were added later in 1969. It has been effective at holding the piezometric level near the ground surface.

All relief well holes drilled were dry for at least their first 10 feet of depth. This agrees with the impervious cap theory discussed previously.

### **Tail Channel Seepage**

Excavation of the Tail Channel slope below the Main Dam exposed several pervious layers of sandy soil (Figure 225). These layers have been seeping water since the filling of the reservoir. Although the seepage was not observed to be carrying any soil particles, the seepage had resulted in minor sloughing and sliding of material imme-

diately above the access road. To remedy the problem, portions of the cut face above the road were excavated in 1986 and replaced with compacted angular gravel underlain by filter fabric. This solution was intended to permit free flow of seepage out of the cut face while preventing both the migration of fine soil particles and the sloughing of saturated soils. The repair has performed as expected to date.

### **Current Evaluation of the Embankment Performance**

The locations of all the instrumentation installed since construction of Thermalito Forebay Dam, are shown on Figures 226 through 229. The current data presented in this report are from Division of Operation and Maintenance *Summary of Semiannual Surveillance Data*, October 1982.

### **Piezometers**

Eighteen piezometers were installed at the Forebay. Most of these were located near the toe of the dam to monitor the ground water conditions (Figure 226).

These piezometers have continued to follow their previously established trends by responding to reservoir levels and precipitation increases without any sharp increases or decreases in pressures. The highest downstream ground water condition exists at P-64 near the Nelson Avenue Bridge. Piezometers 144 and 122 (also near the Nelson Avenue Bridge) average approximately 2 feet lower than P-64. Piezometer 116 and 143 were taken out of service along with Piezometers 142 and 163. Since the time of installation, Piezometers 61 and 68 have gone dry.

### **Embankment Toe Drain Outlets**

The toe drains are continuous between Stations 45 + 00 and 155 + 00 and between Stations 4 + 20 and 15 + 37 with five toe drain outlets (Figures 226 and 227). These drain outlets respond to precipitation, indicating good drainage on the downstream side. During the winter of 1982, the average flow was 30 gpm whereas summer flows averaged 12 gpm.

### **Seepage Relief System**

The seepage relief system was installed late in 1968 to reduce the high ground water that had developed south of

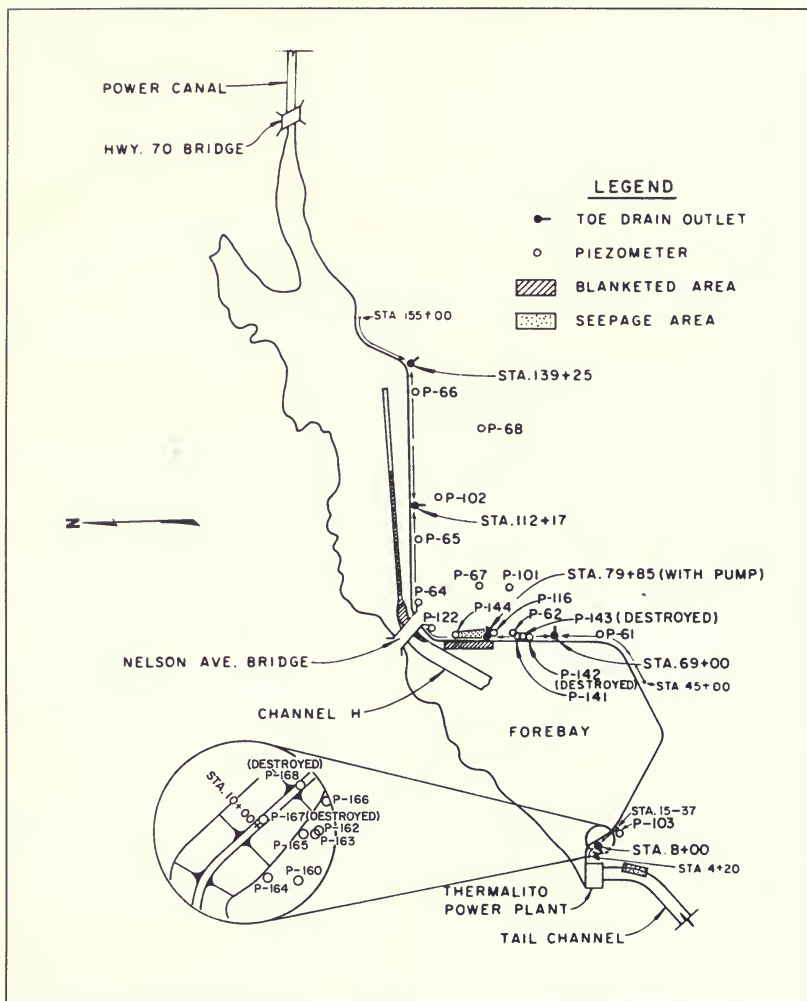


Figure 226. Location of Piezometers and Toe Drain Outlets along Thermalito Forebay Dam

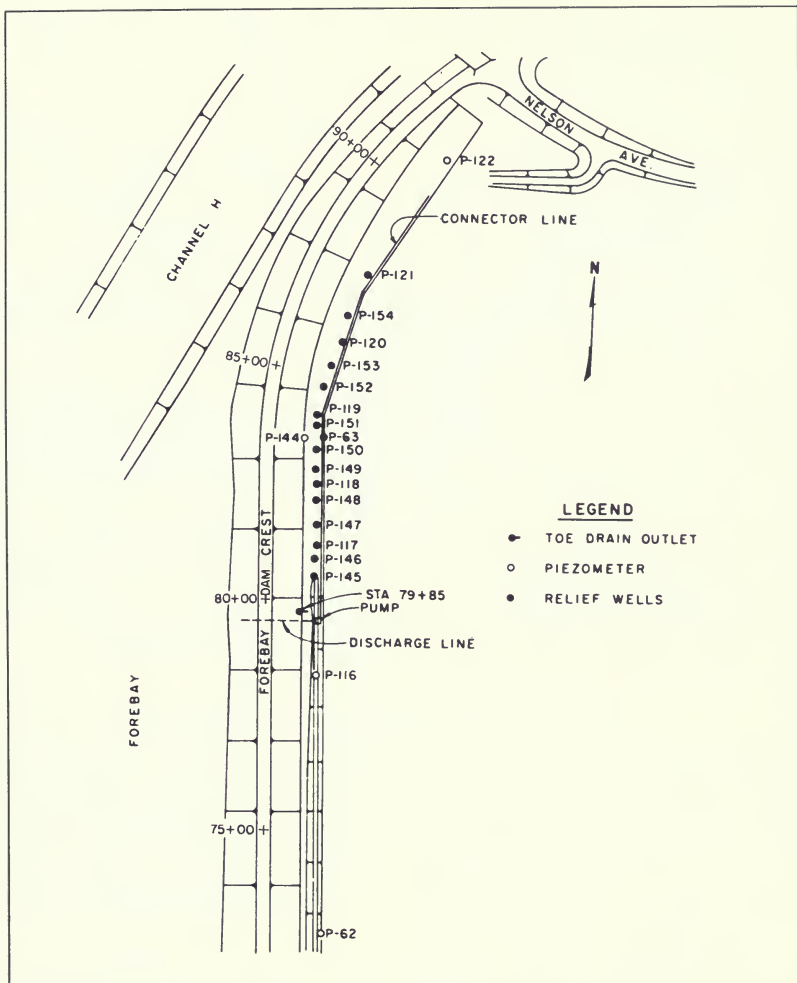


Figure 227. Location of Seepage Relief System at Thermalito Forebay Dam

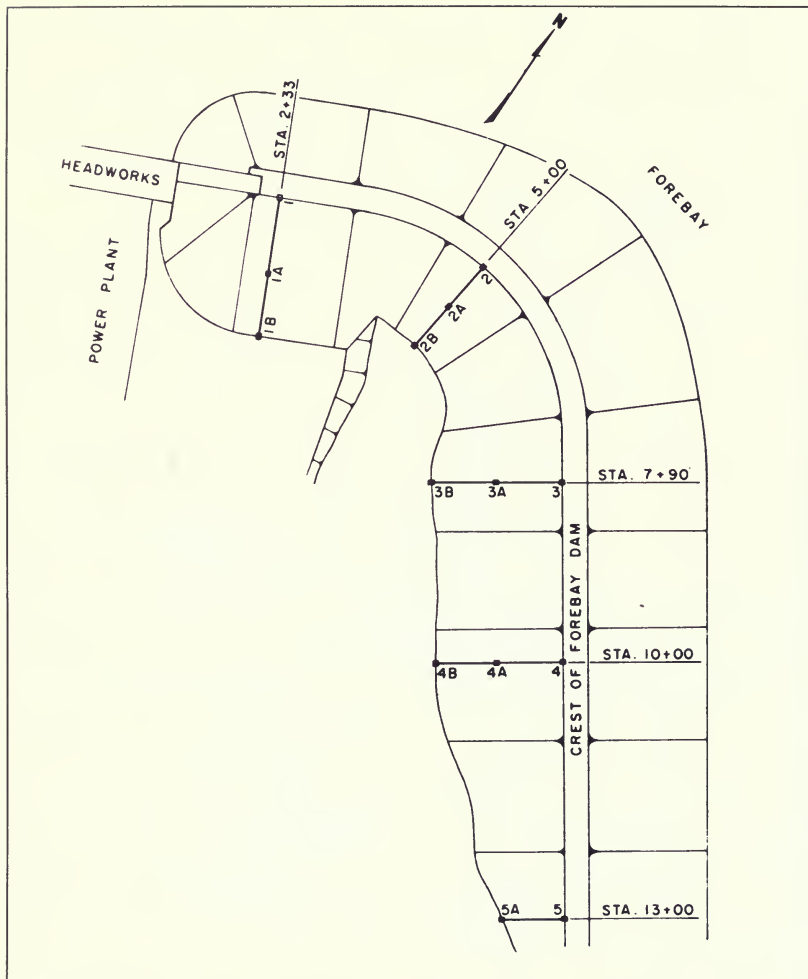


Figure 228. Location of Survey Monuments at Thermalito Forebay Main Dam



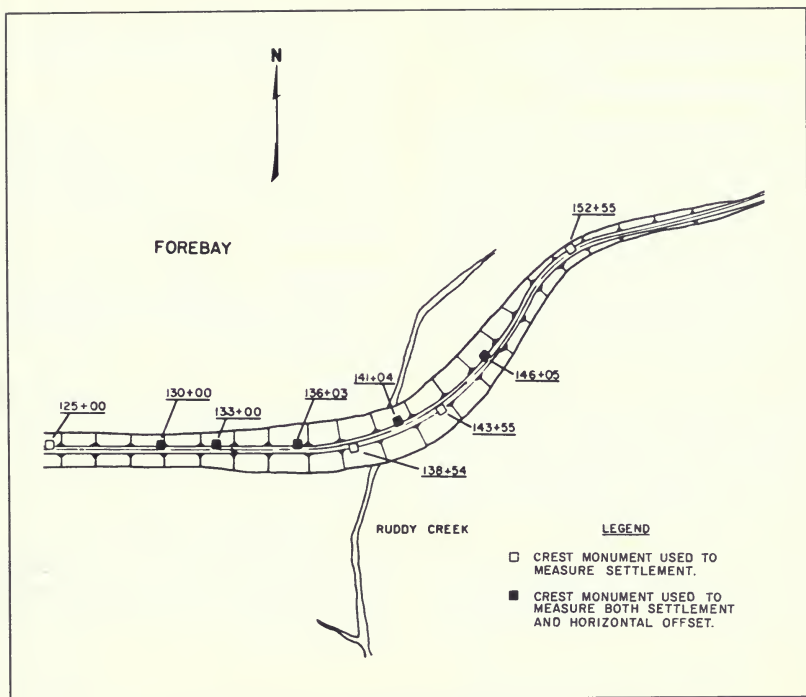


Figure 229. Location of Crest Monuments at Thermalito Forebay Ruddy Creek Area

the Nelson Avenue Bridge. The system currently consists of 16 relief wells, collector line, sump, 100 gpm pump, and discharge line to the reservoir (Figure 227). The ground water elevation is held below Elevation 210 feet by the seepage relief system as confirmed by readings in the affected piezometers (P-116, P-144, and P-122). The pumping rate to maintain this water level is fairly constant at approximately 75 gpm.

#### Tail Channel Seepage Area

Prior to 1986, the seepage in the tail channel cut was monitored at the two culverts in the tail channel. At these

culverts only seepage flows above the service road were measurable. This is estimated to have been approximately 30 percent of the known seepage area determined from geological records (Figure 225). This seepage was measured at tail channel Stations 28 + 41 and 24 + 45, and flows were somewhat erratic. The erratic readings were caused by various factors, one being that the ditches were periodically cleared. This clearing and regrading process changed the flow pattern so that an increased flow in one culvert could cause a corresponding decrease in the other. The sum of the two flows was approximately 140 gpm. This total seepage did not seem to be increasing

when compared to low precipitation periods of previous years, thus indicating a stable condition.

### **Crest and Embankment Monuments**

Fourteen monuments are located on the high embankment adjacent to the Thermalito Powerplant Intake Structure (Figure 228). There are five crest monuments (Nos. 1 through 5) and nine embankment monuments (Nos. 1A through 5A and 1B through 4B) on the downstream slope. Elevations are taken at all of these monuments and horizontal offsets are measured at Crest Monuments 3, 4, and 5. Nine crest monuments were installed between Stations 125+00 and 152+55 on the Ruddy Creek and Low Dams in June 1973 (Figure 229).

### **Vertical and Horizontal Movements**

The results of surveys between December 1967 and July 1982 indicate only minor movements have taken place at the monuments. The maximum vertical movement at the Main Dam was 0.06 feet of settlement measured in July 1981 at Crest Monument 4 (Station 10+00). The maximum vertical movement measured at either the Ruddy Creek Dam or Low Dam was 0.02 feet.

Horizontal offsets measured at three crest Main Dam monuments show a maximum movement of 0.07 feet downstream measured between August 1968 and July 1982. Monitoring of crest monuments at the Ruddy

Creek and Low Dams from June 1973 to July 1982 indicated maximum horizontal offsets of 0.02 feet downstream at Station 130+00 and 0.02 feet upstream at Station 146+05.

Figures 230 through 234 present the deformations measured over time for the surveyed monuments. As these figures show, no abrupt change in deformation resulted after the occurrence of the 1975 Oroville earthquake.

### **General Conditions**

#### **A. Inspections**

The field division personnel make frequent inspections while obtaining instrumentation readings and other activities at the dams.

#### **B. Riprap**

The riprap at the dam appears to be in excellent condition determined by visual inspection.

#### **C. Rodent Activity**

None.

### **Assessment of Performance**

Based on the analysis of performance, the data contained in this report, and inspections of this facility, Thermalito Forebay Dam is in good condition, well maintained, and performing satisfactorily.

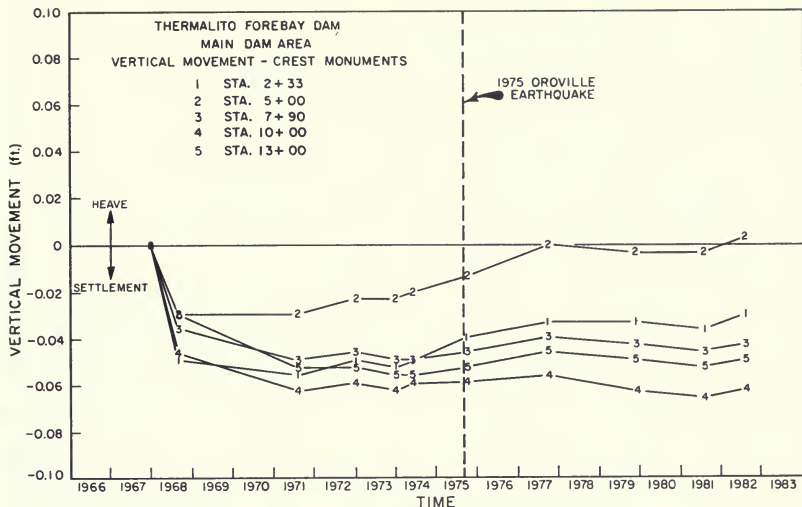


Figure 230. Vertical Movements Measured at Thermalito Forebay Main Dam Crest Monuments

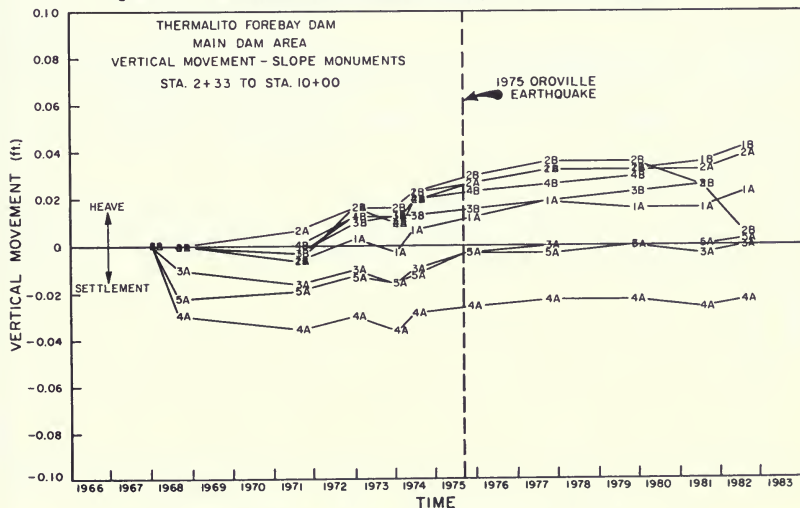


Figure 231. Vertical Movements Measured at Thermalito Forebay Main Dam Slope Monuments

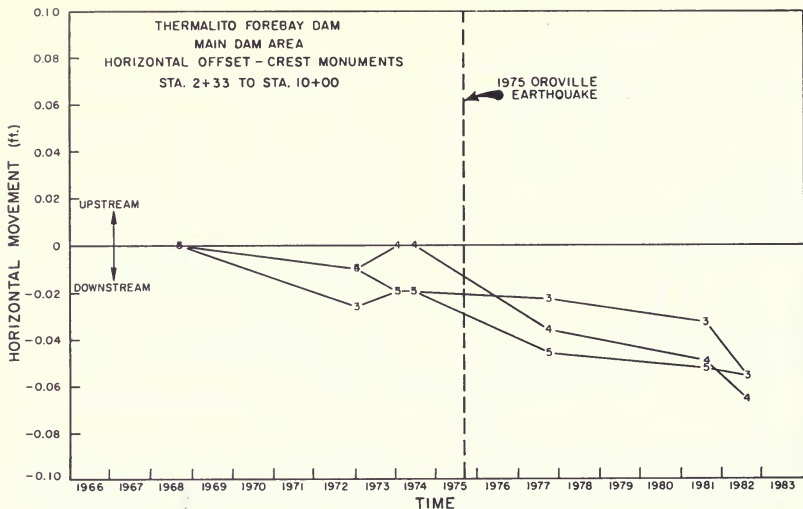


Figure 232. Horizontal Movements Measured at Thermalito Forebay Main Dam Crest Monuments

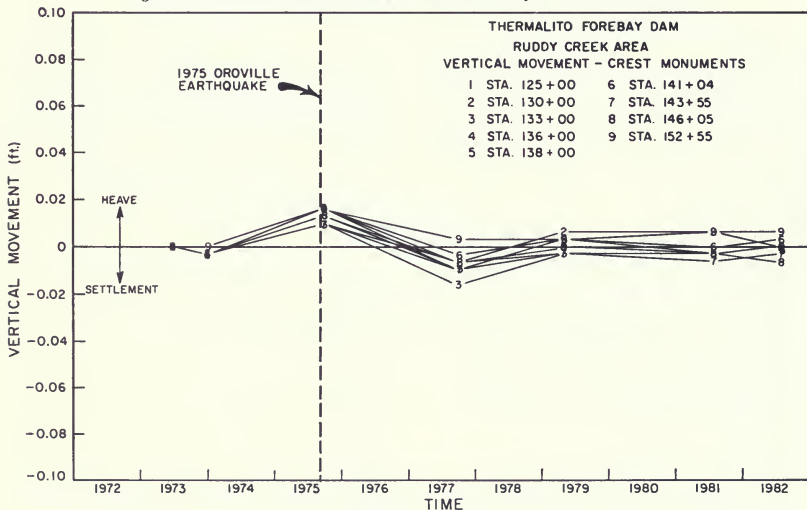


Figure 233. Vertical Movements Measured at Thermalito Forebay Ruddy Creek Area Crest Monuments

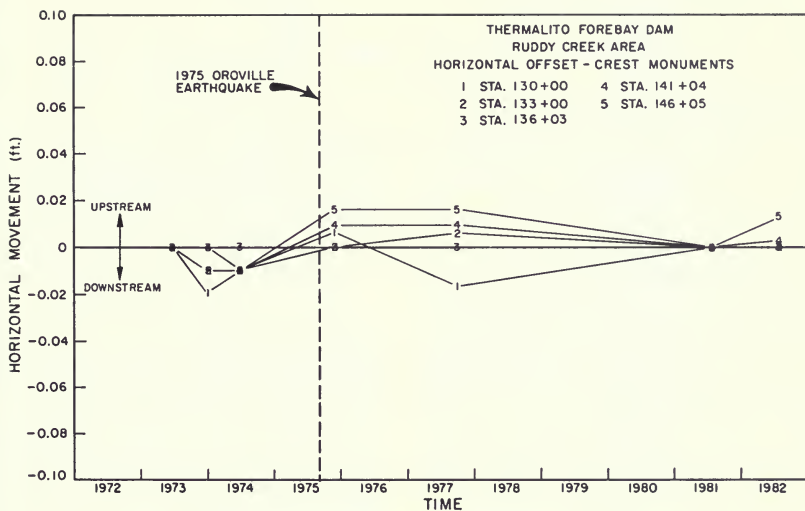
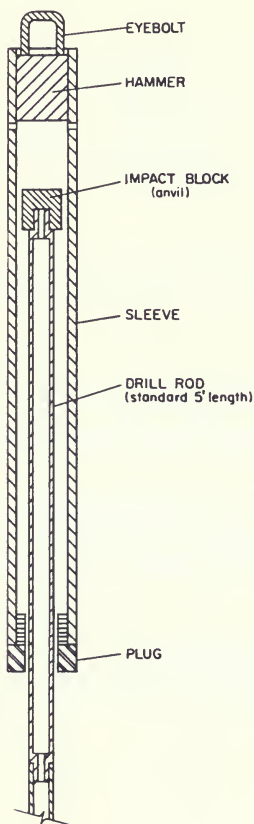
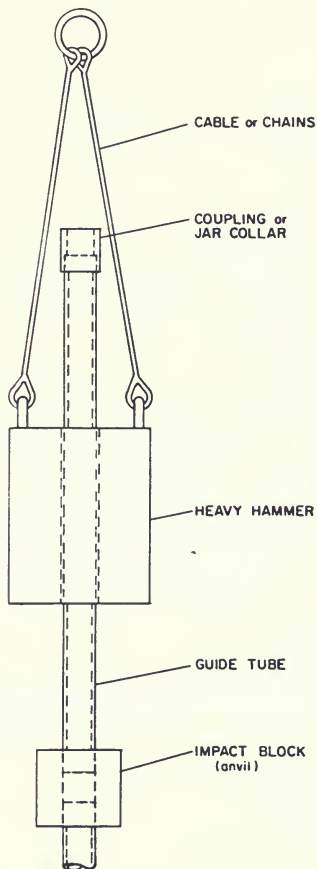


Figure 234. Horizontal Movements Measured at Thermalito Ruddy Creek Area Crest Monuments



a) SAFETY HAMMER



b) DONUT HAMMER

Figure 235. Configuration of SPT Hammers (Adapted from Steinberg, 1981)

### 3. EXPLORATION, SAMPLING, AND FIELD TESTING

#### Introduction

The exploration program was principally performed to locate and delimit foundation materials beneath the embankment that could conceivably liquefy. The major tool in this endeavor was the Standard Penetration Test (SPT). Sandy materials were considered suspect if their corrected SPT blowcounts were less than 30.

#### Standard Penetration Test Procedures

The SPT test consists of driving a 2.0-inch O.D. split- spoon sampler into the soil at the bottom of a borehole. The sampler is driven by raising a 140-lb. hammer weight 30 inches and letting it drop onto an anvil mounted on the drill rods connected to the sampler. The SPT blowcount or N value is the number of such drops or blows required to drive the sampler the last 12 inches of an 18-inch drive. To ensure that consistent test procedures were followed, all tests were supervised by a DWR geologist. Almost all of the SPT tests performed at Thermalito Forebay Dam employed the following test procedures:

- a. SPT boreholes were drilled using bentonite drilling mud and a 4.5-inch upward deflecting, baffled drag bit.
- b. Mobile B-61 drill rigs and both upset wall and parallel wall NW drill rods were used.
- c. The split spoon samplers had 2.0-inch outside diameters, 1.38-inch I.D. at the drive shoe, and a 1.5-inch I.D. within the barrels (i.e. room for liners but no liners used).
- d. 140-lb. safety hammers were used together with 30-inch drops (mark painted on hammer guide rods). The SPT hammers were raised and released using 2 wraps of a 1-inch "new" manila rope around a rotat-

ing 8-inch-diameter cathead. The "new" ropes were used in an attempt to maintain uniform energy.

#### SPT Blowcount Corrections for Use with Seed and Idriss (1982) Correlation

The SPT correlation used to predict liquefaction resistance at Thermalito is the one developed by Seed and Idriss (1982). To account for procedural differences between the tests performed at Thermalito Forebay Dam and the tests used in developing this correlation, correction factors were applied to the SPT blowcounts. These procedural differences principally involve the amount of hammer energy delivered to the drill rods and the configuration of the SPT sampler. In the Seed and Idriss (1982) correlation, the results were apparently intended for use with traditional American SPT hammer equipment. The traditional American SPT hammer has been a "donut" shaped hammer (see Figure 235). Typically, a "donut" hammer, when used with an "old" rope wrapped two to three times around a rotating cathead, delivers to the drill rods approximately 45 percent of the theoretical free-fall energy of a 140-lb. weight falling 30 inches (see Kovacs et al., 1981).

At Thermalito Forebay Dam, "safety" hammers were used to obtain SPT blowcounts (see Figure 235). Since "safety" hammers are more efficient than "donut" hammers in transmitting energy, the blowcounts need to be corrected. Figure 236 presents results from comparison tests conducted at Thermalito Afterbay, which show that a "donut" hammer produces about a 35 percent higher blowcount than does a "safety" hammer for the same rope and cathead release system.

The SPT test energies at Thermalito are also higher than traditional American practice because "new" ropes were used throughout the exploration program. To estimate the SPT energies used in the evaluations of Thermalito Afterbay and Forebay Dams, velocity measurements

were made by the United States Bureau of Standards at Thermalito Afterbay in 1982 (Reference 52). Results showed that the safety hammers used at Thermalito had approximately 70 percent of the theoretical free-fall energy at hammer impact. Attempts to measure the energies delivered through the anvil were unsuccessful. However, safety hammers are generally very efficient and average approximately 95 percent in the amount of energy transmitted through the anvil to the drill rods. Consequently, a rod energy of about 67 percent of the theoretical free-fall energy can be assumed for the Thermalito SPT tests ( $70\% \times 0.95 = 67\%$ ).

The other principal difference between the Thermalito SPT procedures and the Seed and Idriss (1982) procedures involves sampler configuration. The data in the Seed and Idriss (1982) correlation were collected with SPT samplers having a constant 1.38-inch inside diameter. However, the Thermalito SPT samplers have a 1.38-inch inside diameter at the shoe but a 1.5-inch inside diameter within the barrel. The effect of having a larger sampler barrel results in a 10 to 35 percent decrease in SPT resistance (Reference 72).

Table 46 summarizes the development of a correction factor to account for procedural differences in SPT testing. Depending on what value is chosen to account for the effect of the different barrel size, the correction factor varies from 1.6 to 2.0. A correction factor of 1.5 was conservatively chosen to match the procedures used in the Seed and Idriss (1982) correlation. An additional correction factor,  $C_N$ , is also used to correct the blowcount for different overburden pressures. Figure 237 presents the  $C_N$  values used to standardize SPT resistance to that which would be obtained at 1 tsf overburden pressure.

### SPT Blowcount Corrections for Use with Seed (1987) Correlation

To estimate the post-earthquake residual strength of liquefied soil, the SPT correlation developed by Seed (1987) was used. In this correlation, a rod energy equal to 60 percent of the theoretical free fall energy is assumed. In addition, a constant 1.38-inch inside diameter is used. To use the Seed (1987) correlation, uncorrected Thermalito SPT blowcounts are increased by 30 percent for

procedural effects (see previous discussion and Table 46).

### SPT Notation

The following notation is used to define the different SPT blowcount expressions:

$N$	=	Uncorrected Thermalito SPT blowcount measured in the field.
$N_1$	=	Thermalito SPT blowcount corrected to 1 tsf overburden pressure, $N_1 = C_N \times N$ (see Figure 237).
$N_{A1}$	=	Thermalito SPT blowcount corrected for both overburden pressure and procedural differences, $N_{A1} = N_1 \times 1.5$ (see Table 46). This is the blowcount applicable with the Seed and Idriss (1982) correlation.
$(N_1)_{60}$	=	Thermalito SPT blowcount corrected for both overburden pressure and procedural differences, $(N_1)_{60} = N_1 \times 1.3$ (see Table 46). This is the blowcount applicable for use with the Seed (1987) correlation.

### Chronological Summary of Field Testing

Field explorations, testing, and sampling were conducted in five distinct programs:

1976  
1978  
1979–1980  
1981–1982  
1984

Most of the boreholes were drilled along the downstream toe of the dam. Figures 238 and 239 present plan views of the dam showing the locations of most of the explorations.

### 1976 Program

The initial investigation was a very limited attempt to define the foundation profile along the Forebay Dam. Five borings, numbered D-9 through D-13, were drilled to



Table 46. Estimated Effects of Procedural Differences on SPT Blowcounts

SPT Procedures employed at Thermalito Forebay Dam	SPT Procedures for use with Seed and Idriss (1982) SPT Correlation++	Correction Factor*	SPT Procedures for use with Seed (1987) SPT Correlation	Correction Factor*
Sampler driven by a 140-lb. "Safety" Hammer raised 30 inches and released using 2 turns of a 1-in. "new" manilla rope around a rotating cathead. Energy delivered to the drill rods estimated to be approximately 67% of the theoretical free fall energy.	Sampler driven by a 140-lb. "Donut" Hammer raised 30 inches and released using 2 to 3 turns of a 1-in. "old" manilla rope around a rotating cathead. Energy delivered to the drill rods estimated to be approximately 45% of the theoretical free fall energy.	1.49	Sampler is driven by a hammer and anvil system where the energy delivered to the drill rods is equal to 50% of the theoretical free fall energy.	1.12
Sampler consists of a 2.0-in. O.D. split spoon with an I.D. at the shoe of 1.38 inches and an I.D. within the barrel of approximately 1.5 inches.	Sampler consists of a 2.0-in. O.D. split spoon with a constant I.D. of 1.38 inches within both the shoe and the barrel.	1.1 to 1.35	Sampler consists of a 2.0-in. O.D. split spoon with a constant I.D. of 1.38 inches within both the shoe and the barrel.	1.1 to 1.35
	TOTAL CORRECTION FACTOR FOR PROCEDURAL DIFFERENCES = $1.49 \times (1.1 \text{ to } 1.35)$ = <u>1.64 to 2.01</u>		TOTAL CORRECTION FACTOR FOR PROCEDURAL DIFFERENCES = $1.12 \times (1.1 \text{ to } 1.35)$ = <u>1.23 to 1.51</u>	
	IN VIEW OF THE NECESSITY TO MAKE ASSUMPTIONS REGARDING PROCEDURES FOR THIS CORRELATION, A CONSERVATIVE VALUE OF <u>1.5</u> WAS ADOPTED.		FOR COMPARISON PURPOSES, AN AVERAGE CORRECTION FACTOR OF <u>1.3</u> WAS ADOPTED.	
Uncorrected Thermalito Forebay SPT blowcounts are given the symbol  N	Thermalito Forebay SPT blowcounts corrected by the 1.5 factor to this set of procedures and also corrected for overburden pressure are given the symbol  N <sub>A1</sub>		Thermalito Forebay SPT blowcounts corrected by the 1.3 factor to this set of procedures and also corrected for overburden pressure are given the symbol  (N <sub>1</sub> ) <sub>60</sub>	

Notes: \* Denotes that this correction factor is the value needed to correct Thermalito Forebay SPT blowcounts for a procedural difference in order to be used with this correlation.

++ Denotes that the hammer energies appropriate for use with this correlation had to be estimated.

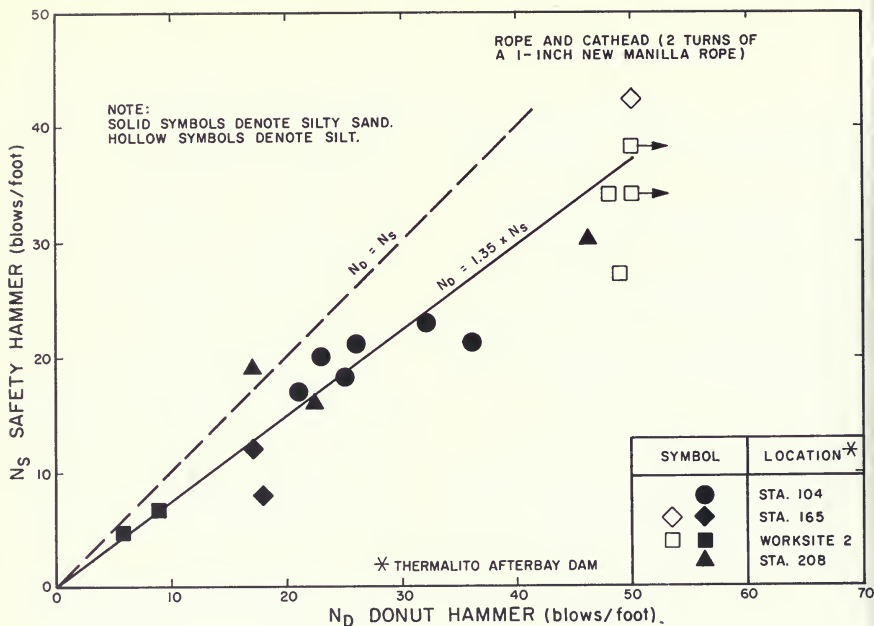


Figure 236. Comparison of SPT  $N$ -Values with Donut and Safety Hammers

depths of 12 feet to 25 feet along the toe of the Low and Ruddy Creek Dams as shown in Figure 239, page 314. Coring for these boreholes was by a Pitcher barrel sampler. These samples were extruded on site for visual classification. From these samples, a general foundation profile was revealed to consist of a 4 to 12-foot-thick surface layer of dense clay underlain by a mixture of well and poorly graded sands, along with clayey and silty sands.

In these sand layers, nine SPT tests were performed and 11 samples for cyclic triaxial testing were obtained with the 2.5-inch DWR thick-walled sampler. All corrected blowcounts ( $N_{A1}$ ) were above 20 blows per foot.

### 1978 Program

Eight borings (TFS-1, TFS-2, and TFS-4 through TFS-4E) were drilled at the Main Dam and two borings (TFS-3 and TFS-3A) were drilled at approximately Station 82 along the Low Dam. As shown in Figures 238 and 239, some of these borings were drilled through the crest as well as along the toe.

At the Main Dam, seven of the borings were drilled for undisturbed sampling of the foundation to depths of 30 to 87 feet. The samples, mainly sands, were obtained for cyclic triaxial testing. These samples included 12 pitcher barrel tubes, 6 Shelby push tubes, and 8 piston samples. In three of the borings, piezometers were installed, which indicated a downstream water table at Elevation 171 feet.

Standard Penetration Tests were performed in only one boring at the toe of the Main Dam. Except for the use of "A" drill rods rather than "NW" rods, the SPT test procedures used in this program were the same as those described in previous sections. Results of the SPT tests showed a 20-foot-thick surface layer of dense clay underlain by 13 feet of suspect sands ( $N_{A1} < 30$ ) in the foundation at the Station 11 area (Figure 240, page 316).

At the Low Dam, two sampling borings—one at the crest and one at the toe—were drilled 50 feet into the foundation near Station 82. Fourteen Pitcher barrel samples were obtained for lab testing. Additional Pitcher tube samples were extruded on the site for visual classification. Both borings encountered a 17-foot-thick surface layer of stiff clay underlain by a 7- to 11-foot layer of compact silty sand in the foundation (Figure 245, page 326).

To define the shear moduli of the foundation, downhole shear wave velocity tests were performed at the Station 11 and 82 areas to depths of 70 to 80 feet. Results presented in Figures 251 and 252 show that the alluvial soils in these areas have shear wave velocities between 740 and 1850 fps. However, sound rock, defined by a minimum shear wave velocity of 2500 fps, was not encountered in the depths explored.

### 1979–1980 Program

This third exploration phase was performed to delimit the suspect sand layer between the Main Dam and the tail channel cut and to define the foundation conditions to a 500-foot depth at the Main Dam. Additional explorations were also made to discover the possible presence of suspect sands along the Low Dam (see Figures 238 through 250, pages 312 through 337).

Five SPT borings were drilled between the Main Dam and the Tail Channel to depths of 50 feet. These borings show a relatively low blowcount sand layer ( $N_{A1} = 12$  to 30) located between Elevations 150 and 165 feet (Figure 241). At the Low Dam, 10 SPT borings were spaced at 1,000-foot intervals. These borings were drilled to depths of 30 to 40 feet into the foundation. Only one of these borings, 79–112 SPT, indicated suspect sands ( $N_{A1} < 30$ ) in the foundation (see Figure 247). The same equipment and procedures were used for standard pene-

tration testing as were employed in 1978. One hundred forty-six bag samples from the SPT tests were subjected to laboratory classification tests.

In the Station 10 area, Borehole 79–10 was drilled to 505 feet to define the foundation characteristics for dynamic response analyses. Eleven SPT tests were performed within the alluvial soil in this borehole and 10 bag samples were collected. Between depths of 82 and 259 feet, basalt was encountered. Sedimentary rock from the Lone Formation was found between 259 and 505 feet. Twenty-one core samples of basalt and Lone Formation were obtained, and downhole shear wave velocities were measured (see Figure 253).

Twenty-six hand-carved samples for cyclic triaxial testing were obtained from foundation sand layers exposed in the tail channel cut slope at the Main Dam. Eighteen samples were hand-carved tubes and eight were hand-carved blocks. As shown in Figure 238, the hand-carved tube samples were obtained closer to the Main Dam than the block samples. It should also be noted that the tube samples contained uncemented sands while the block samples were obtained from partially cemented sands. SPT borings located near both sampling sites indicated  $N_{A1}$  values of between 23 and 33 (Figures 240 and 241).

### 1981–1982 Program

This exploration program was designed to finish identifying all possible areas of suspect sands, obtain samples of these sands, and determine the ground water elevation at the Main Dam. As before, areas of suspect sands were identified by the SPT borings, and disturbed samples of low blowcount soils were obtained with the SPT split-spoon sampler. Undisturbed samples were recovered with a hydraulic fixed-piston sampler. To determine if the suspect sands were below the ground water table, standpipe piezometers were installed in the sand layers at the Main Dam, both at the toe and beneath the crest.

At the Main Dam, SPT borings were used to determine the extent of the suspect foundation sands identified in previous exploration programs. At the end of this program, the maximum spacing between SPT borings along the Main Dam was less than 100 feet (see Figure 238.) Along the Low and Ruddy Creek Dams, SPT borings were placed every 250 feet in an effort to discover possi-

ble suspect sands. Up to four different Mobile B-61 drill rigs were used during this program. To ensure a legitimate comparison among SPT values taken by different drill rigs, a blowcount correlation study with the four rigs was performed at two sites at Thermalito Afterbay. All rigs obtained SPT blowcounts within 3 blows per foot of the average blowcount. This minor variation was attributed principally to material variations (see Chapter III). SPT test procedures used in this program were those outlined at the beginning of this section.

Between 1981 and 1982, a total of 30 SPT borings were drilled at the Main Dam and 64 at the Low and Ruddy Creek Dams (see Figures 238 and 239). Laboratory classification tests were conducted on 880 SPT samples obtained from these borings. "Undisturbed" samples were obtained with a hydraulic fixed piston sampler. Three-

inch-diameter, 24-inch-long stainless steel Shelby tubes were used. Sampling locations were chosen in suspect sand layers, where several SPT borings defined soil layers with consistent blowcounts over a horizontal extent. Such areas were generally established by drilling three SPT boreholes in a triangular pattern, approximately 10 to 20 feet on a side. If the SPT blowcount obtained in all three boreholes for a particular elevation were relatively close, then piston samples would be obtained from the interior of the SPT borehole triangle. Piston samples were taken at the same depths as were SPT tests in order to relate laboratory strength with penetration test resistance.

Figures 254 through 260 present SPT data and borehole locations for the 1981-82 "undisturbed" sampling sites. Table 47 (see page 338) summarizes the average SPT blowcount assigned to the samples. Due to the variation

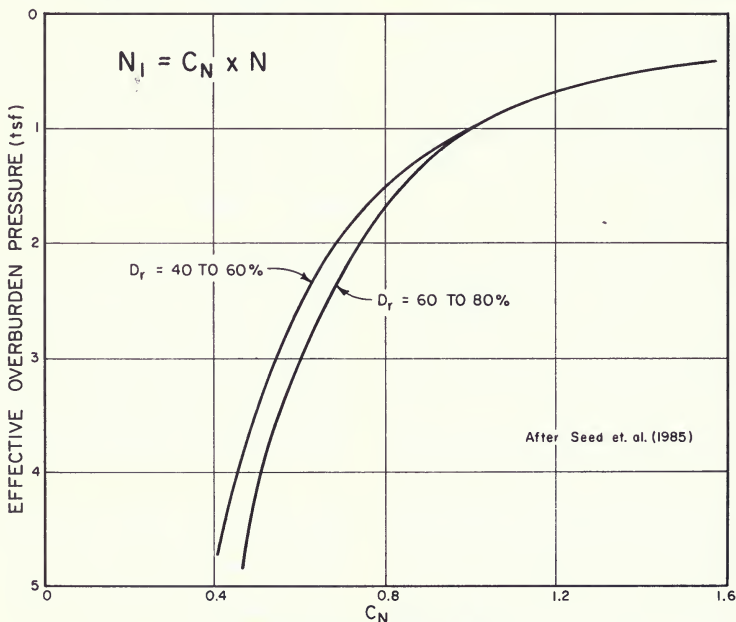


Figure 237. Chart for Determining Values of  $C_N$

of suspect sands in both horizontal and vertical extent, consistent sample sites were difficult to find (see Figures 242 through 250). Approximately 10 percent of the samples were lost during sampling due to the sample falling out of the tube or gravel severely bending the tube. Of the retrieved samples, 83 percent had full recovery. The remaining retrieved samples had 90 percent recovery.

To minimize disturbance of the piston samples, great care was taken in their handling. Sampling was supervised by an engineer and a geologist. After the sample was removed from the boring, it was trimmed, measured, and placed in a sample transportation box. This box was padded with foam around each tube to reduce disturbance during transportation. For samples of fine soil, solid packers were placed on both ends of the samples. For samples of sandy soils, perforated packers with filter paper were placed on the bottom end of the samples to allow drainage. Samples of sandy soils were allowed to drain for one week before they were transported to the lab. After the drainage period, the samples were measured and quantity of drainage water noted. The sample box was then placed on a mattress in a van and tied down with ropes to prevent tipping during the approximately 100-mile drive to the lab.

### **Cone Penetrometer Soundings**

In 1982, eleven cone penetrometer soundings were performed near Stations 9, 68, 74, and 112. These soundings were intended to delimit potential suspect sands. Although layers with low cone resistance were found, the high resistance measured on the penetrometers friction sleeve indicated that the soils were clayey. Since other explorations indicated that the suspect soils were cohesionless in situ, the cone penetrometer results were not used; instead, additional SPT boreholes were used to define suspect sand layers.

### **1984 Program**

In 1984, three borings were drilled at the Station 10 + 50 (84F-10, 84F-C11 and 84F-C11A) and three borings

were drilled at the Low Dam in the Station 112 Area (84F-112SPT, 84F-C112SPT, and 84F-113SPT). These borings were drilled to obtain site specific embankment and foundation data for the determined critical sites of the seismic evaluation (Figures 238 and 239). Fourteen undisturbed push samples of the Main Dam embankment and eight undisturbed samples of the Low Dam embankment were obtained to determine embankment static strengths. Four additional undisturbed push samples at the Main Dam and eight undisturbed push samples at the Low Dam were obtained in shallow foundation clays and clayey/silty sands to determine static and cyclic strengths of this material. Standard Penetration Tests were also performed in foundation materials in the Low Dam borings to enhance previous SPT data and layering definition. Bag samples of this material were taken for laboratory classification. In addition, piezometers were installed at the Low Dam crest and toe within the foundation silty sand layer to better define the phreatic surface through the dam.

### **Characteristics of Red Bluff Formation Soils**

Over the years, the exploration programs have revealed the complexity of the Red Bluff formation. At the Main Dam, this alluvial formation is approximately 80 feet thick and lies above the basaltic Lovejoy Formation. The Red Bluff Formation is composed generally of unconsolidated fluvial (stream deposited) sediments representing a great variety of source rocks originating in the Sierra Nevada and the nearby foothills. These sediments vary not only by soil type but also by density and areal extent, as shown in Figures 241 through 250.

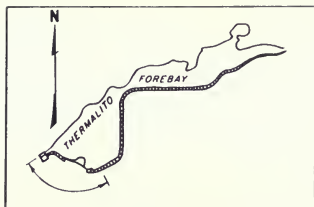
Near the project area, the ancestral Feather River wandered between its present course and basaltic extensions of Table Mountain to the north. Ancient flood plain deposits dominate the valley lowlands. Depending on the river's velocity, volume, and runoff area, different particle sizes were dropped at different locations on the floodplain surface.

**NOTE:** Figures 238 through 250 follow. Text continues on page 338.

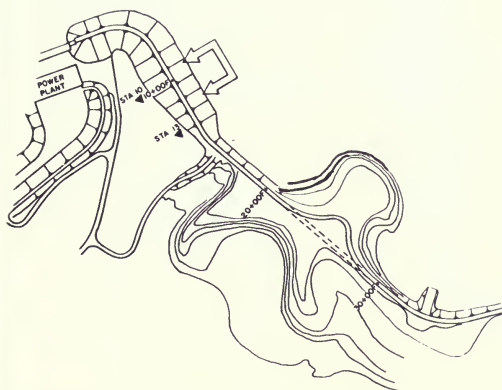


DETAIL OF BORINGS  
AT MAIN DAM

Figure 238. Thermalito Forebay  
Plan And Location  
Station 7 To



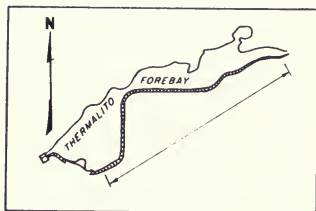
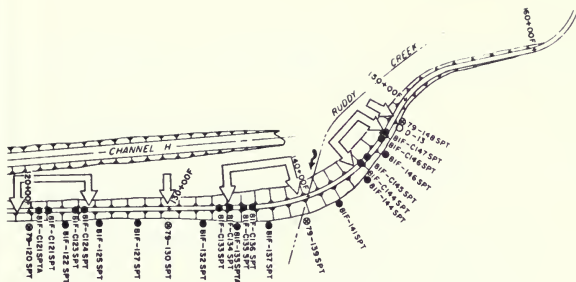
LOCATION MAP



Low Dam  
Of Spt Borings  
Station 40







LOCATION MAP

- LEGEND
- LOW BLOW/COUNT LOCATIONS ( $N_{60} \leq 30$ )
  - 1978 SPT BORINGS
  - 1979-80 SPT BORINGS
  - 1981-82 SPT BORINGS
  - 1984 SPT BORINGS
  - ▲ PISTON SAMPLING SITE

Low Dam  
Of Spt Borings  
Station 150

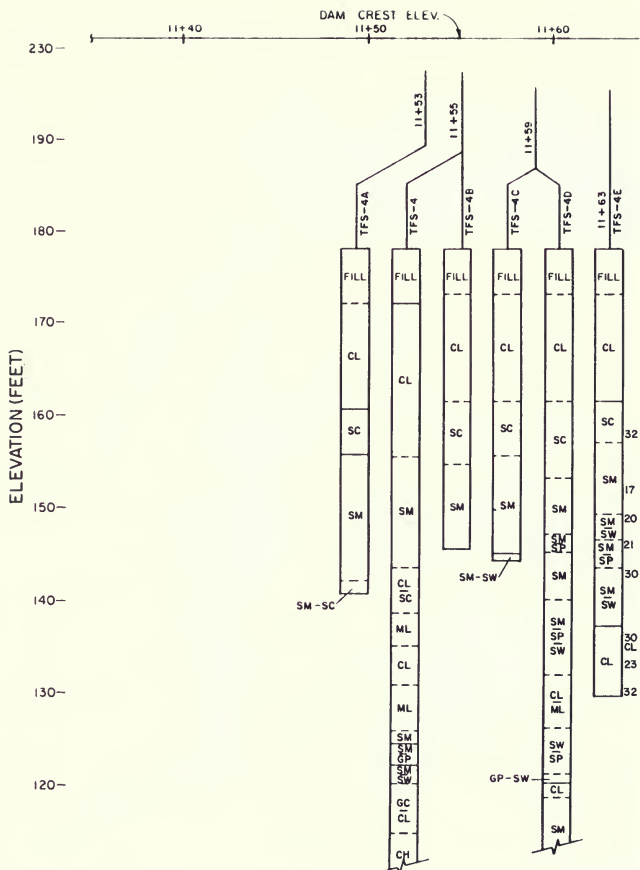
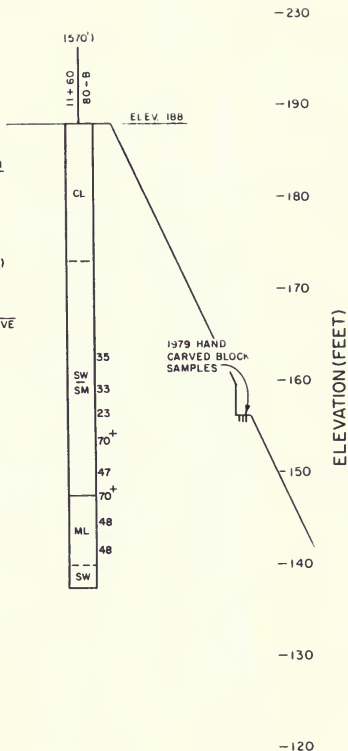
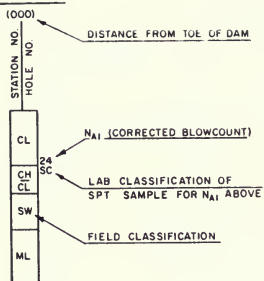


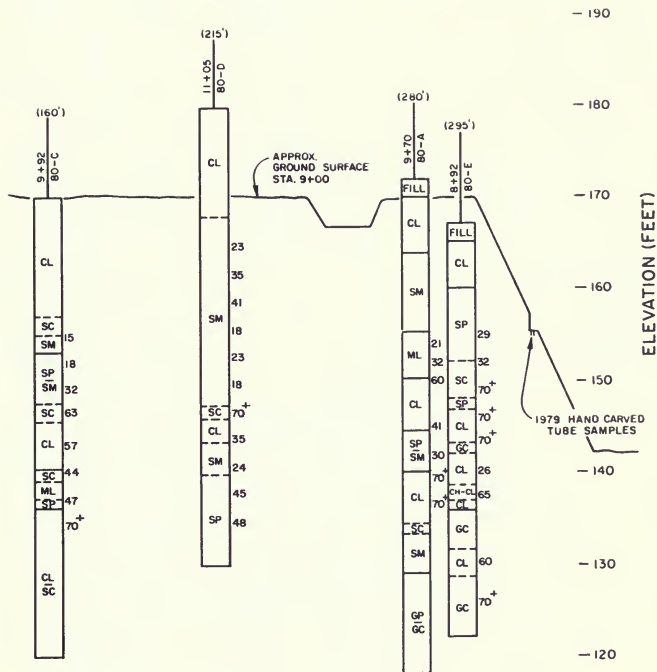
Figure 240. Thermalito Forebay Boring Profile At Station 11 + 50

# LEGEND



Thermalito Forebay  
Boring Profile At The Tail Channel

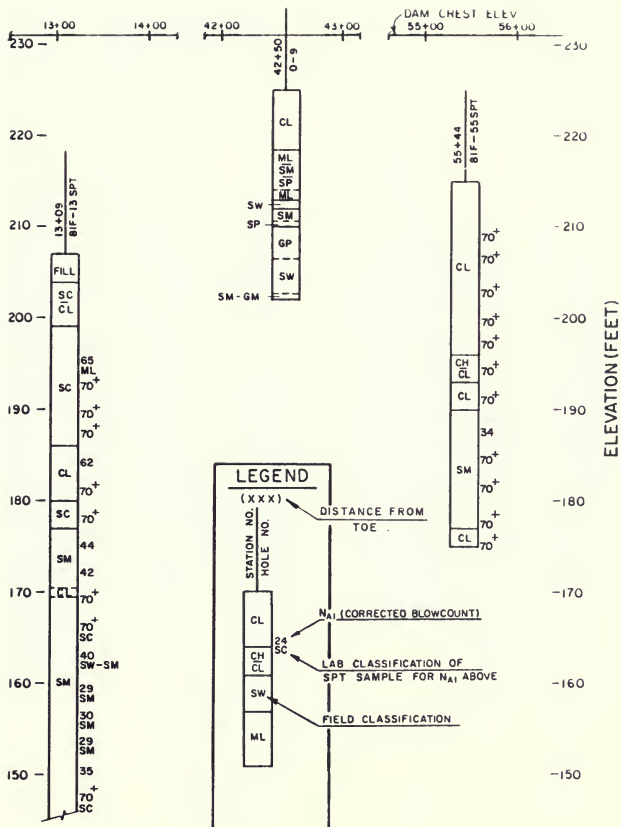




NOTE: FOR LEGEND SEE FIGURE 242

— Main Dam  
 — 11 Area  
 Dam To Tail Channel





Dam Boring Profiles  
Station 56+50

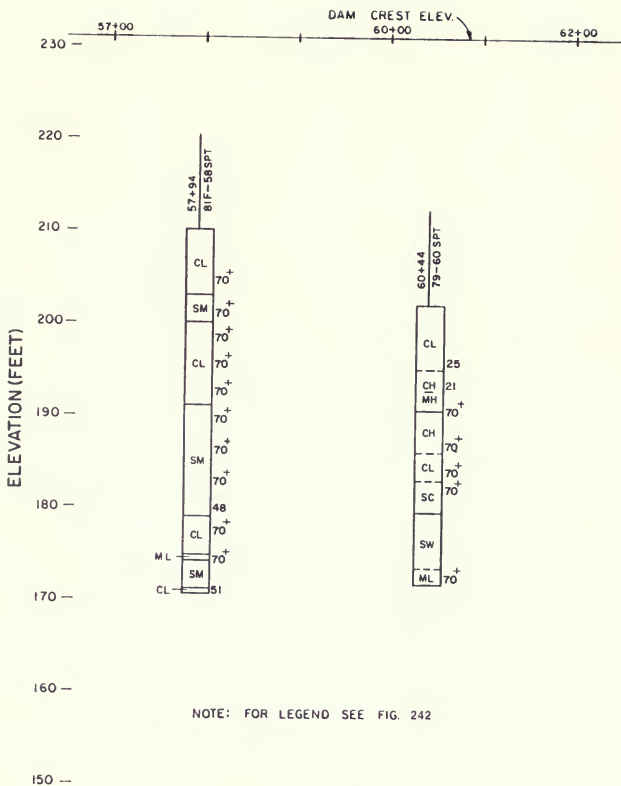


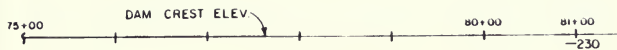
Figure 243. Thermalito Forebay  
Station 56+50 —





- 323 -





-220

-210

-200

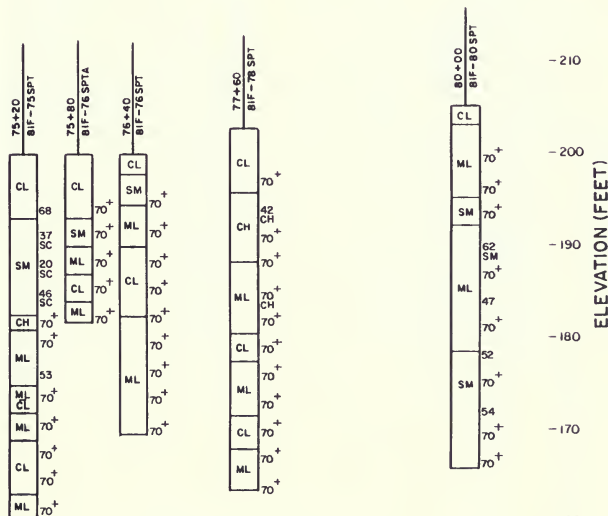
-190

-180

-170

-160

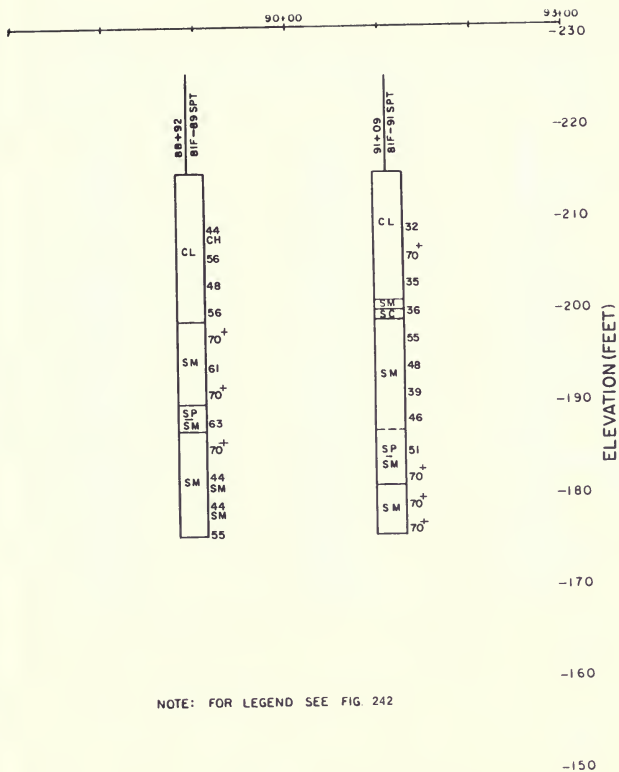
-150



NOTE: FOR LEGEND SEE FIG. 242

Dam Boring Profiles  
Station 81+00





Dam Boring Profiles  
Station 93+00

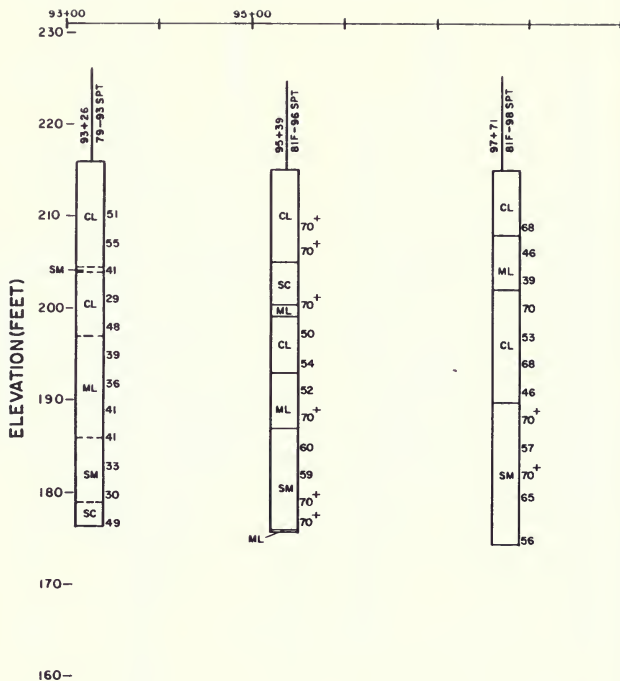
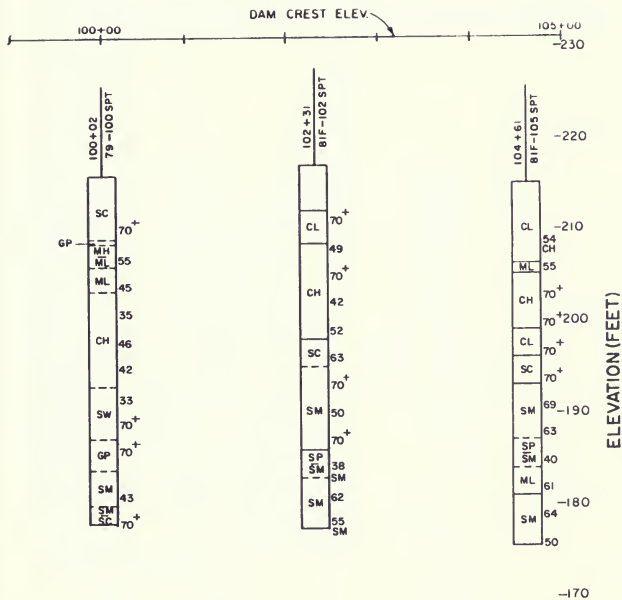


Figure 246. Thermalito Forebay  
Station 93+00 —



NOTE: FOR LEGEND SEE FIG. 242

Dam Boring Profiles  
 Station 105+00

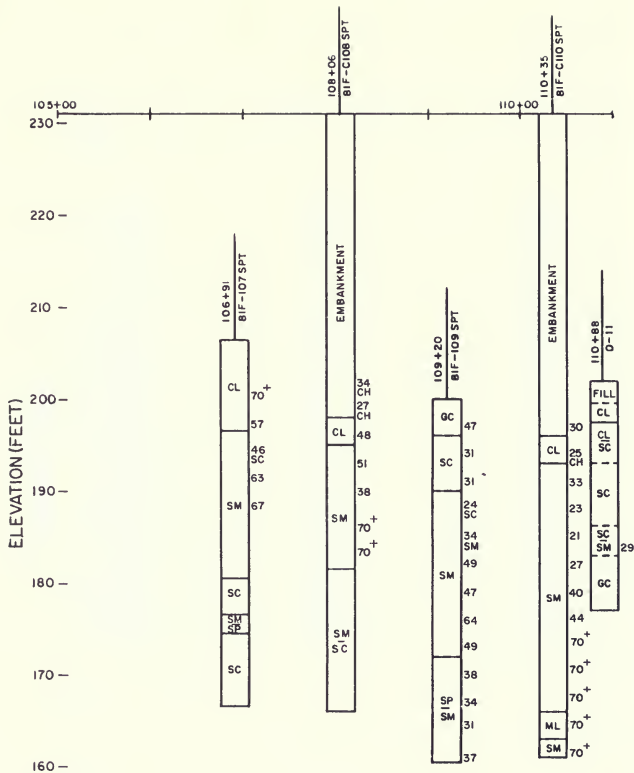


Figure 247. Thermalito Forebay  
Station 105+00 —





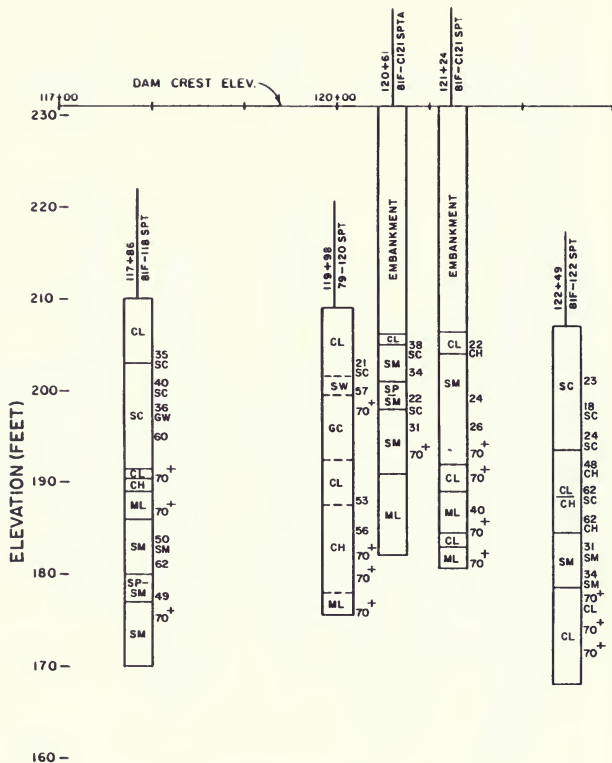
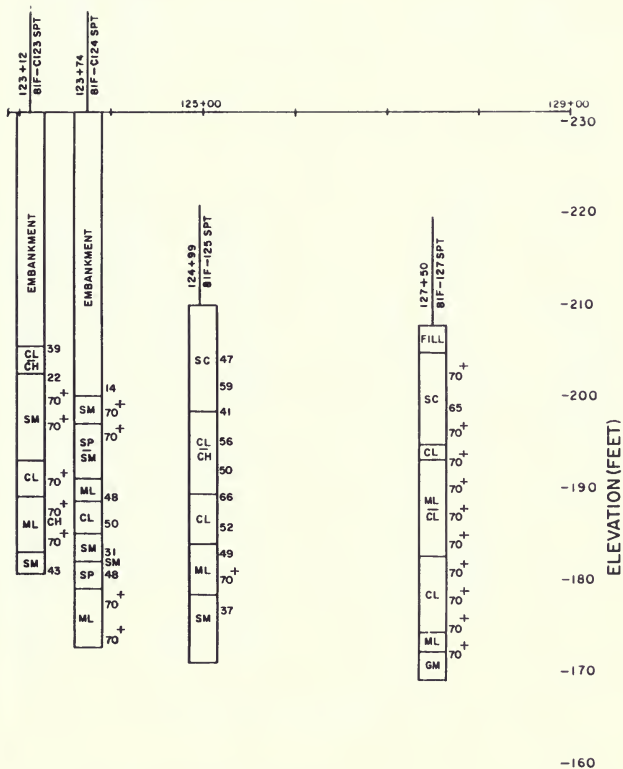


Figure 248. Thermalito Forebay  
Station 117+00 —



Dam Boring Profiles  
Station 129+00

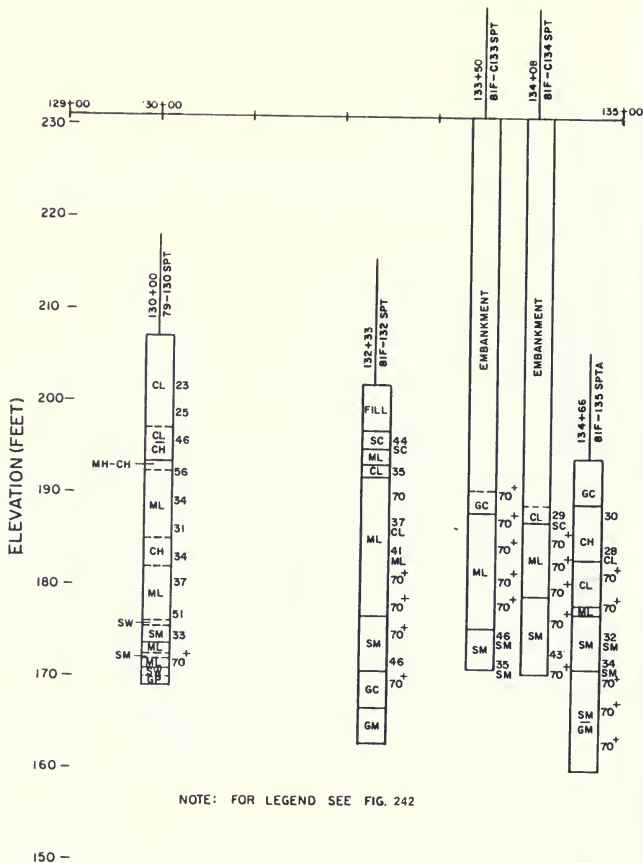
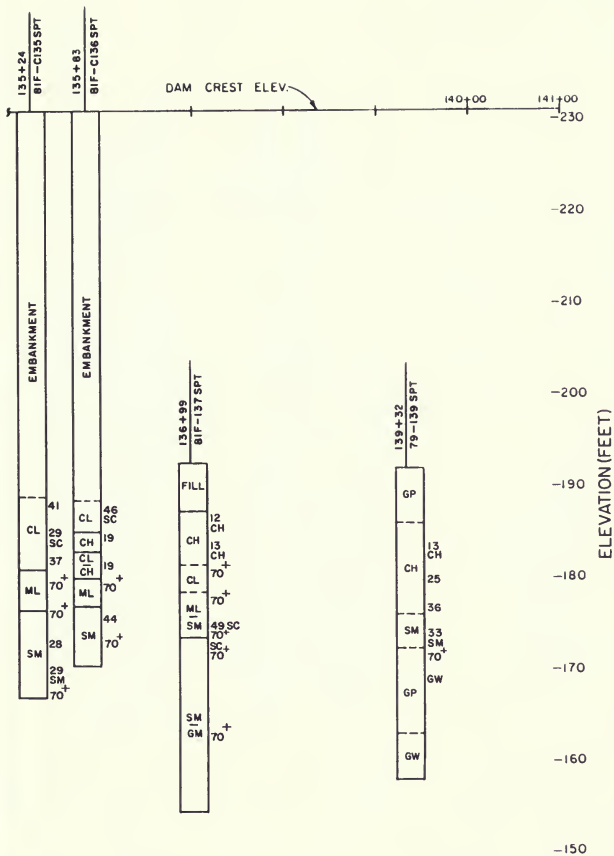


Figure 249. Thermalito Forebay  
Station 129+00 —



Dam Boring Profiles  
Station 141+00

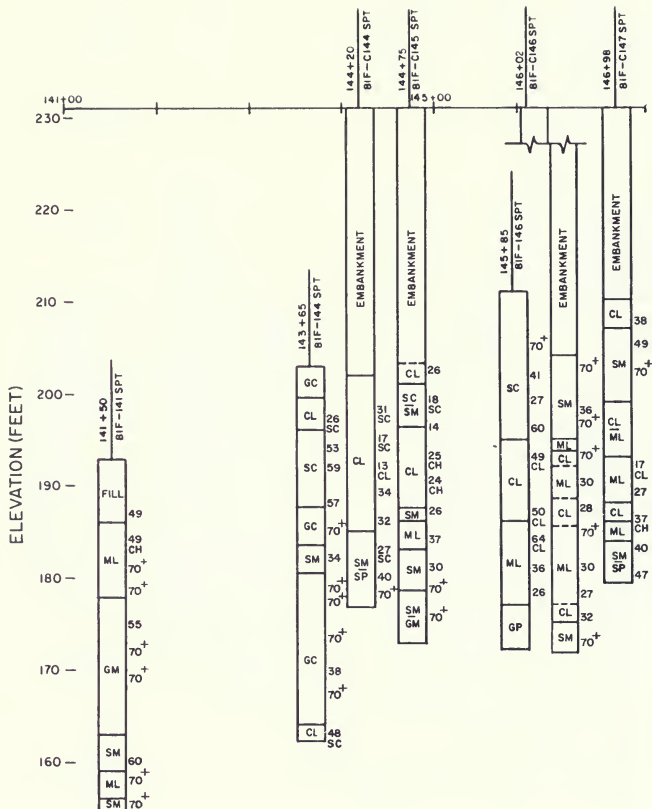
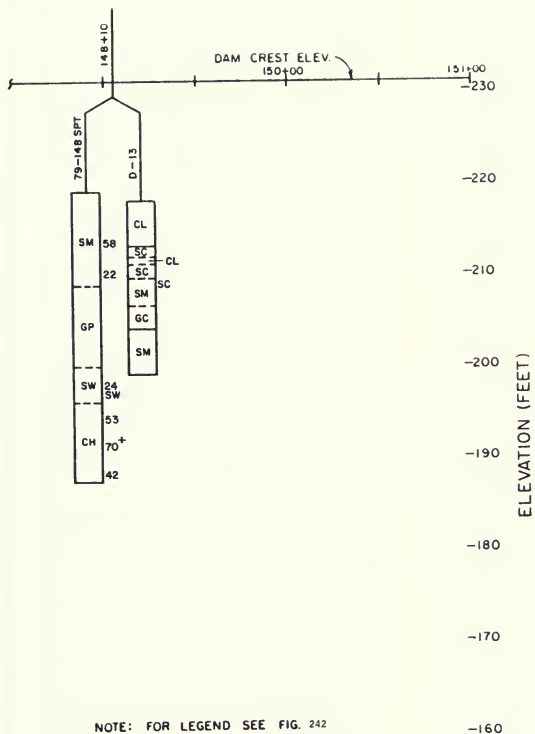


Figure 250. Thermalito Forebay  
Station 141+00 —



Dam Boring Profiles  
Station 151 + 00

Table 47. Suspect Soil Characteristics at 1981-82 Piston Sampling Locations

Soil	Sampling Location	Sampling Depth (feet)	Sampling Elevation (feet)	Mean $N_{A1}$
SM	10 + 00	17 <sup>2</sup>	163	25
(SC)		20	160	28
SM	13 + 00	47 <sup>2</sup>	160	30
(SC)		50	157	30
(SM-SP)		53	154	33
(SM-SW)		56	151	39
SC	68 + 00	9 <sup>2</sup>	191	17
(SC)		12	188	19
SP	74 + 00	12 <sup>2</sup>	180	20
(SC)				
SM	112 + 00	47 <sup>1</sup>	184	26
(SC)		56	175	17
SM	113 + 00	49 <sup>1</sup>	182	27
(SC)		53	178	20
(SC)		56	175	26

Soil classification characteristics within parentheses indicate that the classification was determined from laboratory tests performed on piston samples. Soil classification symbols without parentheses indicate that the classification was determined using field classification techniques applied to SPT samples.

$N_{A1}$  = Blowcounts corrected to 1 tsf effective overburden pressure and corrected for procedural differences.

<sup>1</sup> Denotes depth measured from crest.

<sup>2</sup> Denotes depth measured from downstream toe.

Through long time periods, a considerable thickness consisting of lenses and discontinuous sediments accumulated. Land surface not actively eroded or rapidly buried (temporarily bypassed by the active river channel) was exposed to surface weathering for sufficient time to develop iron-oxide surface staining and local claypans. Subsequent repeated cycles of sediment deposition resulted in the burial of numerous soil horizons within the formation.

Clays and silts are frequently intermixed with more granular sediments, usually derived from more distant sources. The source for much of the fines is more local and is probably supplied from friable formations located uphill from the Forebay. Both the local Ione Formation and volcanic tuffs have provided a significant contribution to the Forebay sediments. The mode of deposition was primarily fluvial but also included significant intermixed



ash falls, mudflows, landslides, and lacustrine deposition. The abundance of soft grains combined with general deep weathering of the Red Bluff commonly results in a granular soil, which, when sufficiently moisturized, becomes plastic upon working between the fingers.

The variety of sediments classified include clays and silts (from nonplastic to high compressibility) sands and fine gravel. Mixed soils are common whereas clean granular soils (those containing less than 5 percent fines) are extremely scarce. Both abrupt and gradational change of soil types occur in short vertical and horizontal distances.

Exploration hole number 79-10 encountered fluvial sediments in the upper 20 feet of the Red Bluff Formation. Below, to a depth of 82 feet, the sediments contained considerable amounts of intermixed clay and gravel. This change in sediment character is attributed to a change in depositional mode with the lower sediments appearing to have been deposited by a combination of mud flows and streams. Because of the mixed grain sizes in this portion of the Red Bluff, it was originally assumed to be a part of the Tuscan Formation, which contains much mudflow material. Recent exploration at the Forebay, with the availability of new samples, has resulted in these sediments being reclassified into the Red Bluff Formation.

Borehole 79-10, the cored 505-foot-deep exploration hole near the Main Dam toe, revealed solid basalt at a depth of 82 feet. Although hard and strong, this volcanic rock was closely to moderately fractured and shattered as a result of movement on the adjacent faults. Two basalt layers and a 9-foot-thick tuff interbed were penetrated by coring. The sampled section is similar to the Middle and Lower Basalt Flows (with included Lower Interflow member) of the Lovejoy Formation, which is located immediately north of Thermalito Powerplant in the Campbell Hills. The cored basaltic section, 177 feet thick, represents a down-faulted block of the strata that comprise the Campbell Hills.

Below the Lovejoy, the core hole encountered 246 feet of Ione Formation—dense clay with numerous silty sand lenses. Organic mudstone, occurring in the upper 18 feet,

originally was identified as a separate formation (Mehrtens) but is now correlated with upper Ione beds of similar lithology found elsewhere in the Sierra foothills.

Comparisons of Red Bluff sediments indicate both similarities and differences in the Main Dam and Low Dam foundations. Lenticular structures and rapid change of material classification in short distances is common to both foundations. At the Main Dam, these soil structures usually occur throughout the surface 30 feet. Underlying sediments are consistently gravelly and are typically deeply weathered and have clay or silt matrices. Sediments in the Low Dam foundation consistently contain clay or clayey sands in the surface 10 to 30 feet. Below the surface clays are usually found weathered silts and sands. Only rarely was gravel encountered in the foundation beneath the Low Dam embankment. The consistent occurrence of fine grained sediments on the surface of the Low Dam foundation is attributed to a sheet-wash deposition or shallow pond filling on an area of low relief.

### General Characteristics of Suspect Soil Sites

Examination of the location where suspect sand layers were found at the Main and Low Dams reveals the complexity of the depositional process. Characteristics of these layers vary considerable both horizontally and vertically. The foundation is generally composed of a 5 to 15-foot thick surface layer of dense clayey sands and clays underlain in places by a layer of relatively loose silty and clayey sand. Below this layer lies a base matrix of dense clays, silts, silty and clayey sands. Of these areas, the site between Stations 111 and 113 contained the lowest and most extensive low blowcount layer.

Table 48 summarizes the characteristics of the 14 sites where suspect sands were found. The exploration program revealed one low blowcount area at the Main Dam between Stations 10 and 11. As shown in Figures 241 and 242, this suspect layer lies generally between Elevations 153 and 165 feet. Along the Low and Ruddy Creek Dams, the explorations discovered 13 sites where low blowcounts were found in silty and clayey sands (see Figures 242 through 250).

Table 48. Suspect Foundation Sites ( $N_{A1} \leq 30$ ) Along Thermalito Forebay Dam

Suspect Site	Borehole No.	Station	Dam Ht. (ft.)	Suspect Material (USCS)	Depth Inter-val (ft.)	Max. Length (ft.)	$N_{A1}$ Range ( $N_{A1} \leq 30$ )	$N_{A1}$ Mean ( $N_{A1} \leq 30$ )	$N_{A1}^*$ Mean All Blows in Depth Interval
Sta. 10-11	81F-10 SPTB	10+09							
	81F-C10 SPT	10+18							
	81F-10 SPT	10+18							
	81F-10 SPTA	10+21							
	79-10	10+24							
	81F-10 SPTC	10+33							
	81F-11 SPTK	10+55							
	81F-11 SPTJ	10+70							
	81F-11 SPTL	10+70	46	SC&SM	20-26	250	12-30	22	25
	81F-11 SPTE	10+84							
	81F-11 SPTB	10+85							
	81F-11 SPTA	10+94							
	81F-11 SPTC	10+97	46	SM	26-31	250	12-30	23	33
	81F-11 SPTF	11+02							
	81F-11 SPT	11+05							
	81F-11 SPTH	11+05							
	81F-C11 SPT	11+18							
	81F-11 SPTG	11+23							
	81F-11 SPTM	11+28							
	81F-11 SPTD	11+33							
Sta. 63	79-60 SPT	60+44	28	CL&CH	0-10	870	10-25	20	20
	81F-63 SPT	62+93							
	81F-65 SPT	65+42							
Sta. 68	81F-67 SPT	66+65	24	SC&SM	7-14	490	17-30	23	28
	81F-67 SPTA	67+28		with					
	81F-68 SPT	67+91		CL&ML					
	81F-68 SPTA	68+41							
	81F-69 SPT	68+91							
Sta. 74	81F-73 SPT	72+80	26	SC	11-15	445	18-25	21	25
	81F-73 SPTA	73+25							
	81F-74 SPTA	73+55							
	81F-74 SPT	73+70							
	81F-C74 SPT	73+70							
	81F-75 SPT1	75+20							
Sta. 93	79-93 SPT	93+26	20	CL	14-16	430	29	29	29
Sta. 109	81F-C108 SPT	108+06	28						
	81F-C110 SPT	110+35							
	81F-109 SPT	109+20		SC/SM	10-15	400	21-24	23	26

Table 48. Suspect Foundation Sites ( $N_{A1} \leq 30$ ) Along Thermalito Forebay Dam (Continued)

Suspect Site	Borehole No.	Station	Dam Ht. (ft)	Suspect Material (USCS)	Depth Inter- val (ft)	Max. Length (ft)	$N_{A1}$ Range ( $N_{A1} \leq 30$ )	$N_{A1}$ Mean ( $N_{A1} \leq 30$ )	$N_{A1}$ * Mean All Blows in Depth Interval
Sta. 112	D-11	110+88	30		6-30	330	11-30	21	21
	81F-C111 SPTA	111+19		SC&SM					
	81F-C111 SPT	111+47		w/some					
	79-112 SPT	111+50		lenses of					
	81F-C112 SPT	111+65		CL&CH					
	84F-C112 SPT	112+00							
	84F-112 SPT	112+00							
	81F-C112 SPTA	112+39							
	84F-113 SPT	112+50							
	81F-C113 SPT	112+56							
	81F-C113 SPTA	112+71							
Sta. 115	81F-114 SPT	113+62	30	SC&SM	5-16	510	12-29	21	27
	81F-C115 SPT	114+68		w/some					
	81F-116 SPT	115+74		ML					
	81F-C117 SPT	116+68							
Sta. 122	79-120 SPT	119+98	30		0-15	710	14-26	22	26
	81F-C121 SPTA	120+61		SC&SM					
	81F-C121 SPT	121+24							
	81F-122 SPT	122+49							
	81F-C123 SPT	123+12							
	81F-C124 SPT	123+74							
Sta. 130	79-130 SPT	130+00	30	CL	0-10	480	23-25	24	24
Sta. 136	81F-C134 SPT	134+08	36	SC, CL	4-14	800	12-30	22	26
	81F-135 SPTA	134+66		& CH					
	81F-C135 SPT	135+24		(Deep	18-25	120	28-29	28	29
	81F-C136 SPT	135+83		SM Lens)					
	81F-137 SPT	136+99							
	79-139 SPT	139+32							
Sta. 145	81F-144 SPT	143+65	30	SC, CL	4-27	450	13-30	22	35
	81F-C144 SPT	144+20		& CH					
	81F-C145 SPT	144+75		w/some					
	81F-146 SPT	145+85		SM					
Sta. 146	81F-146 SPT	145+85	20	ML	20-28	210	17-30	26	26
	81F-C146 SPT	146+02							
	81F-C147 SPT	146+98		ML & CL	29-34	220	26-30	28	30
Sta. 148	79-148 SPT	148+10	12	SM & SW	7-23	200	22-24	23	23

\*70+ blowcounts not included in  $N_{A1}$  average.

-6- Note: Depth intervals measured from foundation surface along downstream toe.

## Installation of Piezometers

Standpipe piezometers were installed at suspect sand sites found at the Main and Low Dams. Table 49 summarizes the locations of piezometers installed during the exploration programs. The locations of piezometers in-

stalled during the explorations at the Main Dam are shown in Figure 261. A typical standpipe piezometer installation is illustrated in Figure 262. The piezometer measurements made at both the Station 10-11 (Main Dam) and Station 112 (Low Dam) areas show that the suspect sands lie beneath the water surface (see Figure 263).

Table 49. Standpipe Piezometers Installed at Thermalito Forebay Dam

Piezometer	Date	Borehole	Station	Location	Ground <sup>1</sup>	Sensing	Tip	Monitoring	
					Surface Elevation (feet)				Elevation (feet)
164	10-14-81	81F-9 SPT A	8+57	20' d/s of Toe	177	110-136	120.0	Capped	---
160	9-11-78	TFS-2	9+55	90' d/s of Toe	170	91.5-110.5	101.0	Capped	---
165	10-27-82	81F-11 SPT B	10+85	15' d/s of Toe	184.5	147.5-161.5	137.0	Capped	---
163	9-22-78	TFS-4B	11+55	51' d/s of Toe	178	145.6-155	150.0	Capped	---
162	9-22-78	TFS-4	11+55	55' d/s of Toe	178	107.5-121	134.0	Capped	---
103	----	----	12+40	70' d/s of Toe	201.5A	----	154.5	Monitored	Semi-Monthly
166	10-22-81	81F-13 SPT C	12+82	28' d/s of Toe	205	144-165	139.0	Capped	---
61	----	----	57+25	60' d/s of Toe	213.6A	----	----	Capped	---
141	----	----	71+40	20' d/s of Toe	207.2A	----	187.8	Monitored	Semi-Monthly
62	----	----	73+00	50' d/s of Toe	211.7A	----	160.7	Capped	---
144	----	----	83+00	5' d/s of Toe	214.1A	----	198.1	Monitored	Semi-Monthly
122	----	----	91+20	5' inside Fence d/s of Toe	216.6A	----	166.5	Monitored	" "
64	----	----	98+05	@ Fenceline @ Toe	221A	----	203.0	Monitored	" "
67	----	----	----	900' s/o Nelson Ave 35' w/o 20th Street	203A	----	166.7	Monitored	" "
65	----	----	109+55	20' d/s of Toe	204.5A	----	162.7	Monitored	" "
102	----	----	----	Southside of Nelson 1075' w/o 16th Street	201.2A	----	149.0	Monitored	" "
112C	6-21-84	84F-C112	112+00	Crest Centerline	231	171.5-192	176.0	Monitored	" "
112T	6-25-84	84F-112 SPT	112+00	@ Toe	201	185.5-199	186.0	Monitored	" "
66	----	----	138+65	20' d/s of Toe	195.8A	----	177.7	Monitored	" "

1 -- values with a Δ symbol next to them indicate a collar elevation which is typically about 3 feet higher than the ground elevation.

Note: Figures 251 through 263 follow. Section 4 begins on page 356.

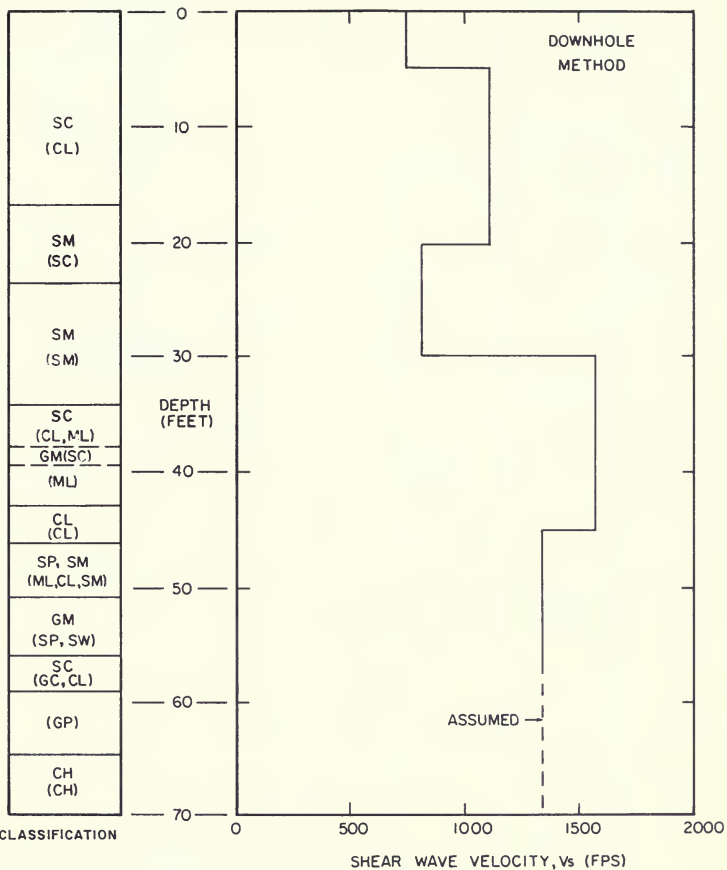


Figure 251. Thermalito Forebay Dam Shear Wave Velocity Test Results - Station 11+50 (Boring TFS - 4)

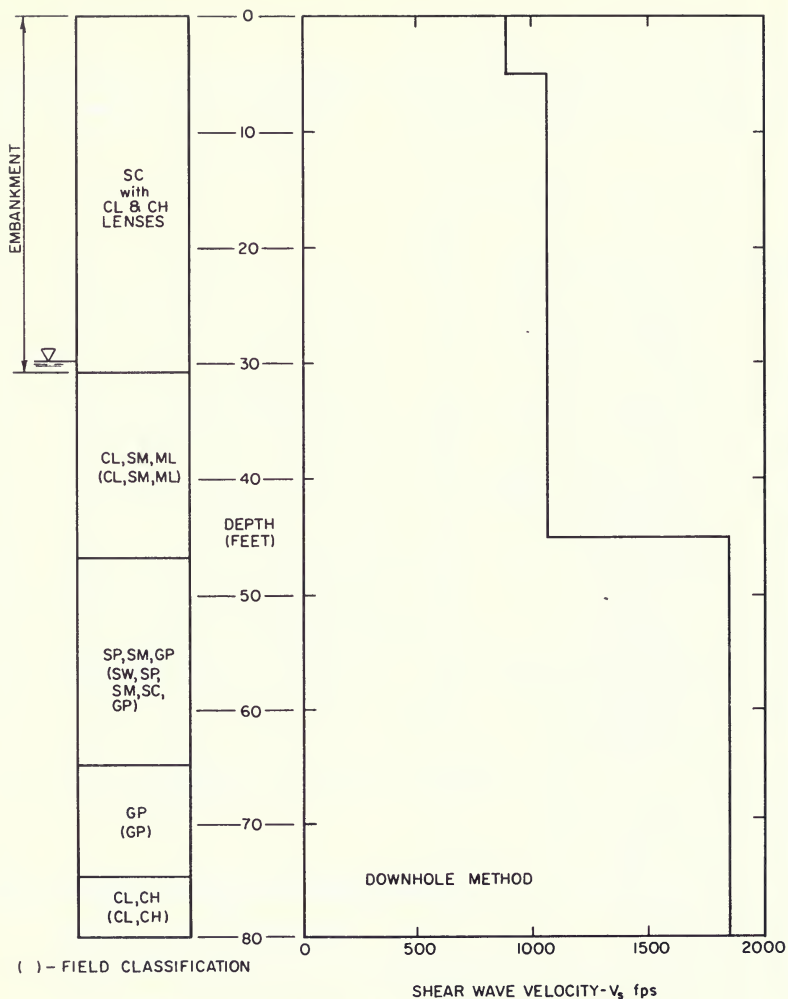


Figure 252. Thermalito Forebay Dam Shear Wave Velocity Test Results - Station 81 + 79 (Boring TFS-3A)

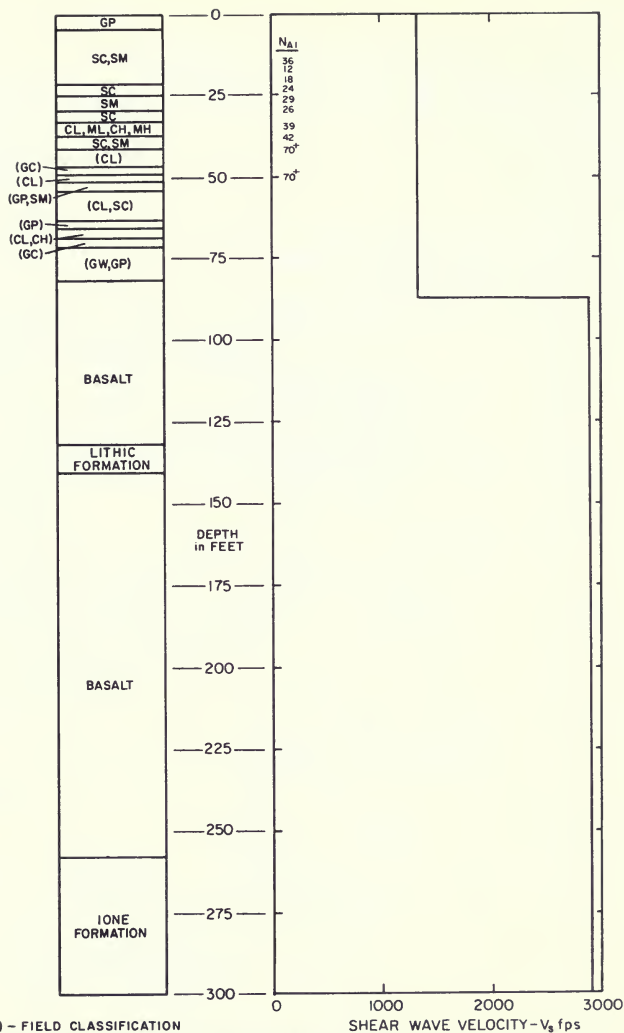


Figure 253. Thermalito Forebay Dam Shear Wave Velocity Test Results - Station 10+00 (Boring 79-10)

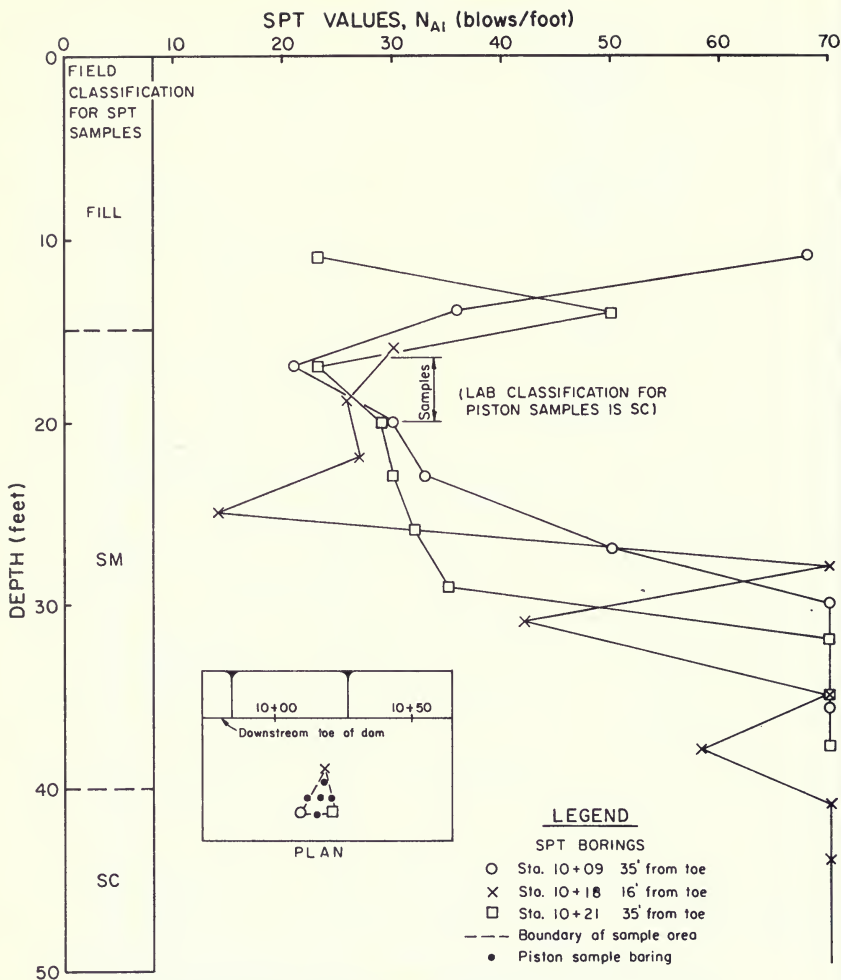
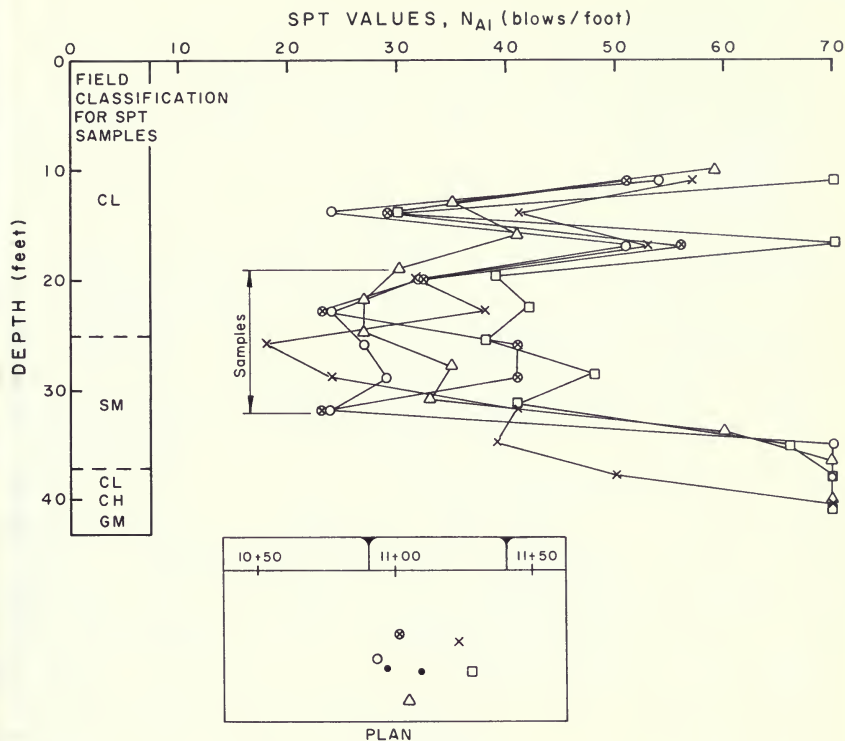


Figure 254. Thermalito Forebay Dam Piston Sampling Site - Station 10+00 Area, Piston Sampling Site





### LEGEND

#### SPT BORINGS

- Sta. 10+94 32' from toe
- ⊗ Sta. 11+02 24' from toe
- × Sta. 11+23 25' from toe
- △ Sta. 11+05 48' from toe
- Sta. 11+28 38' from toe
- Piston sample borings

Figure 255. Thermalito Forebay Dam Piston Sampling Site - Station 11+00 Area, Piston Sampling Site

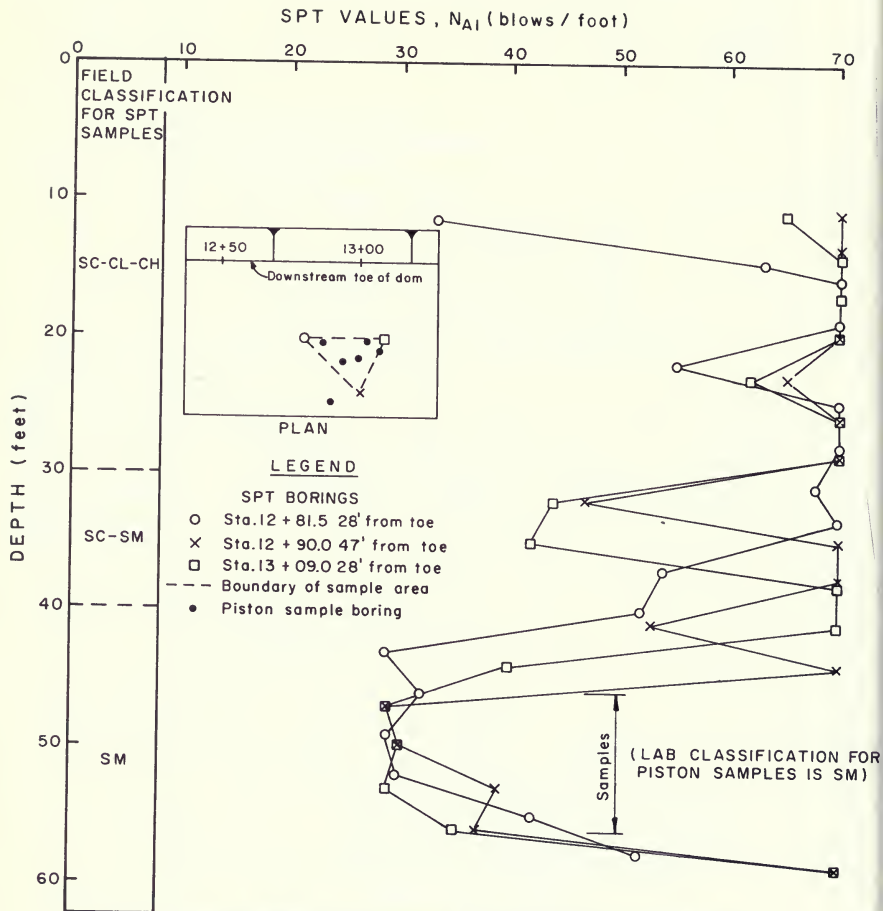


Figure 256. Thermalito Forebay Dam Piston Sampling Site - Station 13 + 00 Area, Piston Sampling Site

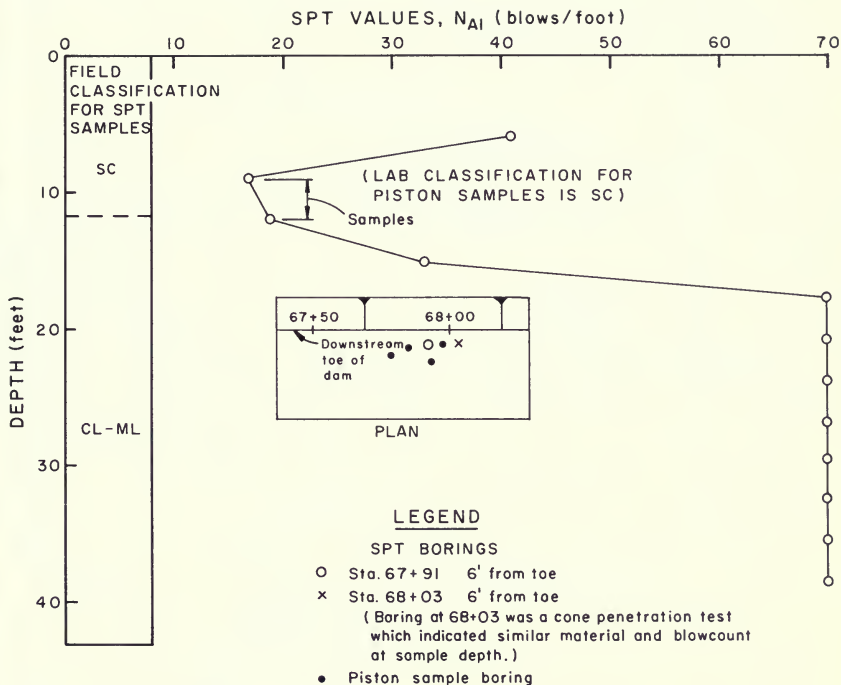
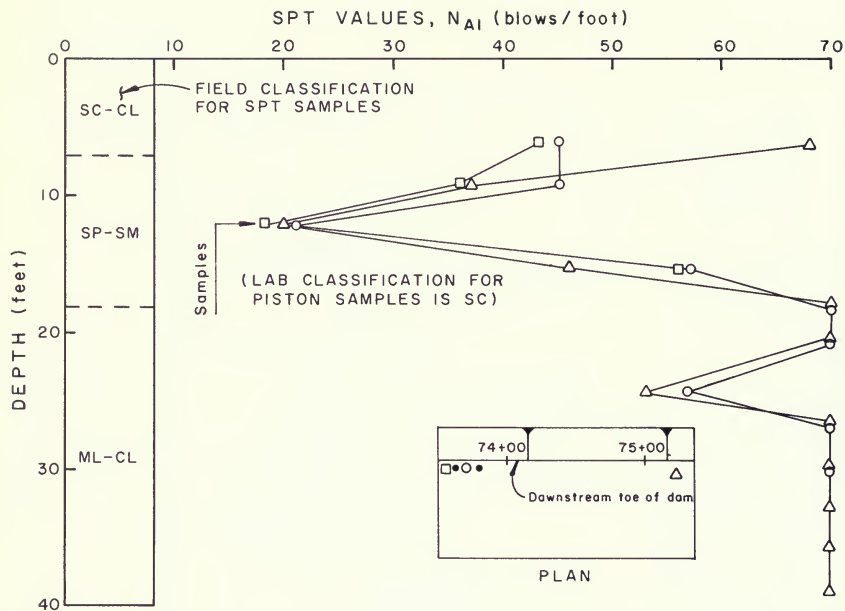


Figure 257. Thermalito Forebay Dam Piston Sampling Site - Station 68+00 Area, Piston Sampling Site



### LEGEND

#### SPT BORINGS

- Sta. 73+55 6' from toe
- Sta. 73+70 6' from toe
- △ Sta. 75+20 6' from toe
- Piston sample boring

Figure 258. Thermalito Forebay Dam Piston Sampling Site - Station 74+00 Area, Piston Sampling Site

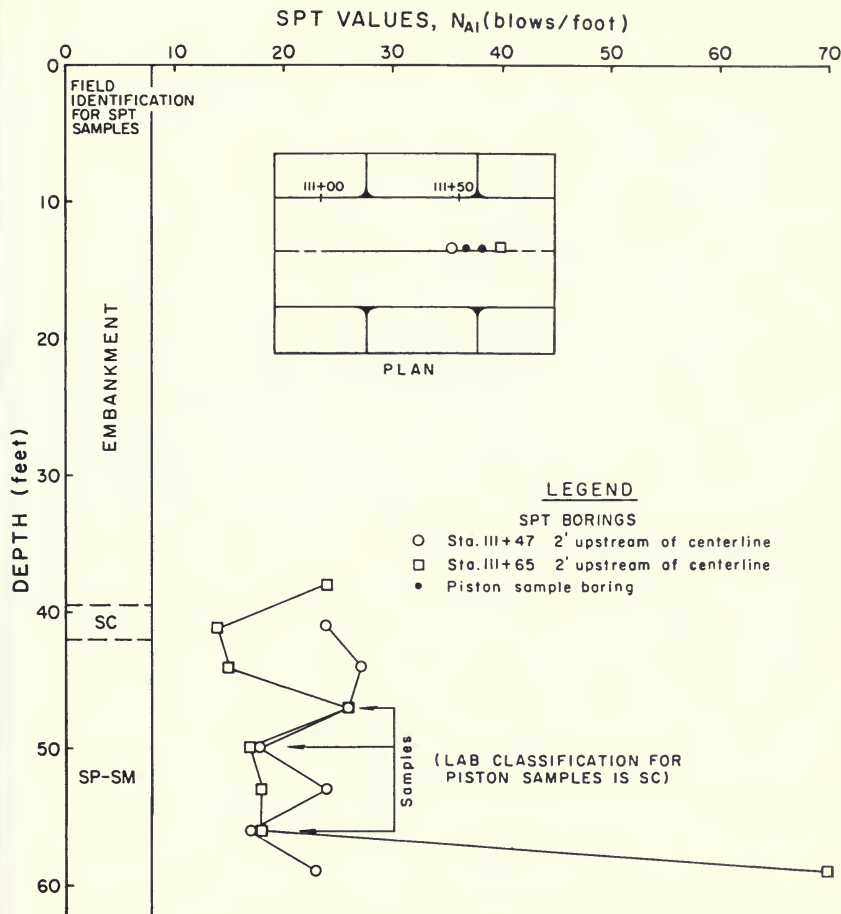


Figure 259. Thermalito Forebay Dam Piston Sampling Site - Station 112+00 Area, Piston Sampling Site

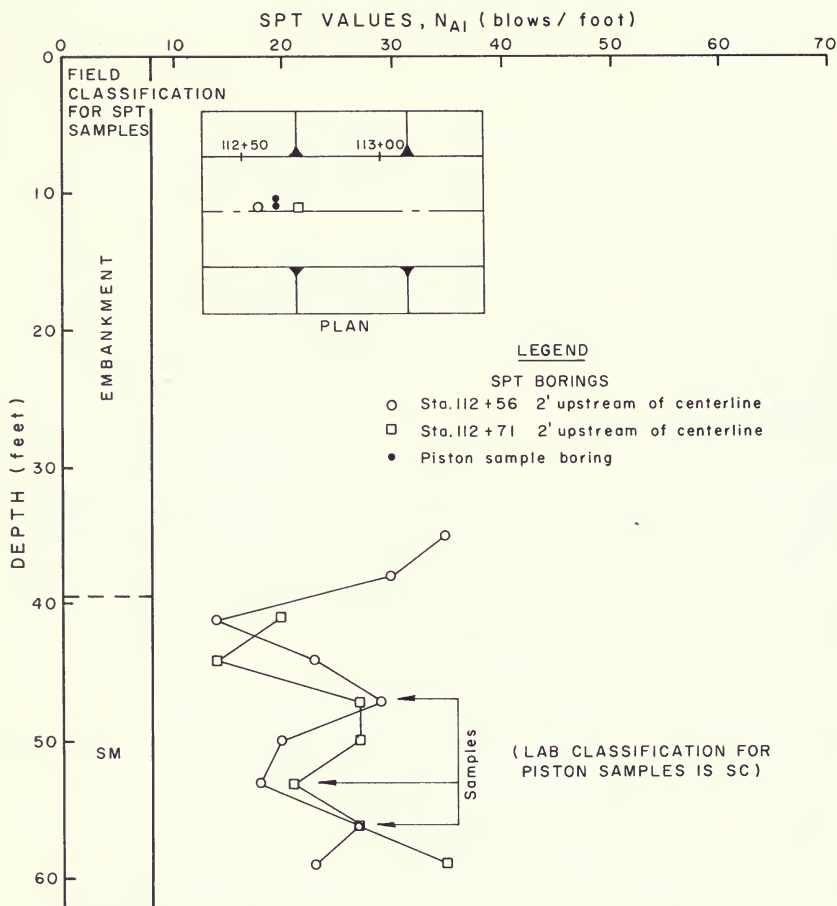


Figure 260. Thermalito Forebay Dam Piston Sampling Site - Station 113+00 Area, Piston Sampling Site

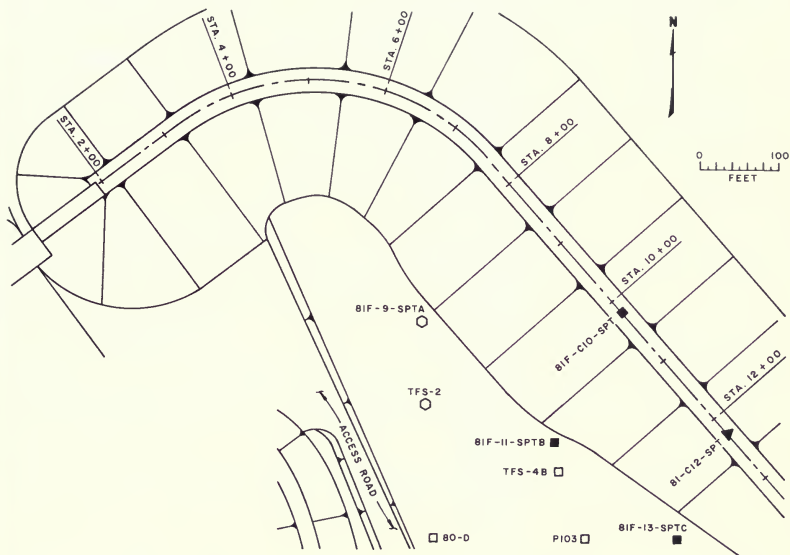


Figure 261. Location of Piezometers Installed at Thermalito Forebay Main Dam

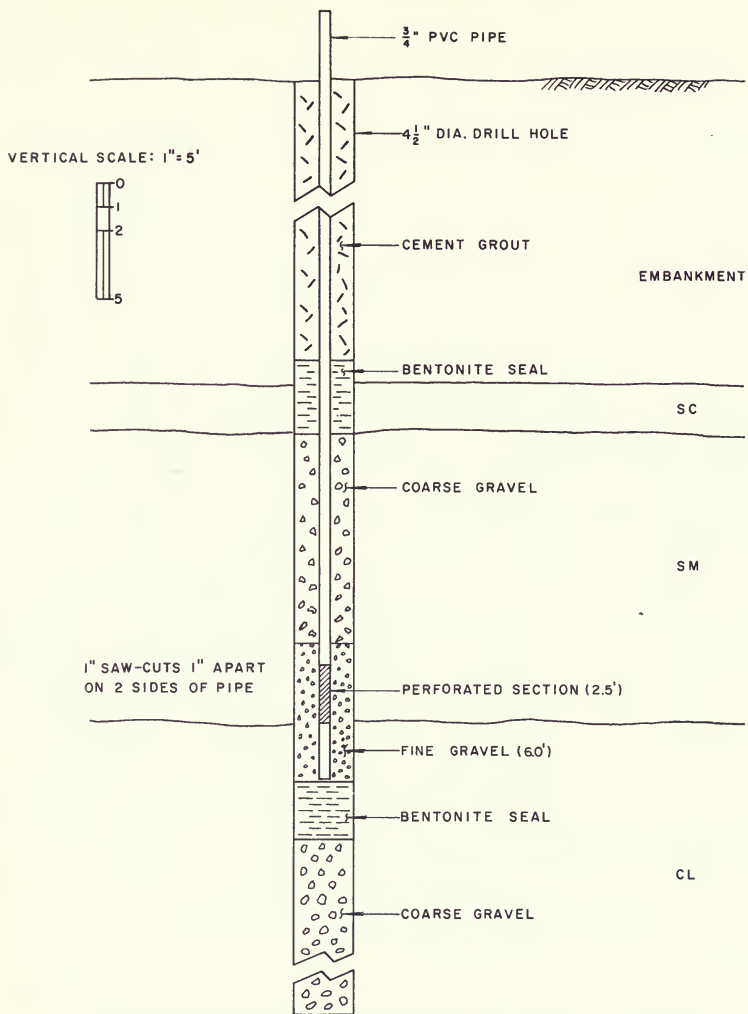


Figure 262. Typical Standpipe Piezometer Installation at Thermalito Forebay Dam Between 1976 and 1984



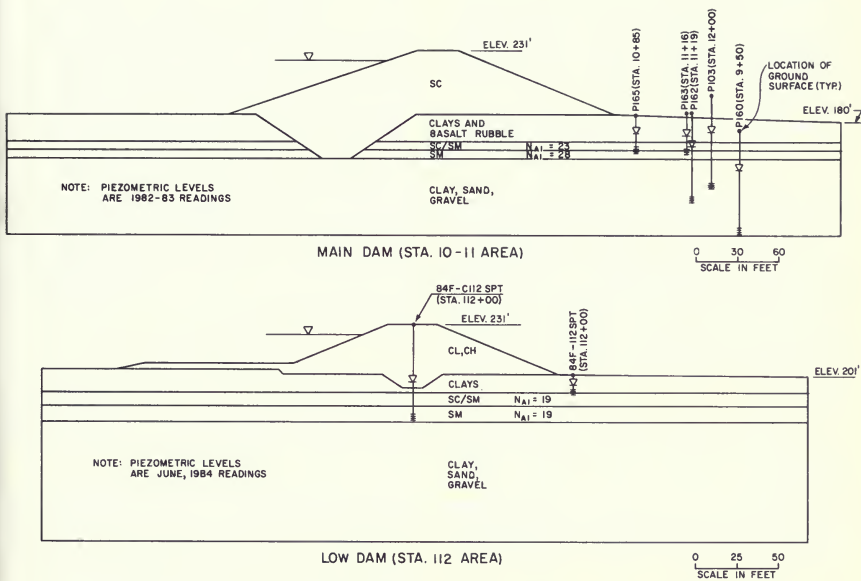


Figure 263. Piezometer Levels Measured at Thermalito Forebay Dam Station 10-11 and 112 Areas

## 4. LABORATORY TESTING AND EVALUATION

### General

Laboratory testing was primarily oriented toward obtaining static and cyclic shear strengths of soils at suspect sites, and to obtain classification data on recovered SPT samples. In some of the later sampling programs, samples were recovered from specific areas and depths in order to correlate laboratory cyclic loading resistances to specific SPT blowcounts. Cyclic and static laboratory shear strength results are summarized in Tables 50 through 52.

### Chronological Summary of Laboratory Testing 1976 Program

This initial testing program provided very preliminary cyclic strength and foundation profile data from eleven samples taken along the Low Dam. These samples were taken in sandy soils ranging from poorly graded to clayey. Sampling was accomplished using a 2.5-inch I.D. DWR thick-walled sampler which is known to cause excessive sample disturbance. Therefore, the cyclic strength data were highly questionable. In addition, the resulting strengths were not related to any specific blowcount value.

A total of six isotropically-consolidated ( $K_c = 1.0$ ) cyclic triaxial tests were performed on the sands at effective confining pressures,  $\sigma'_{3c}$ , of 1.0 and 3.0 ksc (Note: 1 ksc is equal to 1.02 tsf). Classification tests and relative density tests were also performed on the test specimens. Cyclic triaxial test results are presented in Table 50 and in Addendum D.

Classification tests were also performed on five additional tube samples, revealing silty and clayey sands, and well to poorly graded sands.

### 1978 Program

This stage of the investigation attempted to define the foundation soil profile and the cyclic loading resistances of foundation sands at the Main Dam (Station 11 + 55) and at the Low Dam (Station 81 + 80). These sites were chosen as the most likely locations to find extensive sand

layers in the foundation based on previous drilling and on construction information.

Specimens for 11 cyclic triaxial tests were obtained by Pitcher barrel, Shelby push, and piston sampling. These samples were considered less disturbed than those obtained in 1976 using the DWR-thick-walled sampler. However, as with the 1976 samples, the 1978 samples were not related to specific SPT blowcount values. In addition, four out of the five tests performed on specimens from Station 81 + 80 were inadvertently tested at excessively low consolidation pressures (e.g. samples obtained at 57 feet were tested at confining pressures equivalent to 10 to 20 feet of overburden pressure). The six test specimens from Station 11 + 55 were isotropically consolidated to effective confining pressures of 1.0 and 3.0 ksc. None of these test specimens were subjected to Atterberg limit tests to determine if the sands were predominantly silty or predominantly clayey. Results from the cyclic tests performed on Station 11 + 55 specimens are presented in Table 50 and also in Addendum D.

### 1979-1980 Program

The third phase of the investigations attempted to define the foundation soil profile and the cyclic loading resistances of foundation sands between the tail channel and the Main Dam.

Undisturbed hand-carved block and tube samples were obtained from the tail channel cut slope and used for cyclic triaxial testing. Eleven isotropically-consolidated ( $K_c = 1.0$ ) and anisotropically-consolidated ( $K_c = 1.5$ ) tests were conducted at effective confining pressures of 1.0 and 3.0 ksc. Classification tests indicated the materials to be principally well and poorly-graded sands. Cyclic test results are shown in Table 50 and also in Addendum D for tests of both the carved tube samples and of the block samples. It should be noted that the block samples were generally partially cemented sands that are not expected to liquefy.

The sampling locations in the tail channel cut were over 250 feet from the toe of the Main Dam. Five SPT borings (80A through 80E) were drilled in the area between the Main Dam and tail channel. Mechanical analyses from

Table 50. Summary of Cyclic Test Results for Thermalito Forebay Dam Foundation Soils

Testing Program	Site	Depth Interval (feet)	N <sub>A1</sub>	(N <sub>1</sub> ) <sub>60</sub>	$\sigma_{3c}'$ (ksc)	K <sub>c</sub>	5% Axial Strain in 8 cycles $\sigma_{dp}$ (ksc)	5% Axial Strain in 15 cycles $\sigma_{dp}$ (ksc)
1976	D Boreholes	8.5 -- 13.0	--	--	1.0	1.0	1.05	0.95
1976	D Boreholes	8.5 -- 15.0	--	--	3.0	1.0	2.22	2.07
1978	TFS-4	28.0 -- 30.0	--	--	1.0	1.0	0.68	0.60
1978	TFS-4	25.5 -- 29.0	--	--	3.0	1.0	1.53	1.42
1979-80	Hand-Carved	0. -- 3.	--	--	1.0	1.0	0.79	0.71
1979-80	Tail Channel	0. -- 3.	--	--	1.0	1.5	0.87	0.83
1979-80	Samples	0. -- 3.	--	--	3.0	1.0	1.76	1.56
1981-82	Station 10	16.0 -- 17.5	25	--	1.0	1.0	1.32	1.16
1981-82	Station 10	16.0 -- 17.5	25	--	1.0	1.5	0.98	0.88
1981-82	Station 10	16.0 -- 17.5	25	--	3.0	1.0	2.36	2.22
1981-82	Station 10	19.0 -- 20.5	28	--	1.0	1.0	1.16	1.02
1981-82	Station 10	19.0 -- 20.5	28	--	1.0	2.0	1.10	1.00
1981-82	Station 10	19.0 -- 20.5	28	--	3.0	1.0	1.95	1.83
1981-82	Station 13	46.0 -- 51.0	30	--	1.75	1.0	0.93	0.83
1981-82	Station 13	46.0 -- 51.0	30	--	2.0	1.0	1.41	1.19
1981-82	Station 13	46.0 -- 51.0	30	--	3.0	1.5	2.36	2.25
1981-82	Station 13	46.0 -- 51.0	30	--	4.0	1.0	2.36	2.18
1981-82	Station 13	52.0 -- 54.0	33	--	1.75	1.0	1.85	1.58
1981-82	Station 13	52.0 -- 54.0	33	--	2.0	1.0	1.96	1.69
1981-82	Station 13	52.0 -- 54.0	33	--	2.0	1.5	1.70	1.48
1981-82	Station 13	52.0 -- 54.0	33	--	2.0	2.0	2.12	1.83
1981-82	Station 13	52.0 -- 54.0	33	--	4.0	1.0	2.36	2.18
1981-82	Station 13	55.0 -- 56.5	39	--	2.0	1.0	2.22	1.85
1981-82	Station 13	55.0 -- 56.5	39	--	4.0	1.0	3.47	3.30
1981-82	Station 68	8.0 -- 17.5	17	--	0.6	1.0	1.05	0.90
1981-82	Station 68	11.0 -- 12.5	19	--	0.6	1.0	1.05	0.94
1981-82	Station 68	11.0 -- 12.5	19	--	1.0	1.0	1.14	1.06
1981-82	Station 74	11.0 -- 12.5	20	--	0.6	1.0	0.81	0.67
1981-82	Station 112	46.0 -- 52.0*	17, 26	--	2.0	1.0	1.27	1.13
1981-82	Station 112	46.0 -- 51.0*	26	--	2.0	1.25	1.51	1.41
1981-82	Station 113	48.0 -- 57.0*	20, 27	--	2.0	1.0	1.53	1.39
1981-82	Station 113	55.0 -- 57.0*	27	--	2.0	2.0	1.97	1.85
1984	Station 112	8.0 -- 10.0	--	--	0.6	1.0	0.93	0.80
1984	Station 112	8.0 -- 10.0	--	--	1.0	1.0	1.00	0.88
1984	Station 112	11.0 -- 13.0	--	--	1.0	1.0	0.72	0.62
1984	Station 112	41.0 -- 51.0	--	--	3.0	1.0	2.14	2.00

Note: All depth intervals are measured from surface of foundation downstream of the dam except for depth intervals marked with an "\*" which are measured from the crest of the dam.

The use of axial strain is in terms of single amplitude values.

**Table 51. Drained Static Shear Strength Summary**

PROGRAM	1984	DESIGN
Failure Criteria	Maximum Obliquity or 5 percent strain, whichever occurs first	Maximum Obliquity or 5 percent strain, whichever occurs first
Failure Stress Conditions	Mohr Circle	Mohr Circle
Station 10-11 Embankment	C' = 0.0 ksc $\phi'$ = 37 deg.	C' = 0.0 ksc $\phi'$ = 33 deg.
Station 112 Embankment	C' = 0.2 ksc $\phi'$ = 26 deg.	C' = 0.15 ksc $\phi'$ = 30 deg.
Clayey Foundation Cap	C' = 0.2 ksc $\phi'$ = 31 deg.	C' = 0.2 ksc $\phi'$ = 32 deg.
Suspect Foundation SC/SM	C' = 0.0 ksc $\phi'$ = 31 deg.	C' = 0.2 ksc $\phi'$ = 32 deg.

**Table 52. Undrained Static Shear Strength Summary**

PROGRAM	1984						DESIGN
Failure Criteria	Peak Deviator Stress or 5 % axial strain whichever occurs first		Peak Deviator Stress or 10 % axial strain whichever occurs first		Peak Deviator Stress or 15 % axial strain whichever occurs first		Peak Deviator Stress or 20 % axial strain whichever occurs first
Failure Stress Conditions	Mohr Circle	$\tau_{ff}$ vs. $\sigma'_{fc}$	Mohr Circle	$\tau_{ff}$ vs. $\sigma'_{fc}$	Mohr Circle	$\tau_{ff}$ vs. $\sigma'_{fc}$	Mohr Circle
Station 10-11 Embankment	C = 0.2 ksc $\phi$ = 21 deg.	C = 0.4 ksc $\phi$ = 21 deg.	C = 0.3 ksc $\phi$ = 21 deg.	C = 0.4 ksc $\phi$ = 25 deg.	C = 0.4 ksc $\phi$ = 22 deg.	C = 0.4 ksc $\phi$ = 28 deg.	C = 0.4 ksc $\phi$ = 16 deg.
Station 112 Embankment	C = 0.5 ksc $\phi$ = 12 deg.	C = 0.5 ksc $\phi$ = 15 deg.	C = 0.5 ksc $\phi$ = 15 deg.	C = 0.5 ksc $\phi$ = 19 deg.	C = 0.6 ksc $\phi$ = 13 deg.	C = 0.6 ksc $\phi$ = 17 deg.	--
Clayey Foundation Cap	C = 0.2 ksc $\phi$ = 23 deg.	C = 0.3 ksc $\phi$ = 26 deg.	C = 0.4 ksc $\phi$ = 21 deg.	C = 0.5 ksc $\phi$ = 24 deg.	C = 0.5 ksc $\phi$ = 18.5 deg.	C = 0.6 ksc $\phi$ = 22 deg.	C = 1.0 ksc $\phi$ = 15 deg.
Suspect Foundation SC/SM	C = 0.1 ksc $\phi$ = 20 deg.	C = 0.1 ksc $\phi$ = 26 deg.	C = 0.2 ksc $\phi$ = 20 deg.	C = 0.2 ksc $\phi$ = 25 deg.	C = 0.2 ksc $\phi$ = 20 deg.	C = 0.2 ksc $\phi$ = 26 deg.	C = 1.0 ksc $\phi$ = 15 deg.

these borings (23 samples) indicated mostly well graded to poorly graded sands.

### 1981-1982 Program

#### Introduction

The purpose of this testing program was to determine the material types in the Red Bluff alluvium and the cyclic loading resistances of low blowcount foundation sands. The testing program included mechanical analysis, Atterberg limits, specific gravity, and cyclic triaxial tests. All

tests were run at the DWR soils laboratory using standard DWR test procedures.

#### Classification Testing - Red Bluff Sediments

Gradation tests were performed on all samples obtained by the SPT split-spoon sampler but Atterberg limits tests were generally only performed on low blowcount samples (i.e.  $N_{A1} < 30$ ). Samples were obtained from a maximum foundation depth of 68 feet at the Main Dam and 40 feet at the Low Dam. Laboratory classifications (for samples with Atterberg limits tests) are shown on the foundation

soil profiles presented in Figures 242 through 250. As discussed in Section 3, the foundation at suspect sites generally consists of a 5- to 15-foot layer of clays and clayey sands underlain by a 5- to 25-foot thick layer of low blowcount silty and clayey sands. Below the suspect sands exists a 50- to 80-foot base matrix of dense clays, silty and clayey gravels, and silty and clayey sands.

### Classification Testing – Low Blowcount Foundation Sands

Mechanical analysis and Atterberg Limits tests were performed on most low blowcount SPT samples. Generally, these samples were classified as silty or clayey sands. Figures 264 and 265 show that the range of gradations for

SPT samples of low blowcount silty sands and clayey sands are similar for the two most critical suspect sites at the Main Dam and the Low Dam.

Field classifications for most of the low blowcount SPT samples were generally silty sand. However, more than half the soils that were field classified as silty sand turned out to be clayey sand by laboratory tests (Atterberg limits tests). This discrepancy is attributed to two causes. First, considerable experience, practice and checking are necessary to differentiate silty sands from clayey sands in the field. Second, many of the sands encountered were tuffaceous and/or weathered, and would become much finer and more clayey under strong finger pressure. Laboratory sample preparation, drying, grinding and rewetting would

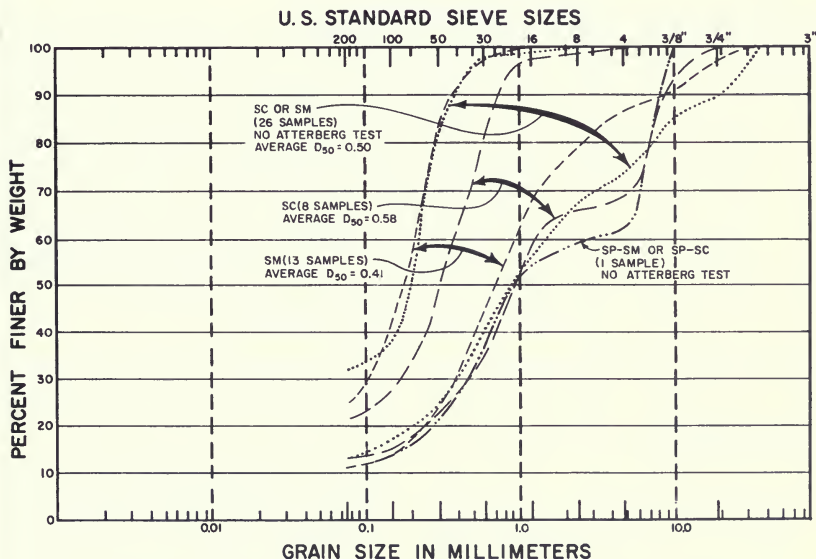
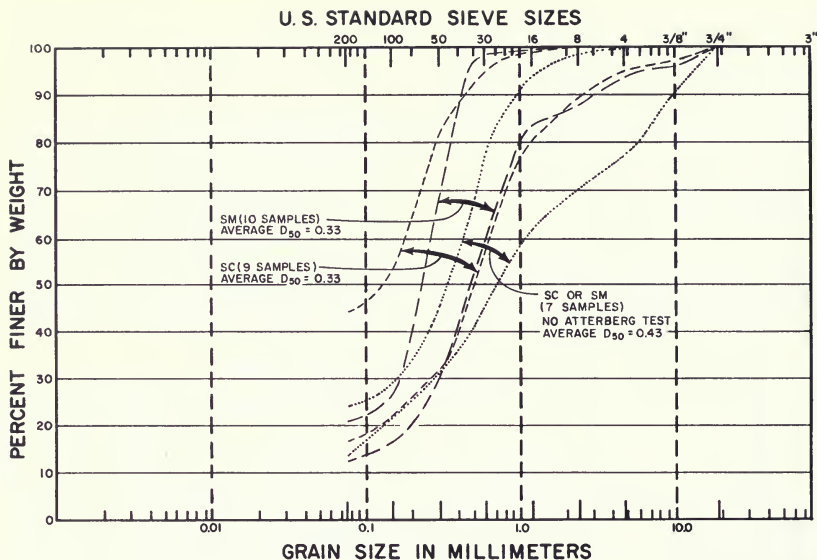


Figure 264. Summary of Gradations for SPT Samples Obtained from the Suspect Foundation Sands at the Thermalito Forebay Main Dam—Station 10-11 Area



CLAY OR SILT FINES	SAND			GRAVEL	
	FINE	MEDIUM	COARSE	FINE	COARSE

Figure 265. Summary of Gradations for SPT Samples Obtained from the Suspect Foundation Sands at the Thermalito Forebay Main Dam - Station 112 Area

cause particle breakage, more fines, and greater plasticity.

### Cyclic Triaxial Testing - Low Blowcount Foundation Sands

Cyclic triaxial tests were performed on low blowcount sands in an attempt to define their resistances to cyclic loading. As stated in Section 3, the 1981-1982 cyclic tests were organized to establish a relationship between SPT blowcount and laboratory test results.

Cyclic triaxial tests were performed on 37 clayey sand and 24 silty sand samples. The clayey sand samples represented  $N_{A1}$  values of 16 to 29 and the silty sand samples

represented  $N_{A1}$  values of 30 to 39, as shown in Table 47. For the same sampling zone, Figures 266 through 272 show that the gradation and plasticity of the piston samples were similar to those of the SPT samples.

Each six-inch-long cyclic triaxial test specimen was obtained from fixed piston tube samples. A maximum of two samples was obtained from each tube. Each test specimen was saturated to obtain a pore pressure parameter  $B$  of at least 0.95. This was obtained except for a few of the clayey samples, where a  $B$  of only 0.91 could be achieved. Consolidation pressures ranged from 0.6 to 4.0 ksc. Each specimen was consolidated to at least the overburden pressure which it was under in the field. Both isotropic and anisotropic tests ( $K_c = 1.0$  to 2.0) were performed to

simulate level ground and sloping ground conditions. Typical traces of cyclic tests for clayey sands and silty sands with SPT  $N_{A1}$  blowcounts of about 30 are shown in Addendum D. Classification tests were performed on the samples after each triaxial test. Cyclic triaxial test results are presented in Table 50 and also in Addendum D.

## 1984 Program

### General

In June 1984, a supplemental sampling program was carried out at the suspected critical sites, Station 10-11 and Station 112. As related in Section 3, tube samples were

obtained from the embankment, clayey foundation cap, and low blowcount clayey sand/silty sand layer.

Additional cyclic triaxial tests were performed on eight specimens from the low blowcount clayey sand at Station 112 (Table 50 and Addendum D). Static triaxial compression tests were also carried out for the clayey embankment and foundation cap soils from the Station 10-11 and Station 112 areas. Additional triaxial compression and post-cyclic triaxial compression tests were performed on specimens of suspect foundation soil from the Station 112 site.

### Static Triaxial Compression Tests

All static triaxial compression tests were performed on saturated, isotropically-consolidated specimens. Speci-

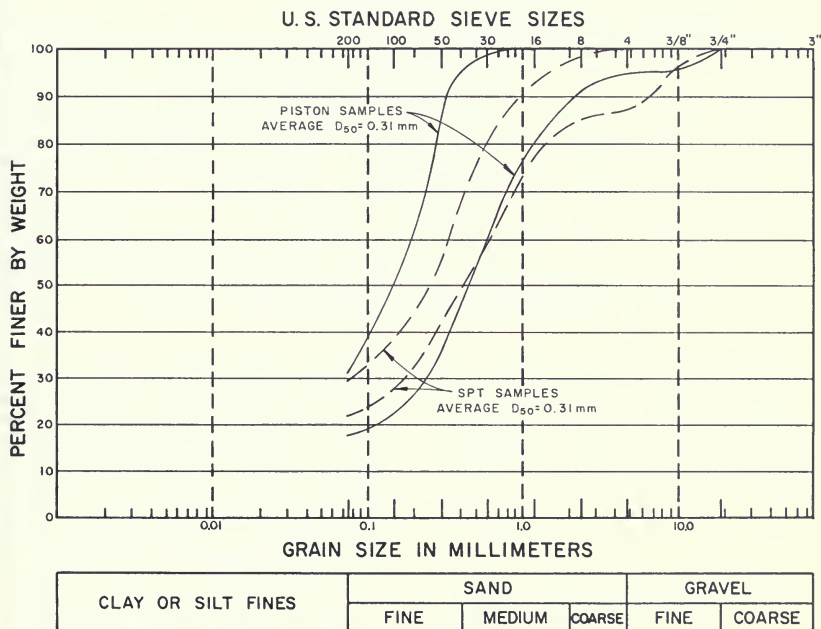
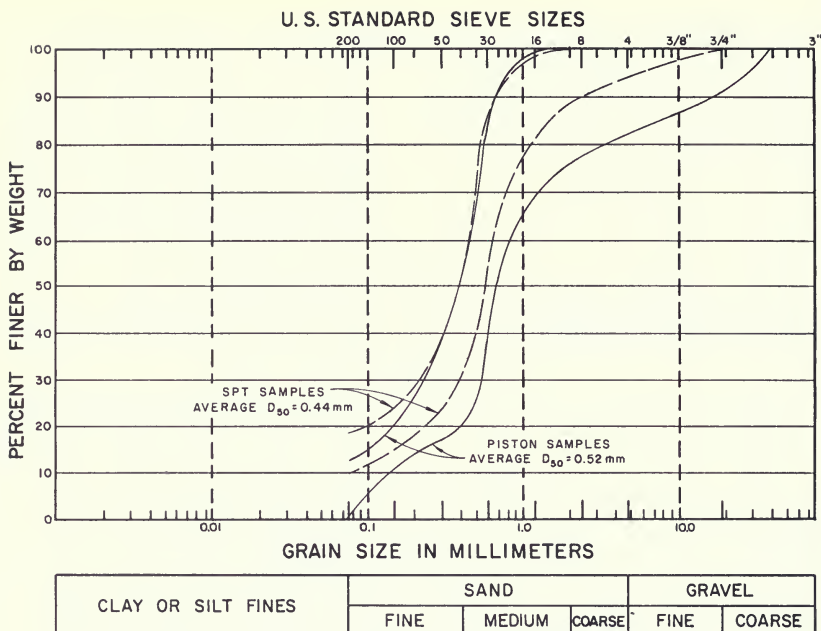


Figure 266. Comparison of Gradations Determined for Piston and SPT Samples Obtained at the Thermalito Forebay Dam Station 10 Sampling Site





*Figure 267. Comparison of Gradations Determined for Piston and SPT Samples Obtained at the Thermalito Forebay Dam Station 13 Sampling Site*

mens were sheared without allowing drainage and with pore pressure measurements. Drained or effective stress strength parameters were obtained using maximum obliquity,  $(\sigma'_1 / \sigma'_3)_{\max}$ , as a failure criterion. Maximum obliquity usually occurred between 2 and 3 percent axial strain.

Undrained strength parameters depended both on the amount of axial strain adopted to define failure (i.e. 5%, 10%, 15% or 20%), and on whether Mohr circle relationships or  $\tau_{ff}$  vs.  $\sigma_{fc}$  relationships were used to define stress relationships.

Figures 273 through 288 present the results from the tri-axial compression test results for specimens of embankment soil, clayey foundation cap, and suspect SC/SM foundation soil obtained from the two critical sites. Static drained test results are shown in the form of Mohr circles in Figures 274, 278, 282, and 286. Undrained strength results are presented in several figures for 5, 10, and 15% axial strain failure criteria and for both Mohr circle and  $\tau_{ff}$  vs.  $\sigma_{fc}$  stress relationships. Tables 51 and 52 summarize the undrained and drained strength results obtained for the different soils tested. Also shown in the tables are the strengths employed during design. In general, the strengths determined in the current study are comparable to, or less than, those employed during design.



## Post-Cyclic Triaxial Tests

Post-cyclic triaxial compression tests were performed on the 1984 cyclic triaxial test specimens of suspect soil from the Station 112 site. These test were performed in an attempt to determine the residual shear strength of the suspect soil should it ever liquefy. All eight specimens were isotropically-consolidated specimens that had been cycled to reach a double amplitude axial strain value of 20 percent. After the loading cycles had been stopped, the specimens were then slowly loaded with increasing axial stress until the specimens reached an axial compression strain of 20 percent. The test data for the post-cyclic loading of the eight specimens are reproduced in Figure 289.

Figure 289 shows that the residual strength of these specimens increases with increased strain. To calculate the residual shear strength, the critical shear resistance was assumed to be on the 45 degree plane within the sample. Accordingly, the residual shear resistance was determined by taking half of the deviator stress for each particular strain level of interest. Because the resistances were relatively low, the test strengths were reduced to account for membrane strength effects. Figure 290 presents the average residual shear resistance for 4 specimens initially consolidated to 3 ksc together with the average resistance for 4 specimens initially consolidated to either 0.6 or 1.0 ksc.

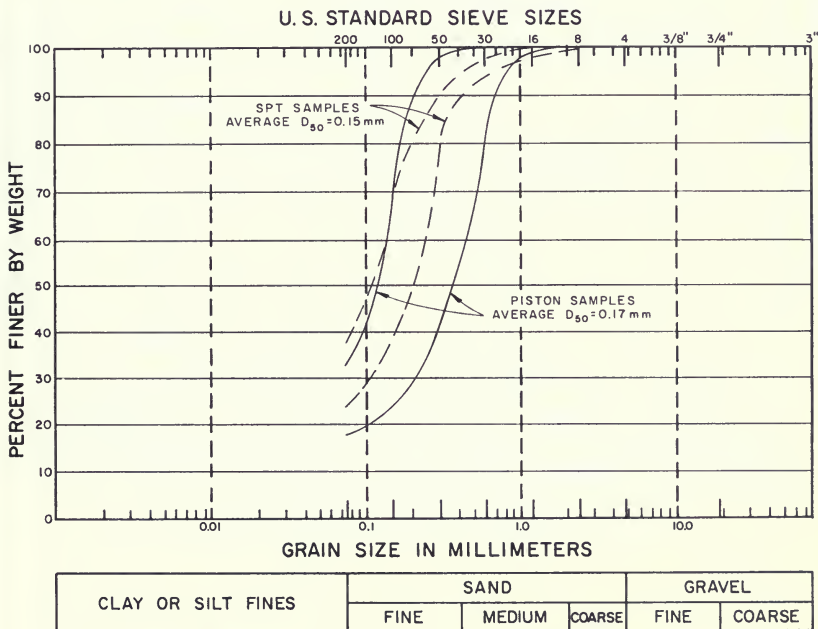
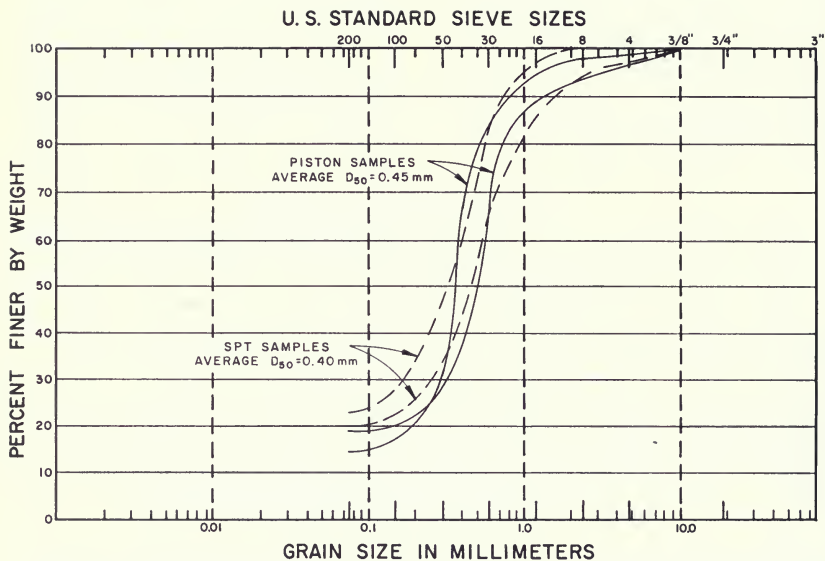
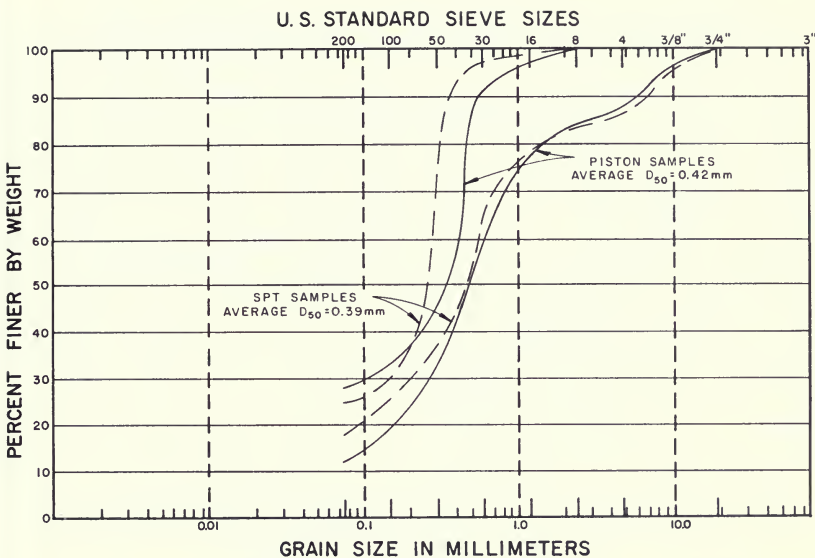


Figure 268. Comparison of Gradations Determined for Piston and SPT Samples Obtained at the Thermalito Forebay Dam Station 68 Sampling Site



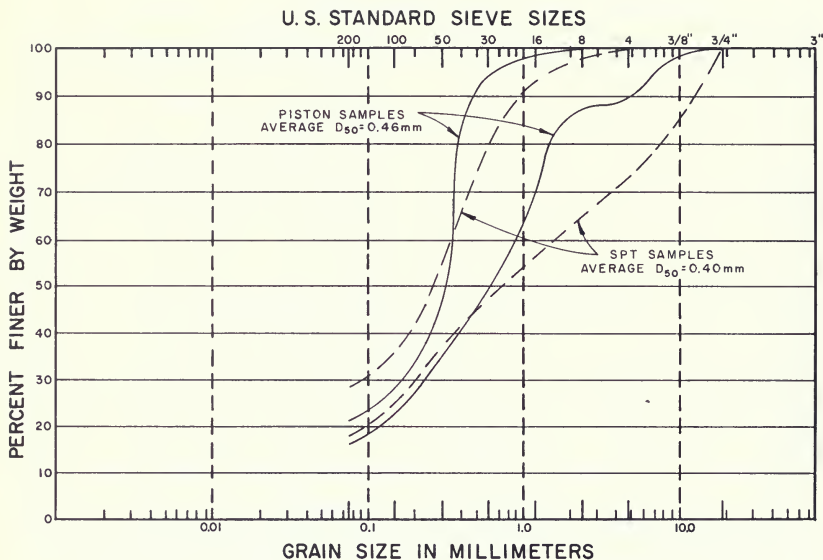
CLAY OR SILT FINES	SAND			GRAVEL	
	FINE	MEDIUM	COARSE	FINE	COARSE

Figure 269. Comparison of Gradations Determined for Piston and SPT Samples Obtained at the Thermalito Forebay Dam Station 74 Sampling Site



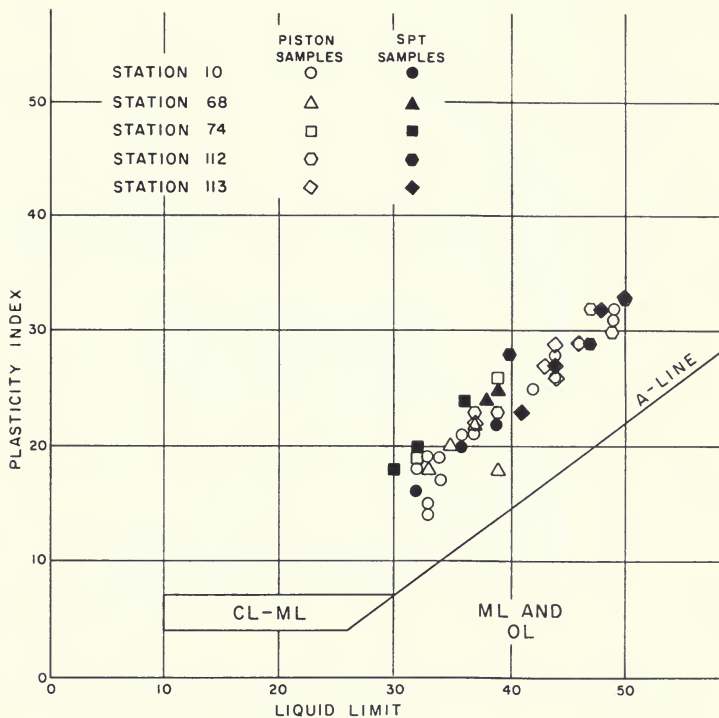
CLAY OR SILT FINES	SAND			GRAVEL	
	FINE	MEDIUM	COARSE	FINE	COARSE

*Figure 270. Comparison of Gradations Determined for Piston and SPT Samples Obtained at the Thermalito Forebay Dam Station 112 Sampling Site*



CLAY OR SILT FINES	SAND			GRAVEL	
	FINE	MEDIUM	COARSE	FINE	COARSE

Figure 271. Comparison of Gradations Determined for Piston and SPT Samples Obtained at the Thermalito Forebay Dam Station 113 Sampling Site



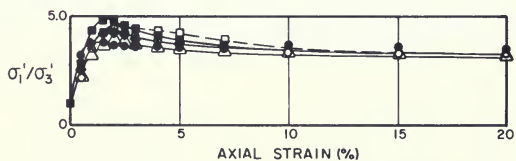
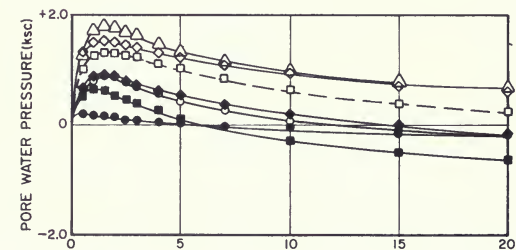
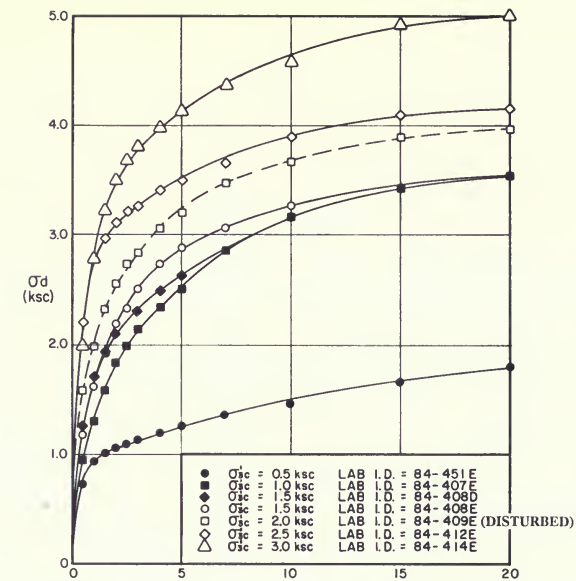


Figure 273. Triaxial Compression Test Results for 1984 Undisturbed Specimens of Thermalito Forebay Main Dam Embankment Material

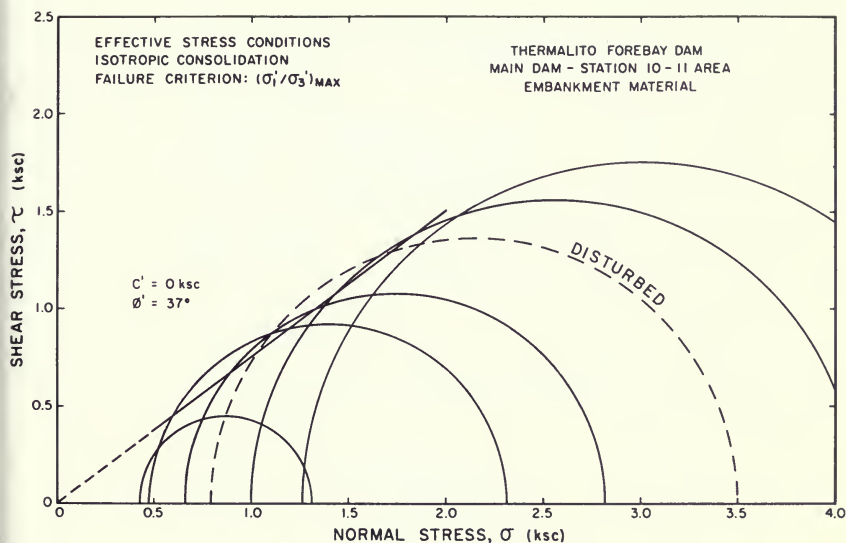
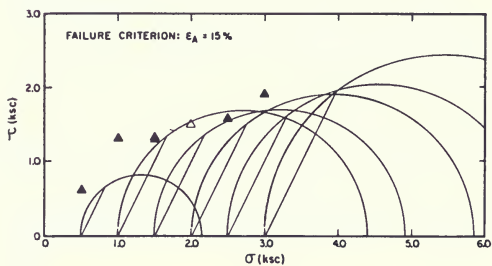
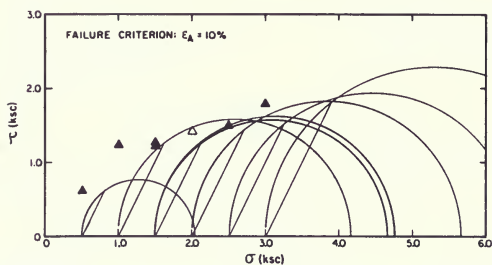
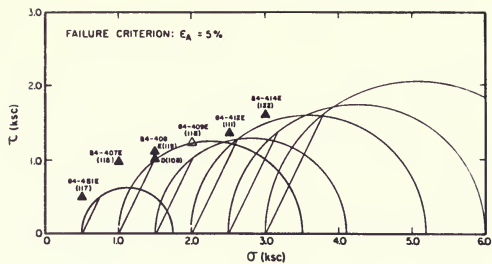


Figure 274. Thermalito Forebay Drained Static Shear Strength Results from ICU Triaxial Tests of Main Dam Embankment Soil

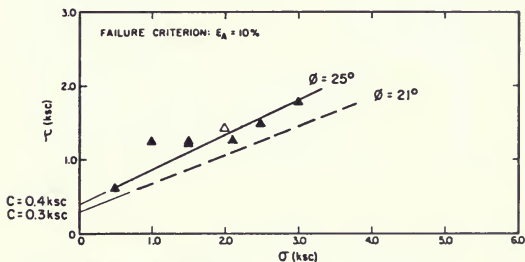
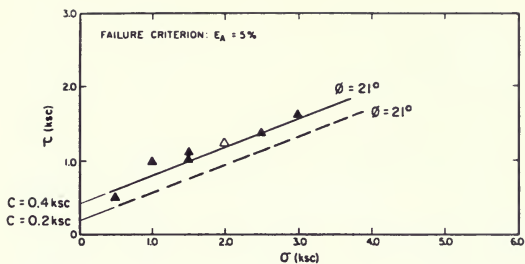


**NOTE:**

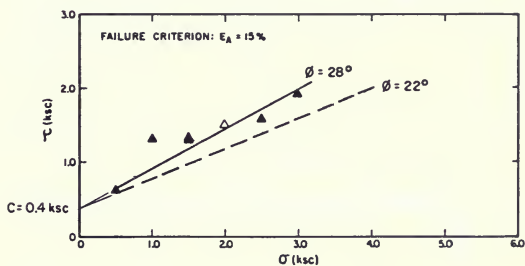
HOLLOW SYMBOL DENOTES DISTURBED SPECIMEN.  
 LAB. SAMPLE NUMBERS ARE SHOWN ABOVE SYMBOLS.  
 CONSOLIDATED DRY DENSITY VALUES ARE SHOWN IN PARENTHESIS.  
 SYMBOLS REPRESENT  $\tau_{ff}$  VS.  $\sigma'_{fc}$  RELATIONSHIP.

Figure 275. Thermalito Forebay Undrained Static Shear Strength Results from ICU Triaxial Tests of Main Dam Embankment Soil





NOTE: HOLLOW SYMBOLS DENOTE  
DISTURBED SPECIMEN



--- STRENGTH REPRESENTATION USING MOHR CIRCLE FAILURE ENVELOPE  
— STRENGTH REPRESENTATION USING  $\tau_{ff}$  VS.  $\sigma_{fc}$  FAILURE ENVELOPE

Figure 276. Thermalito Forebay Undrained Static Shear Strength Determined from ICU Triaxial Tests of Main Dam Embankment Soil

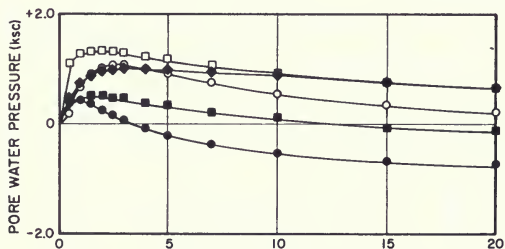
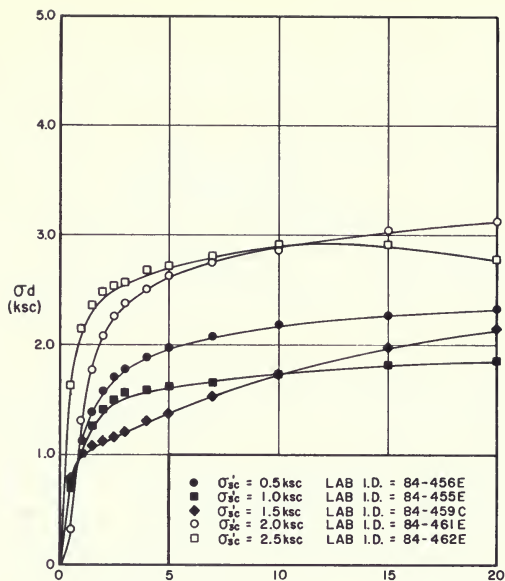


Figure 277. ICU Triaxial Compression Test Results for 1984 Undisturbed Specimens of Thermalito Forebay Low Dam Embankment Soil

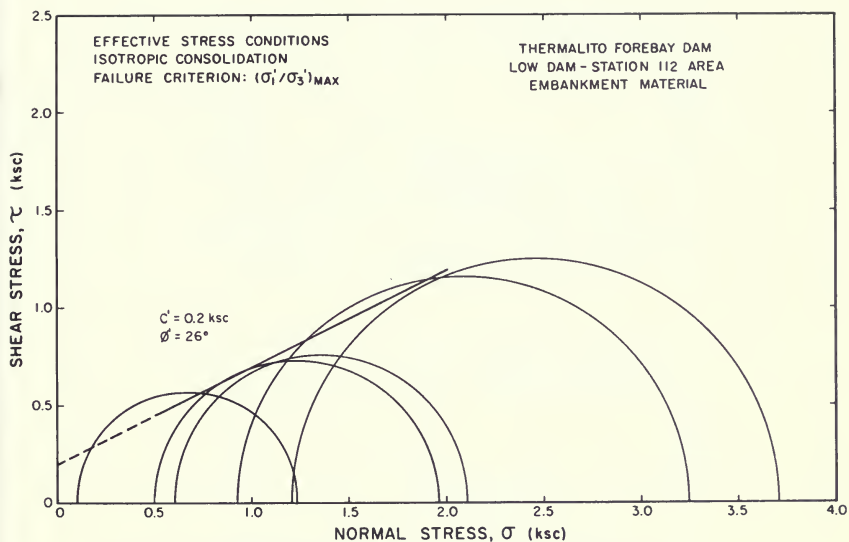
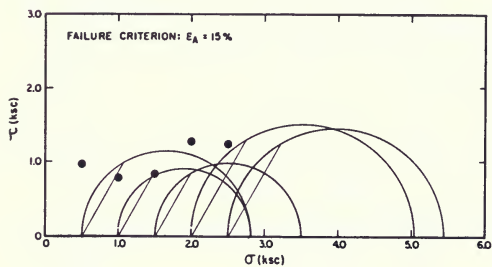
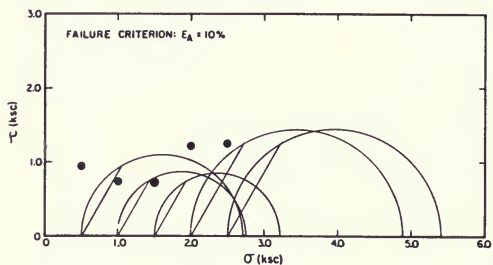
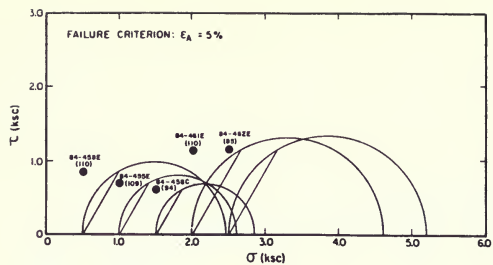


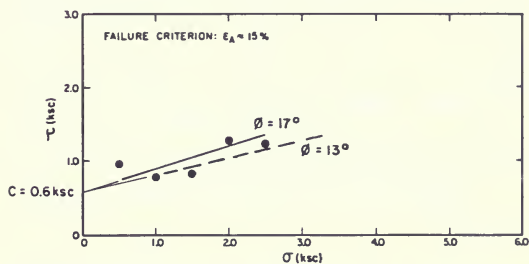
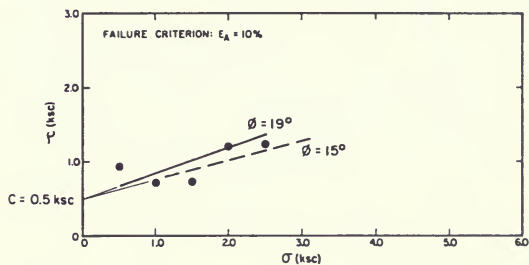
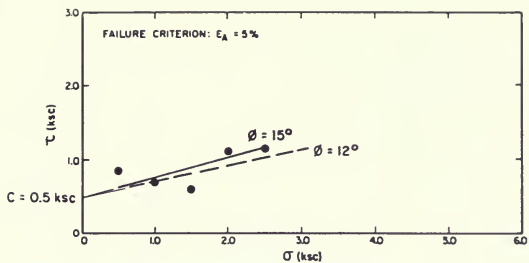
Figure 278. Thermalito Forebay Drained Static Shear Strength Determined from ICU Triaxial Tests of Low Dam Embankment Material



**NOTE:**

LAB SAMPLE NUMBERS ARE SHOWN ABOVE SYMBOLS.  
CONSOLIDATED DRY DENSITY VALUES ARE SHOWN IN PARENTHESIS.  
SYMBOLS REPRESENT  $\tau_{tf}$  VS.  $\sigma'_{fc}$  RELATIONSHIP.

Figure 279. Thermalito Forebay Undrained Static Shear Strength Results from ICU Triaxial Tests of Low Dam Embankment Soil



— — — STRENGTH REPRESENTATION USING MOHR CIRCLE FAILURE ENVELOPE  
 ————— STRENGTH REPRESENTATION USING  $\tau_{11}$  VS.  $\sigma_{1c}'$  FAILURE ENVELOPE

Figure 280. Thermalito Forebay Undrained Static Shear Strength Determined from ICU Triaxial Tests of Low Dam Embankment Soil

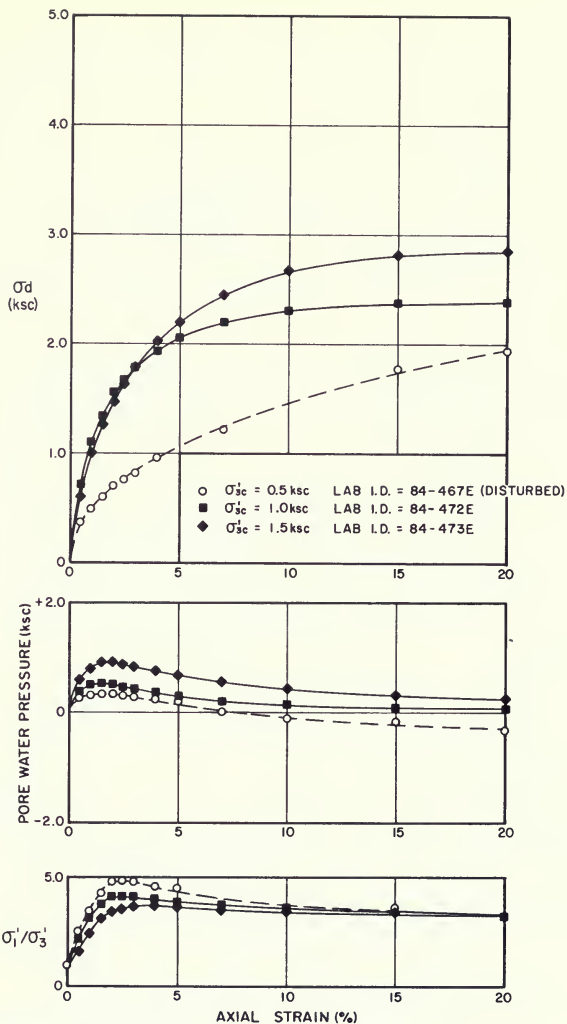


Figure 281. ICU Triaxial Compression Test Results for 1984 Undisturbed Specimens of Thermalito Forebay Clayey Foundation Cap Soil

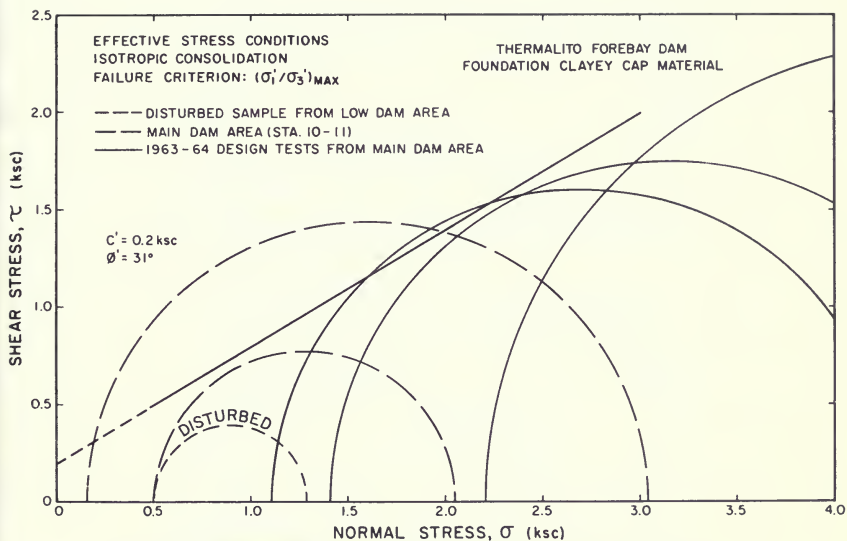
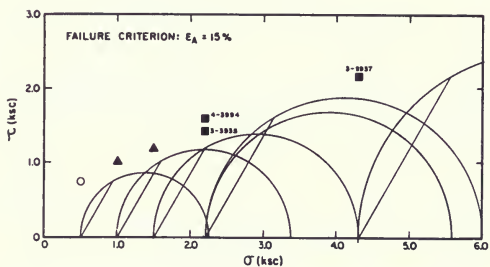
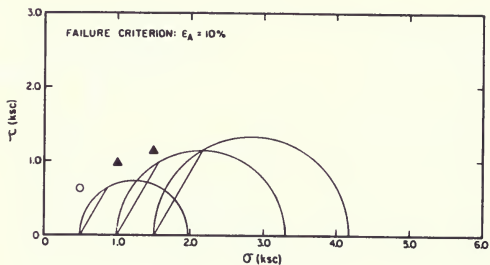
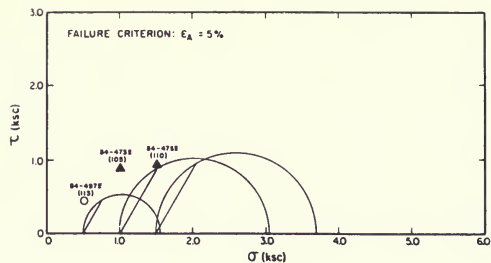


Figure 282. Thermalito Forebay Drained Static Shear Strength Determined from ICU Triaxial Tests of Non-Liquefiable Clayey Foundation Cap Soil



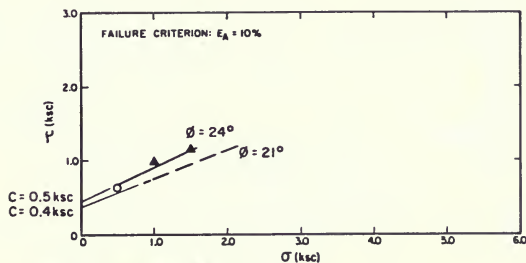
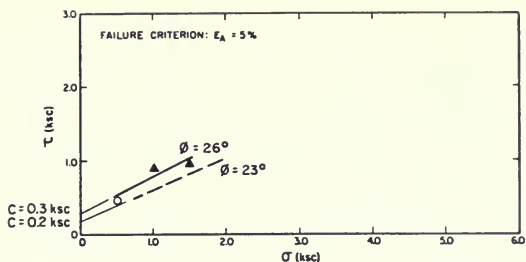
- ▲ 1984 SAMPLES FROM MAIN DAM AREA (STATION 10-11)
- 1963-64 DESIGN TESTS FROM MAIN DAM AREA
- O DISTURBED SAMPLE FROM LOW DAM

**NOTE:**

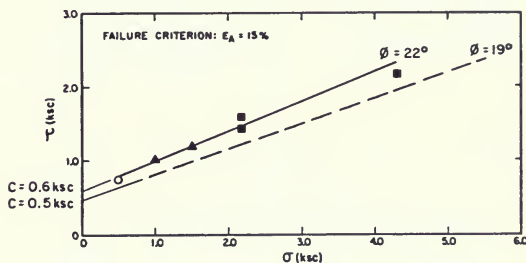
LAB. SAMPLE NUMBERS ARE SHOWN ABOVE SYMBOLS.  
CONSOLIDATED DRY DENSITY VALUES ARE SHOWN IN PARENTHESES.  
SYMBOLS REPRESENT  $\tau_{ff}$  VS.  $\sigma_{fc}$  RELATIONSHIP.

Figure 283. Thermalito Forebay Undrained Static Shear Strength Results from ICU Triaxial Tests of Non-Liquefiable Clayey Foundation Cap Soil





NOTE: HOLLOW SYMBOLS DENOTE  
DISTURBED SPECIMEN



- LOW DAM AREA (STATION 112)
- ▲ MAIN DAM AREA (STATION 10-11)
- 1963-64 DESIGN TESTS FROM MAIN DAM AREA

--- STRENGTH REPRESENTATION USING MOHR CIRCLE FAILURE ENVELOPE  
— STRENGTH REPRESENTATION USING  $\tau_{11}$  VS.  $\sigma_{11}$  FAILURE ENVELOPE

Figure 284. Thermalito Forebay Undrained Static Shear Strength Determined from ICU Triaxial Tests of Non-Liquefiable Clayey Foundation Cap Soil

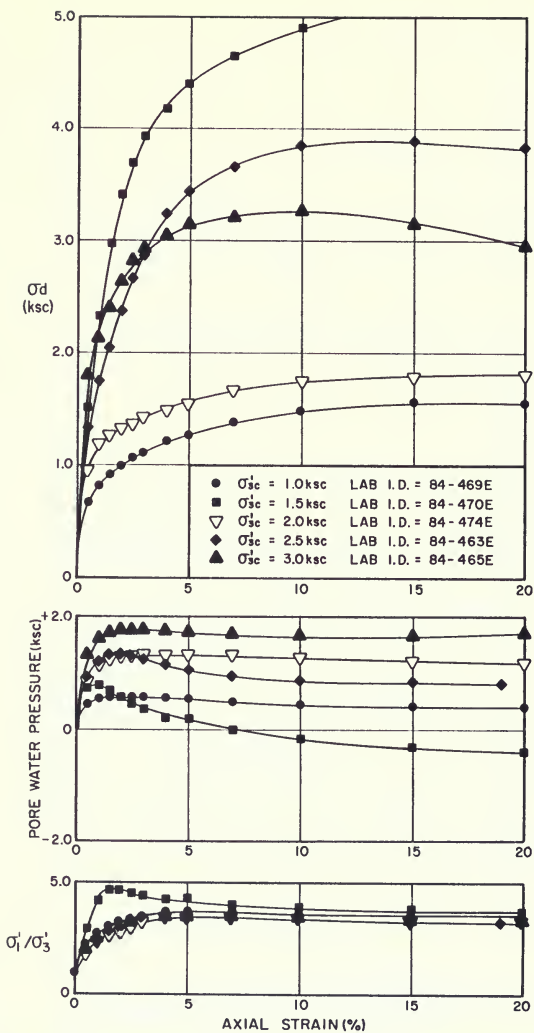


Figure 285. ICU Triaxial Compression Test Results for 1984 Undisturbed Specimens of Thermalito Forebay Suspect SC/SM Foundation Sand

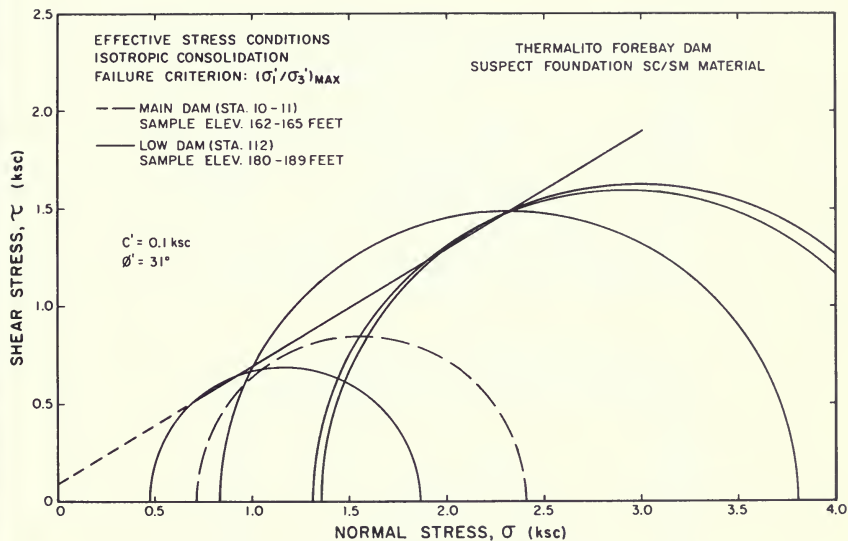
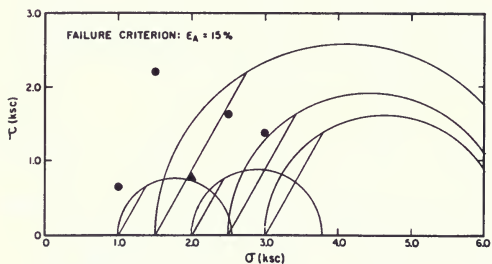
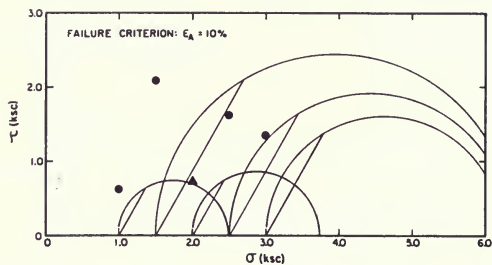
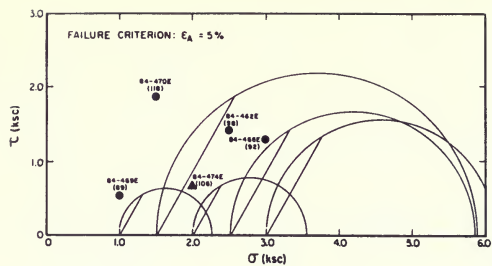


Figure 286. Thermalito Forebay Drained Static Shear Strength Determined from ICU Triaxial Tests of Suspect Foundation SC/SM Sand

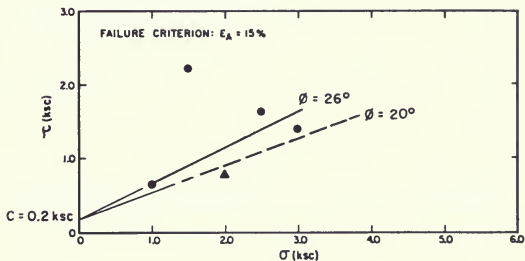
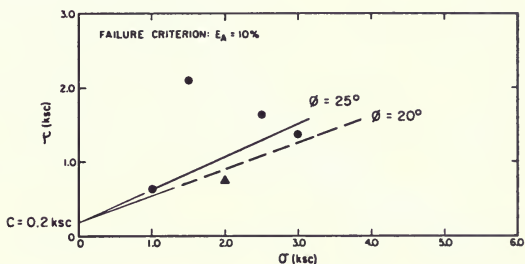
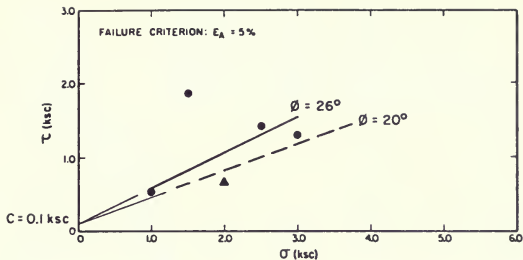


● LOW DAM AREA (STATION 112)  
 ▲ MAIN DAM AREA (STATION 10-11)

**NOTE:**

LAB. SAMPLE NUMBERS ARE SHOWN ABOVE SYMBOLS.  
 CONSOLIDATED DRY DENSITY VALUES ARE SHOWN IN PARENTHESIS.  
 SYMBOLS REPRESENT  $\tau_{ff}$  VS.  $\sigma'_{fc}$  RELATIONSHIP.

Figure 287. Thermalito Forebay Undrained Static Shear Strength Results from ICU Triaxial Tests of Suspect Foundation SC/SM Sand



- LOW DAM AREA (STATION 112)
- ▲ MAIN DAM AREA (STATION 10-11)
- STRENGTH REPRESENTATION USING MOHR CIRCLE FAILURE ENVELOPE
- STRENGTH REPRESENTATION USING  $\tau_{if}$  VS.  $\sigma'_{ic}$  FAILURE ENVELOPE

Figure 288. Thermalito Forebay Undrained Static Shear Strength Determined from ICU Triaxial Tests of Suspect Foundation SC/SM Sand

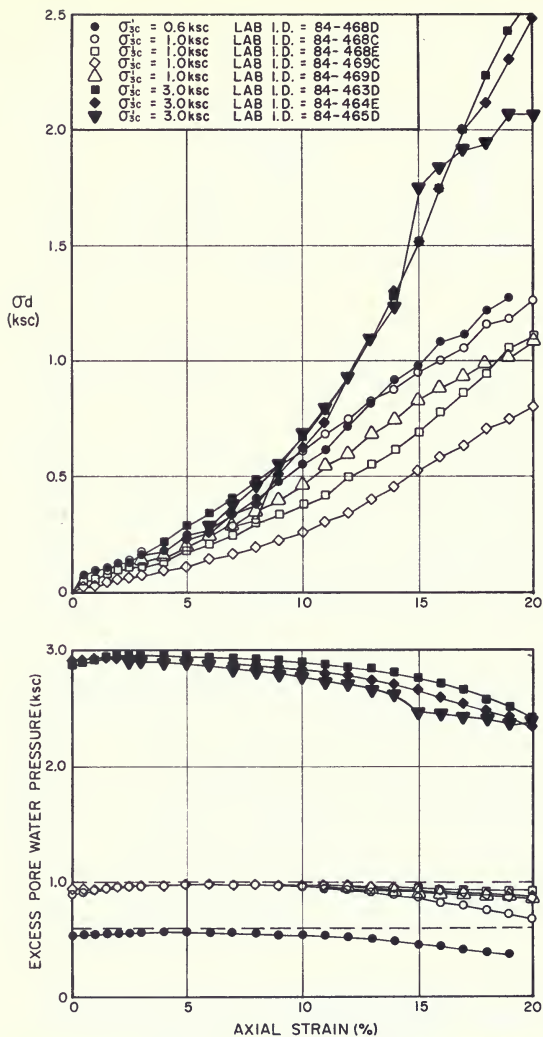


Figure 289. Post-Cyclic Static Triaxial Compression Test Results for 1984 Undisturbed Specimens of Thermalito Forebay Low Dam (Station 112) Suspect SC/SM Foundation Sand

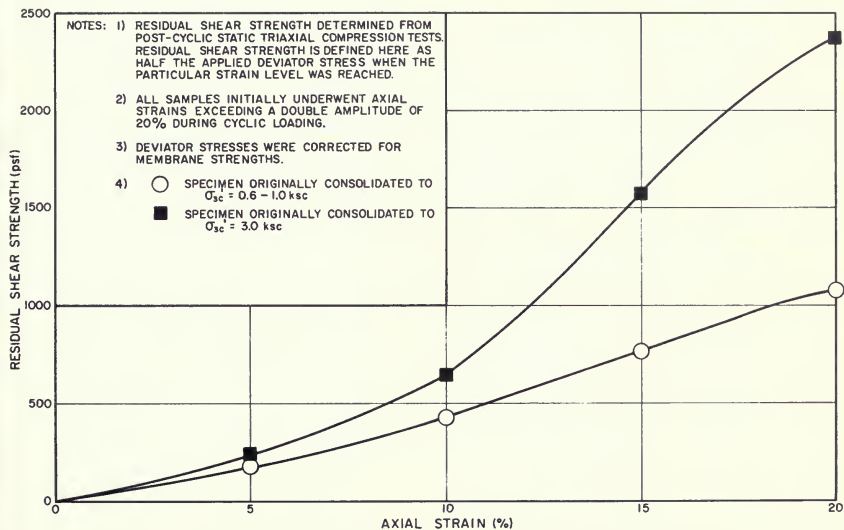


Figure 290. Residual Shear Strength Determined From Post-Cyclic Triaxial Tests Performed on 1984 Specimens of Thermalito Forebay Low Dam (Station 112) Suspect SC/SM Foundation Sand

## 5. IDENTIFICATION AND MODELING OF CRITICAL AREAS

### Introduction

Two areas were selected for detailed analyses. One area was located at the Main Dam and one area was located at the Low Dam. The sites selected contained the thickest and lowest SPT blowcount sand layers. Simplified models for the two critical sites were developed for use in analyses of static stresses, dynamic stresses, liquefaction, and post-earthquake stability.

### Identifying Potential Liquefaction Sites

A SPT  $N_{A1}$  blowcount of 30 was adopted for preliminary screening of all the boring profiles in order to identify all sites needing further examination for evaluating liquefaction potential. Because of the tendency for some soils to break down and become more plastic with remolding, all soils with  $N_{A1} < 30$ , even clays, were considered suspect in this initial screening stage.

#### Identification of Most Critical Area at the Main Dam

Figure 291 presents a plan view of the Main Dam illustrating the locations of SPT boreholes and the lowest  $N_{A1}$  value obtained for each borehole. This figure shows low blowcounts ( $N_{A1} < 30$ ) only in an area between Station 10 and 12. Low blowcounts appear to extend from the foundation beneath the crest to areas beyond the downstream toe. The  $N_{A1}$  values and soil types in this area are shown again in detail in Figures 292 through 295. These figures show a low blowcount zone of clayey and silty sands lying principally between Elevations 153 and 165 feet.

#### Identification of Most Critical Area at the Low Dam

Thirteen low blowcount sites ( $N_{A1} \leq 30$ ) were identified along the Low Dam during the exploration programs, as shown in Figures 243 through 250. Table 48 (page 340) listed the sites along with brief physical descriptions and representative blowcounts. The most critical of these thirteen sites is the Station 112 area, which has an

18-foot-thick foundation layer of low blowcount sands. Figures 296 and 297 present SPT and soil type data obtained from the boreholes placed at this site. This site was selected after considering embankment height, foundation material, average SPT  $N_{A1}$  blowcount, thickness of the low blowcount layer, and fines content. Station 112 is most critical in all criteria except for dam height as compared with Station 136 (30 feet vs. 36 feet). However, Figures 296 and 297 reveal much more extensive and consistently low blowcount foundation material at the Station 112 area than at Station 136 (Figure 249, page 334).

### Assumptions For Developing Simplified Models

1. The silty, gravelly, clayey sand embankment is modeled as a dense clayey material that will neither liquefy nor develop significant pore pressures during an earthquake. This assumption is based on the fact that the excavation, working, and compaction of the soil imparted sufficient strain to break down the weathered material into a dense, plastic mass. Studies of the performance of compacted, clayey materials (Seed et al., 1978) have shown that these materials perform very well during earthquake shaking.
2. Low blowcount clayey sands beneath the foundation cap are considered potentially liquefiable. Normally, the reverse would be assumed because of the traditional good performance of clayey materials. However, due to the weathered and friable nature of these materials, it may be quite possible that the plasticity found in the field or in the lab resulted from remolding the material. Therefore, for the purposes of these analyses, clayey sands will be assumed to behave as silty sands in situ.
3. Cyclic loading resistances of low blowcount materials will be defined principally by the Seed and Idriss (1982) SPT correlation with liquefaction potential. Correlation curves for magnitude 6.5 earthquakes are shown in Figure 298. The two curves shown in this figure are for clean sand ( $D_{50} > 0.25$  mm) and silty sand ( $D_{50} < 0.15$  mm). It can be seen that the silty sand curve gives higher resistance than the clean sand curve. Since the curves are parallel, the effect is



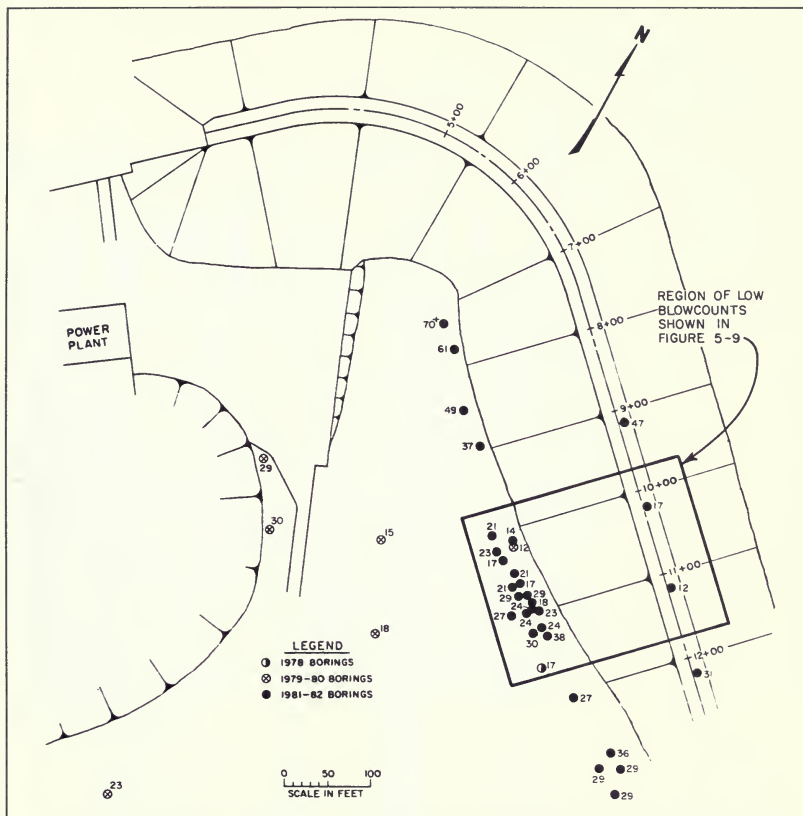
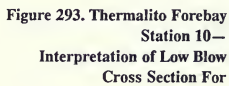


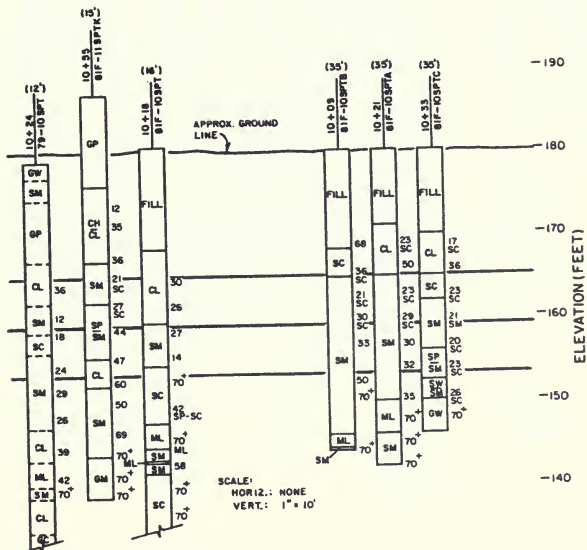
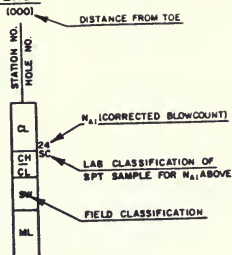
Figure 291. Minimum Corrected SPT Resistance Measured Within Borings Drilled at Thermalito Forebay Main Dam







# LEGEND



Main Dam  
11 Area  
Count Sand Layer  
Stations 10+08 To 10+70

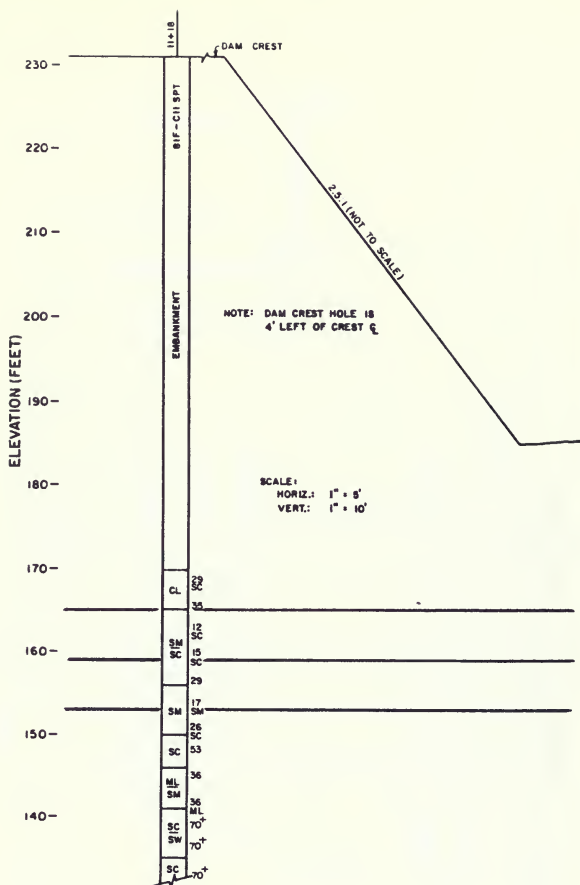


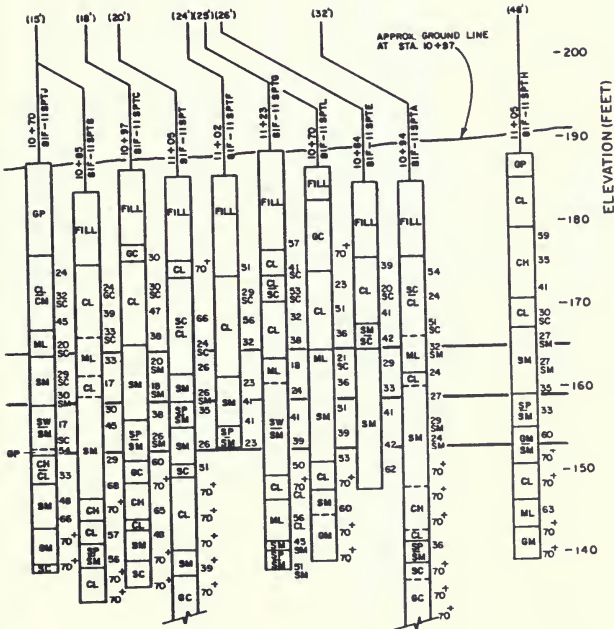
Figure 294. Thermalito Forebay  
Station 10—  
Interpretation of Low Blow  
Cross Section For

-230

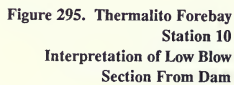
-220

NOTE: FOR LEGEND SEE FIGURE 293

-210



Main Dam  
11 Area  
Count Sand Layer  
Stations 10 + 70 To 11 + 23







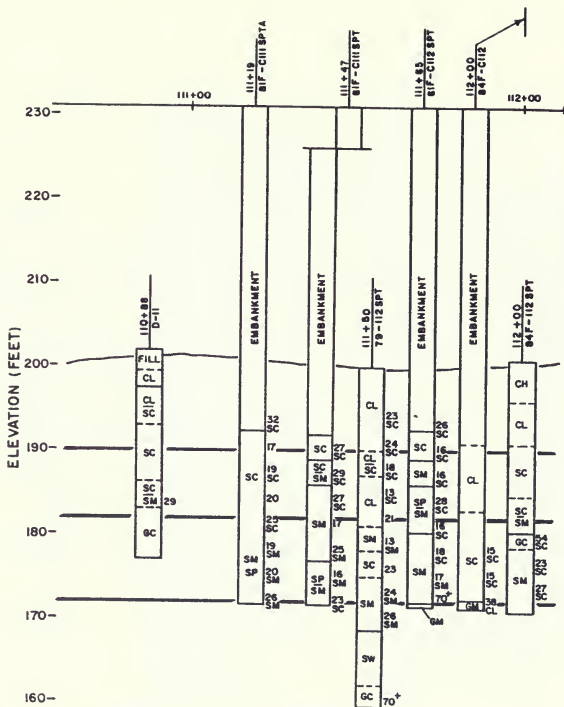
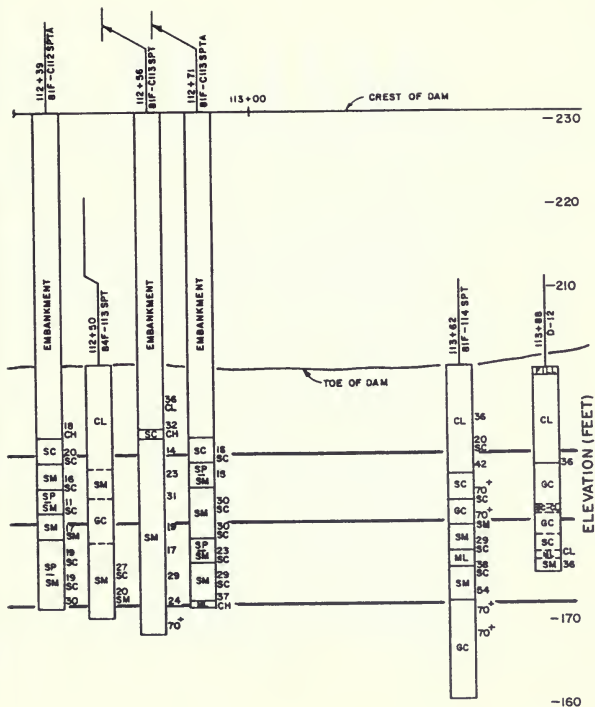
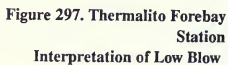


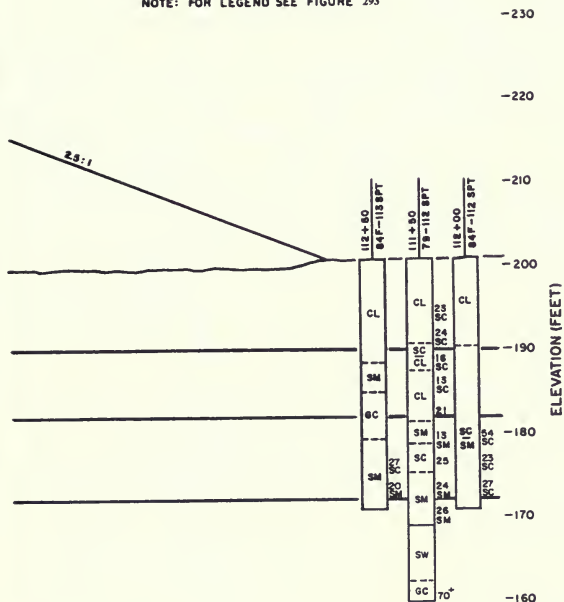
Figure 296. Thermalito Forebay  
Station  
Interpretation of Low Blow



Low Dam  
112 Area  
Count Sand Layer—Profile



NOTE: FOR LEGEND SEE FIGURE 293



Low Dam  
112 Area  
Count Sand Layer—Cross Section

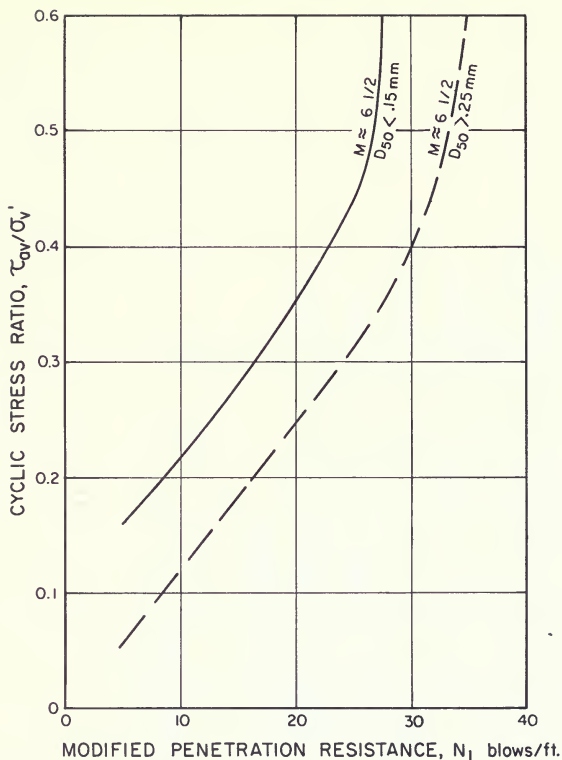


Figure 298. Correlation Between SPT Resistance and Field Liquefaction Behavior of Sands under Level Ground Conditions During Magnitude 6.5 Earthquakes (modified from Seed and Idriss, 1982)

equivalent to adding 7.5 blows per foot to a silty sand blowcount and using the clean sand curve. Recent research by Seed et al. (1985) has shown that curves based on fines content (fraction passing the No. 200 sieve) also show increased strength for silty sands. Silty sands with 15 percent fines have increased strengths equivalent to clean sands with blowcounts about five blows per foot higher. Figures 264 and 265 (pages 359 and 360) show that the suspect materials have fines contents ranging generally between 15 and 40 percent. Even with some particle breakdown, it

can be reasonably assumed that the materials generally have at least 15 percent fines.

Therefore, the cyclic strength of the suspect material will be determined by adding five blows per foot to the blowcounts and by using the clean sand curve in Figure 298. The strength obtained will be in the form of a cyclic stress ratio,  $CSR_1$ , that is appropriate for level ground conditions at about 1 tsf effective overburden pressure. This stress ratio will be modified for different stress conditions using cyclic triaxial test results.

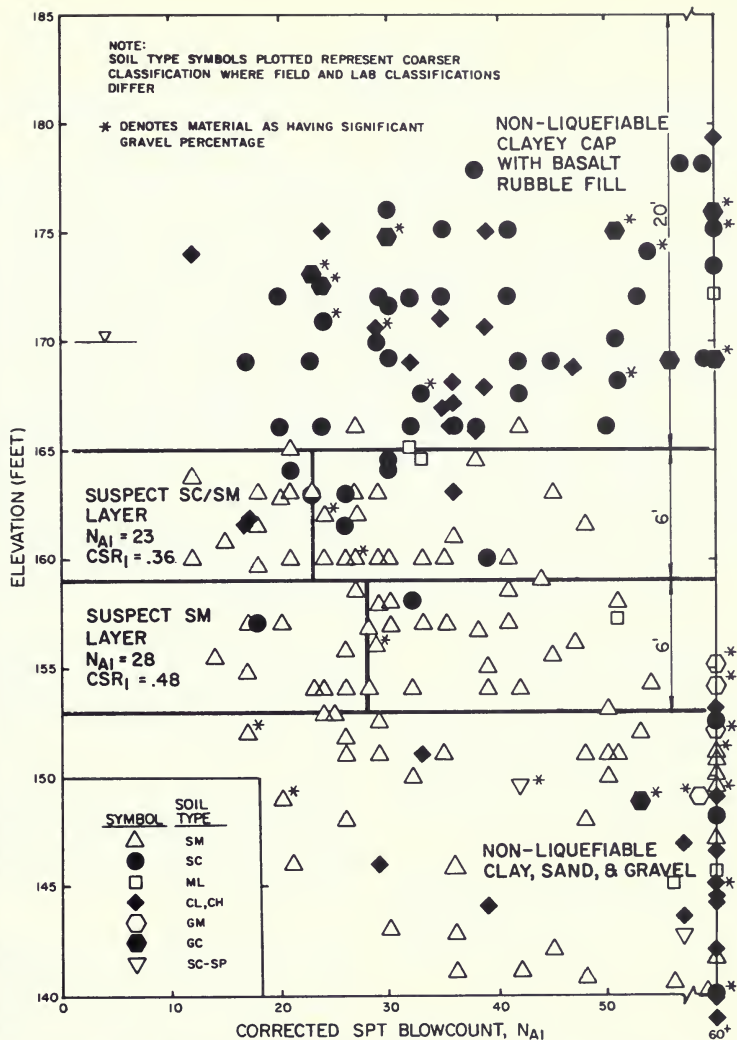


Figure 299. Corrected Standard Penetration Test Resistance for Suspect Sands Located Between Stations 10 and 12 at the Thermalito Forebay Main Dam.

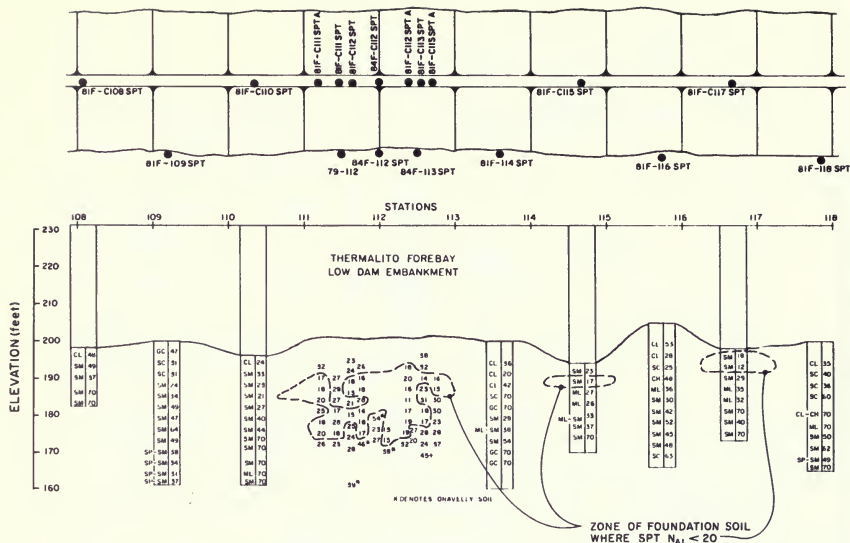


Figure 300. Cross-Section Profile of Corrected Standard Penetration Resistance for Foundation Sands Located Between Stations 108 and 118 at the Thermalito Forebay Low Dam

### Simplified Foundation Model Main Dam — Station 10–11

The SPT results from 21 borings within the rectangle of low blowcounts in Figure 291 are shown together in Figure 299. The blowcount symbols shown in Figure 299 represent the coarsest or least plastic of either the field or laboratory classification (i.e., if the field classification was SM and the lab classification was SC, the point would be plotted as SM).

Figure 299 shows that the upper 20 feet of the foundation is a high blowcount clayey material with some gravel particles. This material is considered non-liquefiable and would be expected to retain its full strength during earthquake shaking. Downstream of the dam, three-quarters of this layer is above the ground water level.

Beneath this clayey cap lies a relatively low blowcount layer of clayey and silty sand about 6 feet thick. This suspect material has been assigned a corrected blowcount,  $N_{A1}$ ,

of 23. This number is equivalent to about the 35th-percentile value, which is commonly used as a conservative average. By adding five blows per foot for fines content, and using the clean sand curve in Figure 298, the resulting cyclic stress ratio,  $CSR_1$ , is about 0.36.

Beneath the first suspect layer is another 6-foot-thick low blowcount layer of silty sand. This layer has been assigned a corrected blowcount,  $N_{A1}$ , of 28, also equivalent to about the 35th-percentile value. Using the same procedures presented above, the resulting stress ratio,  $CSR_1$ , is about 0.48.

Beneath the two suspect layers is an intermixed material of clays, sands, and gravels that have both high shear wave velocities and high blowcounts. This material is considered non-liquefiable and would be expected to retain its full strength during earthquake shaking. This dense soil extends between 32 and 88 feet deep. Beneath this soil is basalt bedrock.



### **Simplified Foundation Model Low Dam — Station 112**

The SPT results obtained from borings between Stations 108 and 118 are presented in Figure 300. This figure shows that a layer of low blowcount sandy soil exists in significant extent only between Stations 111 and 113. Presented together in Figure 301 are the SPT results from borings between Station 111 and 113. The blowcount symbols shown in this figure represent the coarsest or least plastic of either the field or laboratory classification.

The upper 11 feet is composed of a relatively high blowcount clayey material. This material is considered non-liquefiable and would be expected to retain its full strength during earthquake shaking.

Beneath the clayey cap are two layers of low blowcount clayey and silty sands with a combined thickness of 18 feet. Although the upper suspect layer appears to be predominately clayey sand, the weathered nature of this material requires it to be treated as a silty sand (i.e. liquefi-

able). Both suspect layers have been assigned a corrected blowcount,  $N_{A1}$ , of 19. This is equivalent to about the 35th-percentile value. By adding five blows per foot for fines content and using Figure 298, the resulting stress ratio,  $CSR_1$ , is about 0.30.

Soils underlying the suspect layers are not well defined because of the small quantity of data. However, the few blowcounts indicate high strength and are assumed to be highly resistant to liquefaction as at Station 10–11. Although there are no on-site data to determine the depth to bedrock, it is assumed that basalt lies approximately 100 feet below the foundation surface.

### **Simplified Embankment – Foundation Models**

Figure 302 shows the foundation layering and embankment sections adopted for the two critical sites. All static finite element analyses, one-dimensional dynamic response analyses, and post-earthquake slope stability analyses, will be based on the models shown in Figure 302.

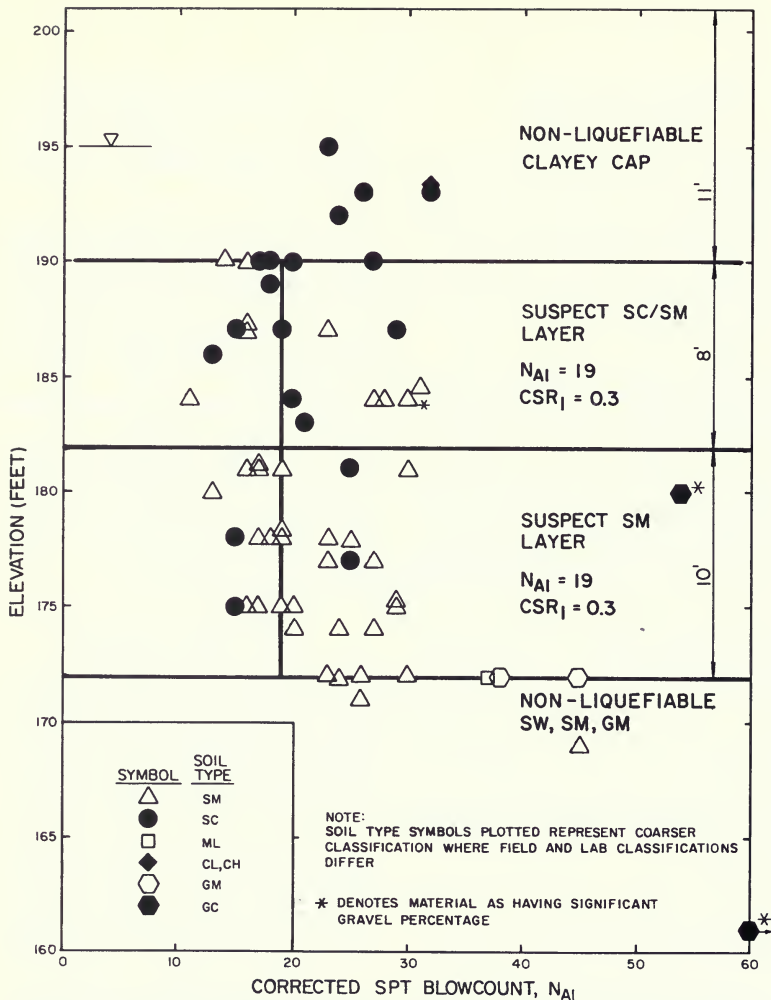
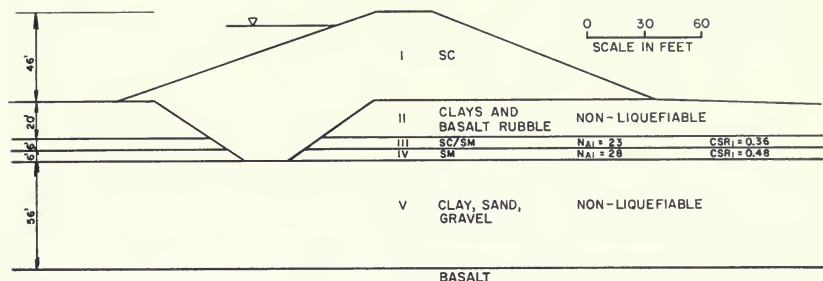
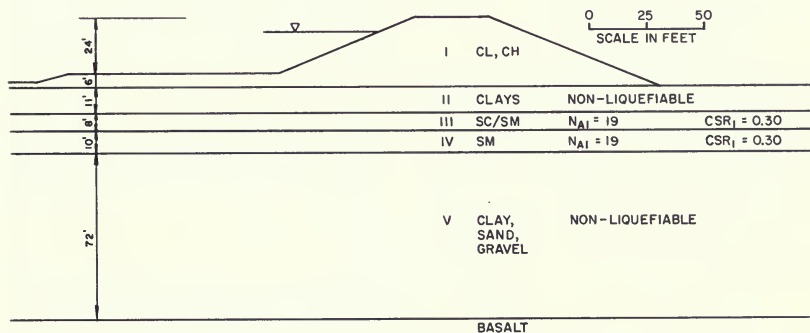


Figure 301. Corrected Standard Penetration Test Resistance for Foundation Sands Located Between Stations 111 and 113 at the Thermalito Forebay Low Dam



### MAIN DAM STATION 10 - 11 AREA



### LOW DAM STATION 112 AREA

Figure 302. Simplified Embankment-Foundation Models Created for the Critical Sites along Thermalito Forebay Main and Low Dams

## 6. STATIC STRESS ANALYSES

### Introduction

Static stress analyses were performed to obtain the pre-earthquake effective stress conditions in the soils at the two critical sites. These stress conditions are used in both the determination of cyclic soil strengths and the predictions of earthquake-induced stresses.

### Method of Analysis

The finite element computer program TWIST was used in conjunction with program NODALFOR to calculate static stresses. Program NODALFOR calculates the resultant hydrostatic water force on each element for input to TWIST. TWIST then adds these water forces to the gravity forces imparted to the soil to obtain the effective static stresses.

Program NODALFOR, developed by the Division of Safety of Dams, calculates the water force on each element. Water pressures at each node are estimated from a flow net and input to the program. The program computes water forces on the sides of each element, based on the assumption of linear variation of pressure between nodes. The resultant force for the element is then distributed to its nodes in proportion to each node's contributing area to the element. The total water force at each node is the sum of the water forces distributed to that node from all of the adjacent elements.

Program TWIST is an in-house, improved version of program 4-CST and uses a quadrilateral element that is subdivided into two incompatible linear strain triangles. The program uses linear material properties.

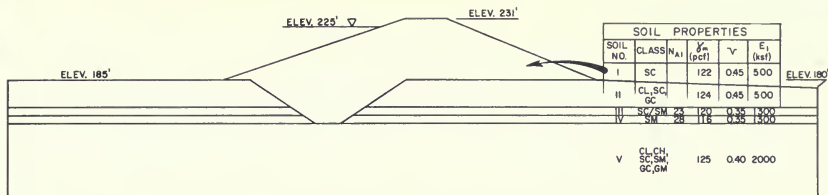
### Models

The dam/foundation models were constructed as two-dimensional finite element meshes for the two critical cross sections as shown in Figures 303 and 304. Layering for the models was determined from Section 5. Young's modulus values were chosen from values published by Wong and Duncan (1974) for drained triaxial test data obtained for similar materials. Factors considered in establishing Young's modulus were gradations, Atterberg limits, densities, and stress ranges. Values for Poisson's ratios were assumed based on general familiarity with published values for similar embankments. Dry density values are averages from construction control testing for the embankment soils, from original design shear test samples for shallow and deep foundation layers, and from 1981 and 1984 triaxial test samples. Flow nets were drawn to represent conditions based on a maximum reservoir elevation of 225 feet and to match piezometer readings, as shown in Figure 305.

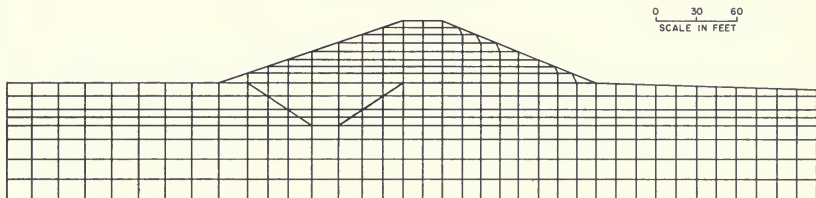
### Results

Program output consists of effective vertical normal stresses, effective horizontal normal stresses, horizontal shear stresses, and alpha values (Alpha is defined as the ratio of the horizontal shear stress divided by the effective vertical normal stress).

Figures 306 and 307 show the pre-earthquake distribution of effective vertical normal stress and alpha values for the two sites. These stress conditions are representative of the maximum operating water level and steady state seepage conditions. Figures 308 and 309 show the specific effective vertical normal stress and alpha values of the suspect sand layers. The stress values for all of the elements are presented in Addendum C.

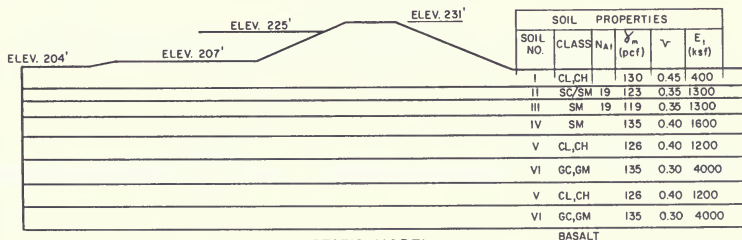


STATIC MODEL (PROGRAM TWIST)

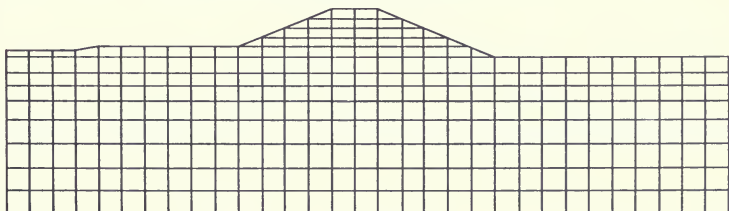


FINITE ELEMENT MESH

Figure 303. Finite Element Model and Mesh Used for Static Stress Analysis of the Thermalito Forebay Main Dam Model (Station 10-11 Area)

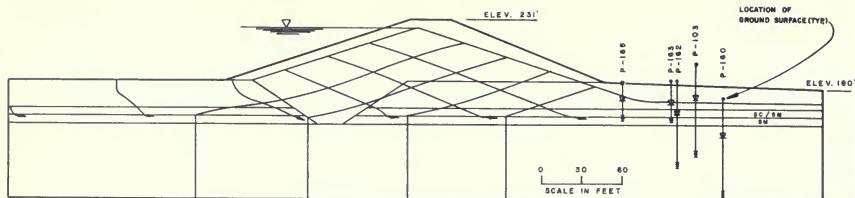


STATIC MODEL  
(PROGRAM TWIST)



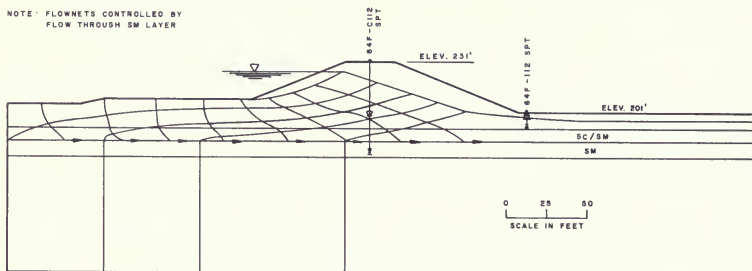
FINITE ELEMENT MESH

Figure 304. Finite Element Model and Mesh Used for Static Stress Analysis of the Thermalito Forebay Low Dam Model (Station 112 Area)



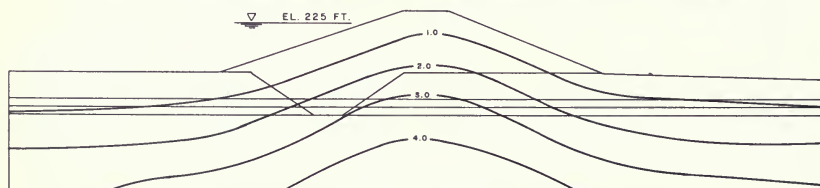
MAIN DAM (STA. 10-11 AREA)

NOTE: FLOWNETS CONTROLLED BY  
FLOW THROUGH SM LAYER

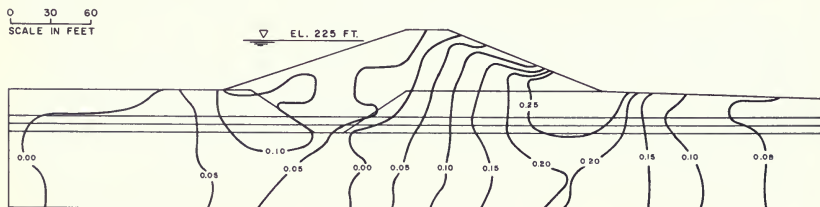


LOW DAM (STA. 112 AREA)

Figure 305. Assumed Flownets Used in Static Stress Analyses of Thermalito Forebay Dam Critical Models



STATIC VERTICAL EFFECTIVE NORMAL STRESSES,  $\bar{\sigma}_y' (tsf)$



ALPHA VALUES ( $\alpha = \tau_{xy}/\bar{\sigma}_y'$ )

Figure 306. Distribution of Effective Vertical Normal Stress and Alpha Values Calculated for Thermalito Forebay Main Dam Model (Station 10-11 Area)

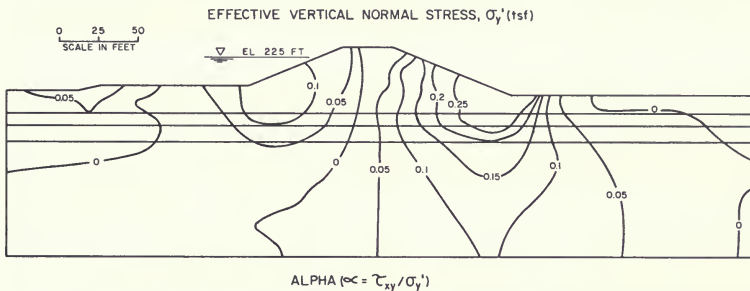
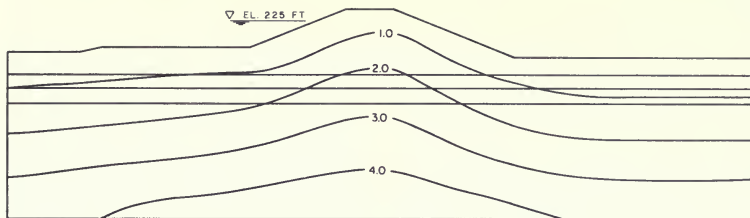
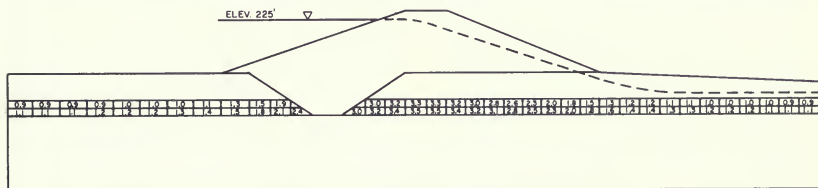
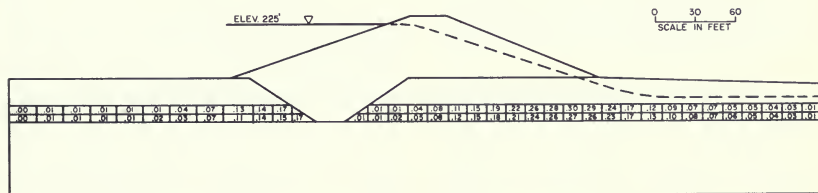


Figure 307. Distribution of Effective Vertical Normal Stress and Alpha Values Calculated for Thermalito Forebay Low Dam Model (Station 112 Area)

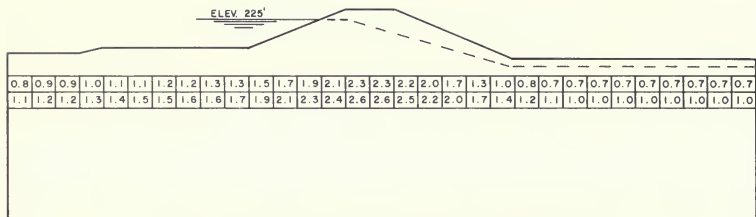


$\sigma_y'$  - EFFECTIVE VERTICAL NORMAL STRESSES (TSF)



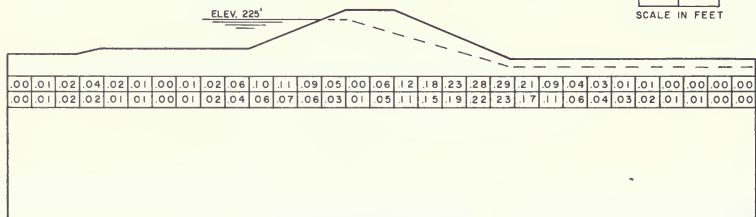
ALPHA ( $\alpha = \tau_{xy}' / \sigma_y'$ )

Figure 308. Pre-Earthquake Stress Conditions Determined for the Suspect Sand Layers in the Thermalito Forebay Main Dam Model (Station 10-11 Area)



$\sigma_y'$  - EFFECTIVE VERTICAL NORMAL STRESSES (TSF)

0 25 50  
SCALE IN FEET



ALPHA ( $\alpha = \tau'_{xy} / \sigma_y'$ )

Figure 309. Pre-Earthquake Stress Conditions Determined for the Suspect Sand Layers in the Thermalito Forebay Low Dam Model (Station 112 Area)



## 7. DYNAMIC RESPONSE ANALYSES

### Introduction

Dynamic response analyses were performed to determine which portions of the suspect foundation layers might liquefy during the postulated earthquake shaking. To perform dynamic response analyses, two major steps are required:

1. Determine the appropriate time history of the base acceleration that should be used to load the dam and its foundation.
2. Using an appropriate dynamic response analysis technique, compute the dynamic displacements, strains, and stresses induced in the dam and foundation by the adopted earthquake motions.

During the several stages of this evaluation several different earthquake motions and dynamic analyses were considered and performed.

### Background on Earthquake Motions Used in Analyses

Initially, the same ground motion was used for the analyses of Thermalito Afterbay and Forebay Dams as was used for the Oroville Dam Analysis. As discussed in Bulletin 203-78 Chapter V, this motion, with a peak acceleration of 0.6g, was to represent the effects of a magnitude 6.5 earthquake generated on the Cleveland Hill Fault, located only a few miles away from Oroville dam (see Figure 310). The accelerogram that was adopted, a combination of the Pacoima (1971) and Taft (1952) records, was to represent a surface rock motion.

Since Thermalito Afterbay Dam has a soil foundation and is farther from the Cleveland Hill Fault than Oroville Dam, different ground motions were adopted for that evaluation in 1980. Three accelerograms were used. Each one was a record of ground motion from a recording site on soil located 10 to 20 miles from the energy source of a magnitude 6.5 earthquake. Each accelerogram was scaled to a peak acceleration,  $a_{max}$ , of 0.35g for the Thermalito Afterbay analyses. See Chapter III of this bulletin for a full discussion of these ground motions. The same accelerograms, scaled to  $a_{max} = 0.4g$  were also used for the

Thermalito Forebay Dam analyses performed during the period 1980-83.

A report describing the selection of the revised ground motions for the Thermalito Afterbay analysis was submitted to the Special Consulting Board for the Oroville Earthquake; the board concurred with the selections in an August 14, 1980 letter from Dr. George Housner, Chairman. However that report considered only the Cleveland Hill Fault, which produced ground cracking during the 1975 Oroville earthquake, as the source for a future earthquake. That is, no mention was made in the report of other possible earthquake sources.

During a subsequent Department internal review, a northerly extension of the Prairie Creek Lineament was also identified as a potential earthquake source. This northerly extension is closer to Thermalito Forebay Dam than is the Cleveland Hill Fault

As discussed in Bulletin 203-78, Chapter II, pages 86 and 87, the Prairie Creek Lineament northerly extension could approach quite close to Thermalito Forebay (Figure 310). Since the location, extent and characteristics of the possible fault associated with the Prairie Creek Lineament extension could be very difficult to determine, due to the thick valley sediments overlying the rock, it was decided to test the dam for an earthquake assumed to be generated by a source on the Prairie Creek Lineament 2-3 miles away. As shown in Figure 311 and in Table 53, average peak accelerations in rock would be 0.54g to 0.61g. Peak ground accelerations on soil surfaces would be expected to be about 10 to 20 percent lower (Reference 64). Accordingly, the three soil surface accelerograms used in the 1980-83 studies were scaled to  $a_{max} = 0.5g$  for the analyses performed in 1983.

In an early review, the Division of Safety of Dams specified that the test accelerogram should include a long period component (fling) if it is to represent ground motions generated by a fault only 2-3 miles from the dam. The question was discussed with the Special Consulting Board for the Oroville Earthquake (a four-member board) who agreed that a long period component generally should be included for such a close source to site distance. The

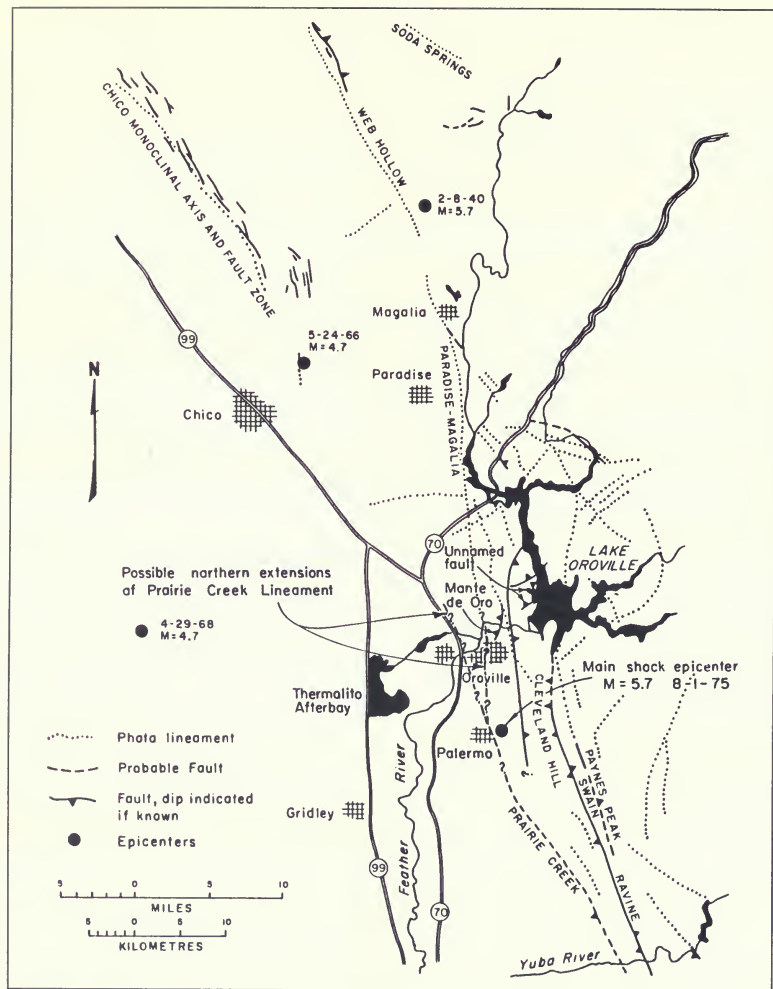


Figure 310. Location of Faults in the Thermalito Area

November 16, 1983 Board report recommended, "While this Board believes that the selected earthquake magnitude of 6.5 at a distance of 5 kilometers is extremely conservative and subject to further study and discussion, it recommends that the eight member Consulting Board for the Oroville Earthquake participate in any further recommendations on earthquake ground motions for reanalysis of Thermalito Forebay Dam and Foundation".

To provide the Department with guidance concerning the earthquake capability of the Prairie Creek Lineament, members of the Special Consulting Board met at the University of California - Berkeley on February 1, 1985. The recommendations derived from this meeting concerning the Prairie Creek Fault were as follows:

"There is little, or no, direct evidence that an active trace of the Prairie Creek Fault extends northwestward of Palermo, adjacent to the Thermalito structures. However, in view of the general tectonic structures and trends in the area, the Board considers it desirable to assume that such an extension exists and that the surface projection of the fault passes about 2.5 miles east of the Forebay Dam. It is also likely that the fault dips to the west as do the other faults in the area such as that observed in the 1975 Cleveland Hill earthquake sequence.

"Because of the lack of a definite surface fault trace north of Palermo, there is a significant limit to the size and recurrence rate of earthquakes likely to be produced by rupture of the assumed fault extension. On this evidence, the Board considers that the maximum nearby earthquake which could reasonably occur on this fault is a shallow Magnitude 6 event with a rupture surface extending down to about 10km. When account is taken of the depths of the likely zone of major energy release on the assumed dipping fault, the closest distance of this dominant seismic source from the Forebay and Afterbay Dams should be, for safety evaluation purposes, as follows:

Forebay Dam — 3 miles  
Afterbay Dam — 7 miles

"For the Afterbay Dam, this distance is the same as that considered in the safety evaluation already performed and thus its adoption does not affect the recommendations contained in the Afterbay Dam Seismic report.

"For the Forebay Dam, the Board suggests that the safety evaluation earthquake motions should have the following characteristics (for a rock outcrop motion):

Peak ground acceleration: 0.45g  
Peak ground velocity: 35 cm/sec

The accelerogram used for analysis should desirably have a "fling" in the early part of the record and an acceleration response spectrum for which the ratio of maximum spectral acceleration,  $(S_a)_{max}$ , to peak ground acceleration,  $a_{max}$ , is about 3 for 5% damping. The general shape of the acceleration response spectrum should be similar to those generally considered representative of rock response spectra. In the vicinity of the dam, however, the maximum ground acceleration on soil deposits should not exceed about 0.55g and the accelerations in rock should be limited as necessary to correspond to this limitation on ground surface motions."

Subsequent to receiving this set of recommendations from the Special Consulting Board, several analyses were performed in 1985 using the Oroville Reanalysis Earthquake scaled to have a peak acceleration of 0.45g. However, an interim review performed by the Division of Safety of Dams indicated strong objections to the use of a MCE for the Prairie Creek Lineament that was any less than the 6.5 value adopted for the Cleveland Hill Fault. The reasons for this position are detailed in a December 26, 1985 memorandum by C. M. dePolo and include evidence of ground cracking and aftershock activity along the fault trace extension following the 1975 Oroville Earthquake.

## Earthquake Motions Adopted for Current Evaluation

To resolve questions regarding earthquake motions and enable the evaluation to proceed to a conclusion, it was decided to use the Oroville Reanalysis Earthquake scaled to have a peak acceleration of 0.6g and a peak velocity of 47 cm/sec. This is the same motion adopted for analyzing Oroville Dam for a near-field magnitude 6.5 earthquake. It is also consistent with the conservative assumption that the Prairie Creek Lineament extends close to Thermalito Forebay Dam and is capable of a future 6.5 magnitude earthquake (see Figure 311 and Table 53). It should be noted that this adopted scaling of peak acceleration rep-

resents a 33 percent increase over the peak acceleration value recommended by the Special Consulting Board.

Figure 312 presents a plot of the Oroville Reanalysis Earthquake scaled to have a peak ground acceleration of 0.6g. This motion has a long period "fling" component located within the first 5 seconds of the record. Figure 313 presents the acceleration response spectrum for this motion together with the scaled mean and 84th percentile (mean plus one standard deviation) response spectra determined for rock sites by Seed et al. (1974).

In general, the Department's approach is to select a mean scaling factor, such as peak acceleration or peak velocity, for use in scaling a design or reanalysis accelerogram. The accelerogram should have an acceleration response spec-

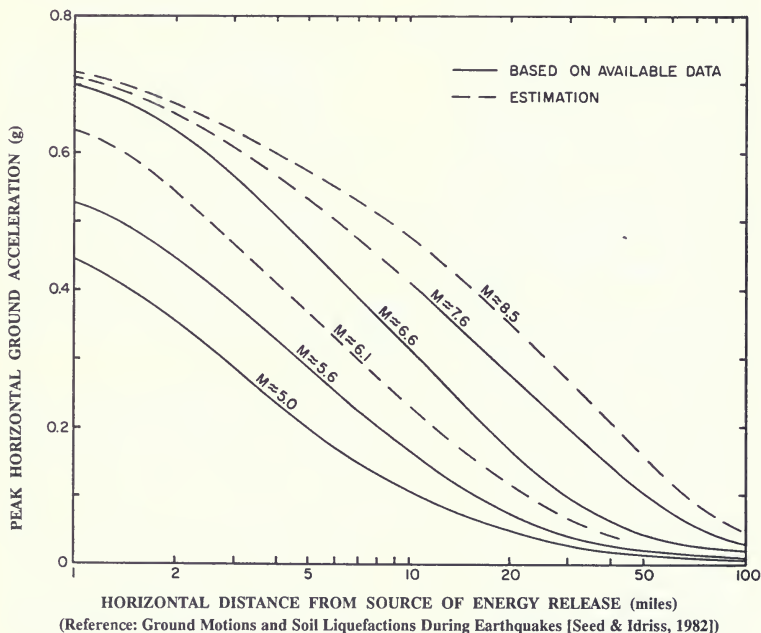


Figure 311. Average Values of Maximum Acceleration in Rock (after Seed and Idriss, 1982)

**Table 53. Average Peak Accelerations Predicted for Magnitude 6.5 Earthquake**

Location	Fault	Horizontal Distance* (Miles)	Average Peak Acceleration** (Rock)
Main Dam	Cleveland Hill	5.5	0.42g
	Prairie Creek Lineament Extension	3.0	0.54g
Low Dam	Cleveland Hill	4.5	0.46g
	Prairie Creek Lineament Extension	2.0	0.61g

\*See Figure 310

\*\*See Figure 311

trum which approaches the 84th percentile spectrum and should exceed the average spectrum for most periods of interest. Although Figure 313 shows that the Oroville Reanalysis Earthquake meets this criteria for most periods, it is also clear that this motion is deficient for periods lower than 0.35 seconds and for periods between 0.5 and 0.8 seconds. The deficiency at very low periods is not particularly significant for the earth structures at Thermalito. However, the deficiency for periods between 0.5 and 0.8 seconds could be a significant nonconservatism because embankment and foundation conditions at some locations along the Forebay exhibit similar natural periods of vibration during strong earthquake shaking.

To address the deficiency of the Oroville Reanalysis Earthquake, it was decided to also perform analyses using a scaled version of the 1940 El Centro record. This record, shown in Figure 314, has been scaled to have a peak acceleration of 0.55g, about ten percent lower than the value used for the Oroville Reanalysis Earthquake, to reflect the fact that this motion is a soil surface motion as opposed to a rock motion. This motion was chosen because its response spectrum, except for low periods, essentially meets the average stiff soil spectrum and meets the 84th percentile spectrum between periods between 0.5 and 1.1 seconds (see Figure 315). Consequently, the El Centro record provides a good complement motion to be used in analyses with the Oroville Reanalysis Earthquake.

The earthquake motions adopted are not necessarily considered to be the expected ground motions, but rather the strongest earthquake motions that could reasonably be postulated for the site, especially considering the uncertainties regarding the Prairie Creek Lineament. The

adopted motions are used with the idea that if the analyses show that the dam will withstand these motions, earthquake performance will have been proven satisfactory without having to expend time and other resources in an effort to determine the specific characteristics of the Prairie Creek Lineament Zone.

### Methods of Analysis

Computer programs SHAKE and QUAD4 were used to determine stresses in the low blowcount sand layers at the two critical dam sites. Both the Oroville Reanalysis Earthquake and the Modified El Centro Record were used as input to each of the programs.

Program SHAKE is a one-dimensional dynamic response analysis based on a solution to the wave equation. The program computes the responses in a system of homogeneous, visco-elastic layers of infinite horizontal extent subjected to vertically traveling shear waves. Each layer is defined by thickness, density, shear modulus, and damping.

The non-linearity of the shear modulus and damping values is accounted for by the use of equivalent linear soil properties (Seed and Idriss, 1970) using an iterative procedure to obtain values for modulus and damping compatible with the effective strains in each layer. Standard normalized curves (Seed and Idriss, 1970), shown in Figure 316, define the non-linear properties of shear modulus and damping with respect to strain.

Program QUAD4 is a finite element analysis that evaluates the seismic response of soil structures using a direct integration scheme for solving equations of motion. Each

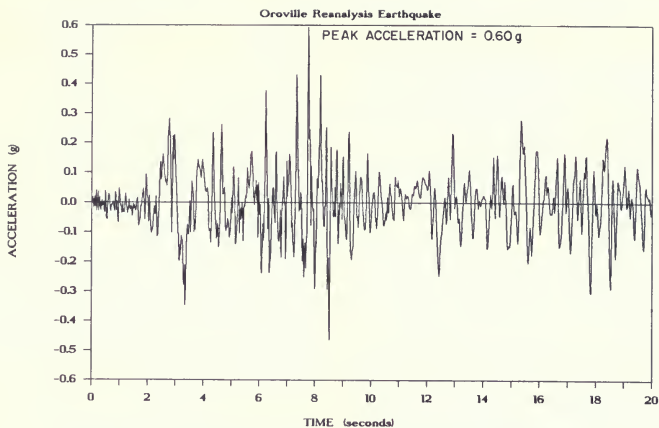


Figure 312. Oroville Reanalysis Earthquake Acceleration Time History—Rock Motion

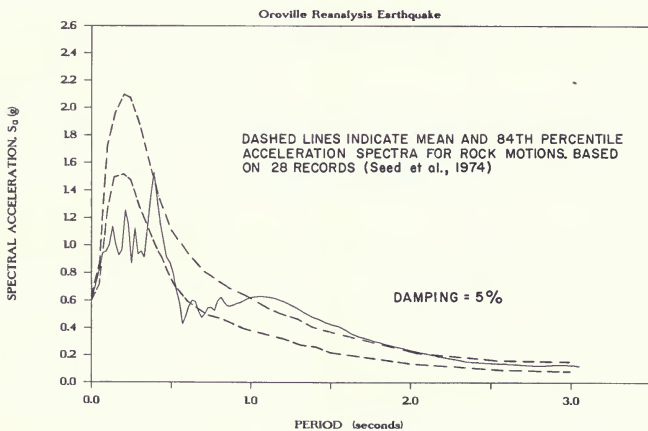


Figure 313. Oroville Reanalysis Earthquake Acceleration Response Spectrum

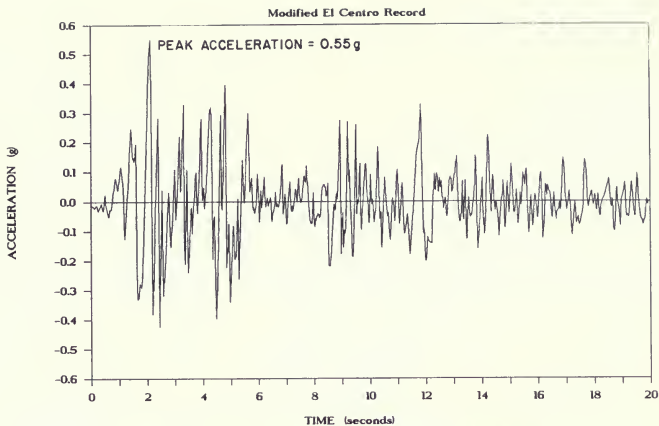


Figure 314. Modified El Centro Earthquake Motion—Ground Motion

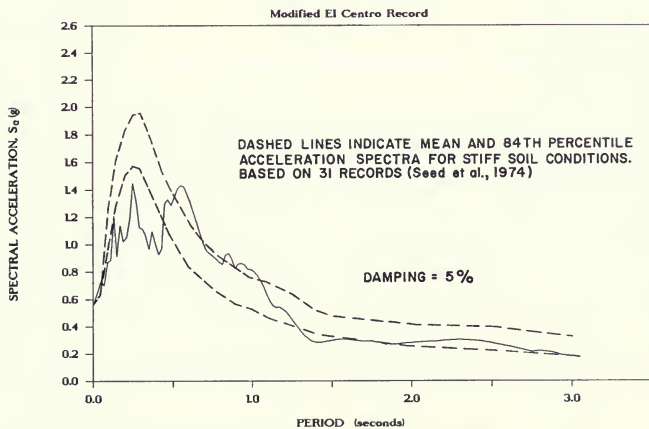


Figure 315. Modified El Centro Acceleration Response Spectrum



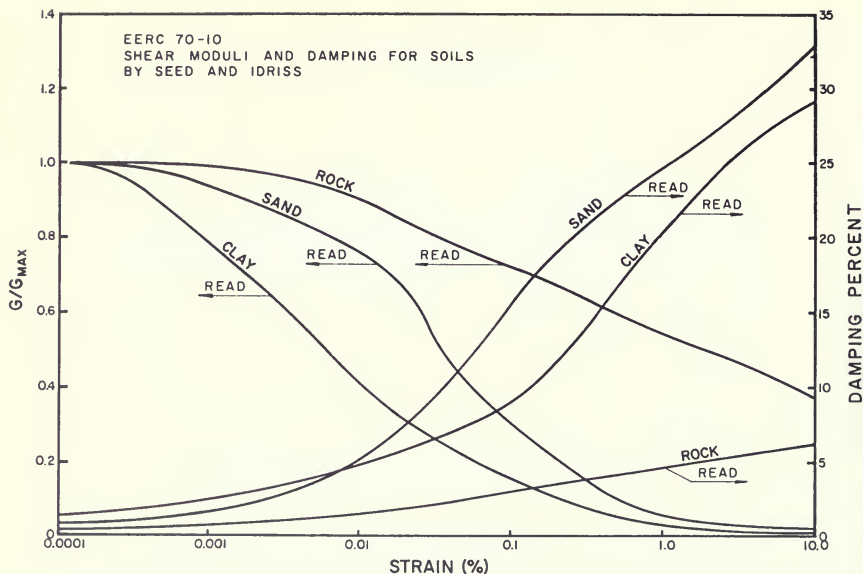


Figure 316. Thermalito Forebay, Standard Modulus Reduction and Damping Curves (after Seed and Idriss, 1970)

element in the mesh is assigned an individual value of damping ratio and shear modulus depending upon the average shear strain anticipated during the earthquake. As with program SHAKE, the QUAD4 program uses an iterative procedure and the equivalent linear method to account for the non-linearity of soil properties. The procedure works by first estimating the average dynamic shear strain that would be induced in each soil layer or element. The shear modulus and damping values associated with that strain value are then used in the analyses for the first iteration. These properties remain constant during the shaking. After the response has been computed, the calculated strain values are compared to the assumed values. If the different strain values produce a difference greater than 5 percent in the corresponding material properties, then the analysis is repeated using the new soil properties.

The material properties used in the SHAKE and QUAD4

analyses are shown in Figures 317 and 318 for the critical sites. The density values for the loose sand layers were obtained from the 1980-1981 piston samples. Density values for other soils came from tests conducted during design. The shear modulus values at low strain ( $G_{\max}$ ) for the Station 10-11 model were obtained from the shear wave velocity data obtained in Boreholes TFS-4D and 79-10 (Figures 251 and 253). From these shear wave velocities and calculated  $G_{\max}$  values, the equivalent  $K_{2\max}$  and ( $G_{\max}/S_u = 2200$ ) modulus parameters were determined and used in the computer analyses to define modulus. Shear modulus parameters for the Station 112 soils were determined using typical values obtained from both the Station 10-11 site and from Thermalito Afterbay sites. For the suspect sand layers, these relationships yielded  $K_{2\max}$  values ranging between 69 to 76 for both the Main Dam and Low Dam models.





## Results from Program SHAKE

SHAKE analyses were performed for eight columns at each of the two critical sites to determine the response across the section of the dam. The soil columns used are illustrated in Figures 317 and 318.

The Oroville Reanalysis Earthquake shown in Figure 312 represents a motion recorded on the surface or outcrop of rock. Consequently, it cannot be used directly as the base rock motion beneath the soil column as the overlying soil has an effect on the base motion induced in the rock. To account for this effect, program SHAKE converts the rock outcrop motion into a base rock sublayer motion for each soil column analyzed (see Figures 319 and 321).

The Modified El Centro record shown in Figure 7-5 represents a motion recorded on the surface of soil in the free-field. To use this motion with program SHAKE, the Modified El Centro record was applied at the surface of a downstream soil column and deconvolved down into an equivalent rock outcrop motion. This equivalent rock outcrop motion was then used to determine base rock sublayer motions for use in analyzing other columns (see Figures 320 and 322).

The acceleration time histories calculated by SHAKE for the selected soil layers within the crest and downstream soil columns are presented in Figures 319 through 322. Peak acceleration values calculated at all soil layers for the columns analyzed are shown in Figures 323 through 326.

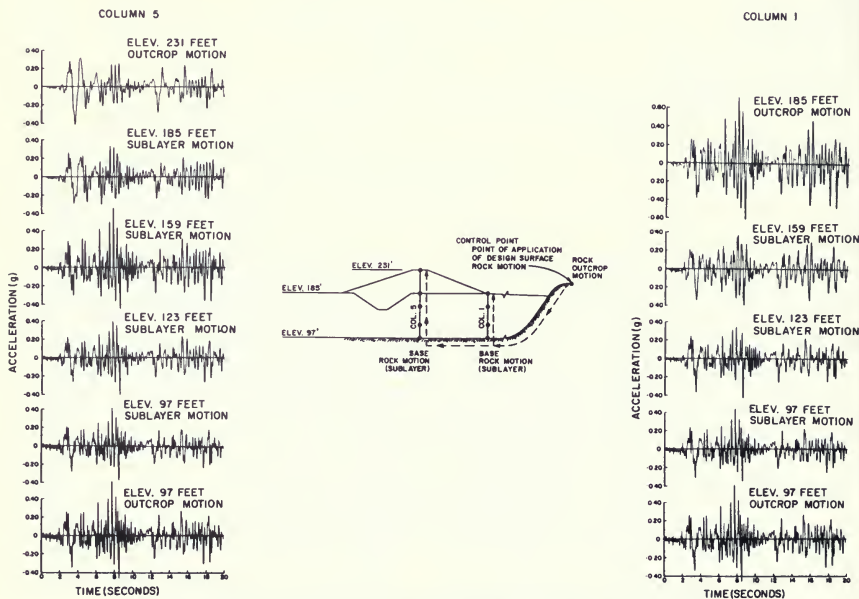


Figure 319. Thermalito Forebay Main Dam Acceleration Response—Computed from Program SHAKE using the Oroville Reanalysis Earthquake Rock Motion

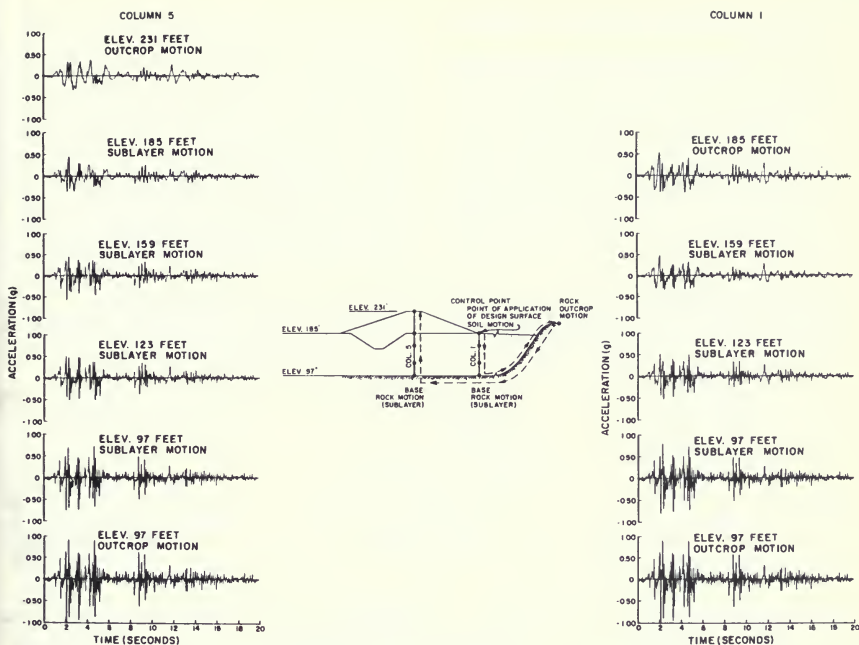


Figure 320. Thermalito Forebay Main Dam Acceleration Response—Computed from Program SHAKE using the Modified El Centro Ground Motion Record

### Results from Program QUAD4

Program QUAD4 is a finite element analysis that employs a base acceleration excitation applied at the bottom row of nodes. As with program SHAKE, it is inappropriate to use rock or soil motions recorded at free-field surfaces for direct application. Consequently, the Oroville Reanalysis Earthquake and El Centro motions shown in Figures 312 and 314 cannot be used directly as base motions. To account for the boundary conditions, the base rock motions calculated by SHAKE at the base of the downstream foundation profile (Column 1) were used in

the QUAD4 analyses for both motions.

Figures 327 through 330 present selected acceleration time histories calculated by QUAD4 for both critical sites and both earthquake motions. Shown in Figures 331 through 334 are comparisons between horizontal shear stress time histories calculated in the suspect layers by both programs SHAKE and QUAD4. Although there are some differences between the two sets of computations, both programs generally give similar patterns of response, and peak values are generally within 10 to 30 percent of each other.

## Dynamic Shear Stresses Adopted for Evaluations

The QUAD4 method of analysis better represents the actual geometry of the embankment and foundation conditions than does program SHAKE (i.e. 2-dimensional vs. 1-dimensional analysis). Consequently, the stresses determined using the QUAD4 analyses are adopted for use in calculating the extent of liquefaction in the foundation soils. The peak dynamic shear stresses calculated within the suspect foundation soils are presented in Figures 335 and 336 for both critical sites and both earthquake motions.

Because two earthquake motions were analyzed, there are two sets of induced stresses for each suspect soil element at the two critical sites. For the suspect foundation soil elements, the two earthquake motions produce peak

dynamic shear stresses that are generally within 10 to 20 percent of each other. Liquefaction determinations could be made using both sets or by using the average of the two sets of stresses calculated for each element. However, it was decided instead to simply use the *larger* of the two sets of stresses as an extra conservatism to account for any of the possible deficiencies inherent in the two earthquake motions. For analyses of the Station 10-11 Main Dam model, the Oroville Reanalysis Earthquake always produced higher stresses within the suspect soils. However, for the Station 112 Low Dam model, the modified El Centro record often produced the higher stresses.

Addendum E presents additional results from the dynamic response analyses performed and compares results between programs SHAKE and QUAD 4.

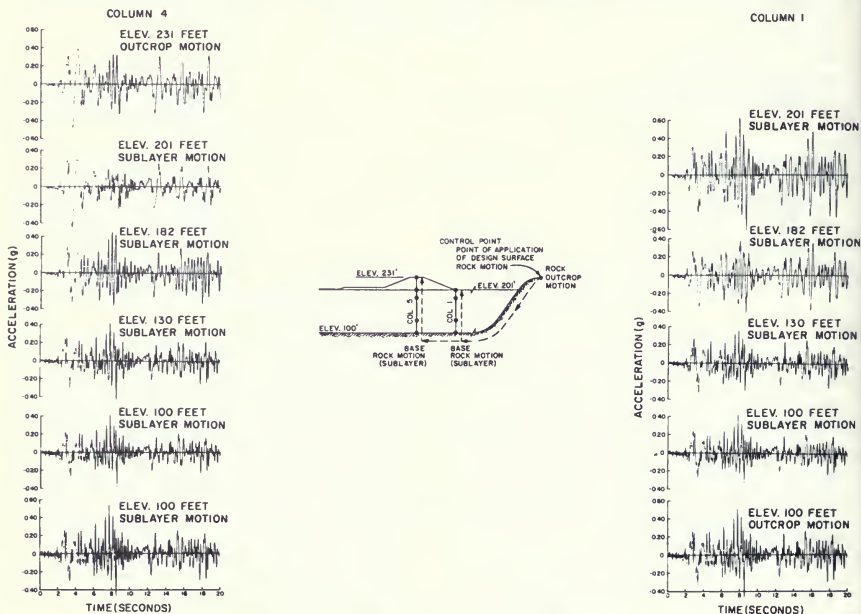


Figure 321. Thermalito Forebay Low Dam Acceleration Response—Computed from Program SHAKE using the Oroville Reanalysis Earthquake Rock Motion

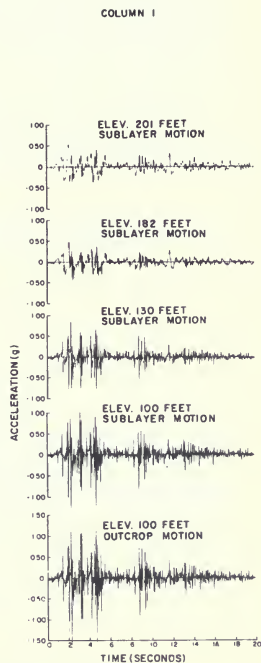
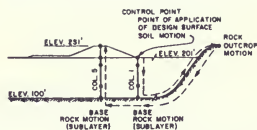
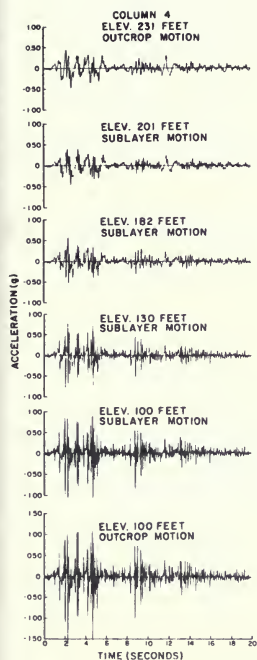


Figure 322. Thermalito Forebay Low Dam Acceleration Response—Computed from Program SHAKE using the Modified El Centro Ground Motion Record



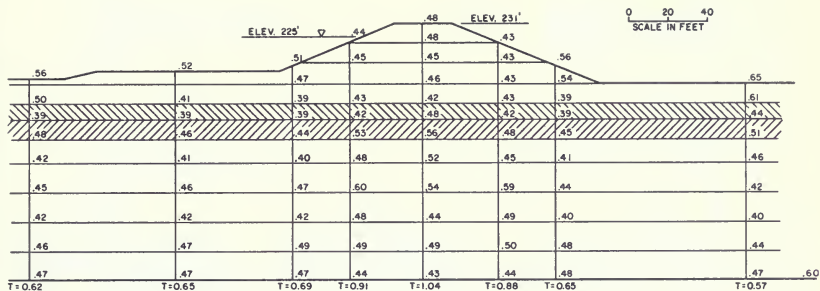


Figure 325. Thermalito Forebay Main Dam Maximum Horizontal Accelerations—Determined from Program SHAKE analyses using the Oroville Reanalysis Earthquake

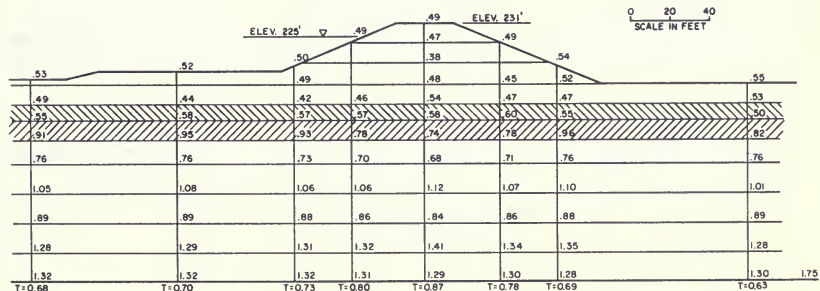


Figure 326. Thermalito Forebay Low Dam Maximum Horizontal Accelerations—Determined from Program SHAKE analyses using the Modified El Centro Record

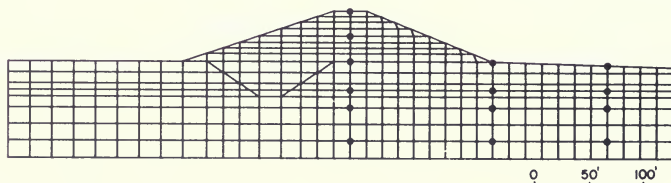
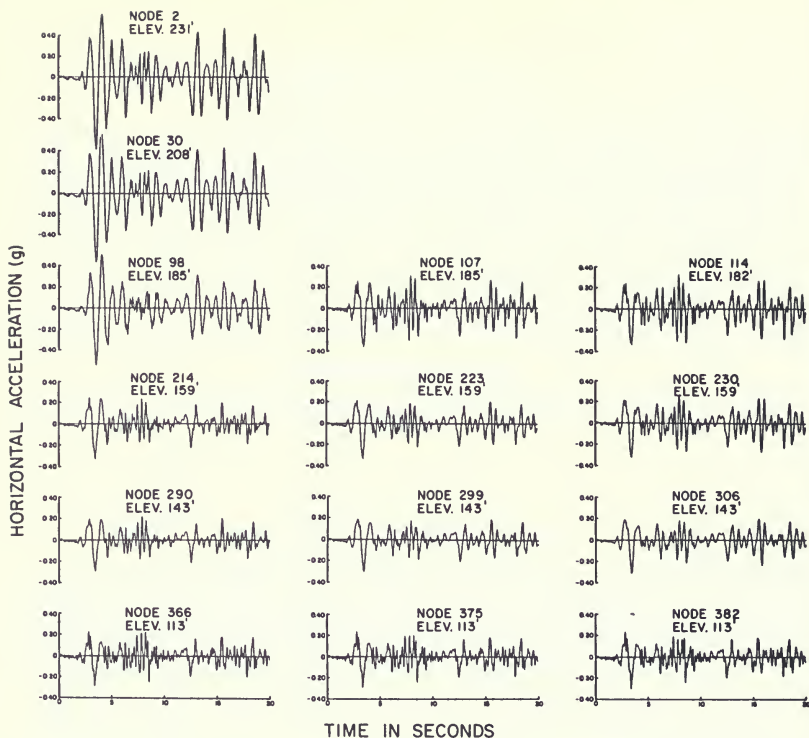


Figure 327. Thermalito Forebay Main Dam—Horizontal Acceleration Time Histories Computed by Program QUAD4 using the Oroville Reanalysis Earthquake



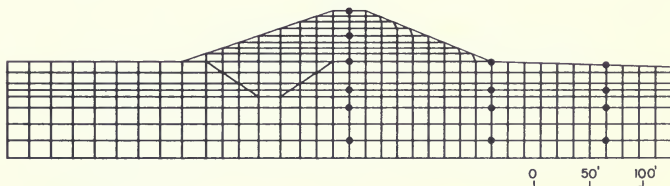
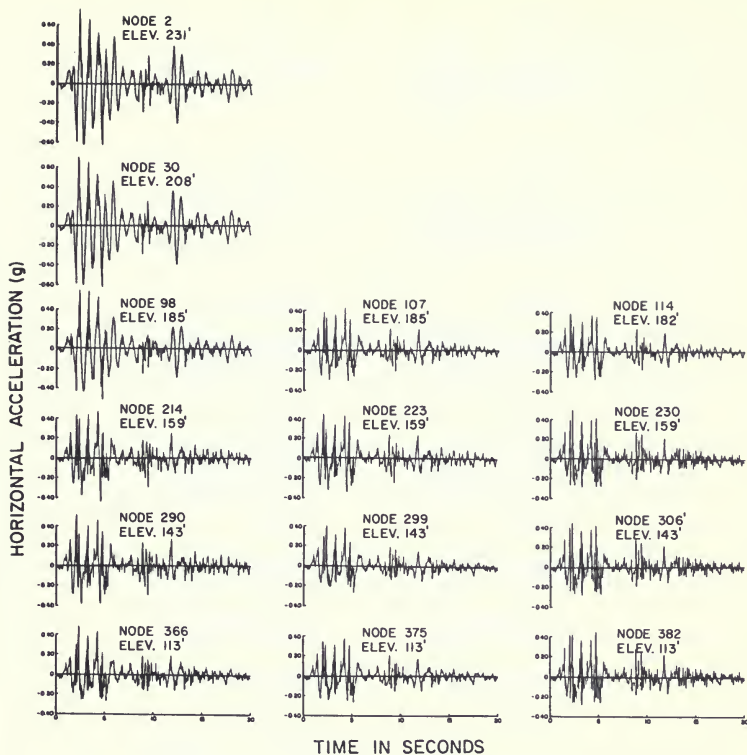


Figure 328. Thermalito Forebay Main Dam—Horizontal Acceleration Time Histories Computed by Program QUAD4 using the Modified El Centro Record

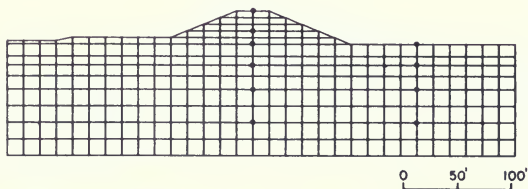
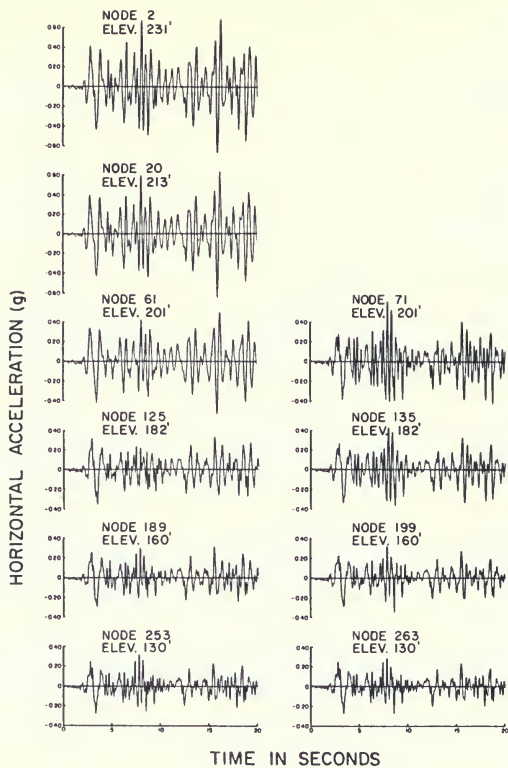


Figure 329. Thermalito Forebay Low Dam—Horizontal Acceleration Time Histories Computed by Program QUAD4 using the Oroville Reanalysis Earthquake

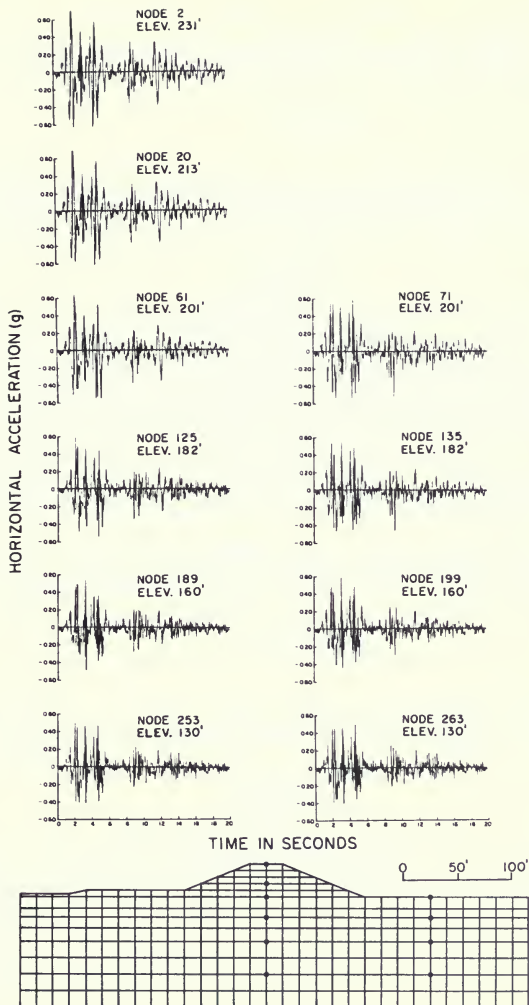


Figure 330. Thermalito Forebay Low Dam—Horizontal Acceleration Time Histories Computed by Program QUAD4 using the Modified El Centro Record

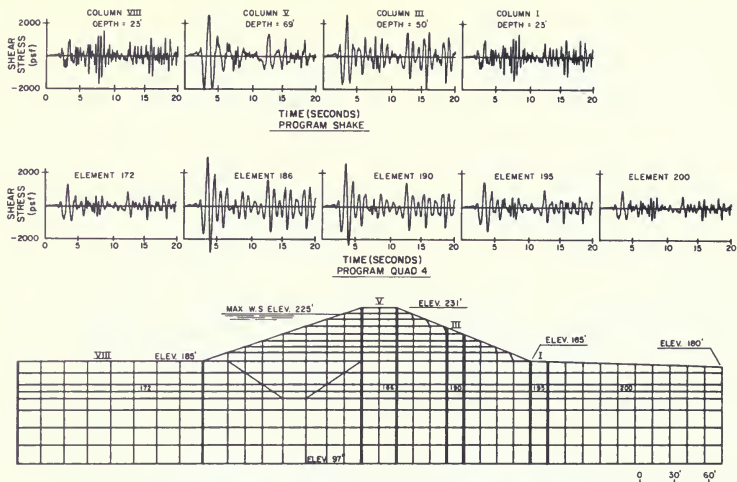


Figure 331. Dynamic Horizontal Shear Stress Time Histories Computed in the Suspect Sand Layers at Thermalito Forebay Main Dam by Programs SHAKE and QUAD4 using the Oroville Reanalysis Earthquake

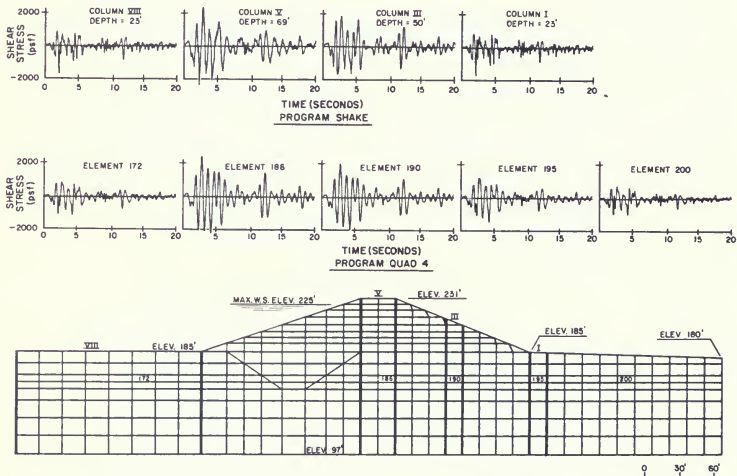


Figure 332. Dynamic Horizontal Shear Stress Time Histories Computed in the Suspect Sand Layers at Thermalito Forebay Main Dam by Programs SHAKE and QUAD4 using the Modified El Centro Record

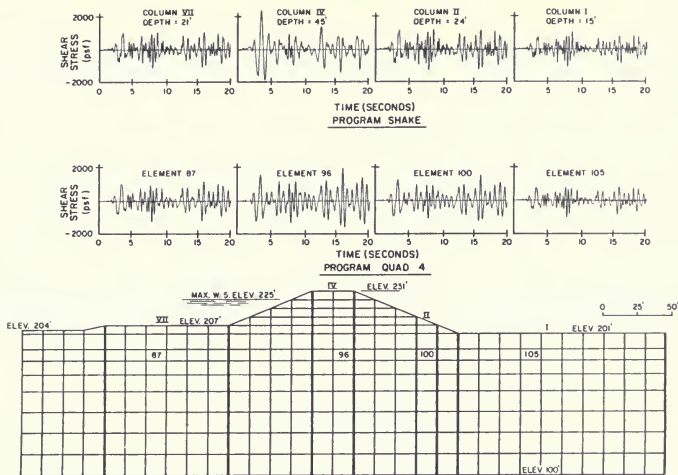


Figure 333. Dynamic Horizontal Shear Stress Time Histories Computed in the Suspect Sand Layers at Thermalito Forebay Low Dam by Programs SHAKE and QUAD4 using the Oroville Reanalysis Earthquake

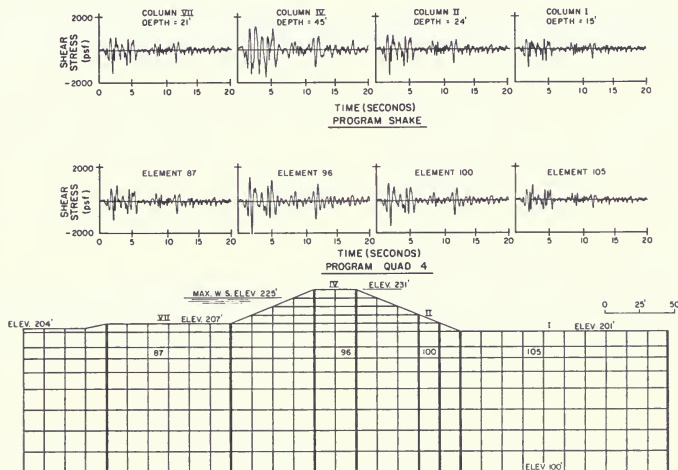
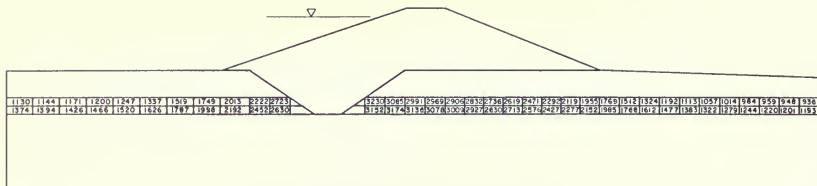


Figure 334. Dynamic Horizontal Shear Stress Time Histories Computed in the Suspect Sand Layers at Thermalito Forebay Low Dam by Programs SHAKE and QUAD4 using the Modified El Centro Record



## 8. DETERMINATION OF PREDICTED ZONES OF LIQUEFACTION

### General

The determination of which portions of the suspect foundation soils might liquefy was performed using the Seed-Lee-Idriss method of analysis (see References 66 and 67). In this approach, the horizontal plane is considered critical and factors of safety are calculated by comparing the earthquake-induced cyclic shear stresses developed on this plane to the cyclic shear strength or liquefaction resistance mobilized on this plane. This general definition

$(FS)_{liq}$  = Factor of safety against liquefaction development

$$(FS)_{liq} = \frac{\text{Cyclic Loading Resistance on Critical Plane for } N_{eq} \text{ cycles}}{\text{Cyclic Loading on Critical Plane for } N_{eq} \text{ cycles}}$$

To convert an irregular, earthquake-induced stress pattern into an equivalent uniform stress pattern, the approach detailed by Seed and Idriss (1982) was used. In this approach, the equivalent average shear stress,  $\tau_{avg}$ , is equal to 65 percent of the maximum shear stress,  $\tau_{max}$ , of the irregular stress pattern. Because large magnitude earthquakes have larger durations of strong shaking, the equivalent number of uniform cycles,  $N_{eq}$ , increases with increasing earthquake magnitude. For a 65 percent averaging factor, Seed and Idriss (1982) suggest a  $N_{eq}$  value of 8 cycles for a magnitude 6.5 earthquake.

### Determination of Cyclic Loading Resistance

Although numerous cyclic triaxial tests were performed on recovered samples of low blowcount suspect soils (see Section 4 and Addendum D), these results were not used to determine cyclic strengths. This is because such tests are now recognized within the engineering profession as being excessively influenced by sample disturbance. A common result from laboratory tests is that the in situ strengths of medium dense and dense soils are underestimated, and the strength of very loose soils is overestimated. This has led to many test programs yielding very similar cyclic loading resistances for soils ranging from medium loose to very dense in situ (e.g. see Castro, 1975).

becomes somewhat complicated because the cyclic loading resistance of soil depends on the number of cycles of loading. Thus, for evaluations of liquefaction potential, both cyclic loading and cyclic resistance must be compared for the same number of cycles of stress. However, earthquake-induced stresses are highly irregular cyclic patterns and it is necessary to convert each pattern into an equivalent number of uniform stress cycles,  $N_{eq}$ , in order to make comparisons. Thus, the factor of safety in this liquefaction evaluation is defined as:

Figure 337 presents the isotropically-consolidated cyclic triaxial test results obtained from 1981-84 Thermalito Forebay Dam foundation samples. Since the cyclic triaxial test does not reproduce field conditions, a correction factor ( $C_r$ ) is used to modify the cyclic triaxial test results. Results presented in Figure 337 show a significant scatter of resistances for different confining pressures, sampling sites, and in situ blowcounts at the sampling sites. Although samples of silty sand indicated a trend of increased laboratory strength with increased SPT blowcount, the reverse trend can be observed for the more clayey SC/SM samples. Also shown on this figure is the cyclic loading resistance determined using SPT correlations for the suspect layer at the Station 112 site. Although the SPT strength matches the overall average of the laboratory data, the SPT strength is for a  $N_{A1}$  blowcount of 19 whereas the laboratory strength is for samples from layers having generally higher  $N_{A1}$  values ranging between 17 and 39. This comparison thus also supports the results of other studies indicating that cyclic triaxial tests can significantly underestimate the cyclic loading resistance of medium dense and dense soils (e.g. see Tokimatsu and Yoshimi, 1981).

The cyclic loading resistances of the suspect foundation sands at the two critical sites were determined in Section 5 using the Seed and Idriss (1982) correlation between SPT blowcount and liquefaction resistance. The cyclic

strengths of the suspect sands, expressed as cyclic stress ratios for level ground overburden pressures

( $CSR_1 = \tau_s/\sigma'_y$ ) are as follows:

Site	Elevation Interval (ft)	35th Percentile SPT $N_{A1}$ (Blows/foot)	Fines Content (%)	Cyclic Stress Ratio for $M = 6.5$ (8 cycles) (s/y)
Station 10-11	159-165	23	> 15%	0.36
	153-159	28	> 15%	0.48
Station 112	172-190	19	> 15%	0.30

The SPT correlation can provide cyclic stress ratios ( $CSR_1$ ) that are appropriate for level ground ( $\alpha = 0$ ) overburden conditions of about 1 tsf. However, the dam foundation at the two critical sites exist generally beneath sloping ground ( $\alpha > 0$ ) and with overburden conditions that are not 1 tsf. To adjust  $CSR_1$  values for the conditions, the following formula suggested by Seed (1983) was used:

$$\tau_s = CSR_1 \times K_o \times K_a = (\tau_s/\sigma'_y) \times \sigma'_y \times K_o \times K_a$$

where:

$\tau_s$  = cyclic loading resistance

$CSR_1$  = average cyclic stress ratio required to cause liquefaction in 8 cycles for a level ground overburden pressure of about 1 tsf—from Seed and Idriss's (1982) correlation:

$$\text{For } N_{A1} = 19, (CSR_1 = \tau_s/\sigma'_y) = 0.30$$

$$\text{For } N_{A1} = 23, (CSR_1 = \tau_s/\sigma'_y) = 0.36$$

$$\text{For } N_{A1} = 28, (CSR_1 = \tau_s/\sigma'_y) = 0.48$$

The  $K_o$  and  $K_a$  corrections are simply scaling factors to account for consolidation conditions. The values of the corrections were obtained for a set of cyclic triaxial tests performed for Thermalito Afterbay silty sands having SPT blowcounts of 20 (see Chapter III). Thermalito Afterbay data was used because there were insufficient good quality anisotropically-consolidated tests available from Thermalito Forebay soils. The tests produced the following corrections: (see next column)

Effective Confining Pressure (tsf or ksc)	K $\alpha = 0$	K $\alpha = 0.18$
1.0	1.00	1.76
2.5	0.70	1.60

These correction factors are either comparable or lower than the typical values reported by Seed (1983). To evaluate elements with overburden pressures different than either 1.0 or 2.5 tsf and/or alpha values different than either 0 or 0.18, the above values were used to develop interpolated or extrapolated values.

### Determination of Liquefaction Factors of Safety

Safety factors against the development of liquefaction were calculated using the approach outlined above and contain the following components:

1. Seed-Lee-Idriss Method defining the horizontal plane as the critical plane (see References 66 and 67).
2. Earthquake-induced cyclic shear stresses on the horizontal plane calculated using finite element analysis QUAD4. The larger of the stresses from analyses using the Oroville Reanalysis Earthquake and Modified El Centro motions was used.
3. The equivalent uniform cyclic stress pattern was 8 cycles with an amplitude equal to 65 percent of the peak stress calculated by QUAD4.
4. The cyclic shear strength was obtained using the Seed and Idriss (1982) SPT correlation, together with the



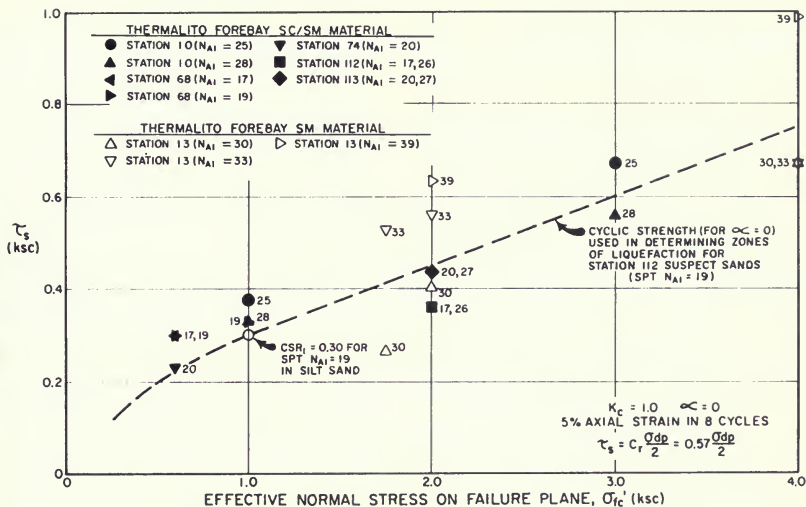


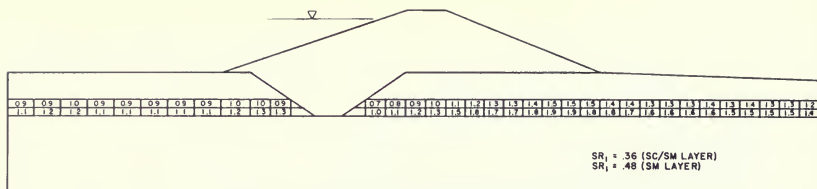
Figure 337. Comparison of Cyclic Triaxial Test Results of Foundation SC/SM Material

35th percentile SPT  $N_{A1}$  blowcount for the suspect soils. The cyclic shear strength was extended to different consolidation conditions using  $K_o$  and  $K_a$  correction factors determined from cyclic triaxial tests performed on Thermalito Afterbay silty sand with an  $N_{A1}$  equal to 20. Figures 338 and 339 present the safety factors in the suspect sands for the two modeled sites. Also shown in these figures are induced pore pressure ratios corresponding to the liquefaction safety factors.

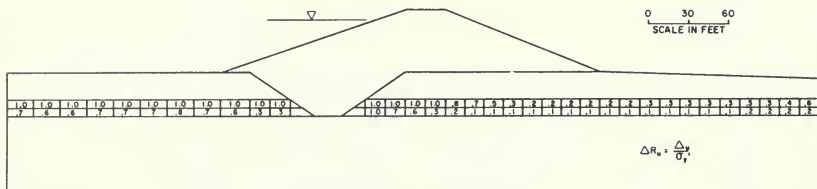
Results for the Station 10-11 Main Dam model (Figure

338) indicate significant zones of liquefaction and excess pore pressure upstream of the dam's centerline, but little liquefaction either beneath the downstream slope or downstream of the dam.

The results for the Station 112 Low Dam model (Figure 339) indicate liquefaction in the suspect layers upstream of the dam's centerline and downstream of the toe. However, beneath the downstream slope and extending somewhat downstream beyond the embankment toe, the suspect soil layer does not completely liquefy, although some excess pore pressures are predicted.

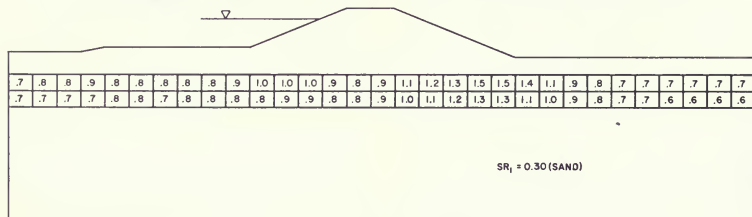


FACTORS OF SAFETY AGAINST LIQUEFACTION,  $\tau_s / \tau_{avg}$ .

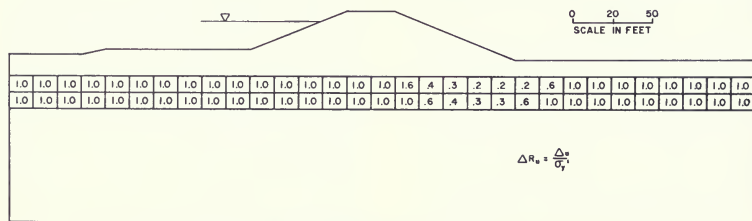


PORE PRESSURE RATIOS,  $\Delta R_u$

Figure 338. Thermalito Forebay Main Dam (Station 10-11 Area) Factors of Safety Against Liquefaction



FACTORS OF SAFETY AGAINST LIQUEFACTION,  $\tau_s / \tau_{avg}$ .



PORE PRESSURE RATIO,  $\Delta R_u$

Figure 339. Thermalito Forebay Main Dam (Station 112 Area) Factors of Safety Against Liquefaction

## 9. POST-EARTHQUAKE SLOPE STABILITY ANALYSES

### Introduction

Post-earthquake slope stability analyses were performed to determine if the earthquake-induced pore pressures and/or liquefaction that might develop in portions of the suspect foundation layers would lead to failure of the embankment. Since these pore pressures would not dissipate immediately after the earthquake, the static shear strength of the foundation sands would remain greatly reduced. The extreme case would be in the liquefied zones, where the strength would be reduced to its residual shear strength.

The post-earthquake slope stability analyses consisted of two steps:

1. Selection of soil strengths to represent the post-earthquake conditions.
2. Calculation of safety factors against sliding on trial failure surfaces through the high pore pressure zones.

No seismic inertial forces (i.e. pseudostatic) were used in these analyses. This was because the predicted zones of liquefaction beneath the embankments correspond to liquefaction factors of safety generally between 0.8 and 1.0. Thus, it required virtually the full duration of significant earthquake shaking to liquefy these zones, leaving very little of the earthquake motions to load the structure after the onset of liquefaction. In addition, the number of equivalent cycles for a magnitude 6.5 earthquake is relatively small (e.g. 8 cycles for  $M = 6.5$  vs. 25 cycles for  $M = 8$ ). These two facts thus indicate that post-liquefaction inertial forces would be relatively small.

### Post-Earthquake Shear Strengths

#### Clayey Embankment and Foundation Cap

Studies of the behavior of embankment dams composed of and/or founded on clayey soils have shown that such soils perform very well during even very strong earthquake shaking (see Seed et al., 1978). Consequently, such soils are believed to not sustain significant strength losses

during earthquake shaking. However, to allow for some possible degradation of strength, the following strength reductions were incorporated in the stability analyses:

1. Undrained shear strengths are considered appropriate for the saturated portions of the clayey soils because the critical period of time for stability problems following an earthquake is believed to be only a few hours. The static undrained strengths of the clayey materials are considered to be those determined using the  $\tau_{ff}$  vs  $\sigma_{fc}'$  stress interpretation of the triaxial compression test results using a 15 percent axial strain failure criterion. To account for possible strength degradation in the clayey soils, a 20% strength reduction was used in modeling these soils in the stability analyses. These reduced strengths are equivalent to those obtained using the Mohr circle stress interpretation of the results together with a 10 percent axial strain failure criterion (see Table 52).
2. To account for the potential development of tensile cracks in the embankment, the soil strength above the phreatic surface was reduced to zero cohesion and a friction angle of 30 degrees.

### Non-Liquefied Suspect Foundation Soils

Portions of the suspect foundation sands were determined to not liquefy during the postulated earthquake loading. These are the zones in Figures 338 and 339 where the factor of safety against liquefaction is greater than 1.0. Nevertheless, these soil zones would be expected to experience some strength loss. To model this strength loss, the excess dynamic pore pressures computed in Section 8 were used together with the drained strengths of the suspect soils.

### Liquefied Suspect Foundation Soils

The portions of the suspect foundation sands that were determined to liquefy in Section 8 are considered to have sustained significant strength losses. The residual strengths of liquefied soils are undoubtedly heavily influenced by the in situ conditions of the soil (e.g. void ratio, relative density, particle cementation, etc.) As with cyclic loading resistance determinations, conventional sampling

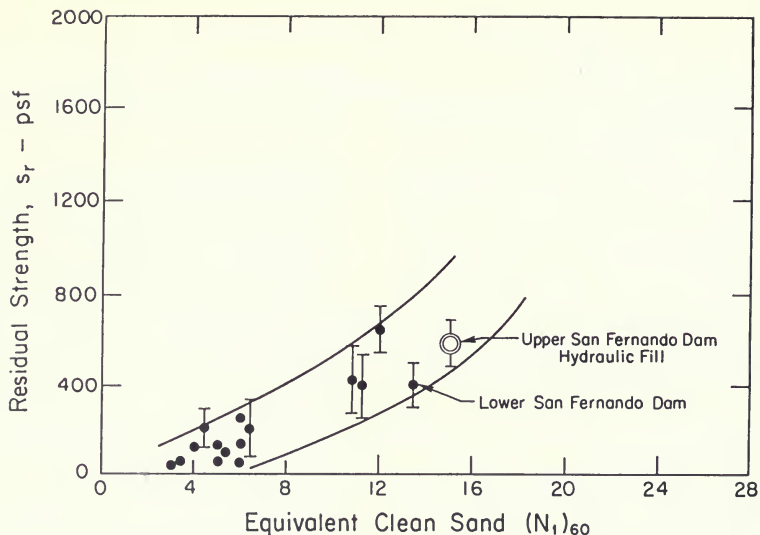


Figure 340. Relationship between Residual Shear Strength and Equivalent Clean Sand SPT Value of  $(N_1)_{60}$  (after Seed et al., 1988)

and testing approaches are not believed to be capable of reliably determining residual shear strengths of liquefied soils. Although Section 3 describes attempts made to determine residual strengths using 1984 Thermalito Forebay samples in post liquefaction triaxial compression tests, these results are not credible because of potential sample disturbance effects. In addition, because these samples were first cyclically loaded to failure, significant void ratio redistribution could have taken place making the post-cyclic test results even more suspect.

At the current (1988) time, only two approaches are generally believed to be theoretically capable of determining the residual shear strength of liquefied soils:

1. The correlation developed by Seed (1987), which is based on the performance of soils during earthquakes. In this correlation, corrected equivalent clean sand SPT resistance  $[(N_1)_{60}]_{CS}$ , is related to

the residual shear strength back-calculated from movements induced in soil structures.

2. The steady-state strength approach outlined by Poulos et al. (1985). In this approach, residual or steady state strengths are determined using undrained triaxial compression tests in conjunction with void ratio corrections to account for void ratio changes caused during sampling and testing. To use this approach, extremely careful sampling and density measurement techniques are required during the sampling, sample handling, and testing phases.

Figure 340 presents the most recent version of the Seed correlation between equivalent clean sand  $[(N_1)_{60}]_{CS}$  corrected SPT blowcount and residual shear strength (see Reference 70). This corrected blowcount employs different corrections than the ones employed in developing the  $N_{A1}$  values used for the Thermalito sites. The differences are as follows:

1. The corrections for test procedures are different. As detailed in Table 46, p. 307, an  $(N_1)_{60}$  blowcount is approximately 13% less than an  $N_{A1}$  blowcount.
2. The Seed (1987) SPT blowcounts represent equivalent clean sand penetration resistance. To convert blowcounts obtained in silty sand with a fines content of about 25%, Seed (1987) suggests adding 2 blows per foot to the measured blowcount.

Presented in Table 54 are the 35th percentile SPT blowcount values corresponding to the suspect foundation sands at the two critical sites. In addition to presenting the blowcounts in terms of both  $N_{A1}$  and  $[(N_1)_{60}]_{CS}$  values, Table 54 indicates the level of residual shear strength that the Seed (1987) correlation would predict. Since the SPT correlation does not actually extend to the blowcount values appropriate to the critical sites at Thermalito Forebay, an extension of the lower bound curve was used.

**Table 54. Residual Shear Strengths Predicted Using the Seed et al. (1988) Correlation**

Site	Elevation Interval (feet)	$N_{A1}$	$(N_1)_{60}$	$[(N_1)_{60}]_{CS}$	Residual Shear Strength Predicted Using Seed Correlation (psf)
Main Dam Station 10-11	159-169	23	20.0	22.0	> 2,000
	153-159	28	24.5	26.5	> 2,000
Low Dam Station	172-190	19	16.5	18.5	> 800

Table 54 indicates that the residual shear strength of the suspect soils at both sites would be greater than 800 psf using the Seed (1987) correlation. Although steady-state strength tests were not performed for Thermalito soils, some insight as to what this alternative approach might have yielded can be obtained by examining Figure 341, developed from data presented by Von Thun (1986). It shows the residual strength predicted using the steady-state approach compared to the corrected equivalent clean sand SPT blowcount of the soils tested. Also shown Figure 341 is the Seed (1987) correlation between corrected SPT blowcount and residual strength.

The data in Figure 341 show that the steady-state strength approach generally gives significantly higher residual strength values than does the Seed (1987) correlation. For the equivalent clean sand SPT blowcounts found within the suspect sands at Thermalito (18.5 to 26.5), the steady-state strength approach gives residual strengths between 1300 and 7500 psf.

In light of the above comparisons, a residual strength value of 800 psf was conservatively adopted for the liquefied zones within the suspect foundation layers at both critical sites.

### Slope Stability Analyses

The post-earthquake slope stability analyses were performed by assuming trial failure surfaces through the embankment and suspect foundation soils. The trial failure surfaces considered in these analyses were oriented to intercept the suspect foundation layers.

Reservoir elevation was assumed to be maximum normal water surface, Elevation 225 feet. This value was assumed because the Forebay reservoir level is generally held at or near this elevation throughout the year.

The Modified Bishop Method using an IBM PC version of computer program BISHOP was used to evaluate circular surfaces. Spencer's Method, using an IBM PC version of computer program STABL, was used to evaluate wedge-shaped surfaces.

Figures 342 and 343 show the most critical of several upstream and downstream surfaces analyzed for the two critical sites studied. Table 55 summarizes the minimum slope stability factors of safety corresponding to the critical surfaces. For both sites, the minimum factor of safety corresponds to a circular surface on the downstream side.

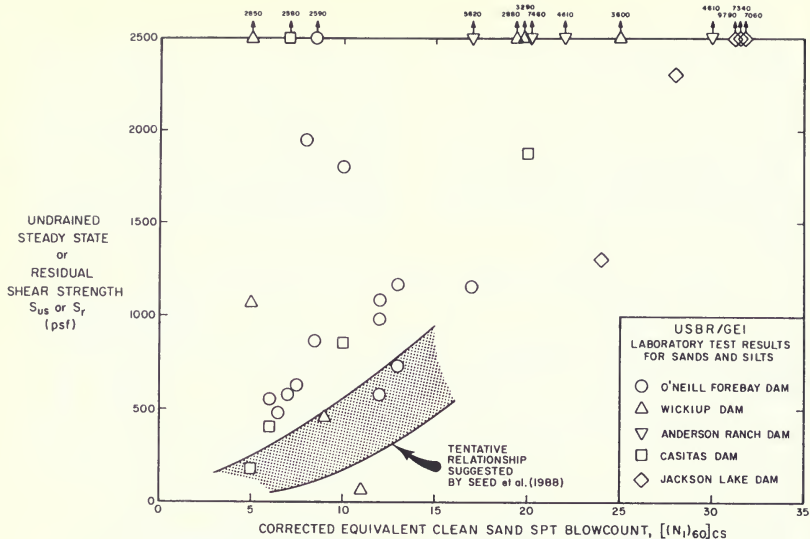


Figure 341. Relationship between Residual Shear Strength and Equivalent Clean Sand Value of  $(N_1)_{60}$   
(after Von Thun, 1986)

SOIL NO.	DENSITY (pcf)	C (psf)	$\phi$	$C'$ (psf)	$\phi'$	$\Delta R_u$
1	134	640	23	-	-	0
2	140	-	-	0	45	0
3	129	-	-	0	30	0
4	127	960	18	-	-	0
5	119	$S_r = 800$	0	-	-	1.0
6	119	-	-	0	31	0.6
7	119	-	-	0	31	0.2
8	131	800	40	-	-	0

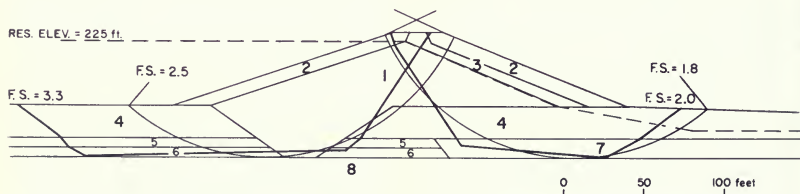


Figure 342. Thermalito Forebay Main Dam--Summary of Critical Failure Surfaces Determined from Post-Earthquake Stability Analyses

SOIL NO.	DENSITY (pcf)	C (psf)	$\phi$	C' (psf)	$\phi'$	$\Delta R_u$
1	128	960	14	-	-	0
2	135	-	-	0	45	0
3	124	-	-	0	30	0
4	127	960	18	-	-	0
5	119	$S_u^* 800$	0	-	-	1.0
6	119	-	-	0	31	0.4
7	131	800	40	-	-	0

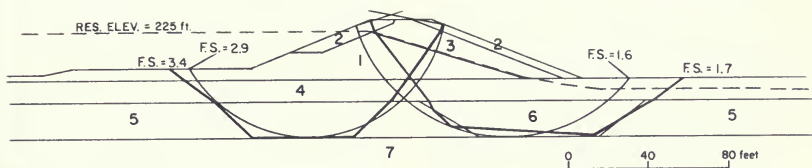


Figure 343. Thermalito Forebay Low Dam—Summary of Critical Failure Surfaces Determined from Post-Earthquake Stability Analyses

Table 55. Summary of Post-Earthquake Slope Stability Analysis

Site	Sliding Surfaces	Upstream Factor of Safety	Downstream Factor of Safety
Station 10–11 Main Dam Model	Circular (PGM BISHOP) [Modified Bishop Method]	2.48	1.81*
	Wedge (PGM STABL) [Spencer's Method]	3.25	2.00
Station 112 Low Dam Model	Circular (PGM BISHOP) [Modified Bishop Method]	2.90	1.60*
	Wedge (PGM STABL) [Spencer's Method]	3.43	1.74

\*Most critical for site analyzed

For the Station 10–11 Main Dam model, the minimum factor of safety is 1.8. For the Station 112 Low Dam model, the minimum factor of safety is 1.6.

Pore pressure redistribution effects were not estimated for the following reasons:

1. Distribution of material types, densities, residual strengths, and permeabilities is very complex within the modeled loose sand layers. Pore pressure redistribution within the layer cannot be estimated with any reasonable degree of certainty. Because of the

added factor of permeability, redistribution estimates are even less certain than estimates of initial induced pore pressures. Although crude simplifying assumptions were made for the Afterbay analyses (Chapter III), the authors were not satisfied that a reasonable answer resulted, and judged that answer to be excessively conservative.

2. The minimum slope stability factors of safety for the two critical sites are between 1.6 and 1.8. Based on the redistribution effects found for Thermalito Afterbay Dam (Chapter III), a factor of safety in excess

of 1.6 would be an ample safety margin for pore pressure redistribution.

3. Since the residual shear strength values used in this study are based on those determined from actual case histories, the effect of pore water pressure redistribution may already be accounted for.

### **Effect Of Residual Shear Strength**

Many analyses of post-earthquake slope stability are sensitive to the values of residual shear strength adopted for zones predicted to liquefy. In an effort to quantify the sensitivity of the computed factor of safety to different values of residual shear strength, additional slope stability analyses were performed. The results of these analyses are presented in Figures 344 and 345.

Figure 344 shows that the Station 10-11 Main Dam analyses are relatively insensitive to changes in residual shear strength. This is because only a relatively small portion of the suspect foundation sands at this site was determined to completely liquefy for the postulated earthquake motions. Figure 345 shows that the Station 112 Low Dam analyses are more sensitive to changes in residual shear strength. However, if the residual shear strength is set at 400 psf, equal to only half of the lower-bound value suggested by Seed (1987) and Seed et al. (1988), the factor of safety drops to 1.4, a margin of safety generally considered acceptable.

Even for a zero residual shear strength assumption (extremely conservative), the factor of safety remains at 1.2 or higher. Accordingly, the analyses show that the embankment will retain adequate sliding stability for the postulated earthquake motion.



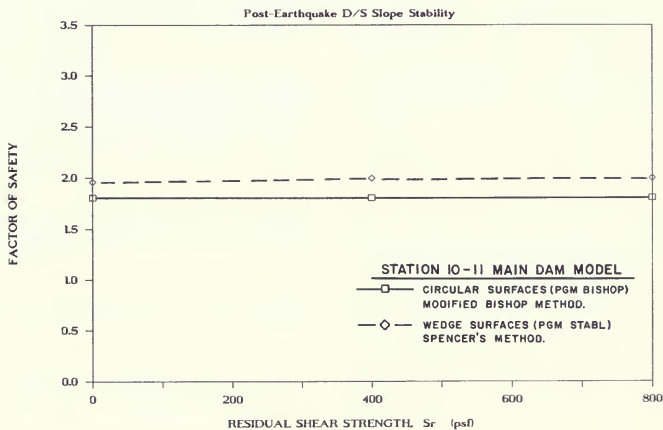
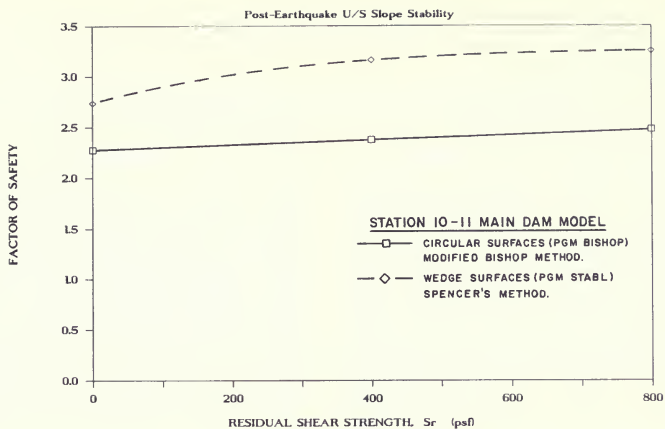


Figure 344. Thermalito Forebay Main Dam—Critical Factors of Safety Vs. Residual Shear Strengths

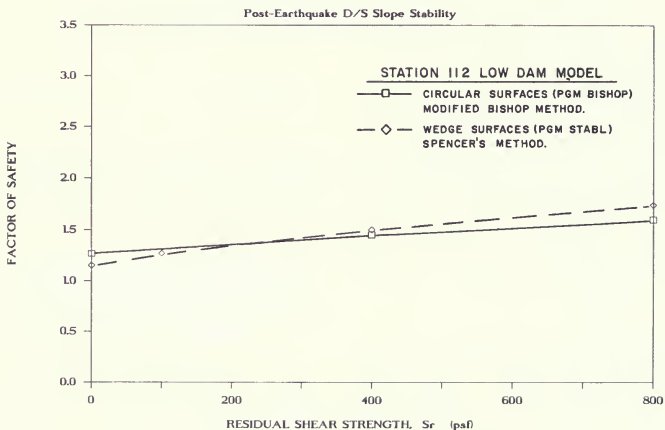
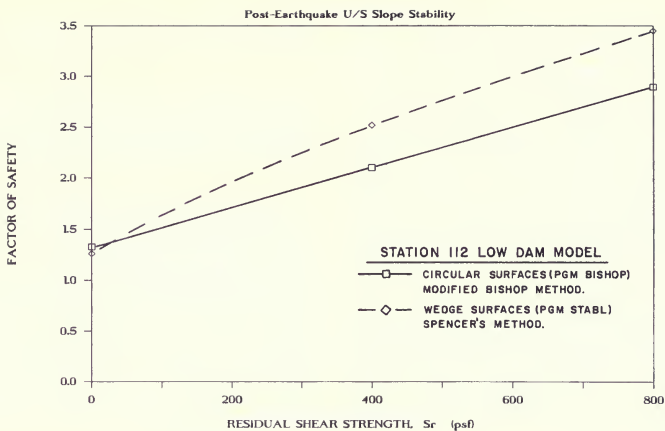


Figure 345. Thermalito Forebay Low Dam—Critical Factors of Safety Vs. Residual Shear Strengths

## 10. EVALUATION OF CONCRETE WINGWALL DAMS

### Introduction

As described in Section 2, two concrete gravity dams or wingwall structures form part of Thermalito Forebay Dam. These two structures flank the Thermalito Powerplant Headworks Structure and are known as the Approach Channel and the Wingwall dams (see Figure 210, page 273). The seismic stability of the headworks structure was found to be adequate in a previous study (see Chapter II of this bulletin). Although a modern concrete gravity dam has never failed during an earthquake, potential failure during seismic shaking was considered to be possible by one of the following two modes:

- a. Seismic shaking resulting in instability or sliding. Because the two dams are founded on relatively fresh basalt, the foundation mass was considered generally competent and highly resistant to sliding. A similar conclusion was reached for the concrete mass. For these reasons, sliding at the concrete/rock interface was considered critical.
- b. Seismic shaking resulting in the generation of large tensile stresses within the concrete mass. Tensile stresses greatly in excess of the concrete's tensile strength could lead to severe cracking and sliding on cracked surfaces.

To evaluate the seismic stability of the two concrete dams for the two potential modes of failure, the following studies were performed:

1. Simplified pseudodynamic sliding analyses were performed for the critical monolith cross section of the two structures.
2. Simplified stress analyses were run to determine the level of earthquake-induced tensile stresses that might develop within the concrete monoliths.
3. The performance of similar structures which have sustained strong earthquake shaking in the past was reviewed.

### Description of Concrete Wingwall Dams

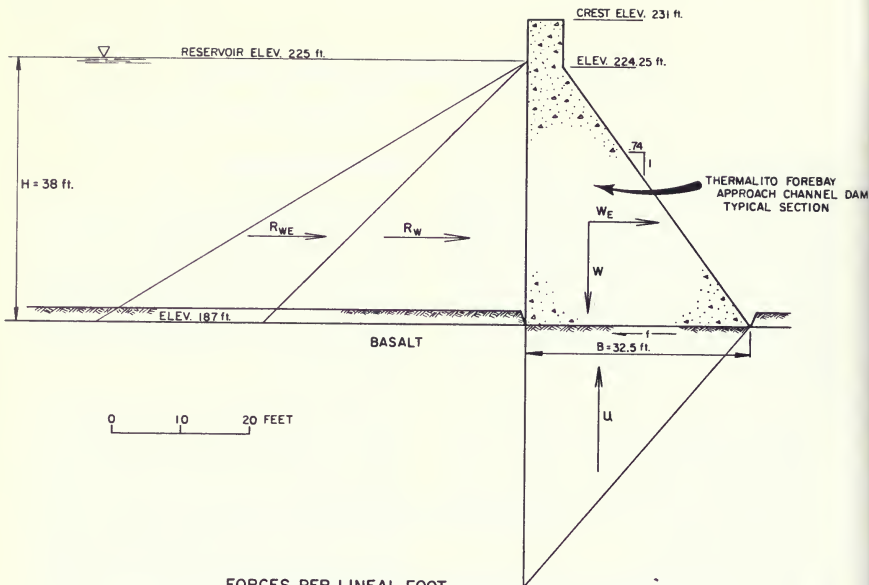
#### Approach Channel Dam

The Approach Channel Dam consists of six monoliths (A-1 through A-6), which block the end of the approach channel. The monoliths are founded on basalt rock ( $T_{vm}$ ), which was described in the "Final Geology Report" as being generally fresh to slightly weathered. During construction, the foundation was stripped to firm rock and cleaned with air jets. Both blanket and curtain grouting were performed.

The monoliths are joined by two 9-inch polyvinyl chloride waterstops which bracket a 5-inch asphalt seal. The northern four monoliths (A-3 through A-6) are less than 44 feet high. However, the two most southern monoliths (A-1 and A-2) have variable geometrics with monolith A-1 increasing to a maximum height of 82 feet (see Figure 223, page 292). Although the two southern monoliths contain a drainage gallery, the following analyses assumed that drainage was obstructed during the earthquake, requiring full uplift pressure to be included in the analyses.

#### Wingwall Dam

The Wingwall Dam consists of three monoliths (A, B, and C) which generally have the same cross section and 51-foot height. However, a small portion of monolith A was extended to have a maximum height of 71 feet (see Figure 222, page 291). The Wingwall Dam is founded on basalt rock similar to the Approach Channel Dam and received similar foundation treatment during construction. As with the Approach Channel Dam, the monoliths are joined by polyvinyl chloride waterstops and an asphalt seal. The eastern end of monolith C butts up against the embankment of the Main Dam at Station 2 + 03 as shown in Figure 224, page 293. The Wingwall Dam does not contain a drainage gallery and, therefore, the full uplift pressure was assumed to act on the base of the monoliths.



### FORCES PER LINEAL FOOT

$\lambda$  = HORIZONTAL EARTHQUAKE ACCELERATION / ACCELERATION OF GRAVITY ( $g$ ) = .6

$$\begin{aligned} R_w &= \text{HYDROSTATIC WATER FORCE} = \frac{1}{2} \gamma_w H^2 \\ &= \frac{1}{2} (.0624 \text{ KIPS/FT.}^3) (38 \text{ FT.})^2 \\ &= 45 \text{ KIPS/FT.} \end{aligned}$$

$$\begin{aligned} R_{WE} &= \text{HYDRODYNAMIC WATER FORCE} = .726 C \lambda \gamma_w H^2 \\ &= .726 (.733) (.6) (.0624 \text{ KIPS/FT.}^3) (38 \text{ FT.})^2 \\ &= 29 \text{ KIPS/FT.} \end{aligned}$$

$$\begin{aligned} W &= \text{WEIGHT OF DAM} = (\text{AREA OF DAM CROSS SECTION})(\gamma_c) \\ &= (1,248 \text{ FT.}^2) (158 \text{ KIPS/FT.}^3) \\ &= 197 \text{ KIPS/FT.} \end{aligned}$$

$$\begin{aligned} W_E &= \text{PSEUDOSTATIC EARTHQUAKE FORCE ON DAM} = \lambda W \\ &= (.6) (197 \text{ KIPS/FT.}) \\ &= 118 \text{ KIPS/FT.} \end{aligned}$$

$$\begin{aligned} U &= \text{UPLIFT WATER PRESSURE FORCE} = \frac{1}{2} 8H \gamma_w \\ &= \frac{1}{2} (32.5 \text{ FT.}) (.0624 \text{ KIPS/FT.}^3) \\ &= 39 \text{ KIPS/FT.} \end{aligned}$$

$$\begin{aligned} S &= \text{COHESION SHEAR STRENGTH OF INTERFACE BETWEEN CONCRETE AND} \\ &\quad \text{BASALT FOUNDATION} = 0.09, 0.5 \text{ KSI} \end{aligned}$$

$$\begin{aligned} f &= \text{SHEAR RESISTANCE AT CONCRETE - BASALT INTERFACE} = SB \\ &\quad CB = (.09 \text{ KSI}) (144 \text{ IN.}^2 / \text{FT.}^2) (32.5 \text{ FT.}) = 421 \text{ KIPS/FT.} \\ \text{OR } CB &= (.5 \text{ KSI}) (144 \text{ IN.}^2 / \text{FT.}^2) (32.5 \text{ FT.}) = 2340 \text{ KIPS/FT.} \end{aligned}$$

Figure 346. Static and Pseudo-Dynamic Forces Acting on Channel Dam - Typical Section

## Concrete Mixes

The interior masses of the concrete monoliths were constructed using a 2.5-sack concrete mix. A relatively thin facing mix of 3-sack concrete, believed to be approximately 3 to 5 feet thick, was apparently placed. The average 1-year compressive strength was found to be about 3800 psi for the 2.5-sack mix and 4500 psi for the 3-sack mix.

## Pseudodynamic Sliding Analyses

### General

During design, many of the Oroville Project concrete dams were analyzed for pseudodynamic sliding and/or overturning. The sliding analyses generally used a concrete/rock interface direct shear strength of 500 psi and a pseudodynamic seismic coefficient of 0.1g. Due to the envelopment of the embankment fill, the Wingwall Dam was apparently not analyzed. However, the Approach Channel Dam was analyzed for both overturning and pseudodynamic loadings. When analyzed for overturning, the force resultant fell within the middle third of the base for both static and pseudodynamic (0.1g) loadings. The sliding factor, or ratio of horizontal to vertical loading, for the operating case with seismic force was found to be from 0.57 to 0.83.

### Re-evaluation of Pseudodynamic Sliding

During design and the re-evaluation of other concrete dams within the Oroville Project (see Bulletin 203-78), the Department analyzed sliding stability using the shear-friction equation:

$$Q = \frac{CA + N \tan \phi}{H}$$

where  $Q$  = Sliding factor of safety  
 $H$  = Summation of total horizontal forces  
 $C$  = Cohesion strength = 500 psi  
 $A$  = Area of base  
 $N \tan \phi$  = Frictional Strength = assumed = to 0

For concrete dams founded on sound rock, the shear resistance was defined as a cohesion strength of 500 psi.

For the re-evaluation of the wingwall dams, a pseudodynamic coefficient of 0.6g, equal to the postulated peak ground acceleration, was used in addition to the static horizontal forces. A hydrodynamic force based on the 0.6g peak acceleration and procedures developed by the U. S. Bureau of Reclamation (see Reference 9) was also incorporated in the sliding analyses. Because the 500 psi represents a relatively high shear resistance, calculations were also made using a reduced cohesion strength of 90 psi. The reduced value, which represents less than 3 percent of the unconfined compressive strength of the concrete, is representative of below average concrete/rock bond strength and was used in an effort to determine the sensitivity of the sliding stability to the assumed shear resistance.

### Approach Channel Dam

Although the variable geometry of the monolith A-1 yields a maximum height of 82 feet, the downstream side of this monolith butts up against basalt rock (see Figure 223, page 292) and thus cannot easily slide downstream. A similar geometric condition exists for portions of monolith A-2. Although monoliths A-3 through A-5 are smaller in height at approximately 44 feet, they do not butt up against basalt on the downstream. Consequently, the sliding analyses assumed that monoliths A-3 through A-5 were critical for sliding. Figure 346 presents a cross section representative of Monolith A-3 together with the static and pseudodynamic forces loading the monolith. Summing up the applied horizontal forces yields the following factors of safety against sliding for monolith A-3:

For a cohesion strength of 500 psi: Sliding F. S. = 12.2  
For a cohesion strength of 90 psi: Sliding F. S. = 2.2

The 2.2 factor of safety is considered both adequate and conservative.

As an additional stability check, the stability of monolith A-1, with a height of 82 feet, was also analyzed by assuming horizontal sliding on a 52-foot horizontal rock surface. The 52-foot length is equal to the inclined length along the actual rock surface. By using this resistance, together with the higher applied static and pseudodynamic horizontal loading corresponding to the 82-foot maximum height of monolith A-1, a conservative estimate of

sliding stability is determined. The calculations for the modified A-1 monolith section yields the following factors of safety against sliding:

For a cohesion strength of 500 psi : Sliding F. S. = 8.1  
 For a cohesion strength of 90 psi : Sliding F. S. = 1.5

As for monolith A-3, the minimum 1.5 factor of safety computed for monolith A-1 using the conservative procedures outlined above is considered adequate.

## Wingwall Dam

Although the Wingwall Dam monoliths are embedded within the embankment fill, simplified sliding analyses were performed in an effort to gain some insight to the possible sliding stability of the monoliths. The calculations were performed in the same manner as for the Approach Channel Dam with the embankment soil ignored in the calculations. The fill was ignored because soil-structure interaction behavior during seismic loadings is not well understood: the potential resistances/loadings of the soil relative to the concrete are very questionable due to strain compatibility problems.

Figure 347 presents a 51-foot high cross section generally representative of all three monoliths of the Wingwall

Dam. Also shown in this figure are the generalized static and pseudodynamic forces used in the stability calculations. Summing up the applied horizontal forces yields the following factors of safety against sliding for the monoliths of the Wingwall Dam:

For a cohesion strength of 500 psi : Sliding F. S. = 13.1  
 For a cohesion strength of 90 psi : Sliding F.S. = 2.4

Figure 222, page 291, shows that the western portion of monolith C expands to a height of about 71 feet. To account for the increased height on this portion, the calculations were repeated by conservatively assuming a uniform monolith height of 71 feet. Summing up the applied horizontal forces yields the following factors of safety against sliding for the higher monolith height:

For a cohesion strength of 500 psi : Sliding F. S. = 8.9  
 For a cohesion strength of 90 psi : Sliding F. S. = 1.6

As for the Approach Channel Dam monoliths, the calculated factors of safety against sliding are considered both adequate and conservative. Table 56 presents a summary of the factors of safety against sliding calculated for the monoliths within both the Approach Channel and Wingwall Dams.

**Table 56. Summary of Pseudostatic Factors in Safety Against Sliding for Concrete Dam Monoliths**

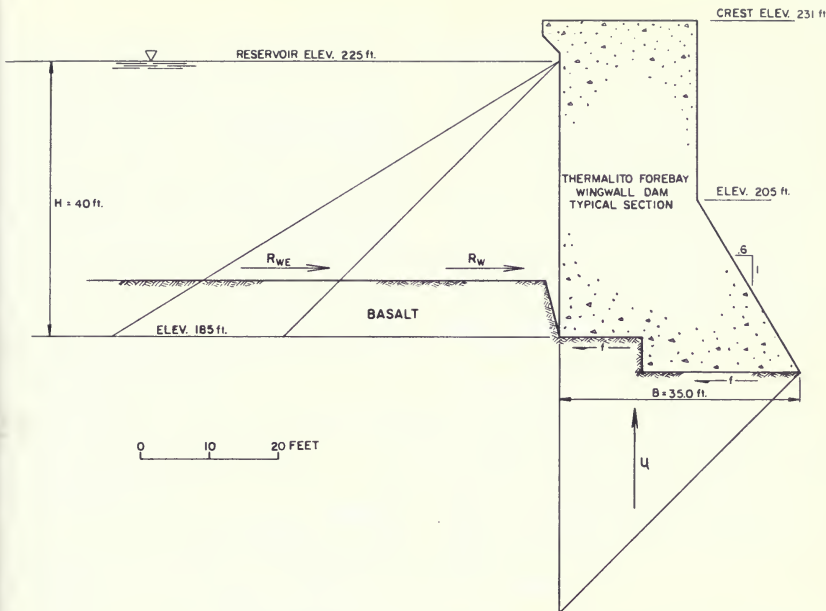
Dam	Monolith	Height (ft)	Cohesion (psi)	Factor of Safety
Approach Channel Dam	Mod. A-1	82	90	1.5
Approach Channel Dam	Mod. A-1	82	500	8.1
Approach Channel Dam	A-3	44	90	2.2
Approach Channel Dam	A-3	44	500	12.2
Wingwall Dam	Mod. A	71	90	1.6
Wingwall Dam	Mod. A	71	500	8.9
Wingwall Dam	C	51	90	2.4
Wingwall Dam	C	51	500	13.1

## Simplified Dynamic Tensile Stress Analyses

### General

The potential for the development of excessive tensile stresses and consequent cracking within the dam was analyzed by performing simplified dynamic stress analyses.

The analyses follow the general procedure outlined by Chopra (1978) and consider that the principal response is estimated using an earthquake design spectrum. This procedure also included the capability of analyzing hydrodynamic forces and the effect of reservoir water on the dam's fundamental period.



### FORCES PER LINEAL FOOT

$\lambda$  = HORIZONTAL EARTHQUAKE ACCELERATION / ACCELERATION OF GRAVITY ( $g$ ) = .6

$R_W$  = HYDROSTATIC WATER FORCE =  $1/2 \gamma_w H^2$   
 =  $1/2 (.0624 \text{ KIPS/FT.}^3)(40 \text{ FT.})^2$   
 = 50 KIPS/FT.

$R_{WE}$  = HYDRODYNAMIC WATER FORCE =  $.726 C \lambda \gamma_w H^2$   
 =  $.726 (.733)(.6)(.0624 \text{ KIPS/FT.}^3)(40 \text{ FT.})^2$   
 = 32 KIPS/FT.

$W$  = WEIGHT OF DAM = (AREA OF DAM CROSS SECTION)( $\gamma_c$ )  
 =  $(1164 \text{ FT.}^2)(.158 \text{ KIPS/FT.}^3)$   
 = 184 KIPS/FT.

$W_E$  = PSEUDOSTATIC EARTHQUAKE FORCE ON DAM =  $\lambda W$   
 =  $(.6)(184 \text{ KIPS/FT.})$   
 = 110 KIPS/FT.

$U$  = UPLIFT WATER PRESSURE FORCE =  $1/2 B H \gamma_w$   
 =  $1/2 (35.0 \text{ FT.})(40 \text{ FT.})(.0624 \text{ KIPS/FT.}^3)$   
 = 44 KIPS/FT.

$S$  = COHESION SHEAR STRENGTH OF INTERFACE BETWEEN CONCRETE AND BASALT FOUNDATION = 0.09, 0.5 KSI

$f$  = SHEAR RESISTANCE AT CONCRETE - BASALT INTERFACE =  $S_B$   
 $S_B = (.09 \text{ KSI})(144 \text{ IN.}^2/\text{FT.}^2)(35.0 \text{ FT.}) = 454 \text{ KIPS/FT.}$   
 OR  $S_B = (.5 \text{ KSI})(144 \text{ IN.}^2/\text{FT.}^2)(35.0 \text{ FT.}) = 2520 \text{ KIPS/FT.}$

Figure 347. Static and Pseudo-Dynamic Forces Acting on Wingwall Dam - Typical Section

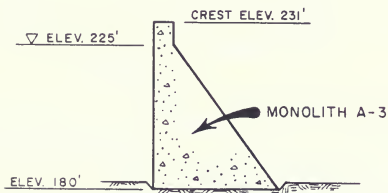
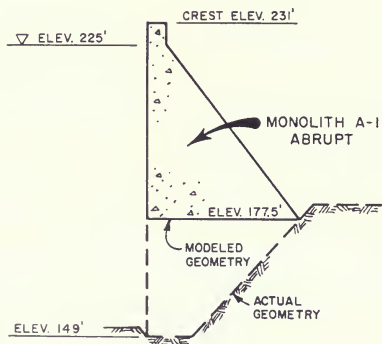
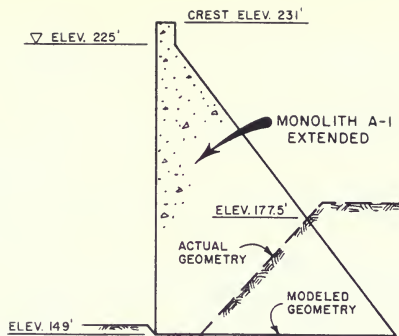


Figure 348. Approach Channel Dam—Modified Cross-Sections used in Simplified Dynamic Tensile Stress Analyses



To estimate the maximum tensile stresses within the concrete dam monoliths, two computer solutions were used: The first is program GRAVDAM, written by the Division of Safety of Dams (Reference 4). The other is Program SMPL, written by Fenves and Chopra (1986). Although both solutions are based on the procedure outlined in the Chopra (1978) study, the two programs also incorporate corrections developed from studies of concrete dams using more sophisticated finite element techniques (see References 42 and 43). A summary of the modifications follows:

Modification	GRAVDAM	SMPL
Influence of foundation stiffness on response is approximated (programs do not use same technique)	X	X
Added damping effects on hydrodynamic forces due to reservoir bottom absorption	X	X
Effects of higher modes approximated		X

In the analyses of the Thermalito Forebay concrete dams, both programs used the 84th percentile acceleration response spectrum determined for rock outcrops by Seed et al. (1974). This response spectrum was computed using 5 percent viscous damping and was scaled to have a peak acceleration of 0.6g at small periods. For calculations using Program SMPL, an alpha value of unity for reservoir sediment effects was conservatively adopted. Although Program SMPL prescribes the use of damping values higher than 5 percent (as high as 23 percent for the parameters and geometries considered in this study) the highest damping value used in the analyses of the Thermalito structures was conservatively set at 5 percent. The simplified analyses are considered to give more conservative results than more detailed finite element analysis techniques (References 33 and 43).

### Analysis Parameters

The value of concrete unit weight and modulus of elasticity ( $E_c$ ) was selected to be 158 pcf and 5 million psi, respectively. These values are the same as those adopted for analyzing the Thermalito Diversion Dam and the Thermalito Powerplant Headworks Structure (see Bulletin

203-78 and Chapter II of this bulletin). The value for the foundation modulus of elasticity ( $E_f$ ) is uncertain. A modulus of 20 million psi would be appropriate to the fresh basalt attributed to the foundation. However, the shear wave velocity test results obtained within the Middle and Lower Basalt flows ( $T_{vm}$  and  $T_{vl}$ ) indicate a modulus of elasticity of only about 1 million psi (see Figure 253). Consequently, values of 1, 5 and 20 million psi were employed for foundation modulus of elasticity in the calculations. A foundation modulus of 20 million psi produces a  $E_f / E_c$  ratio of 4, indicating a relatively rigid foundation. A foundation modulus of 1 million psi produces a  $E_f / E_c$  ratio of 0.2, indicating a relatively flexible foundation.

### Approach Channel Dam

Tensile stress calculations were made for both the highest monolith (A-1) and for the typically-sized monolith (A-4) in the Approach Channel Dam (see Figure 348). Because the variable geometry of monolith A-1 was not in a form readily analyzed by the computer methods, two different modified cross sections were used for the calculations (see Figure 348).

### Wingwall Dam

As with the sliding calculations, it was recognized that the tensile stress computations were not directly applicable due to the fact that the Wingwall Dam monoliths were partially embedded within embankment fill. The presence of the fill and soil-structure interaction effects probably affect the dynamic stress calculations even more than for the sliding calculations. However, tensile stress calculations were also performed on this structure in an effort to gain some insight on the potential for the development of tensile cracking within the concrete. It was thought that as long as the predicted tensile stresses were very significantly below the tensile strength of the concrete, analytical uncertainties would not be important.

Because the three Wingwall Dam monoliths (A through C) have very similar cross sections, only one geometry was used in the tensile stress analyses (see Figure 349). The relatively small portion of monolith A, which increases in height near the headworks structure, was considered to have a minimal effect on the total response of the monolith.

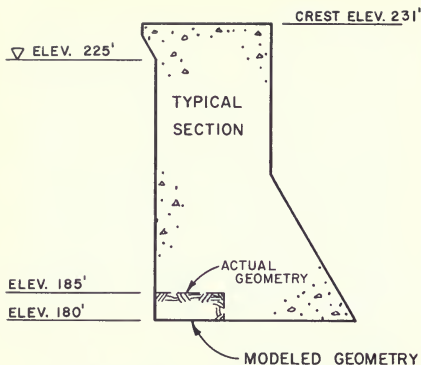


Figure 349. Wingwall Dam—Modeled Cross Section used in Simplified Dynamic Tensile Stress Analyses

### Computed Tensile Stresses

Table 57 summarizes the results from the dynamic tensile stress analyses. The results are presented in the form of combined static and peak dynamic stresses found within the monolith analyzed. Figures 350 and 351 present typical distributions of combined stresses for the two dams.

In general, computer programs GRAVDAM and SMPL gave comparable stress results for analyses of the Approach Channel Dam. The peak tensile stresses were generally found near the base of the monoliths for this dam. The maximum tensile stress computed in this structure was 394 psi.

In the analyses of the Wingwall Dam, program GRAVDAM gave significantly higher tensile stresses than program SMPL. The reason for this was not determined, although it may be related to the fact that there is a significantly greater mass in the upper portion of this dam than in the Approach Channel Dam. This feature is reflected by the fact that the location of highest tensile stress in the Wingwall Dam is located at the downstream change in slope instead of at the base the dam as at the Approach Channel Dam (see Figures 350 and 351). The maximum tensile stress computed for the Wingwall Dam is 356 psi.

Dynamic tensile stresses are generally considered acceptable if the combined static and dynamic peak stresses are less than 15 percent of the unconfined compressive strength of the concrete (Reference 80). For the 3-sack shell and 2 1/2-sack mass concrete within the Thermalito Forebay concrete dams, 15 percent of the unconfined compressive strength would be approximately 675 and 570 psi, respectively. The results of the various solution

Table 57. Summary of Maximum Tensile Stresses

Dam	Monolith	Height (feet)	Concrete $E_c$ ( $10^6$ psi)	Foundation $E_f$ ( $10^6$ psi)	Peak Tensile Stresses (psi)			
					GRAVDAM		SMPL	
					U/S	D/S	U/S	D/S
Approach Channel	A-1 Extended	82	5	20	279	243 (T=0.074)	-	-
				5	304	274 (T=0.085)	-	-
				1	360	333 (T=0.123)	394*	386 (T=0.115)
Approach Channel	A-1 Abrupt	53.5	5	20	84	80 (T=0.46)	-	-
				5	94	97 (T=0.53)	-	-
				1	149	147 (T=0.076)	133	140 (T=0.072)
Approach Channel	A-3	44	5	20	58	60 (T=0.036)	-	-
				5	59	63 (T=0.042)	-	-
				1	96	101 (T=0.061)	71	71 (T=0.056)
Wingwall	A,B,C	51	5	20	190	167 (T=0.44)	90	85 (T=0.042)
				5	228	204 (T=0.050)	94	89 (T=0.048)
				1	356*	329 (T=0.072)	137	132 (T=0.056)

\*Denotes highest tensile stress calculated for dam.

T Denotes fundamental period in seconds.

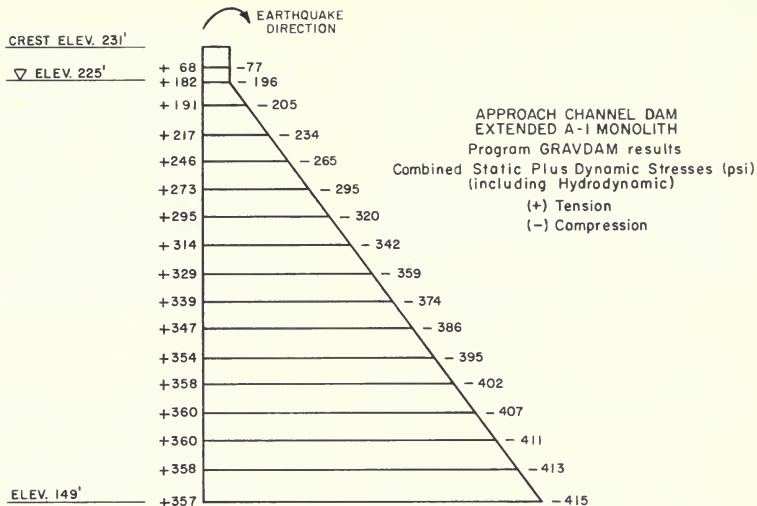


Figure 350. Typical Distributions of Combined Static plus Maximum Dynamic Stresses Calculated for the Approach Channel Dam Monoliths

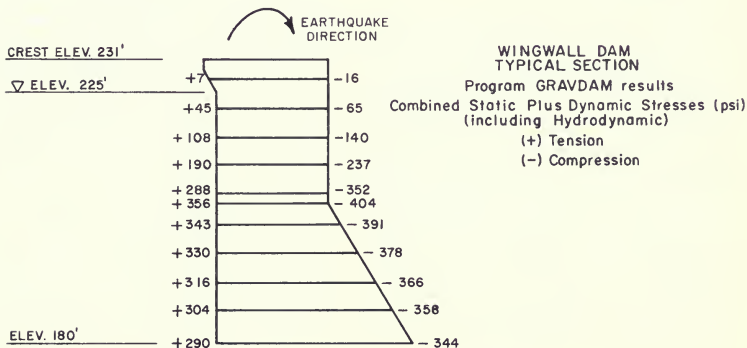


Figure 351. Typical Distributions of Combined Static plus Maximum Dynamic Stresses Calculated for the Wingwall Dam Monoliths

methods, input properties, and geometries yielded a maximum tensile stress of 394 psi (combined static plus peak dynamic). This value is in good accord with the peak tensile stresses estimated for the concrete gravity monoliths within Thermalito Diversion Dam (see Bulletin 203-78) and for the concrete headworks structure (see Chapter II of this bulletin). Since this tensile stress represents only 9 to 11 percent of the unconfined compressive strength, the monoliths would not be expected to develop significant cracking during the postulated earthquake shaking.

### Performance of Concrete Dams During Earthquake Shaking

There are not many histories of performance available for concrete dams that have sustained strong earthquake damage. However, three dams have experienced very strong shaking but remained stable:

1. **Lower Crystal Springs Dam.** This dam is a gravity arch dam approximately 140 feet high. It was located approximately 1000 feet away from the rupture of the San Andreas Fault during the 1906 San Francisco Earthquake ( $M > 8$ ). Despite what must have been very strong earthquake loading, this dam survived undamaged (Reference 33).
2. **Koyna Dam.** This dam is concrete gravity structure with a maximum height of approximately 340 feet and is located in central India. In 1967, it experienced strong shaking from a magnitude 6.5 earthquake. This earthquake was estimated to have produced a transverse peak acceleration of 0.5g in the rock surface. In non overflow monoliths, where tensile stresses were estimated to have been as high as 1400 psi (about equal to 40 percent of the unconfined compressive strength of the concrete), significant tension cracks were produced on the faces of the monoliths; but the monoliths remained stable. In the overflow monoliths where stresses were estimated to have been as high as 440 psi (about equal to 13 percent of the unconfined compressive strength, *no significant cracking or damage was found* (Reference 35).
3. **Pacoima Dam.** This dam is a concrete arch dam approximately 365 feet high. It is located in southern California near the epicenter of the 1971 San Fer-

nando Earthquake ( $M = 6.6$ ). During this earthquake, peak horizontal accelerations of 1.2g were measured on the rock abutments. Although analyses carried out at the University of California, Berkeley indicated that tensile stresses were in excess of 750 psi, no evidence of cracking was found (see Chapter II of this bulletin).

The peak tensile stress estimated for the small Thermalito concrete dams is approximately half of the estimated stresses corresponding to the no-damage cases listed above. This comparison further supports the prediction of no significant tension cracking within the concrete monoliths.

### Predicted Deformations

The results of the pseudodynamic sliding and tension stress analyses indicate that the monoliths within both the Approach Channel and Wingwall dams will be adequately stable during the postulated earthquake shaking. As the monolith joints are not grouted, they will tend to respond independently. Consequently, there may be some relative deformations between monoliths. However, since the dams are composed of concrete and founded on relatively fresh basalt, permanent deformations are expected to be less than a few millimeters. Consequently, differential deformations are also expected to be minor with the polyvinyl chloride waterstops and the asphalt seal being expected to adequately accept this level of deformation. Even if the waterstops and asphalt seal fail, no short-term adverse effects are expected as the concrete and rock formations are composed of non-erodible materials. This would be in line with the good performance summarized above for other concrete dams.

The condition not accounted for in the above case histories or evaluations is the transverse geometric relationship of the Approach Channel Dam relative to the Thermalito Headworks structure. As shown in Figure 210, page 273, monolith A-1 of the Approach Channel Dam overlaps the headworks structure at a right angle by approximately 20 to 26 feet. This arrangement is not typical of concrete dams and there is the possibility of some "pounding" damage caused by the two structures vibrating out of phase. This possibility is not easily evaluated and is probably beyond quantitative analysis at the present time. The judgmental evaluation of this potential be-

havior is that it probably would not lead to a failure of the dam. This judgment is based on the following:

1. The expected level of relative dynamic deformations between the two very stiff structures will be relatively small (less than about 1/4 inch).
2. There is probably a partial gap existing within the joint between the two structures due to the contraction of the concrete during setting. This gap would absorb some of the "pounding" displacement.
3. There is a relatively small number of significant loading cycles in a magnitude 6.5 event.

4. A limited amount of cracking and spalling of concrete in this overlap would not lead to failure of the structure (see report on Koyna Dam in Reference 35).

### Prediction of Performance

The simplified evaluations and case-histories outlined above indicate that the concrete dams will perform adequately during the postulated earthquake shaking. Only minor cracking and/or spalling of the concrete is expected. Permanent deformations are expected to be less than a few millimeters.

Table 58. Components of the Seismic Stability Analysis

COMPONENT	VALUES CONSIDERED	VALUE SELECTED	ASSESSMENT
I. EARTHQUAKE LOADING			
a) Critical Fault	<ul style="list-style-type: none"> <li>- Prairie Creek Lineament</li> <li>- Closest Northward Extension</li> <li>- Prairie Creek Lineament</li> <li>- More Distant Northward Extension</li> <li>- Cleveland Hill Fault</li> </ul>	Prairie Creek Lineament Closest Northward Extension	CONSERVATIVE
b) Maximum Event	<ul style="list-style-type: none"> <li>- Magnitude 5.7</li> <li>- Magnitude 6</li> <li>- Magnitude 6.5</li> </ul>	Magnitude 6.5	CONSERVATIVE
c) Peak Acceleration	<ul style="list-style-type: none"> <li>- Scale Up 1975 Peak from Magnitude 5.7 to Magnitude 6.5</li> <li>- Mean Value from Published Correlations for Magnitude 6.5 Strike-slip and Thrust Faults</li> <li>- Mean plus 1 Standard Deviation Value from Published Correlations for Magnitude 6.5 Strike-slip and Thrust Faults</li> </ul>	Mean Value from Published Correlations for Magnitude 6.5 Strike-slip and Thrust Faults	AVERAGE
d) Accelerograms	<ul style="list-style-type: none"> <li>- Modified 1975 Oroville Record</li> <li>- Oroville Reanalysis Earthquake (<math>a_{max} = 0.60g</math>)</li> <li>- Modified El Centro Record (<math>a_{max} = 0.55g</math>)</li> </ul>	Use both Oroville Reanalysis Earthquake ( $a_{max} = 0.60g$ ) <u>and</u> Modified El Centro Record ( $a_{max} = 0.55g$ ) and use the <u>higher</u> of the two sets of stresses	CONSERVATIVE
II. MODELLING OF LOW BLOWCOUNT FOUNDATION LAYERS			
a) Definition of Liquefiable Soils	<ul style="list-style-type: none"> <li>- Silty Sands Liquefiable and Clayey Sands <u>Nonliquefiable</u></li> <li>- Both Silty <u>and</u> Clayey Sands Liquefiable</li> </ul>	Both Silty <u>and</u> Clayey Sands Liquefiable	CONSERVATIVE
b) Characteristic Blowcount	<ul style="list-style-type: none"> <li>- Mean Blowcount</li> <li>- 35th Percentile Blowcount</li> <li>- Lowest Blowcount</li> </ul>	35th Percentile Blowcount	CONSERVATIVE
c) Thickness of Suspect Soil Layers	<ul style="list-style-type: none"> <li>- Average Thickness</li> <li>- Maximum Thickness</li> </ul>	Maximum Thickness	CONSERVATIVE

Table 58. Components of the Seismic Stability Analysis (Continued)

COMPONENT	VALUES CONSIDERED	VALUE SELECTED	ASSESSMENT
III. CYCLIC STRENGTH			
a) Determination	<ul style="list-style-type: none"> <li>- Cyclic Triaxial Tests of Undisturbed Samples</li> <li>- Published Correlations Between Liquefaction and Penetration Test Resistance</li> </ul>	Published Correlations Between Liquefaction and Penetration Test Resistance	NO DIFFERENCE FOR LOW DAM MODEL  UNCONSERVATIVE FOR MAIN DAM MODEL
IV. METHOD OF LIQUEFACTION ANALYSIS			
a) General Approach	<ul style="list-style-type: none"> <li>- Seed-Lee-Idriss Method (Horizontal Plane)</li> <li>- Casagrande/Castro (Critical Void Ratio)</li> <li>- Leps/Bennett (<math>\sigma_1</math> and/or <math>\sigma_m</math>)</li> </ul>	Seed-Lee-Idriss Method (Horizontal Plane)	*
b) Dynamic Response Analysis	<ul style="list-style-type: none"> <li>- Equivalent Linear Total Stress Analysis</li> <li>- Non-Linear Effective Stress Analysis</li> </ul>	Equivalent Linear Total Stress Analysis	*
V. POST-EARTHQUAKE SLOPE STABILITY			
a) Strength of Non-Liquefied Clayey Embankment and Surface Cap	<ul style="list-style-type: none"> <li>- Mohr Circle Interpretation using 15% Strain Failure Criterion</li> <li>- 80% of <math>\tau_{ff}</math> vs. <math>\sigma_{fc}</math> Interpretation using 15% Strain Failure Criterion</li> <li>- <math>\tau_{ff}</math> vs. <math>\sigma_{fc}</math> Interpretation using 15% Strain Failure Criterion</li> </ul>	80% of $\tau_{ff}$ vs. $\sigma_{fc}$ Interpretation using 15% Strain Failure Criterion	CONSERVATIVE
b) Strength of Partially Liquefied Foundation Sands	<ul style="list-style-type: none"> <li>- Drained Strength used together with Calculated Excess Pore Pressures</li> <li>- Drained Strength used with no Excess Pore Pressures</li> <li>- Undrained Strength</li> </ul>	Drained Strength used together with calculated excess pore pressures	*
c) Residual Strength of Liquefied Foundation Sands	<ul style="list-style-type: none"> <li>- Mean Value Suggested by Seed (1987) Correlation with SPT</li> <li>- Lower Bound Value Suggested by Seed (1987) Correlation with SPT</li> <li>- Values Suggested by Steady-State Strength Results for Similar Soils</li> </ul>	Lower Bound Value Suggested by Seed (1987) Correlation with SPT	CONSERVATIVE

NET STABILITY FACTOR OF SAFETY = 1.6 CONSERVATIVE

\* Value is integral part of procedure (Seed-Lee-Idriss) Calibrated against observed behavior of Chabot, Sheffield, Lower San Fernando, and Upper San Fernando Dams.



## 11. PREDICTION OF EMBANKMENT PERFORMANCE

### General

The prediction of performance for a dam during strong earthquake shaking involves consideration of several possible modes of failure. The major portion of this chapter has been devoted to investigating the possibility of embankment instability due to foundation liquefaction. Section 10 also addressed potential stability and cracking behavior in the concrete wingwall dams. However, the possibility for excessive earthquake induced embankment settlement and/or cracking also needs to be addressed.

### Summary of Predicted Embankment Stability

Table 58 summarizes the many steps of the seismic stability analysis where choices were made from a range of alternatives. In only two of the thirteen steps were average values chosen from the range of alternatives. The remaining eleven steps used either conservative choices or values that were integral parts of the Seed-Lee-Idriss procedure. Table 58 denotes the choice of SPT cyclic strengths over laboratory test results as "unconservative" because the SPT data yielded higher strengths. However, the use of the laboratory test alternatives is not considered acceptable because of sample disturbance effects on dense soils. Consequently, the final result of the analysis—a minimum 1.6 factor of safety against sliding—is considered acceptable and conservative.

### Predicted Level of Permanent Earthquake-Induced Deformations

The results of the post-earthquake slope stability analyses showed that the embankment would remain stable despite the development of extensive zones of liquefaction within the foundation. Consequently, large deformations are not predicted. In addition, the presence of a dense, clayey surface cap of soil within the foundation mitigates against the possibility that the embankment would either sink into the foundation or that large flows of liquified sand would flow out from under the dam.

The level of permanent earthquake-induced deformations that might be produced at Thermalito Forebay Earthquake can be estimated by examining the performance of Upper San Fernando Dam during the 1971 San

Fernando Earthquake ( $M_L=6.6$ ). The Upper San Fernando Dam is a hydraulic fill embankment that was shaken severely by the 1971 earthquake. The earthquake was estimated to produce peak ground accelerations of about 0.6g at the dam site and to have induced extensive zones of liquefaction within the hydraulic fill. Despite the development of the liquefied zones, the dam suffered deformations averaging to about 6 feet of horizontal movement and about 2.5 feet of settlement (see Seed et al., 1973; Addendum F).

The most critical site along Thermalito Forebay Dam is the Station 112 area of the Low Dam. Both the Station 112 suspect sands and the Upper San Fernando Dam hydraulic fill were analyzed and found to have similar zones of liquefaction. Presented below is a comparison of the materials and zoning at the two sites:

	Thermalito Forebay Dam Station 112	Upper San Fernando Dam
Embankment Height (ft)	30	70
Thickness of Liquefiable Zone (ft)	18	40
Liquefiable Soil	Silty and Clayey Sand ( $N_1$ ) <sub>60</sub> = 16.5	Silty Sand ( $N_1$ ) <sub>60</sub> = 9-13
Earthquake	M = 6.5 $a_{max}$ = 0.6g	M = 6.6 $a_{max}$ = 0.6g

Because the earthquake loading is essentially the same, the same 6-foot horizontal and 2.5-foot vertical deformations would be predicted for the Station 112 embankment if this site had the same liquefiable soil with the same thickness as at Upper San Fernando Dam. However, the thickness of the liquefiable soils at the Station 112 site is only 18 feet compared to 40 feet at Upper San Fernando Dam. This difference alone would reduce the predicted deformations to about 1 foot vertical and 2.5 feet horizontal. In addition, the corrected SPT blowcount for the Station 112 liquefiable soil is significantly higher than the SPT blowcount determined for the Upper San Fernando Dam hydraulic fill. This fact, coupled with the fact that the reservoir loading (depth) and embankment height at Thermalito is much less, leads to an estimate of 1 foot or less for permanent deformations in either the vertical or horizontal directions.



## **Predicted Effects Due to Differential Settlement and Embankment Cracking**

Case histories have shown that earthquakes have often induced longitudinal cracking in the crest of embankment dams. However, these cracks are generally less than 1-inch wide and extend only a few feet below the surface. Earthquake-induced transverse cracking is relatively rare. Transverse cracks did not appear in the surfaces of the San Fernando Dams, Hebgen Dam, La Marquesa Dam (Chile), or La Palma Dam (Chile), despite severe ground motions and earthquake-induced settlements exceeding several feet.

Transverse cracking is expected only when there are significant abrupt deformations induced in the embankment (e.g. as at some abutment contacts). Although deformations are predicted to be as much as 1 foot at Station 112, this is not predicted as a differential movement. Rather, as the soils at the site are considered transitional over several hundred feet (see Figure 300, page 402), the deformations are not expected to be abrupt. Consequently, Station 112 and most other Thermalito Forebay sites, in line with the case histories quoted, are not predicted to develop transverse cracks.

However, the possibility of transverse cracking requires examination at the Main Dam for the following reasons:

1. Faults exist in the foundations directly beneath the right end of the dam.
2. Foundation conditions change abruptly from rock under the right end of the Main Dam to 80 feet of alluvium under the left end of the Main Dam.
3. The embankment of the Main Dam abruptly connects to the concrete Wingwall Dam attached to the headworks structure.

## **Potential Cracking Due to Fault Displacement**

Geologic mapping of 1964 construction excavations revealed three fault traces in the bottom of the cutoff trench between grouting stations 5 + 50 and 6 + 50 (see Figures 352 and 353). These faults offset rock assigned to the Tertiary "Middle Basalt Flow" unit but did not offset the Plio-Pleistocene "Basalt Rubble" conglomerate or

the Red Bluff floodplain deposits exposed in the walls of the excavation. These three faults strike northeast-southwest and dip 80 degrees to the southeast. Drill hole data indicate that these are normal faults and that the southeast block has dropped 40 to 60 feet relative to the northwest block.

Southwest of the trench exposures the fault traces are concealed for a distance of about 300 feet by the Basalt Rubble and the Red Bluff formations. If these faults are projected to the southwest beyond the concealed area, they roughly coincide with the trace of Fault "B" mapped in the power plant excavation (see Figure 352). Fault "B" is also a normal fault with an 80 degree dip to the southeast. Faults "A" and "H-J" in the power plant area have similar strikes to the faults in the cutoff trench, but dip 70 degrees to the northwest.

The faults beneath the Main Dam embankment are considered inactive. The predominant trend of these faults cuts across to the trend of major faults in the Oroville area suggesting that they did not form as a result of the present tectonic regime. In addition, the faulting has not affected the overlying cenozoic age units exposed during construction. Alan J. Busacca, a recent University of California graduate student, performed analyses of Late Cenozoic sediments near Oroville and tentatively determined the age of the gravelly sediments at the Thermalito Powerplant area to be 1.6 to 3.4 million years (personal communication, 1981). This age is based on the degree of soil profile development, radiometric age dating of volcanic ash beds, and geomorphic indicators. These old faults are considered inactive and do not present a significant hazard to the stability of the embankment.

## **Potential Cracking Due to Foundation Bedrock Profile**

The depth of Red Bluff sediments overlying basalt rock is about 80 feet under most of the Main Dam, but decreases to zero under the right end. Figures 352 and 353 show in plan and sections how the slope of the rock surface was determined under the dam centerline projected from about Station 7 + 00 to the Approach Channel.

There is only a 70-foot-long reach, labeled C on Figure 354 (Section A-A), which is not well defined by close-by



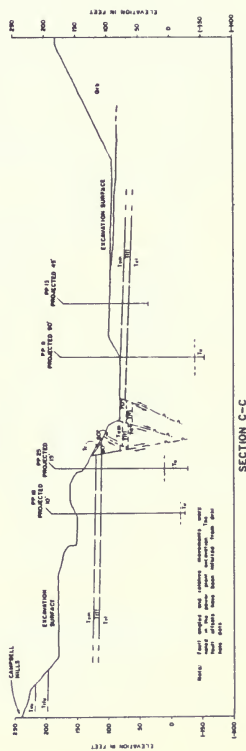
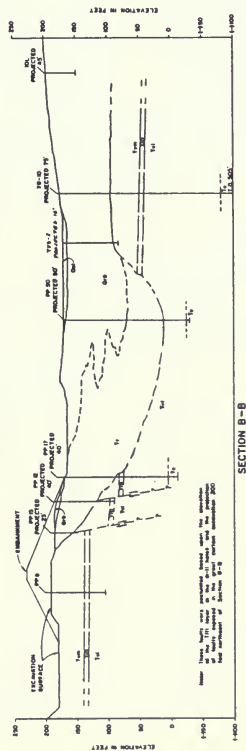
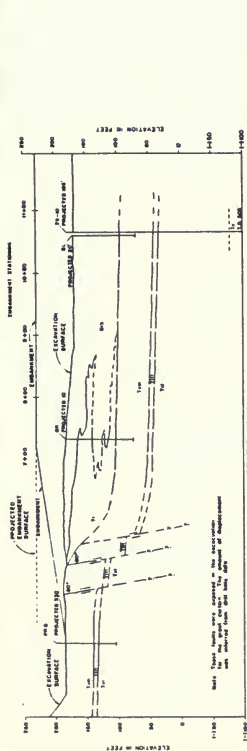
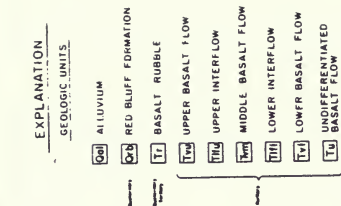


Figure 353. Geologic Sections along Thermalito Forebay Main Dam

borings or foundation trench exposures. This happens to be the critical reach where the basalt dips under the alluvium. This dipping rock surface is well defined by three borings in Section B-B located 300 feet from Section A-A (see Figures 211 and 212, pages 274 & 275). The dip is somewhat flatter than 1:1 at B-B, and was projected to A-A as 1:1.

The rock foundation on the right side of the Main Dam is identified as a moderately-weathered and fractured basalt ( $T_{vm}$ ). The anticipated earthquake shaking is not expected to cause any significant settlement within this material or in the inactive faults or shears in the formation.

The Red Bluff formation ( $Q_{rb}$ ) will tend to settle more due to earthquake shaking. But since no layer at the Main Dam is predicted to completely liquefy, the maximum anticipated settlement should be much less than one foot.

Providing a buffer between the basalt foundation and the Red Bluff formation is the Basalt Rubble layer ( $T_r$ ). This

material consists of loose to moderately consolidated basalt fragments within a clay matrix. The deformation properties of this material, although unknown, are believed to be intermediate between the Red Bluff and the rock ( $T_{vm}$ ). Because of the clay matrix and the absence of sands, the settlements due to the earthquake shaking in the Basalt Rubble will probably be very small.

The estimated slope of the contact between the rock and the rubble is 1:1, or flatter, which is less than abutment slopes of many embankment dams. The contact between the Basalt Rubble and the Red Bluff Formation ( $Q_{rb}$ ) is projected to be between 10:1 and 3:1. (see Figure 354).

Differential settlement and cracking along the Main Dam due to changing foundation materials is not believed to be significant. This is because the contact slopes between differing foundation materials is flatter than that accepted for abutment slopes of embankment dams and because the maximum predicted earthquake-induced settlement would be less than a foot.

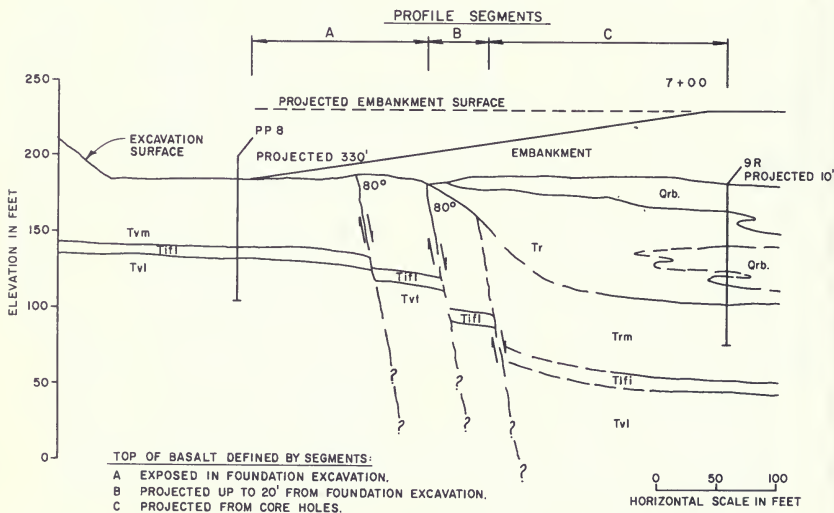


Figure 354. Detailed Bedrock Profile for Thermalito Forebay Main Dam along Section AA (Figures 352 and 353)

Potential Cracking at the Wingwall/Embankment Contact

As described in Sections 2 and 10, the embankment of Thermalito Forebay Dam meets and wraps around the concrete Wingwall Dam connected to the powerplant headworks structure. Due to the different stiffnesses of the concrete and earth structures, it is not outside the realm of possibility that a small transverse crack could develop during severe earthquake shaking along the concrete/soil boundary. Factors suggesting otherwise include the fact that this boundary does not differ greatly from some steep abutment contacts on dams that did not develop transverse cracks during strong shaking (e.g. Coyote and Leroy Anderson Dams). In addition, the wrapping of embankment material around the concrete dam mitigates against the development of a continuous transverse crack through the entire embankment contact. There is only a

20-foot transverse length between concrete and soil for the upper half of the dam. However, at maximum reservoir elevation, a transverse crack would have to pass through a total lengths of 56 feet of soil (see Figure 214, page 279).

Notwithstanding the above reasoning, it is judged that even if a small transverse crack formed, it would not lead to the failure of the dam. The reasoning for this conclusion is as follows:

- 1. The Zone 1F embankment material is a gravelly, clayey sand with approximately 45 percent fines. The Atterberg limits test results plot above the "A" line with an average PI of about 16 percent. Such a soil is considered to have relatively high erosion resistance.
- 2. Based on past performances of earth dams during earthquakes, any earthquake-induced transverse

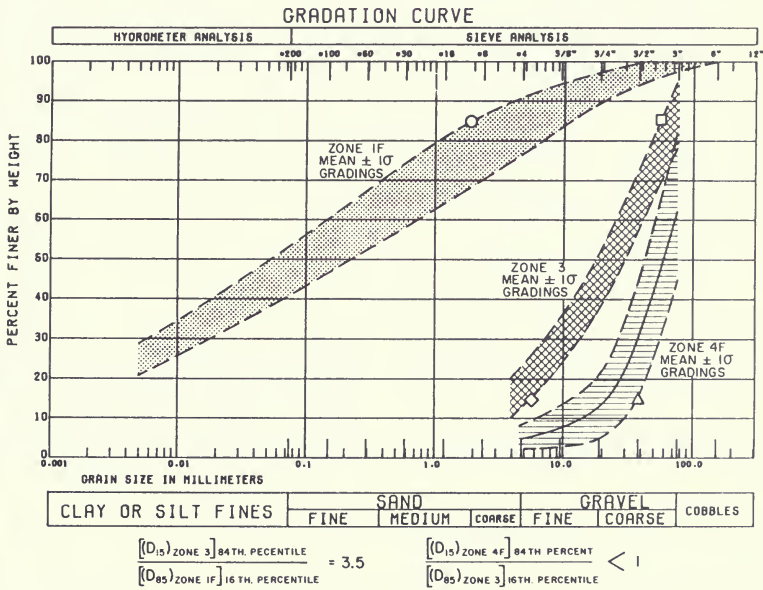


Figure 355. Comparison of Gradations for Thermalito Forebay Main Dam Embankment Soils

crack at this site would be expected to be less than 1-inch wide. Upstream of the Zone 1F soil are layers of Zone 3 and Zone 4F cohesionless soil (minimum horizontal thickness equals 12 feet for each zone, see Figure 214). These soils would possibly act as crack fillers by being washed into the small crack, leading to the larger sizes becoming wedged in, with successively smaller sizes becoming trapped until the crack seals. More importantly, these upstream zones would induce significant head losses in any significant flow passing through a transverse crack, thus reducing velocities through an open crack.

- Most significantly, downstream of and wrapped around the Zone 1F soil are layers of Zone 3 and Zone 4F soil (minimum horizontal thickness equals 12 feet for each zone). Although the extreme specification limits for the Zone 1F and Zone 3 soils do not meet accepted filter criteria, the 84th percentile value (mean plus 1 standard deviation) of the filter zones do meet accepted criteria for filtering the 16th percentile value (mean minus 1 standard deviation) of the base zones. The gradation parameters relating to the filter criteria are presented in Table 59 and Figure 355.

Table 59. Summary of Filter Parameters for Main Dam Embankment Soils

Gradation Parameters	Zone 1F	Zone 3	Zone 4F
No. of Gradation Samples	215	67	47
Mean - 1σ (16th Percentile) $D_{85}$ (mm)	1.7	55	
Mean (50th Percentile) $D_{85}$ (mm)	5.5	75	
Mean (50th Percentile) $D_{15}$ (mm)		4	23
Mean + 1σ (84th Percentile) $D_{15}$ (mm)		6	38

$$\text{Piping Criteria: } \frac{(D_{15}) \text{ Filter}}{(D_{85}) \text{ Base}} < 5$$

$$\frac{[(D_{15}) \text{ Zone 3}] \text{ 84th Percentile}}{[(D_{85}) \text{ Zone 1F}] \text{ 16th Percentile}} = 3.5 \text{ o.k.}$$

$$\frac{[(D_{15}) \text{ Zone 4F}] \text{ 84th Percentile}}{[(D_{85}) \text{ Zone 3}] \text{ 16th Percentile}} = < 1 \text{ o.k.}$$

In light of the above considerations, differential settlement and/or embankment cracking are not considered to pose significant hazards.

### Summary of Predicted Embankment Performance For Magnitude 6.5 Earthquake

#### Embankment Stability

Based on historical performance of clayey embankments, Thermalito Forebay Dam would perform well for any magnitude earthquake if there were no foundation weaknesses. At several short reaches along the dam, seismic

analyses predict "liquefaction" in zones within suspect foundation silty sands and clayey sands. Post-earthquake, slope stability analyses for these conditions show a minimum safety factor of 1.6. Therefore, the dam is considered safe against post earthquake slide failures resulting from induced pore pressure increases. Historical evidence is generally consistent with this finding.

#### Embankment Deformation

Maximum movements are expected to be less than 1 foot in any direction.

### **Embankment Cracking**

The inactive faults, the 1:1 dipping rock surface under the right end of the dam, and the embankment/concrete wingwall contact are not expected to produce unacceptable differential movements. In the unlikely event of a

continuous transverse crack in the Main Dam embankment, the presence of upstream and downstream filter zones are considered capable of preventing failure of the dam. Only minor surface cracking is predicted for the postulated earthquake shaking.



## REFERENCES FOR CHAPTER V

1. Ahmad, Rashid (1976) "Computer Program TWIST, users manual, Division of Safety of Dams, California Department of Water Resources, 1976.
2. Ambraseys, N. N. (1960), "On the Seismic Behavior of Earth Dams," Proceedings of the Second World Conference on Earthquake Engineering, Japan, 1960.
3. Banerjee, Nani G., Seed, H. Bolton, and Chan, Clarence K. (1979), "Cyclic Behavior of Dense Coarse-Grained Materials in Relation to the Seismic Stability of Dams," Earthquake Engineering Research Center, Report No. UCB/EERC-79/13, University of California, Berkeley.
4. Beaty, Mike (1987) "Program GRAVDAM," users manual, Division of Safety of Dams, California Department of Water Resources, 1987.
5. Bennett, M. J., Youd, T. L. Harp, E. L., and Weiczorek, G. F. (1981), "Subsurface Investigation of Liquefaction, Imperial Valley Earthquake, California, October 15, 1979," U. S. Geological Survey Open File Report 81-502, 1981.
6. Bennett, W. J. (1977), "Dynamic Analysis Proposal," Office Memorandum, Division of Safety of Dams, Department of Water Resources.
7. Brady, A. G., Perez, V., and Mork, P. N. (1980), "The Imperial Valley Earthquake, October 15, 1979. Digitization and Processing of Accelerograph Records." Seismic Engineering Data Report 80-703. United States Geological Survey, Menlo Park, California, April, 1980.
8. Bureau of Reclamation (1976) "Dynamic Analysis of Embankment Dams," manuscript prepared for submission to the International Commission on Large Dams for publication, United States Department of the Interior, December 31, 1976.
9. Bureau of Reclamation (1976) "Design of Gravity Dams," United States Department of the Interior, 1976.
10. California Department of Transportation (1979), "Report of Down-Hole Shear Wave Investigation at Thermalito Afterbay and Forebay," Report Prepared for the Department of Water Resources.
11. California Department of Transportation (1980), "Down-Hole Shear Wave Velocity Results for Thermalito Afterbay," Data Report Prepared for the Department of Water Resources.
12. California Department of Water Resources (1962), "Basic Data Compilation Report — Exploration Drilling — Thermalito Afterbay," August 31, 1962.
13. California Department of Water Resources (1964), "Interim Exploration Data, Soil Permeability Investigation — Thermalito Forebay and Afterbay." April 9, 1964.
14. California Department of Water Resources (1965a), "Thermalito Forebay and Afterbay Geology and Construction Materials Data," Project Geology Report D-48, May, 1965.
15. California Department of Water Resources (1965b), "Interim Exploration Data, Columbia Soil Area, Thermalito Afterbay," August 18, 1962.



16. California Department of Water Resources (1964) "Plans and Specifications for Construction of Thermalito Power Plan," Specification No. 64-37, 1964.
17. California Department of Water Resources (1965) "Plans and Specifications for Construction of Thermalito Forebay and Afterbay Dams," Specification No. 65-27, 1965.
18. California Department of Water Resources (1966) "Final Foundation Grouting Report, Intake Structure Thermalito Powerplant," Specification No. 64-37, June, 1966.
19. California Department of Water Resources (1968a) "Final Geologic Report on Foundation Conditions and Grouting Thermalito Forebay and Afterbay — Appendix A to Final Construction Report," Project Geology Report No. C-31, July, 1968.
20. California Department of Water Resources (1968b) "Summary of Concrete Mixes Used at Thermalito Powerplant," Data report for Specifications No. 64-37, 1968.
21. California Department of Water Resources (1968c), "Final Construction Report on Thermalito Forebay and Afterbay — Oroville Division," August, 1968.
22. California Department of Water Resources (1968a), "Final Construction Report on Thermalito Powerplant," Specification No. 64-37, July 1969.
23. California Department of Water Resources (1969b), "Thermalito Afterbay Seepage Control Memorandum Report," August, 1969.
24. California Department of Water Resources (1973), "Thermalito Afterbay—Draft Final Design Report," 1973.
25. California Department of Water Resources (1977), "Performance of the Oroville Dam and Related Facilities During the August 1, 1975 Earthquake," Bulletin 203.
26. California Department of Water Resources (1979), "The August 1, 1975 Oroville Earthquake Investigations," Bulletin 203-78.
27. California Department of Water Resources, "Basic Data Report — Exploration For Seismic Stability Reevaluation — Thermalito Forebay and Afterbay," Project Geology Report.
28. California Department of Water Resources, "Soils Laboratory Report — Laboratory Test Results for Seismic Stability Reevaluation — Thermalito Forebay and Afterbay."
29. California Department of Water Resources, "Thermalito Afterbay — Vibroflotation Test Program to Densify Foundation Sands."
30. California Department of Water Resources, Thermalito Forebay Dam Performance Reports No. 1 through 7.
31. Casagrande, A. (1975), "Liquefaction and Cyclic Deformation of Sands — A Critical Review," Paper Presented at the Fifth Panamerican Conference Soil Mechanics and Foundation Engineering, Buenos Aires, Argentina, November, 1975.
32. Castro, G. (1975) "Liquefaction and Cyclic Mobility of Saturated Sands," Journal of the Geotechnical Engineering Division, ASCE, Vol. 107, No. GT6, June, 1975.

33. Chopra, A.K., "Earthquake Resistant Design of Concrete Gravity Dams," *Journal of the Structural Division, ASCE*, Vol. 104, No. ST6, June, 1978.
34. Chopra, Anil K. and Chakrabarti, P. (1972) "The Earthquake Experience at Kozna Dam and Stresses in Concrete Gravity Dams," *Earthquake Engineering and Structural Dynamics*, Vol. 1, No. 2, Oct. — Dec., 1972.
35. Chopra, Anil K. and Chakrabarti, P. (1973) "The Koyna Earthquake and the Damage to Koyna Dam," *Bulletin of the Seismological Society of America*, Vol. 63, No. 2, April, 1973.
36. Clark, K. R. (1969), "Research on Undisturbed Sampling of Soils, Shales, Air Drilling Techniques, and Data on Penetration Resistance Testing — Third Progress Report on Soil Sampling Research," Report No. EM-770, United States Department of the Interior, Bureau of Reclamation, July, 1969.
37. De Alba, P., Seed, H.B., Retamal, E., and Seed R.B. (1987) "Residual Strength of Sand from Dam Failures in the Chilean Earthquake of March 3, 1985," *Earthquake Engineering Center*, Report No. UCB/EERC 87-11, University of California, Berkeley, September, 1987.
38. DePolo, Craig (1985) "Memorandum of Seismotectonic Review — Thermalito Forebay Dam, No. 1-54," Division of Safety of Dams, Department of Water Resources, December 26, 1985.
39. Douglas, B. J., Olsen, R. S., and Martin, G. R. (1981) "Evaluation of the Cone Penetrometer Test for Use in SPT—Liquefaction Potential Assessments," Preprint From the ASCE Annual Convention, St. Louis, October, 1981.
40. Ertec Western, Inc. (1981), "Cone Penetrometer Test Investigations and Analyses, Thermalito Afterbay, Oroville, California," Report Submitted to the State of California, Department of Water Resources, July, 1969.
41. Ertec Western, Inc. (1982), "Cone Penetrometer Test Investigations and Analyses, Thermalito Afterbay Vibroflotation Program, Oroville, California," Report Submitted to the State of California, Department of Water Resources, January, 1982.
42. Fenves, Gregory and Chopra, Anil K. (1984) "Earthquake Analysis and Response of Concrete Gravity Dams," Report No. UCB/EERC 84/10, Earthquake Engineering Research Center, University of California, Berkeley, August 1984.
43. Fenves, Gregory and Chopra, Anil K. (1986) "Simplified Analysis for Earthquake Resistant Design of Concrete Gravity Dams," Report No. UCB/EERC 85/10, Earthquake Engineering Research Center, University of California, Berkeley, June, 1986.
44. Yoshimi Y., Tokimatsu, K., Kaneko, O., and Makihara, Y. (1984) "Undrained Cyclic Shear Strength of a Dense Niigata Sand," *Soils and Foundations*, Vol. 24, No. 4, 1984.
45. Hudson, E. E. and Brady, A. G. (1971), "Strong Motion Earthquake Accelerograms — Digitized and Plotted Data," Vol. II — Part A, Report No. EERL 71-50, Earthquake Engineering Research Laboratory, California Institute of Technology, Pasadena, California, September, 1971.
46. Idriss, I. M. and Power, M. S. (1978), "Peak Horizontal Accelerations, Velocities, and Displacements on Rock and Stiff Soil Sites for Moderately Strong Earthquakes."
47. Kovacs, W. D. (1981), "Results and Interpretation of SPT Practice Study," *Geotechnical Testing Journal*, GTJODJ, Vol. 4, No. 3, September, 1981.

48. Kovacs, W. D., Salomone, L. S., and Yokel, F. Y. (1981), "Energy Measurement in the Standard Penetration Test," NBS Building Science Series 135, National Bureau of Standards, Washington, D. C.
49. Lee, Kenneth L. and Idriss, Izzat M. (1975) "Static Stresses by Linear and Nonlinear Methods," Journal of the Geotechnical Engineering Division, American Society of Civil Engineers, Vol. 101, No. GT9, September, 1975.
50. Leps, Thomas M. (1973), "Butt Valley Dam — Evaluation of Seismic Stability," Report for Pacific Gas and Electric Company by Thomas M. Leps, Inc., August, 1973.
51. McMasters, Joe (1976) "Computer Program NODALFOR," Users manual, Division of Safety of Dams, California Department of Water Resources, 1976.
52. National Bureau of Standards (1983), "SPT Energy Evaluations (Performed at Thermalito Afterbay, Oroville, California, January 11–12, 1982)," Report Submitted to the Department of Water Resources.
53. Poulos, Steve J., Castro, Gonzalo, and France, John W. (1985) "Liquefaction Evaluation Procedure," Journal of the Geotechnical Engineering Division, ASCE, Vol. 111, No. GT6, June, 1985.
54. Pyke, Robert M., Knuppel, Lee A., and Lee, Kenneth L. (1978), "Liquefaction of Hydraulic Fills," Journal of the Geotechnical Engineering Division, American Society of Civil Engineers, Vol. 104, No. GT11, November, 1978.
55. Sarmiento, John (1981), "U. S. Geological Survey Cone Penetration Program for Thermalito Afterbay, Oroville California," U. S. Geological Survey Report MS-98, Menlo Park, California.
56. Schmertmann, John H. (1979), "Statics of SPT," Journal of the Geotechnical Engineering Division, American Society of Civil Engineers, Vol. 105, GT5, May, 1979.
57. Schnabel, P. B., Lysmer, John, Seed, H. Bolton (1972), "SHAKE, a Computer Program for Earthquake Response Analysis of Horizontally Layered Sites," Earthquake Engineering Research Center, Report No. EERC 72-12, University of California, Berkeley.
58. Seed, H. Bolton (1968), "Landslides During Earthquakes Due to Soil Liquefaction," Journal of the Soil Mechanics and Foundations Division, American Society of Civil Engineers, Vol. 92, SM3, March, 1968.
59. Seed, H. B. (1976), "Evaluation of Soil Liquefaction Effects During Earthquakes," Presented at the ASCE Annual Convention and Exposition, Philadelphia, PA, September 27–October 1.
60. Seed, H. Bolton (1979), "Considerations in the Earthquake-Resistant Design of Earth and Rockfill Dams," Geotechnique, 29, No. 3.
61. Seed, H. Bolton (1983) "Earthquake—Resistant Design of Earth Dams," Proceedings of the Symposium on Seismic Design of Embankment and Caverns, ASCE, Philadelphia, Pennsylvania, May 6–10, 1983.
62. Seed, H.B. and Idriss I.M. (1970), "Soil Moduli and Damping Factors for Dynamic Response Analyses," Earthquake Engineering Research Center, Report No. EERC 70-10, University of California, Berkeley, December.
63. Seed, H.B., and Idriss, I.M. (1981), "Evaluation of Liquefaction Potential of Sand Deposits Based on Observations of Performance in Previous Earthquakes," Presented at the ASCE Annual Convention and Exposition, St. Louis, Missouri, October.

64. Seed, H.B. and Idriss I.M. (1982) "Ground Motions and Soil Liquefaction During Earthquakes," monograph, Earthquake Engineering Research Institute, Berkeley, California, 1982.
65. Seed, H.B., Idriss, I.M., Makdisi, R.I., and Banerjee, N. (1975), "Representation of Irregular Stress Time Histories by Equivalent Uniform Stress Series in Liquefaction Analyses," Earthquake Engineering Research Center, Report No. EERC 75-29, University of California, Berkeley, October, 1975.
66. Seed, H.B., Lee, K.I., and Idriss, I.M. (1969), "An Analysis of the Sheffield Dam Failure," Journal of the Soil Mechanics and Foundations Division, ASCE, Vol. 95, No. SM6, November.
67. Seed, H.B., Lee, K.I., and Idriss, I.M., and Makdisi, F.I. (1973), "Analysis of the Slide in the San Fernando Dams During the Earthquake of February 9, 1971," Earthquake Engineering Research Center, Report No. 73-2, University of California, Berkeley, June.
68. Seed, H.B., Makdisi, F.I., and DeAlba, P. (1978), "Performance of Earth Dams During Earthquakes," Journal of the Geotechnical Division, ASCE, Vol. 104, No. GT7, September.
69. Seed, H.B., Murarka, R., Lysmer, J., and Idriss, I.M. (1975), "Relationships Between Maximum Velocity, Distance From Source, Local Site Conditions for Moderately Strong Earthquakes," Earthquake Engineering Research Center, Report No. EERC 75-17, University of California, Berkeley.
70. Seed, H. Bolton, Seed, Raymond B., Harder, Leslie F., and Jong, Hsien Lian (1988) "Re-evaluation of the Slide in the Lower San Fernando Dam in the Earthquake of February 9, 1971," Earthquake Engineering Research Center.
71. Seed, H. Bolton, Singh, Sukhmander, Chan C.K., and Vilela, F.F. (1982) "Considerations in Undisturbed Sampling of Sands," Journal of the Geotechnical Engineering Division, ASCE, Vol. 108, No. GT2, February, 1982.
72. Seed, H. Bolton, Tokimatsu K., Harder, L.F. and Chung, R.M. (1985) "Influence of SPT Procedures in Soil Liquefaction Resistance Evaluations," Journal of the Geotechnical Engineering Division, ASCE, Vol. 111, No. GT12, December 1985.
73. Seed, H.B., Ugas, C., and Lysmer, J. (1974), "Site Dependent Spectra for Earthquake—Resistant Design," Earthquake Engineering Research Center, Report No. EERC 74-11, University of California, Berkeley.
74. Singh, S., Seed, H. B., and Chan C..K. (1979), "Undisturbed Sampling and Cyclic Load Testing of Sands," Earthquake Engineering Research Center, Report No. UCB/EERC 79/33, University of California, Berkeley, December, 1979.
75. Singh, S., Seed, H.B., and Chan C.K. (1982) "Undisturbed Sampling of Saturated Sands by Freezing," Journal of the Geotechnical Engineering Division, ASCE, Vol. 108, GT2, February, 1982.
76. Smith, D. (1979), "Dynamic Analysis of Castaic Dam," Office Report, Division of Safety of Dams, Department of Water Resources.
77. Steinberg, S. (1981), "Energy Calibration and Hammer Influence on SPT," Paper Presented at the Engineering Foundation Conference on Updating Subsurface Sampling of Soils and Rocks and Their Insitu testing, Santa Barbara, California, January 3-8, 1982.
78. Tokimatsu, K. and Yoshimi, H. (1981), "Field Correlation of Soil Liquefaction with SPT and Grain Size," Proceedings International Conference on Recent Advances in Geotechnical Earthquake Engineering and Soil Dynamics, St. Louis, MO., April 26-May 2.

79. Trifunac, M.D. and Brune, J.N., (1970), "Complexity of Energy Release During the Imperial Valley, California, Earthquake of 1940," Bulletin of the Seismological Society of America, Vol. 60, No. 1, February, 1970.
80. United States Army Corps of Engineers (1985) "Earthquake Analysis and Design of Concrete Gravity Dams," Engineer Technical Letter No. 1110-2-303, Department of the Army, Washington, D.C., August, 1985.
81. Vaid, Y.P. and Finn, W.D. Liam (1979), "Effect of Static Shear on Liquefaction Potential," Journal of the Geotechnical Engineering Division, ASCE, Vol. 105, GT10, October 1979.
82. Von Thun, J. Lawrence (1986) "Analysis of Dynamic Compaction Foundation Treatment Requirements, Stage I, Jackson The Dam," Technical Memorandum No. TM-JL-230-26, Bureau of Reclamation, Engineering and Research Center, Division of Dam and Waterway Design, Embankment Dams Branch.
83. Vrymoed, J.L., and Calzascia, E.R. (1978), "Simplified Determination of Dynamic Stresses in Earth Dams," Proceedings of the ASCE Geotechnical Engineering Division Specialty Conference on Earthquake Engineering and Soil Dynamics, Pasadena, California, June, 1978.
84. Wong, K.S. and Duncan, J.M. (1974), "Hyperbolic Stress-Strain Parameters for Nonlinear Finite Element Analysis of Stress and Movements in Soil Masses," Report No. TE-74-3, University of California, Berkeley.
85. Woodward-Clyde Consultants (1980), "Shear Wave Velocity Measurements at Oroville, California," Report Submitted to the Department of Water Resources, July, 1980.
86. Yoshimi Y., Tokimatsu, K., Kaneko, O., and Makihara, Y. (1984) "Undrained Cyclic Shear Strength of Dense Niigata Sand," Soils and Foundations, Vol. 24, No. 4, 1984.
87. Youd, T.L., and Perkins, D.M. (1978), "Mapping Liquefaction-Induced Ground Failure Potential," Journal of the Geotechnical Engineering Division, ASCE, Vol. 104, No. GT4, April, 1978.

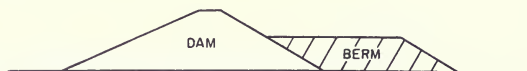


## **ADDENDA TO CHAPTER V**

- A. Glossary**
- B. Explorations for Thermalito Forebay Seismic Evaluations**
- C. Static Stress Finite Element Analysis**
- D. Cyclic Triaxial Test Summaries**
- E. Dynamic Stress Analysis**
- F. Examination of the Performance of Upper San Fernando Dam During the Earthquake of February 1, 1971**

## ADDENDUM A. GLOSSARY

- accelerogram — a record from an accelerometer showing acceleration with time
- accelerometer — an instrument for measuring accelerations during earthquakes or other dynamic events
- alluvium — soils deposited by running water
- bentonite — a highly plastic clay resulting from the decomposition of volcanic ash. It is used commercially as a drilling fluid additive
- berm — a strip of ground placed along a dam for added stability



- blowcount — *see* Standard Penetration Test
- borrow area — location away from the work site where earth construction materials are obtained
- cathead — a rotating device on the back of a drill rig used for hoisting and lowering drilling equipment
- cyclic triaxial test — a laboratory test performed by applying a pulsating load to a sample to estimate the soil's strength during an earthquake
- dredge tailings — refuse material, separated as residue, acquired during mining operations
- dynamic analysis — analysis performed to determine the behavior of a structure during an earthquake
- fluvial — produced by a river action
- geophone — device used to record shock waves
- lens — thin layer of soil or rock
- lenticular — masses of soil or rock existing in one or more thin layers or lenses
- liquefaction — denotes a condition where a soil will undergo strength loss due to the development of high pore water pressures
- N—value — *see* Standard Penetration Test
- nodal force — force acting at a node that is part of a finite element model



- overburden — material overlying a deposit or structure
- penetrometer — an instrument for determining a soil's material properties by measuring the soil's resistance to penetration



## GLOSSARY (continued)

permeability	— relative value used to estimate the rate at which water flows through a soil
phreatic surface	— uppermost line of seepage through a soil mass where there is zero water pressure in the soil
piezometer	— instrument for measuring water pressures in a soil
piston sampler	— device for collecting relatively undisturbed soil samples
pitcher barrel	— device for collecting relatively undisturbed silt and clay soil samples
pluviation	— when applied to soil testing, pluviation usually denotes pouring soil loosely through air or water
pore pressure	— water pressure within the soil
refraction	— the deflection of a wave from a straight path as it passes from one medium to another of a different velocity
riprap	— rock placed on dam slope to protect against erosion
scarify	— to break up and loosen the surface
SH waves	— horizontal shear waves generated during shear wave velocity testing
shear strength	— the property of a material which keeps it from dislocating and deforming
shear wave	— test for determining the material properties velocity test of soil or rock by measuring the speed at which shear waves propagate through the ground
shelby tube	— cold drawn steel tube used to sample soils
slurry	— a watery mixture of an insoluble matter such as mud, lime, or plaster of paris
split—spoon	— thick walled steel tube split lengthwise and sampler used in soil sampling operations
Standard Penetration Test (SPT)*	— a test where a 2.0-inch O.D. soil sample is driven into a soil mass by raising a 140—lb hammer 30 inches and allowing it to drop onto an anvil connected to the drill rods connected to the sampler. The number of blows required to drive the sampler the last 12 inches of an 18-inch drive is called the SPT blowcount or N value. The test is used to determine soil properties.

\* Since several different expressions for SPT blowcounts are required in this report, the following notation will be used.

$N$  = Uncorrected Thermalito SPT blowcount measured in the field

$N_1$  = Thermalito SPT blowcount corrected to 1 tsf overburden pressure,  $= C_N \times N$  (see Figure 237.)

$N_{A1}$  = Thermalito SPT blowcount corrected for both overburden pressure and procedural differences,  
 $N_{A1} = N_1 \times 1.5$  (see Table 46). This is the blowcount applicable for use with the Seed and Idriss (1982) correlation.

## GLOSSARY (continued)

$(N_1)_{60}$  = Thermalito SPT blowcount corrected for both overburden pressure and procedural differences,  
 $(N_1)_{60} = N_1 \times 1.3$  (see Table 46). This is the blowcount applicable for use with the Seed (1987) correlation.

- surficial — occurring on the earth's surface
- toe — location where the edge of a slope meets existing ground
- vibroflotation — a process for densifying loose granular materials with a vibratory probe. During this process existing material is densified and new material is added to occupy the empty space produced

**ADDENDUM B. EXPLORATIONS FOR THERMALITO FOREBAY  
SEISMIC EVALUATIONS**

**Thermalito Forebay Seismic Evaluations**  
**Borings from the 1976, 1978, 1979-80, 1981-82, and 1984 Investigations**

Exploration	Station	Offset	Drilled By	Date Drilled
81F-7 SPT	7+00	25' from toe	Continental	4/13-14/82
81F-8 SPT	7+85	15' from toe	Continental	8/19-24/81
81F-9 SPT A	8+57	20' from toe	Continental	10/12-14/81
80-E	8+92	250' from toe	Caltrans	7/18-22/80
81F-9 SPT	9+00	15' from toe	Continental	8/14-18/81
TFS-1	9+00	5' downstream of C <sub>L</sub> -crest	Caltrans	8/30-9/1/78
81F-C9 SPT	9+18	4' upstream of C <sub>L</sub> -crest	Continental	9/17-24/81
TFS-2	9+55	90' from toe	Caltrans	8/5/78
80-A	9+70	275' from toe	Caltrans	7/15/80
80-C	9+92	160' from toe	Caltrans	7/16-17/80
81F-10 SPT B	10+09	35' from toe	Continental	1/29-2/1/82
81F-10 PS C	10+10	29' from toe	Continental	2/10/82
81F-10 PS	10+15	35' from toe	Continental	2/5/82
81F-10 PS A	10+16	29' from toe	Continental	2/8/82
81F-10 PS B	10+17	22' from toe	Continental	2/9/82
81F-C10 SPT	10+18	4' upstream of C <sub>L</sub> -crest	Continental	8/25-9/2/81
81F-10 SPT	10+18	16' from toe	Continental	8/10-13/81
81F-10 SPT A	10+21	35' from toe	Continental	1/28-29/82
81F-10 PS D	10+22	29' from toe	Continental	2/11/82
79-10	10+24	12' from toe	Caltrans	2/28/80
81F-10 SPT C	10+33	35' from toe	Continental	2/2/82
84F-10	10+45	15' from toe	Hogate	6/27/84
84F-C11	10+50	13.5' S/O C <sub>L</sub> -crest	Hogate	6/18-20/84
84F-C11A	10+50	On C <sub>L</sub> -crest	Hogate	6/26/84
81F-11 SPT K	10+55	15' from toe	Continental	1/7-13/82

**Thermalito Forebay Seismic Evaluations (Continued)**  
**Borings from the 1976, 1978, 1979-80, 1981-82, and 1984 Investigations**

Exploration	Station	Offset	Drilled By	Date Drilled
81F-11 SPT J	10+70	15' from toe	Continental	12/31/81-1/7/82
81F-11 SPT L	10+70	25' from toe	Continental	1/14-15/82
81F-11 SPT E	10+84	26' from toe	Continental	11/18-19/81
81F-11 SPT B	10+85	15' from toe	Continental	10/23-27/81
81F-11 SPT A	10+94	32' from toe	Continental	10/12-14/81
81F-11 PS B	10+96	35' from toe	Continental	10/9/81
81F-11 SPT C	10+97	18' from toe	Continental	10/28-29/81
81F-11 SPT F	11+02	24' from toe	Continental	11/19-20/81
81F-11 SPT	11+05	20' from toe	Continental	8/3-7/81
81F-11 SPT H	11+05	48' from toe	Continental	12/29-31/81
80-D	11+05	200' from toe	Caltrans	7/17-18/80
81F-11 PS A	11+10	37' from toe	Continental	10/8/81
81F-C11 SPT	11+18	4' upstream of C <sub>L</sub> -crest	Continental	9/2-10/81
81F-11 SPT G	11+23	25' from toe	Continental	12/22-28/81
81F-11 SPT M	11+28	38' from toe	Continental	1/18-20/82
81F-11 SPT D	11+33	25' from toe	Continental	11/17-18/81
TFS-4A	11+53	52' from toe	Caltrans	9/13/78
TFS-4B	11+55	51' from toe	Caltrans	9/13-14/78
TFS-4	11+55	55' from toe	Caltrans	9/12-13/78
TFS-4C	11+59	58' from toe	Caltrans	9/14/78
TFS-4D	11+59	51' from toe	Caltrans	9/15/78
80-B	11+60	570' from toe	Caltrans	7/16/80
TFS-4E	11+63	55' from toe	Caltrans	9/18-19/78
81F-12 SPT	12+11	34' from toe	Continental	7/23-29/81
81F-C12 SPT	12+18	4' upstream of C <sub>L</sub> -crest	Continental	9/11-17/81
81F-13 SPT C	12+82	28' from toe	Continental	10/20-22/81

**Thermalito Forebay Seismic Evaluations (Continued)**  
**Borings from the 1976, 1978, 1979-80, 1981-82, and 1984 Investigations**

Exploration	Station	Offset	Drilled By	Date Drilled
81F-13 PS C	12+88	51' from toe	Continental	12/14/81
81F-13 PS A	12+88	28' from toe	Continental	12/9/81
81F-13 SPT A	12+90	47' from toe	Continental	10/7-8/81
81F-13 PB	12+93	28' from toe	Continental	11/20-25/81
81F-13 PS B	12+93	36' from toe	Continental	12/11/81
81F-13 PS E	12+99	35' from toe	Continental	12/17/81
81F-13 PS	13+03	28' from toe	Continental	12/1/81
81F-13 PS D	13+06	34' from toe	Continental	12/21/81
81F-13 SPT	13+09	28' from toe	Continental	7/30-8/3/81
81F-13 SPT B	13+19	45' from toe	Continental	10/9-12/81
D-9	42+50	3' from toe	Caltrans	4/1/76
81F-55 SPT	55+44	6' from toe	Continental	9/24-25/81
81F-58 SPT	57+94	6' from toe	Continental	9/28/81
79-60 SPT	60+44	6' from toe	Caltrans	12/14-17/79
81F-63 SPT	62+93	6' from toe	Continental	9/29-30/81
81F-65 PB A	65+36	6' from toe	Continental	2/82
81F-65 SPT	65+42	6' from toe	Continental	9/30-10/2/81
81F-65 PB	65+48	6' from toe	Continental	2/82
81F-67 SPT	66+65	6' from toe	Continental	11/25-30/81
81F-67 SPT A	67+28	6' from toe	Continental	1/7/81
81F-68 PS	67+79	9' from toe	Continental	2/3/82
C10	67+79	6' from toe	Ertec	1/28/82
81F-68 PS A	67+85	6' from toe	Continental	2/4/82
81F-68 SPT	67+91	6' from toe	Continental	10/2-5/81
81F-68 PS B	67+94	11' from toe	Continental	2/4/82
81F-68 PS C	67+97	6' from toe	Continental	2/4/82
C9	68+03	6' from toe	Ertec	1/28/82
81F-68 SPT A	68+41	6' from toe	Continental	1/5-6/81

**Thermalito Forebay Seismic Evaluations (Continued)**  
**Borings from the 1976, 1978, 1979-80, 1981-82, and 1984 Investigations**

Exploration	Station	Offset	Drilled By	Date Drilled
81F-69 SPT	68+91	6' from toe	Continental	11/30/81
79-70 SPT	70+40	7.5' from toe	Caltrans	12/11-12/79
D-10	71+00	3' from toe	Caltrans	4/1-2/76
C8	71+29	6' from toe	Ertec	1/28/82
81F-71 SPT	71+35	6' from toe	Continental	2/12/82
81F-73 SPT	72+80	6' from toe	Continental	11/16-17/81
81F-73 SPT A	73+25	7' from toe	Continental	1/26-27/82
81F-74 SPT A	73+55	6' from toe	Continental	2/16/82
C7	73+58	6' from toe	Ertec	1/28/82
81F-74 PS	73+64	6' from toe	Continental	2/26/82
81F-74 SPT	73+70	6' from toe	Continental	1/4-5/82
81F-C74 SPT	73+70	2' upstream of C <sub>L</sub> -crest	Continental	4/19-20/82
81F-74 PS-A	73+76	6' from toe	Continental	2/26/82
C6	73+82	6' from toe	Ertec	1/28/82
81F-75 SPT	75+20	6' from toe	Continental	11/13-16/81
81F-76 SPT A	75+80	6' from toe	Continental	1/26/82
81F-76 SPT	76+40	6' from toe	Continental	12/31/81
81F-78 SPT	77+60	6' from toe	Continental	11/12-13/81
81F-80 SPT	80+00	6' from toe	Continental	11/11-12/81
TFS-3	81+79	25' from toe	Caltrans	9/8/78
TFS-3A	81+79	10' downstream of C <sub>L</sub> -crest	Caltrans	9/19-20/78
79-82 SPT	82+38	32' from toe	Caltrans	12/12-13/79
81F-85 SPT	84+57	36' from toe	Continental	11/10/81
81F-87 SPT	86+74	19' from toe	Continental	11/6/81
81F-89 SPT	88+92	50' from toe	Continental	11/10-11/81
81F-91 SPT	91+09	6' from toe	Continental	11/5/81

**Thermalito Forebay Seismic Evaluations (Continued)**  
**Borings from the 1976, 1978, 1979-80, 1981-82, and 1984 Investigations**

Exploration	Station	Offset	Drilled By	Date Drilled
79-93 SPT	93+26	8' from toe	Caltrans	12/10-11/79
81F-96 SPT	95+39	8' from toe	Continental	11/4/81
81F-98 SPT	97+71	7' from toe	Continental	11/3/81
79-100 SPT	100+02	18' from toe	Caltrans	12/5/79
81F-102 SPT	102+31	10' from toe	Continental	10/30/81
81F-105 SPT	104+61	31' from toe	Continental	10/28-29/81
81F-107 SPT	106+91	29' from toe	Continental	10/29-30/81
81F-C108 SPT	108+06	4' upstream of C <sub>L</sub> -crest	Continental	12/1-3/81
81F-109 SPT	109+20	6' from toe	Continental	11/2/81
81F-C110 SPT	110+35	2' downstream of C <sub>L</sub> -crest	Continental	12/3-7/81
D-11	110+88	4' from toe	Caltrans	4/2/76
81F-C111 SPT A	111+19	On C <sub>L</sub> -crest	Continental	2/16/82
C-5	111+38	2' upstream of C <sub>L</sub> -crest	Ertec	1/28/82
81F-C111 SPT	111+47	2' upstream of C <sub>L</sub> -crest	Continental	2/5-8/82
79-112 SPT	111+50	8' from toe	Caltrans	12/5-6/79
C4	111+50	2' upstream of C <sub>L</sub> -crest	Ertec	1/28/82
81F-C112 PS	111+53	On C <sub>L</sub> -crest	Continental	2/23/82
81F-C112 PS A	111+59	On C <sub>L</sub> -crest	Continental	2/19/82
C3	111+62	2' upstream of C <sub>L</sub> -crest	Ertec	1/28/82
81F-C112 SPT	111+65	2' upstream of C <sub>L</sub> -crest1	Continental	2/9-10/82
84F-112 SPT	112+00	17' from toe	Hogate	6/22-25/84
84F-C112 SPT	112+00	On C <sub>L</sub> -crest	Hogate	6/20-21/84



**Thermalito Forebay Seismic Evaluations (Continued)**  
**Borings from the 1976, 1978, 1979-80, 1981-82, and 1984 Investigations**

Exploration	Station	Offset	Drilled By	Date Drilled
81F-C112 SPT A	112+39	2' upstream of C <sub>L</sub> -crest	Continental	2/11-12/82
C2	112+44	2' upstream of C <sub>L</sub> -crest	Ertec	1/28/82
84F-113 SPT	112+50	C <sub>L</sub> access road	Hogate	6/25-26/84
81F-C113 SPT	112+56	2' upstream of C <sub>L</sub> -crest	Continental	12/7-9/81
81F-C113 PS	112+62	2' upstream of C <sub>L</sub> -crest	Continental	2/17/82
81F-C113 PS A	112+62	5' upstream of C <sub>L</sub> -crest	Continental	2/25/82
C1	112+68	2' upstream of C <sub>L</sub> -crest	Ertec	1/28/82
81F-C113 SPT A	112+71	2' upstream of C <sub>L</sub> -crest	Continental	2/3-4/82
81F-114 SPT	113+62	6' from toe	Continental	10/27-28/81
D-12	113+88	5' from toe	Caltrans	4/6/76
81F-C115 SPT	114+68	On C <sub>L</sub> crest	Continental	12/23-28/81
81F-116 SPT	115+74	6' from toe	Continental	10/26-27/81
81F-C117 SPT	116+68	6' downstream of C <sub>L</sub> -crest	Continental	12/28-30/81
81F-118 SPT	117+86	6' from toe	Continental	10/23-26/81
79-120 SPT	119+98	5' from toe	Caltrans	12/6/79
81F-C121 SPT A	120+61	On C <sub>L</sub> -crest	Continental	1/8/82
81F-C121 SPT	121+24	2' upstream of C <sub>L</sub> -crest	Continental	12/9-10/81
81F-122 SPT	122+49	8' from toe	Continental	10/23-26/81
81F-C123 SPT	123+12	On C <sub>L</sub> -crest	Continental	1/11-13/82
81F-C124 SPT	123+74	4' upstream of C <sub>L</sub> -crest	Continental	12/11-15/81
81F-125 SPT	124+99	10' from toe	Continental	10/22-23/81

**Thermalito Forebay Seismic Evaluations (Continued)**  
**Borings from the 1976, 1978, 1979-80, 1981-82 , and 1984 Investigations**

Exploration	Station	Offset	Drilled By	Date Drilled
81F-127 SPT	127+50	6' from toe	Continental	10/22-23/81
79-130 SPT	130+00	12' from toe	Caltrans	12/7/79
81F-132 SPT	132+33	6' from toe	Continental	10/21/81
81F-C133 SPT	133+50	2' upstream of C <sub>L</sub> -crest	Continental	12/15-16/81
81F-C134 SPT	134+08	On C <sub>L</sub> -crest	Continental	1/13-14/82
81F-135 SPT A	134+66	6' from toe	Continental	10/16-19/81
81F-C135 SPT	135+24	On C <sub>L</sub> -crest	Continental	1/15-19/82
81F-C136 SPT	135+83	2' upstream of C <sub>L</sub> -crest	Continental	12/16-17/81
81F-137 SPT	136+99	8' from toe	Continental	10/19-20/81
79-139 SPT	139+32	4' from toe	Caltrans	12/3-4/79
81F-141 SPT	141+50	6' from toe	Continental	10/15-16/81
81F-144 SPT	143+65	6' from toe	Continental	10/14-16/81
81F-C144 SPT	144+20	On C <sub>L</sub> -crest	Continental	11/19-21/81
81F-C145 SPT	144+75	2' upstream of C <sub>L</sub> -crest	Continental	12/18-21/81
81F-146 SPT	145+85	5' from toe	Continental	10/20-22/81
81F-C146 SPT	146+02	On C <sub>L</sub> -crest	Continental	1/22-25/82
81F-C147 SPT	146+98	On C <sub>L</sub> -crest	Continental	12/21-22/81
D-13	148+10	4' from toe	Caltrans	4/6-7/76
79-148 SPT	148+10	10' from toe	Caltrans	12/4-5/79

## **ADDENDUM C. STATIC STRESS FINITE ELEMENT ANALYSES**

The static stresses presented in this addendum are values generated by the static finite element program TWIST. Stresses are presented in units of tons per square foot and are shown for the two models analyzed (Station 10-11, and Station 112). The suspect sand layers are highlighted on each figure.

Figure 356. Element Numbers for Finite Element Mesh of Thermalito Forebay Main Dam

Figure 357. Node Numbers for Finite Element Mesh of Thermalito Forebay Main Dam

Figure 358. Static Vertical Effective Normal Stresses,  $\sigma_y'$  (tsf) for Thermalito Forebay Main Dam

Figure 359. Static Horizontal Effective Normal Stresses,  $\sigma_x'$  (tsf) for Thermalito Forebay Main Dam

Figure 360. Static Major Effective Principal Stresses,  $\sigma_1'$  (tsf) for Thermalito Forebay Main Dam

Figure 361. Static Minor Effective Principal Stresses,  $\sigma_3'$  (tsf) for Thermalito Forebay Main Dam

Figure 362. Static Horizontal Effective Shear Stresses,  $\tau_{xy}$  (tsf) for Thermalito Forebay Main Dam

Figure 363. Static Maximum Effective Shear Stresses,  $\tau_{\max}$  (tsf) for Thermalito Forebay Main Dam

Figure 364. Static Principal Stress Orientation for Thermalito Forebay Main Dam

Figure 365. Element Numbers for Finite Element Mesh of Thermalito Forebay Low Dam

Figure 366. Node Numbers for Finite Element Mesh of Thermalito Forebay Low Dam

Figure 367. Static Vertical Effective Normal Stresses,  $\sigma_y'$  (tsf) for Thermalito Forebay Low Dam

Figure 368. Static Horizontal Effective Normal Stresses,  $\sigma_x'$  (tsf) for Thermalito Forebay Low Dam

Figure 369. Static Major Effective Principal Stresses,  $\sigma_1'$  (tsf) for Thermalito Forebay Low Dam

Figure 370. Static Minor Effective Principal Stresses,  $\sigma_3'$  (tsf) for Thermalito Forebay Low Dam

Figure 371. Static Horizontal Effective Shear Stresses,  $\tau_{xy}$  (tsf) for Thermalito Forebay Low Dam

Figure 372. Static Maximum Effective Shear Stresses,  $\tau_{\max}$  (tsf) for Thermalito Forebay Low Dam

Figure 373. Static Principal Stress Orientation for Thermalito Forebay Low Dam

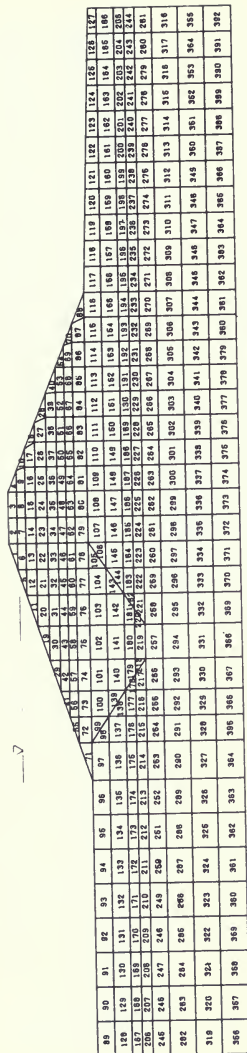


Figure 356. Element Numbers for Finite Element Mesh of Thermalito Forebay Main Dam

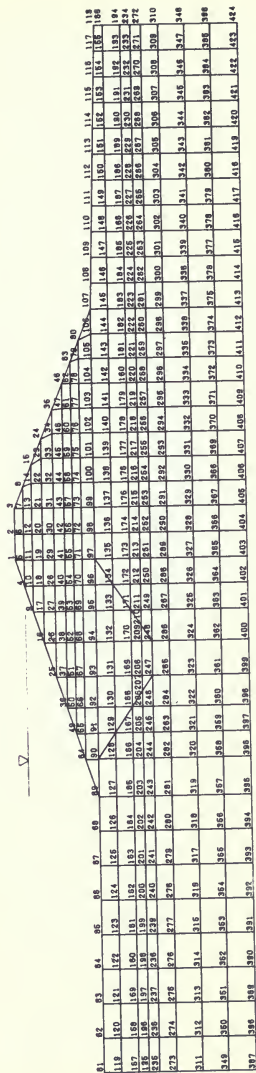
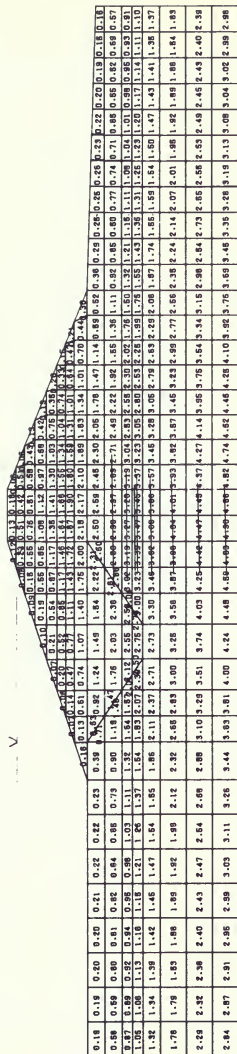


Figure 357. Node Numbers for Finite Element Mesh of Thermalito Forebay Main Dam



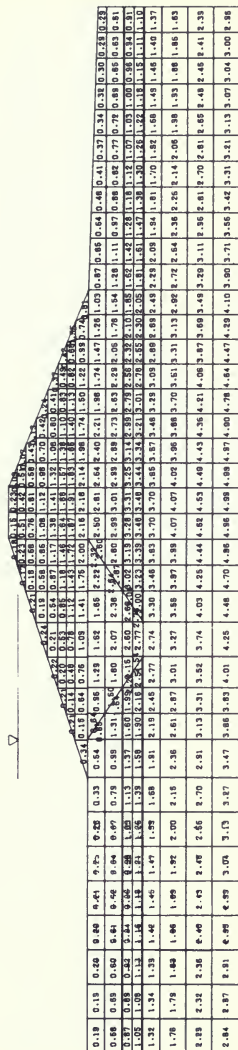
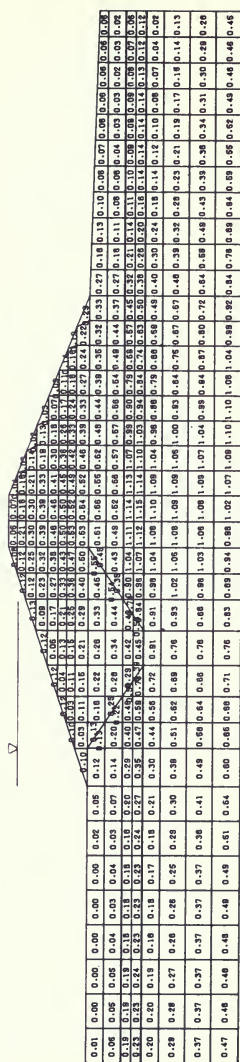


Figure 360. Static Major Effective Principal Stresses,  $\sigma_1'$  (tsf) for Thermalito Forebay Main Dam



Figure 361. Static Minor Effective Principal Stresses,  $\sigma_2'$  (tsf) for Thermalito Forebay Main Dam





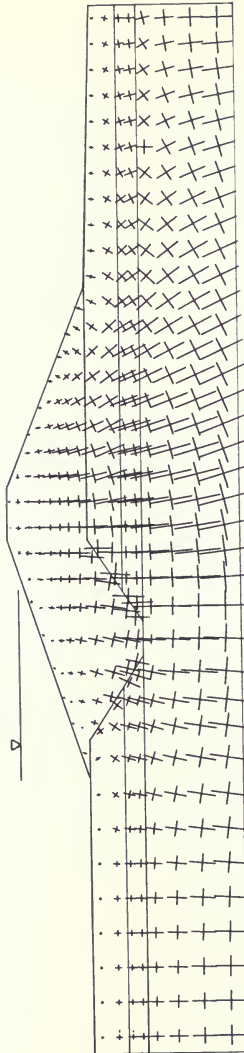
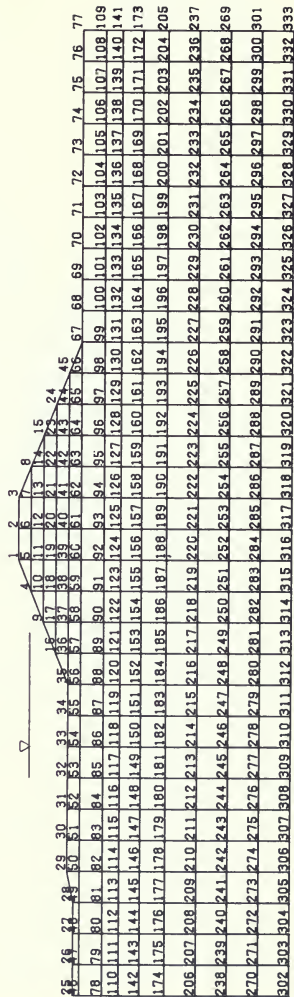
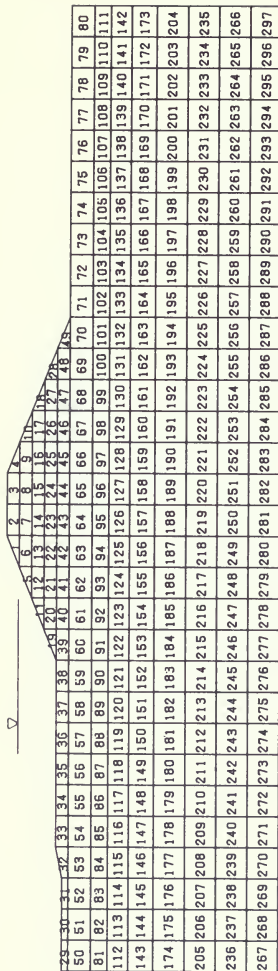


Figure 364. Static Principal Stress Orientation for Thermalito Forebay Main Dam



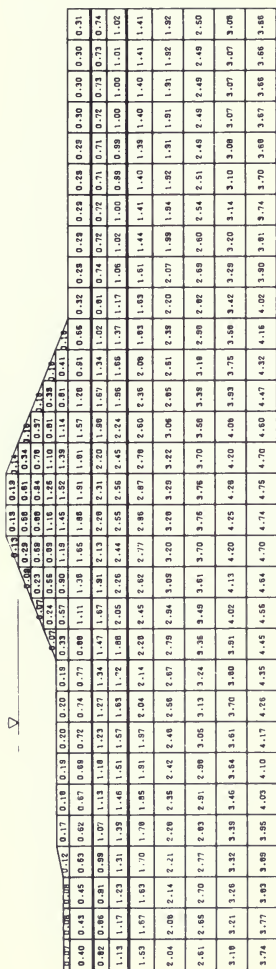


Figure 367. Static Vertical Effective Normal Stresses,  $\sigma'_v$  (tsf) for Thermaito Forebay Low Dam

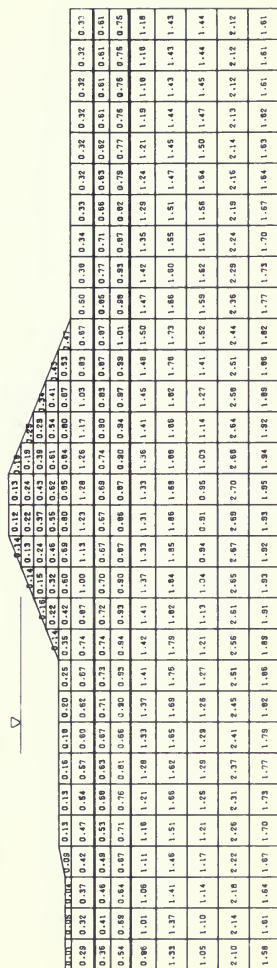


Figure 368. Static Horizontal Effective Normal Stresses,  $\sigma'_x$  (tsf) for Thermaito Forebay Low Dam





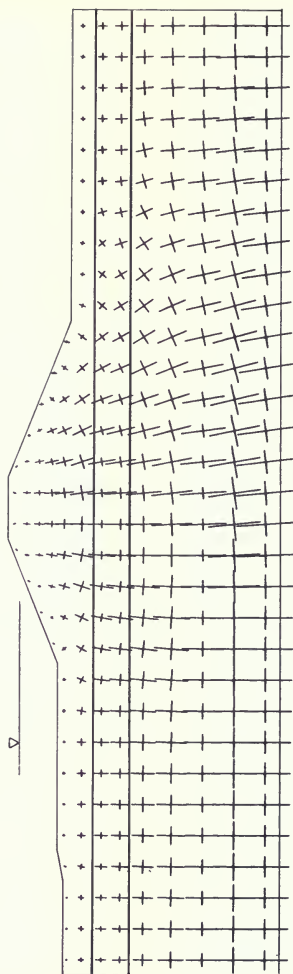


Figure 373. Static Principal Stress Orientation for Thermalito Forebay Low Dam

## **ADDENDUM D. CYCLIC TRIAXIAL TEST SUMMARIES**

Cyclic triaxial test data are summarized in Tables 61 through 65 and Figures 374 through 401 for the different testing programs from 1976 to 1984 at Thermalito Forebay Dam. An index to these tables and figures is given below. This information supplements the material in Section 4 (Chapter V).

### Tables

- 60. Cyclic Triaxial Test Summary for 1976 Undisturbed Samples
- 61. Cyclic Triaxial Test Summary for 1978 Undisturbed Samples
- 62. Cyclic Triaxial Test Summary for 1979–1980 Undisturbed Samples
- 63. Cyclic Triaxial Test Summary for 1981–1982 Undisturbed Samples
- 64. Cyclic Triaxial Test Summary for 1984 Undisturbed Samples

### Figures

- 374. Typical Triaxial Test Records ( $K_c = 1.0$ )
- 375. Typical Cyclic Triaxial Test Records ( $K_c > 1.0$ )
- 376. 1976 SC/CM Samples ( $\sigma'_{3c} = 1.0 \text{ ksc}$ ,  $K_c = 1.0$ )
- 377. 1976 SC/SM Samples ( $\sigma'_{3c} = 3.0 \text{ ksc}$ ,  $K_c = 1.0$ )
- 378. 1978 SC/SM Samples from Station 11 + 55 ( $\sigma'_{3c} = 1.0 \text{ ksc}$ ,  $K_c = 1.0$ )
- 379. 1978 SC/SM Samples from Station 11 + 55 ( $\sigma'_{3c} = 3.0 \text{ ksc}$ ,  $K_c = 1.0$ )
- 380. 1980 SP, SW, SM, SC Hand Carved Samples from Tail Channel ( $\sigma'_{3c} = 1.0 \text{ ksc}$ ,  $K_c = 1.0$ )
- 381. 1980 SP, SW, SM, SC Hand Carved Samples from Tail Channel ( $\sigma'_{3c} = 1.0 \text{ ksc}$ ,  $K_c = 1.5$ )
- 382. 1980 SP, SW, SM, SC Hand Carved Samples from Tail Channel ( $\sigma'_{3c} = 3.0 \text{ ksc}$ ,  $K_c = 1.0$ )
- 383. 1981–82 SC/SM Samples from Station 10 ( $\sigma'_{3c} = 1.0 \text{ ksc}$ ,  $K_c = 1.0$ ,  $N_{A1} = 25, 28$ )
- 384. 1981–82 SC/SM Samples from Station 10 ( $\sigma'_{3c} = 1.0 \text{ ksc}$ ,  $K_c = 1.5, 2.0$ ,  $N_{A1} = 25, 28$ )
- 385. 1981–82 SC/SM Samples from Station 10 ( $\sigma'_{3c} = 3.0 \text{ ksc}$ ,  $K_c = 1.0$ ,  $N_{A1} = 25, 28$ )
- 386. 1981–82 SW/SM Samples from Station 13 ( $\sigma'_{3c} = 1.75 \text{ ksc}$ ,  $K_c = 1.0$ ,  $N_{A1} = 30, 33, 39$ )
- 387. 1981–82 SW/SM Samples from Station 13 ( $\sigma'_{3c} = 2.0 \text{ ksc}$ ,  $K_c = 1.0$ ,  $N_{A1} = 30, 33, 39$ )
- 388. 1981–82 SW/SM Samples from Station 13 ( $\sigma'_{3c} = 2.0 \text{ ksc}$ ,  $K_c = 1.5, 2.0$ ,  $N_{A1} = 33$ )
- 389. 1981–82 SW/SM Samples from Station 13 ( $\sigma'_{3c} = 3.0 \text{ ksc}$ ,  $K_c = 1.5$ ,  $N_{A1} = 30, 33$ )
- 390. 1981–82 SW/SM Samples from Station 13 ( $\sigma'_{3c} = 4.0 \text{ ksc}$ ,  $K_c = 1.0$ ,  $N_{A1} = 30, 33, 39$ )



# Figures (continued)

391. 1981-82 SC/SM Samples from Station 68 ( $\sigma'_{3c} = 0.6ksc, K_c = 1.0, N_{A1} = 17$ )
392. 1981-82 SC/SM Samples from Station 68 ( $\sigma'_{3c} = 0.6ksc, K_c = 1.0, N_{A1} = 19$ )
393. 1981-82 SC/SM Samples from Station 68 ( $\sigma'_{3c} = 1.0ksc, K_c = 1.0, N_{A1} = 19$ )
394. 1981-82 SC/SM Samples from Station 74 ( $\sigma'_{3c} = 0.6ksc, K_c = 1.0, N_{A1} = 20$ )
395. 1984 SC/SM Samples from Station 112 ( $\sigma'_{3c} = 0.6ksc, K_c = 1.0$ )
396. 1984 SC/SM Samples from Station 112 ( $\sigma'_{3c} = 1.0ksc, K_c = 1.0$ )
397. 1981-82 SC/SM Samples from Station 112 ( $\sigma'_{3c} = 2.0ksc, K_c = 1.0, N_{A1} = 17, 26$ )
398. 1981-82 SC/SM Samples from Station 112 ( $\sigma'_{3c} = 2.0ksc, K_c = 1.25, N_{A1} = 26$ )
399. 1984 SC/SM Samples from Station 112 ( $\sigma'_{3c} = 3.0ksc, K_c = 1.0$ )
400. 1981-82 SC/SM Samples from Station 113 ( $\sigma'_{3c} = 2.0ksc, K_c = 1.0, N_{A1} = 20, 27$ )
401. 1981-82 SC/SM Samples from Station 113 ( $\sigma'_{3c} = 2.0ksc, K_c = 2.0, N_{A1} = 27$ )

Table 60. Cyclic Triaxial Test Summary for 1976 Undisturbed Samples

Bore- Hole	Field Sample	Depth (feet)	Lab. Sample No.	CDD** (pcf)	No. D <sub>50</sub> (mm)	200 Sieve (Z)	L.L. (Z)	P.I. (Z)	USCS Class	B Value	U <sub>b</sub> (ksc)	σ <sub>3c</sub> ' (ksc)	K <sub>c</sub>	σ <sub>dp</sub> (ksc)	N <sub>A1</sub>	Number of Cycles at 5% Strain	Number of Cycles at 10% Strain
D-9	L-1	14 <sup>3-14</sup> <sup>8</sup>	76-123	95.1	.14	32	--	--	SC, SM	.90	7.0	3.0	1.0	1.75	--	55	64
D-10	L-1	8 <sup>7-9</sup> <sup>2</sup>	76-124	99.8	.60	6	--	--	SP-SM, SF-SC	.95	7.0	3.0	1.0	2.03	--	17	31
D-11	L-2	12 <sup>5-13</sup> <sup>0</sup>	76-127	108.2	.54	29	--	--	SC, SM	.90	9.0	1.0	1.0	1.43	--	1	2
D-12	L-4	10 <sup>3-10</sup> <sup>8</sup>	76-131	87.5	.17	44	--	--	SC, SM	.95	7.0	1.0	1.0	1.00	--	11	14
D-13	L-1	8 <sup>8-9</sup> <sup>3</sup>	76-132	92.8	.40	35	49	29	SC	.95	8.0	1.0	1.0	1.00	--	13	20
D-13	L-2	8 <sup>3-8</sup> <sup>8</sup>	76-133	90.4	.20	35	36	20	SC	.95	7.0	1.0	1.0	0.75	--	34	49

\*\* Consolidated Dry Density

U<sub>b</sub> = Back Pressure

NP = Non-Plastic

Table 61. Cyclic Triaxial Test Summary for 1978 Undisturbed Samples

Bore- Hole	Field Sample	Depth (feet)	Lab. Sample No.	CDD** (pcf)	No. D <sub>50</sub> (mm)	200 Sieve (Z)	L.L. (Z)	P.I. (Z)	USCS Class	B Value	U <sub>b</sub> (ksc)	σ <sub>3c</sub> ' (ksc)	K <sub>c</sub>	σ <sub>dp</sub> (ksc)	N <sub>A1</sub>	Number of Cycles at 5% Strain	Number of Cycles at 10% Strain
TFS-3A	S-8	54 <sup>4-57</sup> <sup>0</sup>	8-648B	95.0	.48	21	--	--	SC, SM	.90	5.5	3.0	1.0	2.48	--	--	--
TFS-3A	S-8	54 <sup>4-57</sup> <sup>0</sup>	8-648C	92.2	.46	23	--	--	SC, SM	.96	5.0	1.0	1.0	1.24	--	11	--
TFS-3A	S-8	54 <sup>4-57</sup> <sup>0</sup>	8-648D	91.3	.47	23	--	--	SC, SM	.92	5.0	1.0	1.0	0.99	--	33	--
TFS-3A	S-8	54 <sup>4-57</sup> <sup>0</sup>	8-648E	93.7	.53	20	--	--	SC, SM	.80	6.0	0.5	1.0	0.53	--	61	--
TFS-3A	S-9	57 <sup>4-58</sup> <sup>1</sup>	8-649E	94.6	.50	23	--	--	SC, SM	.82	5.0	0.5	1.0	0.53	--	300	--
TFS-4A	S-3	25 <sup>5-26</sup> <sup>8</sup>	8-657D	88.4	--	--	--	--	--	.93	4.0	3.0	1.0	1.50	--	9	11
TFS-4A	S-3	25 <sup>5-26</sup> <sup>8</sup>	8-657E	89.4	.18	28	--	--	SC, SM	.96	4.0	3.0	1.0	1.26	--	34	37
TFS-4A	S-4	28 <sup>3-30</sup> <sup>0</sup>	8-658C	92.9	.31	30	--	--	SC, SM	.92	4.0	1.0	1.0	0.48	--	41	47
TFS-4A	S-4	28 <sup>3-30</sup> <sup>0</sup>	8-658D	91.6	.25	26	--	--	SC, SM	--	5.0	1.0	1.0	0.73	--	6	9
TFS-4A	S-4	28 <sup>3-30</sup> <sup>0</sup>	8-658E	93.2	.23	30	--	--	SC, SM	.95	4.0	1.0	1.0	1.00	--	2	4
TFS-4C	S-1	28 <sup>3-29</sup> <sup>1</sup>	8-662C	93.3	.26	25	--	--	SC, SM	.95	4.0	3.0	1.0	1.75	--	3	4

\*\* Consolidated Dry Density

U<sub>b</sub> = Back Pressure

NP = Non-Plastic

Table 62. Cyclic Triaxial Test Summary for 1979-1980 Undisturbed Samples

1980 Samples\*

Bore- Hole	Field Sample	Depth (feet)	Lab. Sample No.	CDD** (pcf)	D <sub>50</sub> (mm)	No. 200 Sieve (Z)	L.L. (Z)	P.I. (Z)	USCS Class	B Value	U <sub>b</sub> (ksc)	$\sigma'_{3c}$ (ksc)	K <sub>c</sub>	$\sigma_{dp}$ (ksc)	N <sub>A1</sub>	Number of Cycles at 5% Strain	Number of Cycles at 10% Strain
LOC. 2	2	2 <sup>5</sup>	80-310A	86.0	.36	9	--	--	SH-SM, SW-SC .95	7.0	1.0	1.5	1.50	--		3	3
LOC. 2	2	2 <sup>5</sup>	80-310B	85.8	.35	7	--	--	SP-SC .93	6.0	1.0	1.0	0.64	--		289	289
LOC. 3	3	2 <sup>5</sup>	80-312B	92.4	.60	12	--	--	SC-SM .93	6.0	1.0	1.0	0.49	--		175	189
LOC. 3	3	2 <sup>5</sup>	80-312C	92.6	.56	9	--	--	SH-SM, SP-SC .95	6.0	1.0	1.0	0.87	--		5	8
LOC. 3	3	2 <sup>5</sup>	80-312D	90.1	.51	9	--	--	SP-SC .95	6.0	1.0	1.5	0.75	--		100+	--
LOC. 3	3	2 <sup>5</sup>	80-312E	--	.61	6	--	--	SH-SM, SW-SC --	--	1.0	1.5	1.25	--		Power went off	
LOC. 3	3	2 <sup>5</sup>	80-312F	92.5	.61	6	--	--	SH-SM, SW-SC .95	7.0	1.0	1.5	0.97	--		5	6
LOC. 3	3	3 <sup>0</sup>	80-313A	94.7	.66	6	--	--	SH-SM, SW-SC .95	5.0	3.0	1.0	1.62	--		6	--
LOC. 3	3	3 <sup>0</sup>	80-313B	99.4	.70	5	--	--	SW .95	5.0	3.0	1.0	1.20	--		47	49
80151	1	--	80-273	86.5	.50	6	--	--	SP-SM, SP-SC .95	7.0	1.0	1.0	0.75	--		100+	--
80151	2	--	80-274	90.6	.55	4	--	--	SP .95	5.5	3.0	1.0	2.95	--		2	3
80151	3	--	80-275	--	.52	5	--	--	SP --	--	1.0	1.0	2.95	--		Membrane Broke	
80151	4	--	80-276	88.8	.52	4	--	--	SP .95	5.5	3.0	1.0	2.00	--		6	8

\* All 1980 samples are handcarved from the tail channel cut: locations 2 &amp; 3 -- carved tubes; location 80151 -- carved chunks

\*\* Consolidated Dry Density

U<sub>b</sub> = Back Pressure

NP = Non-Plastic

Table 63. Cyclic Triaxial Test Summary for 1981-1982 Undisturbed Samples

Bore- Hole	Field Sample	Depth (feet)	Lab. Sample No.	CDP** (pcf)	D <sub>50</sub> (mm)	200 Slieve (I)	L.L. (I)	P.I. (I)	USCS Class	B Value	U <sub>b</sub> (ksc)	$\sigma'_{3c}$ (ksc)	K <sub>c</sub>	$\sigma_{dp}$ (ksc)	N <sub>A1</sub>	Number of Cycles at 5% Strain	Number of Cycles at 10% Strain
81F-10FSA	PS-1	16 <sup>2</sup> -17 <sup>2</sup>	82-675B	95.8	.31	28	44	26	SC	.95	9.5	1.0	1.0	1.29	25	35	40
81F-10FSA	PS-2	19 <sup>2</sup> -20 <sup>2</sup>	82-674C	98.9	.44	18	33	15	SC	.95	9.5	1.0	1.0	0.99	28	17	21
81F-10FSA	PS-2	19 <sup>2</sup> -20 <sup>2</sup>	82-674B	93.9	.33	20	32	18	SC	.95	8.0	1.0	1.0	1.44	28	3	5
81F-10FSA	PS-1	16 <sup>2</sup> -17 <sup>2</sup>	82-624C	89.6	.15	25	34	17	SC	.95	9.0	1.0	1.0	0.83	25	54	61
81F-10FSA	PS-2	19 <sup>2</sup> -20 <sup>2</sup>	82-678C	98.2	.37	19	44	28	SC	.94	9.5	1.0	1.0	1.19	28	11 Bent Tip	15
81F-10FSA	PS-1	16 <sup>2</sup> -17 <sup>2</sup>	82-673C	83.0	.15	31	--	NP	SM	.95	9.0	1.0	1.0	1.32	25	8	9
81F-10FSA	PS-1	16 <sup>2</sup> -17 <sup>2</sup>	82-679C	94.9	.22	28	36	20	SC	.95	9.5	1.0	1.0	0.99	25	19	24
81F-10FSA	PS-1	16 <sup>2</sup> -17 <sup>2</sup>	82-624B	96.8	.37	29	49	32	SC	.91	9.5	3.0	1.0	2.21	25	15	16
81F-10FSA	PS-1	16 <sup>2</sup> -17 <sup>2</sup>	82-677C	97.5	.35	28	49	31	SC	.93	9.5	3.0	1.0	3.00	25	1.5 Tube Damaged	2
81F-10FSA	PS-2	19 <sup>2</sup> -20 <sup>2</sup>	82-678B	96.1	.20	29	33	19	SC	.95	8.0	3.0	1.0	2.67	29	1	1.5
81F-10FSA	PS-2	19 <sup>2</sup> -20 <sup>2</sup>	82-680C	97.9	.35	24	34	19	SC	.94	9.5	3.0	1.0	1.95	28	5	6.5
81F-10FSA	PS-2	19 <sup>2</sup> -20 <sup>2</sup>	82-680A	102.2	.31	25	37	21	SC	.93	9.5	3.0	1.0	2.30	28	3.5	Gravel 4.5
81F-10FSA	PS-1	16 <sup>2</sup> -17 <sup>2</sup>	82-679B	100.9	.33	30	42	25	SC	.95	9.5	3.0	1.0	2.30	25	10	14
81F-10FSA	PS-2	19 <sup>2</sup> -20 <sup>2</sup>	82-926C	96.2	.45	20	34	17	SC	.95	9.0	1.0	1.5	1.15	28	1.5 Soft/wet	2.5
81F-10FSA	PS-1	16 <sup>2</sup> -17 <sup>2</sup>	82-925C	98.4	.33	30	46	29	SC	.95	9.0	1.0	1.5	0.77	25	126+	126+
81F-10FSA	PS-1	16 <sup>2</sup> -17 <sup>2</sup>	82-825B	94.5	.29	30	39	22	SC	.95	9.5	1.0	1.5	0.77	25	58	69
81F-10FSA	PS-2	19 <sup>2</sup> -20 <sup>2</sup>	82-678B	94.3	.31	20	36	21	SC	.93	9.5	1.0	2.0	1.00	28	15	48
81F-11FSA	PS-3	23 <sup>2</sup> -26 <sup>2</sup>	81-1534C	89.7	.29	15	--	--	SM	.90	9.5	1.2	1.0	0.99	26	6	--
81F-11FSA	PS-4	28 <sup>2</sup> -28 <sup>2</sup>	81-1535C	100.3	.50	17	--	--	SM	.89	9.5	1.2	1.0	0.83	35	8	13
81F-11FSA	PS-3	27 <sup>2</sup> -28 <sup>2</sup>	81-1537C	94.0	.41	16	--	--	SM	.95	9.5	1.2	1.0	0.60	35	14	20
81F-11FSA	PS-4	31 <sup>2</sup> -31 <sup>2</sup>	81-1538C	102.3	.46	15	--	--	SM	.95	N/A	1.2	1.0	0.60	26	57	--
81F-13FSA	PS-2	49 <sup>2</sup> -51 <sup>2</sup>	81-2508B	91.2	.53	7	--	NP	SP-SM	.95	9.0	1.75	1.0	1.01	30	101+	101+
81F-13FSA	PS-2	49 <sup>2</sup> -51 <sup>2</sup>	81-2508C	94.3	.51	9	--	NP	SH-SM	.95	9.5	1.75	1.0	0.72	30	100+	100+
81F-13FSA	PS-1	46 <sup>2</sup> -47 <sup>2</sup>	81-2503C	85.1	.50	10	--	NP	SH-SM	.95	9.5	1.75	1.0	1.03	30	4	6
81F-13FSA	PS-2	49 <sup>2</sup> -50 <sup>2</sup>	81-2504C	100.5	.64	9	--	NP	SH-SM	.95	8.0	1.75	1.0	0.98	30	8.5	12.5
81F-13FSA	PS-1	47 <sup>2</sup> -48 <sup>2</sup>	81-2507C	97.2	.59	8	--	NP	SH-SM	.95	9.5	1.75	1.0	0.72	30	42	53
81F-13FSA	PS-3	52 <sup>2</sup> -53 <sup>2</sup>	81-2505C	95.4	.58	9	--	NP	SP-SM	.95	9.5	1.75	1.0	1.30	33	34	40
81F-13FSA	PS-3	52 <sup>2</sup> -53 <sup>2</sup>	81-2505B	94.5	.58	11	--	NP	SH-SM	.95	9.5	1.75	1.0	1.74	33	10	13
81F-13FSA	PS-4	55 <sup>2</sup> -56 <sup>2</sup>	81-2506B	89.6	.51	9	--	NP	SP-SM	.95	9.5	1.75	1.0	1.33	39	100+	--
81F-13FSA	PS-4	55 <sup>2</sup> -56 <sup>2</sup>	81-2506C	87.6	.51	10	--	NP	SH-SM	.95	9.5	1.75	1.0	1.33	39	250+	250+
81F-13FSA	PS-2	49 <sup>2</sup> -50 <sup>2</sup>	82-132C	88.7	.34	13	--	NP	SM	.93	9.5	2.0	1.0	0.99	30	126+ Bent Tip	126+
81F-13FSA	PS-2	49 <sup>2</sup> -50 <sup>2</sup>	82-135C	99.4	.55	10	--	NP	SH-SM	.95	9.0	2.0	1.0	1.61	30	5	8
81F-13FSA	PS-1	46 <sup>2</sup> -47 <sup>2</sup>	82-134C	90.4	.41	10	--	NP	SP-SM	.95	9.5	2.0	1.0	1.38	30	9	11
81F-13FSA	PS-2	49 <sup>2</sup> -50 <sup>2</sup>	81-2504B	88.6	.39	13	--	NP	SM	.95	9.0	2.0	1.0	1.97	30	4.5	6
81F-13FSA	PS-1	49 <sup>2</sup> -50 <sup>2</sup>	81-2509B	93.6	.59	9	--	NP	SH-SM	.95	9.5	2.0	1.0	0.82	30	100+	100+
81F-13FSA	PS-2	49 <sup>2</sup> -50 <sup>2</sup>	82-128C	95.9	.60	9	--	NP	SH-SM	.95	9.5	2.0	1.0	1.18	30	11.5	15
81F-13FSA	PS-2	52 <sup>2</sup> -53 <sup>2</sup>	81-2510C	91.6	.54	9	--	NP	SH-SM	.94	9.5	2.0	1.0	1.67	33	17	20
81F-13FSA	PS-3	52 <sup>2</sup> -53 <sup>2</sup>	82-136C	95.1	.51	10	--	NP	SH-SM	.95	9.5	2.0	1.0	1.93	33	8.5	10
81F-13FSA	PS-2	52 <sup>2</sup> -53 <sup>2</sup>	81-2510B	93.6	.42	10	--	NP	SP-SM	.94	9.5	2.0	1.0	1.46	33	28	32
81F-13FSA	PS-4	55 <sup>2</sup> -56 <sup>2</sup>	82-130B	94.0	.58	10	--	NP	SH-SM	.93	9.5	2.0	1.0	1.34	39	57	65
81F-13FSA	PS-4	55 <sup>2</sup> -56 <sup>2</sup>	82-130C	97.1	.68	10	47	21	SH-SM	.93	9.5	2.0	1.0	1.51	39	19	26
81F-13FSA	PS-3	55 <sup>2</sup> -56 <sup>2</sup>	81-2511C	97.3	.56	10	--	NP	SP-SM	.97	9.5	2.0	1.0	2.04	39	18	24
81F-13FSA	PS-4	55 <sup>2</sup> -56 <sup>2</sup>	82-137C	91.9	.56	11	--	NP	SP-SM	.95+	9.0	2.0	1.0	2.12	39	9	11.5
81F-13FSA	PS-1	46 <sup>2</sup> -47 <sup>2</sup>	82-131C	89.5	.60	9	--	NP	SH-SM	.93	9.5	4.0	1.0	3.19	30	1	1
81F-13FSA	PS-1	46 <sup>2</sup> -47 <sup>2</sup>	82-134B	91.2	.40	12	--	NP	SM	.95	8.0	4.0	1.0	2.44	30	8.5	10
81F-13FSA	PS-1	46 <sup>2</sup> -47 <sup>2</sup>	82-127B	92.9	.52	9	--	NP	SH-SM	.95	9.0	4.0	1.0	2.07	30	13	15

\*\* Consolidated Dry Density

U<sub>b</sub> = Back Pressure

NP = Non-Plastic

Table 63. Cyclic Triaxial Test Summary for 1981-1982 Undisturbed Samples (Continued)

Bore- Hole	Field Sample	Depth (feet)	Lab. Sample No.	CDD** (pcf)	D <sub>50</sub> (mm)	200 Sieve (%)	L.L.	P.I.	USCS (I)	B Class	U <sub>b</sub> Value (ksc)	$\sigma_{a'}$ (ksc)	K <sub>c</sub>	$\sigma_{dp}$ (ksc)	N <sub>A1</sub>	Number of Cycles at 5% Strain	Number of Cycles at 10% Strain
G1F-13PSC	PS-3	52 <sup>1</sup> -53 <sup>2</sup>	82-129C	87.7	39	9	--	NP	SH-SM	.95	9.5	4.0	1.0	3.31	33	1	2
G1F-13PSC	PS-3	52 <sup>1</sup> -53 <sup>2</sup>	82-129B	96.9	51	12	--	NP	SM	.91	9.5	4.0	1.0	2.91	33	40	44
G1F-13PSD	PS-4	55 <sup>2</sup> -55 <sup>2</sup>	82-133C	92.1	34	8	--	NP	SH-SM	.90	9.5	4.0	1.0	3.48	39	8	--
G1F-13PSA	PS-4	52 <sup>1</sup> -54 <sup>2</sup>	82-126C	96.5	46	13	37	19	SC	.91	9.5	2.0	1.5	2.04	33	5	8
G1F-13PSC	PS-2	49 <sup>3</sup> -50 <sup>2</sup>	82-128B	95.7	58	10	--	NP	SP-SM	.93	9.5	3.0	1.5	1.80	30	66	79
G1F-13PSD	PS-1	46 <sup>2</sup> -47 <sup>2</sup>	82-131B	89.9	58	--	--	NP	SM	.95	9.0	3.0	1.5	3.17	30	1	1
G1F-13PSC	PS-1	46 <sup>2</sup> -47 <sup>2</sup>	82-127C	91.6	48	11	--	NP	SH-SM	.95	9.5	3.0	1.5	2.50	30	17	20
G1F-13PSE	PS-3	52 <sup>1</sup> -53 <sup>2</sup>	82-136B	97.1	68	8	--	NP	SH-SM	.95	9.5	3.0	1.5	3.07	33	1.5	3
G1F-13PSA	PS-3	52 <sup>1</sup> -54 <sup>2</sup>	82-126B	93.8	46	10	36	17	SH-SC	.94	9.5	2.0	2.0	2.34	33	8	11
G1F-65PB	PB-1	7 <sup>2</sup> -8 <sup>2</sup>	82-670D	95.4	--	61	42	26	CL	.95	9.0	0.6	1.0	0.60	42	100+	--
G1F-65PB	PB-1	7 <sup>2</sup> -8 <sup>2</sup>	82-670D	93.3	--	57	44	30	CL	.93	9.5	0.6	1.0	1.20	42	90	--
G1F-65PBA	PB-1	8 <sup>2</sup> -9 <sup>2</sup>	82-671B	92.6	--	66	47	31	CL	.95	8.0	0.6	1.0	0.72	42	50	100+
G1F-65PBA	PB-1	8 <sup>2</sup> -9 <sup>2</sup>	82-671D	91.0	--	69	48	29	CL	.95	9.5	0.6	1.0	0.45	42	100+	100+
G1F-65PBA	PB-1	8 <sup>2</sup> -9 <sup>2</sup>	82-671F	94.2	--	67	46	31	CL	.91	9.5	2.0	1.0	1.27	42	100+	100+
G1F-68PSB	PS-2	11 <sup>1</sup> -12 <sup>2</sup>	82-673C	88.9	11	30	37	22	SC	.95	9.0	0.6	1.0	1.21	19	12	18
G1F-68PSB	PS-2	11 <sup>1</sup> -12 <sup>2</sup>	82-673B	87.6	11	29	35	16	SC	.95	9.0	0.6	1.0	1.00	19	21	30
G1F-68PSC	PS-2	11 <sup>1</sup> -12 <sup>2</sup>	82-630C	88.7	11	31	39	18	SC	.92	9.5	0.6	1.0	0.70	19	60	70
G1F-68PSC	PS-2	11 <sup>1</sup> -12 <sup>2</sup>	82-630B	94.3	11	33	33	18	SC	.95	8.0	0.6	1.0	1.00	19	7	14
G1F-68PSB	PS-1	8 <sup>2</sup> -9 <sup>2</sup>	82-628C	97.9	37	18	35	20	SC	.91	9.5	0.6	1.0	1.25	17	4.5	7.5
G1F-68PSC	PS-1	8 <sup>2</sup> -9 <sup>2</sup>	82-629C	99.9	19	25	37	22	SC	.92	9.5	0.6	1.0	0.85	17	52	71
G1F-68PSC	PS-1	8 <sup>2</sup> -9 <sup>2</sup>	82-628B	97.3	18	30	38	24	SC	.92	9.5	0.6	1.0	1.00	17	26	50
G1F-68PS	PS-1	8 <sup>2</sup> -9 <sup>2</sup>	82-625B	99.3	25	22	36	21	SC	.92	9.5	0.6	1.0	0.85	17	14	19
G1F-68PS	PS-1	8 <sup>2</sup> -9 <sup>2</sup>	82-625C	98.5	36	23	45	30	SC	.92	9.5	0.6	1.0	0.53	17	23	32
G1F-68PSA	PS-1	8 <sup>2</sup> -9 <sup>2</sup>	82-626B	97.7	20	25	33	21	SC	.92	9.5	0.6	1.0	1.08	17	9	13
G1F-68PSA	PS-1	8 <sup>2</sup> -9 <sup>2</sup>	82-626C	98.9	25	24	39	24	SC	.92	9.5	0.6	1.0	0.63	17	25	36+
G1F-68PSA	PS-2	11 <sup>1</sup> -12 <sup>2</sup>	82-627B	92.6	23	16	--	NP	SM	.95	9.0	1.0	1.0	1.09	19	12	16
G1F-68PSA	PS-2	11 <sup>1</sup> -12 <sup>2</sup>	82-627C	92.2	10	36	37	21	SC	.95	9.0	0.6	1.0	0.54	19	19	34
G1F-68PS	PS-2	11 <sup>1</sup> -12 <sup>2</sup>	82-672B	91.8	22	13	--	NP	SM	.95	9.5	0.6	1.0	1.18	19	3	8
G1F-68PS	PS-2	11 <sup>1</sup> -12 <sup>2</sup>	82-672C	87.1	13	29	--	NP	SM	.95	9.0	0.6	1.0	0.83	19	54	66
G1F-74PSA	PS-1	11 <sup>1</sup> -12 <sup>2</sup>	82-937C	97.7	41	14	32	19	SC	.93	9.5	0.6	1.0	0.45	20	46	70
G1F-74PSA	PS-1	11 <sup>1</sup> -12 <sup>2</sup>	82-937B	104.4	49	19	39	26	SC	.93	9.5	0.6	1.0	0.58	20	21	34
G1F-74PS	PS-1	11 <sup>1</sup> -12 <sup>2</sup>	82-936B	102.8	51	17	35	23	SC	.95	9.5	0.6	1.0	0.42	20	63 Disturbed	80+
G1F-74PS	PS-1	11 <sup>1</sup> -12 <sup>2</sup>	82-936C	103.4	47	19	--	--	SM,SC	.95	9.0	0.6	1.0	0.60	20	30 Samples	--
G1F-C112PSA	PS-1	46 <sup>2</sup> -47 <sup>2</sup>	82-928C	93.0	47	18	47	32	SC	.94	9.5	2.0	1.0	1.30	26	6	9
G1F-C112PS	PS-1	46 <sup>2</sup> -46 <sup>2</sup>	82-927C	102.5	47	28	50	33	SC	.95	9.0	2.0	1.0	0.95	26	190	200
G1F-C112PSA	PS-3	54 <sup>2</sup> -55 <sup>2</sup>	82-930C	87.7	36	13	39	23	SC	.94	9.5	2.0	1.0	0.71	17	--	--
G1F-C112PSA	PS-3	54 <sup>2</sup> -55 <sup>2</sup>	82-930B	91.4	32	21	37	23	SC	.93	9.5	2.0	1.0	1.19	17	11	13
G1F-C113PSA	PS-3	55 <sup>2</sup> -56 <sup>2</sup>	82-942C	94.5	49	21	46	29	SC	.95+	9.0	2.0	1.0	1.58	27	7	10
G1F-C113PS	PS-3	55 <sup>2</sup> -56 <sup>2</sup>	82-933C	94.0	45	18	43	27	SC	.95	8.0	2.0	1.0	1.50	27	15	21
G1F-C113PS	PS-3	55 <sup>2</sup> -56 <sup>2</sup>	82-933B	99.3	60	17	44	26	SC	.95	8.8	2.0	1.0	1.29	27	11.5	15
G1F-C113PS	PS-2	52 <sup>2</sup> -52 <sup>2</sup>	82-932C	84.1	31	17	37	22	SC	.95	9.0	2.0	1.0	1.48	20	8	10
G1F-C113PSA	PS-2	52 <sup>2</sup> -52 <sup>2</sup>	82-941C	85.1	31	17	44	29	SC	.95	8.0	2.0	1.0	1.16	20	53	60
G1F-C112PSA	PS-1	46 <sup>2</sup> -47 <sup>2</sup>	82-928B	96.4	50	23	49	30	SC	.92	9.5	2.0	1.25	1.98	26	1.5	3.5

\*\* Consolidated Dry Density

U<sub>b</sub> = Back Pressure

NP = Non-Plastic

Table 63. Cyclic Triaxial Test Summary for 1981-1982 Undisturbed Samples (Continued)

Bore- Hole	Field Sample	Depth (feet)	Lab. Sample No.	CDD** (pcf)	No.		L.L.	P.I.	USCS	B	U <sub>b</sub>	$\sigma'_{3c}$	K <sub>c</sub>	$\sigma_{dp}$	N <sub>A1</sub>	Number of Cycles at 5% Strain	Number of Cycles at 10% Strain
					D <sub>50</sub> (mm)	200 Sieve (Z)											
81F-C113FSA	FS-3	55 <sup>1</sup> -56 <sup>4</sup>	82-942B	99.1	.61	20	44	27	SC	.95	8.0	2.0	2.0	2.50	27	1.5	3
81F-C112FSA	FS-2	51 <sup>4</sup> -52 <sup>2</sup>	82-929B	92.8	.40	18	38	23	SC	.95	9.5	2.0	1.0	1.18	17	11	13
81F-C112FSA	FS-2	51 <sup>4</sup> -52 <sup>2</sup>	82-929C	88.5	.39	18	39	23	SC	.84	9.5	2.0	1.0	0.86	17	16	19
81F-C113FS	FS-1	48 <sup>4</sup> -49 <sup>8</sup>	82-931C	91.2	.42	19	45	31	SC	.95	9.5	2.0	1.0	1.99	27	1.5	2
81F-C112FS	FS-2	48 <sup>0</sup> -50 <sup>3</sup>	82-938B	95.7	.45	24	--	--	SM,SC	.95	9.5	2.0	1.0	1.46	17	4	6
81F-C112FS	FS-2	49 <sup>0</sup> -50 <sup>3</sup>	82-938C	91.6	.34	19	35	22	SC	.94	9.5	2.0	1.0	1.87	17	1.5	2.5
81F-C112FS	FS-3	55 <sup>1</sup> -56 <sup>4</sup>	82-939B	92.0	.22	20	--	--	SM,SC	.95	8.0	2.0	1.0	1.74	17	4.5	7
81F-C112FS	FS-3	55 <sup>1</sup> -56 <sup>4</sup>	82-939C	88.7	.24	17	--	NP	SM	.95	9.0	2.0	1.0	1.12	17	15	17
81F-C113FSA	FS-1	48 <sup>1</sup> -49 <sup>4</sup>	82-940B	98.8	.49	17	47	30	SC	.95	9.0	2.0	1.0	0.99	27	89	98
81F-C113FSA	FS-1	48 <sup>4</sup> -49 <sup>8</sup>	82-940C	92.4	.38	24	46	32	SC	.95	9.5	2.0	1.0	1.52	27	16	20

\*\* Consolidated Dry Density

U<sub>b</sub> = Back Pressure

NP = Non-Plastic

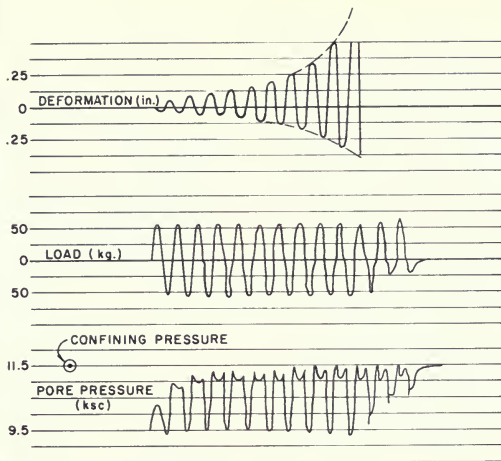
Table 64. Cyclic Triaxial Test Summary for 1984 Undisturbed Samples

Bore- Hole	Field Sample	Depth (feet)	Lab. Sample No.	CDD** (pcf)	No.		L.L.	P.I.	USCS	B	U <sub>b</sub>	$\sigma'_{3c}$	K <sub>c</sub>	$\sigma_{dp}$	N <sub>A1</sub>	Number of Cycles at 5% Strain	Number of Cycles at 10% Strain
					D <sub>50</sub> (mm)	200 Sieve (Z)											
84F-112SPT	S-3	8 <sup>2</sup> -10 <sup>0</sup>	84-468D	101.5	.14	45	62	45	SC	.86	7.0	0.6	1.0	1.00	--	5.5	12
84F-112SPT	S-3	8 <sup>2</sup> -10 <sup>0</sup>	84-468E	107.4	.20	42	52	37	SC	.96	6.0	1.0	1.0	1.30	--	3.5	7.5
84F-112SPT	S-3	8 <sup>2</sup> -10 <sup>0</sup>	84-468C	--	.12	47	62	46	SC	--	5.5	1.0	1.0	1.15	--	3	6
84F-112SPT	S-4	11 <sup>0</sup> -13 <sup>0</sup>	84-469D	87.1	.15	43	39	25	SC	.96	6.0	1.0	1.0	1.17	--	1.5	3.5
84F-112SPT	S-4	11 <sup>0</sup> -13 <sup>0</sup>	84-469C	84.2	.11	46	42	27	SC	--	4.0	1.0	1.0	0.87	--	2	3.5
84F-C112SPT	S-9	41 <sup>2</sup> -43 <sup>2</sup>	84-463D	103.5	.21	44	63	45	SC	.85	5.5	3.0	1.0	1.71	--	81	100
84F-C112SPT	S-10	43 <sup>0</sup> -47 <sup>2</sup>	84-464E	104.8	.23	41	55	37	SC	.86	5.5	3.0	1.0	1.62	--	105	120
84F-C112SPT	S-11	49 <sup>4</sup> -51 <sup>0</sup>	84-465D	87.3	.24	37	52	38	SC	.86	5.5	3.0	1.0	2.03	--	12.5	15.5

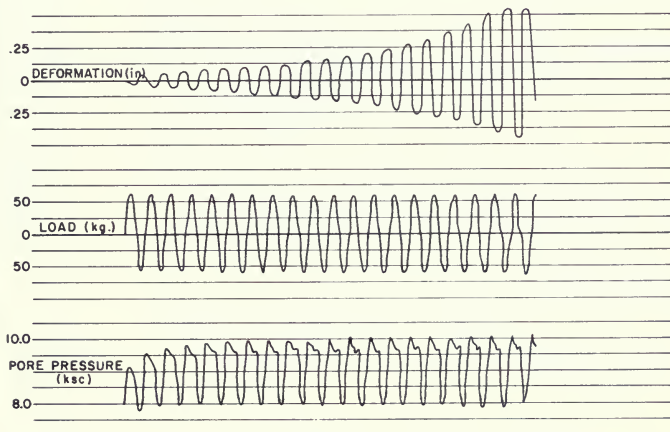
\*\* Consolidated Dry Density

U<sub>b</sub> = Back Pressure

NP = Non-Plastic

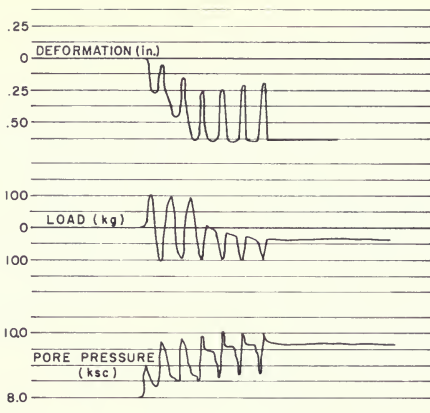


SM ( $N_{A1} = 30$ )  
 $\sigma'_{3c} = 2.0 \text{ ksc}$   
 BORING 8IF-13-PSE  
 DEPTH 47 ft.



SC ( $N_{A1} = 29$ )  
 $\sigma'_{3c} = 2.0 \text{ ksc}$   
 BORING 8IF-C113-PS  
 DEPTH 56 ft.

Figure 374. Typical Triaxial Test Records ( $K_c = 1.0$ )



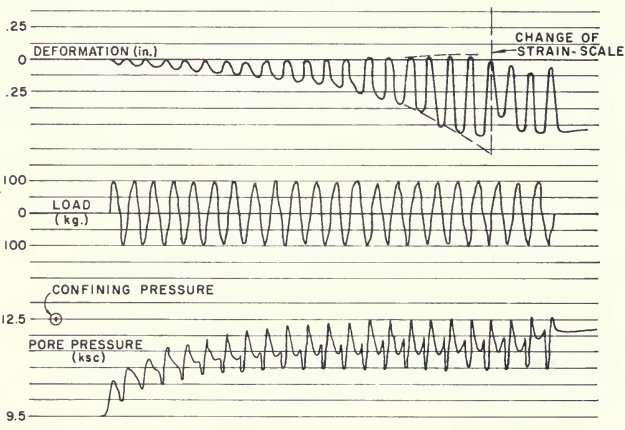
SC ( $N_{AI}=33$ )

$K_C = 2.0$

$\sigma'_{3c} = 2 \text{ ksc}$

BORING 8IF-CII3-PSA

DEPTH 56 ft.



SM ( $N_{AI}=30$ )

$K_C = 1.5$

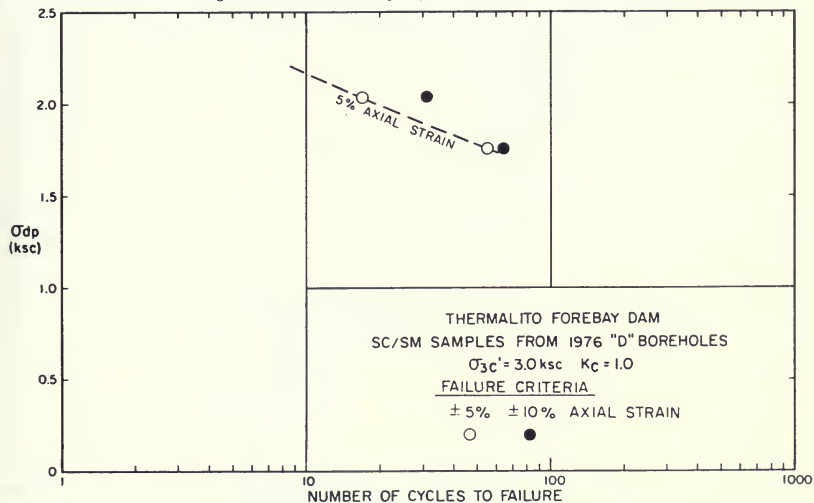
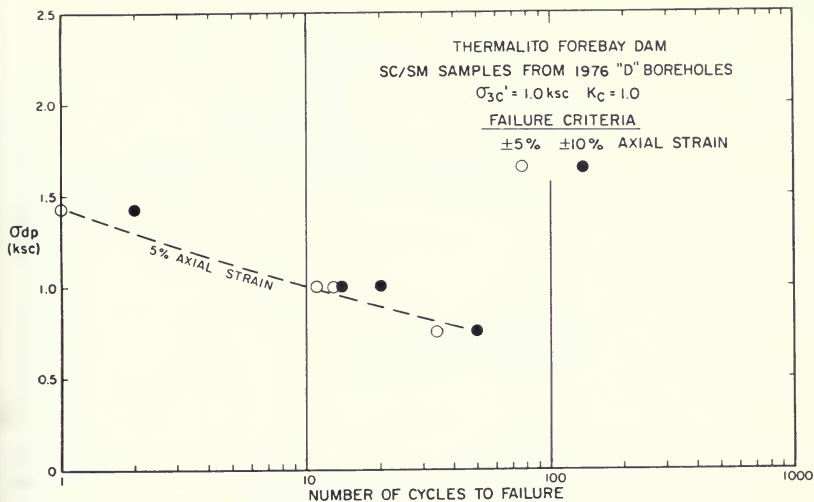
$\sigma'_{3c} = 3 \text{ ksc}$

BORING 8IF-I3-PCS

DEPTH 47 ft.

Figure 375. Typical Cyclic Triaxial Test Records ( $K_C > 1.0$ )





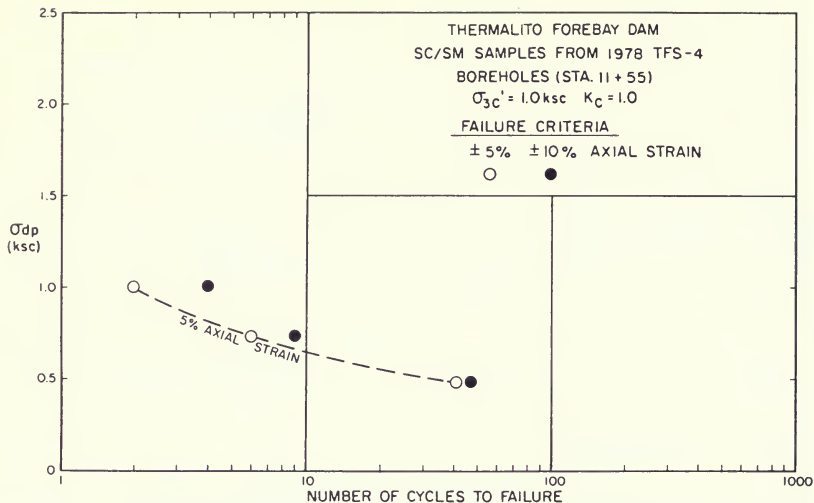


Figure 378. 1978 SC/SM Samples from Station 11 + 55 ( $\sigma'_{3c} = 1.0 \text{ ksc}$ ,  $K_C = 1.0$ )

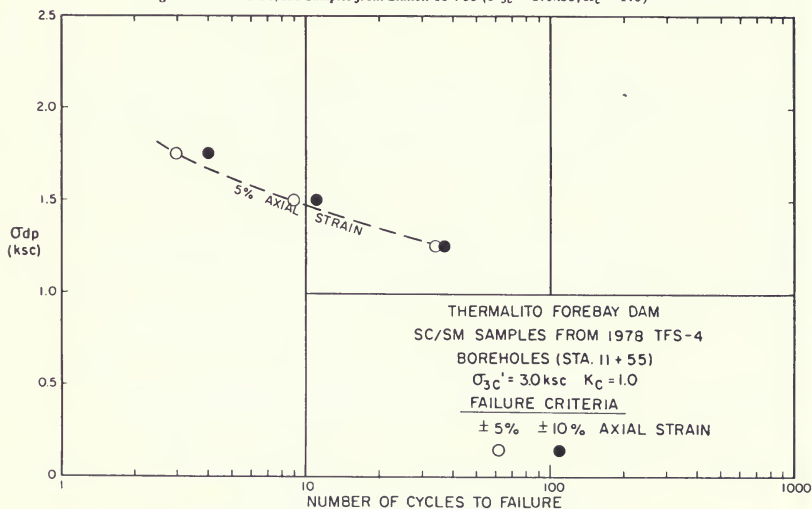


Figure 379. 1978 SC/SM Samples from Station 11 + 55 ( $\sigma'_{3c} = 3.0 \text{ ksc}$ ,  $K_C = 1.0$ )

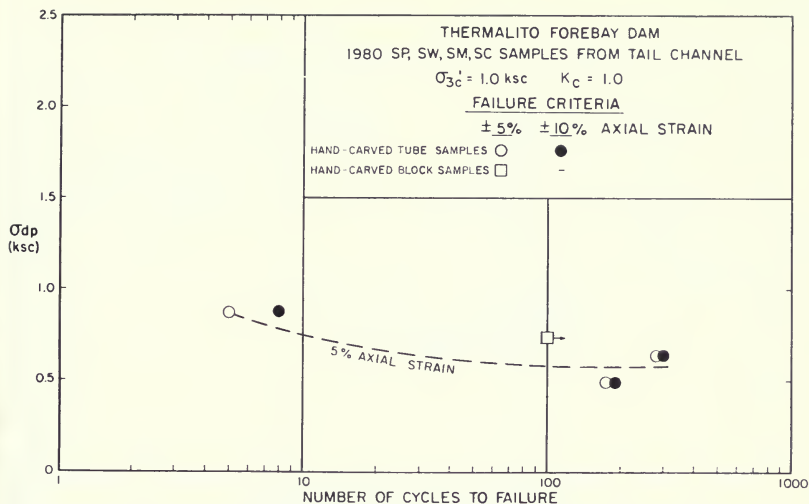


Figure 380. 1980 SP, SW, SM, SC Hand Carved Samples from Tail Channel ( $\sigma'_{3c} = 1.0 \text{ ksc}$ ,  $K_c = 1.0$ )

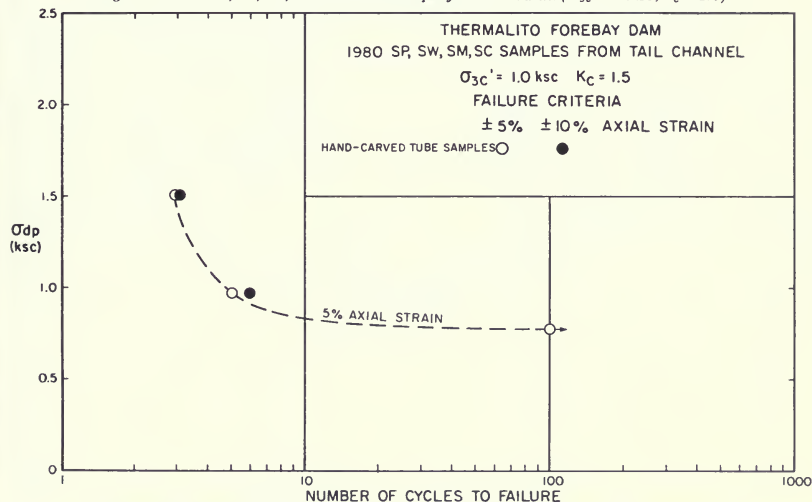


Figure 381. 1980 SP, SW, SM, SC Hand Carved Samples from Tail Channel ( $\sigma'_{3c} = 1.0 \text{ ksc}$ ,  $K_c = 1.5$ )

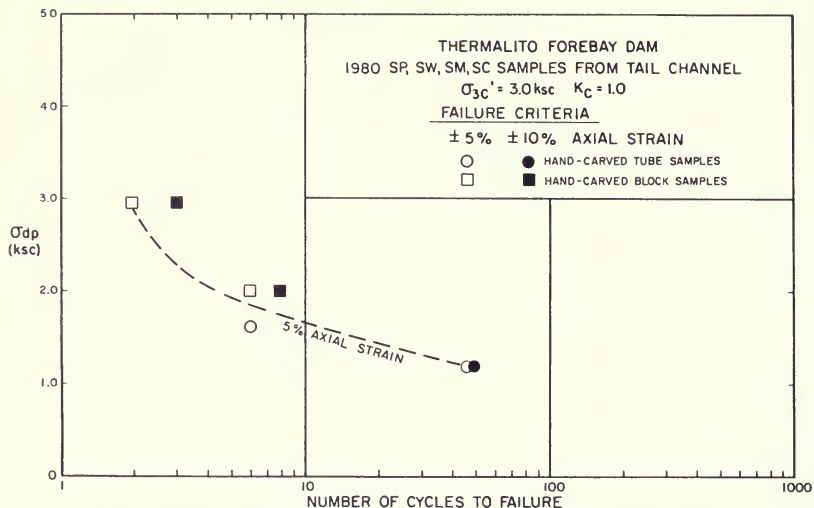


Figure 382. 1980 SP, SW, SM, SC Hand Carved Samples from Tail Channel ( $\sigma'_{3C} = 3.0 \text{ ksc}$ ,  $K_C = 1.0$ )

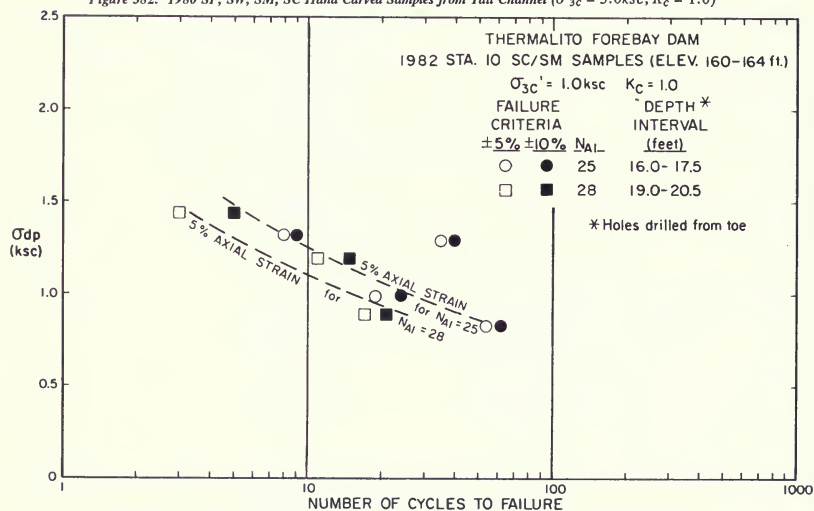


Figure 383. 1981-82 SC/SM Samples from Station 10 ( $\sigma'_{3C} = 1.0 \text{ ksc}$ ,  $K_C = 1.0$ ,  $N_{A1} = 25, 28$ )

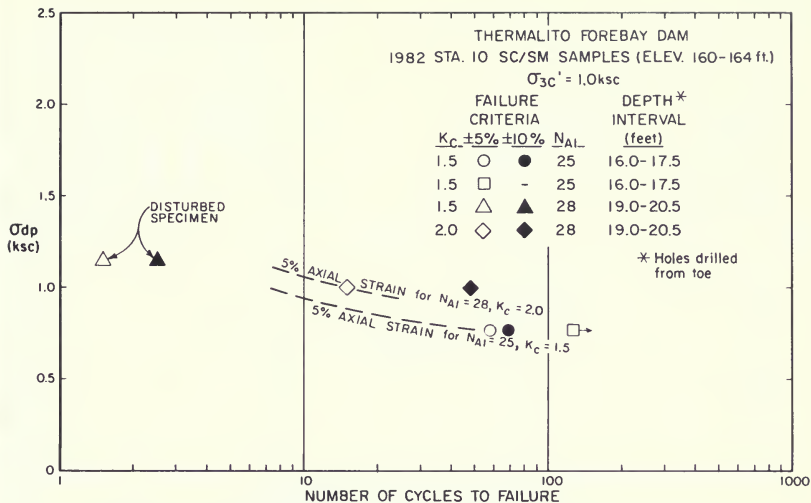


Figure 384. 1982-82 SC/SM Samples from Station 10 ( $\sigma'_{3c} = 1.0 \text{ ksc}$ ,  $K_c = 1.5, 2.0$ ,  $N_{A1} = 25, 28$ )

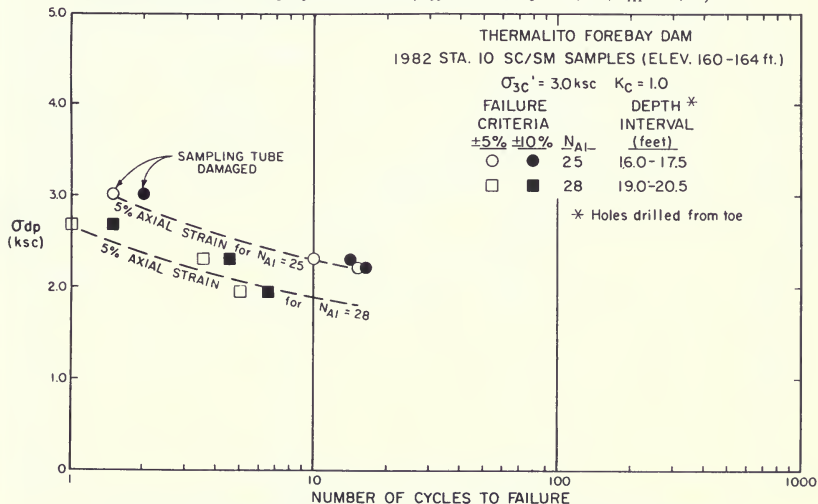


Figure 385. 1981-82 SC/SM Samples from Station 10 ( $\sigma'_{3c} = 3.0 \text{ ksc}$ ,  $K_c = 1.0$ ,  $N_{A1} = 25, 28$ )

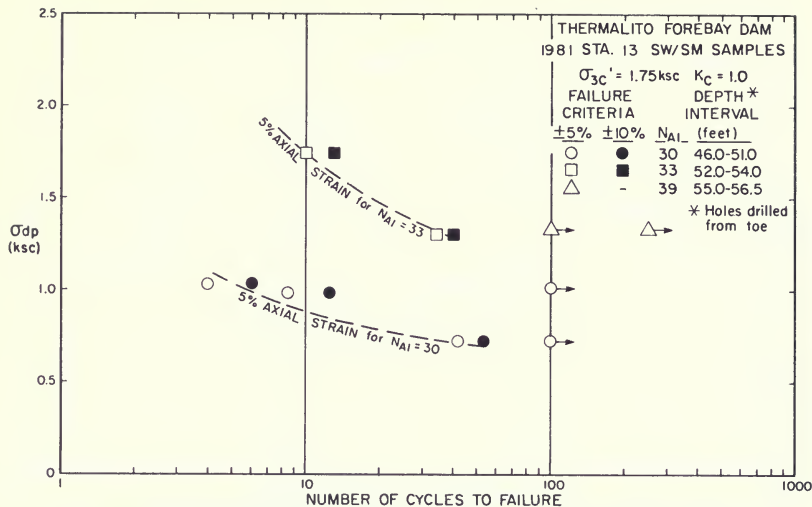


Figure 386. 1981-82 SW/SM Samples from Station 13 ( $\sigma'_{3c} = 1.75 \text{ ksc}$ ,  $K_c = 1.0$ ,  $N_{AI} = 30, 33, 39$ )

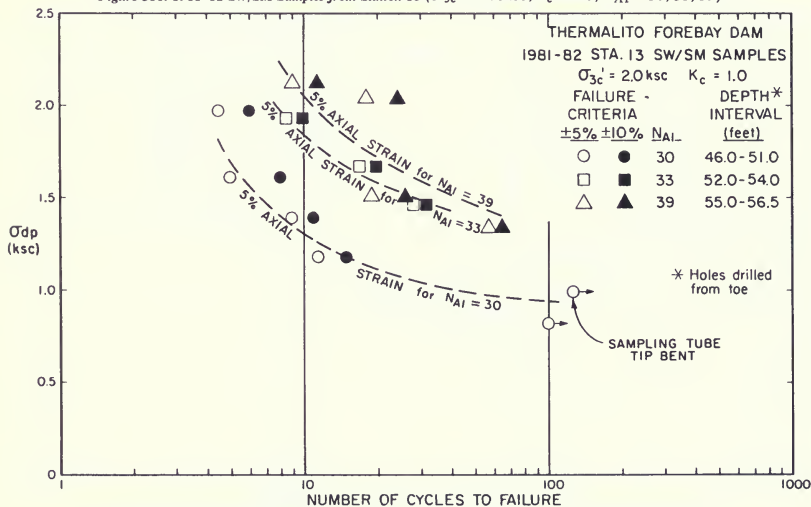


Figure 387. 1981-82 SW/SM Samples from Station 13 ( $\sigma'_{3c} = 2.0 \text{ ksc}$ ,  $K_c = 1.0$ ,  $N_{AI} = 30, 33, 39$ )

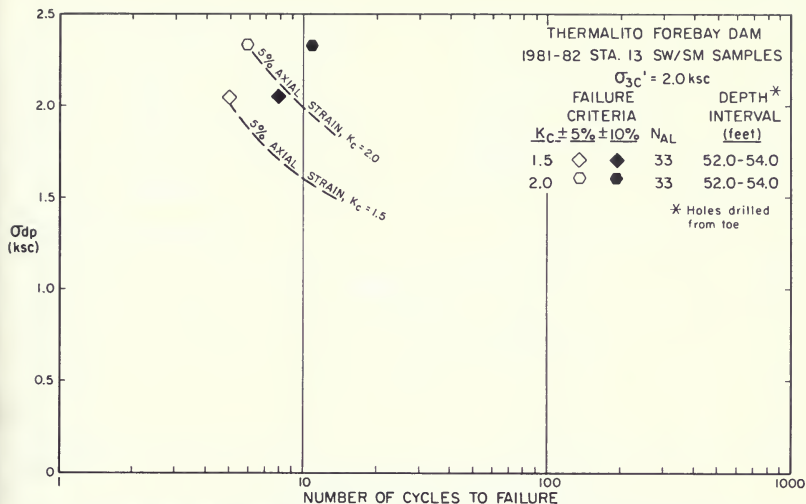


Figure 388. 1981-82 SW/SM Samples from Station 13 ( $\sigma'_{3c} = 2.0 \text{ ksc}$ ,  $K_C = 1.5, 2.0$ ,  $N_{A1} = 33$ )

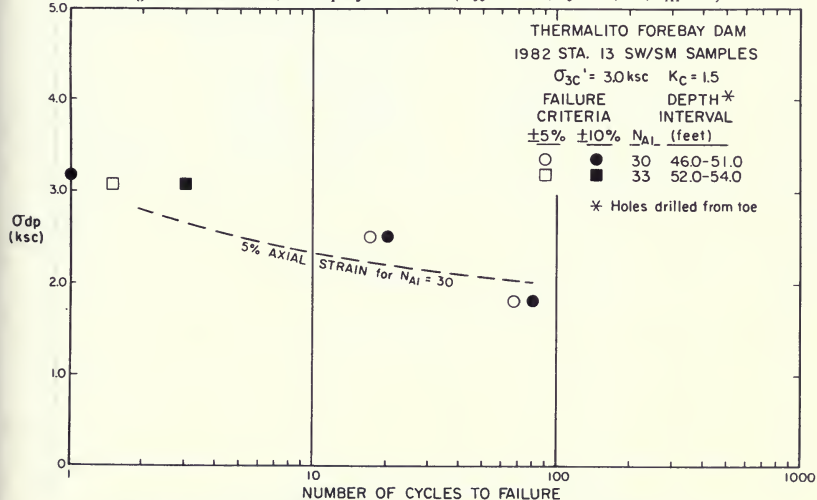
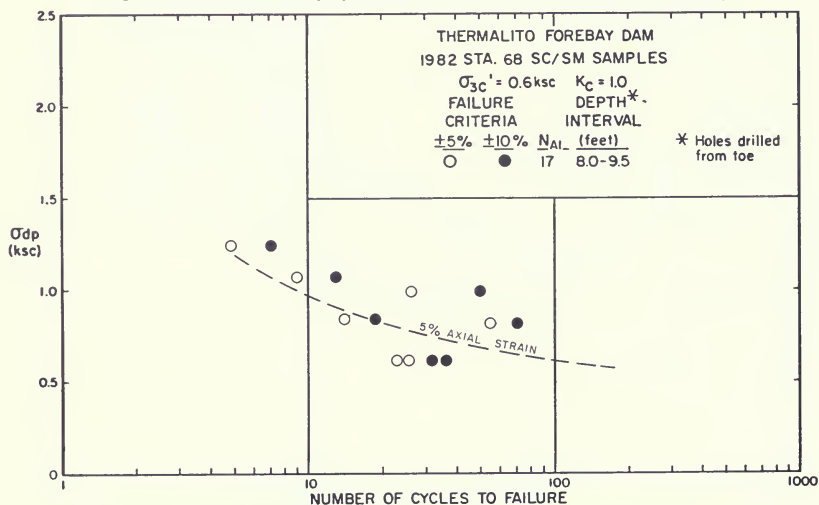
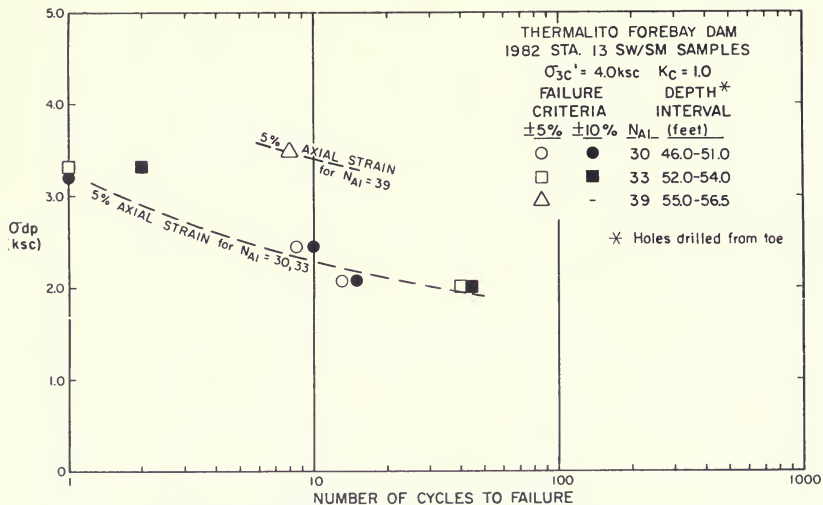


Figure 389. 1981-82 SW/SM Samples from Station 13 ( $\sigma'_{3c} = 3.0 \text{ ksc}$ ,  $K_C = 1.5$ ,  $N_{A1} = 30, 33$ )





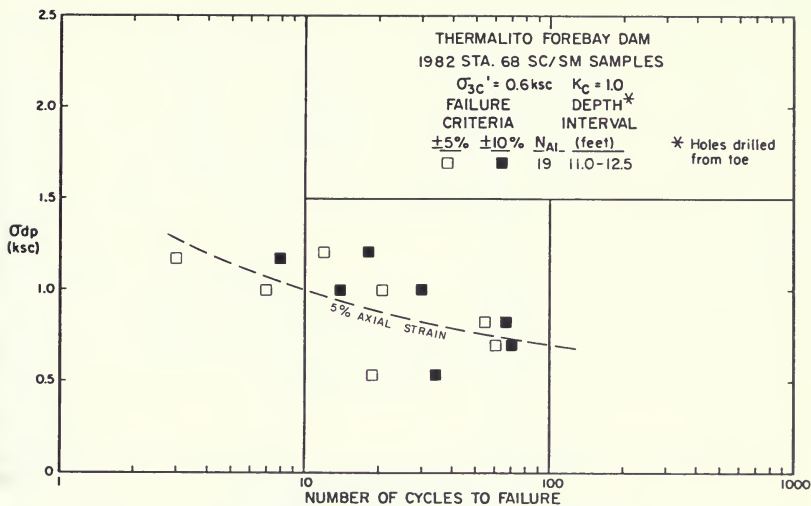


Figure 392. 1981-82 SC/SM Samples from Station 68 ( $\sigma'_{3c} = 0.6 \text{ ksc}$ ,  $K_c = 1.0$ ,  $N_{A1} = 19$ )

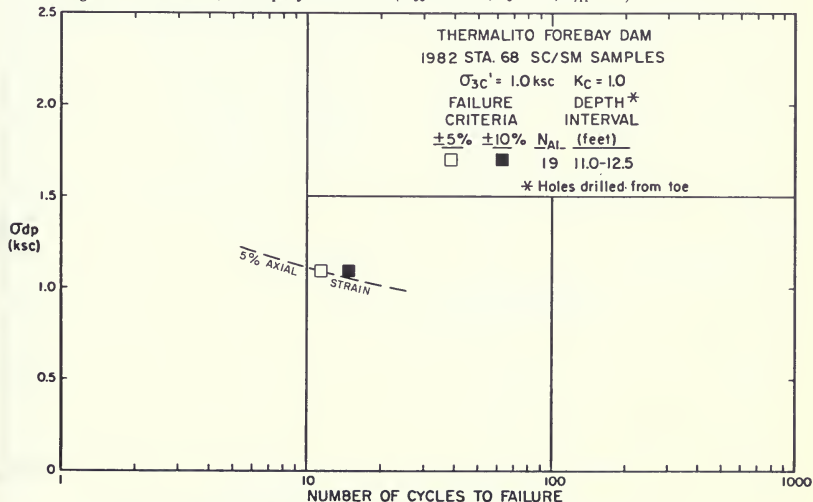


Figure 393. 1981-82 SC/SM Samples from Station 68 ( $\sigma'_{3c} = 1.0 \text{ ksc}$ ,  $K_c = 1.0$ ,  $N_{A1} = 19$ )

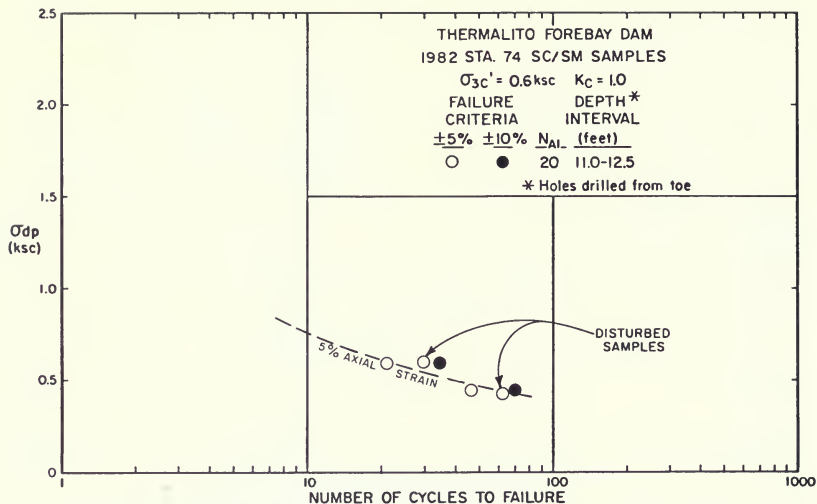


Figure 394. 1981-82 SW/SM Samples from Station 74 ( $\sigma'_{3c} = 0.6 \text{ ksc}$ ,  $K_C = 1.0$ ,  $N_{A1} = 20$ )

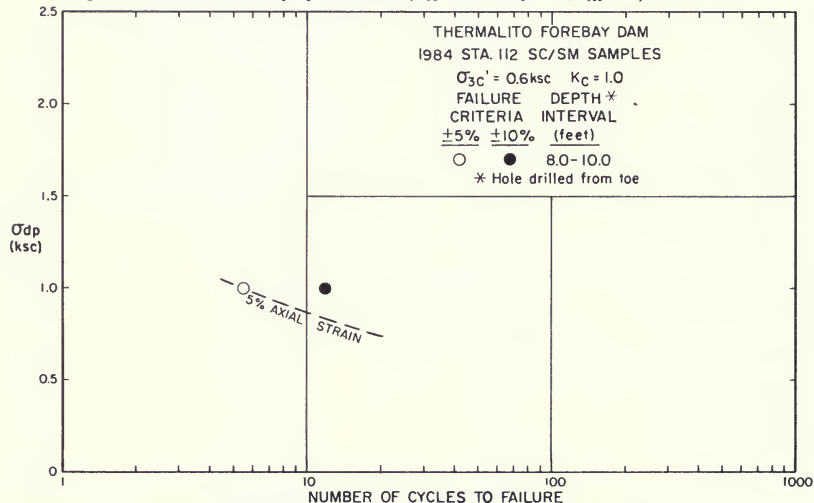


Figure 395. 1984 SC/SM Samples from Station 112 ( $\sigma'_{3c} = 0.6 \text{ ksc}$ ,  $K_C = 1.0$ )

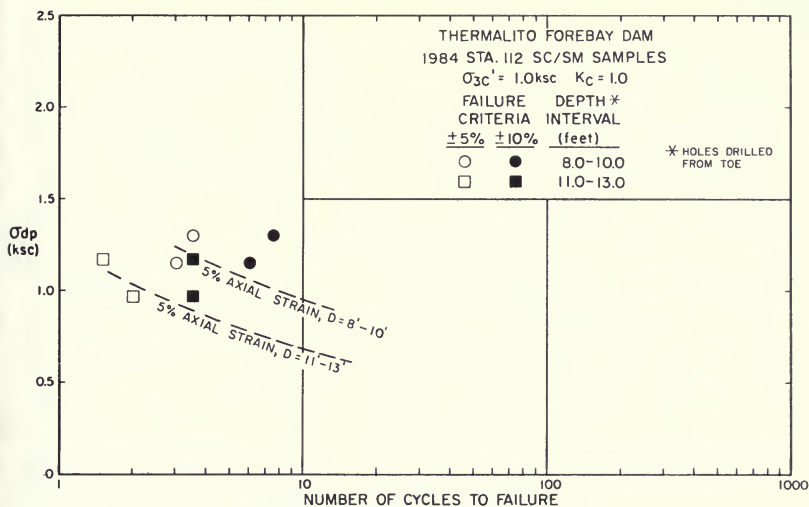


Figure 396. 1984 SC/SM Samples from Station 112 ( $\sigma'_{3c} = 1.0 \text{ ksc}$ ,  $K_c = 1.0$ )

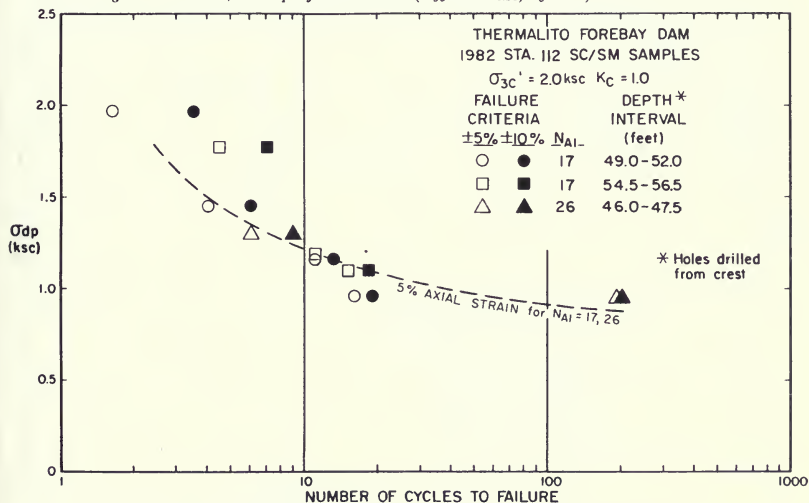


Figure 397. 1981-82 SC/SM Samples from Station 112 ( $\sigma'_{3c} = 2.0 \text{ ksc}$ ,  $K_c = 1.0$ ,  $N_{A1} = 17, 26$ )

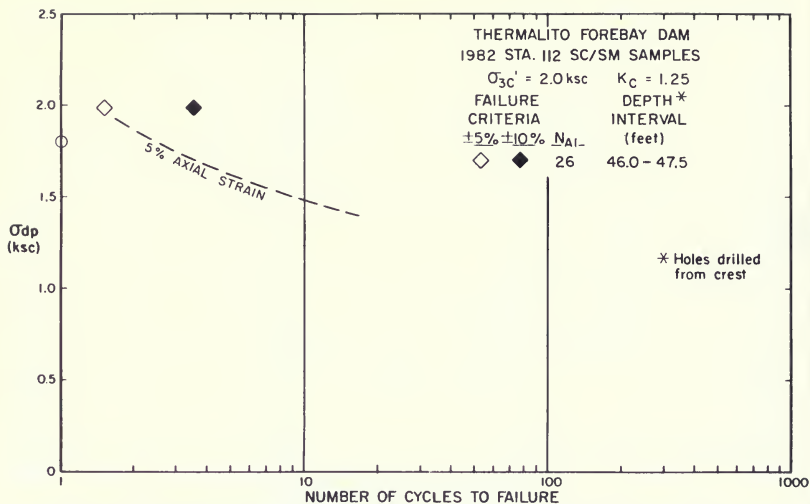


Figure 398. 1981-82 SC/SM Samples from Station 112 ( $\sigma'_{3c} = 2.0 \text{ ksc}$ ,  $K_c = 1.25$ ,  $N_{A1} = 26$ )

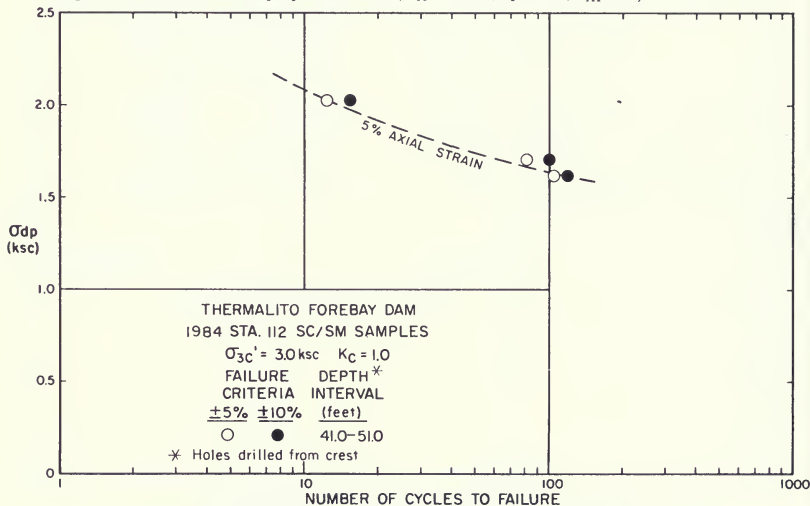


Figure 399. 1984 SC/SM Samples from Station 112 ( $\sigma'_{3c} = 3.0 \text{ ksc}$ ,  $K_c = 1.0$ )

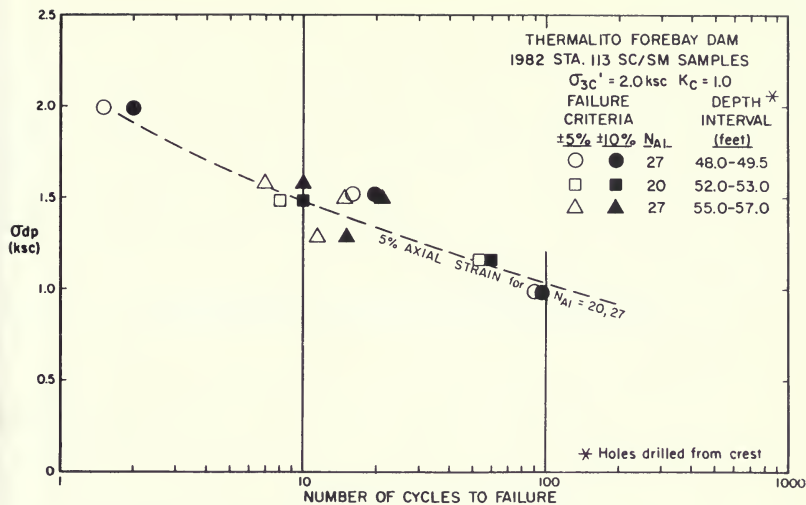


Figure 400. 1981-82 SC/SM Samples from Station 113 ( $\sigma_{3c}' = 2.0 \text{ ksc}$ ,  $K_C = 1.0$ ,  $N_{A1} = 20, 27$ )

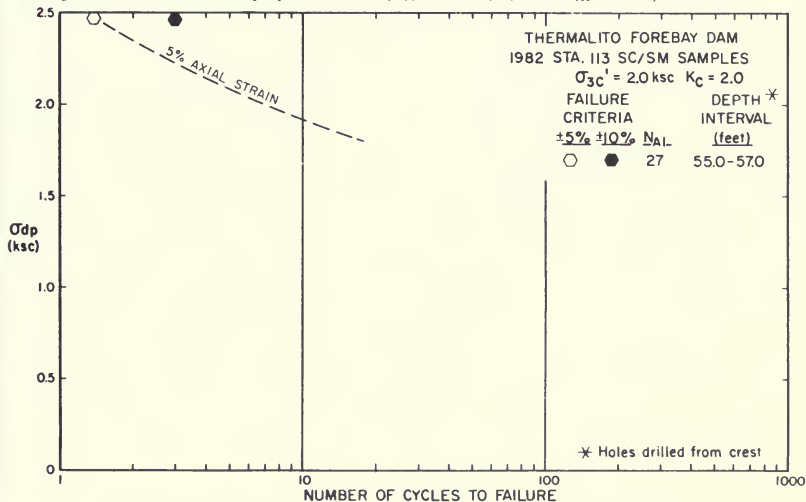


Figure 401. 1981-82 SC/SM Samples from Station 113 ( $\sigma_{3c}' = 2.0 \text{ ksc}$ ,  $K_C = 2.0$ ,  $N_{A1} = 27$ )



## **ADDENDUM E. DYNAMIC STRESS ANALYSES**

## ADDENDUM E. DYNAMIC STRESS ANALYSES

Dynamic stresses, strains and accelerations calculated using programs SHAKE and QUAD4 are presented in the figures shown below. Also included are comparisons between results obtained by program SHAKE and program QUAD4. Program SHAKE uses a one-dimensional dynamic response analysis technique. Since Program SHAKE assumes horizontal soil layers with infinite extent, eight SHAKE columns were used to approximate both the Main Dam and the Low Dam Sections at Thermalito Forebay. Program QUAD4 is a dynamic finite element analysis. The soil layers and properties in SHAKE were made identical to those elements in the QUAD4 analysis at the column locations. Both the Oroville Reanalysis Earthquake motion and the Modified El Centro Earthquake motion were used with each program.

**Figure 402** (a) Maximum Horizontal Accelerations,  $a_{\max}$  (g), Computed by Program SHAKE using the Oroville Reanalysis Earthquake—Main Dam

(b) Maximum Horizontal Accelerations,  $a_{\max}$  (g), Computed by Program SHAKE using the Modified El Centro Record—Main Dam

**Figure 403** (a) Maximum Horizontal Accelerations,  $a_{\max}$  (g), Computed by Program QUAD4 using the Oroville Reanalysis Earthquake—Main Dam

(b) Maximum Horizontal Accelerations,  $a_{\max}$  (g), Computed by Program QUAD4 using the Modified El Centro Record—Main Dam

**Figure 404** (a) Comparison of Maximum Horizontal Accelerations Computed by Programs SHAKE and QUAD4 using the Oroville Reanalysis Earthquake—Main Dam

(b) Comparison of Maximum Horizontal Accelerations Computed by Programs SHAKE and QUAD4 using the Modified El Centro Record—Main Dam

**Figure 405** (a) Maximum Horizontal Shear Stresses,  $(\tau_{xy})_{\max}$  (psf), Computed by Program SHAKE using the Oroville Reanalysis Earthquake—Main Dam

(b) Maximum Horizontal Shear Stresses,  $(\tau_{xy})_{\max}$  (psf), Computed by Program SHAKE Using the Modified El Centro Record—Main Dam

**Figure 406** (a) Maximum Horizontal Shear Stresses,  $(\tau_{xy})_{\max}$  (tsf), Computed by Program QUAD4 Using the Oroville Reanalysis Earthquake—Main Dam

(b) Maximum Horizontal Shear Stresses,  $(\tau_{xy})_{\max}$  (tsf), Computed by Program QUAD4 using the Modified El Centro Record—Main Dam

**Figure 407** (a) Comparison of Maximum Horizontal Shear Stresses,  $(\tau_{xy})_{\max}$ , Computed by Programs SHAKE and QUAD4 using the Oroville Reanalysis Earthquake—Main Dam

(b) Comparison of Maximum Horizontal Shear Stresses,  $(\tau_{xy})_{\max}$ , Computed by Programs SHAKE and QUAD4 using the Modified El Centro Record—Main Dam

**Figure 408** (a) Maximum Shear Strains,  $\gamma_{\max}$  (%), Computed by Program SHAKE using the Oroville Reanalysis Earthquake—Main Dam

(b) Maximum Shear Strains,  $\gamma_{\max}$  (%), Computed by Program SHAKE using the Modified El Centro Record—Main Dam



**Figure 409** (a) Maximum Shear Strains,  $\gamma_{\max}$  (%), Computed by Program QUAD4 using the Oroville Reanalysis Earthquake—Main Dam

(b) Maximum Shear Strains,  $\gamma_{\max}$  (%), Computed by Program QUAD4 using the Modified El Centro Record—Main Dam

**Figure 410** (a) Comparison of Maximum Shear Strains,  $\gamma_{\max}$  , Computed by Programs SHAKE and QUAD4 using the Oroville Reanalysis Earthquake—Main Dam

(b) Comparison of Maximum Shear Strains,  $\gamma_{\max}$  , Computed by Programs SHAKE and QUAD4 using the Modified El Centro Record—Main Dam

**Figure 411** (a) Maximum Horizontal Accelerations,  $a_{\max}$  (g), Computed by Program SHAKE using the Oroville Reanalysis Earthquake—Low Dam

(b) Maximum Horizontal Accelerations,  $a_{\max}$  (g), Computed by Program SHAKE using the Modified El Centro Record—Low Dam

**Figure 412** (a) Maximum Horizontal Accelerations,  $a_{\max}$  (g), Computed by Program QUAD4 using the Oroville Reanalysis Earthquake—Low Dam

(b) Maximum Horizontal Accelerations,  $a_{\max}$  (g), Computed by Program QUAD4 using the Modified El Centro Record —Low Dam

**Figure 413** (a) Comparison of Maximum Horizontal Accelerations Computed by Programs SHAKE and QUAD4 using the Oroville Reanalysis Earthquake—Low Dam

(b) Comparison of Maximum Horizontal Accelerations Computed by Programs SHAKE and QUAD4 using the Modified El Centro Record—Low Dam

**Figure 414** (a) Maximum Horizontal Shear Stresses,  $(\tau_{xy})_{\max}$  (psf), Computed by Program SHAKE using the Oroville Reanalysis Earthquake—Low Dam

(b) Maximum Horizontal Shear Stresses,  $(\tau_{xy})_{\max}$  (psf), Computed by Program SHAKE using the Modified El Centro Record—Low Dam

**Figure 415** (a) Maximum Horizontal Shear Stresses,  $(\tau_{xy})_{\max}$  (psf), Computed by Program QUAD4 using the Oroville Reanalysis Earthquake—Low Dam

(b) Maximum Horizontal Shear Stresses,  $(\tau_{xy})_{\max}$  (psf), Computed by Program QUAD4 using the Modified EL Centro Earthquake—Low Dam

**Figure 416** (a) Comparison of Maximum Horizontal Shear Stresses,  $(\tau_{xy})_{\max}$  , Computed by Programs SHAKE and QUAD4 using the Oroville Reanalysis Earthquake—Low Dam

(b) Comparison of Maximum Horizontal Shear Stresses,  $(\tau_{xy})_{\max}$  , Computed by Programs SHAKE and QUAD4 using the Modified El Centro Record—Low Dam

**Figure 417** (a) Maximum Shear Strains,  $\gamma_{\max}$  (%), Computed by Program SHAKE using the Oroville Reanalysis Earthquake—Low Dam

(b) Maximum Shear Strains,  $\gamma_{\max}$  (%), Computed by Program SHAKE using the Modified El Centro Record—Low Dam

**Figure 418** (a) Maximum Shear Strains,  $\gamma_{\max}$  (%), Computed by Program QUAD4 using the Oroville Reanalysis Earthquake—Low Dam

(b) Maximum Shear Strains,  $\gamma_{\max}$  (%), Computed by Program QUAD4 using the Modified El Centro Record—Low Dam

**Figure 419** (a) Comparison of Maximum Shear Strains,  $\gamma_{\max}$  , Computed by Programs SHAKE and QUAD4 using the Oroville Reanalysis Earthquake – Low Dam

(b) Comparison of Maximum Shear Strains,  $\gamma_{\max}$  , Computed by Programs SHAKE and QUAD4 using the Modified El Centro Record – Low Dam

NOTE: T = NATURAL PERIOD (IN SECONDS) OF SOIL  
COLUMN DURING FINAL ITERATION

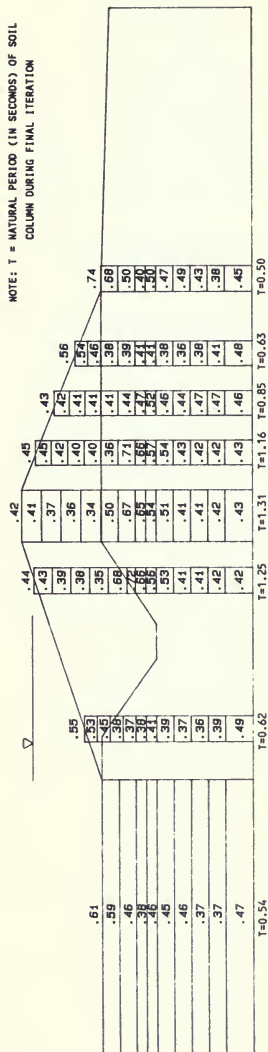


Figure 402. (a) Maximum Horizontal Accelerations,  $a_{max}$  (g), Computed by Program SHAKE using the Oroville Reanalysis Earthquake—Main Dam

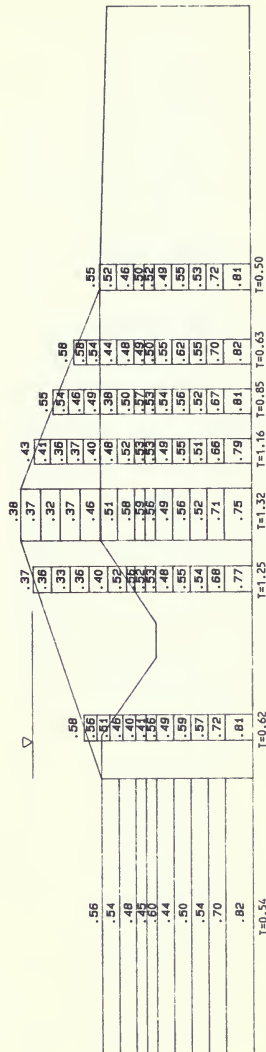


Figure 402. (b) Maximum Horizontal Accelerations,  $a_{max}$  (g), Computed by Program SHAKE using the Modified El Centro Record—Main Dam

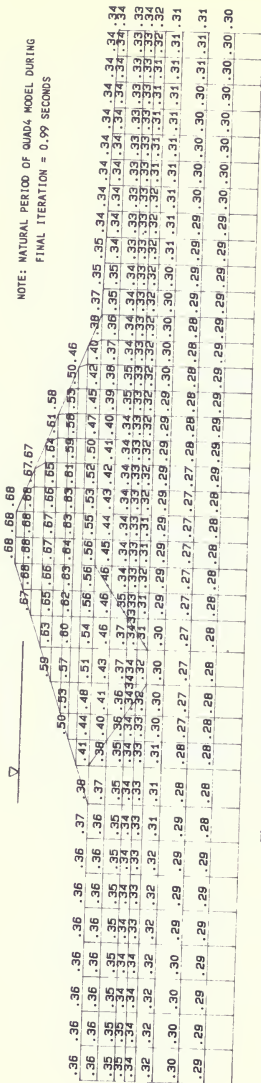


Figure 403. (a) Maximum Horizontal Accelerations,  $a_{max}$  (g), Computed by Program QUAD4  
using the Orowille Reanalysis Earthquake—Main Dam

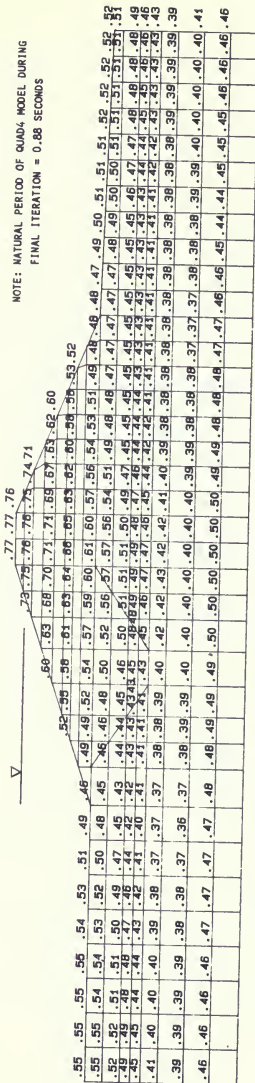


Figure 403. (b) Maximum Horizontal Accelerations,  $a_{max}$  (g), Computed by Program QUAD4  
using the Modified El Centro Record—Main Dam

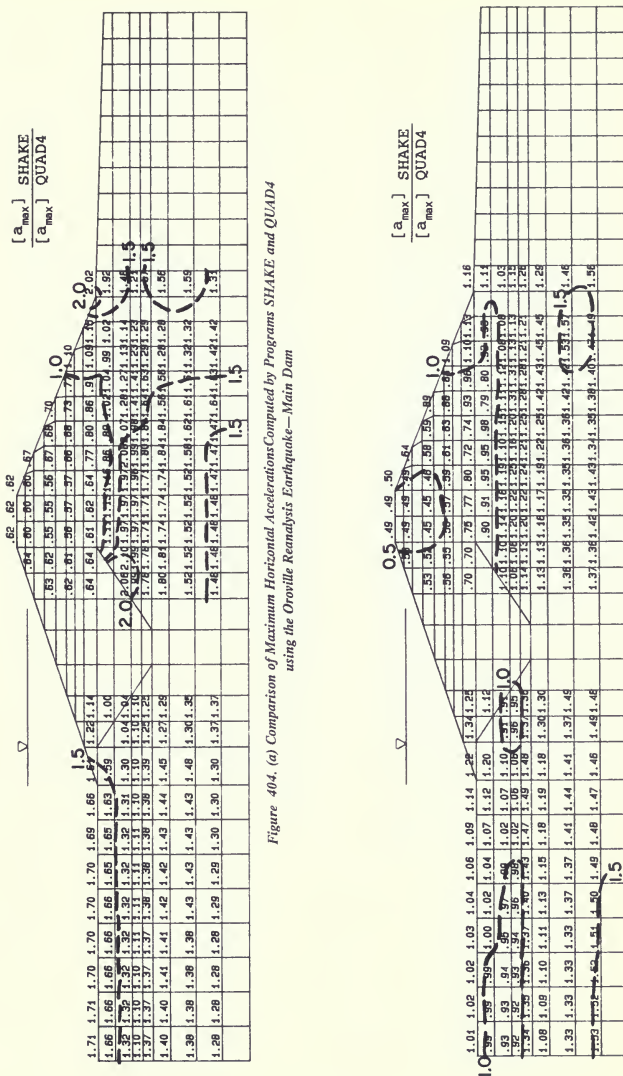


Figure 404. (a) Comparison of Maximum Horizontal Accelerations Computed by Programs SHAKE and QUAD4 using the Orville Reanalysis Earthquake—Main Dam

Figure 404. (b) Maximum Horizontal Accelerations Computed by Programs SHAKE and QUAD4 using the Modified El Centro Record—Main Dam

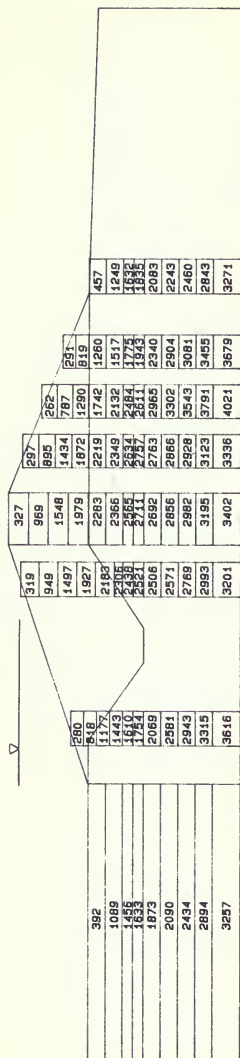
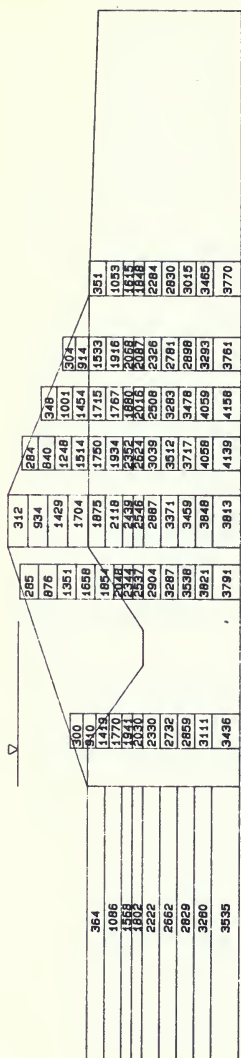
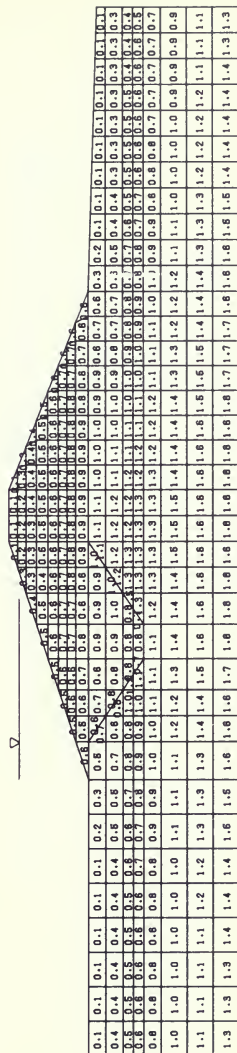
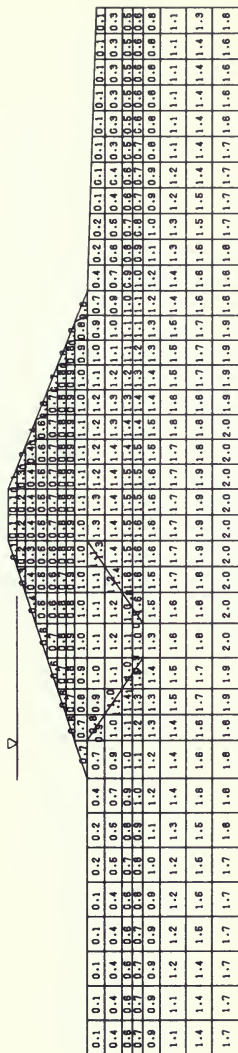


Figure 405. (a) Maximum Horizontal Shear Stresses,  $(\tau_{xy})_{\max}$  (psf), Computed by Program SHAKE using the Oroville Reanalysis Earthquake—Main Dam







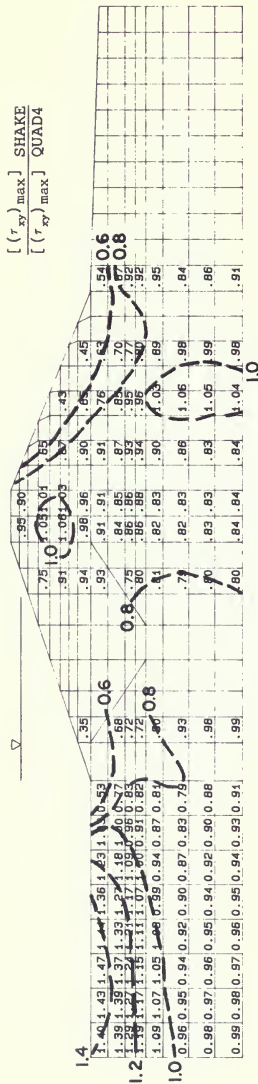


Figure 407. (a) Comparison of Maximum Horizontal Shear Stresses,  $(\tau_{xy})_{\max}$ , Computed by Programs SHAKE and QUAD4 using the Orville Reanalysis Earthquake—Main Dam

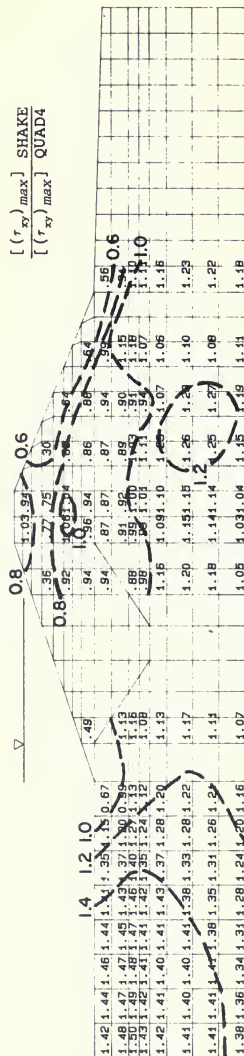
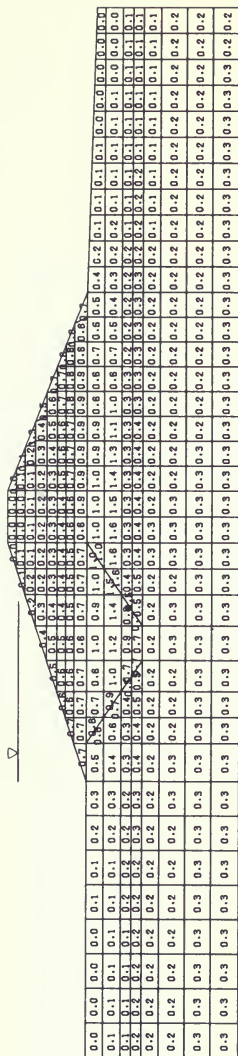
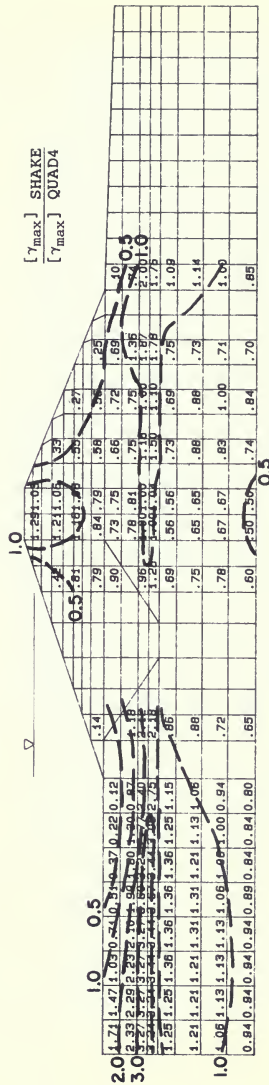
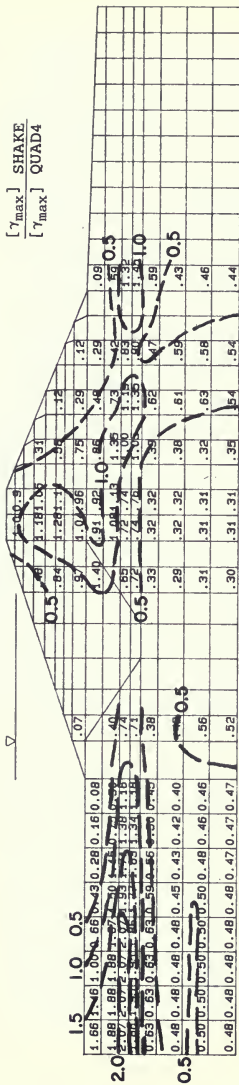


Figure 407. (b) Comparison of Maximum Horizontal Shear Stresses,  $(\tau_{xy})_{\max}$ , Computed by Programs SHAKE and QUAD4 using the Modified El Centro Record—Main Dam









NOTE: T = NATURAL PERIOD (IN SECONDS) OF SOIL COLUMN DURING FINAL ITERATION

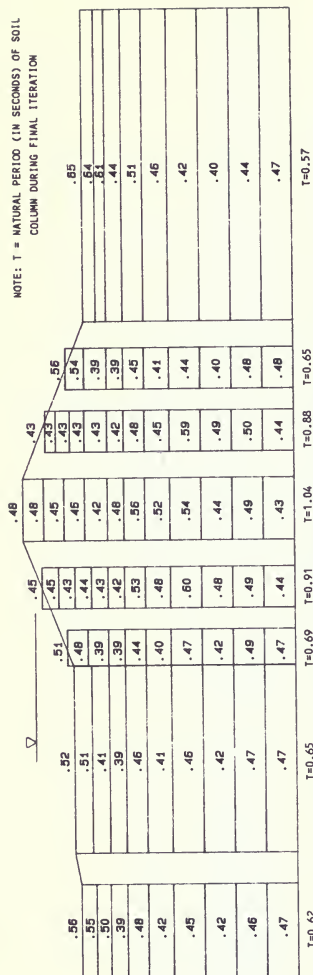


Figure 411. (a) Maximum Horizontal Accelerations,  $a_{max}$  (g), Computed by Program SHAKE using the Oroville Reanalysis Earthquake—Low Dam

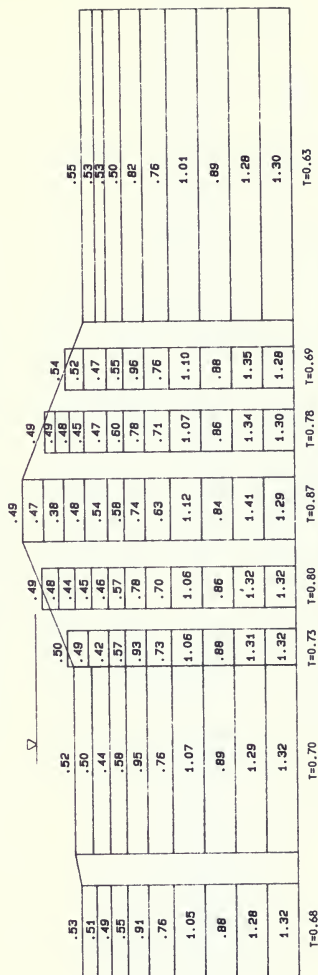


Figure 411. (b) Maximum Horizontal Accelerations,  $a_{max}$  (g), Computed by Program SHAKE using the Modified El Centro Record—Low Dam

[illegible]

Figure 412. (a) Maximum Horizontal Accelerations,  $a_{\max}$  (g), Computed by Program QUAD4 using the Oroville Reanalysis Earthquake—Low Dam

	60	70	80	90	100	110	120	130	140	150	160	170	180	190	200	210	220	230	240	250	260	270	280	290	300	310	320	330	340	350	360	370	380	390	400	410	420	430	440	450	460	470	480	490	500	510	520	530	540	550	560	570	580	590	600	610	620	630	640	650	660	670	680	690	700	710	720	730	740	750	760	770	780	790	800	810	820	830	840	850	860	870	880	890	900	910	920	930	940	950	960	970	980	990	1000																																												
61	62	63	64	65	66	67	68	69	70	71	72	73	74	75	76	77	78	79	80	81	82	83	84	85	86	87	88	89	90	91	92	93	94	95	96	97	98	99	100	101	102	103	104	105	106	107	108	109	110	111	112	113	114	115	116	117	118	119	120	121	122	123	124	125	126	127	128	129	130	131	132	133	134	135	136	137	138	139	140	141	142	143	144	145	146	147	148	149	150	151	152	153	154	155	156	157	158	159	160	161	162	163	164	165	166	167	168	169	170	171	172	173	174	175	176	177	178	179	180	181	182	183	184	185	186	187	188	189	190	191	192	193	194	195	196	197	198	199	200

Figure 412. (b) Maximum Horizontal Accelerations,  $a_{\max}$  (g), Computed by Program QUAD4 using the Modified El Centro Record—Low Dam

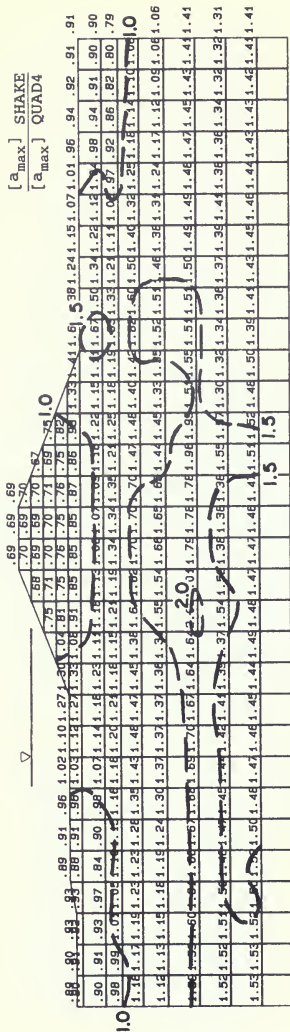


Figure 413. (a) Comparison of Maximum Horizontal Accelerations Computed by Programs SHAKE and QUA/4 using the Orville Reanalysis Earthquake—Low Dam

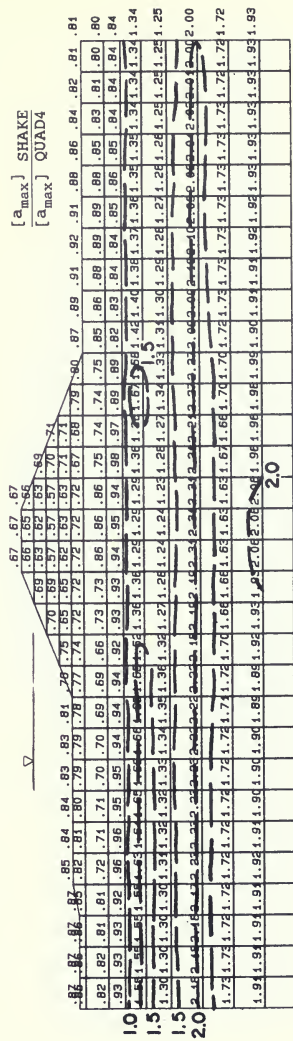


Figure 413. (b) Comparison of Maximum Horizontal Accelerations Computed by Programs SHAKE and QUA/4 using the Modified El Centro Record—Low Dam

252	284	333	237	322	202	338	248
755	837	820	718	962	813	889	721
1071	1130	1216	1186	1532	1024	989	248
1336	1436	1520	1561	1963	1486	1068	721
1768	1869	1991	1916	2354	1911	1275	1068
			2259	2616	2307	1559	1394
			2726	2921	2770	2015	1734
2370	2511	2636	3179	3236	3224	2602	2194
2907	3011	3114	3500	3472	3556	3165	2820
3363	3453	3534	3763	3644	3925	3563	3369
3655	3736	3828	4029	3741	4093	3921	3690

Figure 414. (a) Maximum Horizontal Shear Stresses,  $(\tau_{xy})_{\max}$  (psf), Computed by Program SHAKE using the Oroville Reanalysis Earthquake—Low Dam

248	289	335	267	316	242	327	217
740	894	1003	792	890	717	1044	604
1211	1342	1438	1457	1463	1130	1519	1097
1570	1603	1609	1553	1696	1451	1796	1536
2130	2153	2146	1708	1943	1827	2363	2207
2627	2981	2924	2115	2380	2220	2734	2767
2989	2945	3091	2517	2875	2510	2964	3263
3511	3449	3534	3588	3873	3615	3550	3673
3898	3886	4029	3871	3962	3985	3951	3984

Figure 414. (b) Maximum Horizontal Shear Stresses,  $(\tau_{xy})_{\max}$  (psf), Computed by Program SHAKE using the Modified El Centro Record—Low Dam



2587	2584	2588	2586	638	620	569	567	634	606	1143	1089	1095	1124	1140	1142	1129	1109	1104	1107	1146	937	883	849	875	877	849	906	952	946	984	268	246
618	625	660	700	734	762	778	805	874	1113	1327	1475	1506	1668	1722	1725	1685	1618	1521	1356	1078	685	415	428	427	430	432	436	441	447	445		
1131	1166	1193	1219	1227	1232	1227	1260	1385	1521	1632	1713	1821	1915	1974	1975	1925	1832	1698	1535	1357	1162	980	391	1023	1048	1074	1093	1110	1115	1121		
1503	1523	1541	1540	1533	1522	1503	1623	1731	1823	1894	1947	2022	2092	2135	2133	2094	1996	1879	1700	1631	1503	1384	1354	1406	1458	1503	1540	1569	1590	1603		
1752	1765	1784	1806	1831	1862	1913	1971	2062	2134	2152	2146	2167	2208	2230	2223	2179	2113	2042	1981	1935	1895	1736	1603	1659	1708	1761	1809	1849	1877	1889		
2265	2268	2293	2305	2331	2364	2408	2458	2513	2549	2559	2551	2548	2550	2549	2538	2517	2491	2466	2443	2421	2378	2309	2243	2186	2138	2103	2088	2137	2176	2186		
2840	2853	2866	2880	2896	2920	2949	2981	3016	3042	3033	3007	2984	2967	2949	2935	2943	2926	2919	2922	2922	2903	2856	2805	2761	2724	2688	2663	2646	2629	2623		
3417	3418	3424	3432	3441	3451	3463	3480	3484	3500	3487	3485	3472	3464	3456	3447	3437	3428	3421	3416	3412	3400	3378	3354	3331	3309	3289	3272	3262	3255	3250		
3845	3853	3865	3871	3875	3884	3896	3904	3918	3928	3925	3915	3904	3897	3890	3880	3871	3863	3858	3847	3832	3813	3796	3777	3761	3752	3744	3737	3735	3734			

Figure 415. (a) Maximum Horizontal Shear Stresses,  $(\tau_{xy})_{\max}$  (psf), Computed by Program QUAD4

using the Orville Reanalysis Earthquake—Low Dam

--	--	--	--	--	--	--	--	--	--	--	--	--	--	--	--	--	--	--	--	--	--	--	--	--	--	--	--	--	--	--	--	--	--	--	--	--	--	--	--	--	--	--	--	--	--	--	--	--	--	--	--	--	--	--	--	--	--	--	--	--	--	--	--	--	--	--	--	--	--	--	--	--	--	--	--	--	--	--	--	--	--	--	--	--	--	--	--	--	--	--	--	--	--	--	--	--	--	--	--	--	--	--	--	--	--	--	--	--	--	--	--	--	--	--	--	--	--	--	--	--	--	--	--	--	--	--	--	--	--	--	--	--	--	--	--	--	--	--	--	--	--	--	--	--	--	--	--	--	--	--	--	--	--	--	--	--	--	--	--	--	--	--	--	--	--	--	--	--	--	--	--	--	--	--	--	--	--	--	--	--	--	--	--	--	--	--	--	--	--	--	--	--	--	--	--	--	--	--	--	--	--	--	--	--	--	--	--	--	--	--	--	--	--	--	--	--	--	--	--	--	--	--	--	--	--	--	--	--	--	--	--	--	--	--	--	--	--	--	--	--	--	--	--	--	--	--	--	--	--	--	--	--	--	--	--	--	--	--	--	--	--	--	--	--	--	--	--	--	--	--	--	--	--	--	--	--	--	--	--	--	--	--	--	--	--	--	--	--	--	--	--	--	--	--	--	--	--	--	--	--	--	--	--	--	--	--	--	--	--	--	--	--	--	--	--	--	--	--	--	--	--	--	--	--	--	--	--	--	--	--	--	--	--	--	--	--	--	--	--	--	--	--	--	--	--	--	--	--	--	--	--	--	--	--	--	--	--	--	--	--	--	--	--	--	--	--	--	--	--	--	--	--	--	--	--	--	--	--	--	--	--	--	--	--	--	--	--	--	--	--	--	--	--	--	--	--	--	--	--	--	--	--	--	--	--	--	--	--	--	--	--	--	--	--	--	--	--	--	--	--	--	--	--	--	--	--	--	--	--	--	--	--	--	--	--	--	--	--	--	--	--	--	--	--	--	--	--	--	--	--	--	--	--	--	--	--	--	--	--	--	--	--	--	--	--	--	--	--	--	--	--	--	--	--	--	--	--	--	--	--	--	--	--	--	--	--	--	--	--	--	--	--	--	--	--	--	--	--	--	--	--	--	--	--	--	--	--	--	--	--	--	--	--	--	--	--	--	--	--	--	--	--	--	--	--	--	--	--	--	--	--	--	--	--	--	--	--	--	--	--	--	--	--	--	--	--	--	--	--	--	--	--	--	--	--	--	--	--	--	--	--	--	--	--	--	--	--	--	--	--	--	--	--	--	--	--	--	--	--	--	--	--	--	--	--	--	--	--	--	--	--	--	--	--	--	--	--	--	--	--	--	--	--	--	--	--	--	--	--	--	--	--	--	--	--	--	--	--	--	--	--	--	--	--	--	--	--	--	--	--	--	--	--	--	--	--	--	--	--	--	--	--	--	--	--	--	--	--	--	--	--	--	--	--	--	--	--	--	--	--	--	--	--	--	--	--	--	--	--	--	--	--	--	--	--	--	--	--	--	--	--	--	--	--	--	--	--	--	--	--	--	--	--	--	--	--	--	--	--	--	--	--	--	--	--	--	--	--	--	--	--	--	--	--	--	--	--	--	--	--	--	--	--	--	--	--	--	--	--	--	--	--	--	--	--	--	--	--	--	--	--	--	--	--	--	--	--	--	--	--	--	--	--	--	--	--	--	--	--	--	--	--	--	--	--	--	--	--	--	--	--	--	--	--	--	--	--	--	--	--	--	--	--	--	--	--	--	--	--	--	--	--	--	--	--	--	--	--	--	--	--	--	--	--	--	--	--	--	--	--	--	--	--	--	--	--	--	--	--	--	--	--	--	--	--	--	--	--	--	--	--	--	--	--	--	--	--	--	--	--	--	--	--	--	--	--	--	--	--	--	--	--	--	--	--	--	--	--	--	--	--	--	--	--	--	--	--	--	--	--	--	--	--	--	--	--	--	--	--	--	--	--	--	--	--	--	--	--	--	--	--	--	--	--	--	--	--	--	--	--	--	--	--	--	--	--	--	--	--	--	--	--	--	--	--	--	--	--	--	--	--	--	--	--	--	--	--	--	--	--	--	--	--	--	--	--	--	--	--	--	--	--	--	--	--	--	--	--	--	--	--	--	--	--	--	--	--	--	--	--	--	--	--	--	--	--	--	--	--	--	--	--	--	--	--	--	--	--	--	--	--	--	--	--	--	--	--	--	--	--	--	--	--	--	--	--	--	--	--	--	--	--	--	--	--	--	--	--	--	--	--	--	--	--	--	--	--	--	--	--	--	--	--	--	--	--	--	--	--	--	--	--	--	--	--	--	--	--	--	--	--	--	--	--	--	--	--	--	--	--	--	--	--	--	--	--	--	--	--	--	--	--	--	--	--	--	--	--	--	--	--	--	--	--	--	--	--	--	--	--	--	--	--	--	--	--	--	--	--	--	--	--	--	--	--	--	--	--	--	--	--	--	--	--	--	--	--	--	--	--	--	--	--	--	--	--	--	--	--	--	--	--	--	--	--	--	--	--	--	--	--	--	--	--	--	--	--	--	--	--	--	--	--	--	--	--	--	--	--	--	--	--	--	--	--	--	--	--	--	--	--	--	--	--	--	--	--	--	--	--	--	--	--	--	--	--	--	--	--	--	--	--	--	--	--	--	--	--	--	--	--	--	--	--	--	--	--	--	--	--	--	--	--	--	--	--	--	--	--	--	--	--	--	--	--	--	--	--	--	--	--	--	--	--	--	--	--	--	--	--	--	--	--	--	--	--	--	--	--	--	--	--	--	--	--	--	--	--	--	--	--	--	--	--	--	--	--	--	--	--	--	--	--	--	--	--	--	--	--	--	--	--	--	--	--	--	--	--	--	--	--	--	--	--	--	--	--	--	--	--	--	--	--	--	--	--	--	--	--	--	--	--	--	--	--	--	--	--	--	--	--	--	--	--	--	--	--	--	--	--	--	--	--	--	--	--	--	--	--	--	--	--	--	--	--	--	--	--	--	--	--	--	--	--	--	--	--	--	--	--	--	--	--	--	--	--	--	--	--	--	--	--	--	--	--	--	--	--	--	--	--	--	--	--	--	--	--	--

Figure 415. (b) Maximum Horizontal Shear Stresses,  $(\tau_{xy})_{\max}$  (psf), Computed by Program QUAD4

using the Modified EL Centro Earthquake—Low Dam



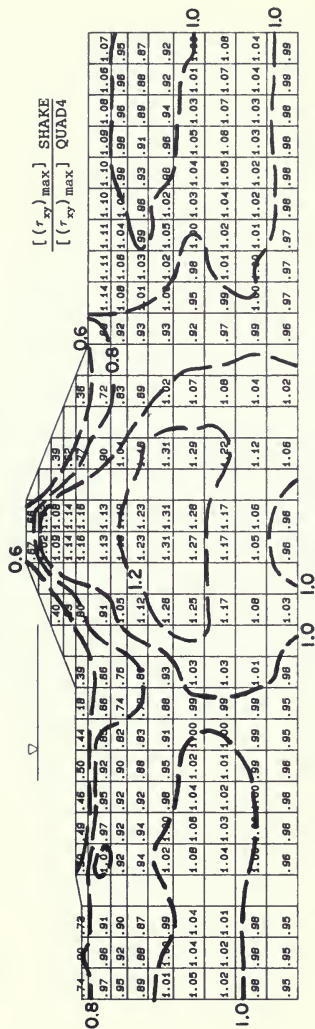


Figure 416. (a) Comparison of Maximum Horizontal Shear Stresses,  $(\tau_{xy})_{\max}$ , Computed by Programs SHAKE and QUAD4 using the Oroville Reanalysis Earthquake—Low Dam

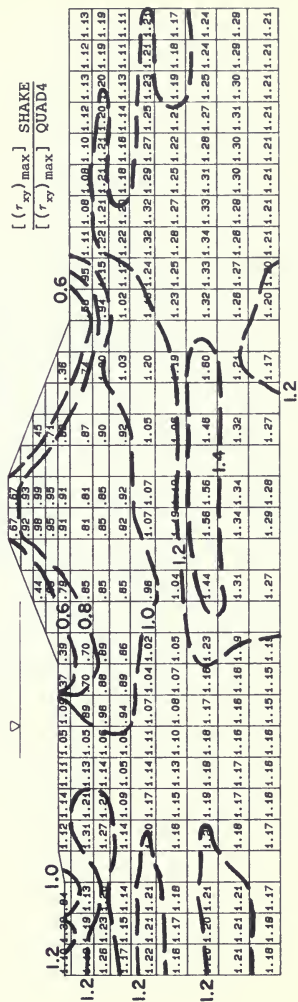



Figure 416. (b) Comparison of Maximum Horizontal Shear Stresses,  $(\tau_{xy})_{\max}$ , Computed by Programs SHAKE and QUAD4 using the Modified El Centro Record—Low Dam



.02	.02	.01	.02	.01
.09	.11	.08	.16	.06
.31	.29	.24	.44	.18
.35	.37	.47	.97	.40
.11	.12	.63	.63	.52
.20	.22	.76	.70	.66
.09	.09	.13	.16	.17
.13	.13	.25	.40	.24
.10	.10	.10	.08	.10
	.14	.17	.16	.15
	.10	.10	.08	.10
				.18
				.08
				.13
				.10

Figure 417. (a) Maximum Shear Strains,  $\gamma_{\max}$  (%), Computed by Program SHAKE using the Oroville Reanalysis Earthquake—Low Dam



.01	.02	.02	.02	.01
.09	.13	.10	.28	.08
.50	.52	.38	.38	.22
.59	.54	.33	.25	.37
.17	.16	.49	.33	.32
.25	.24	.15	.10	.33
.10	.09	.23	.30	.47
.14	.13	.11	.10	.15
.11	.11	.12	.10	.27
			.10	.08
			.18	.15
			.10	.10
				.11
				.01
				.06
				.28
				.50
				.17
				.27
				.11
				.18
				.11

Figure 417. (b) Maximum Shear Strains,  $\gamma_{\max}$  (%), Computed by Program SHAKE using the Modified El Centro Record—Low Dam



Figure 418. (a) Maximum Shear Strains,  $\gamma_{max}$  (%), Computed by Program QUAD4 using the Orville Reanalysis Earthquake—Low Dam



Figure 418. (b) Maximum Shear Strains,  $\gamma_{max}$  (%), Computed by Program QUAD4 using the Modified El Centro Record—Low Dam

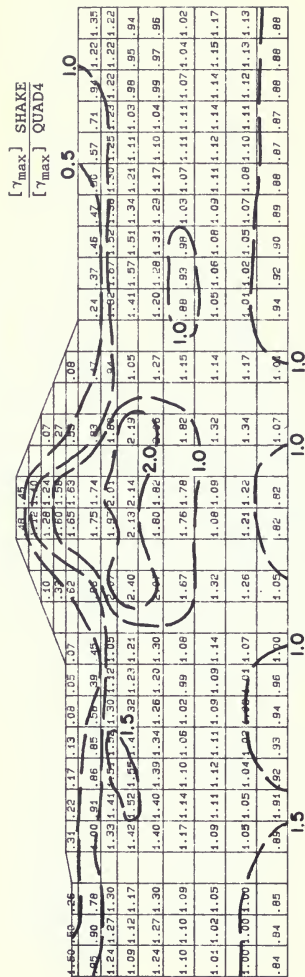


Figure 419. (a) Comparison of Maximum Shear Strains,  $\gamma_{\max}$ , Computed by Programs SHAKE and QUAD4 using the Orville Reanalysis Earthquake—Low Dam

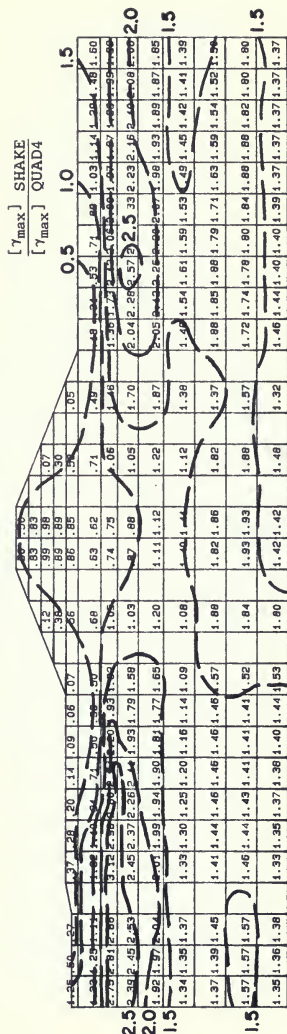


Figure 419. (b) Comparison of Maximum Shear Strains,  $\gamma_{\max}$ , Computed by Programs SHAKE and QUAD4 using the Modified El Centro Record—Low Dam

**ADDENDUM F**

**EXAMINATION OF THE PERFORMANCE OF  
UPPER SAN FERNANDO DAM  
DURING THE EARTHQUAKE OF FEBRUARY 9, 1971**

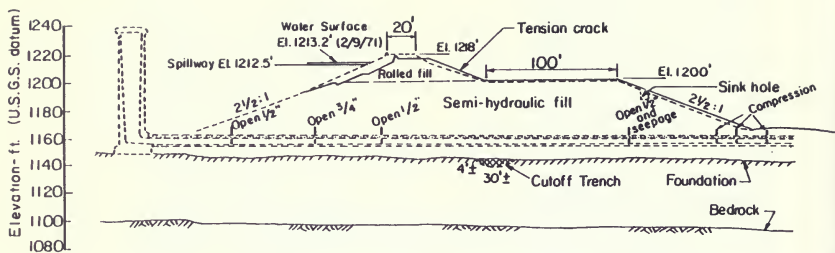


Figure 420. Cross-Section Through Upper San Fernando Dam (after Seed et al., 1973)

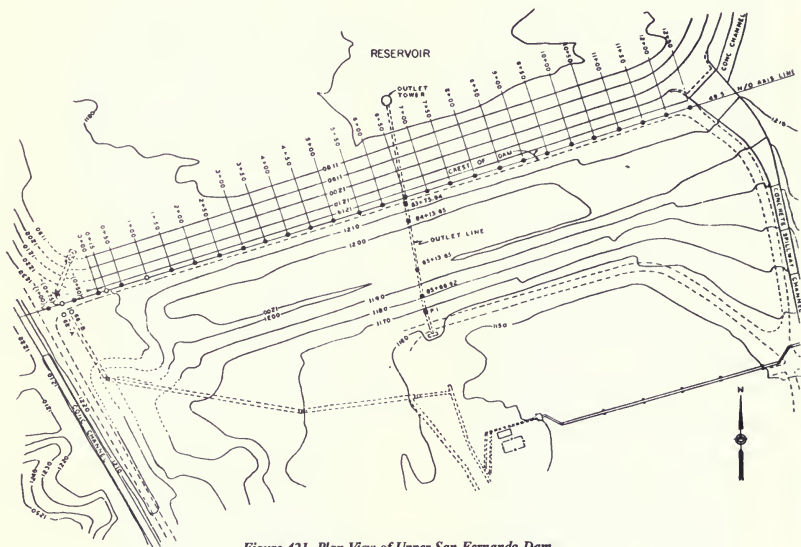


Figure 421. Plan View of Upper San Fernando Dam

## ADDENDUM F

# EXAMINATION OF THE PERFORMANCE OF UPPER SAN FERNANDO DAM DURING THE EARTHQUAKE OF FEBRUARY 9, 1971

### 1. INTRODUCTION

#### Description of Upper San Fernando Dam

Upper San Fernando Dam is a hydraulic fill embankment about 75 feet high with a reservoir capacity of approximately 1,850 acre-feet. The dam is part of the Van Norman Lake Complex, which serves as a water distribution center for the city of Los Angeles.

Construction of the dam began in 1921 using the "semi-hydraulic" fill method. This construction method generally consisted of placing material in dikes at the upstream and downstream toes and spreading the material in between by sluicing it with jets of water. Using this technique, the finer material tended to be deposited in the middle of the dam to form the core, and the coarser material remained near the outer portions of the dam to form the embankment shells. By the end of 1921, the dam was raised to approximately elevation 1200 feet. Although the original design called for adding hydraulic fill up to elevation 1238 feet, this plan was changed. Instead, the dam was completed only to elevation 1218 feet by the addition of an 18-foot-high rolled fill parapet crest section on the upstream side of the dam. A typical cross-section of Upper San Fernando Dam is shown in Figure 420. A plan view of the dam is shown in Figure 421.

#### Earthquake of February 9, 1971

On February 9, 1971, a Magnitude 6.6 earthquake occurred in the San Fernando area. The epicenter was located approximately 6 miles northeast of the Van Norman Dam Complex. Seed et al. (1973) estimated that the maximum rock surface acceleration at the site of the dam was between 0.55 and 0.69g. This same earthquake resulted in a large upstream slide in the Lower San Fernando Dam (see Seed et al., 1973, 1988).

#### Earthquake-Induced Displacements

As a result of the earthquake, the Upper San Fernando Dam developed significant settlements and downstream movements. The downstream movement of the dam led to the development of several longitudinal cracks along the upstream slope of the parapet crest and running nearly the full length of the dam. According to Seed et al. (1973), the upstream cracks appeared to be multiple shear scarps. There was no embankment breach resulting in the loss of water from the reservoir.

Figure 422 shows settlement measurements made before and after the earthquake for stations along the crest. Similarly, Figure 423 shows horizontal measurements made before and after the earthquake for the same stations. These figures indicate a maximum earthquake-induced settlement of 3.2 feet together with a maximum horizontal movement of 5.0 feet downstream for monuments along the crest.

For the monuments set on the embankment crest, the pattern of earthquake-induced settlements matches relatively well the height of the hydraulic fill. However, the downstream movements reflect a simple uniform bowing out of the fill irrespective of its height.

Figure 424 shows settlement of the embankment surface downstream of the crest along the outlet line. Except for Outlet Station 84 + 13.95, located above the clayey central core material, settlement decreases with distance from the crest, from approximately 3 feet at the crest to approximately 0 at Station P.I. This trend also reflects hydraulic fill height since the height of the fill decreases past Outlet Station 85 + 14. These same monuments indicated horizontal movements as much as 7 feet downstream.

# UPPER SAN FERNANDO DAM

Settlement Records before and after EQ

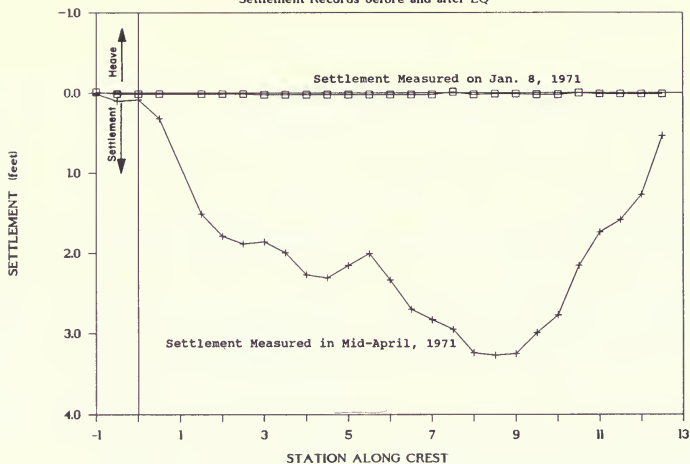


Figure 422. Upper San Fernando Dam—Settlement Records Before and After Earthquake

# UPPER SAN FERNANDO DAM

Horiz. Offset before and after EQ

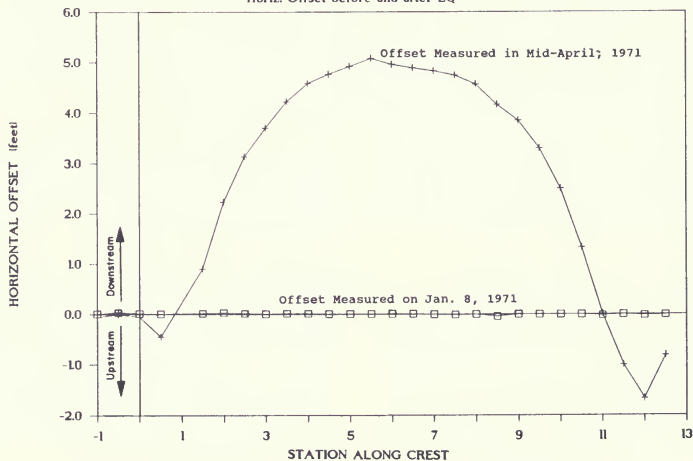


Figure 423. Upper San Fernando Dam—Horizontal Offset Before and After Earthquake



# UPPER SAN FERNANDO DAM

Settlement Records before and after EQ

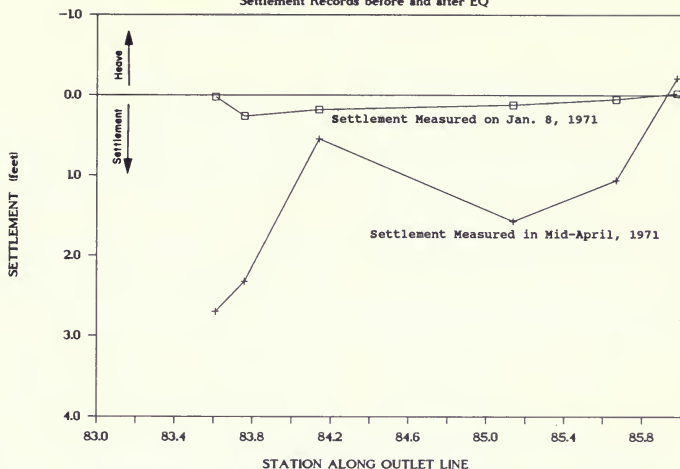


Figure 424. Upper San Fernando Dam—Settlement Records Before and After Earthquake

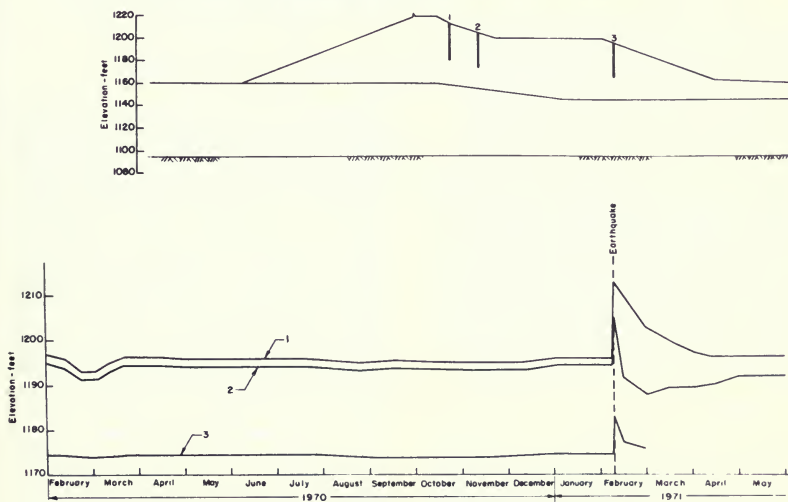


Figure 425. Recorded Pore Pressures—Upper San Fernando Dam (adapted from Seed et al., 1973)

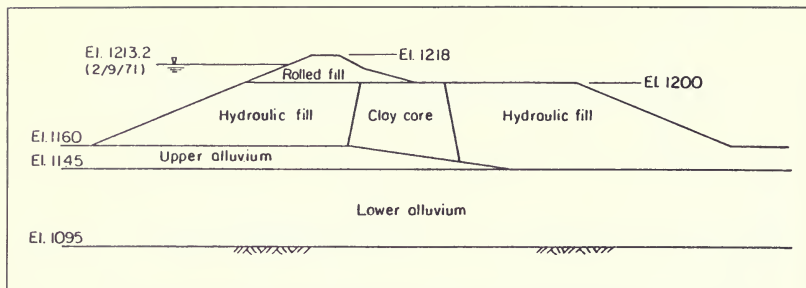


Figure 426. Idealized Cross-Section Through Upper San Fernando Dam (after Serff et al., 1976)

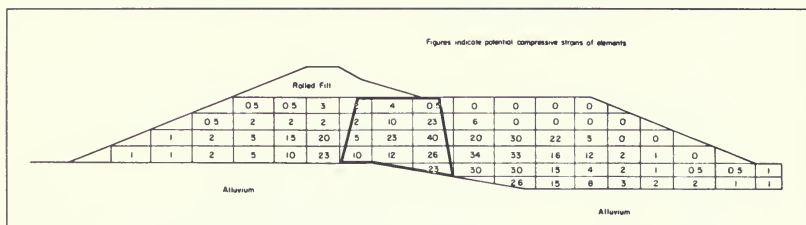


Figure 427. Strain Potential in Hydraulic Fill—Upper San Fernando Dam (after Seed et al., 1973)

## Earthquake-Induced Pore Pressure Changes

Figure 425 (after Seed et al., 1973) shows locations and recorded pore pressures measured in three standpipe piezometers. During the earthquake, water flowed out the tops of Piezometers 1 and 2 and, consequently, the actual maximum values could not be measured. However, the maximum recorded changes in pressure were at least 17 feet and 12 feet, respectively, for Piezometers 1 and 2. Evidence that liquefaction developed in the embankment is also indicated by several sand boils that formed in fill placed beyond the downstream toe.

## 1973 Liquefaction Evaluation

The significant deformations and pore pressures measured after the earthquake, together with the development of sand boils near the toe of the dam, indicated that some amount of earthquake-induced liquefaction was

triggered in the dam. To investigate this behavior, a comprehensive liquefaction evaluation was performed by Seed et al. (1973). The results of these analyses are described fully by Seed et al. (1973) and Serff et al. (1976).

Figure 426 shows the idealized model used in the 1973 evaluations. Figure 427 presents zones of compressive strain potential predicted by the evaluations. Complete liquefaction, as evidenced by the development of 100% pore water pressure increase, would be expected for compressive strain potentials greater than about 3 to 5 percent. Figure 427 shows that significant zones of liquefaction would be predicted within the bottom half of the hydraulic fill. This appears to be in relatively good accord with the behavior observed. Although large compressive strain potentials are shown within the heavy lines denoting the approximate boundaries of the clayey core, it is not clear if the bulk of the core zone actually liquefied since the material in this zone is predominantly clayey.

## 2. 1971 POST-EARTHQUAKE DRILLING EXPLORATIONS

### Introduction

Following the 1971 earthquake, the California Department of Water Resources conducted a field and laboratory exploration program in both the Upper and Lower San Fernando Dams. The field explorations were conducted principally during April and May 1971.

Table 65 summarizes information concerning the boreholes drilled after the earthquake at Upper San Fernando Dam. Figures 428 and 429 present plan and profile sections showing the boring locations.

As reported in the Seed et al. (1973) studies, the 1971 field explorations indicated that the soils within the hydraulic fill ranged from coarse sands to clays, generally grading from coarse to fine soils moving from the slope surface towards the central core. Figure 430 shows the range of grain size curves for the sandy and silty soils found in the outer shell zones within the hydraulic fill.

### Standard Penetration Testing

#### SPT Test Procedures

Standard Penetration Testing (SPT) was performed in the dam after the earthquake by the California Department of Water Resources. The drilling was performed in April and May 1971, approximately 2 to 3 months after the February 9, 1971 earthquake. The SPT tests were performed in mud-filled boreholes, which were drilled with a 5.6-inch tricone drill bit. The SPT split-spoons used had 2.0-inch O.D.'s and 1.38-inch I.D.'s at the shoe. However, it is believed that the barrel I.D.'s above the shoe were 1.5 inches in order to make space for liners, but that no liners were used. It is also believed that the samplers were driven into the soil using 140-lb. safety hammers raised and released with a 2-wrap rope and cathead technique.

#### Procedural and Overburden Corrections to Measured SPT Blowcount

Recent SPT correlations with liquefaction resistance and residual strength have been presented in terms of a cor-

rected SPT blowcount,  $(N_1)_{60}$ . The corrected blowcount represents the value that would be obtained in a soil under a level ground overburden pressure of 1 tsf. It also represents the value that would be obtained using a SPT hammer that delivers to the drill rods an impact energy equal to 60 percent of the theoretical free-fall energy of a 140-lb. weight falling 30 inches. Further, this standardized blowcount also represents a test result using a 2.0-inch O.D. sampler with a constant I.D. of 1.38 inches. Because the SPT tests conducted at Upper San Fernando Dam in 1971 were performed using somewhat different test procedures and conditions, it is necessary to correct the measured blowcounts to obtain equivalent  $(N_1)_{60}$  values. The following corrections were made to the Upper San Fernando Dam SPT data:

1. Because 140-lb. safety hammers used with a 2-wrap rope and cathead release deliver average energies of about 60 percent of the theoretical value to the drill rods, no correction was made for energy.
2. Because the SPT sampler used was believed to have a 1.5-inch barrel I.D. (i.e. space for liners but no liners used), the measured blowcounts were increased as suggested by Seed et al. (1985). The amount of increase varied with the value of the blowcount with blowcounts of about 10, with a 10 percent correction, and blowcounts of 40 or more with a 35 percent correction.
3. To correct for the different overburden pressures which exist at different testing depths, a correction factor, denoted as  $C_N$ , was used. The values of  $C_N$  used for the overburden correction were those suggested by Seed et al. (1983) for moderately dense soils ( $D_r = 40$  to 60 percent). Because borings A-1, A-4, B-1, B-4, B-5, C-1, C-4, and C-5 were drilled in sloping ground, the vertical overburden pressure was increased by 15 percent to account for increased lateral stresses.

#### Corrected Post-Earthquake SPT Blowcounts

Figure 431 presents corrected  $(N_1)_{60}$  blowcounts as a function of test elevation for all 1971 SPT tests performed at Upper San Fernando Dam, save for those conducted in

Table 65. Summary of 1971 Drilling Explorations at Upper San Fernando Dam

Borehole	Station	Horizontal Offset— from Axis <sup>1</sup>	Surface Elevation (feet)	Maximum Depth (feet)	No. of SPT Tests
A-1	3+80	80' u/s	1205.4	105.0	13
A-2	3+87	50' u/s	1216.2	127.9	20
A-3	3+67	16' d/s	1199.8	120.3	18
A-4	3+73	90' d/s	1199.8	111.5	14
B-1	7+46	83' u/s	1205.6	115.0	13
B-2	7+42	50' u/s	1215.2	130.0	15
B-3	7+50	15' d/s	1199.1	121.5	15
B-4	7+69	102' d/s	1198.7	115.9	18
B-5	7+67	185' d/s	1169.5	87.5	14
B-6	7+57	271' d/s	1148.8	67.9	7
C-1	9+42	84' u/s	1206.2	121.0	17
C-2	9+43	50' u/s	1215.8	140.0	11
C-3	9+43	15' u/s	1201.1	100.8	13
C-4	9+17	101' d/s	1198.8	115.0	11
C-5	9+71	162' d/s	1177.6	88.4	13
C-6	9+73	280' d/s	1149.0	83.9	11
C-7	9+80	474' d/s	1144.1	73.5	8
L-1	(drilled in slide area E/o Reservoir—not used)				
L-2	(drilled in Powerhouse Tailbay—not used)				

<sup>1</sup> Offset is measured from original axis-line. (The original axis line is 49.5 feet d/s of crest centerline)

Boreholes A-3, B-3, and C-3. These three boreholes were located in the central core section which consists of predominantly clayey soils, generally not thought to be liquefiable. The hollow symbols in Figure 431 indicate that the blowcount, despite being performed outside of the core, was obtained in predominantly clayey soil. Small symbols indicate that the borehole location is upstream of the central core, large symbols indicate that the borehole location is downstream of the clay core, and asterisks next to symbols denote that the material contains gravel. No significant difference is observed in the blowcount data obtained upstream versus downstream of the core.

Figure 431 indicates that the upper half of the hydraulic fill has somewhat lower blowcounts than the lower half and that blowcounts increase sharply as the soil tested changes from the fill to the alluvial foundation. Figure 432 shows mean and median values in the upper, middle,

and lower intervals of the hydraulic fill for the non-clayey soils (i.e. solid symbols only). These mean and median values are also presented in Table 66, along with blowcount values for intervals above and below the hydraulic fill.

#### Average Pre-Earthquake SPT Blowcount

The blowcount data summarized in Table 66 were taken after the February 1971 earthquake. The density of the soil was probably changed by the earthquake as evidenced by settlement records. Consequently, the blowcounts shown above need to be reduced in order to obtain the pre-earthquake blowcount values.

If it is assumed that horizontal movements were caused by shearing and that lateral strains are small, then the volu-

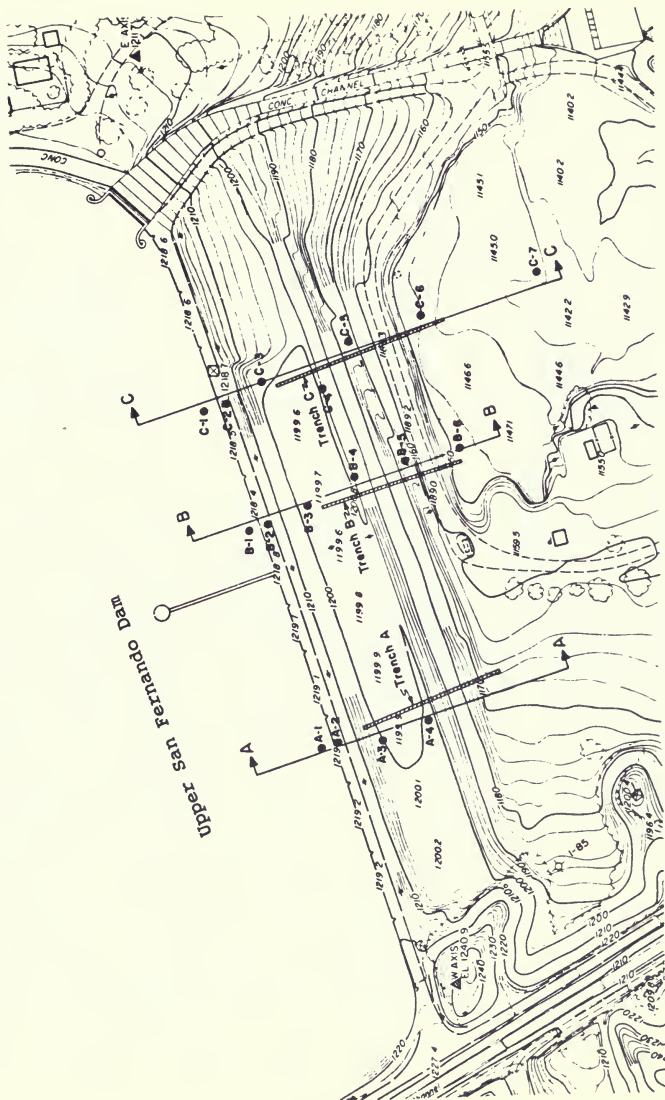


Figure 428. 1971 Borehole Locations at Upper San Fernando Dam—Plan View (after Seed et al., 1973)

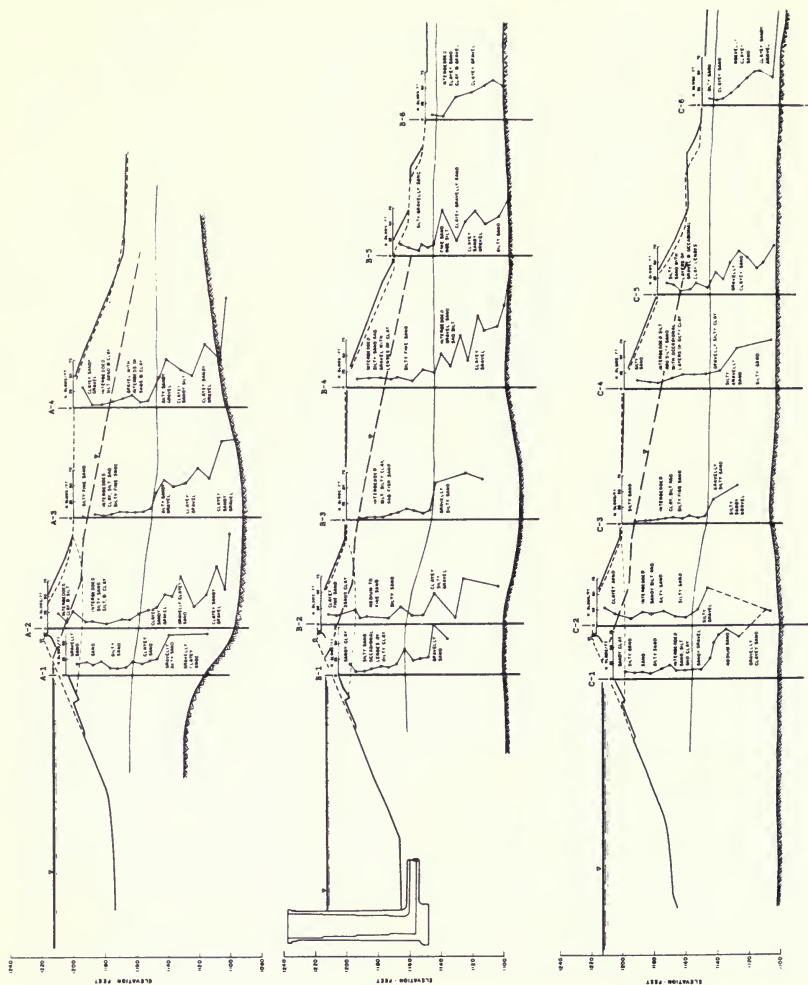


Figure 429. 1971 Borehole Locations at Upper San Fernando Dam—Profile Views (after Seed et al., 1973)

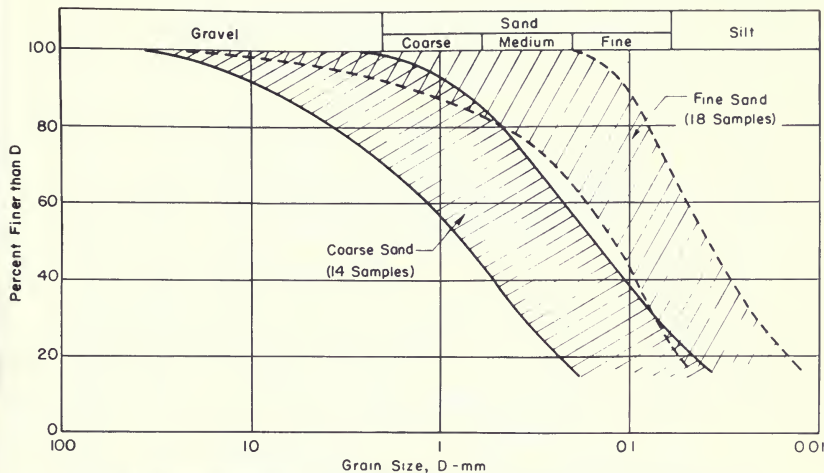


Figure 430. Ranges of Grain Size Distribution Curves for Sand, Hydraulic Fill (after Seed, et al., 1973)

metric strain in the cohesionless shell zones can be determined by calculating values of vertical strain in the hydraulic fill. Table 67 summarizes the vertical strain computations.

The data presented in Table 67 show that the average vertical strain along the crest in the vicinity of the 1971 boreholes is approximately 5.7 percent. It should be noted that the strains computed along the crest may be too high because the calculations ignore the possibility that some of the measured settlements could have occurred in the rolled fill. The data in Table 67 also show that the average vertical strain in the vicinity of the boreholes downstream of the crest is about 3.1 percent (excluding Station 84 + 13.95 above the clayey core). The overall average vertical strain in both areas is about 4.6 percent. In light of these results, a reasonable average post-earthquake volumetric strain in the hydraulic fill would be approximately 4.5 percent.

For the silty sand material that constitutes the principal portions in the shell zones within Upper San Fernando Dam, the range between maximum and minimum dry densities was found to be about 36 pcf (see Seed et al., 1973). The average post-earthquake relative density was also determined to be about 54 percent, corresponding to a void ratio of approximately 0.75. Using the above parameters, together with a post-earthquake volumetric strain of 4.5 percent, results in a void ratio change of approximately 0.08. This void ratio change corresponds to a relative density change of about 12 percent, say, from 42 percent prior to the earthquake to about 54 percent after the earthquake.

Studies by Skempton (1986) and by Marcuson and Bieganousky (1977) indicate that such a change in relative density corresponds to a change in blowcount value of about 4 to 5 blows per foot. Accordingly, pre-earthquake blowcounts in the hydraulic fill can be estimated by subtracting 4.5 blows from the measured post-earthquake values as performed in Table 68.



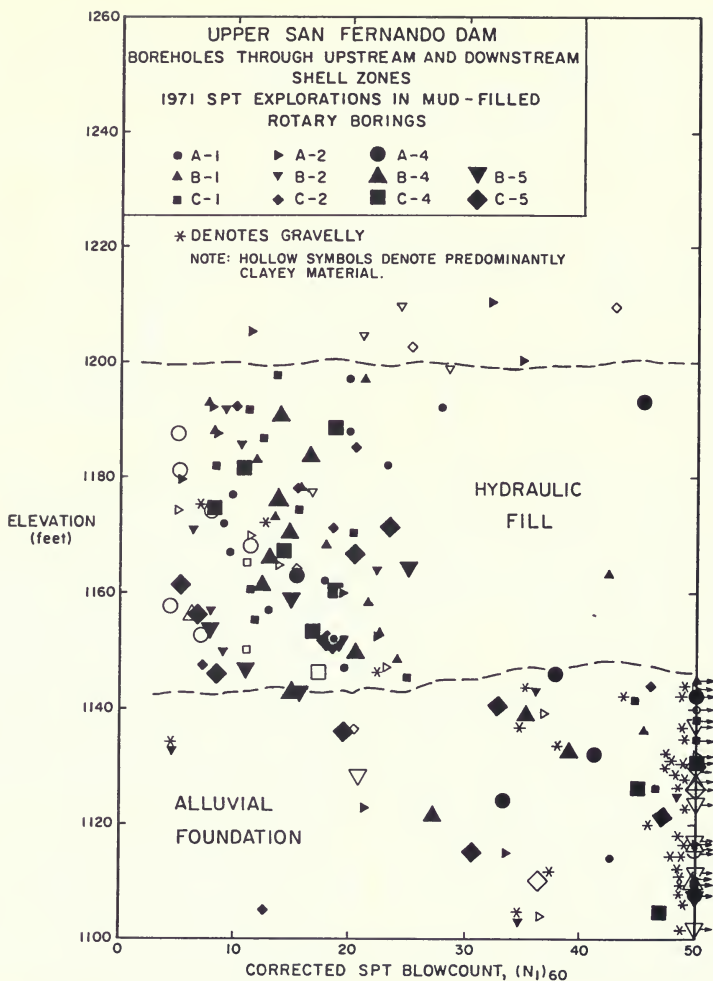


Figure 431. Corrected SPT Blowcounts for Boreholes Drilled through the Upstream and Downstream Shell Zones of Upper San Fernando Dam



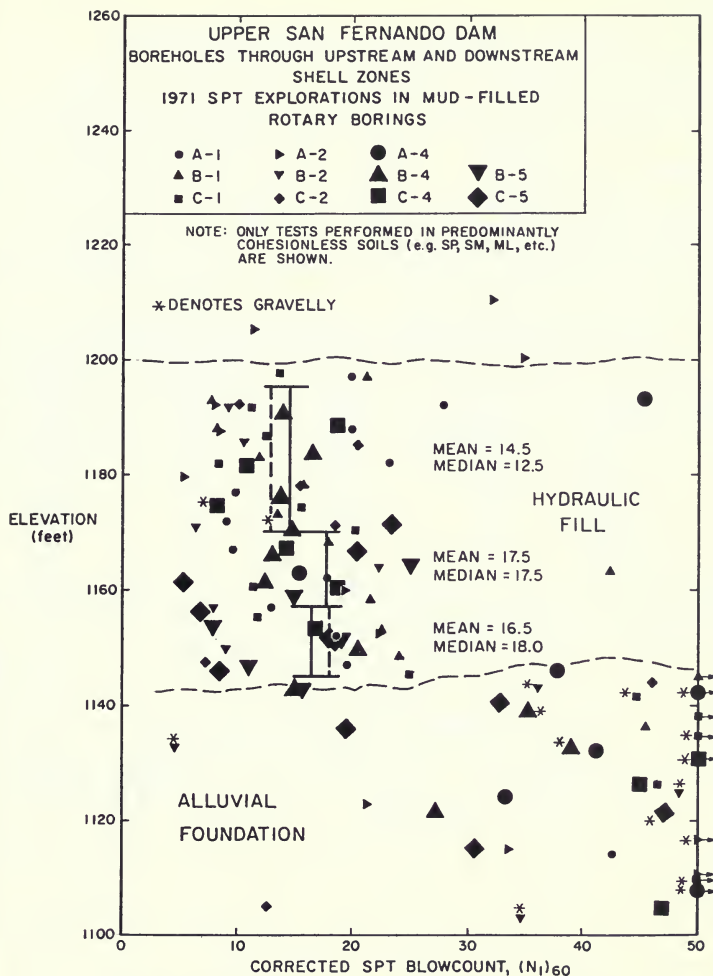


Figure 432. Mean and Median Corrected SPT Blowcount Values for Layers of Hydraulic Fill in Upper San Fernando Dam (Non-Clayey Soils only)

Table 66. 1971 Post-Earthquake SPT Blowcount Data (Non-Clayey Soils)

Material	Elevation (feet)	Mean ( $N_1$ ) <sub>60</sub> , 1971 Data	Median ( $N_1$ ) <sub>60</sub> , 1971 Data	No. of Tests
Rolled Fill	1195-1215	22.0	20.5	6
Hydraulic Fill	1170-1195	14.5	12.5	34
Hydraulic Fill	1157-1170	17.5	17.5	17
Hydraulic Fill	1145-1157	16.5	18.0	21
Alluvium/Sedimentary Rock	1090-1145	43.5	43.5	34

Table 67. Computations of Earthquake-Induced Vertical Strains in Hydraulic Fill

Borehole	Station <sup>1</sup>	Location	Settlement (feet)	Hydraulic Fill Thickness (feet)	Vertical Strain (%)
A-2	3+80	Crest	2.18	45	4.8
B-2	7+42	Crest	2.94	48.5	6.1
C-5	9+43	Crest	3.01	48.5	6.2
—	6+50	Crest	2.68	48.5	5.5
—	83+75.94◆	D/S	2.07	50	4.1
—	84+13.95◆	D/S	0.37	53	0.7*
—	85+13.85◆	D/S	1.45	57	2.5
—	85+16.92◆	D/S	1.01	38.5	2.6

<sup>1</sup> Stations with a ◆ symbol are measured along the outlet line. All other stations are measured along the crest (see Figure 421).

\*Denotes this monument is located above the clay core.

Table 68. Determination of Average Pre-Earthquake SPT Blowcounts in the Hydraulic Fill of Upper San Fernando Dam

Elevation Interval (feet)	Average Post-EQ SPT Blowcount ( $N_1$ ) <sub>60</sub>	Blowcount Change	Estimated Average Pre-EQ SPT Blowcount ( $N_1$ ) <sub>60</sub>
1170-1195	≈ 13.5	-4.5	≈ 9
1157-1170	≈ 17.5	-4.5	≈ 13
1145-1157	≈ 17.5	-4.5	≈ 13

### 3. POST-EARTHQUAKE SLOPE STABILITY ANALYSES

#### General

Post-earthquake slope stability analyses were performed to develop an estimate of the residual shear strength,  $S_r$ , of the hydraulic fill following liquefaction. The basic approach was to assume trial values of  $S_r$  within the liquefied zones and determine factors of safety against downstream sliding. The estimated value of  $S_r$  would be that value which produced a factor of safety of unity, corresponding to being barely stable.

Although the fill did develop significant lateral movement and the appearance of slide scarps near the upstream edge of the parapet crest, the movements were limited and failure of the dam did not develop. Consequently, the conditions following the earthquake correspond to a factor of safety somewhat higher than unity. Thus, back-calculations assuming a factor of safety of unity underestimate the true residual strength by some

amount. However, because the lateral movements of between 5 and 7 feet correspond to shear strains of at least 11 to 16 percent, the level of conservatism is probably low.

#### Stability Model and Parameters

The model used for the post-earthquake stability analyses was developed from the 1971 borehole information and results of the liquefaction evaluation conducted by Seed et al. (see Figure 427). Figure 433 shows the slope stability model divided into different soil zones. The properties used to model the different zones are summarized in Table 69.

The post-earthquake shear strengths of the various soil were developed using the following assumptions:

**Rolled Fill (Zone I):** The rolled fill within the parapet crest was found to have sustained extensive cracking. Consequently, this zone was assigned zero cohesive

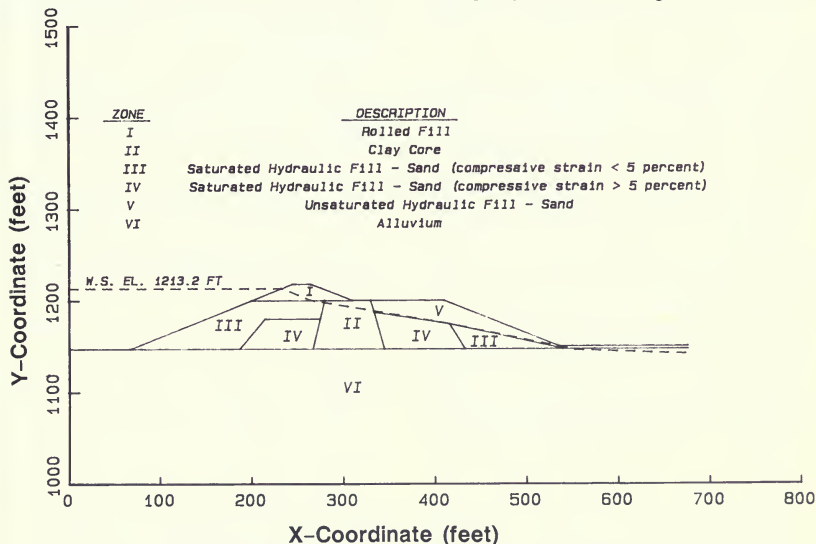


Figure 433. Post-Earthquake Stability Model—Upper San Fernando Dam

**Table 69. Soil Properties Assumed in Post-Earthquake Slope Stability Analyses  
of Upper San Fernando Dam**

Zone	Material	Density (pcf)	Strength	
			Cohesion (psf)	Friction Angle (degrees)
I	Rolled Fill	130	0	30
II	Central Clayey Core			
	Hydraulic Fill	122	600	0
III	Partially Liquefied	122 (a)	0	20.6
	Hydraulic Fill—Sand <sup>1</sup>	122 (b)	$S_r$	0
IV	Liquefied Hydraulic Fill—Sand <sup>2</sup>	122	$S_r$	0
V	Unsaturated Hydraulic Fill—Sand	122	0	37
VI	Alluvium	129	0	37

<sup>1</sup>Saturated, Compressive Strain Potential < 5 percent

<sup>2</sup>Saturated, Compressive Strain Potential > 5 percent

strength and a friction angle of 30 degrees reflective of this condition.

**Saturated Clay Core (Zone II):** This zone was assigned an undrained shear strength of 600 psf, which was developed from the numerous torvane test performed by Seed et al. (1973) on tube samples of clayey fill (see Figure 434).

**Partially-Liquefied Hydraulic Fill (Zone III):** The saturated portions of the hydraulic fill with compressive strain potentials of less than 5 percent were not considered to have developed complete liquefaction. Nevertheless, some amount of excess pore pressure and/or strength losses were undoubtedly sustained in these zones. To account for this strength loss, the slope stability analyses were performed with two different strength assumptions. The first assumption was that the strength in this material was equal to half of the drained strength. The second assumption was that this material had a strength equal to the residual shear strength in the completely liquefied zone.

**Liquefied Hydraulic Fill (Zone IV):** The saturated portions of the hydraulic fill with compressive strain potentials of 5 percent or more were assumed to have completely liquefied and to exhibit only a residual shear

strength. Different trial values of residual shear strength were assumed to obtain a range of calculated factors of safety against sliding.

**Unsaturated Hydraulic Fill (Zone V):** The full drained strength ( $\phi = 37$  degrees) as determined by Seed et al. (1973) was assigned to the unsaturated hydraulic fill soils.

**Foundation Alluvium (Zone VI):** The foundation alluvium was determined to have very high SPT resistance. This material would be expected to retain its full static strength following the earthquake. Accordingly, this material was conservatively assigned a friction angle of 37 degrees with no cohesion intercept.

### Determination of Residual Shear Strength

Slope stability analyses were computed using an IBM PC version of computer program STABL, which employed the Modified Bishop Method. Figure 435 presents factors of safety determined as a function of the residual shear strength assumed for the liquefied zones. Curves were plotted for the two different strengths assumed for the partially-liquefied hydraulic fill (Zone III). Based on Figure 435, the residual strength of the liquefied soil (i.e. Zone IV) required for stability (F.S. = 1.0) would have to be between 500 and 700 psf, depending on the strength



# Upper San Fernando Dam

## Downstream Stability Summary

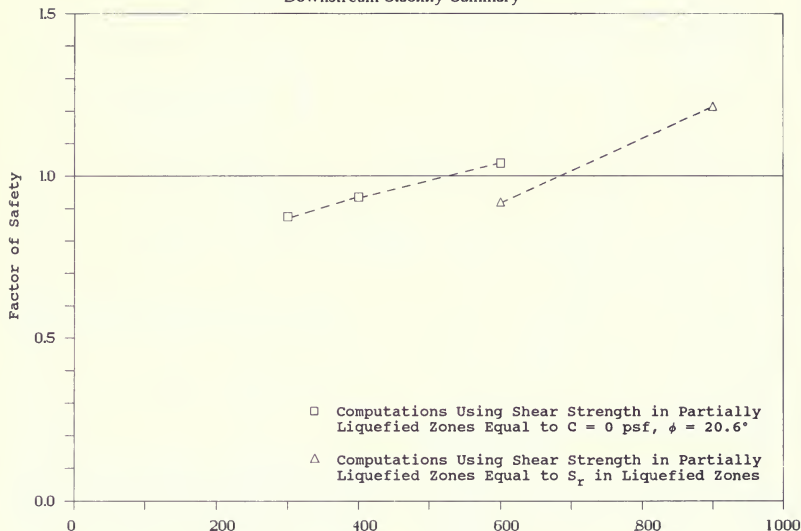


Figure 435. Residual Shear Strength in Liquefied Zone,  $S_r$  (psf)

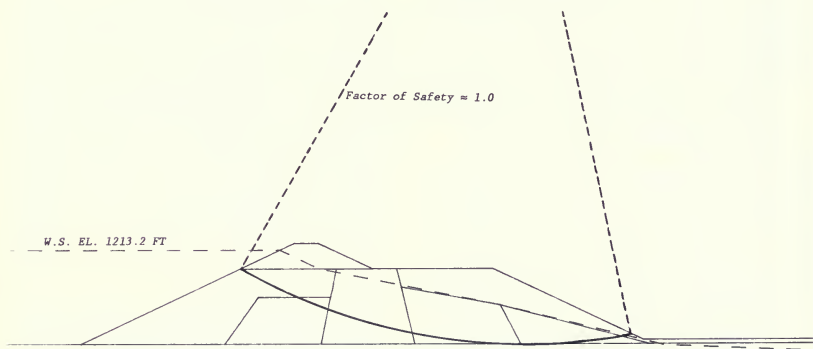


Figure 436. Upper San Fernando Dam, Post-EQ Stability Analysis—Location of Critical Failure Surfaces

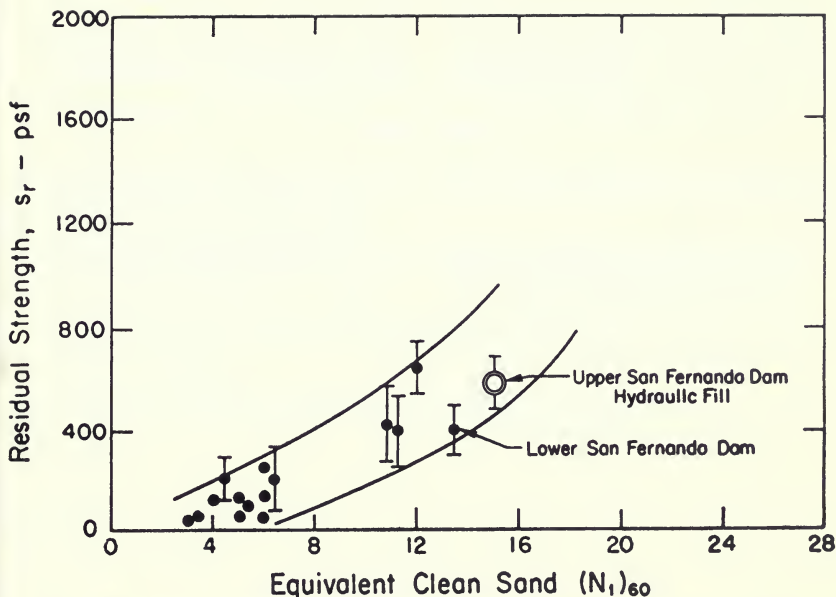


Figure 437. Relationship Between Residual Strength and Equivalent Clean Sand Value of  $(N_1)_{60}$  (after Seed et al., 1988)

assumed to model Zone III. The minimum residual shear strength for the liquefied soil, therefore, is approximately 600 psf.

Figure 436 shows the location of the critical failure surfaces.

#### Comparison of Estimates of Residual Strength for Upper San Fernando Dam with Correlation Developed By Seed et al. (1988)

The previous sections estimated the undrained residual shear strength for the liquefied silty sand hydraulic fill of Upper San Fernando Dam to be approximately 600 psf. The corrected pre-earthquake SPT blowcount for the

lower elevations through which sliding would take place was estimated to be approximately 13.

Presented in Figure 437 is the correlation between equivalent clean sand SPT blowcount and residual strength suggested by Seed et al. (1988). To correct silty sand blowcounts to clean sand blowcounts, Seed (1987) suggests increasing the actual  $(N_1)_{60}$  blowcounts by small increments depending on the fines content. For an average fines content of approximately 25 percent (see Figure 430), the blowcount increment is 2 blows per foot. This would make the equivalent clean sand pre-earthquake blowcount in the hydraulic fill shell zones equal to approximately 15.

Figure 437 shows that the estimated residual strength for the Upper San Fernando Dam hydraulic fill falls near the lower bound of the values suggested by the Seed et al. (1988) correlation. As noted previously, this result contains some degree of conservatism due to the fact that the

Upper San Fernando Dam did not fail. However, this amount of conservatism is expected to be small in light of the deformations sustained and the good agreement between this result and the results determined for Lower San Fernando Dam.

#### 4. CONCLUSIONS

The work presented above leads to the following determinations:

1. The pre-earthquake SPT blowcounts that would have been measured in the silty sand comprising the hydraulic fill of the Upper San Fernando Dam would average between 9 and 13 blows per foot.

2. The residual shear strength of the liquefied portions of the hydraulic fill was estimated to be between 500 and 700 psf, which is in good accord with the lower bound values suggested by Seed et al. (1988). This result is also in good accord with the values determined for the similar soils in Lower San Fernando Dam.



## REFERENCES

1. Marcuson, W. F., III and Bieganousky, W. A. (1977) "Laboratory Standard Penetration Tests on Fine Sands," *Journal of the Geotechnical Engineering Division*, ASCE, Vol. 103, No. GT6, June, 1977.
2. Seed H. Bolton, Idriss, I. M., and Arango, Ignacio (1983) "Evaluation of Liquefaction Potential Using Field Performance Data," *Journal of the Geotechnical Engineering Division*, ASCE, Vol. 109, No. GT3, March, 1983.
3. Seed, H. Bolton, Lee, K. L., Idriss, I. M. and Makdisi, F. (1973) "Analysis of the Slides in the San Fernando Dams During the Earthquake of Feb. 9, 1971," Report No. EERC 73-2, Earthquake Engineering Research Center, University of California, Berkeley, June 1973.
4. Seed, H. Bolton, Seed, Raymond B., Harder, L. F., and Jong, Hsing-Ling (1988) "Re-evaluation of the Slide in the Lower San Fernando Dam in the Earthquake of Feb. 9, 1971," Earthquake Engineering Research Center, University of California, Berkeley.
5. Serff, Norman, Seed, H. Bolton, Makdisi, F. I., and Chang, C.-Y. (1976) "Earthquake Induced Deformations of Earth Dams," Report No. EERC 76-4, Earthquake Engineering Research Center, University of California, Berkeley, September, 1976.
6. Skempton, A. W. (1986) "Standard Penetration Test Procedures and the Effects of Overburden Pressure, Relative Density, Particle Size, Ageing and Overconsolidation," *Geotechnique*, Vol. 36, No. 3, 1986.

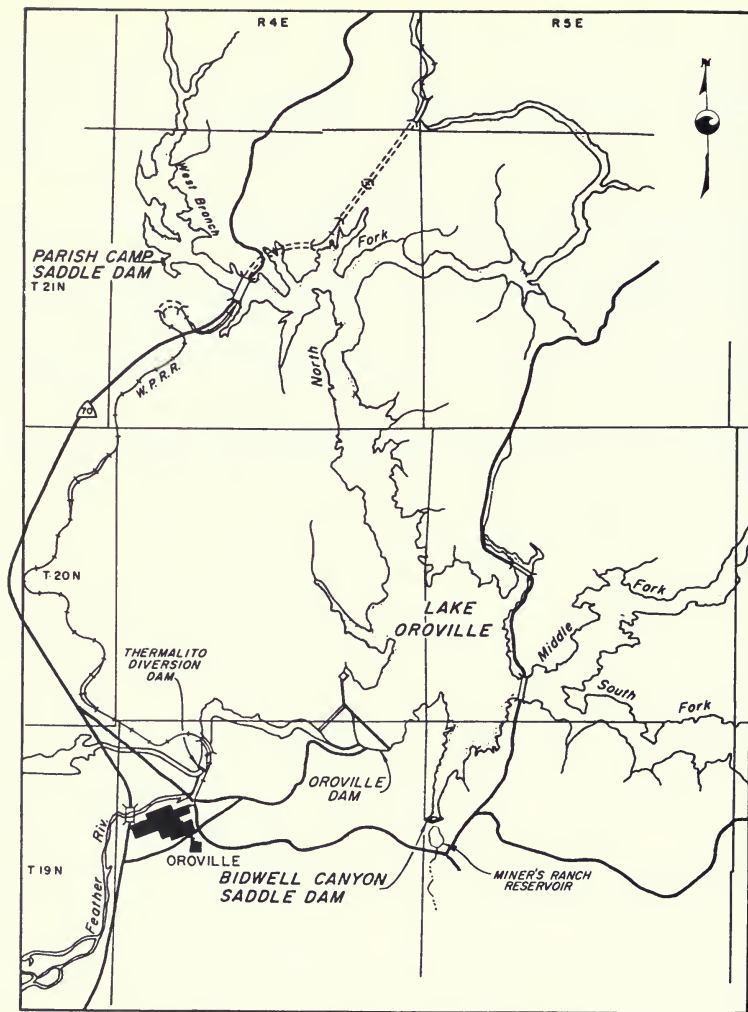


Figure 438. Vicinity Map—Bidwell Canyon and Parish Camp Saddle Dams

# CHAPTER VI. SEISMIC EVALUATION OF BIDWELL CANYON AND PARISH CAMP SADDLE DAMS AND EFFECTS OF POSSIBLE FAULT MOVEMENTS IN OROVILLE PROJECT DAM FOUNDATIONS

## 1. EXECUTIVE SUMMARY

### Conclusions

1. Bidwell Canyon Saddle Dam and Parish Camp Saddle Dam would perform satisfactorily during earthquake shaking as severe as the Oroville Reanalysis Earthquake ( $a_{max} = 0.6g$ ).
2. All of the Oroville Project Dams would perform satisfactorily if the postulated fault offsets in their foundations were to occur.

### Background

Bidwell Canyon and Parish Camp Saddle Dams are small embankments that help retain Oroville reservoir at high

elevations (see Figure 438). Detailed analytical studies were deemed unnecessary and, therefore, were not carried out for these two structures.

Prior to the 1975 Oroville Earthquake ( $M_L = 5.7$ ), the possibility of fault movement was considered nil in the foundations of the Oroville Project Dams. However, since ground cracking was associated with the 1975 earthquakes, the question of foundation fault movements has been reconsidered. This subject, together with the evaluation of Parish Camp and Bidwell Canyon Saddle Dams, is addressed in more detail in the following sections.

## 2. SEISMIC EVALUATION OF PARISH CAMP SADDLE DAM

Parish Camp Saddle Dam is located on the West Branch arm of Oroville Reservoir approximately 12 miles north of Oroville Dam (see Figure 438). At Parish Camp Saddle Dam, the lowest original ground elevation is at Elevation 900 feet, the same elevation as the maximum operating pool of the reservoir. Therefore, the dam retains water only during rare intervals when flood operations raise the reservoir above this level. Throughout its 20-year history of operation, Oroville Reservoir has never exceeded Elevation 900 feet.

Parish Camp Saddle Dam has a maximum height of 27 feet and a crest length of 270 feet, and is constructed of compacted, clayey soils. The foundation consists generally of moderately weathered to decomposed phyllite, together with a small portion of relatively dense metavol-

canic rock on the left abutment. The weathered phyllite has a fairly high clay content. Dams built of and on similar materials have performed well during strong earthquake shaking without exhibiting significant strength losses. Further examination of the performance of dams composed of similar materials and exposed to similar levels of earthquake shaking show that the maximum permanent deformation that might be induced in the Parish Camp embankment after a magnitude 6.5 earthquake would be between 1 and 6 inches in any direction (see Seed et al., 1978; Tepel et al., 1984).

In light of the large freeboard and good stable materials present at this dam, this dam would be expected to perform satisfactorily for virtually any level of earthquake shaking.

### 3. SEISMIC EVALUATION OF BIDWELL CANYON SADDLE DAM

#### General

Bidwell Canyon Saddle Dam is located at the head of the Bidwell Canyon arm of the reservoir approximately 1.5 miles southeast of Oroville Dam (see Figure 438). The upstream slope (north side) contains Oroville Reservoir with a normal pool at Elevation 900 feet while the downstream slope (south side) holds the Miners' Ranch Reservoir with a maximum pool at Elevation 888 feet. In its 20-year history, the surface of Oroville Reservoir has never exceeded Elevation 900 feet. The plan and profile are shown in Figure 439.

#### Embankment

Bidwell Canyon Saddle Dam consists of two separate embankments: the Main Dam section is on the east and the West Dam section is on the west (Figure 439). The Main Dam was constructed on top of the existing Miners' Ranch Dike, which was completed in 1962. The combined height is 47 feet above the low point of the saddle. The West Dam meets the Main Dam at a knoll in the middle of Bidwell Bar Saddle and is only 24 feet above the lowest ground elevation in the west saddle (Figure 440).

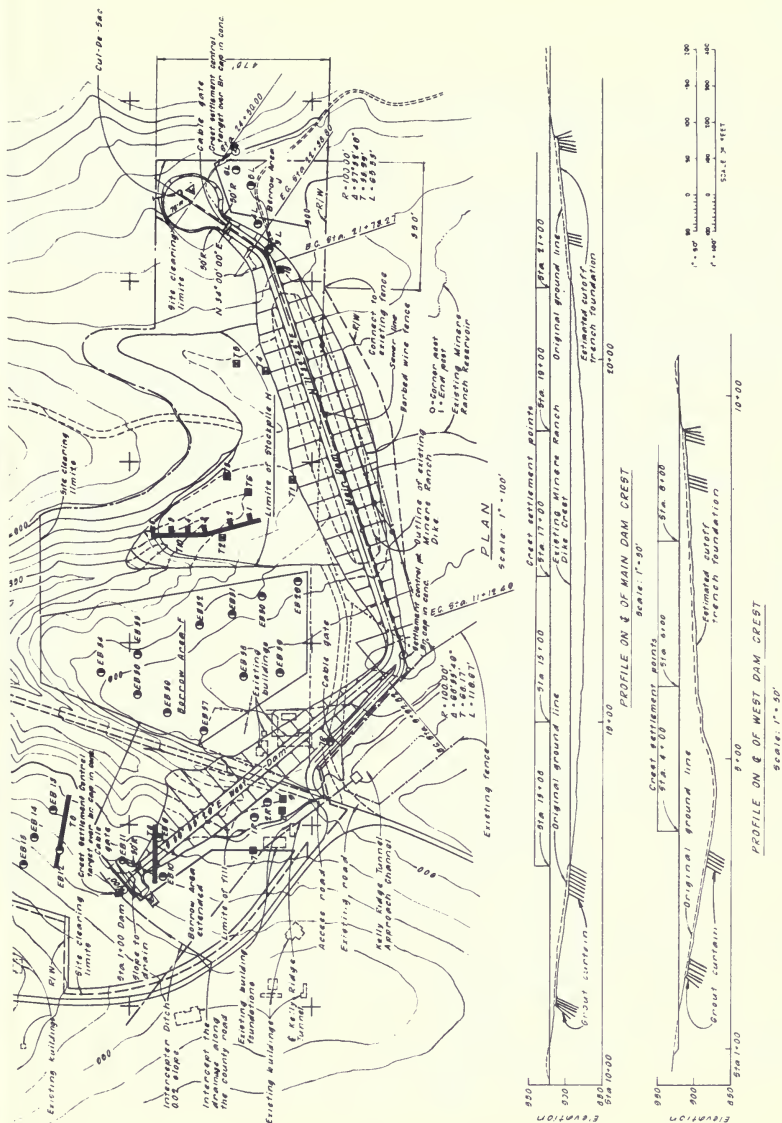
The Main Dam was built as a zoned embankment matching the existing Miners' Ranch Dike zoning, which has a central core of clayey, gravelly sand (Zone 1B), flanked by Zone 2B sand/gravel transition zones and Zone 3B sandy gravel shells. A stockpile of clean cobbles was left on the upstream side of the dike to serve as the toe for Bidwell Canyon Main Dam.

The West Dam has a Zone 1B core of clayey, gravelly sand flanked by Zone 1B/S "shell" zones of clayey gravel and an upstream Zone 2B transition and Zone 3B sandy gravel layer. In essence, it is a protected homogeneous dam. A 1.5-foot-thick drainage blanket within the downstream section at Elevation 895 feet contains an 8-inch perforated collector pipe that drains into Miners' Ranch Reservoir through an 8-inch pipe.

Impervious borrow for the inner core, Zone 1B, was strongly weathered, decomposed amphibolite (sandy clay to clayey sand). The outer core Zone 1B/S came from the same borrow source, but it was the deeper and slightly less weathered material with a higher rock content, and classified as clayey sand to clayey gravel. Table 70 presents the level of compaction achieved during construction.

Table 70. As-Built Properties of Bidwell Canyon Saddle Dam

Dam	Zone	Relative* Compaction	Number of Tests
Main	1B (Core)	97.9	17
	2B (Filter)	97.2	4
	3B (Shell)	103.0	9
West	1B (Core)	96.0	13
	1B/S (Shell)	95.3	10
	2B (Filter)	100.5	2
	3B (Shell)	106.0	2
*DWR Standard			
Zone 1B, 1B/S		20,000 ft-lb/ft <sup>3</sup>	
Zone 2b, 3B		Vibrated Maximum Density	



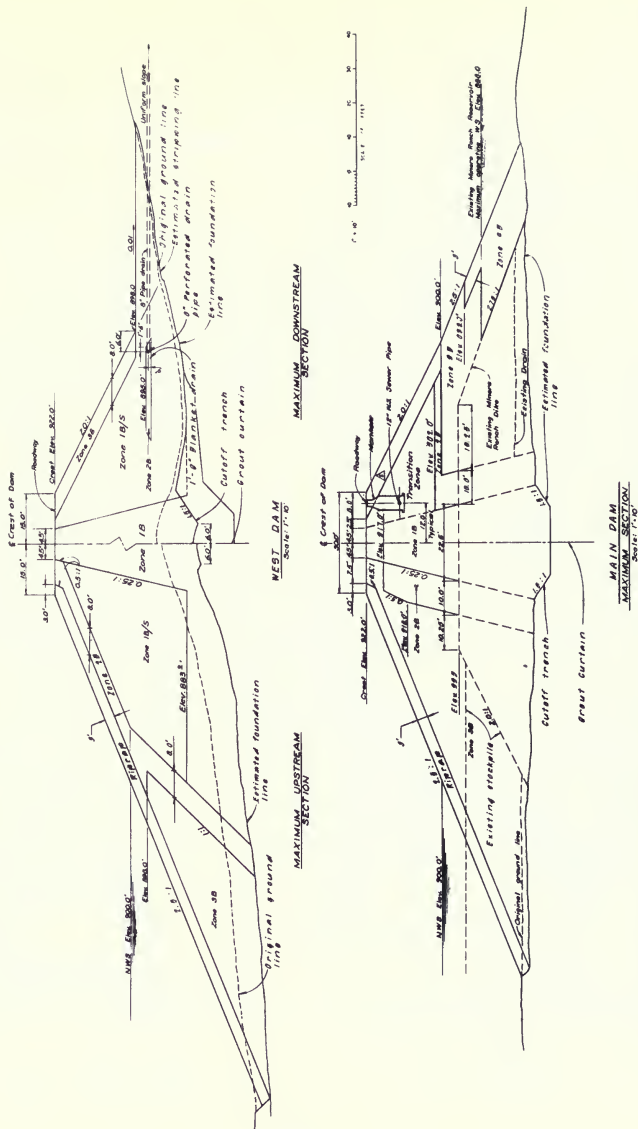


**Figure 440. Bidwell Canyon Saddle Dam—Sections and Details**

Pervious borrow (Zone 3B) came from several nearby sources including rock spoils from tunnel excavation and rejected oversize material from impervious borrow excavations. Filter material, Zone 2B, was composed of dredger tailings. Zone 4B, the Main Dam downstream toe, is composed of clean, coarse, dredger-tailing cobbles. All riprap placed on the dams was fresh, hard, and durable metamorphic rock. Material gradations and plasticity are shown in Figures 441 through 443.

### Foundation

Bidwell Canyon Saddle Dam is founded on a metavolcanic rock consisting mainly of a foliated amphibolite. The amphibolite varies considerably in the degree of weathering throughout the foundation. Fresh exposures

generally are dense and tough with a dark bluish or greenish gray color. In other areas, the amphibolite has weathered to a reddish-brown clayey soil (see Figure 444).

As described in Project Geology Report C-32, the foundation rock contains planes of nearly vertical foliation, at one-inch intervals, which strike about normal to the dam axis. There are several narrow shear zones mapped in the foundation ranging up to one-foot-wide and paralleling the foliation (see Figure 445). The largest shear zone crossing the dam foundation is located on the right abutment of the West Dam. The foliation in this shear zone is more intense, resulting in a soft, but fresh and impermeable, schist. This sheared zone is approximately 20 feet wide.

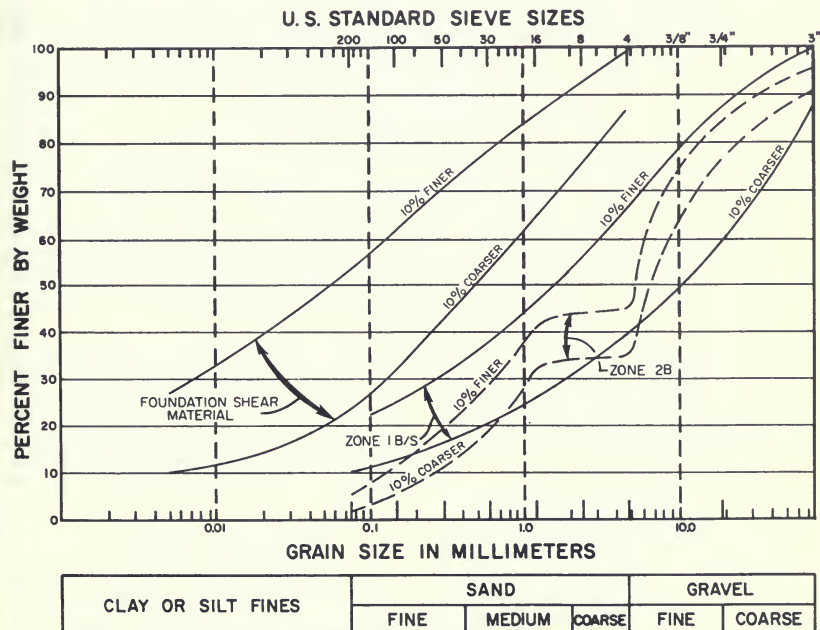
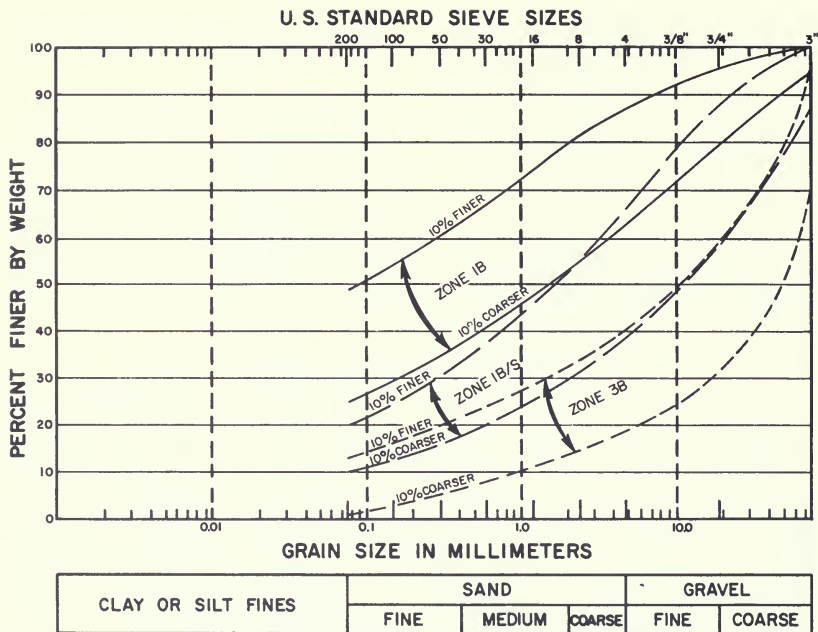


Figure 441. Bidwell Canyon Saddle Dam—Gradation Curves





*Figure 442. Bidwell Canyon Saddle Dam—Gradation Curves*

Periodic surveys made along the crest of the dam indicate more settlement at the West Dam than at the Main Dam. In particular, the location of the maximum displacement coincides with the large shear zone discovered during construction at the West Dam. Profiles of these settlements are shown in Figure 446.

When Oroville Reservoir is below the upstream toe of the Main Dam, water from Miners' Ranch Reservoir seeps through the foundation and surfaces close to the upstream toe of the Main Dam embankment. The estimated seepage is about 10 gpm on the average. Much of the flow, however, is probably ground water seepage from the left abutment. During extreme drought periods, such as in 1976-1977, the upstream toe has standing water on the ground surface.

Ground cracking and displacements from the August 1975 Oroville Earthquake sequence occurred south of Bidwell Canyon Saddle Dam. Initial cracking from the earthquake was discovered along the Swain Ravine Lineament fault zone west of Cleveland Hill (see Figure 447). A year later, cracking had propagated several miles northward and was discovered only 1.3 miles south of the dam.

### Seismic Evaluation

It has been postulated that the shear zone in the foundation of the West Dam is the surface expression of the Swain Ravine Lineament fault system. This would mean that the Bidwell Canyon Saddle Dam would be about the same distance as Oroville Dam from the zone of energy



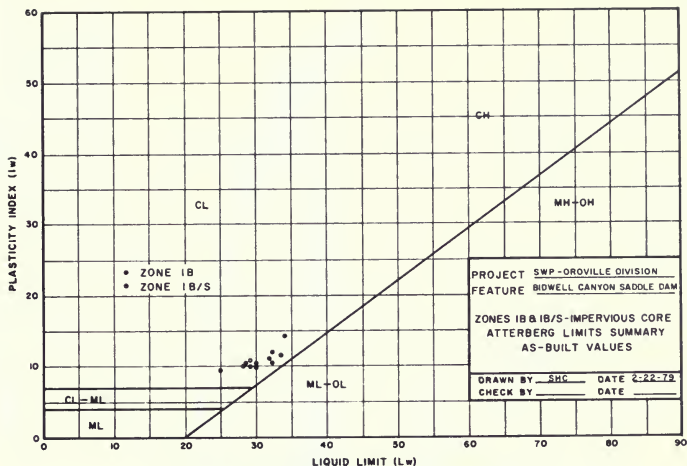


Figure 443. Bidwell Canyon Saddle Dam—Atterberg Limits

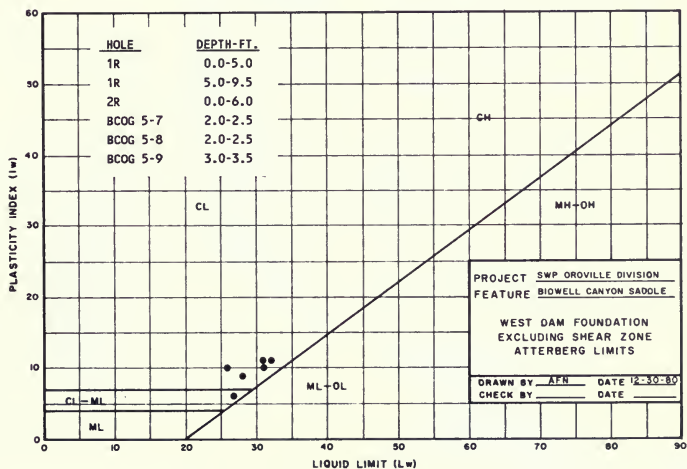


Figure 444. Bidwell Canyon Saddle Dam—Atterberg Limits



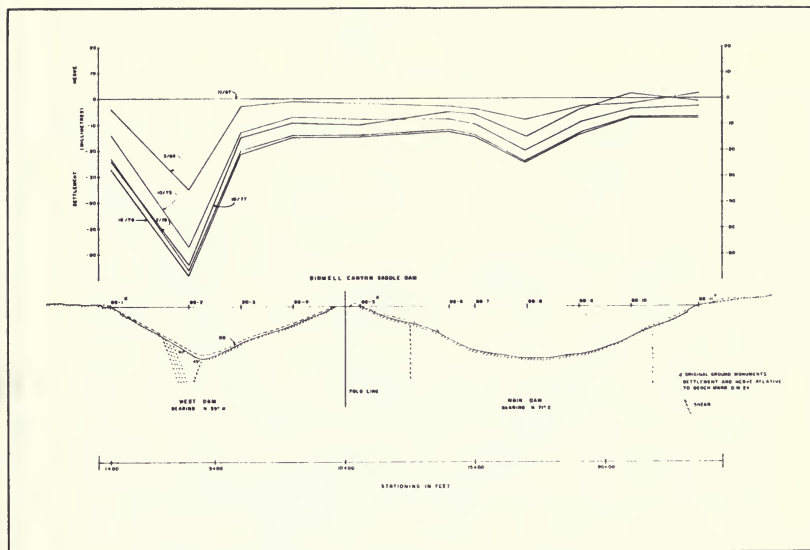


Figure 446. Changes in Crest Elevations of Bidwell Canyon Saddle Dam

release of an earthquake on the Cleveland Hill Fault (i.e. the zone of energy release would be only a few miles beneath the dam). Consequently, an appropriate ground motion for use in re-analyzing Bidwell Canyon Saddle Dam is the Oroville Reanalysis Earthquake which produces a peak ground acceleration on rock surfaces in the free field of 0.6g (see Chapters III and V of this bulletin)

A key assumption in the seismic evaluations of the Oroville and Thermalito dams was that the compacted clayey embankment materials would perform satisfactorily in the strong earthquake shaking adopted. This assumption was based on the findings of Seed et al. (1978) who studied the historical performance of dams subjected to strong earthquake shaking.

This assumption is equally valid for Bidwell Canyon Saddle Dam. Both the West Dam, composed almost entirely

of compacted clayey soil, and the Main Dam, containing a compacted clayey core and dense, sandy gravel shells, would be expected to perform satisfactorily during earthquake shaking as strong as the Oroville Reanalysis Earthquake ( $a_{max} = 0.6g$ ) without exhibiting significant strength losses. Examination of the performance of dams composed of similar materials and exposed to similar levels of earthquake shaking shows that the maximum permanent deformation that might be induced in the Bidwell embankments after the postulated Magnitude 6.5 earthquake would be between 1 and 6 inches in any direction (see Seed et al., 1978; Tepel et al., 1984).

In light of the large freeboard and good stable materials present at this dam, this dam would be expected to perform satisfactorily for virtually any level of earthquake shaking.

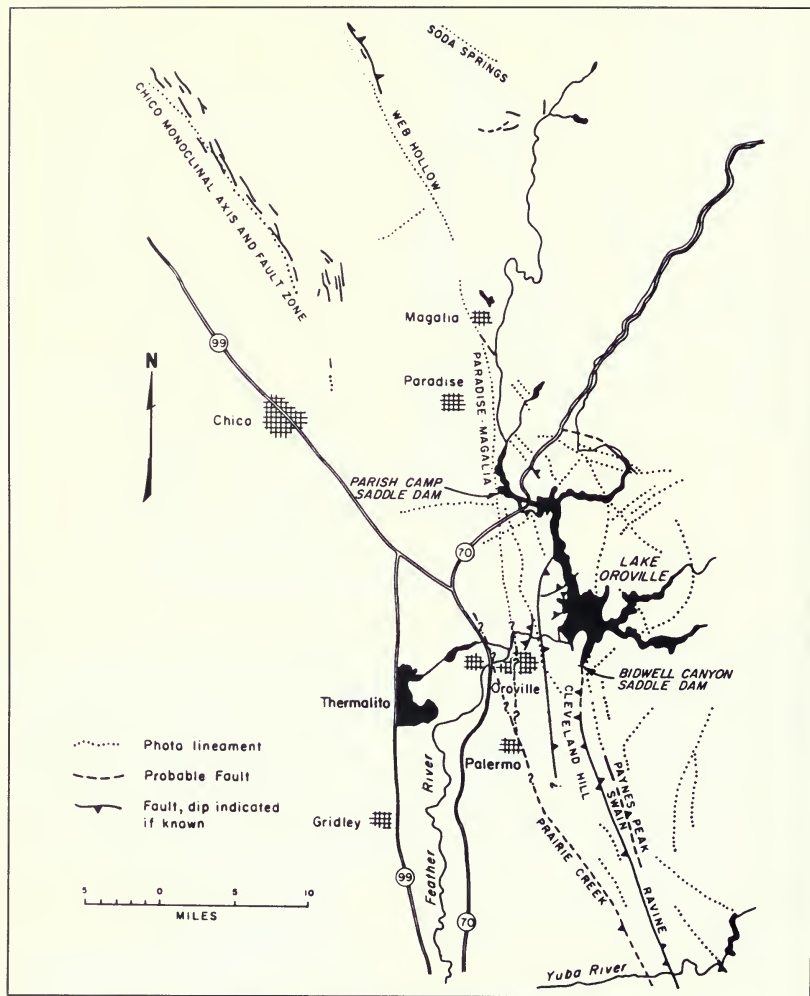


Figure 447. Lineaments and Faults in the Northwestern Sierra Foothills

## 4. EFFECTS OF POSSIBLE FAULT MOVEMENTS ON OROVILLE PROJECT DAMS

### Possible Fault Movements

Estimates of maximum credible fault displacement in the Oroville area are presented in a memorandum from Pro-

ject Geology Chief, J. W. Marlette, to Civil Design Chief, Ernest C. James, dated December 11, 1978:

"This memorandum is in response to an inquiry from Mr. Bill Hammond on the amount of fault displacement that should be considered for reanalysis of various structures in the Oroville Division. Estimated amounts of displacement cited in this memorandum should be considered as maximum credible events with slight probability of occurrence.

"No detailed discussion of regional geologic conditions and tectonic framework is made herein. For detail on geologic environment, see Bulletin 203-78, Chapter III 'Geologic Investigations.'

"The maximum fault displacement expected would be along the Swain Ravine Lineament fault zone. The maximum estimated displacement that might occur along this fault zone is estimated to be 15 centimetres (6 inches) vertical displacement and 2.5 centimetres (1 inch) horizontal extension or opening. The 15 centimetres (6 inch) vertical displacement is derived from an interpretation made by Woodward-Clyde Consultants in one of their trenches where they felt there was 1.5 feet of cumulative displacement that resulted from at least three, and possibly more, fault movements during the last 100,000 years. This is the maximum displacement seen in the Oroville investigations and is about three times larger than the vertical displacement resulting from the 1975 Oroville Earthquake. Assuming the worst case, (displacement caused by only three movements), this suggests an average of 15 centimetres (6 inches) vertical movement for each occurrence. The 2.5-centimetre (1 inch) opening is an arbitrary estimate based primarily on approximately average 2.5-centimetre (1 inch) opening along ground cracking after the 1975 Oroville earthquake. We think it unlikely that horizontal opening would increase much with somewhat greater earthquake and/or vertical displacement.

"The only structure that would be affected by the 15-centimetre (6-inch) movement is the Bidwell Bar Canyon Saddle Dam. Although we were unable to trace faulting continuously to the Bidwell Bar Canyon Saddle Dam, we are making a worst-case assumption and presume the shear zone uncovered during the foundation excavation at the west end of the dam is part of the Swain Ravine Lineament fault system. Therefore, the 15-centimetre (6 inches) vertical displacement and 2.5-centimetre (1 inch) horizontal opening should be assumed to take place on this shear. Attached is a map of the Bidwell Bar Saddle Dam showing the location of the shear. We do not envision displacement distributed evenly throughout the shear, but instead anticipate it would be localized sharply somewhere within the shear.

"It is possible that movement along the Swain Ravine Lineament fault zone could be accompanied by sympathetic movements along other smaller local faults. There is no way to precisely evaluate how large such displacements would be but, intuitively, they should be smaller than displacements along the main fault zone. We estimate sympathetic movement to be several orders of magnitude smaller than movements along the main fault zone so would estimate a maximum of 5 centimetres (2 inches) vertical displacement and 2.5 centimetres (1 inch) horizontal extension or separation. Displacements of this size might take place underneath the main Oroville Dam along the pre-existing shears and faults mapped in the foundation. These small displacements also might occur along any faults that might be obscured in the bedrock underlying Thermalito Afterbay, if movements were to occur along the Prairie Creek Lineament fault zone [Note: this was meant to refer to Thermalito Forebay Dam as the Prairie Creek Lineament fault zone passes near the Forebay and not the Afterbay]. It should be emphasized that such displacements in the bedrock probably would not be propagated up through the soft, younger sedimentary deposits overlying the bedrock. Consequently, displacement at the surface probably would consist of slight, almost imperceptible changes in ground elevation.

"For all other structures in the Oroville Division, which have small faults or shears in their foundations, displacements would be very small compared to what might be expected along the main Swain Ravine Lineament fault zone. Assume 2.5 centimetres (1 inch) vertical movement and 0.6-centimetre (1/4-inch) horizontal opening for analysis of these structures.

"The above estimates of fault displacement are not precise — in fact, they should be regarded as conjectural. They do represent our opinion of the worst movement credible in the existing tectonic framework, as we understand it today. The estimated future displacements are larger by several times than those produced by the 1975 Oroville Earthquake."

Before addressing the possible effects of fault movements, it is important to re-emphasize that sympathetic movement on subsidiary faults is less likely than displacement on the primary fault (Swain Ravine or possibly Prairie Creek—see Figure 447) during the postulated earthquake, which in itself is a very unlikely event. However, if such sympathetic movement should occur, the movement

would probably be normal fault displacement on north-south trending subsidiary faults.

A further description and clarification of the ground cracking that might be associated with the postulated fault movements was provided by the Special Consulting Board for the Oroville Earthquake in its letter report dated February 22, 1985:

"In its report of January 14, 1981, the Board noted that normal-fault displacements in the project area 'will necessarily be associated with a component of horizontal extension at the surface.' In saying this, the Board did not mean to imply that horizontal extension would be caused by the opening of significant tensile cracks in the bedrock, but only that shear failure on a dipping bedrock fault plane, with the foot-wall relatively raised, would necessarily be reflected in gross horizontal extension at the surface. Although such shear failure at depth might result in shallow tensile cracks in the overlying soils, weathered materials, or artificial embankments, tensile effects would not extend to large depths. The Board does not feel it to be appropriate to assume significant tensile opening of fissures in bedrock, such as is currently envisaged by the Department at, e.g., Bidwell Canyon Saddle Dam. We recommend instead that only shear failures be assumed in firm bedrock, with possible tensile failure being limited to surficial materials."

#### **Evaluation of Possible Effects of Fault Movements**

All of the Oroville Project dams are predicted to perform satisfactorily should the postulated fault displacements occur. Individual structures are addressed below:

##### **Oroville Dam**

The Oroville Dam Core is composed of a compacted, clayey gravel and is blanketed by wide upstream and downstream transition zones composed of sand and gravel. The width of each transition zone ranges from 10 feet near the crest to over 140 feet at the foundation level. Bracketing the transition zones are large gravel shell zones (8-inch maximum particle size). The core material is not highly erodible and the transition and drain zones would be expected to prevent progressive erosion following a foundation displacement even if a crack opened through the core.

##### **Bidwell Canyon Saddle Dam**

A more detailed consideration is warranted for Bidwell Canyon Saddle Dam because predicted fault displacements are the greatest for this structure (6 inches vertical, 1 inch horizontal extension).

The Main Dam is judged to be satisfactory since it has basically the same zoning as Oroville Dam. The core material is not highly erodible and the upstream and downstream transition and drain zones would be expected to prevent progressive erosion should a crack open through the core. Further, the shear zone where the displacements are being postulated lies beneath the West Dam and not the Main Dam.

The West Dam, however, is more nearly a homogeneous cross section comprised primarily of Zone 1B and Zone 1B/S, respectively a clayey gravelly sand and a clayey gravel (see Figures 442 and 443). Although most of the foundation is composed of more competent material, the

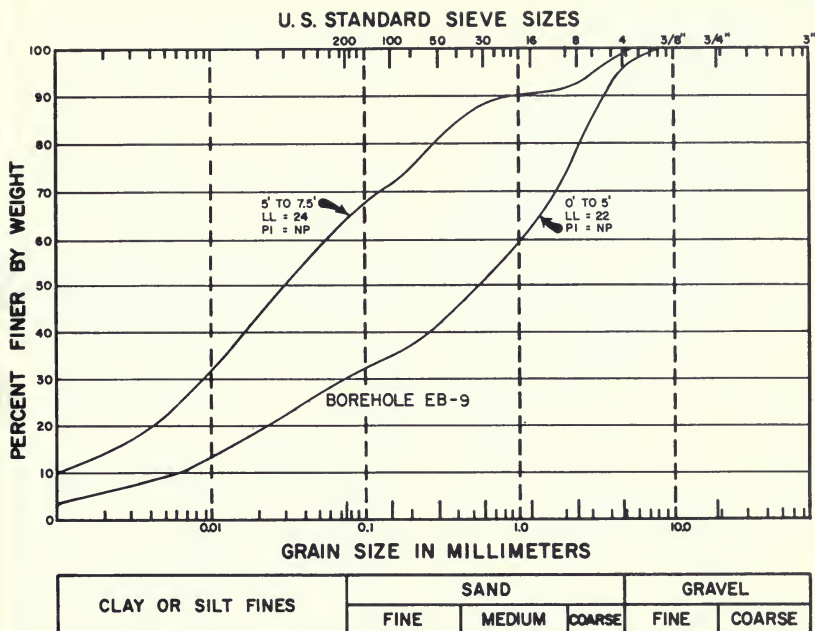


*Figure 448. Bidwell Canyon Saddle Dam—West Dam Shear Zone Gradations*

large shear zone discovered during construction contains both silty sand and sandy silt (Figure 448).

Figure 449 shows a plan view of the shear zone found in the foundation beneath the West Dam. As previously discussed, this shear zone has been postulated to be the surface expression of the Swain Ravine Fault System. It is assumed that the worst case would be a shallow crack opening along this line in the foundation, and possibly in the base of the embankment. Based on the Consulting Board's recommendations and on the observed cracking in surface soils on the Cleveland Hill Fault in 1975, the largest crack that can be envisioned would be one inch wide and a few feet deep.

The amount of water that could enter the shear zone is limited for the following reasons:

- As shown in Figure 449, the upstream end of the crack would daylight on the right abutment at approximately Elevation 905 feet, about 5 feet above maximum operating reservoir surface (Elevation 900 feet). Along the right abutment, the shear zone extends upstream and uphill and is above reservoir level. Consequently, the reservoir does not have direct access to the shear zone.
- One possible way for the reservoir water to enter the shear zone would be seepage through the foundation



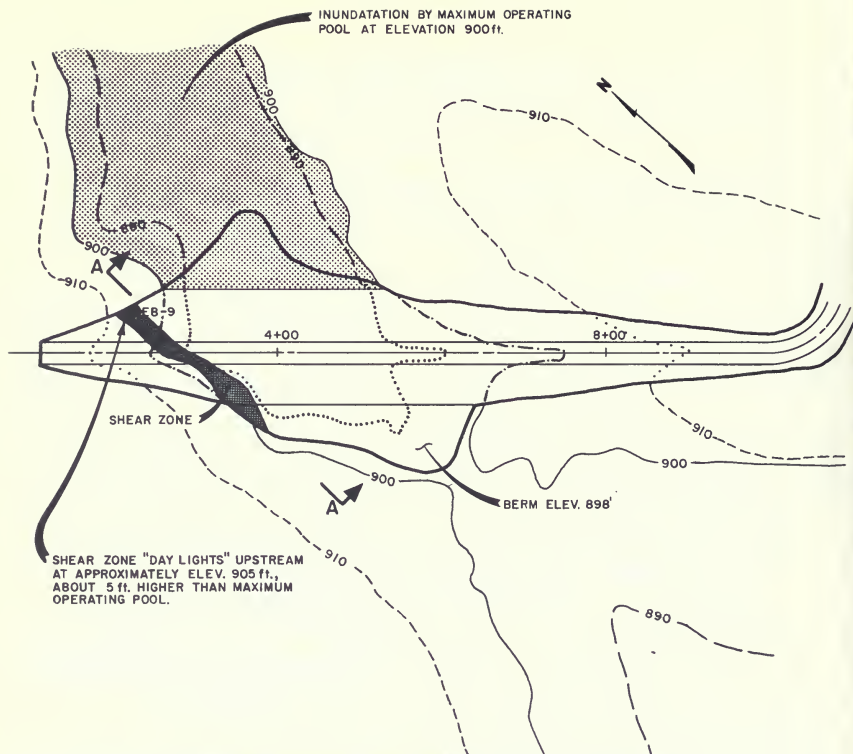


Figure 449. Plan View of Bidwell Canyon Saddle Dam—West Dam Shear Zone Details

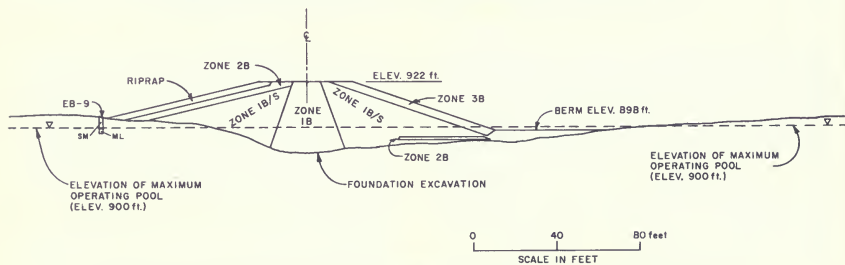


Figure 450. Cross Section AA of Bidwell Canyon Saddle Dam Along West Dam Shear Zone (see Figure 449)



rock and/or the clayey Zone 1B/S embankment material. As both materials presumably have relatively low permeabilities, the amount of water which could enter the crack in the shear zone by this method would be minor.

- The only other way for reservoir water to enter the shear zone would be through a subsidiary crack through the clayey Zone 1B/S embankment material, which would connect the crack within the shear zone to the reservoir. Such a crack, oriented in such an unfavorable manner, would be highly unlikely. Further, if such a crack did develop, the size of the subsidiary crack would be expected to be several times smaller than the 1-inch opening being postulated for the shear zone. The smaller size, in relatively non-erodible clayey gravel and at small head, would act to limit the amount of water which could be introduced into the shear zone crack.

In the very unlikely event that a significant amount of water could enter the shear zone, it should be noted that the crack would first traverse approximately 180 feet of embankment (see Figures 449 and 450). At the downstream toe, the crack would be at the 898-foot elevation berm and then in natural ground above Elevation 900 feet for a further distance of 500 feet. Altogether the crack would be 680 feet long before “daylighting” at Elevation 900 feet downstream. Elevation 900 feet is the nominal storage elevation, and has never been exceeded in the 20-year history of reservoir operation. Furthermore, the surface of Oroville Reservoir has exceeded elevation 898 feet only six times, for a total cumulative period of only 5 months.

Water flowing in the crack would have a gradient that would be less than 0.01. Using Mannings’ equation for flow in an open channel, the velocity calculated for a crack of the size described was found to be less than 0.5 fps. Permissible velocities in unlined canals in fine sand are generally 1.5 fps (see, for example, *Handbook of Hydraulics* by Brater and King). If the crack collapsed or plugged up downstream of the 898 berm, water would flow out of the crack and spread out at a very low velocity across the 898 berm. Even if this latter behavior should occur, the gradient would still remain at about 0.01 or less through the embankment, and the velocity within the shear zone crack would also remain low. Consequently, it is considered extremely unlikely that the shear zone crack

would experience velocities high enough to erode the silty soils found within the zone.

In light of the above reasoning, if the postulated cracking occurred in the West Dam foundation, the possibility of erosional failure of the dam would be practically nil.

### **Parish Camp Saddle Dam**

As mentioned previously, Parish Camp Saddle Dam retains water only during rare intervals when flood operations raise the reservoir above Elevation 900 feet. The foundation is composed primarily of weathered phyllite, material containing a fairly high clay content. Because reservoir retention is relatively rare, foundation and embankment materials not highly erodible, and the maximum credible surface crack opening is so small (1/4 inch), the expected performance of this structure is judged to be satisfactory.

### **Thermalito Diversion Dam, Thermalito Fish Barrier Dam, and Thermalito Powerplant Headworks**

These dams are all concrete gravity structures founded on rock and are considered capable of surviving fault displacements of one-inch vertical offset and 1/4-inch extension.

### **Thermalito Forebay and Afterbay Dams**

These two structures are compacted clay embankments built on alluvial material. The sediments beneath these two dams vary between 70 and 200 feet thick. Although the previously cited Project Geology memorandum states that displacements in bedrock probably would not be propagated up through sedimentary deposits, the Consulting Board called to our attention that earthquake displacements have been observed at the ground surface where considerable depth of alluvium overlaid bedrock. However, it should also be noted that the fault displacements in the rock at depth in these locations were probably much greater than the 1 to 2 inches of rock displacement postulated for the rock surfaces lying at depth beneath the Thermalito embankments. Consequently, the postulated rock displacements are not anticipated to propagate through the alluvium and reach the surface.

In the unlikely event that the minor displacements are propagated to the surface, the following considerations are appropriate:

- The predicted fault extension in rock was estimated to be one inch for Thermalito Forebay and 1/4 inch

for Thermalito Afterbay. The extension component could not cause a crack or opening to be propagated to the ground surface. A 70 to 200-foot-deep crack, open one inch from top to bottom is not possible in sediments composed of layers of gravel, sand and/or clay.

- It is reasonable to assume that deformations would propagate to ground surface – but reduced from the

predicted offset in base rock. This could lead to very small shear displacements at the ground surface.

Since Thermalito Forebay and Afterbay Dams are compacted clay embankments, they should accommodate very small foundation displacements with at most very minor cracking (small fraction of an inch), which would not lead to progressive erosion. It is judged that these dams would perform satisfactorily for the postulated fault movements.

### References

1. Brater, Ernest F. and King, Horace Williams (1976) *Handbook Of Hydraulics*, Sixth Edition, McGraw-Hill Book Company.
2. Seed, H. B., Maksisi, F. I. and DeAlba, P. (1978) "The Performance of Earth Dams During Earthquakes," *Journal of the Geotechnical Engineering Division*, ASCE, Vol. 104, No. GT7, July, 1978.
3. Tepel, R. E., Volpe, R. L., and Bureau, G. (1984) "Performance of Anderson and Coyote Dams during the Morgan Hill Earthquake of 24 April 1984," California Division of Mines and Geology, Special Publication 68.

## **APPENDIX A**

### **REPORTS PREPARED BY THE SPECIAL CONSULTING BOARD FOR THE OROVILLE EARTHQUAKE BETWEEN 1979 AND 1989**

February 27, 1979

Mr. H. H. Eastin, Chief  
Division of Operations and Maintenance  
Department of Water Resources  
P. O. Box 388  
Sacramento, CA 95802

Re: Review of Studies - Seismic Safety of Thermalito Afterbay,  
Forebay and Related Structures

Dear Mr. Eastin:

At meetings on February 26 and 27, 1979, the undersigned members of the Special Consulting Board for the Oroville Earthquake received briefings from Department engineers on the status of seismic stability studies of certain features of the Oroville-Thermalito Reservoir complex other than Oroville Dam. Studies of the latter had been completed and are in process of being published as Department Bulletin 203-78. The studies currently in progress principally address conditions applicable to features of Thermalito Forebay and Afterbay. The basic thrust of the following comments is intended to be supportive of an early completion of the Department's studies, and thereupon a development of the Department's conclusions as to adequacy of the existing construction.

A list of DWR participants in the meetings is presented on attached sheets.

Question No. 1. Does the Board agree with the tentative conclusions of the studies presented?

Response. The Board was much interested in the progress which has been made in additional testing and analyses of foundation conditions under the Thermalito Afterbay, the Thermalito Forebay, and the Thermalito Powerplant headworks structure. Much detailed work has been done and was reported upon. The Board believes, however, that before final conclusions can be drawn, the stress and strength comparisons should all be based on the condition of existing foundation loadings; that is, with the embankments in place; and that the results of these additional analyses should be the basis for the conclusions to be drawn. The Board will be interested to review the resulting conclusions.

In the interim, while there is need for further study of foundation conditions under the Afterbay Dam, particularly at Site 1, the Board considers that it would be prudent to minimize operation of the Afterbay reservoir above El. 128, and to set some elevation above which no operation will go.

The latter conclusion is based on the Board's present understanding of the following operating conditions:

1. All irrigation service outlets can be served from a minimum Afterbay reservoir level of El. 124.
2. Contracturally, pump-back to the Forebay is required at any time, but this mode of operation is rarely used. Hence, no significant

Mr. H. H. Eastin  
Page 2  
February 27, 1979

practical loss would result from restricting pump-back from Thermalito Afterbay.

3. River regulation requires availability of 18,000 to 20,000 acre-feet of Afterbay or Forebay storage, particularly over weekends.

The capacity of the Afterbay at El. 124 is 15,157 acre-feet. The capacity at El. 128 is 25,182 acre-feet. The capacity at El. 131 is 35,555 acre-feet. The difference between the capacity at El. 124 and El. 131 is 20,398 acre-feet.

By operating the Forebay so as to use 8,000 acre-feet of its capacity for re-regulation, and accepting 18,000 acre-feet as the combined storage for re-regulation, operation of the Afterbay reservoir could be held below El. 128 without significant operating hardship.

Question 2. Does the Board have any suggestions or comments concerning the studies?

Response. 1. Seismic Stability Studies

After consideration of the Department's presentations of the effects of estimated variations in the several input parameters utilized in the dynamic stress analysis of the Afterbay Dam, the Board's reaction is that a very conservative approach has been adopted for each parameter. There is always a practical question in such an approach whether conservatism may unconsciously be pyramided to unnecessary levels. Our comments are detailed under subsection 3 below.

A most important detail of the stability analysis may be the estimated dynamic shear strength of the foundation sands. For the purposes of preliminary analysis to date, this parameter has been based on cyclic tests on isotropically consolidated sand samples. The construction of the embankment, and the imposition of reservoir loading on the embankment, however, introduce shear stresses in the foundation which may well be of such magnitude as to justify the adoption of dynamic shear strengths based on anisotropic loading conditions. As illustrated in the Department's July 1966 report on this subject, even a modest level of anisotropic consolidation is sufficient to double the estimated dynamic shear strength of the sand.

Accordingly, the Board considers that it would now be advisable to prepare a finite element analysis of stresses applicable to site TAS-1, from which appropriate consolidation ratios ( $K_c$ ) prior to earthquake loading could be plotted as a contour chart. This information, when utilized together with the relationship of dynamic strength to  $K_c$  illustrated, for example, in Fig. 19 of the July 1966 report, would then provide an improved basis for estimating overall stability of the postulated potential sliding wedge of Thermalito Afterbay embankment-plus-foundation. For best confirmation of dynamic strength values under anisotropic loading

Mr. H. H. Eastin  
Page 3  
February 27, 1979

conditions, we recommend making a few more borings at Site 1, taking undisturbed samples, and testing the samples under an appropriate range of anisotropic loading.

## 2. Foundation Displacements During Seismic Events

Studies to evaluate the potential effect of foundation displacements on structures of the project have been based on qualified judgement by the Department's geologic staff concerning maximum fault displacements. The maximum movements postulated are six inches vertical displacement and one inch horizontal extension along the Swain Ravine Lineament. That fault trends toward Bidwell Canyon Saddle Dam, but could not be traced continuously to the dam. A shear zone at the west end of the dam was mapped during construction, and a worst case assumption was made that these maximum displacements could occur at that location. It was also assumed that sympathetic movement could occur along other, small, local faults in the vicinity of Oroville Dam; movements postulated are two inches vertical and one inch horizontal. For all other areas of the project including the Forebay and Afterbay which have small faults and shears in some structure foundations, displacements at bedrock level are postulated to be one inch vertical and one-quarter inch horizontal extension. The geologist's qualification was that these estimates are conjectural and imprecise. The Board agrees in this qualification; however, we believe that the judgements are sufficiently conservative, in view of all data available. Evaluations of structures under these postulated displacements have not been completed; however, data presented and tentative conclusions discussed indicate that the maximum foundation movements could be safely accommodated by the structures.

## 3. Parameters.

Several conservatisms have been introduced into the analysis of the Afterbay Dam. In addition to the very conservative earthquake motions assumed for this modest structure, it appears that factors in addition to those discussed above that have a high degree of conservatism include: (1) use of  $k_2$  values that may be high for the materials they represent, and (2) assumption that 5% strain is the upper bound permissible. Although the Board encourages that these analyses be conservative, it also cautions that compounded conservatisms can result in unrealistic answers. The Board recommends that the Department objectively review those areas of the analysis where judgements have been made, particularly those judgements which have great sensitivity in the final conclusions of the analysis. Values and assumptions used in the analysis should be as realistic as possible and should represent the actual conditions as closely as possible.

Question 3. Does the Board have any other comments or recommendations to make at this time?

Mr. H. H. Eastin  
Page 4  
February 27, 1979

Response. 1. Continuing Studies.

The Board would be interested to be furnished a list of the physical and analytical work which remains to be done before definitive conclusions can be drawn and the amount of time and the schedule required to accomplish it.

2. Possible Remedial Measures.

Pending implementation of possibly needed remedial measures, the Board considers that an interim decision to limit the Afterbay levels to elevations below El. 128, except for unusual, very short time situations, would be prudent.

In regard to possible structural modifications of the Afterbay or Forebay Dams, it seems premature to offer comments until the Department has arrived at definite conclusions that modifications are indicated to be advisable.

In regard to the several subsidiary structures on which we were briefed, such as the Afterbay River Outlet, Ridwell Canyon Dam, and Parish Camp Dam, we tend to share the tentative opinions expressed to us that no important deficiencies relative to seismic stability or foundation displacements are evident, and hence that no modifications will be needed.

Respectfully submitted:

  
Wallace L. Chadwick

  
Thomas M. Lepa

  
Alan L. O'Neill

Members, Board of Consultants



21 June 1979

Mr. Gordon W. Dukleth, Chief  
Division of Design and Construction  
Department of Water Resources  
Sacramento, California

REPORT ON THERMALITO AFTERBAY SEISMIC SAFETY ANALYSIS AND CEDAR SPRINGS SEISMIC  
SAFETY ANALYSIS

The Special Consulting Board for the Oroville Earthquake met in Sacramento on May 24 and 25, 1979. DWR personnel gave presentations on studies that have been made, or are underway, on the seismic and geologic setting, and on the seismic safety analysis of Thermalito Afterbay Dam. A presentation was also made on Thermalito Afterbay operations. The Board's answers to specific questions are as follows:

Thermalito Afterbay Dam

Question #1. What earthquake ground motion does the Board recommend for the seismic safety analysis of Thermalito Afterbay Dam and foundation?

Answer. Because insufficient information is presently available on the soil and rock beneath the Dam, the Board is not able to recommend a specific ground motion at the base of Thermalito Afterbay Dam. The nature of such motion will be influenced by the properties of the underlying soil and rock, hence, the characteristics of this material must be determined before appropriate ground motion at the base of the Dam can be developed. However, as a guide to DWR personnel, the Board makes the following statement: If the Afterbay Dam were founded on rock, the Board would recommend a free-field surface ground motion of about three-quarters the Reanalysis Earthquake accelerogram. However, it is founded on deep alluvium,



The Board feels that useful information might also be obtained if DWR made a preliminary seismic safety analysis using the N-S component of the El Centro, 1940 accelerogram as the free-field surface ground motion at the Afterbay. This accelerogram was recorded four miles from the causative fault, and the El Centro earthquake had a magnitude somewhat greater than the Reanalysis Earthquake.

Question #2. Does the Board have any comments on the studies completed to date on the seismic stability of Thermalito Afterbay Dam?

Answer. The extensive studies completed to date have been performed with diligence and are certainly worthwhile; however, the Board believes that a number of questions concerning input parameters to the analysis need to be answered before the results can be accepted with confidence. Specifically, in the analysis two parameters of great sensitivity to the end results are the ground motions which would occur at the ground surface and the shear modulus of the deep soil column beneath the Dam. A better understanding of the deep soil column properties would permit a more specific response to questions regarding input ground motions and would also permit selection of shear modulus values with a greater degree of confidence. The Board is aware that additional costs would be incurred if further explorations were made to obtain the necessary information. As long as the Department and its contractors are willing to operate the reservoir under the current restrictions, there is no urgency to perform those explorations. However, when the Department determines that full reservoir operation is desirable, it will be necessary to make deep borings as described later in this report.

Question #3. Does the Board have any other comments or recommendations to make at this time?

Answer. The Board considers that the studies so far made are not sufficient to permit a firm conclusion to be drawn as to the earthquake safety of the Dam at full reservoir. Accordingly, it would seem that at least two options are available, as follows:

a) The Department could indefinitely defer the fairly expensive additional exploration and study which we visualize to be an essential element of a convincing analysis, and consequently would be required to continue operation of the Afterbay at substantially reduced levels for the indefinite future. Based on the limited information presently available, operating at reservoir levels between elevations 124 and 131, as currently adopted, is considered to be reasonably safe.

b) Further investigations of study parameters could be undertaken with the objective of developing improved analytic evaluations of the seismic safety of the dam. If this course is adopted, the Board recommends that it include the following items.

1. At least one deep boring of about 500 ft should be made at Test Site 1, with the primary objective of obtaining in situ measurements of shear wave velocity at all depths. These data are needed to provide a supportable basis for estimating the shear modulus parameter  $K_{2\max}$  which is one of the most uncertain parameters in the analysis made to date. It would undoubtedly be valuable to expand this program to include two additional holes of similar depth, located at distances of about 200 ft on each side of the initial boring.

2. Install two seismic sensors in one of the deep borings, one at the bottom and one at the top, together with recording equipment which would be capable of evaluating ground accelerations at the two depths for even moderate seismic events. The purpose would be to obtain in situ verification of the relationship at this site between the bottom level and the ground surface level earthquake motions, perhaps in the near future.
3. Install a strong-motion accelerograph at an appropriate location along the N-S leg of the Afterbay Dam near the downstream toe of the Dam. This would extend the present strong-motion accelerograph instrumentation to a pertinent location on deep alluvium.
4. Make at least five borings through the crest of the dam, opposite the borings made recently near the downstream toe, to obtain a comparison between  $SP\bar{\alpha}$  values under the dam and those obtained previously in the downstream area. The new borings should probably be near Test Site 1 and should extend about 40 ft below the base of the Dam. The purpose would be to determine whether the embankment loading has densified the shallow sands appreciably and thereby increased the  $SP\bar{\alpha}$  values.
5. Make an evaluation of the dynamic shear characteristics of the silty Columbia soil underlying the eastern end of the E-W leg of the Dam. If undisturbed samples for cyclic shear testing cannot practicably be recovered from open test pits, appropriate borings should be made. The purpose of the sampling and testing would be to verify the present assumption that this material has

superior strength in comparison to that of the clean sands at Test Site 1.

6. Following collection and evaluation of basic data from the foregoing (except 2 and 3) and the final establishment of an appropriate Reanalysis Earthquake for Thermalito Afterbay, final computations of foundation liquefaction tendency at Site 1 should be made, in the general manner utilized in the studies at this meeting. This evaluation together with all supporting assumptions and data should be submitted to the Board for comment.
7. The Board was presented the results of analyses to determine the factors of safety for a Site 1 sand layer under various accelerations using a ten cycle exposure and 10% strain for both undisturbed and remolded samples. The Board believes that it is desirable to supplement these analyses, if possible, by analyses using strengths indicated by in situ blow counts, as further evaluated by the additional testing suggested in item 4 above.

The seismic safety analysis of the Thermalito Forebay Dam was not considered at this meeting. It is understood that this will be presented to the Board at a later date.

#### CEDAR SPRINGS DAM

The Board was also given a presentation by DWR personnel on the seismic and geologic setting, and the seismic safety analysis of Cedar Springs Dam. The answers to specific questions about the seismic safety analysis of

Cedar Springs Dam are as follows:

Question #1. What earthquakes should be considered in the seismic safety analysis of Cedar Springs Dam, and what test accelerograms are recommended for the dynamic analysis?

Answer. The Board recommends that two earthquakes be considered in the seismic safety analysis of Cedar Springs Dam: 1) A magnitude 8+ event should be assumed to be centered on the San Andreas fault at its closest point to the Dam. For the dynamic analysis, either of the two test accelerograms previously specified by the Board for structures close to the San Andreas fault should be used. 2) A magnitude  $6\frac{1}{2}$  local event should be considered on a fault close to the Dam. The test accelerogram for this earthquake should be the same as that proposed earlier by the Board for the reanalysis of Oroville Dam. Additionally, it is accepted that this ground shaking may be accompanied by up to three feet of surficial shear displacement in any direction on a fault through the Dam foundation.

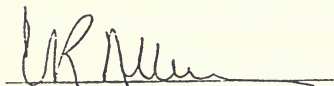
The Board would feel more confident in the assignment of design parameters for the local earthquake if the geologic relationships were better understood between the faults traversing the foundation and other nearby structures such as the Cleghorn fault. In this regard, we remind the Department of the Board's recommendation of April 8, 1965, that "a high-quality detailed geologic map of the reservoir area be completed as soon as possible.

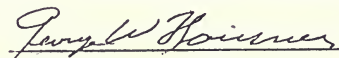
Question #2. Does the Board have any other comments or recommendations to make at this time?

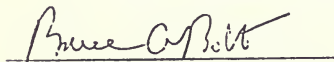
Answer. The Board was shown a diagram illustrating the slip circle considered to be critical and which was used in analyzing the safety of

Cedar Springs Dam by the pseudo-static loading method. It was noted that this circle crosses the downstream filter, the core and the upstream transition into the foundation, including rocks of the Harold formation. It is questioned whether this circle is the most critical. It is understood that other circles and wedges were also analyzed and the Board would be interested to learn the results of an analysis of a wedge through the upstream sand and gravel transition and the sand and gravel drain blanket under the upstream shell. The Board recommends, however, that before reliance is placed on safety factors determined as discussed above, consideration be given to other methods of analysis now current in the technology.

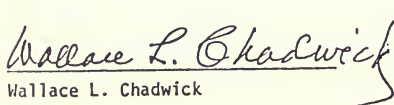
The recommendations presented in this report supersede those of previous reports.

  
Clarence R. Allen

  
George W. Housner, Chairman

  
Bruce A. Bolt

  
Thomas M. Leps

  
Wallace L. Chadwick

  
Allen L. O'Neill

  
H. Bolton Seed

GEORGE W. HOUSNER  
1201 EAST CALIFORNIA BLVD.  
PASADENA, CALIFORNIA 91125  
August 14, 1980

Mr. Gordon W. Dukleth, Chief  
Division of Design and Construction  
Department of Water Resources  
P.O. Box 388  
Sacramento, California 95802

Dear Mr. Dukleth:

Subject: Seismic Analysis of Thermalito Afterbay  
Dam and Foundation

The committee on Thermalito Dam has reviewed the draft copy of the section "Design Earthquake" of the Thermalito Afterbay Dam - Evaluation of Seismic Stability Report. The following steps are planned for the analysis:

(1) A surface ground motion having 0.35g peak acceleration will be specified for the ground surface in the vicinity of Thermalito Dam. This ground motion will be in the form of magnitude 6.5± earthquakes.

(2) A corresponding base rock motion will be determined at depth so that when this is used as input the calculated surface motion will reproduce the specified 0.35g recorded accelerogram. The stresses and strains in the materials beneath the surface of the ground will be calculated and the ability of the soil to survive under these deformations will be analyzed.

(3) The same base rock input motion will be used to excite a soil column beneath the dam, including the dam overburden. The calculated stresses and strains will then be used to determine the ability of the soil material to survive.

The Committee feels that the foregoing is an appropriate method of analyzing the ability of the soil material to survive the dynamic stresses and strains. Several ground surface accelerograms should be used in the analysis, and one of these should be a record obtained on relatively hard ground.

Yours truly,

  
GEORGE W. HOUSNER, Chairman  
Committee on Thermalito Dam

G/H:md

cc: Committee Members

14 January 1981

Mr. Gordon W. Dukleth, Chief  
Division of Design & Construction  
Department of Water Resources  
Sacramento, California 95802

Re: Supplement to Bulletin 203-78

The Special Consulting Board for the Oroville Earthquake met in the Department offices in Sacramento January 8 & 9, 1981. The purpose of the meeting was to review with your staff the basis for their drafts of chapters 11 through 15 of Supplement to Bulletin 203-78 presenting results of the August 1, 1975 Oroville Earthquake Investigations. The Board appreciated your attendance at the sessions.

The Board's comments on the five principal features which were presented are covered separately in the following sections:

1. Thermalito Afterbay Dam Concrete Structures Seismic Evaluation.

The Board has reviewed the draft of chapter 13 of the supplement to Bulletin 2-3-78, and was given a presentation on the seismic analyses of these structures. Pseudo-static analyses of the structures were made for a lateral force coefficient of 0.3, (equivalent to a constant, horizontal acceleration of 0.3g) under combined earthquake and gravity loads. In general, the calculated stresses are below yield point in the reinforcing steel and below allowable stresses in concrete. The only locations where relatively high stresses were found in reinforcing steel were in the lower portion of the tension sides of the counterforts supporting the side walls of the gate structure. At those locations the maximum calculated tensile stress was 1.5 times the yield stress, but did not exceed the ultimate stress, assuming a cracked section. It was concluded that this would mean, that in a dynamic stress condition, as distinguished from a static condition, the concrete would probably crack and the reinforcing bars would undergo some permanent extension, but the structure would not collapse and it would be in a repairable condition.

The Board considers these analyses to be appropriate for exhibiting the seismic resistance of the structures and agrees that their earthquake resistance is satisfactory. The draft report does not contain any information on the foundation conditions of these structures and the Board recommends that this be added to the report.

2. The Thermalito Power Plant Headworks Structure.

This is a concrete gravity section with many openings for the passage and control of flowing water. The complex structure has been analyzed for a M6.5 earthquake centered about four miles away, as previously recommended by the Special Consulting Board. Professor A. K. Chopra, under contract to the Department, determined the lateral earthquake forces using advanced technology which included the dynamic properties of the system at various water levels and various values of the modulus of elasticity of concrete.



The dam monolith was idealized as a finite element system and hydro-dynamic effects were included. The Chopra report provided lateral forces applied to various units of the structure. The Department staff evaluated the stresses in the structure caused by the seismic forces, both taken alone and in combination with static stresses. The working stress method was used, treating the structure as uncracked, and neglecting the effect of the reinforcing steel. The maximum allowable tensile stress in the concrete was 550 psi, which was 10% of the ultimate strength  $f_c$ . The maximum allowable compressive stress was 2,475 psi, which is 45% of  $f_c$ , plus a  $\frac{1}{3}$  increase under seismic conditions. The characteristics of the basaltic rock foundation material were assumed equivalent to those of the concrete in the structure. The maximum shear stress was set at  $1.1\sqrt{f_c}$ , or 81.6 psi, plus  $\frac{1}{3}$  increase for seismic conditions. The maximum confined direct shear strength of the concrete was set at 35% of  $f_c$ , or 1,925 psi.

Stresses were computed for all critical elements of the structure including walls and piers. The maximum concrete tensile stress obtained was 333 psi and maximum compressive stress was 432 psi, both below the allowable stresses. The maximum average shear in the structure as a whole was 99.3 psi and the maximum on any individual member was 113 psi, only a few percent above the allowable. In the wall of the downstream end of the water-passage opening, overturning moment on the structure produced a compression of 940 psi and a tension of 460 psi in the basaltic rock base.

The Board agrees that the foregoing analyses demonstrate that the Thermalito Power Plant Headworks would perform satisfactorily under the prescribed earthquake with possibly some minor local cracking. The draft of Chapter XV does not mention the fault that reportedly lies beneath the bases of the penstocks and on which minor sympathetic movements have been considered credible. The Board recommends that this fault be discussed in the draft. The Board also recommends that consideration be given to the seismic stability of the traveling gantry crane and its ability to handle the gates.

3. Seismic Evaluation of Bidwell Canyon and Parish Camp Saddle Dams and Effects of Possible Fault Movements in Oroville Project Dam Foundations.

The Board concurs in the conclusion that the two saddle dams would perform satisfactorily during earthquake shaking as severe as would be generated by the Oroville Reanalysis Earthquake. Postulated fault displacements were presented as 15 centimeters beneath the Bidwell Canyon Saddle Dam (West Dam) resulting from movement along the Swain Ravine faults, and sympathetic movement from 2.5 centimeters to 5 centimeters beneath other project dams. The Board concurs with these estimated surficial fault displacement parameters for the various faults and shears in the project area. However, we suggest (1) emphasis be placed on the fact that movement on any individual subsidiary fault is even less likely than displacement on the Swain Ravine fault during the postulated earthquake, which is in itself a very unlikely event, (2) a statement be inserted

noting that normal fault displacements will necessarily be associated with a component of horizontal extension at the surface, and (3) modification be made of the inference that bedrock fault displacements will necessarily die out in overlying alluvial deposits.

4. Thermalito Afterbay Dam.

The Board concurs that the investigations and analyses to date indicate that the postulated M6.5 Oroville Reanalysis Earthquake is capable of causing a significant degree of liquefaction in the shallow, saturated, sandy foundation stratum at four or more locations along the 13km long dam. The Board accepts the Department's judgment that no significant liquefaction would result, however, from a local M5.7 event.

The Board also concurs that the recently completed survey of foundation conditions, which employed borings at 1,000 ft spacing, is not sufficient either to identify all potentially inadequate foundation areas or to determine the lateral extent of such areas. Hence, the Department's expressed intent to extend the survey by drilling and SPT testing of a substantial number of interspersed borings is endorsed. The spacing of the holes should be such as to define the extent of each clearly identifiable weak foundation area, so as to delimit the scope of needed corrective construction.

The Board presently considers that in those areas where it may be shown that stabilization or reinforcement is justified, the most practicable and effective procedures would be either placement of a substantial upstream berm of rock fill or densification of the sand layers.

The Board was advised that plans are proceeding regarding the recommended installation of two seismic sensors in the 500 ft deep boring at Site 1, one at the top and one at the bottom. In review, the Board recommends the installation of a third sensor at a depth of about 70 ft.

During the interim, while the investigations of the Afterbay and Forebay dams are being completed, the Board reiterates the statement in its report of June 21, 1979, "Based on the limited information presently available, operating at reservoir levels between elevations 124 and 131 as currently adopted is considered to be reasonably safe". However, the Board believes that it is reasonably safe to operate the Forebay without limitation, in accord with current practice. In each case, the related outlet works should be maintained so as to permit as rapid lowering of the reservoir level as would be practicable possible.

5. Thermalito Forebay Dam.

The general approach to assessing the seismic stability of Thermalito Forebay Dam is appropriate and would have been adequate if it had led to a clearer determination of the adequacy or inadequacy of the structure to withstand the postulated earthquake. However, since the approach that was followed

leads to a conclusion of marginal stability, even with the incorporation of soil strengths which are not necessarily the worst which may occur in the foundation, more detailed studies which will eliminate some of the assumptions made in the present investigation are required before a final assessment of seismic stability can be made. In particular, the Board considers that the following supplementary studies are desirable:

a) A number of borings should be made along the length of the dam to confirm the present indication that the conditions at Station 10+00 are likely to be representative of the most critical conditions.

b) If such a conclusion is confirmed by these borings, a detailed cross section through the dam and its foundation at Station 10+00 (or whichever location is found to be more critical) should be developed by means of borings made at appropriate intervals across that section of the dam. Standard penetration tests should be made in these borings to determine the possible continuity or lack of continuity of any loose layers of sand encountered.

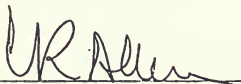
c) Special efforts should be directed toward obtaining good quality, undisturbed samples for cyclic load testing in areas of high and low penetration resistance with a view to exploring further the possibility of a correlation between cyclic strength characteristics and penetration resistance in the sandy soils of the Red Bluff foundation material, thereby facilitating an extrapolation of the cyclic loading test data to other areas for which only penetration resistance data are available.

d) Every effort should be made in the conduct of the supplementary studies to back up judgmental decisions with field or laboratory test data.

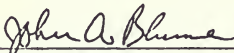
On the basis of the results obtained, studies similar to those already performed should be conducted for an established cross section through the dam and its foundation. Interpretation of these studies and their extrapolation to other zones of the dam can then be used to provide a more definitive assessment of seismic stability than is presently available.

The Board notes that the results of current investigations are encouraging and it may well be that the Forebay Dam has adequate stability to withstand the postulated earthquake. However, it is also considered that more definitive studies along the lines discussed above are required before such a decision can be made with an adequate degree of assurance for important structures of this type.

In the discussion of the Forebay Dam, some attention should be given to the nature and geometry of the contact between the underlying volcanic rocks and the Red Bluff formation, and to the possible effect of this relationship on the stability of the dam under seismic shaking. Mention should also be made of faults beneath the dam on which displacements are considered credible.



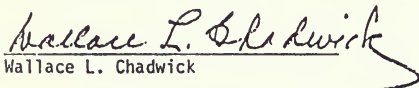
Clarence R. Allen



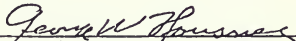
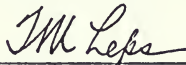
John A. Blume



Bruce A. Bolt



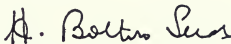
Wallace L. Chadwick

  
George W. Housner

Thomas M. Leps



Alan O'Neill



H. Bolton Seed

WALLACE L. CHADWICK  
200 HOWE BUILDING  
180 SOUTH LAKE AVENUE  
PASADENA, CALIFORNIA 91101

March 19, 1982

Mr. Gordon W. Dukleth, Chief  
Division of Design and Construction  
Department of Water Resources  
P. O. Box 388  
Sacramento, California 95802

Dear Gordon:

At the close of yesterday's meeting of the Board of Consultants on Thermalito Project, the Board met briefly and prepared the attached notes for consideration of your staff in finalizing its report. Xerox copies were furnished to Keith Barrett yesterday.

Thanks to you and all of your associates for the courtesies and assistance which we enjoyed.

Very truly yours,



WLC:ecs  
Attach.

cc: Harry B. Seed, w/attach.  
Tom M. Leps, w/attach.  
Alan L. O'Neill, w/attach.

March 25, 1982

THE FOLLOWING WAS TYPED BY DWR FROM NOTES PREPARED BY THE CONSULTING BOARD FOR THERMALITO AFTERBAY SEISMIC STABILIZATION AT THE MEETING OF MARCH 18, 1982.

Wallace L. Chadwick

1. Summary description of development of changes in conclusions over last 18 months.
2. Assure that use of lowest values, which have been included in averages, would not significantly change results.
3. Submit final draft for review and meet with Board to review and accept conclusions.

Tom M. Leps

Consider the possibility that a rapid transfer of pore pressure may occur in the liquified-to-partially liquified sand stratum at the end of the seismic event, with possibly critical increases occurring quickly in the partially liquified portions under the outer slopes of the embankment.

The strength of the clay hardpan layer was estimated to conform to  $C=0$ ,  $\phi = 37$  deg. In fact, this formation must have a considerable cohesive strength, and hence the assumption appears to be unreasonably conservative.

The several considerations which have been used to define the "Design Earthquake" are endorsed as being reasonably conservative.

The extensive program of dynamic triaxial testing of undisturbed "sand" specimens (150 tests) is considered to have provided a fully satisfactory evaluation of dynamic shear strength.

Harry B. Seed

Probably the main reason why the report concludes the dam to be stable is the high values of cyclic loading resistance exhibited by soils with relatively low values of penetration resistance. It is important to justify why this result is reasonable by comparison with the entire base of data available on this subject -- not just the results of Tokimatsu and Yoshimi which do not necessarily reflect lower bound acceptable values.

I believe the cyclic load test data are as high as they are because:

1. The penetration test procedure used in this project did seem to deliver more energy than "standard" procedures because of the

very good techniques used in the field. Both the Ertec and Kovacs reports lend support to this and it means in effect that other agencies making the same studies would have obtained blow counts about 30 percent higher than those measured by DWR personnel.

2. The soils involved are basically silty sands, which for given values of liquefaction resistance, are now recognized to give lower N-values than clean sands.

My interpretation of mean grain sizes for the different sets of samples leads to the following results:

DWR "N"	$\frac{\text{Seed}}{D_{50}}$	$\frac{\text{DWR}}{D_{50}}$
4.	= 0.2	= 0.3
8	= 0.2	= 0.3
12	= 0.25	= 0.3
16.5	= 0.34	= 0.3
27	= 0.6	= 0.6

DWR interpretations give slightly higher values for  $D_{50}$  as shown in the right hand column. I think it would be desirable to look over the curves again to examine carefully the small discrepancies which could well be the basis for a better explanation of the relatively high cyclic loading resistance values. I would be glad to examine the data with you to resolve this problem because I believe it is very important.

If a convincing line of logic is developed in the report, based on some changes in style of presentation, I believe the results can be clearly explained and justified.

Redistribution of pore pressure in a short period following the earthquake.

July 7, 1982

Mr. Gordon W. Dukleth, Chief  
Division of Design and Construction  
Department of Water Resources  
P. O. Box 388  
Sacramento, California 95802

Re: Thermalito Afterbay and Forebay Dams  
Seismic Stability Evaluations

Dear Mr. Dukleth:

In accordance with your letters of June 14, and June 18, 1982; your Consulting Board for Thermalito Afterbay and Forebay Dams Seismic Stability Evaluations met at Sacramento on July 1, 1982. The meeting was conducted by your Mr. K. G. Barrett. The purpose of the meeting was to provide an opportunity for your staff to brief the Board on the present status of the studies and preliminary conclusions relative to the following:

1. Thermalito Afterbay Dam (Partial draft report furnished)
2. Thermalito Afterbay Concrete Structures (Final draft submitted)
3. Thermalito Forebay Dam (Studies well along; Completion in September).

A copy of the meeting agenda and a list of participants in the meeting are attached.

In general, the Board was favorably impressed with the



exceptional extent and detailed attention to state-of-the-art analysis which characterize the investigations, analyses and evaluations which were presented. In review of the present status, the Board believes that it should be possible for the Department to complete each of the three evaluations noted above, and submit them to the Board in Draft form for final comments, by November. Following completion of that phase, we suggest that the drafts be submitted to the full Board on the Oroville Earthquake for final comments and endorsement.

In regard to Item 2 above, identified as Chapter XIII, "Thermalito Afterbay Dam Concrete Structures, Seismic Evaluation", this Board is satisfied, as a result of the briefing it received and its review of this chapter, that the structures are acceptably stable, and that the chapter is now in final form.

Reference is now made to three questions which you have requested the Board to respond to, in consideration of the documents furnished to the Board and the July 1 technical briefings. The questions are listed on an attached sheet. Following are the Board's responses.

Response No. 1.

The Board is not yet in a position to concur with the conclusions (1) that Thermalito Afterbay Dam would be acceptably safe under the postulated M 6.5 earthquake conditions and (2) that it would be safe to restore full use of the reservoir. Basically, we take this position because we have not yet been furnished with

a completed draft report; in particular, we have not had an opportunity to review the proposed, 100-page Addendum which we were advised will include the full details of the step-by-step, seismic stability analyses. We must fully understand and concur with the analyses before endorsing the Department's findings. In this regard, we urge that the text of all portions of your evaluations be thoroughly edited, with the objective of making the presentation as simply worded and as complete as possible, so that it may be followed and comprehended by non-experts. In particular, also, we would recommend that, wherever it is decided that empirical "correction" factors or "average" values must be utilized, the justification therefor be clearly stated.

The foregoing comments represent, in part, the Board's recognition that the evaluations being now finalized by the Department will be published in a document to be available to the general public, and will represent engineering at the forefront of the state-of-the-art. Accordingly, every reasonable effort should be made to make the evaluations complete, understandable and credible.

Response No. 2.

The Board agrees with the conclusion that the Thermalito Afterbay Concrete Structures are acceptably safe against serious damage during the postulated reanalysis earthquake.

Response No. 3

In regard to your studies of the seismic stability of

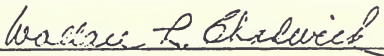
Mr. Gordon W. Dukleth  
July 7, 1982  
Page 4

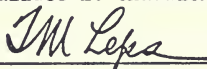
Thermalito Forebay Dam, the Board was favorably impressed with the extent, thoroughness and apparent conservatism of the investigations presented to it orally on July 1. We consider, however, that having not had an opportunity to review the studies in the detail which they will deserve, which review will of course be impossible without having at hand a full draft of your report, it would be premature for the Board to express a judgment.

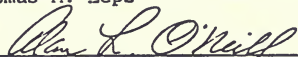
We are satisfied that there seems to be no risk of fault displacement affecting the right abutment of the dam, but we have not yet been provided with a full assessment of the potential of transverse cracking near the right abutment due to differential settlement of foundation soils causable by seismic shaking.

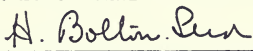
We assume that you may wish to have a final meeting of this Board, possibly in November.

Respectfully submitted,

  
Wallace L. Chadwick

  
Thomas M. Leps

  
Alan L. O'Neill

  
H. Bolton Seed

Board of Consultants  
July 2, 1982

Attachments: Agenda  
List of Participants  
List of Questions

November 15, 1983

Mr. John H. Lawder, Chief  
Division of Design and Construction  
Department of Water Resources  
P.O. Box 288  
Sacramento, CA 95802

Re: Thermalito Afterbay and Forebay Dams  
Seismic Stability Evaluations

Dear Mr. Lawder:

In accord with prior arrangements, your Consulting Board for Thermalito Afterbay and Forebay Dams Seismic Stability Evaluations met in your offices in Sacramento on November 15 and 16, 1983. A copy of the meeting agenda and a list of those persons who attended are attached.

The purposes of the meeting were to update the Board on the most recent work of the Department and the conclusions therefrom concerning Chapter XII of Bulletin 202-78 as that work will be presented in a supplement to that Bulletin, and to present the current status of evaluation of the Forebay Dam.

The Board was asked specific questions to which responses will be made with references to each such question.

Question 1

Does the Board concur with the conclusions stated in Chapter XII, Thermalito Afterbay Seismic Analysis?

Mr. John H. Lawder  
November 16, 1983  
Page -2-

Response

Chapter XII of the Supplement to Bulletin 203-78 on Thermalito Afterbay Seismic Evaluation has three conclusions which are presented on page 1 of the Report. These conclusions are discussed separately below:

Conclusion 1. -- "The strengths of the foundation sands are higher than the values used in the preliminary (1981 Report) evaluation of Station 107".

Since the 1981 preliminary report a detailed investigation program involving 223 SPT borings, 26 borings for piston sampling of sands and 211 cone penetrometer soundings has been conducted, together with a careful laboratory investigation of the liquefaction characteristics of the sands and silty sands in the foundation of the Afterbay Dam. Careful studies have also been made of procedural details involved in the conduct of the SPT tests.

These studies have clearly demonstrated that the SPT procedures used in the DWR investigation deliver more energy to the drill-rods than is customary in past U.S. practice in performing this test and therefore lead to lower values of penetration resistance than would be obtained using conventional procedures. Furthermore, it has been generally recognized in the past few years that silty sands have a greater resistance to liquefaction than clean sands having the same penetration resistance.

These factors, among others, have been carefully considered in evaluating the results of the 1981-82 investigations and they provide convincing evidence, which is supported by findings on other projects and in other countries, that the cyclic loading resistance of the foundation sands for the Afterbay Dam is higher (by about 20 to 25 percent) than the values indicated by the previous (1981) studies. The Board considers that the method of evaluating this resistance used in the present report is appropriate for seismic safety evaluation purposes.

Conclusion 2. -- "The stability of the dam is satisfactory for the maximum earthquake shaking anticipated. Only minor cracking or movements are predicted for the postulated shaking."

The Board considers the wording adequately expresses a generalized finding, but recommends that it be modified so as to convey a decision to reinforce any local reaches of the dam where sharp downstream angles in the axis alignment, such as at the southwest corner of the reservoir, are concluded to be focal points of potential transverse cracking during major seismic events. This thought might be expressed by adding a sentence stating: "short reaches of the dam, at sharp angles in the axis alignment, will be locally reinforced to supplement resistance to transverse cracking."

Conclusion 3. -- "Is it safe to restore full use of the reservoir?"

The Board believes that from the standpoint of seismic stability of the Afterbay Dam and its foundations, it will be safe to restore full use

of the reservoir provided care is taken to ensure that the ground water conditions on the downstream side of the dam are similar to those considered in the seismic evaluation studies and that soil is not pumped from the foundation by the ground water control system.

Question 2. -- "What earthquake ground motions (accelerograms) do the Board recommend using for analysis of Thermalito Forebay Dam and Foundation?"

Response

The Board was briefed in some detail on the rationale and procedure used in selection of the earthquake magnitude and acceleration for reanalysis of the Forebay Dam and Foundation. While this Board believes that the selected earthquake magnitude of 6.5 at a distance of 5 kilometers is extremely conservative and subject to further study and discussion, it recommends that the eight member Consulting Board for the Oroville Earthquake participate in any further recommendations on earthquake ground motions for reanalysis of Thermalito Forebay Dam and Foundation.

Question 2. -- "Does the Board concur with the findings presented for Thermalito Forebay Seismic Analysis with respect to:

- Identification and Modeling of Critical Areas?
- Adopted Soil Strengths?
- Shape and Effect of Foundation Bedrock Profile at Main Dam?"

Response

(a) Identification and Modeling of Critical Areas

The Board considers the approach presented by Mr. Hammond for establishing an idealized soil profile to be used for analysis to be reasonable and appropriate. It has not been possible for the Board to evaluate all of the details of the variable soil conditions but we believe that the overall approach is sound and the results seem to be consistent with such evaluation as we have been able to make in the limited time available. We would caution however against the use of over-conservatism in evaluating variable foundation conditions for soils of the types involved.

(b) Adopted Soil Strength

Final selection of soil strengths for analysis of the Forebay Dam has not yet been made but in view of the relatively dense nature of the soils in the foundation of this dam, the Board notes again the need to avoid excessive conservatism in selection of cyclic loading resistance values, by cumulative compounding of slightly conservative safety margins selected at different stages of the analysis. In particular it is noted that careful consideration needs to be given to the effects of sample disturbance on the values of cyclic loading resistance determined by laboratory tests, among other factors. The Board notes that the effective penetration resistance values for the foundation sands are almost twice as high as those of the San Fernando dam sands and on this basis it would seem highly improbable that failure could occur in these materials for



design earthquake motions comparable to those which occurred at San Fernando in 1971. A careful review of all analytical details involved in the Forebay Dam analysis would therefore seem appropriate.

(c) Shape and Effect of Foundation Bedrock Profile at Main Dam .

Based on the detailed review presented by Mr. Akers of bedrock and adjacent overburden conditions at the right abutment of the dam, and on the extensive overburden studies southeasterly therefrom presented by Mr. Hammond, together with consideration of the clearly favorable curvature of the axis of the dam at the abutment, the Board concurs with the finding that the moderately steep bedrock profile in this location has no significant influence on the seismic safety of the dam.

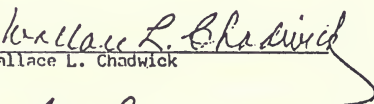
Question 4. -- "When all analyses are completed to the satisfaction of the Small Board, will it be appropriate to obtain concurrence signatures of all eight Board Members on Chapter X, Introduction (Summary of Conclusions and Recommendations) by mail after mailing each Board Member a final draft of the Bulletin Report?"

Response

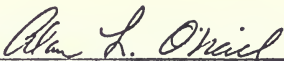
Many meetings have been held, and information has been exchanged, between the Small Board and the Department since the last meeting of the eight member Board. This Board recommends that the eight members of the Board be contacted to determine if a meeting should be held wherein those members not participating on the Small Board can be briefed and have questions answered prior to providing concurrence signatures on Chapter X.


The Board assumes that there may later be a meeting with the full Consulting Board for Oroville-Thermalito Dams Seismic Evaluation.

Respectfully submitted,

  
Wallace L. Chadwick

  
Thomas M. Leps

  
Alan L. O'Neill

  
H. Bolton Seed

Board of Consultants

November 16, 1993

Attachments: Agenda  
List of Participants  
List of Questions

THE SPECIAL CONSULTING BOARD FOR THE OROVILLE EARTHQUAKE

2 November, 1984

Mr. Keith G. Barrett, Chief  
Design Office  
Dept. of Water Resources  
P.O. Box 388  
Sacramento, California 95802

Dear Mr. Barrett:

The Special Consulting Board for the Oroville Earthquake met in the Resources Building on October 19, 1984 and heard presentations on seismic evaluations as outlined in the attached Agenda. Since several presentations dealt with assumed faulting and assumed magnitudes, and since Dr. Bruce Bolt was not in attendance, it was decided that the Board would not submit its report until Dr. Clarence Allen and Dr. H. Bolton Seed had an opportunity to discuss these matters with Dr. Bolt so that he could participate in the Board's report. Among the points at question were 1) extension of the Swaine Ravine fault to Bidwell Canyon Saddle Dam, 2) opening of a vertical crack during faulting, 3) type of anticipated displacement and earthquake magnitude on Prairie Creek fault/lineament, 4) possible extension of Prairie Creek fault/lineament.

The Board also has some questions about the ability of the Forebay Dam foundation in the vicinity of Station 112 to withstand ground motions as strong as the Oroville Reanalysis Earthquake on the Prairie Creek fault/lineament. The Board wishes to give further consideration to the appropriate reanalysis ground motions and/or methods of strengthening. A question was also raised as to whether the Division of Safety of Dams and the Design Office were in agreement with the Supplements to Bulletin 203-78 so that the final report would represent the findings of the Department. It is our understanding that this matter will be clarified in the next month or so.

It is also our understanding that a revised copy of Chapter VI will be sent shortly to the members of the Board which will answer some of the questions that were raised at the meeting.

After discussions with Dr. Bolt and review of revised Chapter VI, the Board will prepare a report. At this time we do not anticipate that another meeting of the Board will be required.

Yours truly,

  
GEORGE W. HOUSNER  
Chairman

cc. Board members

THE SPECIAL CONSULTING BOARD FOR THE OROVILLE EARTHQUAKE  
22 February 1985

Mr. Keith G. Barrett, Chief  
Design Office  
Dept. of Water Resources  
P.O. Box 388  
Sacramento, California 95802

Dear Mr. Barrett:

The Special Consulting Board for the Oroville Earthquake met in the Resources Building on October 19, 1984 and later met at the Seismographic Station at the University of California-Berkeley on February 1, 1985 to consider certain items having to do with the seismic reanalysis of the Oroville Forebay Dam and Afterbay Dam. The present report covers the following items.

Prairie Creek Fault

There is little, or no, direct evidence that an active trace of the Prairie Creek Fault extends northwestward of Palermo, adjacent to the Thermalito structures. However, in view of the general tectonic structures and trends in the area, the Board considers it desirable to assume that such an extension exists and that the surface projection of the fault passes about 2.5 miles east of the Forebay Dam. It is also likely that the fault dips to the west as do the other faults in the area such as that observed in the 1975 Cleveland Hill earthquake sequence.

Because of the lack of a definite surface fault trace north of Palermo, there is a significant limit to the size and recurrence rate of earthquakes likely to be produced by rupture of the assumed fault extension. On this evidence, the Board considers that the maximum nearby earthquake which could reasonably occur on this fault is a shallow Magnitude 6 event with a rupture surface extending down to about 10km. When account is taken of the depths of the likely zone of major energy release on the assumed dipping fault, the closest distance of this dominant seismic source from the Forebay and Afterbay Dams should be, for safety evaluation purposes, as follows:

Forebay Dam : 3 miles

Afterbay Dam : 7 miles

For the Afterbay Dam, this distance is the same as that considered in the safety evaluation already performed and thus its adoption does not affect the recommendations contained in the Afterbay Dam Seismic report.


For the Forebay Dam, the Board suggests that the safety evaluation earthquake motions should have the following characteristics (for a rock outcrop motion):


Peak ground acceleration: 0.45g

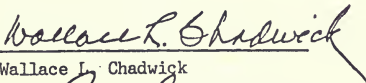
Peak ground velocity: 35 cm/sec

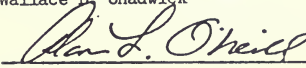
The accelerogram used for analysis should desirably have a "fling" in the early part of the record and an acceleration response spectrum for which the ratio of maximum spectral acceleration,  $(S_a)_{max}$ , to peak ground acceleration,  $a_{max}$ , is about 3 for 5% damping. The general shape of the acceleration response spectrum should be similar to those generally considered representative of rock response spectra. In the vicinity of the dam, however, the maximum ground acceleration on soil deposits should not exceed about 0.55g and the accelerations in rock should be limited as necessary to correspond to this limitation on ground surface motions.

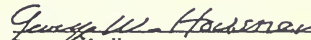
In its report of January 14, 1981, the Board noted that normal-fault displacements in the project area "will necessarily be associated with a component of horizontal extension at the surface." In saying this, the Board did not mean to imply that horizontal extension would be caused by the opening of significant tensile cracks in the bedrock, but only that shear failure on a dipping bedrock fault plane, with the footwall relatively raised, would necessarily be reflected in gross horizontal extension at the surface. Although such shear failure at depth might result in shallow tensile cracks in the overlying soils, weathered materials, or artificial embankments, tensile effects would not extend to large depths. The Board does not feel it to be appropriate to assume significant tensile opening of fissures in bedrock, such as is currently envisaged by the Department at, e.g., Bidwell Canyon Saddle Dam. We recommend instead that only shear failures be assumed in firm bedrock, with possible tensile failure being limited to surficial materials.

  
Clarence R. Allen

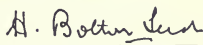
  
Bruce A. Bolt

  
Wallace L. Chadwick

  
Alan L. O'Neill

  
George W. Housner

  
Thomas M. Leps

  
H. Bolton Seed

cc. W. Hammond

SPECIAL CONSULTING BOARD  
FOR THE OROVILLE EARTHQUAKE

5 January 1989

Mr. John H. Lawder, Chief  
Division of Design and Construction  
Department of Water Resources  
1416 Ninth Street  
P.O. Box 942836  
Sacramento, California 94236-0001

Dear Mr. Lawder:

As requested, the Board has reviewed the following chapters of Bulletin 203-88, Supplement to Bulletin 203-78 "The August 1, 1975 Oroville Earthquake Investigations."

Chapter 1, Introduction, July 1988

Chapter 2, Seismic Evaluation of the Thermalito Power Plant Headworks

Chapter 3, Thermalito Afterbay Dam Seismic Evaluation

Chapter 4, Thermalito Afterbay Dam Concrete Structures Seismic Evaluation

Chapter 5, Thermalito Forebay Dam Seismic Evaluation, July 1988

Chapter 6, Seismic Evaluation of Bidwell Canyon and Parish Camp Saddle  
Dams and Effects of Possible Fault Movements in Oroville Project Dams  
Foundations, July 1988.

A meeting was held in the DWR building in Sacramento on November 18, 1988 with members of your staff making explanatory presentations and answering final questions from the Board members. The responses were fully adequate.

Based on its reviews the Board concurs with the conclusions presented in Chapters 1-6 of Bulletin 203-88 and with the adequacy of the remedial measures proposed.

Respectfully submitted,



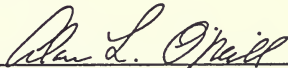
Clarence R. Allen



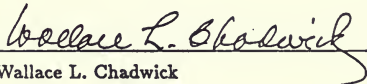
Thomas M. Leps



Bruce A. Bolt



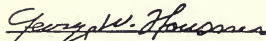
Alan L. O'Neill



Wallace L. Chadwick



H. Bolton Seed



George W. Housner









## CONVERSION FACTORS

Quantity	To Convert from Metric Unit	To Customary Unit	Multiply Metric Unit By	To Convert to Metric Unit Multiply Customary Unit By
Length	millimetres (mm)	inches (in)	0.03937	25.4
	centimetres (cm) for snow depth	inches (in)	0.3937	2.54
	metres (m)	feet (ft)	3.2808	0.3048
	kilometres (km)	miles (mi)	0.62139	1.6093
Area	square millimetres (mm <sup>2</sup> )	square inches (in <sup>2</sup> )	0.00155	645.16
	square metres (m <sup>2</sup> )	square feet (ft <sup>2</sup> )	10.764	0.092903
	hectares (ha)	acres (ac)	2.4710	0.40469
	square kilometres (km <sup>2</sup> )	square miles (mi <sup>2</sup> )	0.3861	2.590
Volume	litres (L)	gallons (gal)	0.26417	3.7854
	megalitres	million gallons (10 <sup>6</sup> gal)	0.26417	3.7854
	cubic metres (m <sup>3</sup> )	cubic feet (ft <sup>3</sup> )	35.315	0.028317
	cubic metres (m <sup>3</sup> )	cubic yards (yd <sup>3</sup> )	1.308	0.76455
	cubic dekametres (dam <sup>3</sup> )	acre-feet (ac-ft)	0.8107	1.2335
Flow	cubic metres per second (m <sup>3</sup> /s)	cubic feet per second (ft <sup>3</sup> /s)	35.315	0.028317
	litres per minute (L/min)	gallons per minute (gal/min)	0.26417	3.7854
	litres per day (L/day)	gallons per day (gal/day)	0.26417	3.7854
	megalitres per day (ML/day)	million gallons per day (mgd)	0.26417	3.7854
	cubic dekametres per day (dam <sup>3</sup> /day)	acre-feet per day (ac-ft/day)	0.8107	1.2335
Mass	kilograms (kg)	pounds (lb)	2.2046	0.45359
	megagrams (Mg)	tons (short, 2,000 lb)	1.1023	0.90718
Velocity	metres per second (m/s)	feet per second (ft/s)	3.2808	0.3048
Power	kilowatts (kW)	horsepower (hp)	1.3405	0.746
Pressure	kilopascals (kPa)	pounds per square inch (psi)	0.14505	6.8948
	kilopascals (kPa)	feet head of water	0.33456	2.989
Specific Capacity	litres per minute per metre drawdown	gallons per minute per foot drawdown	0.08052	12.419
Concentration	milligrams per litre (mg/L)	parts per million (ppm)	1.0	1.0
Electrical Conductivity	microsiemens per centimetre (uS/cm)	micromhos per centimetre	1.0	1.0
Temperature	degrees Celsius (°C)	degrees Fahrenheit (°F)	(1.8 × °C) + 32	(°F - 32)/1.8

State of California—Resources Agency  
Department of Water Resources  
P.O. Box 942836  
Sacramento CA 94236-0001



UNIVERSITY OF CALIFORNIA, DAVIS



3 1175 02041 2659

